Silver Coordination Compounds with a Family of Ditopic Ligands of Varying Flexibility: about Chains, Rings, Helices and Polycatenanes

Inauguraldissertation

zur

Erlangung der Würde eines Doktors der Philosophie

vorgelegt der

Philosophisch-Naturwissenschaftlichen Fakultät

der Universität Basel

von

Jorge Luis SAGUE DOIMEADIOS

aus Holguin, Kuba

BASEL, 2006

Genehmigt von der Philosophisch-Naturwissenschaftlichen Fakultät

Auf Antrag von

Prof. Dr. Katharina M. FROMM

Prof. Dr. Edwin C. CONSTABLE

Basel, den 6 Juni 2006

Prof. Dr. Hans-Jakob Wirz

A Mia Lyuba

Acknowledgements

Some of these results have been reported in these publications [1-4]:

- Fromm K. M.*et al.*, *Zeitschrift fuer Anorganische und Allgemeine Chemie*, **2005**, *631*, (10), 1725-1740.

- Fromm K. M., Doimeadios J. L. S., Robin A. Y., *Chemical Communications (Cambridge, United Kingdom)*, **2005**, (36), 4548-4550.

- Fromm K. M., Doimeadios J. L. S., Robin A. Y., *CrystEngComm***, 2006,** 8(5), 403.

- Sague, J.L. and Fromm, K. M., *Crystal Growth & Design*, **2006**, 6(7), 1566.

Contents

A - Introduction on coordination polymer networks

A - I - What is a coordination polymer network?

In the journey from molecular to supramolecular design old ideas were broken and new proposals possessing a higher degree of complexity have been implemented.

Within the last two decades the theoretical principles of the supramolecular chemistry field have been established (and are continuously developing) after the pioneer work of Jean Marie Lehn [5-7], Dietrich [8, 9], Behr [10, 11], Sauvage [8, 12-14] and Cheney [12, 15] from macrocycles and cryptates to complexes of alkaline metals, anions or protons.

The scientific community working in the 80s did not imagine the impact of their research in the future of chemistry. One of the merits of these researchers was to open a new exciting field in chemistry, but also to induce other scientists at that time to the idea that it was possible to overcome control of extremely weak intermolecular forces in order to direct the formation of assemblies containing metal ions with specific functions or properties.

One of the first attempts to describe the use of metal ions and all their possible combinations with an organic ligand, forming large molecular assemblies was introduced in 1994 by Constable, who brought the term 'metallosupramolecular chemistry' into daily scientific language [16-18]. From the coordinative point of view, such structures could possess diverse dimensionalities, discrete zero-dimensional structures or polymeric three-dimensional arrays in the crystalline and solution state.

The diversity of intermolecular forces present depends on which states we are working in: i) in solution for instance, in the generation of dimensionality, the complexation of the metal cation by the organic ligand depends basically on a cooperative effect, the concentrations used or the solvents, ii) in the crystalline state, however, other weak forces are relevant and should not be neglected (hydrogen bond, aromatic-aromatic, metal-aromatic, metal-metal).

In the supramolecular chemistry field, chemical effects due to molecular recognition like: i) steric complementarity (shape and size, convex and concave domains) ii) interactional complementarity (complementary binding sites, hydrogen bonds, electrostatic charge/dipole, dipole/dipole) in the correct disposition, iii) large contact areas, iv) multiple coordination sites and v) strong overall

---

binding, can direct the formation of a particular assembly between several combinations. The control and rational use of these interactions remain so far a challenge for modern chemistry.

Several new definitions have appeared during the last three decades. Most of these definitions are already implanted in the scientific mind, others are still waiting to be generally accepted. The use of definitions like 'self-assembly' and 'self- organization' brings some discussion in the literature [19-21]. Lehn defined 'self-assembly' as "the spontaneous association of a well delimited number of species generating *polymolecular assemblies*" and 'Self-organization' basically as "a set of intersecting self-assemblies". One should keep in mind that this definition is subjected to the theoretical and empirical development of the supramolecular chemistry field [22, 23].

Gaining more insights and controlling weak supramolecular forces present in nature will permit chemists to construct large supramolecular aggregates with specific functions able to emulate proteins.

Nowadays, the supramolecular chemistry field is facing a new paradigm: the control of the last level in matter organization.

A - II - An overview on the crystalline state

In the state of art of supramolecular chemistry the major star is without any doubt the crystal and the structure it brings to life. In comparison, less attention has been paid to the liquid state, and to what happens when extremely weak forces take control over a conglomerate of particles to bring them into an infinite ordered mode

A notable difference between the atomic or molecular level of matter and the supramolecular level arises from the nature of the forces which control the properties of atoms or molecules and supramolecular aggregates. Atomic forces and/or ionic and covalent forces have been well studied. However, the establishment of a hierarchy in the weak supramolecular forces (like hydrogen bonds, π–π stacking, or metal-metal interactions) is nowadays a subject of controversy (Figure 1).
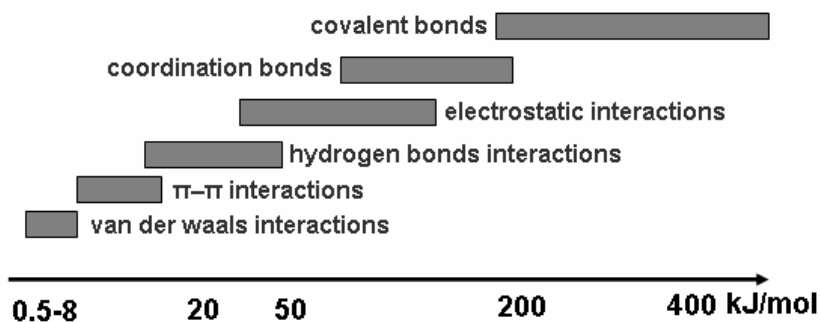
Figure 1. Schematic distribution of some supramolecular forces base on the energy

In the crystalline array, it is quite difficult to differentiate the importance between all these extremely weak supramolecular forces which are present and stabilize the packing in the solid state. A common approach is to separate and analyze all of them. But the fact that almost all these forces act usually in a concomitant manner just makes the picture more complicated.

The basic force in the crystalline array of metallosupramolecular arrays is the *ligand-metal interaction*. This interaction can be thermodynamically or kinetically dependent. In the case concerning the coordination of the silver cation to an N-donor pyridine derivative ligand, this interaction involves the donation of the nitrogen lone electron pair to the silver cation.

The preference of the Ag(I) for linear coordination geometry makes the generation of linear supramolecular arrays possible when ditopic ligands are used as building blocks. This basic interaction should be considered as the main 'cement' of the crystalline state.

Electrostatic interactions are present mostly due to the coordination of the metal by the counter ion. The here considered anions have the ability to interact with the metal cation in different modes (mono-, bi- or both versus different cations). The nature of this interaction depends usually on the shape and charge distribution of the anion. The energy involved in the silver-anion bond can vary over a wide range and depends on the particular crystalline array. General conclusions are difficult to extract in order to predict the formation of one particular structure over others. Even poorly coordinating anions can distort the supramolecular structure and because of this, this force is considered important for long-range structural orders [24-33].

The nature and strength of *hydrogen bond interactions* have been discussed since 1930. It was Taylor in 1982 who highlighted the importance of C–H bonds in crystals after an exhaustive study on crystal data obtained by neutron diffraction. The author concluded that it exists a clear evidence

Silver Coordination Compounds with a Family of Ditopic Ligands of Varying Flexibility: About Chains, Rings, Helices and Polycatenanes

7

of C–H···X interactions (X = N, S, and Cl) and they were indeed of attractive nature [34]. Hydrogen bonds are directional and can involve multiple acceptor and donor atoms [35-51].

When aromatic systems are present in the supramolecular array the stabilization of the crystalline array through *π–π interactions* is feasible. The different types and the nature of aromatic interactions has been widely discussed in the literature [52-56]. This interaction, according to the Hunter–Sander's model, exists due to an electrostatic attraction of aromatic π-electrons to a positively charged ring π-frame. One can distinguish between three stacked arrangements: face to face, offset and T-shape conformation (Figure 2)
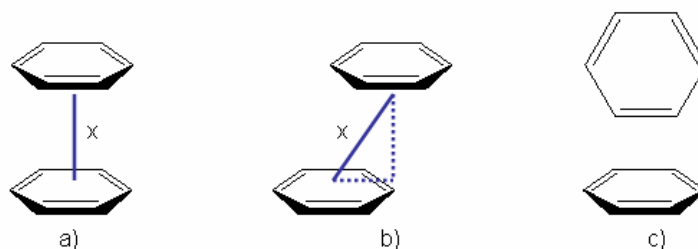
Figure 2. Aromatic stacking: a) face to face, b) offset and c) T-shape conformation. "x" represents distances centroid-centroid, normally between 3.3 and 3.8 Å.

The case of the T-shape conformation illustrates a common problem in supramolecular chemistry since the potential presence of a weak C–H···π bond should not be neglected and consequently it is rather difficult to differentiate the border between these two interactions.

Even if some recent examples show ligand unsupported Ag–Ag interactions [57, 58], the tendency of d^{10} cations to form $M(d^{10})$-$M(d^{10})$ bonds [59, 60] and the nature of this *metal-metal bond* have been debated in the literature. Some calculations estimate the energy involved in the Ag–Ag bond to be about 5 kJmol^{-1}, depending on the ligand used in the coordination of the silver cation [61, 62].

Other forces like *metal–π interactions* depend as well on the aromatic system present in the complex. The broader this system is, the stronger the aromatic interaction with the silver cation is [63, 64].

Because the ligand we use in this work is based on pyridine rings, which is not comparable to polyaromatic systems concerning the ability to coordinate Ag(I), we must expect rather a scattered presence of this kind of interaction in our complexes.

Coulombic interactions are basically repulsive forces present in the crystalline packing. The reasons are better understood if one visualizes the coordination polymer as locally charged species which are separated by ligands with different geometries. The charge on the cation can be delocalized into the

ligand, and it should be neutralized by the counter ion if this is enough coordinative. The use of non-coordinating counter ions, however, may lead to a significant coulombic repulsion within the crystal due to the less delocalization of this charge. This can alter the supramolecular array to a great extend, and it is an important factor to survey.

A - III - Application of coordination polymer in metal-organic framework (MOF)

One particular field where metallosupramolecular chemistry has found wide application is the creation of three-dimensional metal-organic frameworks (MOF's). The next chapters will focus on the different motifs and types of coordination polymers. Here, some recent research and applications of MOF coordination polymers in modern chemistry will be shortly highlight.

Inorganic porous materials have found application in industrial processess and domestic life during the past two decades. Zeolite based materials are an excellent example of this kind of materials which are able to allocate several guest molecules in their internal channels depending on the size and shape of these pores. Several researchers have focused on the chemical or physical modification of the size and shape of these pores, envisaging some selectivity in the guest recognition process and consequently applications like catalysis, storage and ion-exchange [65, 66]. The synthesis of new materials in which rather rigid organic ligands were used with metal cations to generate porous metal-organic frameworks has attracted some attention since the last decade [67-81]. The possibility to play with the coordination geometry of the metal cation and almost with an infinite number of ligands has the potential to generate an enormous variety of porous materials.

The inclusion of an organic ligand will easily allow tuning of the physical and chemical properties of the metal-organic framework, which is important for application in magnetism, catalysis or absorption/desorption processess of guest molecules just to mention a few examples [82] (Figure 3).

Silver Coordination Compounds with a Family of Ditopic Ligands of Varying Flexibility:
About Chains, Rings, Helices and Polycatenanes

9
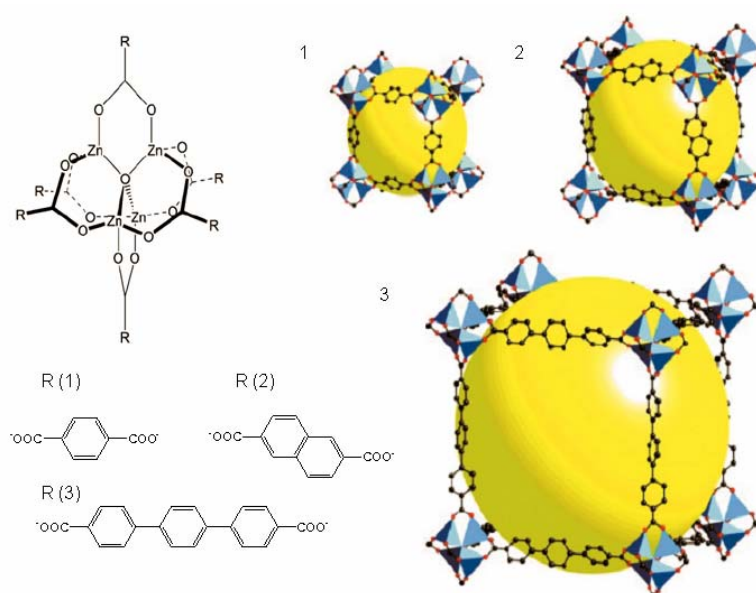
Figure 3. MOF generated after coordination of Zn(II) with ditopic ligands possesing carboxilates functions

The use of rigid ligands should avoid the presence of network isomerism in the generation of porous metal-organic frameworks. Some usual ligands employed are listed in Figure 4. The nature of the heteroatoms present in the ligand is related to the metal to be coordinated. Other aspects concerning the nature of the metal cations, and the lability of their coordination sphere are an important factor, mostly because metal cations which do not impose a rigid geometry can affect the predictability of the resulted network.
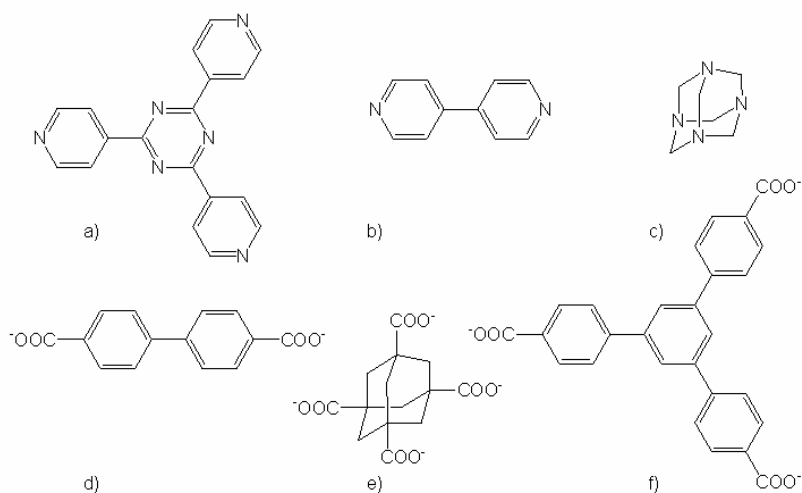
Figure 4. Rigid ligands used to generate MOF's motifs

Silver Coordination Compounds with a Family of Ditopic Ligands of Varying Flexibility: About Chains, Rings, Helices and Polycatenanes

10

The silver cation often possesses a low coordination number [83] and some ability to form metal-metal bonds. A MOF containing linear silver coordinated with a ditopic ligand, where Ag–Ag bonds (2.970(2) Å) were present [84], was synthesized (Figure 5).
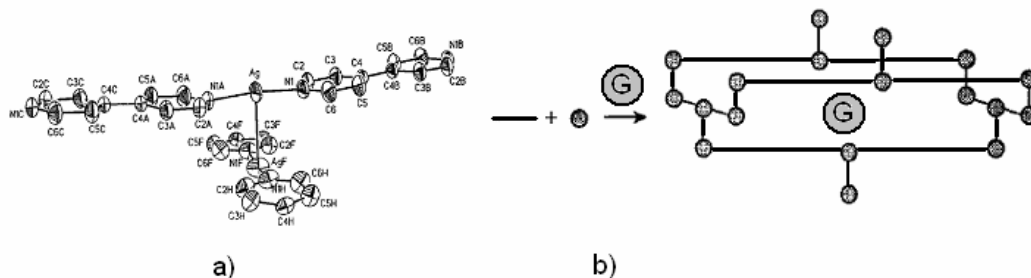
Figure 5. a) building block unit including the asymmetric unit present in crystalline [Ag(4,4'-bpy)*NO₃] b) a schematic representation of the assembly of metal ions (dark-gray spheres) and organic ligands (dark rods) to yield diamond-like frameworks with rectangular channels where a guest molecule G occupies the voids.

Bulky counter ions [74, 85-87] and ligands [88-92] have been used to avoid interpenetration, which is a common problem found in the creation of MOFs.

A new, more "supramolecular" approach is coming through the field of porous metal-organic frameworks. If the use of rigid ligands avoids the presence of network isomerism in the porous structure, what about if we can indeed control some supramolecular weak forces like hydrogen bonds or π-stacking to create a dynamic MOF?

The synthesis of dynamic porous frameworks is an active field of research in chemistry. They are usually categorized in three main types: i) dynamic MOFs, which have the property that after removing the guest molecules the network collapses due to the close packing force, but it can be regenerated under the initial conditions [93-97]; ii)) dynamic MOFs of ''guest-induced transformation'' type, where the guest molecules absorbed in the network have the property of structurally shifting the network after simultaneous exchange with other guest molecules [98, 99], and iii) dynamic MOFs of ''guest-induced reformation'' type, in which the removal of guest molecules from the pore induces a structural change in the network to a different one. However, absorption of the initial guest molecules reverts the network to the original one [93, 100-110] (Figure 6).
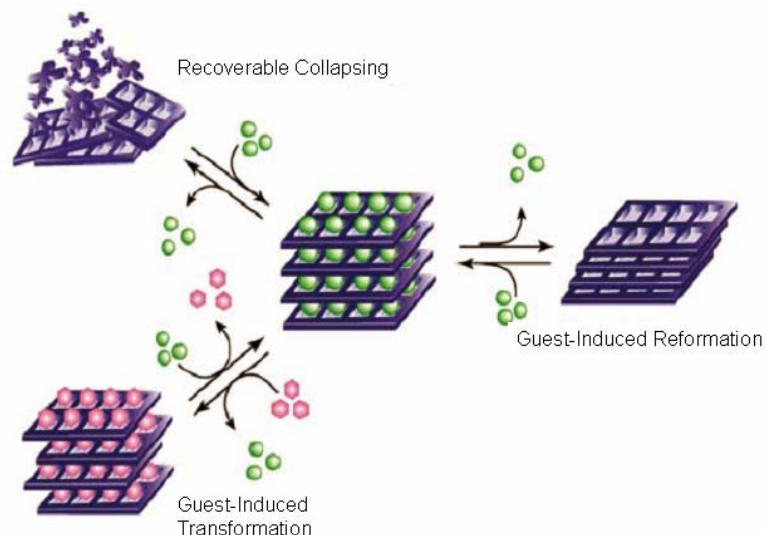
Figure 6. Schematic representation of some dynamic MOF types

The future potential applications of these dynamics MOFs is enormous from domestic life to industrial processes (new materials for the storage of hydrogen at ambient conditions, heterogeneous catalysis, adsorption and ion-exchange processes [78, 111]). However, further research is required to define the importance of all factors participating in the generation of the MOF (ligand, anion and weak supramolecular forces) in order to get insight of the formation process and make possible an accurate prediction of the final product [112-114].

A - IV - Interest of silver(I) metal-organic networks

In metal-organic chemistry, the silver ion has been widely used due to the soft acceptor characteristic of this cation, as well as the flexible coordination sphere which it posseses. The latter allows this metal to be coordinated by a variety of ligands which possess several geometries and heteroatoms like sulphur, phosphor and nitrogen to generate a diverse number of topologies, which are interesting from the structural point of view in crystal engineering.

For decades silver has had several applications due to its antibacterial properties and more recently, in the field of catalysis. Deposition of monolayered silver complexes and posterior reduction of the metal cation should generate nanoparticles where the distances between metals could be controlled

via the ligand. This approach has found potential applications in the functionalization of surfaces envisaging catalysis and medical uses.

A - V - What and why and how?

In our group we are interested in studying the coordination pattern of silver salts with a serie of organic ligands of a same family. These ligands were only differentiated by the linking chain between two group, isonicotinic or nicotinic acid. The length of the polyether can be increased or decreased to generate more or less flexibility, and was expected to induce more or less complexity in the final supramolecular array.

What was known about silver coordination polymers at that time? Quite a lot [115-117]. Silver is a soft cation (according to HSAB theory). From the coordination point of view that means that it prefers soft donating atoms, like nitrogen, phosphor and sulfur. The use of pyridine derived ligands should lead to linear type of networks, in which the anion could influence the final dimensionality of the supramolecular motif . Increasing the number of potential coordination sites in the lateral chain will induce more complicated arrays. Formally one can imagine a large variety of combinations and new structures.

The metal cation allow coordination geometries from linear to bi-pyramidal depending of the ligand used and the reaction condition, as well as electrostatic requirements directly responsible for the assembly and stability of the supramolecular array. This last condition can be manipulated in order to bring new chemical or physical properties.

Silver salts are considered to provide a linear coordination motif [118-124], but tetrahedral [33, 125, 126], trigonal bipyramidal [127-129] and even square planar motifs[130, 131] are found in practical laboratory work.

The counter ion has another important effect on the final network design. Several studies have been carried to test the bridging ability to coordinate one or more metal atoms, the facility to form hydrogen bonds, size and shape [25, 30, 33, 119, 124, 126, 132, 133]. For this work, we chose four different counter ions and played with almost all previous discussed possibilities (Figure 7) to influence the crystal packing.

Silver Coordination Compounds with a Family of Ditopic Ligands of Varying Flexibility:
About Chains, Rings, Helices and Polycatenanes

13
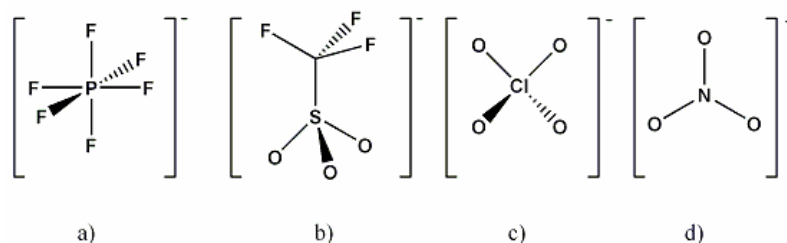
Figure 7. Counter ion types.Changing shape and size will allow us to explore the impact of each one on the network

The hexafluorophosphate counter ion is the least coordinating one, however it is the most voluminous with 109 Å^3 [134]. Generally, it is difficult to find networks where the PF_6^- coordinates several metal cations or coordinates in a multidentate way; it is more often observed to be placed in cavities in the structure. Due to the "symmetric" electronic distribution in a "sphere type" volume, its coordination ability is considered to be weak [135].

The triflate, with less than 109 Å^3 is quite similar from the point of view of hydrogen bonds forming facility; however, this counter ion can coordinate more strongly the silver cation using its oxygen atoms. The trifluoromethane part of the molecule avoids the possibility of effective coordination in a bidentate or more complex coordination mode with other hydrogen atoms.

Perchlorate (82 Å^3) offer less acceptors atoms for hydrogen bonds but introduces more complexity in the network bridging individual chains or rings into a more sophisticated network.

The award as "master of bridging" belongs so far to the nitrate (volume 64 Å^3): mono-, bi- and tridentate, nothing is impossible for this counter ion. The only problem is that it can form bonds with solvent molecules as well with a great facility. Working in aqueous medium, when nitrate anions are present, there is an enormous probability to find water molecules inside the crystalline structure coordinated to this anion. The solvent can distort or direct the overall motif in an unusual or unexpected way. A rapid search in the Cambridge Structural Database (CSD) affords more than 40% structures possessing nitrate, and having water at the same time.

A - VI - Why ligands of this type?

Ligand design is important in this sense. Dramatic variations in the overall coordination type are due to imperceptible changes on the ligand planning [121, 132, 133, 136-142]. For the topology of the

polymeric networks is determinant the control of the geometry of the polydentate ligand and the potential complementary interactions with the metal cation. The anion and the solvent are an important choice to take into account [33, 126, 132, 136, 143-145].

With a view to possible industrial applications, our ligands were constructed based on relatively simple starting materials. Nicotinic and isonicotinic acid were assembled with polyethylene glycol through an ester function (Figure 8). Flexibility was envisaged at this point due to the increasing rotational freedom around C–C and C–O bonds. The fact that every ligand contains nitrogen and oxygen atoms allows the coordination of different cations depending on the desirable properties we expect to confer to the overall array.
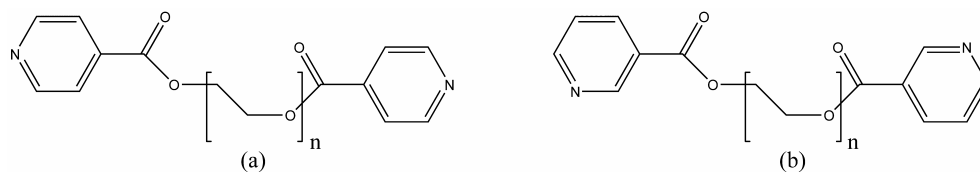
Figure 8. Ligands synthesized for this work. a) based on the Isonicotinic acid b) based on the Nicotinic acid. (n= 1,2,3 and 4)

Several research groups are working with similar ligands as building blocks for supramolecular coordination arrays [146-148]. This, more than being a problem is in fact very stimulant, since the results found in all these groups share with our group just a few structures which are identical or similar, based on their topology.

The very beginning idea behind this work was based on the synthesis and characterization of double salt complexes for non linear optical (NLO) applications [149-151]. A flexible ligand wrapping around a cation through programmed specific binding sites and a second cation, like silver, acting as closing key was the first design. The main problem was to design a ligand with two different kinds of coordination sites, what would permit to differentiate two dissimilar metals.

Based on the well known hard–hard or soft–soft principle in HSAB-theory terms, the ligand should include two different heteroatoms which differ in their coordination ability. Oxygen and nitrogen atoms are present in most available organic compounds, like polyethylene glycol and pyridil moieties, they have been extensively used in different tecton construction, separated [152-158] and together [159]. In addition to this, it is possible to play with different lengths in the spacer in order to

study the stability of the complexation process itself and the ability to differentiate several cations [160] (Figure 9).
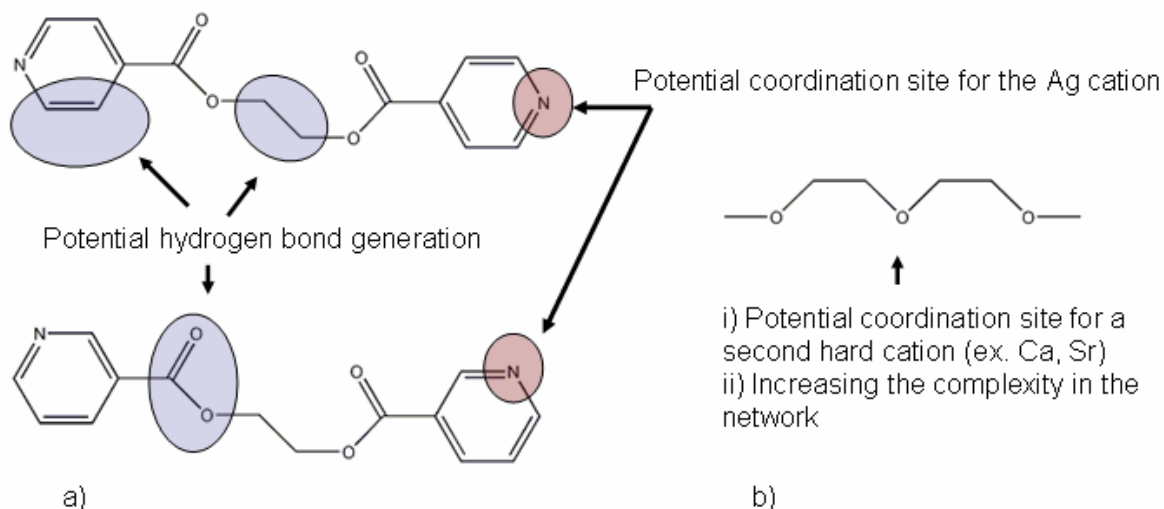
Figure 9. Potential coordination sites present in the ligands

We synthesized a family of ligands based on the isonicotinic and nicotinic acid, linked with polyethylene glycol of variable lengths (Figure 10).
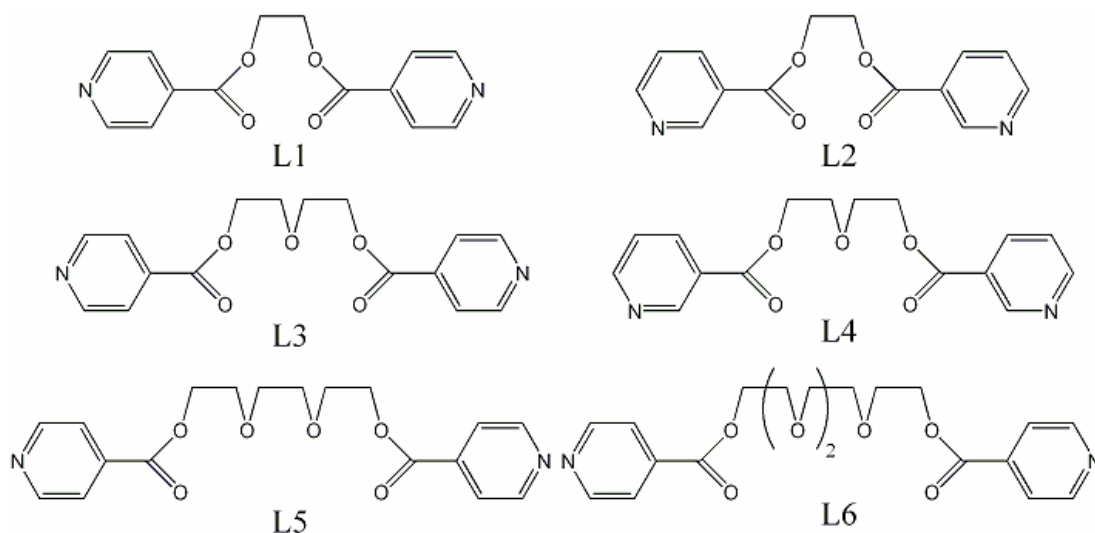
Figure 10. Ligands synthesized to generate supramolecular metal-organic arrays with Ag(I)

DFT calculation for the ligand **L1**, presented by Dr. Robin in her PhD thesis, evidence that the energetic difference between the syn and the staggered conformation is rather small. In almost all

---

crystalline arrays was found a predominantly linear array of type (-L-Ag)$_n$, which may be expanded in a 2D sheet via interaction with the counter ion [161].

We realized very easily that a change in the polyethylene glycol length would affect the whole supramolecular array, and we expected this change would occur in a logical way like: growing the length of the spacer, boost in the dimensionality.

That is not always, however, the case as we will see in the discussion part of this work.

A - VII - Aim of the Thesis

While searching possibilities of creating "supramolecular architectures" in which different metal cations can be caught by an organic ligand, envisaging catalysis, formation of polyelectrolytes, and other applications, it was a matter of fact that certain ligands are able to form more than one supramolecular array in the same reaction vessel [162], even some other crystals, acting like "living structures" changing form when left in the reaction mixture [161, 163, 164].

"Supramolecular polymorphism" or "Supramolecular isomerism" is a common phenomena in coordination polymer. Network isomerism or polymorphism appears and disappears almost without a clear idea of what happened. Just as in the same way is pretty difficult to predict the formation of a crystalline array based on the knowledge of the organic ligand, the metal salt and the crystallization conditions that are employ. A previous work of Dr. Robin in our group, for instance, shown the difficulty arised on the control of the co-crystallized solvent in a family of silver(I) compounds which crystallize concomitantly in water [161]. That place two relates question: working in similar circumstances concerning the reactants and reaction conditions, are the number of possible topological combinations infinite or rather quantized? If the answer is affirmative than, until which point can we gain control over the forces involved in the complexation process and further crystallization of the products?

The crystallization of silver(I) network polymers can be achieved by different methods, but two main approaches are the most common ones: i) varying the solvent, ii) varying temperature. Other techniques were implemented for several authors, we tried almost all of them and the results will be discussed later.

Silver Coordination Compounds with a Family of Ditopic Ligands of Varying Flexibility:
About Chains, Rings, Helices and Polycatenanes

17

B - Results and discussion

Coordination polymers obtained were synthesized using three major techniques: i) slow evaporation from a solvent or a mixture of solvents, ii) solvent diffusion (different solvents containing each of them the ligand or the silver salts; diffusion of one solvent into a second one containing the ligand and the silver salt already dissolved, and solvent diffusion in a "H"-shaped tube) iii) based on microwave synthesis (Figure 11).
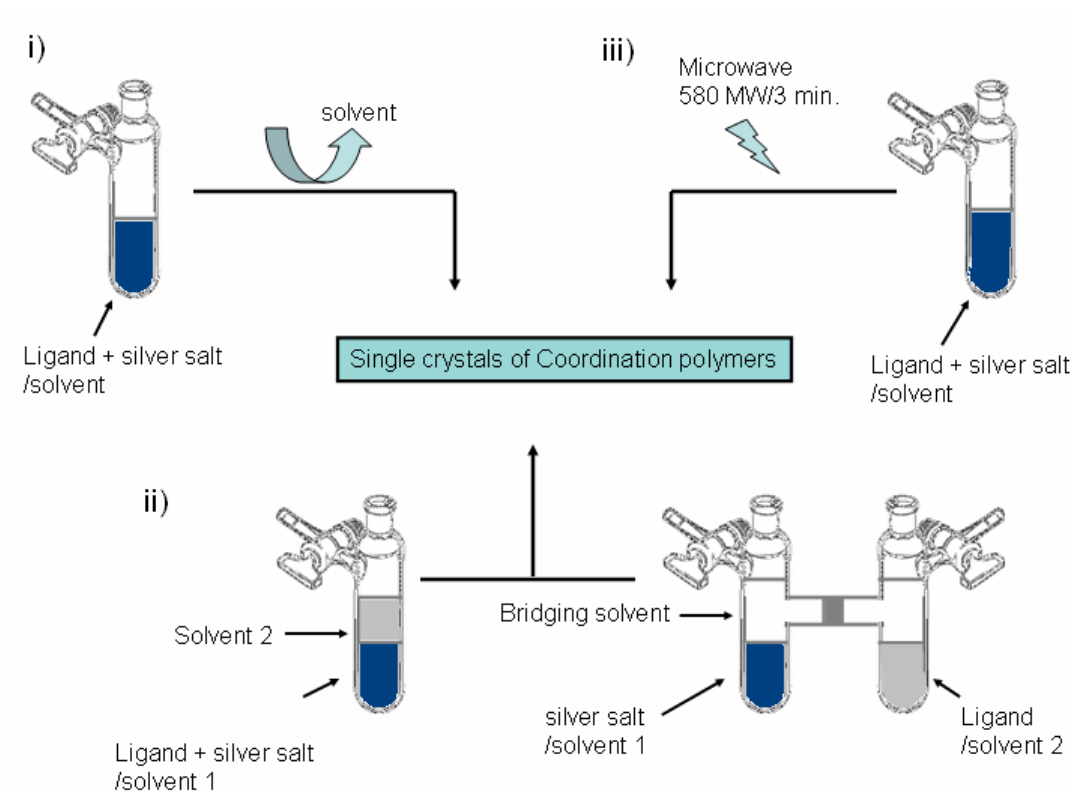
Figure 11. Crystallization technique used to obtain single crystal structures. i) slow diffusion ii) solvent diffusion and iii) synthesis using microwave radiation

In the *slow evaporation technique* a solution with the ligand and the silver salt was left to slowly evaporate. A rapid evaporation affords precipitation rather than crystallization. *Solvent diffusion* involves the slow deposition of one or more solvent layers (containing or not one of the chemical species) over a second solution (containing one or both chemical species); the slower the deposition to generate sheets, the better the results.

The use of an "H"-shaped tube is a special case of solvent diffusion, mostly due to the control on the diffusion rate exerted by the frit which connects both sides of the tube. The crystals obtained by this technique offer an excellent quality for X-ray diffraction measurements. Due to the concentration and solvent gradient, the appearance of network isomers or polymorphs is favored. A solution containing the ligand and the silver salt can be subjected to a microwave radiation for less than four minutes and single crystals of the complex are obtained immediately in the vessel or after filtrating the solution. Due to the rapid growth of crystals (within 2-3 days) and the small quantity of materials needed, the *microwave technique* offers great advantages against the other techniques previously discussed. Only the small size of the crystal obtained can be problematic using this technique, but with the modern area detectors present in actual X-ray diffractometers this problem can been overcome in most cases.

B - I - Ligands

Single mono-crystals of the ligands were grow by slow evaporation of a mixture of solvent DCM:n-Hexane in different ratio. Different crystals of the same batch were tested to determine polymorphism.

B - I.1 - Crystallographic structures of ethane-1,2-diyl diisonicotinate (L1)

This ligand was previously synthesized and characterized by Dr. Robin while working on her PhD project [162]. It crystallizes in the monoclinic system, space group $P2_1/n$ (No. 14). The asymmetrical unit cell contains half of a molecule, and one molecule in the unit cell packing (Figure 12).
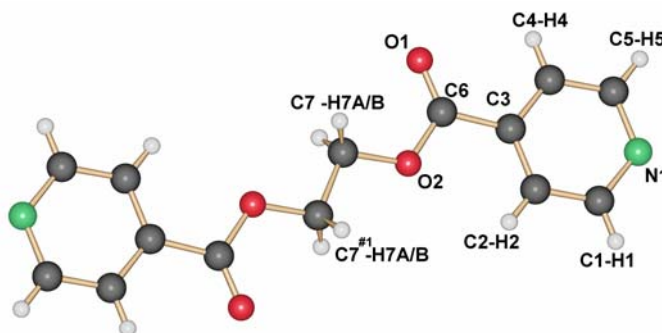
Figure 12. Schakal view of the ligand L1. The representation is based on its crystal structure

Silver Coordination Compounds with a Family of Ditopic Ligands of Varying Flexibility:
About Chains, Rings, Helices and Polycatenanes

19

The ligand is contained in a plane with an inversion centre in the geometrical middle of the bond C7–C7$^{#1}$. The ethylene moiety adopt in the crystalline state an anti (staggered) conformation, with both carbonyl oxygen atoms pointing to opposite direction within the molecule (O2–C7–C7$^{#1}$–O2$^{#1}$, 180.0(9)°) (Table B-I.1).

Table B-I.1 Most important Bond lengths [Å] and angles [°] for **L1**

N(1)–C(1)	1.390(3)	C(1)–N(1)–C(2)	120.0(7)
N(1)–C(2)	1.390(3)	O2–C7–C7$^{#1}$–O2$^{#1}$	180.0(9)
C(7)–C(7)$^{#1}$	1.498(2)		
Symmetry transformations used to generate equivalent atoms: #1 3-x, 1-y, 1-z			

Weak hydrogen bonds exist between hydrogen atoms of the aromatic ring or the ethylene moiety and the carbonyl oxygen and the nitrogen atoms of the pyridine rings, which act as donor atoms (Table B-I.2).

Both hydrogen bonds types differ in their final function: whereas the C–H⋯N bonds are important to maintain individual ligand molecules stacked in a sheet (perpendicular to the plane generated by the ring atoms), the C–H⋯O bonds hold these formed sheets attached together (Figure 13).
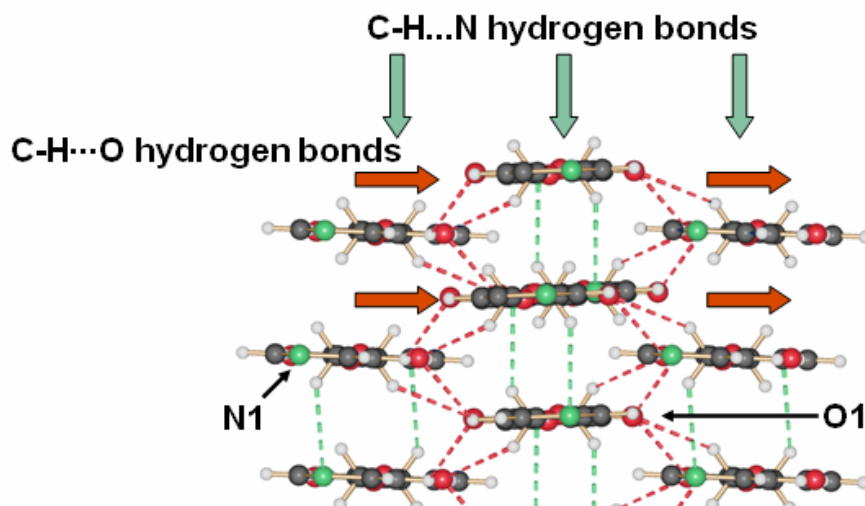
Figure 13. Hydrogen bonds formed after coordination of the hydrogen atoms (white) to the nitrogen (green) and oxygen atoms (red)

Table B-I.2 Hydrogen bond data for **L1** [length (Å) and angle (°)]

D–H⋯Acceptor	d (D–H)	d (H⋯A)	d (D⋯A)	Angle D–H⋯A
Hydrogen bonds formed between ligands				
C5–H5⋯N1[#2]	0.93	2.75(8)	3.58(1)	148.4(1)
C7–H7A⋯N1[#3]	0.97	2.88(9)	3.61(1)	133.1(8)
C4–H4⋯O1[#4]	0.93	2.74(9)	3.26(7)	116.5(8)
C7–H7B⋯O1[#3]	0.97	2.91(6)	3.71(9)	140.6(8)

Symmetry transformation used to generate equivalent atoms: #2 1-x, -y, -z #3 2-x, -y, -z #4 -0.5+z, 0.5-y, -0.5+z

Due to the planar extension of the ligand, some weak π–π interactions are expected. The closest aromatic-aromatic distance present is 4.32 Å, which rejects any evidence of interaction (Table B-I.3).

Table B-I.3 π–π stacking for **L1**

π–π interaction	d_{R-R} (Å)	ρd_{R-R} (Å)	α	β
Inter π–π stacking between aromatic rings of different ligands				
Ring (N1,C1,C2,C3,C4,C5)⋯Ring (N1,C1,C2,C3,4,C5)[#5]	4.32	3.55	34.65	34.65

Symmetry transformation used to generate equivalent atoms: #5 1-x, -y, 2-z

B - I.2 - Crystallographic structures of ethane-1,2-diyl dinicotinate (L2)

Crystals in the form of needles appear after slow diffusion of hexane into a solution of THF containing the ligand. The ligand crystallizes in the orthorhombic system, space group $P2_12_12$ (No. 18), with half of the molecule in the asymmetrical unit cell with a C_2 axis in the geometrical middle of the C7–C7[#1] bond (Figure 14). The ethylene moiety is in a gauche (Staggered) conformation (Table B-I.4).
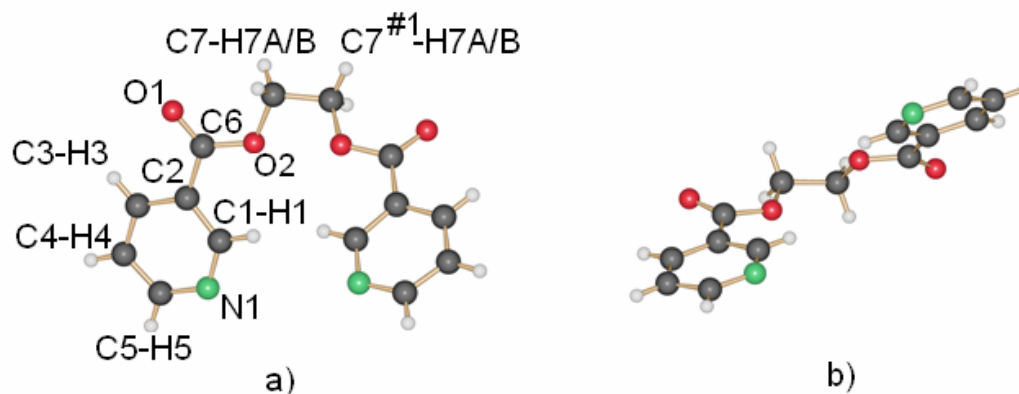
Figure 14. Schematic representation of the ligand L2. Nitrogen atoms are represented in green, oxygen atoms in red

In the crystalline state **L2** possesses a "U"-shape with both nitrogen atoms (green) pointing to the inside of the "U". Within the molecule, the carbonyl group is twisted against the aromatic ring (C2–C3–C6–O2, 14.2(1)°). Both aromatic rings are contained in planes which are not parallel to each other (43.9° between both planes).

Principal angles and distances are given in Table B-I.4.

Table B-I.4 Most important bond lengths [Å] and angles [°] for **L2**

N(1)–C(1)	1.322(2)	C(1)–N(1)–C(2)	115.7(7)
N(1)–C(2)	1.318(2)	O2–C7–C7#1–O2#1	58.5(9)
C(7)–C(7)#1	1.488(1)		

Symmetry transformations used to generate equivalent atoms: #1 –x, -y, z

Aromatic-aromatic interactions are discarded due to the distances between rings (more than 5.8 Å, centroid-centroid distances). Weak hydrogen bond interactions are present in the crystalline motif (Figure 15).

Silver Coordination Compounds with a Family of Ditopic Ligands of Varying Flexibility: About Chains, Rings, Helices and Polycatenanes

22

view a direction
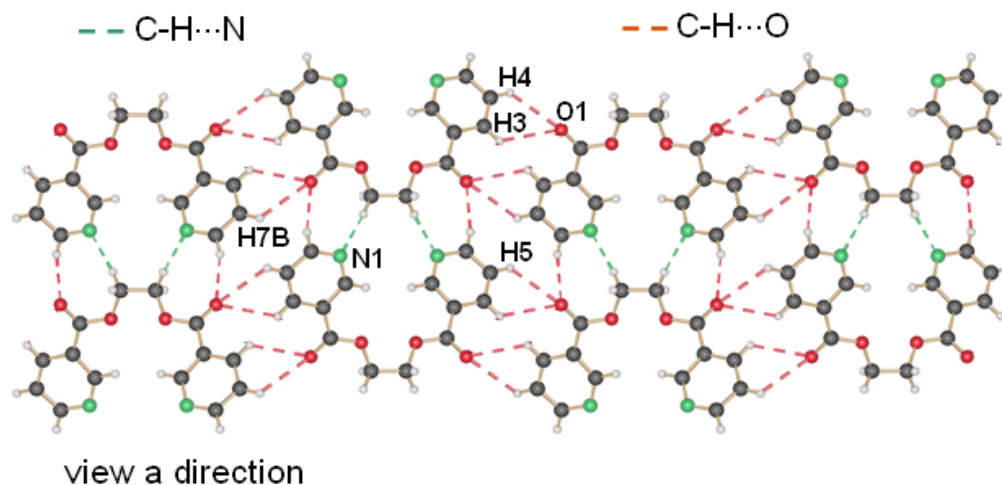
Figure 15. Hydrogen bond interactions present in the crystalline structure of L2. Nitrogen atoms are represented in green, oxygen atoms in red, hydrogen atoms in white

Whereas the nitrogen atoms of the pyridine rings interact with the spatially closely situated hydrogen atoms of the ethylene part of the ligands (C7–H7B···N1), the oxygen atoms of the carbonyl group form weak hydrogen bonds with hydrogen atoms attached to the aromatic rings (C3–H3···O1[#2], C4–H4···O1[#2] and C5–H5···O1[#3]) (Table B-I.5).

Table B-I.5 Hydrogen bond data [length (Å) and angle (°)] for **L2**

D–H···Acceptor	d (D–H)	d (H···A)	d (D···A)	Angle D–H···A
Hydrogen bond formed between ligands				
C7–H7B···N1	0.97	2.64(1)	3.59(2)	167.7(8)
C3–H3···O1[#2]	0.93	2.73(8)	3.33(7)	123.0(7)
C4–H4···O1[#2]	0.93	2.70(3)	3.31(5)	124.0(7)
C5–H5···O1[#3]	0.93	2.60(6)	3.50(5)	162.8(9)
Symmetry transformation used to generate equivalent atoms: #2 0.5+x, 0.5-y, 1-z #3 1+x, y, -1+z				

B - I.3 - Crystallographic structures of 2,2'-oxybis(ethane-2,1-diyl) diisonicotinate (L3)

Rod like crystals of **L3** appear on the wall of the reaction vessel after purification on a silica gel chromatography column (recrystallization on hexane:ethyl acetate 7:1). The ligand crystallizes in the monoclinic space group $P2_1/n$ (No. 14). The asymmetric unit contains one molecule, and 2 molecules are present in the unit cell (Figure 16).

Silver Coordination Compounds with a Family of Ditopic Ligands of Varying Flexibility: About Chains, Rings, Helices and Polycatenanes

23

View b direction
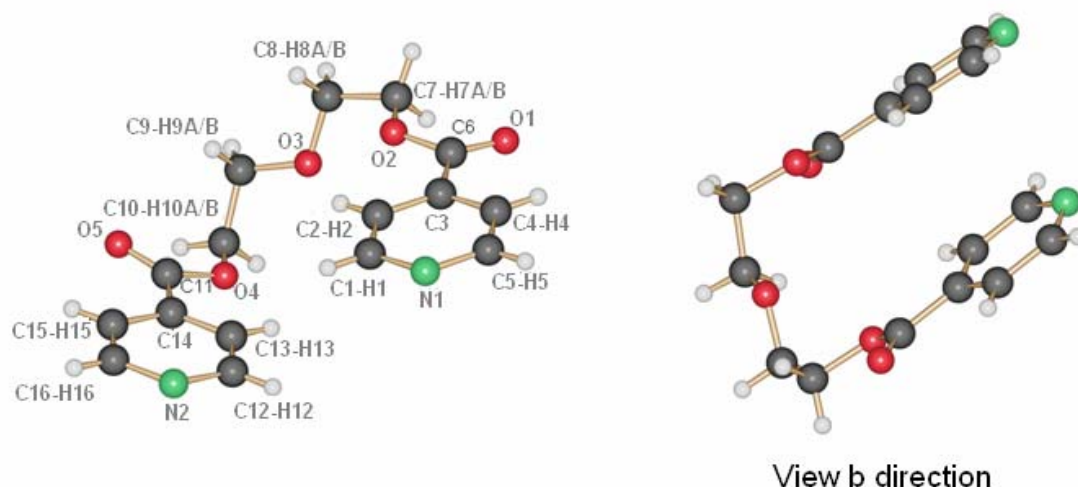
Figure 16. Schematic representation of the crystal structure of ligand L3

In the crystalline state, and as a difference compared with **L2**, the torsion angles C2–C3–C6–O2 (10.0(1)°) and C13–C14–C11–O4 (11.6(9)°) of the carbonyl group are twisted with respect to the plane formed by the aromatic carbon atoms.

In the diethylene glycol spacer, all ethylene groups are in a gauche (staggered) conformation. The ligand possesses a marked U-shape, this conformation suggests the existence of a dipolar moment in the molecule. This, however, is annulated by a second molecule, related to the first one via an inversion center.

The closest ring distance of 4.49 Å, evidences absence of aromatic-aromatic interactions.

Hydrogen bond forces are present and stabilize the crystalline packing. Nitrogen atoms of the pyridine rings coordinate hydrogen atoms located at the ethylene moiety of a frontal ligand molecule (C9–H9B···N1[#1] and C10–H10A···N1[#2]). Other hydrogen bonds are formed between the oxygen atom of the carbonyl groups and ethylene hydrogen atoms of a second ligand, which is located parallel to the first one (C10–H10A···N1[#2], C9–H9A···O1[#4] and C8–H8B···O1[#4]) (Figure 17).

Silver Coordination Compounds with a Family of Ditopic Ligands of Varying Flexibility:
About Chains, Rings, Helices and Polycatenanes

24

········ C-H···O
········ C-H···N

View b direction
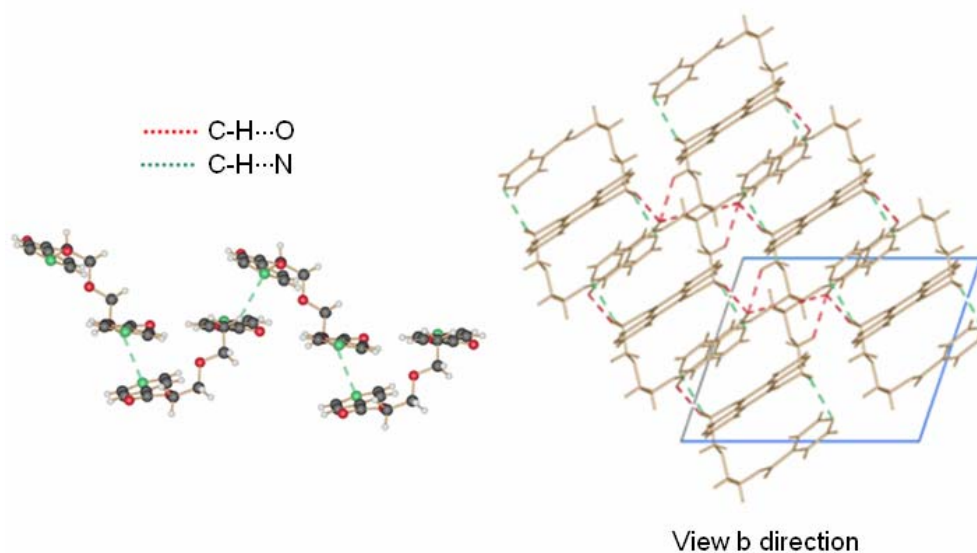
Figure 17. Hydrogen bonds within the crystalline structure of L3. Nitrogen atoms are represented in green, oxygen atoms in red and hydrogen atoms in white

Table B-I.6 Most important bond lengths [Å] and angles [°] for **L3**

N(1)–C	1.390(0)	C(1)–N(1)–C(2)	119.9(1)
N(2)–C	1.390(2)	C(12)–N(2)–C(16)	120.0(1)
		C(7)–C(8)–O(3)–C(9)	171.5(1)

Table B-I.7 Hydrogen bond data [length (Å) and angle (°)] for **L3**

D–H···Acceptor	d (D–H)	d (H···A)	d (D···A)	Angle D–H···A
Hydrogen bonds formed between ligands				
C9–H9B···N1[#1]	0.97	2.77(6)	3.72(7)	167.5(1)
C10–H10A···N1[#2]	0.97	2.81(9)	3.64(0)	143.7(1)
C10–H10B···O1[#3]	0.97	2.75(6)	3.67(4)	158.8(1)
C9–H9A···O1[#4]	0.97	2.57(5)	3.34(9)	136.7(1)
C8–H8B···O1[#4]	0.97	2.62(4)	3.35(2)	132.1(1)
Symmetry transformation used to generate equivalent atoms: #1 2-x, -y, 1-z #2 1.5-x, -0.5+y, 0.5-z #3 0.5+x, -0.5+y, 0.5+z #4 2.5-x, -0.5+y, 0.5-z				

B - I.4 - Crystallographic structures of 2,2'-oxybis(ethane-2,1-diyl) dinicotinate (L4)

Brown needles of **L4** were collected after slow evaporation of a DCM solution containing the ligand. **L4** crystallizes in the monoclinic space group C2/c (No. 15). The asymmetrical unit cell contains half a molecule, with one molecule in the unit cell packing (Figure 18).

Silver Coordination Compounds with a Family of Ditopic Ligands of Varying Flexibility: About Chains, Rings, Helices and Polycatenanes

25
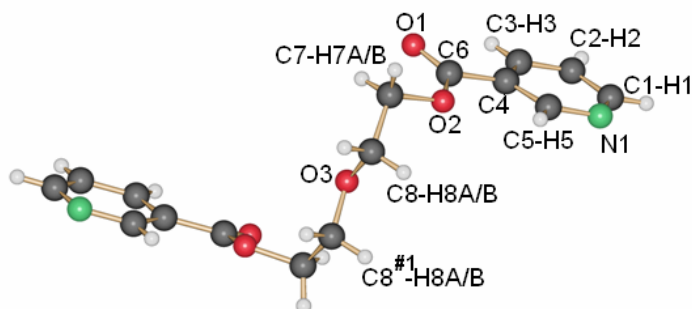
Figure 18. Schematic representation of the ligand L4 based on crystallographic data

In the crystalline packing the ligand possesses a semi-extended position with both nitrogen atoms pointing in the same direction.

The diethylene moiety is perpendicular to the plane formed by both π-systems. The planes formed by the aromatic rings are nearly parallel (7.32 Å distance between planes). The torsion angle in the diethylene chain is 78.8(1)° (O2–C7–C8–O3). This value is typical of a gauche (staggered) conformation.

The carbonyl group remains almost in the plane formed by the atoms of the pyridine ring (C5–C4–C6–O2, 9.0(1)°). Oxygen atoms of the diethylene moiety and nitrogen atoms of the pyridine rings are able to form hydrogen bonds with spatially close hydrogen atoms (C1–H1···O3$^{\#2}$, C8–H8A···O1$^{\#3}$, C7–H7B···O1$^{\#4}$ and C8–H8A···N1$^{\#5}$, C8–H8B···N1$^{\#6}$) (Figure 19) (Table B-I.9).
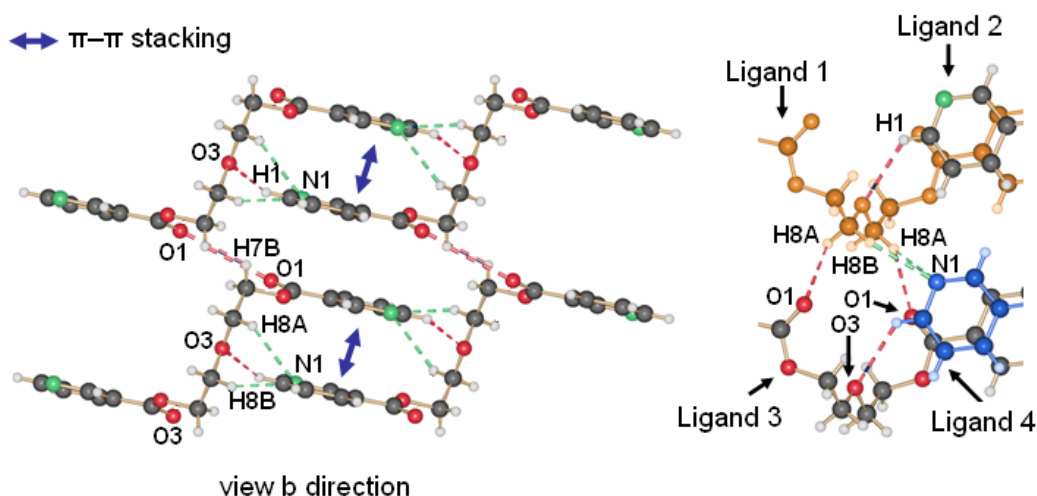
Figure 19. Hydrogen bonds formed by the nitrogen and oxygen atoms and hydrogen atoms located in the pyridine ring and the diethylene glycol moiety

Weak π–π interactions are present between stacked ligands, and stabilize the packing in the crystalline state.

Table B-I.8 Most important bond lengths [Å] and angles [°] for **L4**

N(1)–C(1)	1.338(2)	C(1)–N(1)–C(2)	116.2(1)
N(1)–C(2)	1.334(3)		
O3–C(8)[#1]	1.414(2)		

Symmetry transformations used to generate equivalent atoms: #1 1-x, y, 1.5-z

Table B-I.9 Hydrogen bond data [length (Å) and angle (°)] for **L4**

D–H⋯Acceptor	d (D–H)	d (H⋯A)	d (D⋯A)	Angle D–H⋯A
Hydrogen bonds formed between ligands				
C1–H1⋯O3[#2]	0.93	2.79(5)	3.49(3)	132.6(8)
C8–H8A⋯O1[#3]	0.97	2.82(4)	3.40(7)	119.1(7)
C7–H7B⋯O1[#4]	0.97	2.71(7)	3.24(3)	114.4(5)
C8–H8A⋯N1[#5]	0.97	2.88(7)	3.75(4)	149.5(6)
C8–H8B⋯N1[#6]	0.97	2.64(4)	3.56(8)	158.2(1)

Symmetry transformation used to generate equivalent atoms: #2 1-x, 1-y, 1-z #3 x, 1+y, z #4 1.5-x, 1.5+y, 1.5-z #5 1-x, -y, -z #6 x, -y, -0.5+z

Table B-I.10 π–π stacking for **L4**

π–π interaction	d_{R-R} (Å)	ρd_{R-R} (Å)	α	B
Inter π–π stacking between aromatic rings of different ligands				
Ring (N1,C1,C2,C3,C4,C5)⋯Ring (N1,C1,C2,C3,C4,C5)[#1]	3.57	3.40	0.03	17.73

Symmetry transformation used to generate equivalent atoms: #7 –x, -y, -z

B - I.5 - Crystallographic structures of 2,2'-(ethane-1,2-diylbis(oxy))bis(ethane-2,1-diyl) dinicotinate (L5)

The ligand **L5** crystallizes after slow evaporation of a THF solution in the triclinic space group P-1 (No. 2). The asymmetric unit cell contains half of the ligand. A centre of symmetry is located in the geometrical middle of the C9–C9[#1] bond. The ligand is extended in a Z-like shape, with the triethylene moiety almost perpendicular to the plane formed by both aromatic rings (about 17 Å distance between nitrogen atoms). Both nitrogen atoms are pointing to opposite directions (Figure 20).

Silver Coordination Compounds with a Family of Ditopic Ligands of Varying Flexibility:
About Chains, Rings, Helices and Polycatenanes

27
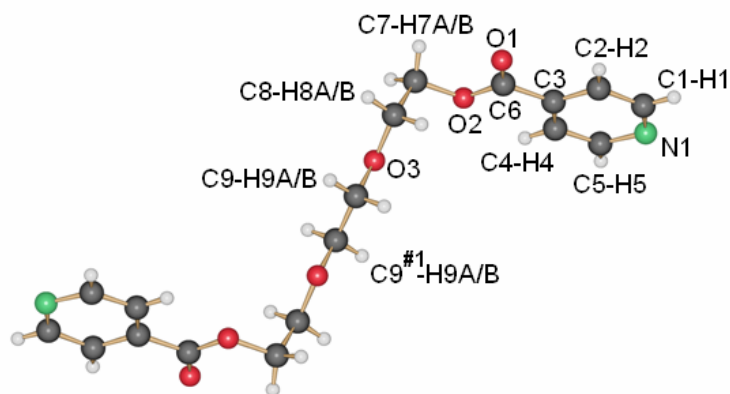
Figure 20. Conformation of the ligand L5 in the crystalline state

Within the ligand, the carbonyl group remains in the plane formed by the aromatic ring atoms (C4–C3–C6–O2, 1.3(3)°). The two ethylene moieties close to the aromatic systems possess a gauche (staggered) conformation (O2–C7–C8–O3), whereas the ethylene moiety located in the middle of the triethylene glycol spacer (O3–C9–C9$^{#1}$–O3$^{#1}$) posses an anti (staggered) conformation.

Individual ligands are stacked via weak π–π contacts between aromatic rings (Figure 21). (See Table B-I.12 for distances).
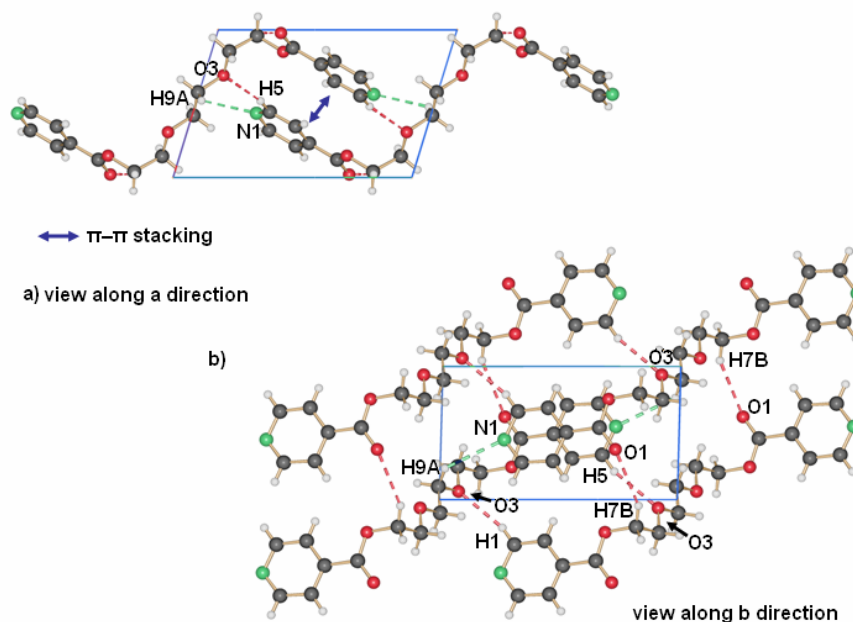
Figure 21. Hydrogen bonds within the crystal structure of L5. Nitrogen atoms are represented in green, oxygen atoms in red and hydrogen atoms in white

Weak hydrogen bonds are present in the motif (Figure 21 a) and b)). The extended conformation of the ligand should improve the formation of hydrogen bonds in the crystalline state. Indeed, oxygen atoms of the triethylene moiety coordinate hydrogen atoms located at the pyridine rings and the ethylene glycol hydrogen atoms. The nitrogen atoms interact with hydrogen atoms of the triethylene chain, which are spatially close enough to generate a three dimensional array in the crystalline motif (Table B-I.13).

Table B-I.11 Most important bond lengths [Å] and angles [°] for **L5**

N(1)–C(1)	1.311(6)	C(1)–N(1)–C(2)	115.7(1)
N(1)–C(2)	1.360(4)	O2–C7–C8–O3	76.2(2)
C(7)–C(7)$^{\#1}$	1.448(5)	O3–C9–C9$^{\#1}$–O3$^{\#1}$	180.0(2)

Symmetry transformations used to generate equivalent atoms: #1 –x, 1-y, 2-z

Table B-I.12 π–π stacking for **L5**

π–π interaction	d_{R-R} (Å)	ρd_{R-R} (Å)	α	β
Inter π–π stacking between aromatic rings of different ligands				
Ring (N1,C1,C2,C3,C4,C5)···Ring (N1,C1,C2,C3,4,C5)$^{\#2}$	3.70	3.39	0.03	23.64

Symmetry transformation used to generate equivalent atoms: #2 1-x, 1-y, 1-z

Table B-I.13 Hydrogen bond data [length (Å) and angle (°)] for **L5**

D–H···Acceptor	d (D–H)	d (H···A)	d (D···A)	Angle D–H···A
Hydrogen bonds formed between ligands				
C9–H9A···N1	0.96	2.80(1)	3.50(4)	129.4(2)
C7–H7B···O1$^{\#3}$	0.96	2.77(7)	3.65(9)	152.9(1)
C9–H9B···O1$^{\#3}$	0.96	2.85(1)	3.69(7)	146.6(2)
C9–H9B···O1$^{\#3}$	0.96	2.70(7)	3.56(9)	148.8(1)
C5–H5···O3$^{\#4}$	0.92	2.49(1)	3.40(1)	164.6(2)

Symmetry transformation used to generate equivalent atoms: #3 1-x, -y, 2-z #4 –x, 1-y, 1-z

B - I.6 - Crystallographic structures of 2,2'-(2,2'-oxybis(ethane-2,1-diyl) bis(oxy)) bis(ethane-2,1-diyl) diisonicotinate (L6)

When a solution in DCM/n-Hexane 1:5 containing the ligand was allowed to evaporate slowly, ligand **L6** crystallized as small rod-like crystals in the bottom of the vessel. The crystal belongs to the orthorhombic system, space group Pbcn (No. 60), and contains half of a molecule in the

asymmetric unit cell (Figure 22). Two molecules are generated in the unit cell. The molecule has a "U"-like shape, with a C_2-symmetry axis going through the O3 atom.
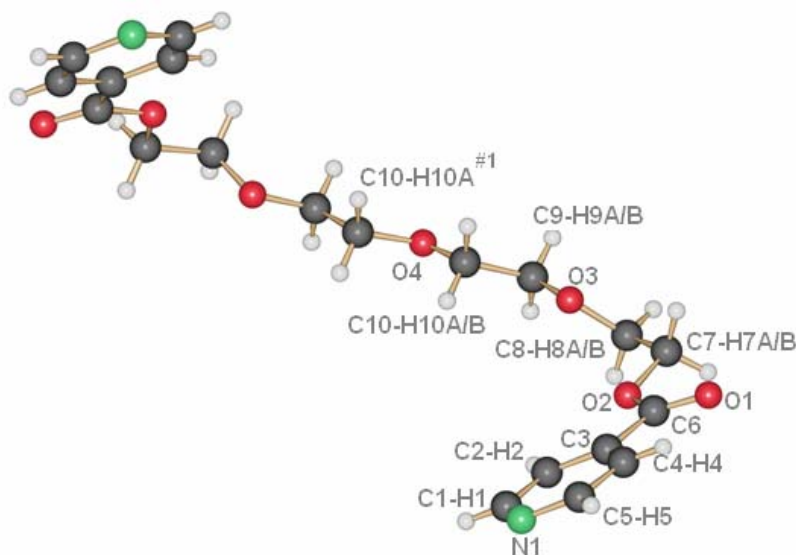
Figure 22. Crystal structure of L6. The ligand, like L6, possesses a "U"-like shape structure

Both pyridine rings are twisted to each other (34.9° angle between planes).

The extension of the tetraethylene chain is due to the anti (staggered) conformation of the two central ethylene moieties (O3–C9–C10–O4 and O4–C10$^{\#1}$–C9$^{\#1}$–O3$^{\#1}$, 176.2(9)°) and the gauche (staggered) conformation of two ethylene moieties (O2–C7–C8–O3 and O3$^{\#1}$–C8$^{\#1}$–C7$^{\#1}$–O2$^{\#1}$, 64.7(1)°). The carbonyl group remains approximately in the plane defined by the aromatic ring (C2–C3–C6–O2, 7.1(3)°).

Table B-I.14 Most important bond lengths [Å] and angles [°] for **L6**

N(1)–C(1)	1.332(2)	C(1)–N(1)–C(2)	116.4(1)
N(1)–C(5)	1.332(2)	C(10)–O4–C(10)$^{\#1}$	110.9(9)
C(10)–O4$^{\#1}$	1.414(2)		
Symmetry transformations used to generate equivalent atoms: #1 1-x, y, 1.5-z			

Aromatic interactions like π–π are discarded due to the distances between pyridine rings (more than 4.3 Å).

The density in the packing and the spatial extension of the ligand afford a high number of potential hydrogen bonds (Table B-I.15). Nitrogen atoms of the pyridine rings coordinate hydrogen atoms of

Silver Coordination Compounds with a Family of Ditopic Ligands of Varying Flexibility: About Chains, Rings, Helices and Polycatenanes

30

the ethylene moiety (C8–H8B···N1$^{\#3}$) and of aromatic rings (C2–H2···N1$^{\#2}$ and C5–H5···N1$^{\#4}$) of close ligands. The same occurs with oxygen atoms located at the tetraethylene glycol chain: they form four hydrogen bonds with aromatic hydrogen atoms (C7–H7A···O1$^{\#5}$, C9–H9B···O1$^{\#6}$, C9–H9A···O3$^{\#2}$ and C7–H7B···O3$^{\#7}$) and another one with an hydrogen atom located at the ethylene part of the lateral chain (C4–H4···O1$^{\#5}$) (Figure 23).
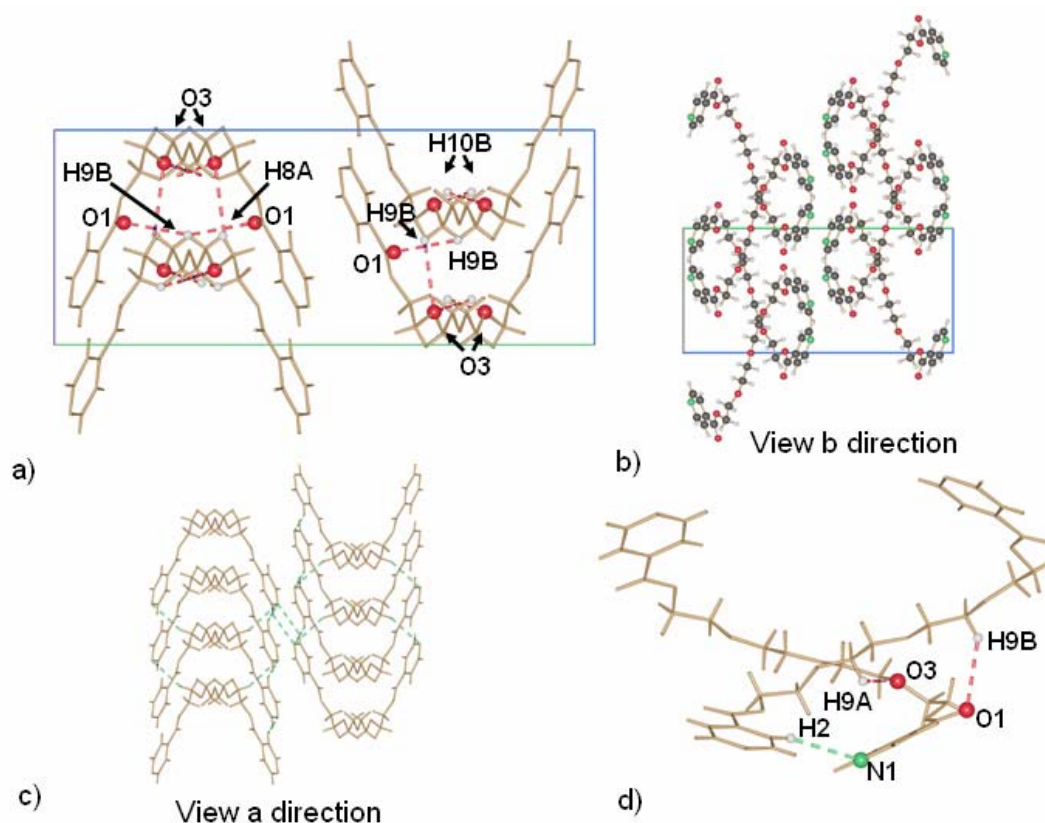
Figure 23. Hydrogen bonds present in the crystal structure of L6. Nitrogen atoms are represented in green, oxygen atoms in red and hydrogen atoms in white

Every single molecule of **L6** may possess a dipole moment due its conformation. This is annulated by a second dipole moment of a second molecule of the next chain in the opposite direction.

Silver Coordination Compounds with a Family of Ditopic Ligands of Varying Flexibility:
About Chains, Rings, Helices and Polycatenanes

31

Table B-I.15 Hydrogen bond data [length (Å) and angle (°)] for **L6**

D–H···Acceptor	d (D–H)	D (H···A)	d (D···A)	Angle D–H···A
Hydrogen bonds formed between ligands				
C2–H2···N1[#2]	0.93	2.76(4)	3.57(6)	146.1(1)
C8–H8B···N1[#3]	0.97	2.99(4)	3.84(0)	146.7(9)
C5–H5···N1[#4]	0.93	2.85(4)	3.65(0)	143.7(1)
C7–H7A···O1[#5]	0.97	2.77(4)	3.66(8)	153.1(1)
C4–H4···O1[#5]	0.93	2.58(3)	3.31(1)	135.2(1)
C9–H9B···O1[#6]	0.97	2.73(5)	3.53(9)	140.5(9)
C9–H9A···O3[#2]	0.97	2.96(6)	3.55(2)	120.1(1)
C7–H7B···O3[#7]	0.97	2.51(4)	3.35(8)	144.7(9)

Symmetry transformation used to generate equivalent atoms: #2 0.5-x, 0.5+y, z #3 x, 1y, z #4 –x, 2-y, 1-z #5 -0.5-x, 0.5+y, z #6 -0.5+x, 0.5+y, 1.5-z #7 –x, y, 1.5-z

B - I.7 - Some aspects about the ligands

All ligands were crystallized in at least two different conditions and several times; no structural isomerism was observed.

This is interesting since when other relatively simple molecules with rotational freedom around bonds crystallize, they may exhibit polymorphism [165-173]. From the structural point of view, the ligands used in this work have two main regions: i) a rigid aromatic ring with an ester function, ii) a flexible polyethylene glycol chain. While the first one is supposed to be controlled in the solid state by interactions like π–π and hydrogen bonds (nitrogen and oxygen atoms as aceptors and aromatic hydrogen atoms as acceptors), the second part is flexible and only maintained by hydrogen bonds.

For some ligands in the crystalline state, the aromatic rings may be stacked (forming sometimes very weak π–π interactions). They tend to form weak ring-ring interactions. Polyethylene glycol, however, tends to maximize the number of hydrogen bonds in order to stabilize the crystalline motif increasing at the same time the density of the unit cell (the presence of solvent was circumvented in all case).

The aromatic rings possess a head-to-head stacking type with **L2,** whereas **L1, L3, L4** and **L5** are head-to-tail stacked (Figure 24).

Silver Coordination Compounds with a Family of Ditopic Ligands of Varying Flexibility:
About Chains, Rings, Helices and Polycatenanes

32
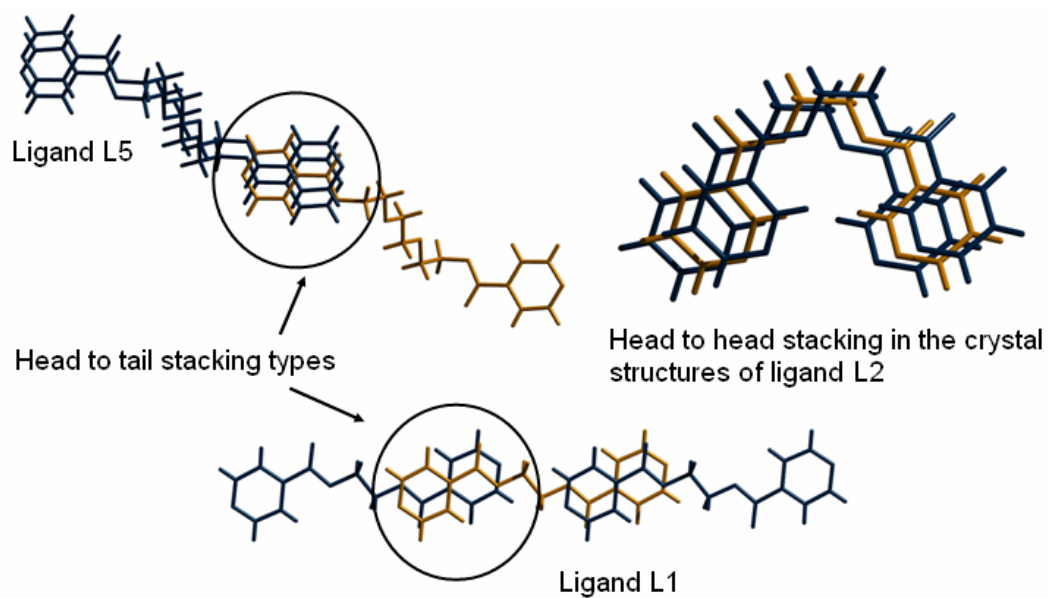
Figure 24. aromatic stacking in the crystal of ligands L1, L2 and L3

The more flexible tetraethylene glycol spacer present in **L6** tends to form hydrogen bonds rather than π–π interactions, avoiding the presence of aromatic stacking in this structure.

Silver Coordination Compounds with a Family of Ditopic Ligands of Varying Flexibility:
About Chains, Rings, Helices and Polycatenanes

33

B - II - Ag (I) complexes with ligands L1 and L2. An overview of the linear motif

Coordination polymers obtained using short ligands are quite common in supramolecular chemistry, and it is in addition one of the most versatile approaches to generate new linear arrays. Multidimensional structures can be obtained by the judicious choice of the ligand and the incorporation of different potential coordination sites within the organic molecule (Figure 25).
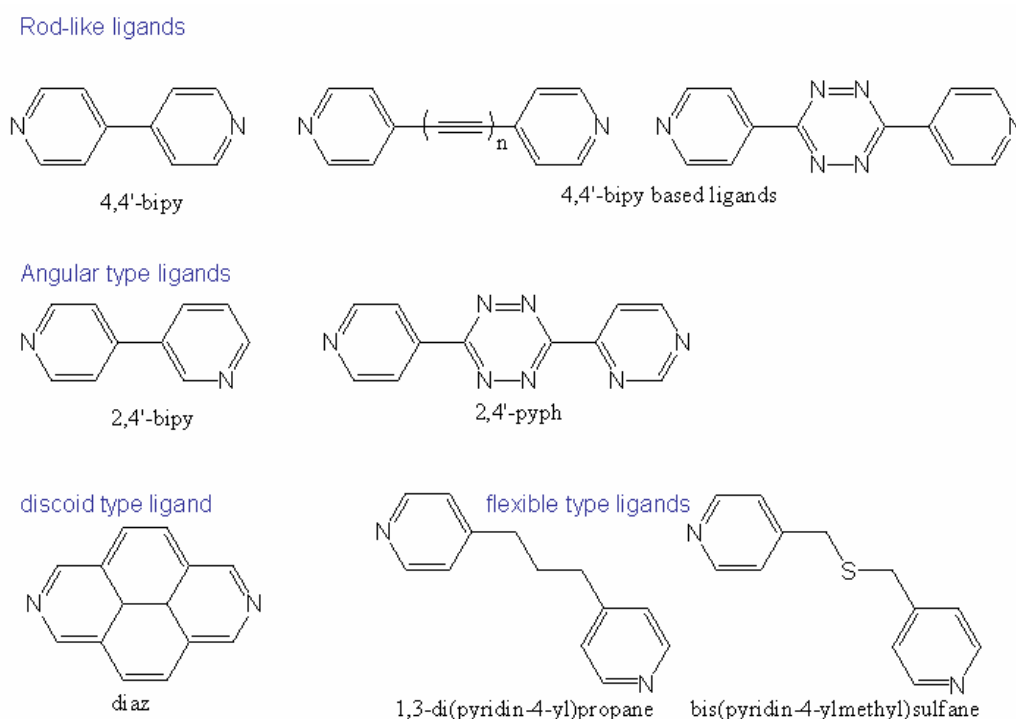
Figure 25. Some rigid ligands used to synthesize polymeric linear motifs

Concepts like self-assembly, complementation and cooperative effects have been successfully applied in supramolecular chemistry to create structures in a wide range of dimensionalities (0D→3D). So far in our group, Dr. Robin working with the ligand ethane-1,2-diyl diisonicotinate (**L1**) was able to obtain a family of complexes [1, 161-163]. In her PhD work, Dr Robin has brought an excellent review from which interesting conclusions can be extracted: first, the preference of the Ag(I) cation for a linear coordination motif, independent of which counter ion was used. The general crystalline motif implies stacking of linear chains to generate 2-D arrays through the counter ion

(this is especially true when NO_3^- was used). They are an evidence of a relationship between the solvent in which the crystals grow, and the coordination mode of the counter ion toward the metal atom. A rough prediction of a coordination array considering just the ligand (geometry, ability to form hydrogen bonds), counter ion and the metal atom remains so far a difficult task.

1D metal-organic polymers are obtained usually when a metal cation is coordinated by a ditopic ligand, generating an infinite array of alternated species (Figure 26 a), c) and d)). In the supramolecular realm most of the ligands that usually generate this kind of array are based on pyridine [84, 141, 174-180], or a five member aromatic ring containing one nitrogen heteroatom [141, 181], or several nitrogen atoms in the aromatic ring [25, 90, 182, 183]. Other soft atoms like sulfur have been used with similar results [184, 185].
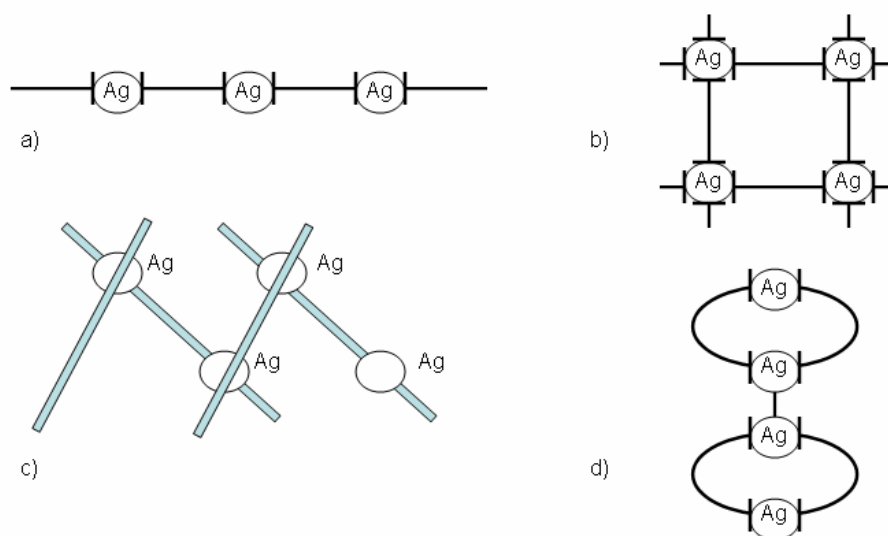
Figure 26. Schematic representation of some crystalline metal-organic motifs found in supramolecular chemistry

To generate angular arrays, the geometry of the ligand is determinant (see 2,4-bipyridine [186] and [187]). The geometry of the ligand plays an important role in the generation of "*off-axis rod*" geometries (see 1,2-bis{2-pyridyl}ethylene [188], or 1,4-bis{2-pyridyl}butadiyne [189]) (Figure 27).

Silver Coordination Compounds with a Family of Ditopic Ligands of Varying Flexibility:
About Chains, Rings, Helices and Polycatenanes

35
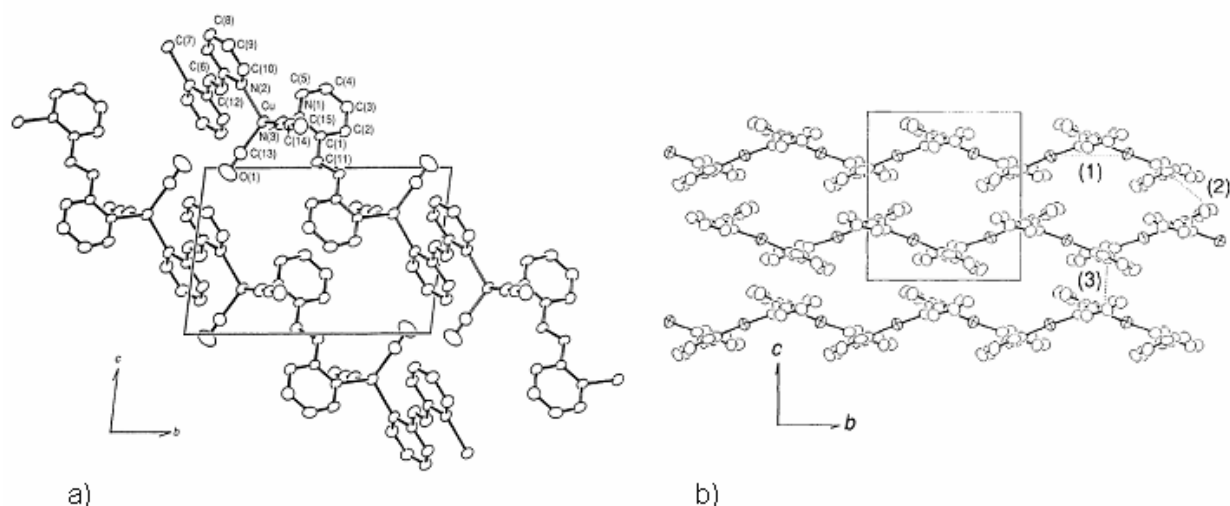
Figure 27. a) An ORTEP view of portions of the macrocations of [{Cu(bpen)(CO)(CH₃CN)(PF₆)}ₙ]. (Thermal ellipsoids enclose 30% probability) b) Projection of the chain structure of [{Cu(bpen)}ₙ] along the "a" axis, showing the framework of the non-planar polymeric chain. Dashed lines show the nearest-neighbor atom contacts: (1) Cu···Cu 7.17; (2) C(1)···C(3') 3.46; (3) C(1)···C(4') 3.69 Å

Another strategy is based on the geometry of the metal cation. When appropriated ligands are used, linear 1D motifs can be obtained. They are based on a metal cation with a tetrahedral (Zn(II) [190-193], Cu(I) [194-197]), an octahedral (Co(II) [198] or a square planar geometry (Pt(II) [199-201], Pd(II) [202, 203]).

Even when the most common coordination geometry of the silver is linear, trigonal [204-206], tetrahedral [142, 207, 208] and square planar [130, 131] geometries have been found in the literature.

Loops and chain motifs emerge in the crystalline state separately and/or concomitantly, but the appearance of these motifs is associated frequently with the use of flexible spacers between the coordination sites in the ligand [209, 210], as well as the anion [211] and the solvent used in the crystallization process [212].

The use of a second metal cation directing the synthesis of the 1D chain has been tested with certain success. It is essential the complementarity between the geometry of both metal cations concerning the coordination sites of the ligand. Some examples are reported for tetrahedral Fe(II)-linear Ag(I) [213] and square-planar Pd(II)-tetrahedral Ag(I) [214] (Figure 28).

Silver Coordination Compounds with a Family of Ditopic Ligands of Varying Flexibility: About Chains, Rings, Helices and Polycatenanes

36
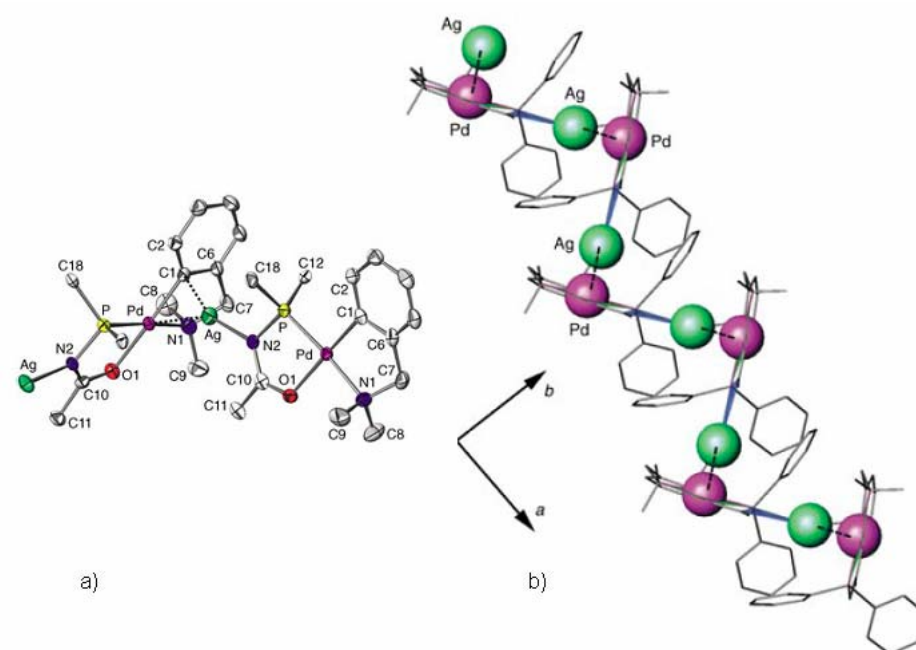
Figure 28. a) ORTEP view of the asymmetrical unit cell Ag₂Pd₂ of the polymeric complex formed with phosphanyl iminolates·(SO3CF3)₂CH₂Cl₂. Only the ipso aryl carbon atoms on P are shown for clarity. Thermal ellipsoids showing 50% of the electron density. b) View through the c axis direction showing the zigzag wire structure of the polymeric complex

Coordination of Ag(I) cations by ligands possessing soft atoms (N, S, P) may result in the formation of metallic Ag–Ag contacts which can alter the final crystalline motif from linear coordination polymer [212] (Figure 29) to an array consisting of fused loops [215]. An extended analysis is shown in the next section (p.40).
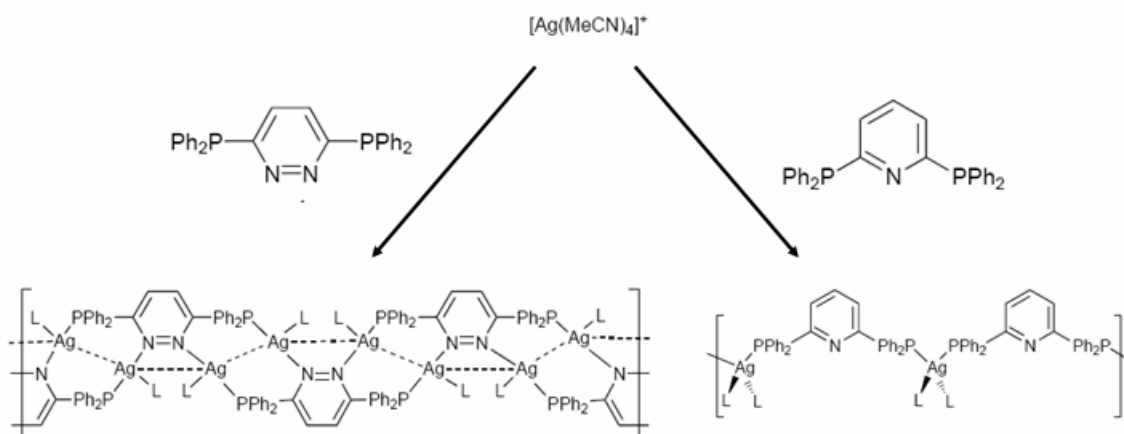
Figure 29. (link picture) Fused loop of polymer {[Ag₂(MeCN)₂(μ-L)]}ₙ[ClO₄]₂ₙ showing silver-silver contacts along the chain direction. (right picture) simple 1D motif of polymer {[Ag(MeCN)₂(μ-L)]}ₙ[ClO₄]ₙ

While a linear coordinated silver cation typically forms straight polymers [117, 183], a trigonal or T-like coordinate Ag(I) [216], and a four-coordinated metal cation can generate ladder-like 1D polymers or more complicated patterns [141, 217].

Within the ligand, when the coordination sites are carefully designed, several functionalities can be included in the linear polymer: complexing new cations [160], anions [141], encapsulating neutral molecules like solvent [218-221], forming hydrogen bonds [222, 223] or just generating exciting news topologies [221, 224, 225].

The coordination of a metal cation by an appropriate ligand may afford interpenetration or polycatenation in the crystalline state (Figure 30). In the supramolecular field some confusion still arises from the use of the adequate nomenclature to name these motifs.

a)   Interlocked adamantane units of two independent diamond like nets.

b) Schematic representation of the multiple rotaxane associations.

c) Inclined interpenetration of sheets.

d) Two interpenetrating nets with three- and six-connected nodes in [Cd(bipy)$_2${Ag(CN)$_2$}$_2$]. Larger circles represent Cd atoms, smaller circles Ag atoms.

bipy ligands
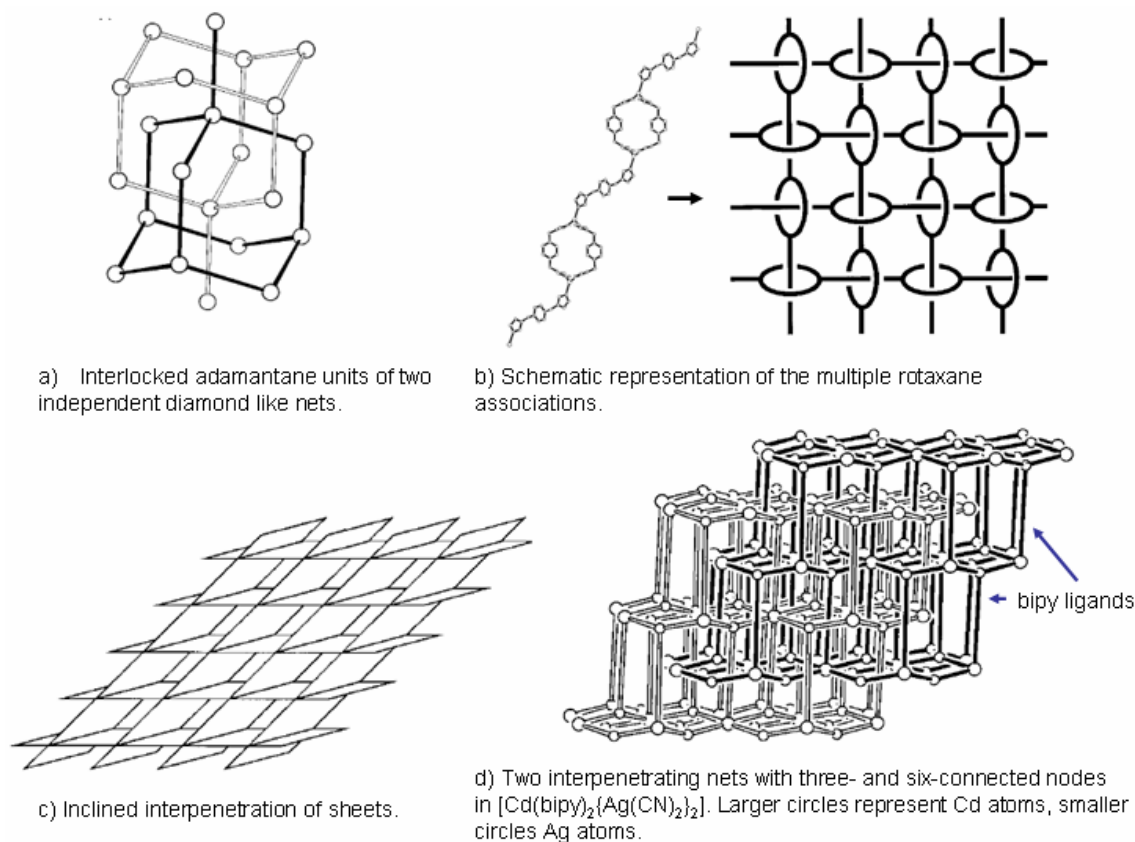
Figure 30. Schematic representation of some common interpenetration motifs reported in the literature

Interpenetrated One-Dimensional Polymers [226, 227], Interpenetrated Two-Dimensional Networks (which are classified into parallel [228-230] or inclined [88, 231]) and Interpenetrated Three-Dimensional Nets [232, 233].

Other types of interpenetration exist and have been well documented in the literature [26, 180, 231, 232, 234-241]. The use of flexible ligands seems to be related with the generation of this kind of motif [242-244], but this requirement is not essential [232, 245] (Figure 31). The presence of a particular metal cation can also favor the formation of a specific type of entanglement [238, 246].
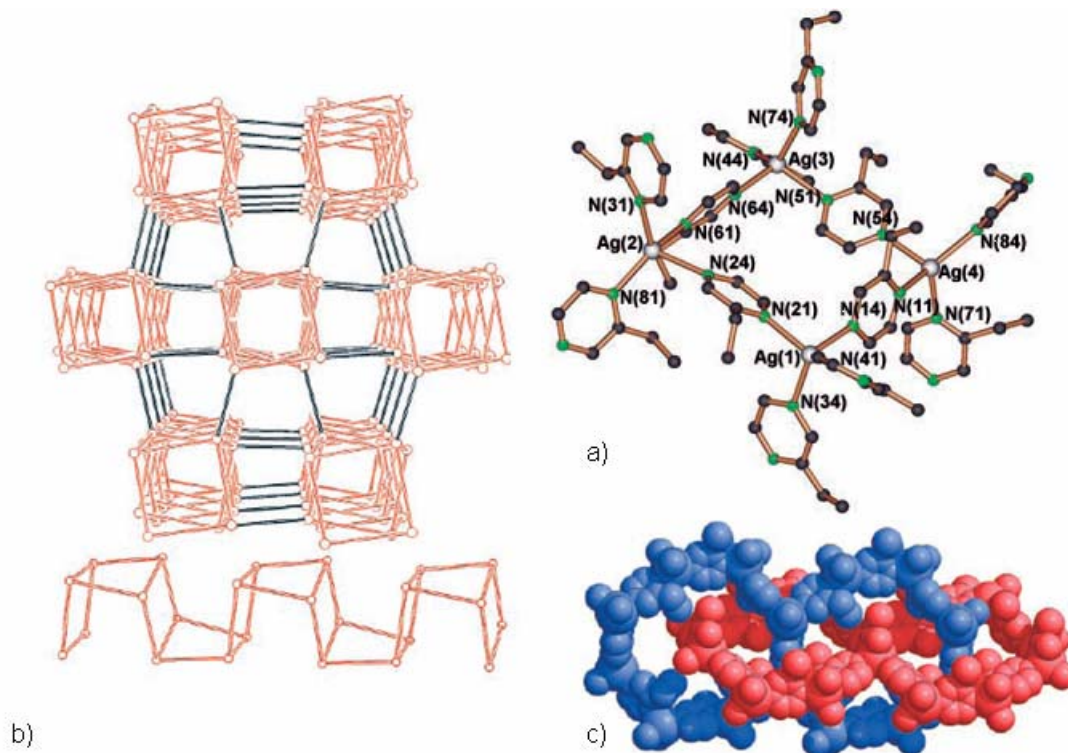
Figure 31. a) A molecular square sub-unit of compound [Ag(2-ethpyz)₂][SbF₆], with partial atomic labeling (only the major components of the disordered ligands are shown for clarity). b) Schematic views of a single ribbon (bottom) and of the overall array (top) derived by joining the ribbons in compound [Ag(2-ethpyz)₂][SbF₆] . The network is shown down the [0 0 1] direction. All the channels (exhibiting distorted square section) contain rows of anions. c) Self-entanglement of two chains of eight-membered rings in compound [Ag(2-ethpyz)₂][SbF₆]

The generation of zero-dimensional metallacycles will be explored in detail within the next chapter of this thesis (p.73).

B - II.1 - Crystal structures and discussion of Ag (I) complexes with ligands L1 and L2

Here, we will first discuss the structures of six compounds obtained with **L1** and **L2** and silver salts. These descriptions are followed by further investigations in solution as well as comparison of the compounds, their crystallization conditions and the literature data.

B - II.2 - {[Ag(L1)NO₃]}ₙ coordination polymer (1)

The first crystals were obtained after evaporation from a solution of silver nitrate and the ligand in acetonitrile. Although the crystals have a cubic shape they do not possess optimal transparency and quality in order to be measured.

Slow diffusion of a THF solution of the ligand and a water solution of silver nitrate through an "H"-shaped tube affords crystals with the same morphology and good enough quality to be measured by X-ray experiments.

The compound **1** crystallizes in the triclinic space group P-1 with an organic ligand, a metal atom and a counter ion in the asymmetric unit. The silver cation has a distorted trigonal coordination sphere with two nitrogen atoms (Ag(1)–N(1), 2.199(6) and Ag(1)–N(2)[#1] 2.194(6) Å), of two ligands **L1**, and one oxygen atoms belonging to the counter ion (Ag-O, 2.602(8) Å). A second counter ion coordinate more weakly the silver cation at 2.697(9) Å (Table B-II.16) (Figure 32).
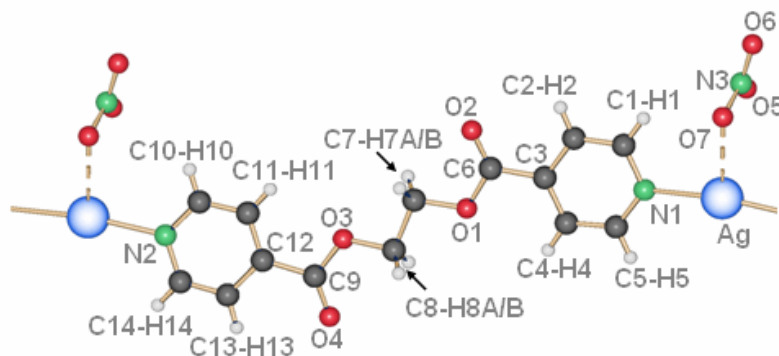
Figure 32. Basic motif of the crystalline structure of complex 1. The ethylene glycol moiety possesess an anti (staggered) conformation

The nitrate molecules coordinate two silver atoms in the same sheet in a monodentate fashion, almost in a symmetrical fashion for both metal atoms (Figure 33 left side).

view perpendicular to the plane containing the metal cations and the counter ions in a sheet
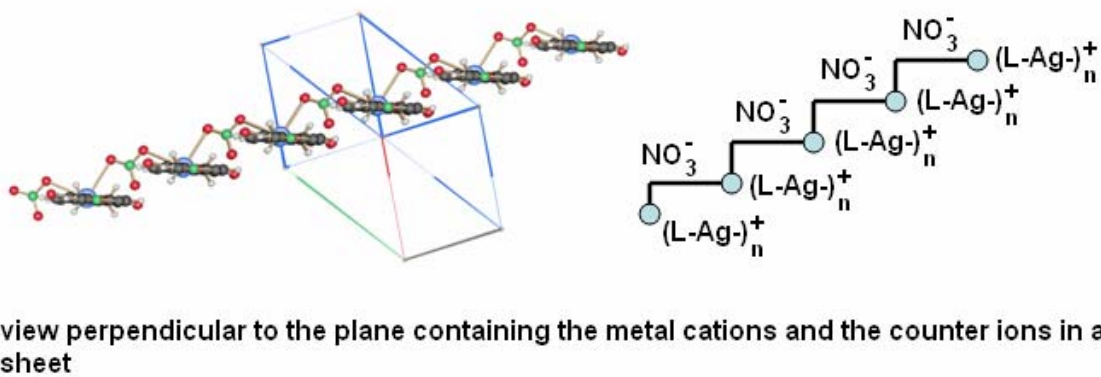
Figure 33. Generation of a two dimensional sheet through the interaction of the nitrate counter ion with the metal cations of parallel polymeric chains {L1-Ag-}$_n$

The maximal extension of the ligand is achieved due to the anti (staggered) conformation of the diethylene glycol moiety. Both tectons **L1** coordinate the metal cation almost in a linear fashion (N1-Ag-N2[#1], 168.9(1)°). The carbonyl group is contained in the plane formed by the aromatic ring with a slightly twisted torsion angle (C4-C3-C6-O1, 4.9(6)°) and (C11-C12-C9-O3, 5.1(6)°) almost the same value founded in **L1** (about 4°)

The ligand molecule is contained in a plane, and this plane is slightly twisted compared to a second plane formed by the atoms O5-Ag-O5[#1] (oxygen belonging to the counter ion). The resulting motif is a staircase like array in which chains (-**L2**-Ag-**L2**-Ag-)$_n$ are linked μ^2- *via* counter ions (Figure 33 rigth side).

These infinite chains are supported by weak π-π interactions with parallel chains situated above and below each chain (Table B-II.17).

Silver Coordination Compounds with a Family of Ditopic Ligands of Varying Flexibility: About Chains, Rings, Helices and Polycatenanes

41

Table B-II.16 Most important bond lengths [Å] and angles [°] present in complex **1**

Ag(1)–N(1)	2.189(6)	N(1)–Ag(1)–N(2)[#1]	168.9(1)
Ag(1)–N(2)[#1]	2.191(6)	O(6)–Ag(1)–O(7)	100.2(1)
Ag(1)–Ag(1)[#2]	4.012(1)	C–N–C	117.1(3)
Ag(1)–O(NO$_2$)	2.596(8), 2.695(9)		
N–C	1.354(4), 1.302(4)		

Symmetry transformations used to generate equivalent atoms: #1 1+x, -1+y, 1+z #2 1-x, 1-y,1-z

Table B-II.17 π–π stacking present in complex **1**

π-π interaction	d_{R-R} (Å)	ρd_{R-R} (Å)	α	β
Inter chain π–π stacking between aromatic rings of the ligand				
Ring (N1,C1,C2,C3,C4,C5)···Ring (N2,C10,C11,C12,C13,C14)[#1]	3.79	3.49	1.56	24.64
Ring (N1,C1,C2,C3,C4,C5)···Ring (N2,C10,C11,C12,C13,C14)[#1]	3.80	3.45	1.56	23.10

Symmetry transformation used to generate equivalent atoms: #1 -X,-Y,-Z

Other supramolecular forces like hydrogen bonds are present within the crystal structure *via* the nitrate counter ion, the carbonyl group and the acidic hydrogen atoms of the aromatic ring (Table B-II.18). The counter ion plays an important role not just reinforcing the formation of the sheet after linking chains together, but also creating a double decker after bonding a hydrogen atom from a second sheet (Figure 34), just like the carbonyl group when it coordinates a hydrogen atom of the ethylene moiety.
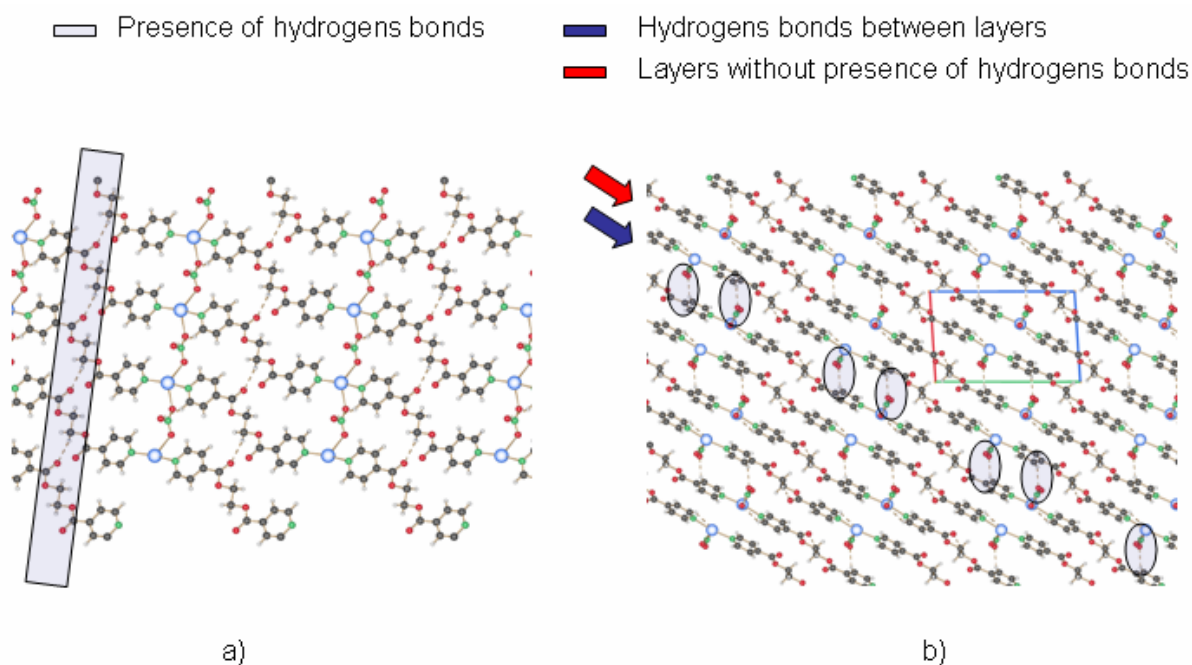
Figure 34. a) Hydrogen bonds formed in the 2-D sheet between the carbonyl oxygen and hydrogen atoms of the ethylene moiety, b) double deck formation due to hydrogen bonds between the nitrate counter ion and hydrogen atoms of the pyridine ring

Table B-II.18 Hydrogen bond data [length (Å) and angle (°)] present in complex **1**

D-H⋯Acceptor	d (D–H)	d (H⋯A)	d (D⋯A)	Angle D-H⋯A
Hydrogen bonds formed in the sheet				
C5–H5⋯O5[#1]	0.93	2.56(2)	3.30(1)	137.5(9)
C8–H8B⋯O2[#1]	0.97	2.52(3)	3.45(1)	162.6(2)
Hydrogen bonds formed between sheets				
C11–H11⋯O6[#2]	0.93	2.56(6)	3.41(1)	152.4(8)
Analysis of X-H⋯Ring Interactions (H⋯Ring < 3.4 Å)				
C7–H7B⋯(N1–C1–C2–C3–C4–C5)[#3]	0.97	3.09(2)	3.80(2)	
Symmetry transformation used to generate equivalent atoms: #1 1+x,y,z, #2 -1-x,1-y,-z, #3 -x,1-y,-z.				

A weak interaction between the hydrogen atom H7B of the ethylene glycol moiety and the aromatic ring situated on the next sheet which is on the top may gives rise to the stabilization of the crystalline array.

B - II.3 - {[Ag(L1)PF₆]}ₙ coordination polymer (2).

The complex **2** crystallizes in the monoclinic space group C2/c (No. 15). The asymmetric unit cell contains two independent ligand molecules with a C_2- plane located in the middle of the C-C bond of the ethylene spacer, a silver cation and a hexafluorophosphate counter ion (Figure 35).
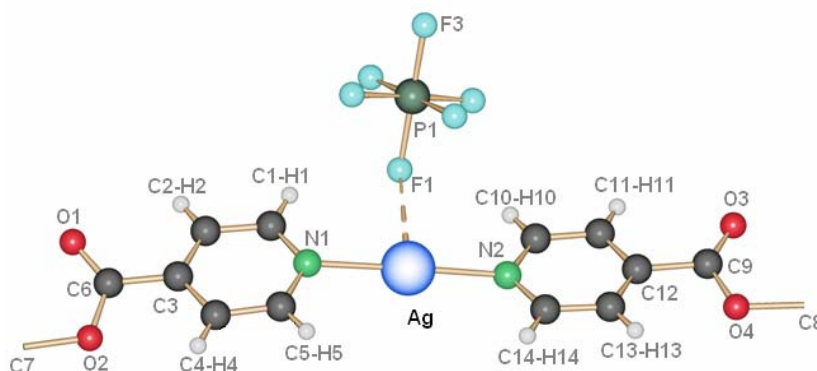
Figure 35. Schematic representation of the coordination geometry of the Ag(I) in complex 2. The poor coordination ability of the PF₆⁻ counter ion determines the almost linear angle N-Ag-N

The two ligands coordinate the silver cation equally (Ag(1)-N(1), 2.163(6) Å, Ag(1)-N(2), 2.132(6) Å). The counter ion is a weak coordinating agent; distances F-Ag(1) are for one counter ion 2.903(5) Å (F(1)-Ag(1)) and 3.091(5) Å (F(2)-Ag(1)) for the next closest PF₆⁻.

The angle N(1)-Ag(1)-N(2) is 178.9(1)°. This linear value is expected due to the poor coordinating ability of this counter ion (Table B-II.19).

Table B-II.19 Most important bond lengths [Å] and angles [°] present in complex **2**

Ag(1)–N(1)	2.163(6)	N(1)–Ag(1)–N(2)	178.9(1)
Ag(1)–N(2)	2.132(6)	C–N–C	116.5(1)
Ag(1)–F(PF₅)	2.903(5), 3.394(5)		
Ag(1)–F(2)[#1]	3.091(5)		
N–C	1.342(3), 1.356(3)		
Symmetry transformations used to generate equivalent atoms: #1 x, -y, -0.5+z			

The metal atom geometry with respect to the **L1** molecules is linear (Figure 35).

The combination (–**L1**-Ag-)ₙ generates a infinite linear polymer in the crystalline state, where the chain is undulated with a periodic distance of 33.95(8) Å (from one silver to the alternate silver

cation) (Figure 36). Aromatic-aromatic interactions through the pyridine ring of the ligand are discarded; the stacking is too far apart to be considered sufficiently stabilizing (closest distance 4.145(6) Å).
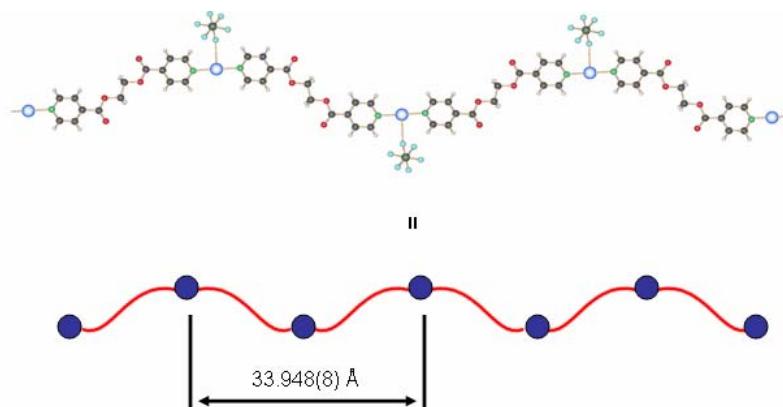
Figure 36. Undulate pattern found in the crystalline state of complex 2. The ethylene glycol moiety possesses an anti (staggered) conformation

These chains are arranged parallel to each other, forming an infinite bi-dimensional sheet due to the weak coordination of the counter ion on two metal atoms. These sheets (above and below) are running in different directions (Figure 37 b, c).

Silver Coordination Compounds with a Family of Ditopic Ligands of Varying Flexibility:
About Chains, Rings, Helices and Polycatenanes

45
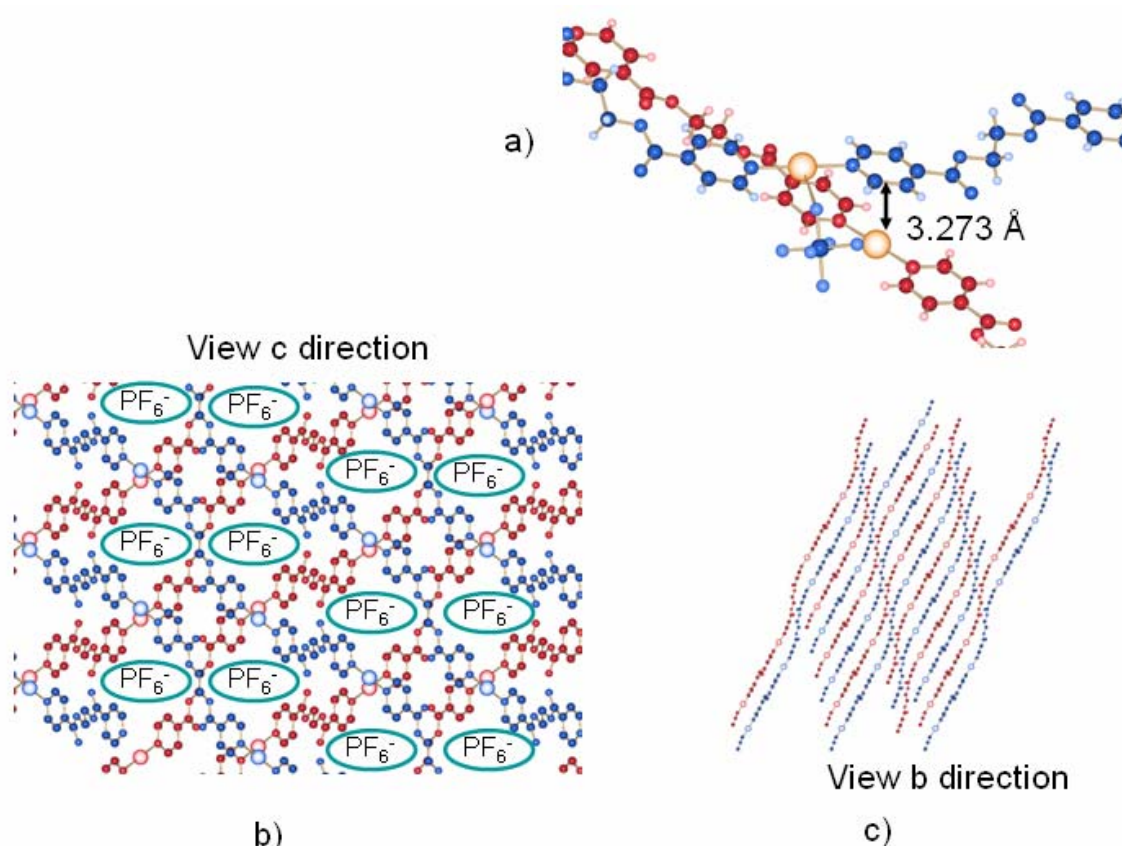
Figure 37. a) Due to the packing the aromatic ring of the ligand remains close to the metal cation; b) two dimensional array due to the coordination of the counter ion. Different directions are represented in red and blue; c) view through the b axis showing sheets running parallel to each others

Due to the position of the sheets, the metal atom is close to the aromatic ring, which suggests some Ag$^+$-π interaction (Table B-II.20) (Figure 37 a).

Table B-II.20 π–π stacking present in complex **2**

Metal-π interaction	$d_{centroid-Ag(1)}$ (Å)	$d_{Ring-Ag(1)}$ (Å)	β
Inter Ag(1)–π stacking between aromatic rings of different chains			
Ring (N1,C1,C2,C3,C4,C5)···Ag(1)[#1]	3.88	2.89	41.9
Ring (N2,C12,C13,C14,C15,C16)···Ag(1)[#2]	3.27	3.16	14.7
Symmetry transformation used to generate equivalent atoms: #1 X,-Y,1/2+Z #2 X,-Y,-1/2+Z			

Following the same analysis, we should anticipate some interaction C-H···π, even if they are relative weak (Table B-II.21).

Table B-II.21 C-H···π interaction present in complex **2**

C-H···π interaction	$d_{\text{C-H···centroid}}$ (Å)	$d_{\text{C···centroid}}$ (Å)	γ
Inter C–H···π stacking between aromatic rings of different chains			
C12–H12···Ring (N1,C1,C2,C3,C4,C5)[#1]	3.18	3.42	9.6
Symmetry transformation used to generate equivalent atoms: #1 x,-y,-1/2+z			

The presence of the hexafluorophosphate is accompanied by the potential formation of hydrogen bonds in the crystalline state (Figure 38). The counter ion within this structure stabilizes the array approaching chains to form sheets, and at the same time acting as a cement linking different sheets through the formation of hydrogen bonds (Table B-II.22).
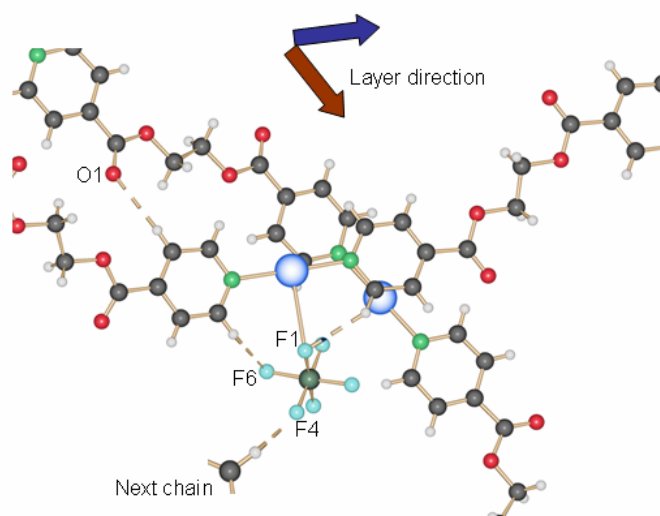
Figure 38. Hydrogen bonds formed after the coordination of the hydrogen atoms from different sheets by the PF_6^- counter ion

Table B-II.22 Hydrogen bond data for **2** [length (Å) and angle (°)]

D-H···Acceptor	d (D–H)	d (H···A)	d (D···A)	Angle D-H···A
Intra chain Hydrogen bonds between the counter ion and the pyridine ring hydrogens				
C1–H1···F6[#1]	0.93	2.51(2)	3.27(1)	140.3(1)
C8–H8···F1[#2]	0.93	2.54(3)	3.32(1)	142.6(2)
Inter chain hydrogen bond formed between the carbonyl oxygen and an hydrogen from the pyridine ring.				
C4–H4···O1[#3]	93	2.60(1)	3.49(1)	163.0(2)
Inter chain hydrogen bond formed between the counter ion and an hydrogen from the pyridine ring				
C11–H11···F4[#2]	0.93	2.46(2)	3.23(1)	141.2(1)
Symmetry transformation used to generate equivalent atoms: #1 x,1-y,-1/2+z, #2 x,-y,-1/2+z, #3 1/2-x,-1/2+y,3/2-z				

B - II.4 - {[Ag(L1)SO₃CF₃]}ₙ coordination polymer (3)

Dr. Robin reported the synthesis of this complex using a "H"-shaped tube, after 2 months of slow diffusion of a THF solution containing the ligand and a water solution where the silver salt was dissolved.

The same reaction could be carried out much faster in the microwave, using THF as solvent at 580 W for five minutes. Single crystals could be isolated and measured in two days. The only problem concerning the microwave synthesis is that the crystal size remained small, even after long periods of incubation.

Complex **3** crystallizes in the monoclinic space group P2₁/c (No. 14). A ligand molecule, a counter ion and a metal atom are contained in the asymmetric unit cell. The Ag(I) is coordinated in a linear fashion by two non-equivalent ligands with very similar distances, **L1** (Ag(1)–N(1) 2.152(5)Å) and **L1A** (Ag(1)–N(1A) 2.154(5)Å). The angle N(1)–Ag(1)–N(1A) of 177.4(1)°, close to 180°, suggests a rather weak interaction with the counter ion (Figure 39).
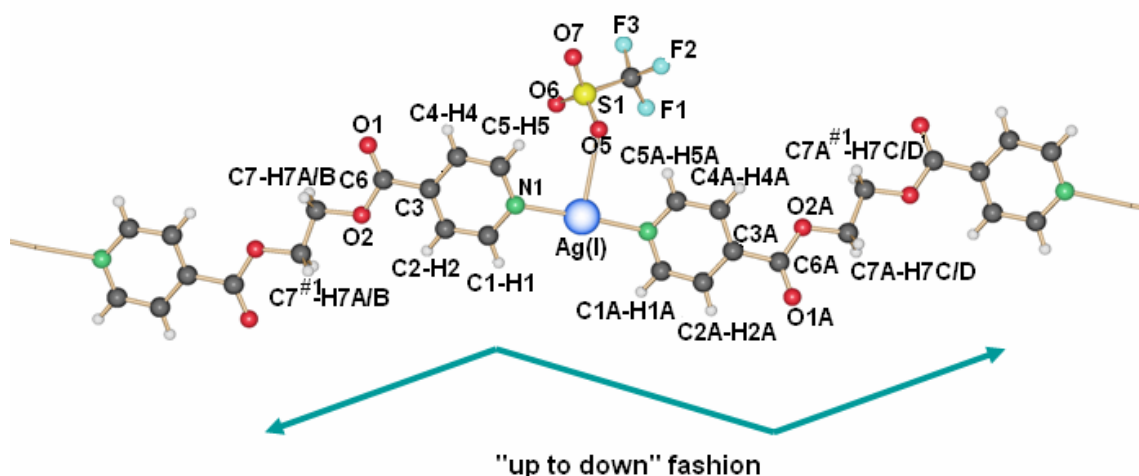
Figure 39. Linear polymeric array obtained after the coordination of the metal cation by two organic ligands in a "Up to down" fashion

The ligand possesses all carbonyl groups almost contained in the same plane, like the aromatic ring (O2–C6–C3–C4, 4.8(2)°). The ethylene moiety has a staggered conformation as well as the ligand **L1A**. In **L1A**, however, the carbonyl groups are slightly twisted compared to the plane of the

Silver Coordination Compounds with a Family of Ditopic Ligands of Varying Flexibility:
About Chains, Rings, Helices and Polycatenanes

48

aromatic rings (O2A–C6A–C3A–C4A, 10.6(2)°). The result is a slightly extension of the ligand length (distance from Ag to Ag 17.423(3) Å versus 17.367(3) Å for **L1**) (Figure 40).
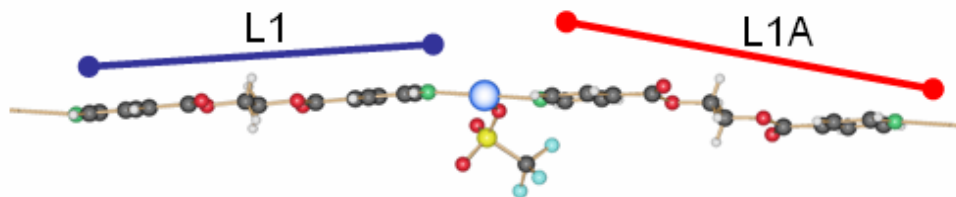
Figure 40. All carbonyl groups in L1 remain in the plane of the aromatic ring. In ligand L1A these carbonyl groups are twisted, so the two ligand are not symmetrical

The principal motif is an infinite $\{-$**L1**$-$Ag$-$**L1A**$-$Ag$-\}_n$ chain in an "up-to-down" mode.

The counter ion coordinates in a mono-dentate way to the metal atom Ag(1)–O(5)[#1] (2.801(5) Å). At the same time, this counter ion coordinates more weakly and in a mono-dentate way a second metal atom of a chain running in almost perpendicular direction above or below that chain (distance Ag(1)–O(7) of 2.822(5) Å).

To better visualize the main motif we should differentiate between two complementary arrays in the crystalline state. One consists of a three-dimensional network. This is formed by chains running in opposite direction. The silver atoms are superimposed but not close enough to form metal-metal bonds (Ag(1)–Ag(1)[#1], 4.758(9) Å). These metal atoms are linked by the counter ion, forming a cage-like structure with empty space of 13.183(1) x 14.262(2) Å^2 within the cage (Figure 41).

Silver Coordination Compounds with a Family of Ditopic Ligands of Varying Flexibility: About Chains, Rings, Helices and Polycatenanes

49
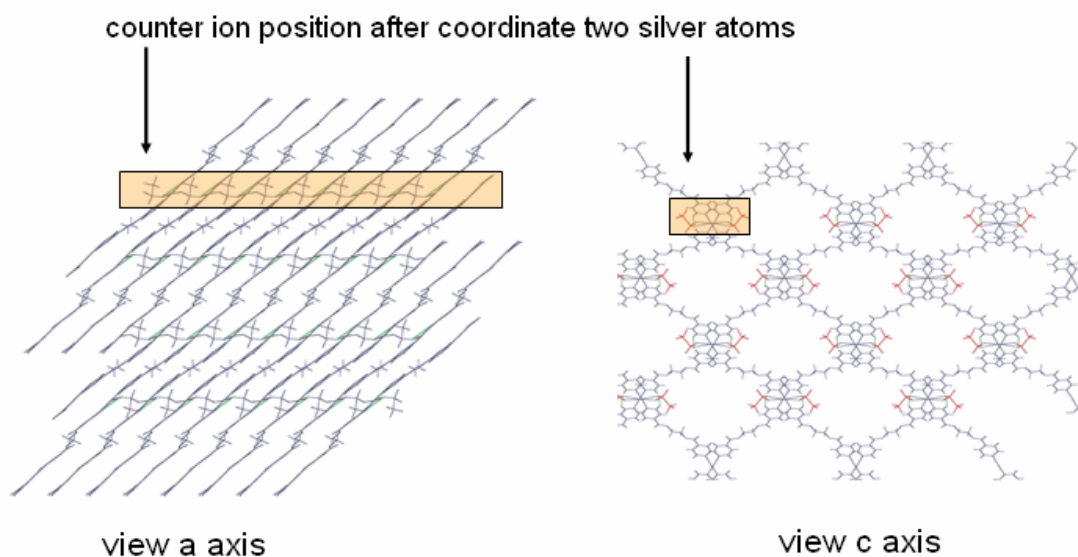
Figure 41. Three dimensional motifs in the crystalline state of 3. a) The counter ion coordinates chains running in opposite direction, b) cage formations within the structure with dimension about 13x14 Å^2

This empty space is occupied by a second motif with the same topology existing in a parallel direction, which interpenetrates the first motif (Figure 42).
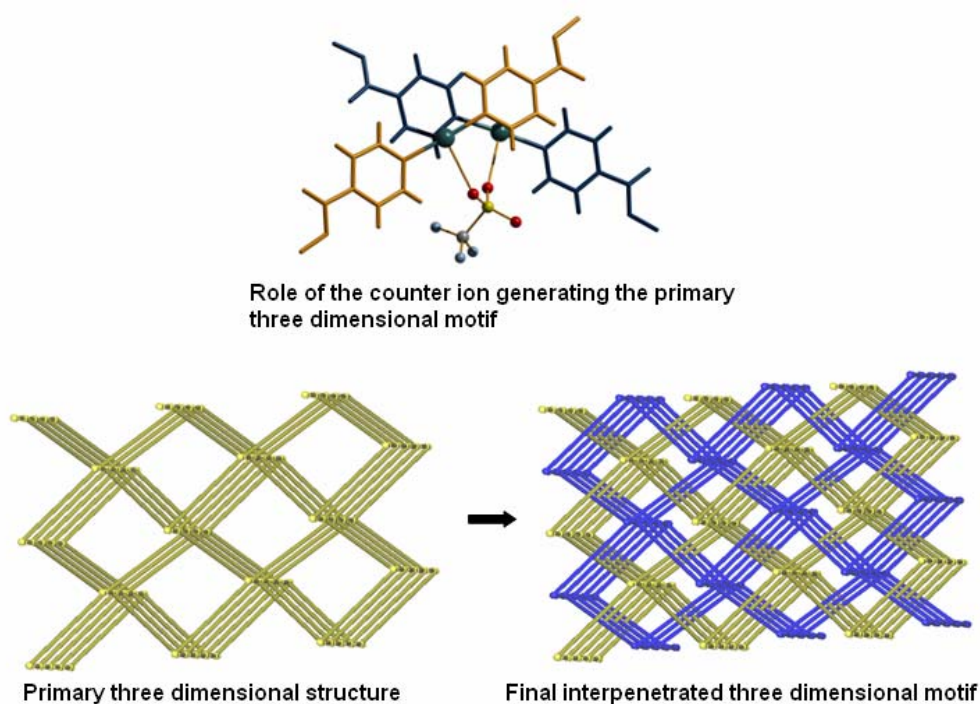
Figure 42. Interpenetration of the two main motifs

Silver Coordination Compounds with a Family of Ditopic Ligands of Varying Flexibility: About Chains, Rings, Helices and Polycatenanes

50

Both motifs are parallel but displaced by 0.43(2) Å in the *c* axis direction. Between the two motifs the relationship is based on the counter ion-metal interactions.

The triflate counter ion possesses two chemical regions ($-SO_3$ and $-CF_3$) which act essentially in a different way from the coordinating point of view. The oxygen atoms ($-SO_3$) coordinate the silver atom, and at the same time form hydrogen bonds with hydrogen atoms of the pyridine ring. These hydrogen atoms are spatially the closest to the oxygen of the counter ion, so this interaction is doubly favored (C1A–H1A⋯O7, 2.586(7) Å; C5A–H5A⋯O5, 2.589(4) Å; C5–H5⋯O5, 2.471(6) Å). The $-CF_3$ part of the molecule, however, is in the opposite direction as the $-SO_3$ and it is spatially directed to hydrogen atoms in the second motif. Potential hydrogen bonds could be formed between sheets from the fluorine atoms of the counter ion to hydrogen atoms of the pyridine ring and lateral chain (C1A–H1A⋯F3, 2.685(5) Å; C2–H2⋯F2, 2.818(5) Å; C4–H4⋯F3, 2.815(5) Å, C1–H1⋯F3, 2.685(5) Å) (Figure 43).
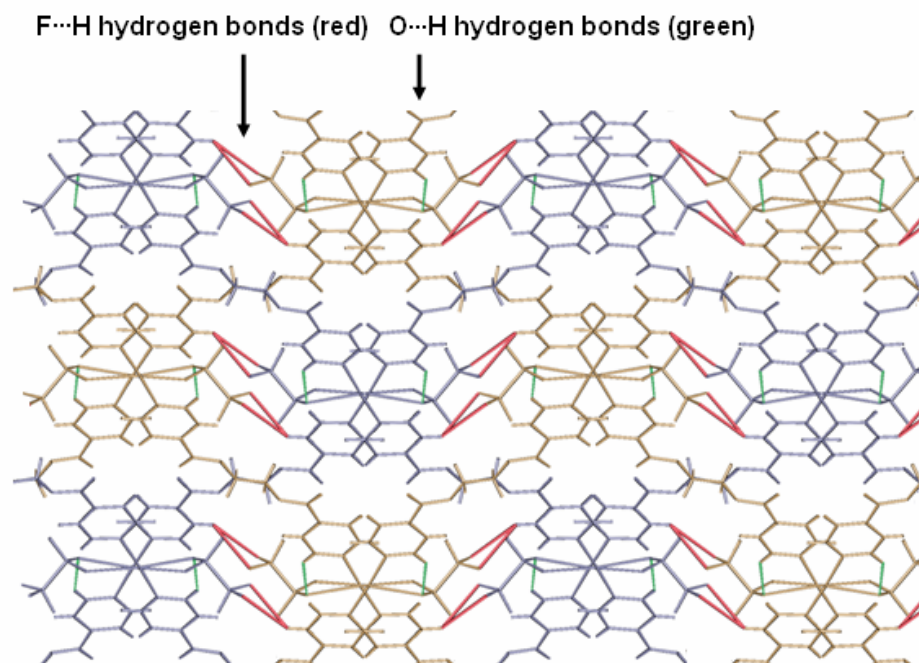
Figure 43. Hydrogen bonds formed within the crystalline structure of 3. O⋯H Hydrogen bonds are represented in green, whereas F⋯H are represented in red color

Silver Coordination Compounds with a Family of Ditopic Ligands of Varying Flexibility:
About Chains, Rings, Helices and Polycatenanes

51

Both motifs are related through hydrogen bonds. The final structure consists of a 3D framework (classify as Ia, Z=2 using TOPOS) with Ag(I) cations acting as node. There are 2 interpenetrated nets, the final network topology of this compound is similar as the one present in the CdSO$_4$ salt.

Table B-II.23 Most important bond lengths [Å] and angles [°] present in complex **3**

Ag(1)–N1	2.152(5)	N1–Ag(1)–N1A	177.4(1)
Ag(1)–N1A	2.153(5)	C–N–C	118.0(1)
Ag(1)–O5(SO$_3$CF$_3$)	2.801(5)		
Ag(1)–O7(SO$_3$CF$_3$)[#1]	2.822(5)		
N–C	1.333(3), 1.338(3)		
Symmetry transformations used to generate equivalent atoms: #1 x, 1.5-y, 0.5+z			

Table B-II.24 Hydrogen bond data for [length (Å) and angle (°)] present in complex **3**

D-H···Acceptor	d (D–H)	d (H···A)	d (D···A)	Angle D-H···A
Intra sheet hydrogen bonds between the anion and the hydrogen atoms of the pyridine ring				
C1A–H1A···O7	0.93	2.59(0)	3.35(6)	140.0(0)
C5–H5···O5[#1]	0.93	2.47(0)	3.22(2)	138.0(2)
C5A–H5A···O5[#1]	0.93	2.59(0)	3.31(3)	135.0(0)
Inter sheet hydrogen bonds between the anion and the hydrogen atoms of the pyridine ring				
C1A–H1A···F3[#2]	0.93	2.68(5)	3.37(0)	131.1(1)
C4–H4···F2[#3]	0.93	2.81(8)	3.55(1)	136.6(1)
C4–H4···F3[#3]	0.93	2.81(5)	3.50(7)	131.8(1)
C1A–H1A···F3[#4]	0.93	2.68(5)	3.37(0)	131.1(1)
C7A–H7D···F1	0.97	2.79(0)	3.60(1)	142.6(1)
C7–H7B···F1[#5]	0.97	2.71(0)	3.44(1)	132.6(1)
Symmetry transformation used to generate equivalent atoms: #1 x, 1.5-y, 0.5+z, #2 1-x, 1-y, z, #3 1-x, 0.5+y, -0.5-z #4 1-x, 1-y, -z #5 1+x, 1.5-y, -0.5+z #6 1-x, 1-y, -z				

Other interactions like aromatic-aromatic are discarded due to the distance between the pyridine rings (closest distance 4.250(3) Å).

B - II.5 - {[Ag(L2)NO$_3$]}$_n$ coordination polymer (4)

This complex crystallizes in the orthorhombic space group Pnma (No. 62), with a silver cation coordinated by two half molecules of ligands and a counter ion situated perpendicular to the plane formed by pyridines rings of both tectons **L2**. A symmetry plane located in the bond connecting the

Silver Coordination Compounds with a Family of Ditopic Ligands of Varying Flexibility:
About Chains, Rings, Helices and Polycatenanes

52

two –CH$_2$- groups of the spacer chain generates a one dimensional infinite polymer of {–**L2**–Ag–}$_n$ type (Figure 44).
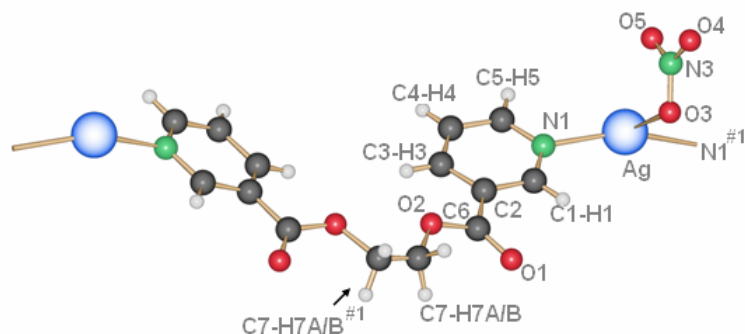
Figure 44. Infinite metal-organic polymeric array in complex 4

The nitrate counter ion coordinates the silver in an asymmetrical –µ^2 (distances Ag-O, 2.602(4) and 2.815(5) Å) and monodentate –µ^1 way in relation to the closest silver cation (Ag$^{#1}$-O, 2.795(6) Å) located in a parallel plane (Figure 45). A two dimensional network of parallel sheets is the final motif in the crystalline state. The distorted trigonal coordination is completed by two nitrogen atoms from each aromatic ring. The bonding strength due to the counter ion is reflected in the distortion of the angle N1-Ag-N1$^{#1}$ 156.9(8)° (ideal 109.5°).
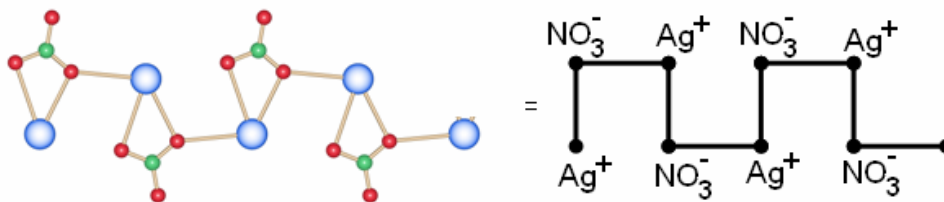
Figure 45. Bidentate-monodentate coordination modes of the nitrate counter ion in compound 4

Concerning the ligand, the most remarkable feature is the almost perfect eclipsed conformation of the ethane groups. The aromatic ring is twisted regarding the carbonyl group (C3-C2-C6-O2, 17.6(1)°). Every single chain is undulated, the next chain conforming the sheet is also undulated, but in the opposite way (Figure 46).

Silver Coordination Compounds with a Family of Ditopic Ligands of Varying Flexibility: About Chains, Rings, Helices and Polycatenanes

53
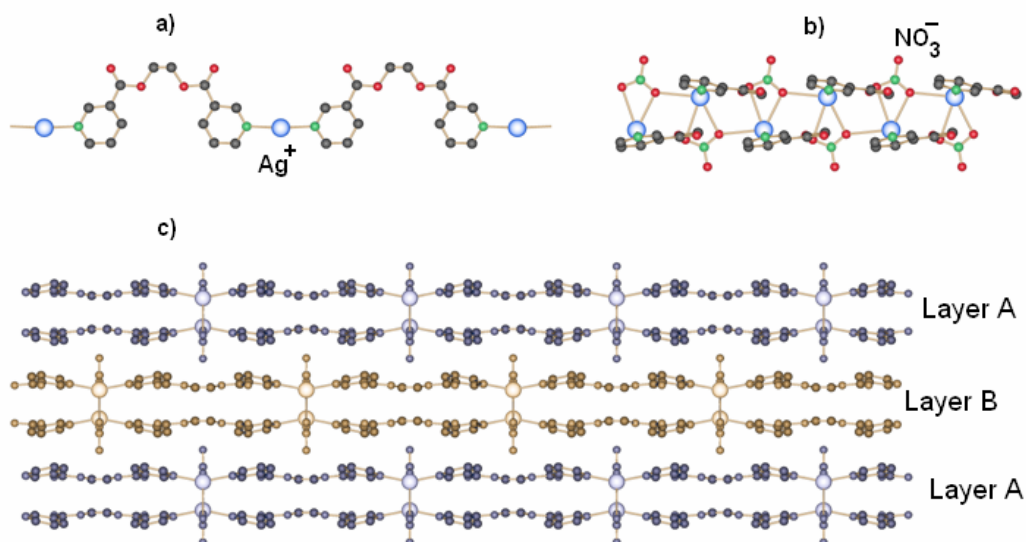
Figure 46. Two dimensional array in compound 4 due to the nitrate counter ion coordination on the metal cations of parallel metal-organic chains

The closest distance between aromatic rings is more than 4 Å, excluding π–π contacts between sheets. The nitrate counter ion is located in such a position that it can form hydrogen bonds with hydrogen atoms from the pyridine ring in the sheet direction, but at the same time with hydrogen atoms located in the ethylene group of the ligand situated in the next perpendicular sheet (Figure 47).
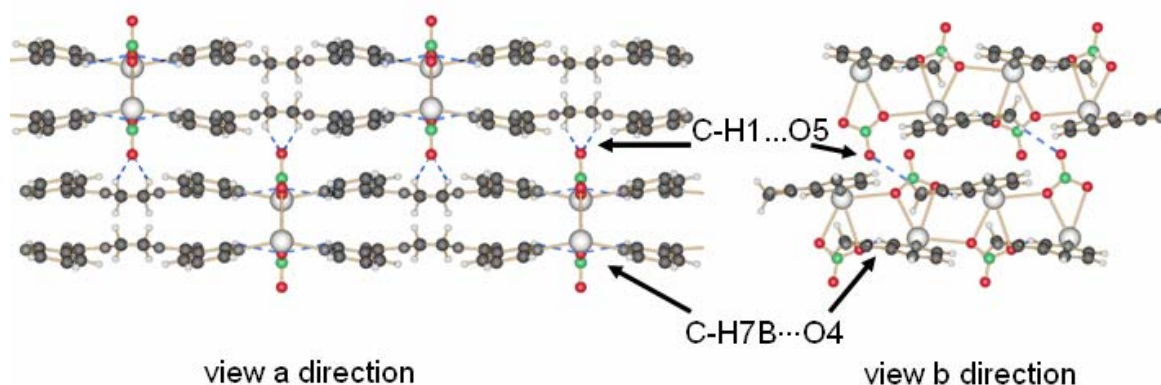
Figure 47. Hydrogen bonds generation in the crystalline array of compound 4. Oxygen atoms represented in red, nitrogen atoms in green

Silver Coordination Compounds with a Family of Ditopic Ligands of Varying Flexibility: About Chains, Rings, Helices and Polycatenanes

54

Both hydrogen bonds are different. The C7-H7B⋯O4 bond is running in the sheet direction as a bridge between ligands coordinating the same silver cation, whereas the C1-H1⋯O5 bond is perpendicular to the sheet direction and acts as a linker between sheets (Figure 47. view *a* direction).

Table B-II.25 Hydrogen bond data [length (Å) and angle (°)] present in complex **4**

D-H⋯Acceptor	d (D–H)	d (H⋯A)	d (D⋯A)	Angle D-H⋯A
Intra sheet hydrogen bond between the counter ion and the pyridine ring hydrogen				
C7–H7B⋯O4	0.97	2.60(1)	3.40(3)	141.2(0)
Inter sheet hydrogen bond formed between the counter ion and hydrogen on the lateral chain.				
C1–H1⋯O5	0.93	2.57(2)	3.32(1)	139.1(2)

Table B-II.26 Most important bond lengths [Å] and angles [°] present in complex **4**

Ag(1)–N(1)	2.190(4)	N(1)–Ag(1)–N(2)$^{\#1}$	156.9(8)°
Ag(1)–O(NO$_2$)	2.602(4), 2.818(5)	C–N–C	117.7(1)°
Ag(1)$^{\#1}$–O(NO$_2$)$^{\#2}$	2.796(3)		
N–C	1.330(2), 1.336(2)		
Symmetry transformations used to generate equivalent atoms: #1 x,0.5-y,z #2 0.5+x,0.5-y,0.5-z.			

B - II.6 - {[Ag(L2)SO₃CF₃]}ₙ (5) coordination polymer and its network isomer (6)

After diffusion of a THF solution of the ligand into a water solution containing the silver trifluoromethanesulfonate salt, single crystals of good quality for X-ray measurements were collected in the ligand side of the "H"-shaped tube.
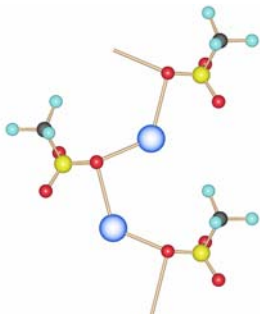
The complex **5** crystallizes in the monoclinic space group P2₁/c (No. 14). The unit cell contains one ligand coordinated through the pyridine rings to a silver cation, and a trifluoromethanesulfonate (triflate) counter ion.

The counter ion coordinates two silver cations in a μ^2- fashion with distances Ag(1)-O(5), 2.67(4)Å and Ag(1)$^{\#1}$-O(5), 2.820(5) Å to the next silver cation in the [0 0 1] direction (viewing along the *c* axis).

Every ligand binds one silver cation with each nitrogen of the aromatic ring (Ag(1)-N, 2.197(4) and 2.182(4) Å). The angle N-Ag-N 154.0(1)° reveals a distorted tetrahedral geometry for the metal

Silver Coordination Compounds with a Family of Ditopic Ligands of Varying Flexibility: About Chains, Rings, Helices and Polycatenanes

55

atom, as well as a strong interaction of the metal atom with the counter ion (Table B-II.27) (Figure 48).
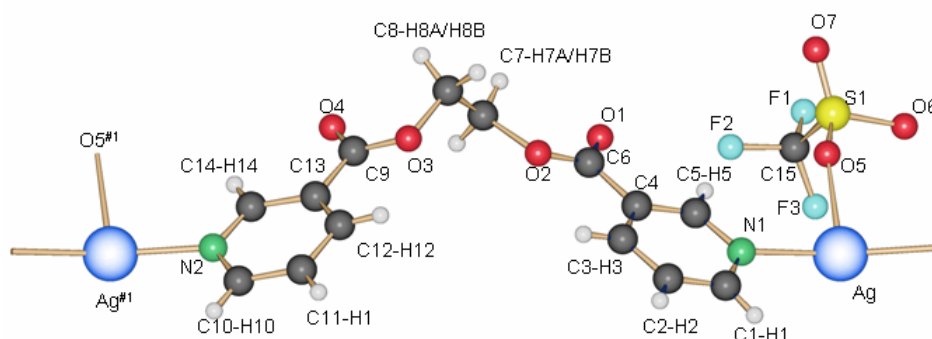
Figure 48. Infinite linear motif in complex 5. The ethylene glycol moiety is in a gauche (staggered) conformation

Within the ligand **L2** the carbonyl group is almost enclosed in the plane of the aromatic ring (C3-C4-C6-C2, 8.8(2)°). The ethylene spacer presents a gauche (staggered) conformation which allows the ligand to be "twisted", forming one-dimensional wave-like metal-organic polymers. The chains are undulating in different directions regarding polymeric chains located above and below (Figure 49).
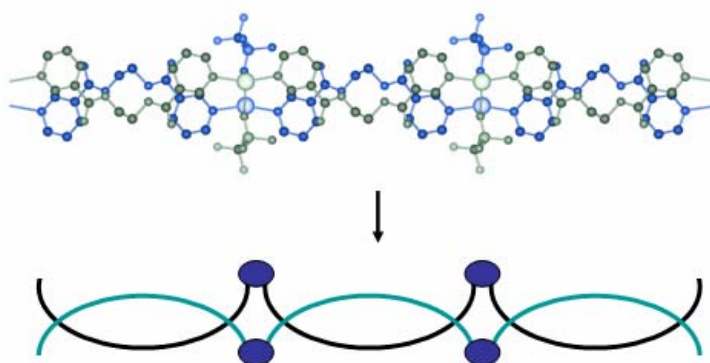
Figure 49. View in the c direction showing different undulating direction between parallel metal-organic chains

The single 1-D chain generated in this way changes into a 2-D motif due to the counter ion role. The $SO_3CF_3^-$ coordinates asymmetrically two silver cations. This two dimensional sheet runs perpendicular to the plane formed by the pyridine rings of the organic ligand (Figure 50).

Silver Coordination Compounds with a Family of Ditopic Ligands of Varying Flexibility: About Chains, Rings, Helices and Polycatenanes

56

staggered conformation
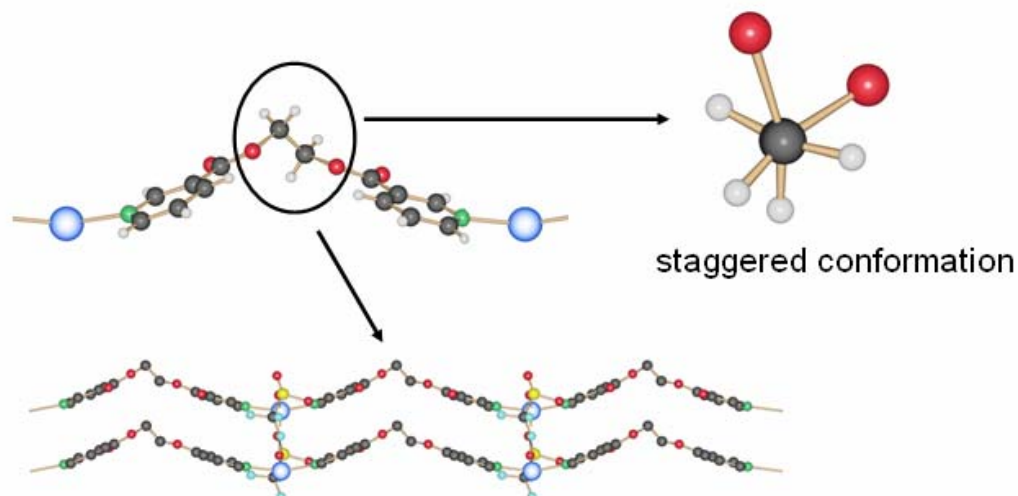
Figure 50. Two dimensional network generation due to the coordination of the metal cations by the counter ions (view *b* direction)

Aromatic interaction of type π-π stacking is excluded due to the displacement of the aromatic rings from one chain to the aromatic rings in the next one (closest distance about 4.587 Å).

Table B-II.27 Most important bond lengths [Å] and angles [°] for compound **5**

Ag(1)-N(1)	2.197(4)	N(1)-Ag(1)-N(2)[#1]	154.0(1)°
Ag(1)-N(2)[#1]	2.182(4)	C-N-C	118.2(1)°
Ag(1)-Ag(1)[#1]	4.02(7)		
Ag(1)-O(SO$_2$CF$_3$)	2.467(4), 2.820(5)		
N-C	1.381(2), 1.348(2)		
Symmetry transformations used to generate equivalent atoms: #1 1+x, y, z			

In the crystalline motif, sheets are displaced with respect to each other in such a way that the counter ions of one sheet are spatially close to the ethylene part of the parallel sheet. The formation of hydrogen bonds in such a way is potentially increased (Table B-II.28). Hydrogen bonds are formed between fluorine and oxygen atoms of the triflate and the hydrogen atoms of the lateral ethylene glycol spacer and hydrogen atoms of the pyridine rings. These interactions seem to be significant holding sheets together and compacting the whole structure (Figure 51).

Schematic representation of hydrogen bonds formed by the counter ion (—)
and metal counter ion bond (⋯)
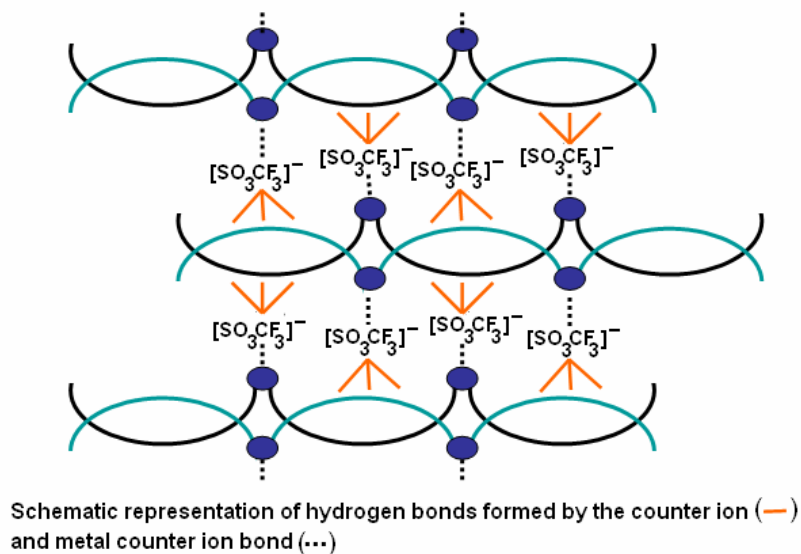
Figure 51. Schematic representation of the hydrogen bonds in the crystalline structure of compound 5

Table B-II.28 Hydrogen bond data for **5** [length (Å) and angle (°)]

D-H⋯Acceptor	d (D–H)	d (H⋯A)	d (D⋯A)	Angle D-H⋯A
Inter sheet hydrogen bonds formed between the counter ion and the pyridine ring hydrogen.				
C1-H1⋯O7[#1]	0.93	2.51(0)	3.29(2)	141.7(0)
C2-H2⋯F2[#2]	0.93	2.50(2)	3.12(0)	124.9(8)
C3-H3⋯F1[#2]	0.93	2.54(1)	3.43(3)	160.5(5)
C11-H11⋯O6[#3]	0.93	2.34(0)	3.07(1)	136.0(2)
Inter sheet hydrogen bonds formed between the counter ion and the pyridine ring hydrogen.				
C7-H7A⋯F1[#4]	0.97	2.52(1)	3.32(4)	140.3(0)
C7-H7B⋯O7[#5]	0.97	2.41(3)	3.19(0)	137.4(1)
Symmetry transformation used to generate equivalent atoms: #1 x,3/2-y,-1/2+z, #2 -x,1/2+y,1/2-z, #3 1-x,1/2+y,1/2-z, #4 -x,1-y,-z, #5 -x,1-y,1-z.				

In the opposite side of the "H"-shaped tube, where the silver solution was placed, single crystals with the same morphology as **5** were obtained and measured. The new complex **6** crystallizes in the monoclinic space group $P2_1/n$ (No. 14). In the asymmetric unit cell, one ligand and one counter ion coordinate a silver cation.

The coordination geometry around the metal atom involves two ligands directly bonded to the silver cation (Ag(1)-N, 2.17(3) and 2.147(1) Å) with an angle N(1)-Ag(1)-N(2) close to linearity

(168.99(1)°), which implies more a T-like coordination type considering the interaction with the triflate counter ion (Ag(1)-O5, 2.762(5) Å) (Figure 52).
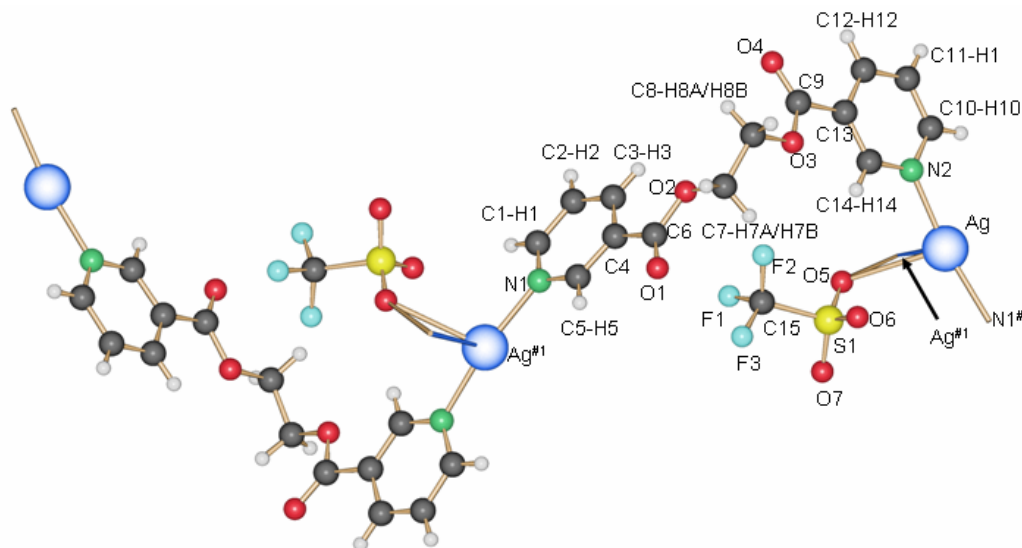
Figure 52. Coordination motif in the crystalline state for complex 6. The linear metal-organic chains are linked through Ag–Ag with adjacent chains. These metal cations are linked through the counter ion

The counter ion coordinates also a second silver cation (Ag(1)$^{\#1}$-O5, 2.897(7) Å). This bond could be responsible for the metal-metal interaction present within the structure (Ag(1)-Ag(1)$^{\#2}$, 3.201(8) Å) (Table B-II.29).

Table B-II.29 Most important bond lengths [Å] and angles [°] present in complex **6**

Ag(1)-N(1)	2.147(7)	N(1)-Ag(1)-N(2)$^{\#1}$	169.0(1)
Ag(1)-N(2)$^{\#1}$	2.147(1)	N(1)-Ag(1)-Ag(1)$^{\#3}$	99.8(8)
Ag(1)-Ag(1)$^{\#2}$	3.201(8)	N(2)$^{\#1}$-Ag(1)-Ag(1)$^{\#1}$	90.1(7)
Ag(1)-O(SO$_2$CF$_3$)	2.762(5), 2.897(9)	C-N-C	117.7(1)
N-C	1.343(5)		

Symmetry transformations used to generate equivalent atoms: #1 0.5-x, -0.5+y, 1.5-z #2 1-x, -y, 2-z #3 1-x, -y, 2-z

The carbonyl group remains in the plane formed by the aromatic ring (O3-C9-C13-C14, 13.7(2)° and 2.72(2)° for O2-C6-C4-C3). The ethylene moiety retains the staggered conformation like in **5**, but the nitrogen atoms in the aromatic ring are pointing both to the same side compared to the conformation of the ligand in **5**. This is important in the generation of helicity within the chain (Figure 53).

Silver Coordination Compounds with a Family of Ditopic Ligands of Varying Flexibility:
About Chains, Rings, Helices and Polycatenanes

59
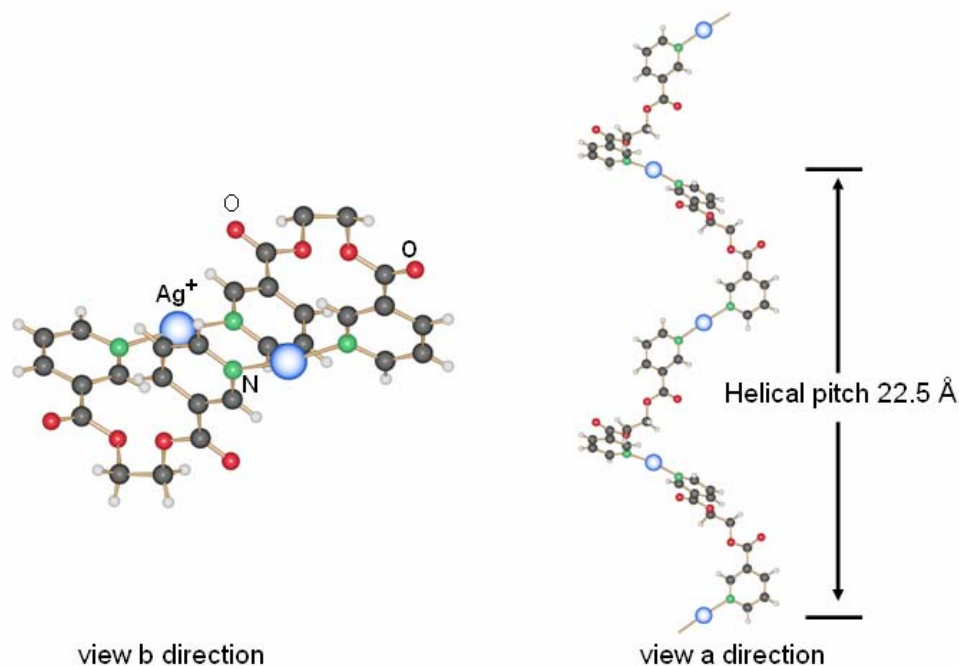
Figure 53. Helical array of one single chain in 6

The shorter ethylene glycol moiety impacts directly in the pitch of the helice. Another important fact concerning **6** is the presence of metal-metal interactions; this one links two chains but exists only every two silver centers (Figure 54), alternating toward a next chain to yield an overall 2-D motif.
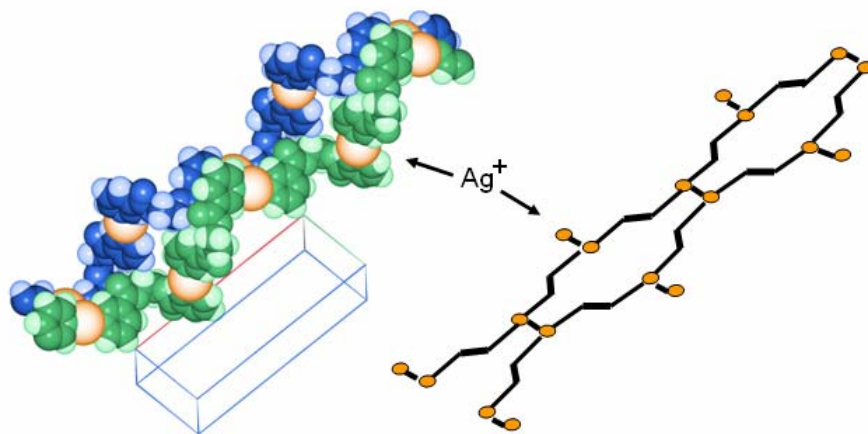
Figure 54. Relationship between single chains through metal-metal bonds

Individual ribbons are joined together by metal-metal interaction through the crystalline motif. This array, when extended, creates a very intricate three-dimensional motif

Figure 55).

Weak aromatic π–π stacking (Table B-II.30) and hydrogen bonds are present. The presence of aromatic π–π stacking and Ag–Ag contacts may be determinant for the final crystal motif in **6**. Hydrogen bonds are formed mostly between the counter ion and hydrogen atoms of the pyridine ring coordinating the same metal cation. (Table B-II.31).
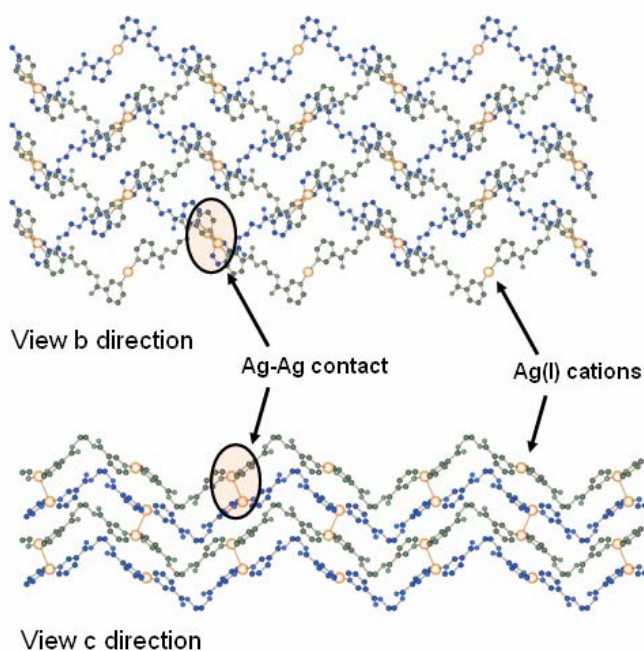
Figure 55. Two dimensional network generated through silver-silver contacts in compound 6.

Table B-II.30 π–π stacking present in complex **6**

π-π interaction	d_{R-R} (Å)	ρd_{R-R} (Å)	α	β
Inter π–π stacking between aromatic rings of different helices.				
Ring (N1,C1,C2,C3,C4,C5)···Ring (N2,C10,C11,C12,C13,C14)[#1]	3.81	3.65	14.66	29.44
Symmetry transformation used to generate equivalent atoms: #1 0.5+x,0.5-y,0.5+z				

Table B-II.31 Hydrogen bond data [length (Å) and angle (°)] present in complex **6**

D–H⋯Acceptor	d (D–H)	d (H⋯A)	d (D⋯A)	Angle D-H⋯A
Intra helice hydrogen bonds between the anion and the pyridine ring hydrogens.				
C1–H1⋯O6[#1]	0.93	2.53(3)	3.29(8)	139.7(6)
C5–H5⋯O5[#2]	0.93	2.48(1)	3.26(2)	141.6(7)
C10–H10⋯O7[#3]	0.93	2.45(2)	3.34(7)	161.5(8)
Intra helice hydrogen bond formed between the carbonyl oxygen atom and the hydrogen atom from the lateral chain.				
C7–H7A⋯O4[#4]	0.97	2.52(4)	3.38(7)	148.1(4)

Symmetry transformation used to generate equivalent atoms: #1 1-x,-y,1-z, #2 x,y,1+z, #3 1/2-x,1/2+y,1/2-z, #4 0.5+x,0.5-y,0.5+z.

B - II.7 - Some considerations about complexes 1, 2, 3, 4, 5 and 6

The use of these two short ligands **L1** and **L2** envisages the creation of linear metal-organic arrays. In these polymers, the role played by the Ag(I) cation and the counter ion is determinant to direct the preferable linear motif. The same ligand combined with other metal cations showing a preference for a tetrahedral geometry affords metallacycles under similar reaction conditions [247].

While in the solid state, the crystalline structure of polymeric complexes remains well established, the presence of these polymeric structures in solution has not been explored with the same intensity. Therefore some conductivity measurements were performed to evaluate the presence and characteristics of these silver complexes in solution. Measurements were performed under standard conditions (see experimental part p.159).

Two solutions (0.01 mmol*L^{-1}) were prepared in THF, the first containing the ligand **L1** (**1***) and the second the salt $AgNO_3$ (**2***). It was necesary to work below this concentration due to the precipitation of the complex. For the first experiment, aliquots of the solution **1*** were added to the solution **2*** until the equivalence point was reached and the conductivity was measured until the value was stabilized (Figure 56). The curve shows a decrease in the conductivity value from which the formation of the complex could be qualitatively estimated. The decrease in the curve is not constant; the values at 0.3 and 0.7 or 1 equivalence could be a consequence of the labile coordination bond Ag–N.
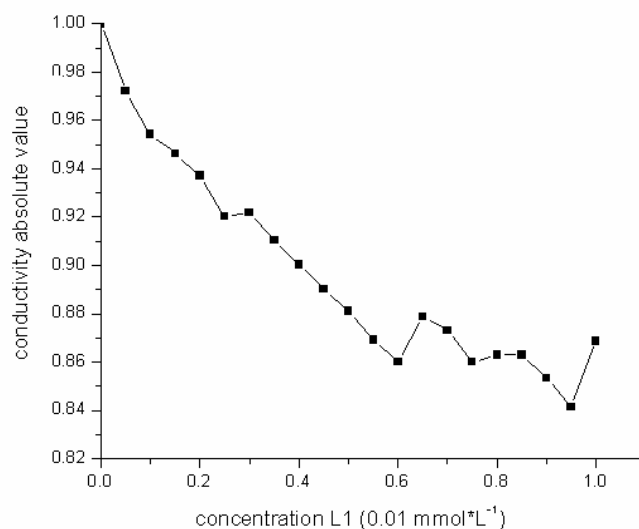
Figure 56. Conductivity measurement performed on a solution containing the ligand L1 and AgNO$_3$

In the second experiment, the formation of the complex over time was evaluated. The same volumes of **1*** and **2*** were mixed together and the conductivity values were measured every hour. When a concentration of 1.00 mmol*L^{-1} was used, the complex precipitated, which is reflected in the anomalous curve obtained. Lower concentration afforded a decrease in the conductivity value against time (Figure 57). These qualitative results suggest the formation of molecular complexes of the silver cation in solution rather than the formation of polymeric arrays.
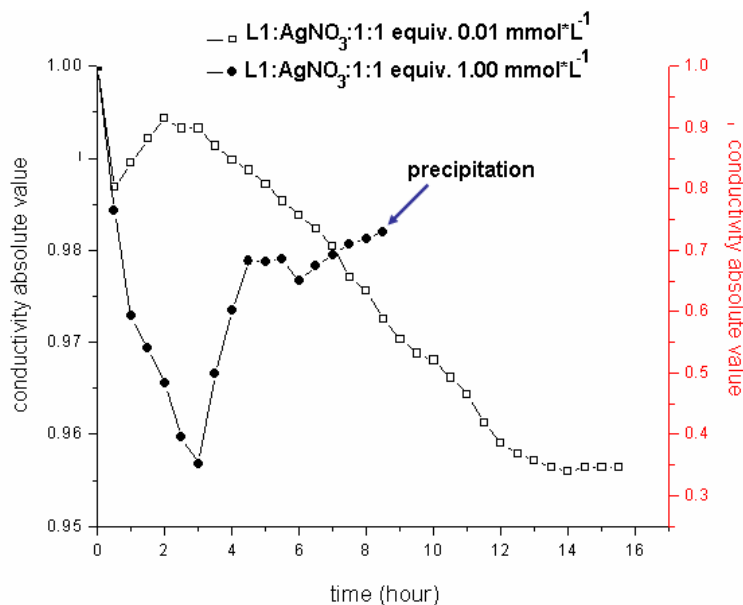
Figure 57. Conductivity measurements versus time (h) in a solution containing the ligand L1 and AgNO$_3$. Higher concentration (1.00 mmol*L^{-1}) affords precipitation (blue arrow)

To determinate quantitatively the extension of the polymer in solution, further refined techniques are needed.

The non-invasive DOSY-NMR (diffusion ordered spectroscopy) technique has been applied by several groups [248-257]. This relates the diffusion coefficient of the species present in solution to the molar mass or hydrodynamic radii of these species. Usually regarding to the shift in intensity of the proton signals in the NMR scale, changes are observed when the strength of the magnetic field is varied.

Based on the diffusion coefficient (DC), the molar mass or hydrodynamic radii of species present in solution can be determinated with a reasonable degree of error and consequently the molecular structure of these species derived. A limitation of this technique is that reliable diffusion coefficients can only be determined for well-resolved resonances. This can be problematic in the analysis of complex mixtures where signal overlapping can complicate the spectra. That was basically the cause why the NMR spectra recorded using THF-d8 were not reliable enough in our case.

NMR samples containing the ligand alone (**3'**) and the ligand with the silver nitrate (**4'**) were prepared and sealed under inert atmosphere (Argon). Two solvents were used for the NMR measurements, THF-d8 and DMSO-d6. All samples were measured in Geneva by Prof. Damien Jeannerat (Figure 58).

Silver Coordination Compounds with a Family of Ditopic Ligands of Varying Flexibility:
About Chains, Rings, Helices and Polycatenanes

64
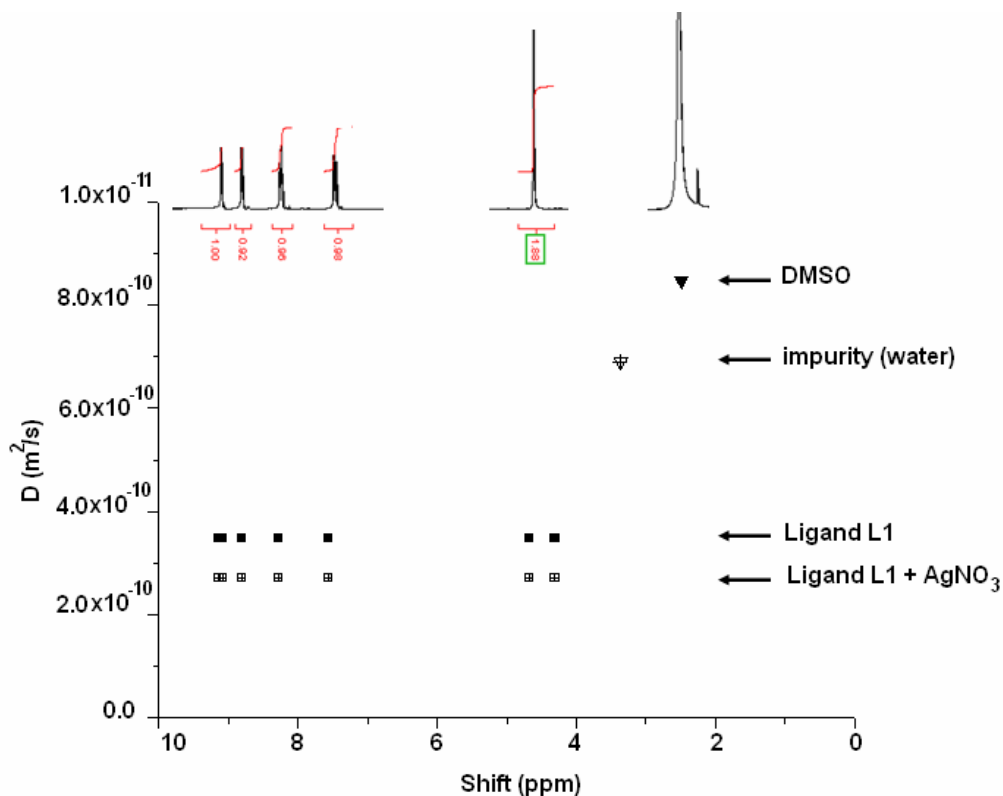
Figure 58. Diffusion coefficients of a sample containing the ligand L1 and a mixture (L1+AgNO₃). The DOSY-NMR technique affords differencse in the values for the ligand and the complex in solution

From the samples measured in THF-d8, only poor conclusions could be drawn. Both, (**3'**) and (**4'**), afford similar DCs. However, samples of (**3***) and (**4***) prepared using DMSO-d6, show significant differences from their diffusion coefficient in the NMR tube.

The variable of the *x*-axis is the chemical shift and that of the *y*-axis is the diffusion coefficient related to molecular properties, such as molecular weight and structure. Figure 58 illustrates that there are two components containing aromatic protons.

The experimental diffusion coefficient (DC) obtained allow via the Einstein-Stokes equation DC = $k_BT/(6\pi\eta r_h)$ the calculation of the hydrodynamic radii. In this formula k_B is the Boltzmann constant, T the temperature in Kelvin, η the viscosity of the solvent employed and r_h the hydrodynamic radii (Table B-II.32).

Silver Coordination Compounds with a Family of Ditopic Ligands of Varying Flexibility: About Chains, Rings, Helices and Polycatenanes

65

Table B-II.32 Hydrodynamic radii calculated based in DOSY-NMR experiments

	Solvent used, Temperature	DC (x 10^{-10} m^2/s)	Hydrodynamic radii (Å)
L1	DMSO-d6,	3.23	3.55
L1+AgNO$_3$	298 K	2.46	4.66
L1	THF-d8,	15.12	2.37
L1+AgNO$_3$	235 K	8.89	4.02

The radii calculated possess a ±5% error. Measure times from 15 to 20 ms.

The DC of the solvent used are in the range reported in the literature (about 8-10 x 10^{-10} m^{2}s^{-1} for DMSO-d6 and THF-d8). To better assess the found DC value, a theoretical model is required.

Prof. Garcia de la Torre at the University of Murcia in Spain is currently modelling our complexes using a version of the program HYDROPRO to simulate some of the properties of these complexes in solution. The future results will allow us to determine if the use of DOSY-NMR is an appropriate tool in the investigation of metal-organic polymers in solution.

The diffusion coefficients found for the ligand alone and the complex are illustrated in Table B-II.32. The relation in the hydrodynamic radii ligand/complex in both cases implies the presence of oligomers (–**L1**–Ag$^+$–)$_n$ (n = 1,2) rather than polymeric species in solution at this concentration.

Further experimental data with different equivalent concentrations of metal to ligand and solvent should afford a more complete answer concerning the question if the polymers are formed in solution previous the crystallization or if the presence of infinite polymeric arrays is just the result of the crystallization process in the crystalline state.

B - II.8 - Impact of the ligand in the crystalline structures of the complexes

In these complexes the geometry of the ligand plays a crucial role in the polymeric motif. The coordination at the silver atom occurs in a linear fashion, using the nitrogen atom located at the pyridine ring.

The ethylene glycol chain acting as spacer provides the ligand with a limited range of torsion angle values (staggered or eclipsed conformation). Indeed, these differences in the torsion angle values are the ones which determine the formation of a linear polymer in complex **1** or the generation of helices in complex **6**.

Ligand **L1** is less dependent than **L2** of the torsion angle value for the generation of straight polymers in the crystalline state (using a metal cation like silver with a linear coordination geometry) (Figure 59).
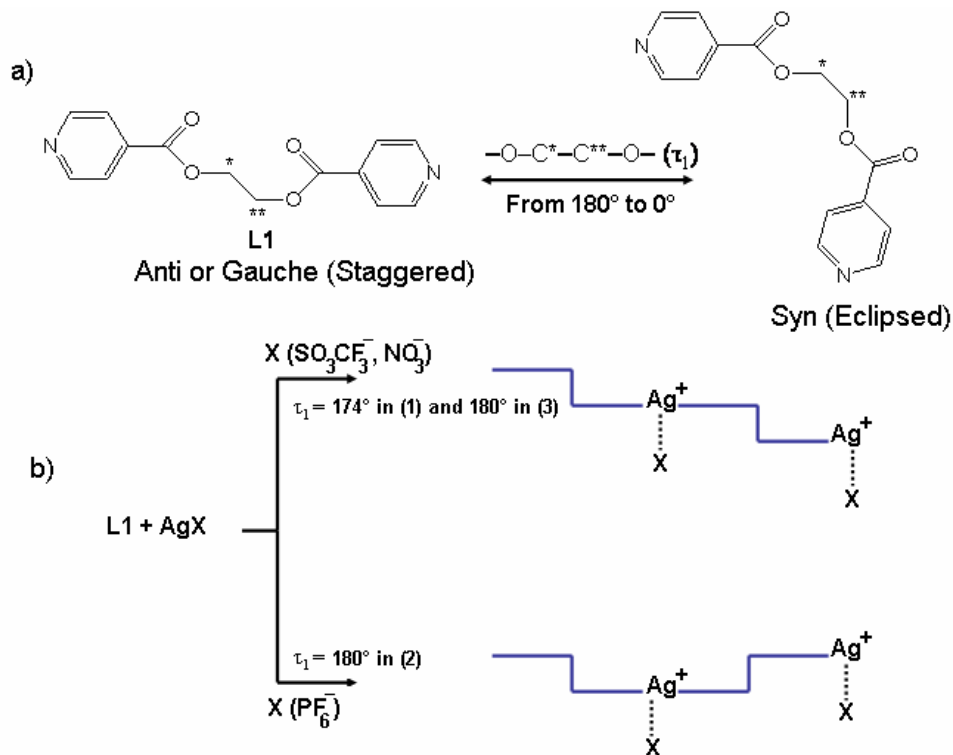
Figure 59. Metal-organic arrays found using ligand L1 and silver salts

The polymeric complexes can present the "up and down"- "up and down" motif (like in complex **1**) or "up and down"-"down and up" distribution (complexes **2** and **3**). In all complexes the ethylene glycol moiety is in the stable anti (staggered) conformation.

The ligand **L2** based on the nicotinic acid is more susceptible to the value of the torsion angle as **L1**. Here we found an ethylene glycol moiety in the less stable Syn (eclipse) conformation (compound **4**) (Figure 60).

Silver Coordination Compounds with a Family of Ditopic Ligands of Varying Flexibility:
About Chains, Rings, Helices and Polycatenanes

67
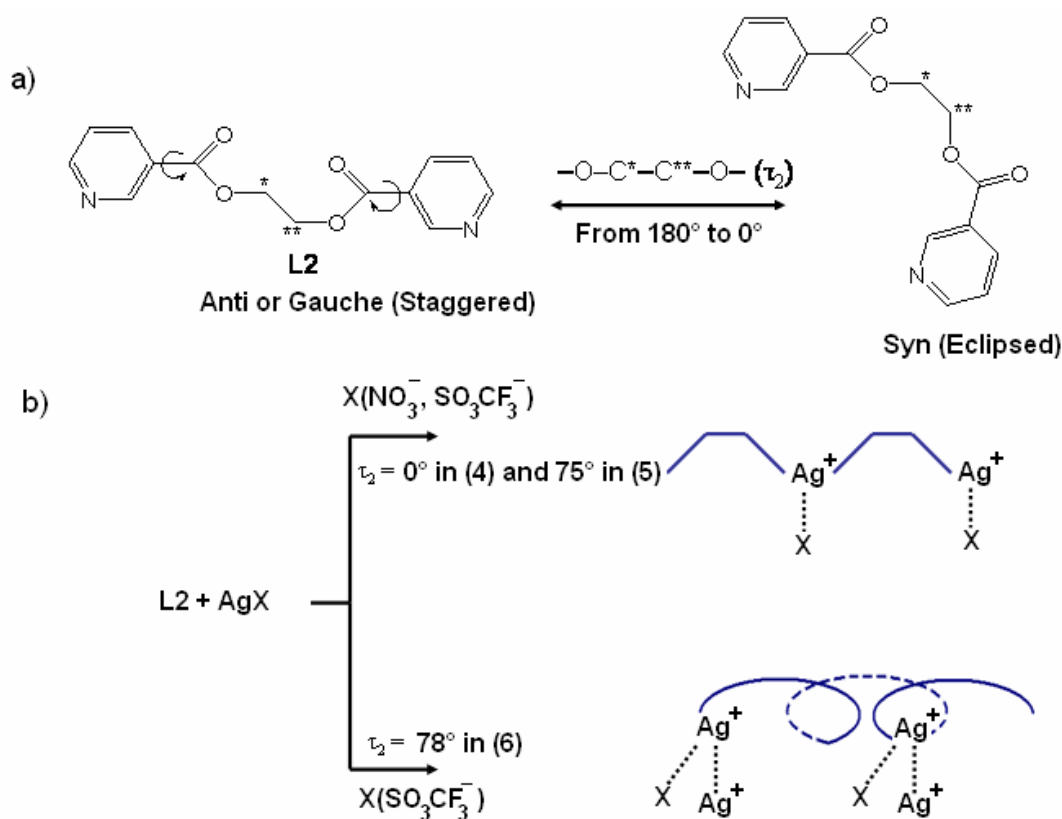
Figure 60. Metal-organic arrays found using ligand L2 and silver salts

In the other two complexes **5** and **6,** the spacer adopts a more favorable gauche (staggered) conformation. The almost 180° rotation around the bond Csp^2-COO- generates in the case of **6** a helical array.

B - II.9 - Counter ion effect on the crystalline structure of the complexes

The importance of the counter ion is not delimited to the coordination abilities over the cation [29, 30, 99, 133, 137, 258-264]. The potential formation of hydrogen bonds and the impact of these in the packing of the crystal structure [32, 265, 266] as well as the volume and shape of the anion acting as template [267-269] are important factors to take into account when a supramolecular design is planned.

Silver Coordination Compounds with a Family of Ditopic Ligands of Varying Flexibility: About Chains, Rings, Helices and Polycatenanes

68

Concerning the coordination abilities of molecules like NO_3^-, PF_6^-, $SO_3CF_3^-$ and ClO_4^- to the silver cation, they exhibit differences in the coordination mode (mono, bidentate or a combination of both using a second cation) and are also different concerning the strength of these interactions.

The stronger coordination of the silver cation by the counter ion is related to the distance Ag–N in the complexes. Complexes obtained using **L1** are consistent with the dependence between the coordination of the silver cation by the counter ion and the bending of the N–Ag–N angle (Figure 61).
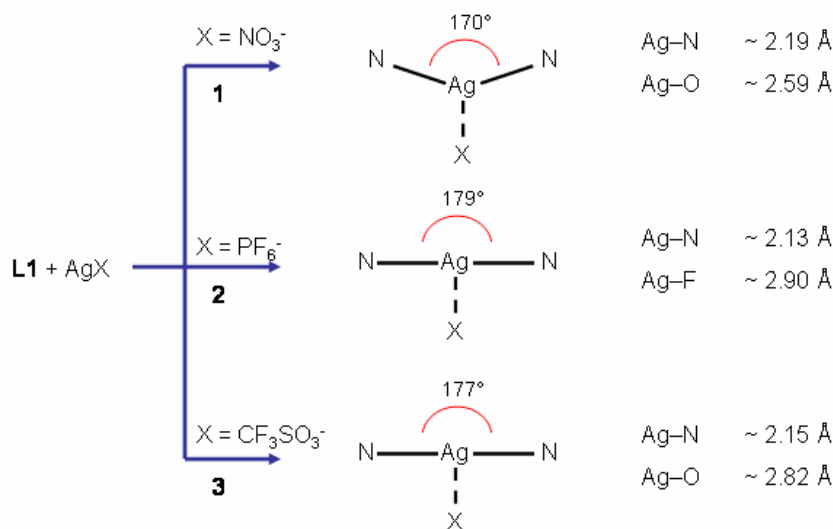
Figure 61. Relationship between the coordination of the counter ion and the bend found in the N–Ag–N angles for complexes using L1 as coordinating ligand

When the nitrate was used as counter ion, the ligand is not so strongly attached to the metal cation [31, 270-272] (Table B-II.33, see values for distances Ag–N for complexes **1** and **4**).

Silver Coordination Compounds with a Family of Ditopic Ligands of Varying Flexibility: About Chains, Rings, Helices and Polycatenanes

69

Table B-II.33 Resume of the interactions present in the compounds **1-6**

Complex	Ag–N distance (Å)	Ag–Ag (Å)	π–π (Å)	Number H-bonds in the structure
1	2.189(6)–2.191(6)	-	3.79	5 (2 *formed by the counter ion and 1 forming C–H⋯π*)
2	2.163(6)–2.132(6)	-	3.27 (Ag⋯π)	5 (3 *formed by the counter ion and 1 forming C–H⋯π*)
3	2.152(5)–2.153(5)	-	-	9 *(formed by the counter ion)*
4	2.190(4)	-	-	2 *(formed by the counter ion)*
5	2.197(4)–2.182(4)	-	-	6 *(3 formed by the counter ion)*
6	2.147(7)–2.147(1)	3.201(8)	3.81	6 *(3 formed by the counter ion)*

Compounds **4**, **5** and **6** as the previous examples, exhibit the same pattern (Figure 62). Even if the distances nitrate-silver in **1** and **4** are similar, the first compound presents a lower value of the N–Ag–N angle against the value found in **4**. The coordination of the counter ion should be responsible for this distortion (the counter ion coordinates one silver cation in **4** and two different silver cations in **1**).
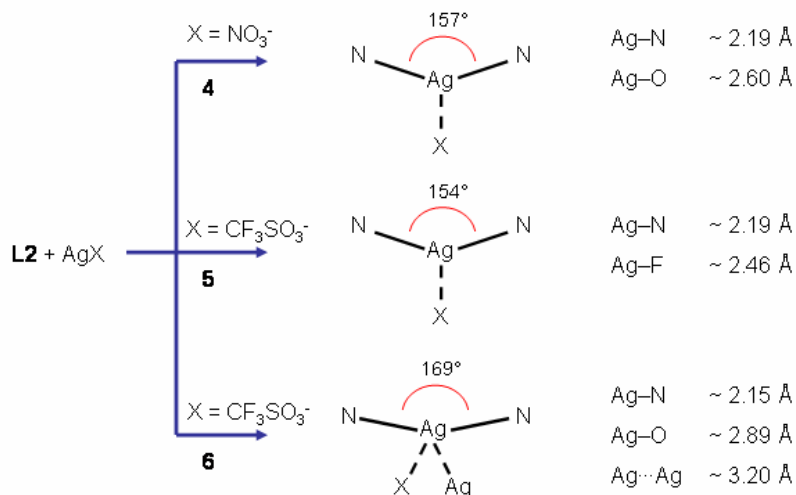
Figure 62. Relationship between the coordination of the counter ion and the bend found in the N–Ag–N angles for complexes using L2 as coordinating ligand

The coordinative weakness of the counter ion to the metal cation (NO_3^- vs. PF_6^-) can be used to generate tri- or tetra coordinated silver cations. Increasing the concentration can afford compounds were the number of ligands coordinating the silver cation is more than two.

The ability of the counter ion to generate hydrogen bonds in the crystalline motif is an important stabilizing factor that should be better studied and understood. Counter ions like hexafluorophosphate are less directional concerning the facility to form hydrogen bonds. Other anions like perchlorate and nitrate are more predictable, since they remain in most of the cases coordinating the metal cation and, consequently, they form hydrogen bonds with the closest hydrogen atoms of the ligand.

Different softwares focused in the prediction of crystalline structures have been implemented with more or less degree of success. These exploit most of these approaches concerning the counter ion ability to coordinate the metal cation and form potential hydrogen bonds with the chemical environment surrounding the cation [273-276].

B - II.10 - Crystallization techniques and solvent effect in compounds 1-6

Usually crystallization in a "H"-shaped tube was employed. When different crystals were obtained, samples of all batches were measured to detect the presence of isomerism or polymorphism. Table B-II.34 shows a resume of results and techniques used.

Table B-II.34 Solvents employed in the crystallization of crystal structures of compounds **1-6**

Complex	Solvent or combination of solvents used	Crystallization techniques
1	Acetonitrile, THF, THF/water, acetonitrile/DCM	Solvent diffusion, slow evaporation in THF, methanol or acetonitrile, solvent diffusion (acetonitrile/DCM).
2	THF/water, THF	Solvent diffusion, slow evaporation in THF.
3	THF/water	Solvent diffusion, slow evaporation, microwave.
4	THF/water, DMSO	Solvent diffusion, slow evaporation in DMSO.
5	THF/water	Solvent diffusion, slow evaporation in THF/water (THF side of the "H"-shaped tube).
6	THF/water	Solvent diffusion, slow evaporation in THF/water (water side of the "H"-shaped tube).

Silver Coordination Compounds with a Family of Ditopic Ligands of Varying Flexibility: About Chains, Rings, Helices and Polycatenanes

71

Some recent works relate the presence of a particular crystal structure with the solvent used in the crystallization process [132, 136, 143-145, 277-279]. In particular, the case of complex **1** was already discussed by Dr. Robin [161, 162]. In her PhD work, Dr. Robin proposed a direct relationship between the polarity of the solvent used and the weaker or stronger coordination of the silver cation by the ligand employed (based on Ag–N distances of several complexes of type $\{[Ag(\mathbf{L1})]NO_3*H_2O\}_n$, X= 0, 1 and 2). This suggests that the initial coordination of the silver salt *via* the solvent should be determining in the final supramolecular motif. Conductivity measurements will allow to bring more clarity in relation to this subject. The main problem is the extremely low concentration needed to avoid the precipitation of the silver polymer (usually $< 10^{-2}$ mmol). More detailed studies are required in order to get insights of this particular topic.

B - III - Ag(I) complexes with ligands L3 and L4. An overview on metallacycles and related network isomers.

While in the last chapter the metal cation dominated the arrangement when short and relatively rigid ligands were used, introducing more torsional freedom in the organic tecton should be relevant for the role played by the ligand in the final network array. However, this is not absolutely true since the different interactions present in the crystal structure are important from the enthalpy point of view as well as other parameters such as the concentration and the method used for the crystallization. In other words, entropy can be decisive to direct discrete or infinite structures. Competition between zero dimensional structures and polymers has been reported [143, 272, 280-286] and the results obtained have been so far reproducible for different silver salts.

Formation of metallacycles has been known for rigid or semi rigid ligands. The final motif depends on other supramolecular forces. Some recent examples are the silver complexes synthesized using 1*H*-[1,10]phenanthrolin-2-one [287], where the crystal structures obtained using metal:ligand 2:2 ratio, show the aromatic tecton stacked through π–π interactions and Ag^+–π interaction. A two dimensional structure is generated with remarkably high electrical conducting properties which do not exhibit photodegradation (Figure 63).
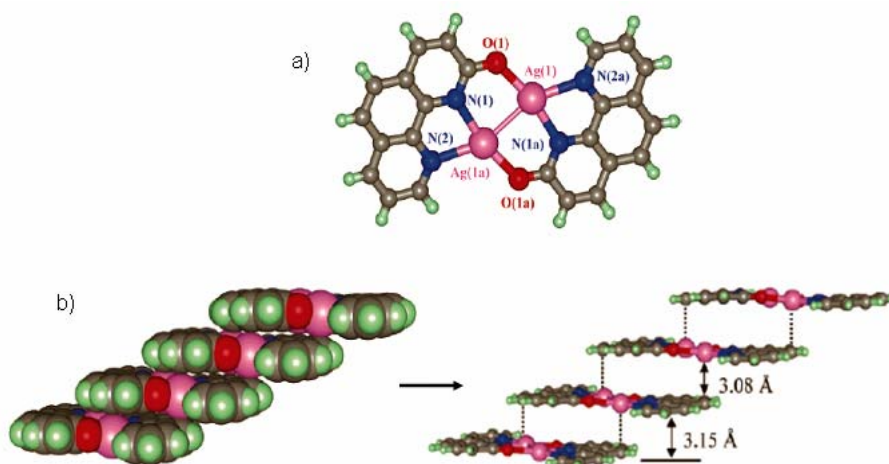
Figure 63. Aromatic-aromatic stacking of zero-dimensional structures of a phenanthrolin-2-one silver complex

Silver Coordination Compounds with a Family of Ditopic Ligands of Varying Flexibility: About Chains, Rings, Helices and Polycatenanes

73

Other ligands incorporate multiple coordinating atoms in the closest possible position in order to increase the variety of coordination types. Oxadiazole-containing ligands have been explored when looking for the role of the counter ion on dimensionality [288, 289]. In all cases the product is independent from the ratio of metal:ligand. Interestingly, the increase of this ratio is associated to an increase of the yield of the products.

The influence of the counter ion in the formation of metallacycle has been induced through the appropriate choice of the counter ion [290]. Subtle anion effects are decisive for the cyclization of silver salts with bis(3-pyridyl)-dimethylsilane [291]. In other cases, the introduction of another metallic cation generates and controlles these kind of arrays [292]. In this sense, the use of ferrocene based ligands is a typical example of rigid metallorganic ligands which generate a broad spectrum of metallacycles with interesting physical and chemical properties [293] (Figure 64).
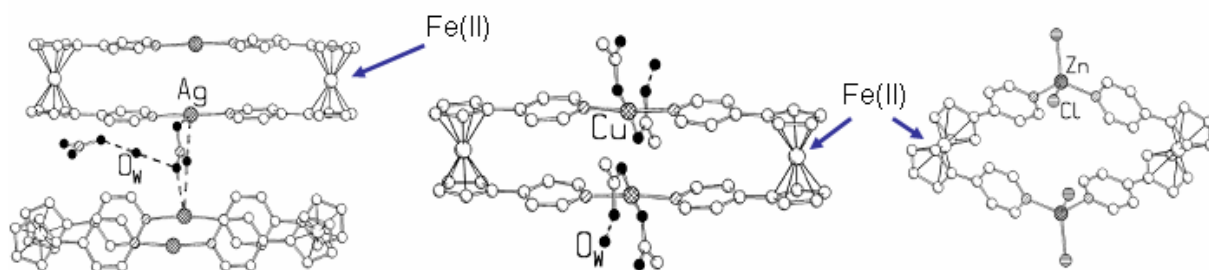
Figure 64. Some ferrocene based-ligands which generate zero-dimensional structures with different metal cations

Sommerer et al. [294] reported in 1995 the synthesis and crystal structure of two novel metal dimmers (using di-2-pyridyl ketone oxime as molecular tecton) within the complex formed with the silver salts. They found the presence of an unidentate nitrate ligand, which was quite remarkable at this time.

More flexible siloxane-based ligands react readily with silver salts to form crystalline complexes, which revealed to be dimers after X-ray single crystal characterization [295].

Interestingly, complexes obtained with this cyclophane based ligand generate zero-dimensional structures, in which two Ag(I) cations are coordinated by two ligand units and a nitrate counter ion. This motif incorporates π–π stacked interactions as well as weak Ag–O (ether oxygen from the lateral chain) [296].

A curious example was reported by *Suzuki et al.* [297], who worked with a pyridine derived ligand (*(4R,5R)*- and (4S,SS)-4,5bis(2-(2-pyridy1)ethyl)- 1,3-dioxolane (R,R-L and S,S-L)) and silver

Silver Coordination Compounds with a Family of Ditopic Ligands of Varying Flexibility: About Chains, Rings, Helices and Polycatenanes

74

trifluoromethanesulfonate (AgSO$_3$CF$_3$). Treatment of the optically pure ligand (R,R-L or S,S-L) with silver(I) salt in methanol gave the R,R-L ligand with a right-handed helicity, while the S,S-L presented a left-handed helicity.

In contrast, a similar reaction with a racemic mixture of the ligands (rac-L), a 1:1 mixture of R,R-L and S,S-L, they obtained a di-silver metallacycle formed via one R,R-L and one SS-L ligand. The same pattern was observed after mixing methanolic solutions of [Ag(R,R-L)](SO$_3$CF$_3$), and [Ag(S,S-L)](SO$_3$CF$_3$) (1: 1), which also provided the same mesoformed dinuclear complex.

Competition between formation of rings and helices was found when two different ligands, a diphosphine based ligand [Ph$_2$P(CH$_2$)nPPh$_2$, n = 1–6] and *trans*-1,2-bis(4-pyridyl)ethylene (bipyen) were reacted with silver salts. Even when a mixture of all components was present in solution, after crystallization just one structure was found. This is formed of macrocyclic rings of type [Ag$_4$(O$_2$CCF$_3$)$_4$\{m-Ph$_2$P(CH$_2$)nPPh$_2$\}$_2$(m-bipyen)$_2$] when n = 1 or 5, but it is a one-dimensional polymer [\{Ag$_2$(O$_2$CCF$_3$)$_2$\{m- Ph$_2$P(CH$_2$)nPPh$_2$\}(m-bipyen)\}x] when n = 6 [140].

The preference of the silver cation to form metallacycles in comparison to other metals was remarked by *He et al.* [298] when they studied the complexation ability of a new bis-bidentate Schiff base ligand, bis[4-(2-pyridylmethyleneamino)phenyl] ether (**L**). The crystal structure shows the formation of silver (I) molecular boxes [Ag$_2$**L**$_2$]$_2$, and molecular helices [Co$_2$**L**$_3$]$_4$ or [Ni$_2$**L**$_3$]$_4$ when cobalt (II) or nickel (II) were used. Mass spectra results obtained from solution seem to corroborate the presence of rings in the solution, despite of the helices found for nickel or cobalt salts.

The linear and multidentate ligands 1,5-bis(8-quinolylsulfanyl)-3-oxapentane (**L$_{q1}$**) and 1,8-bis(8-quinolylsulfanyl)-3,6-dioxaoctane (**L$_{q2}$**) are both excellent examples of the contradiction between flexibility and complexity. A more flexible ligand does not mean an increase in the dimensionality in the final supramolecular array: when the two ligands were reacted with silver(I) perchlorate, both of them afforded the simple mononuclear complexes [Ag(**L$_{q1}$**)]ClO$_4$ and [Ag(**L$_{q2}$**)]ClO$_4$, respectively. With silver(I) nitrate, novel metallosupramolecular complexes [Ag$_4$(**L$_{q2}$**)$_2$(η^1-NO$_3$)$_2$(η^2-NO$_3$)$_2$] and [Ag$_4$(**L$_{q1}$**)(**L$_{q2}$**)(η^1-NO$_3$)$_2$(η^2-NO$_3$)$_2$]H$_2$O were obtained. In these, the coordination motifs [Ag(**L$_{q1}$**)] and [Ag(**L$_{q2}$**)] are spontaneously self-assembled by sulfur bridged silver(I) ions to form tetrametallotricyclic molecules, which contain the same or mixed building blocks [299] (Figure 65).
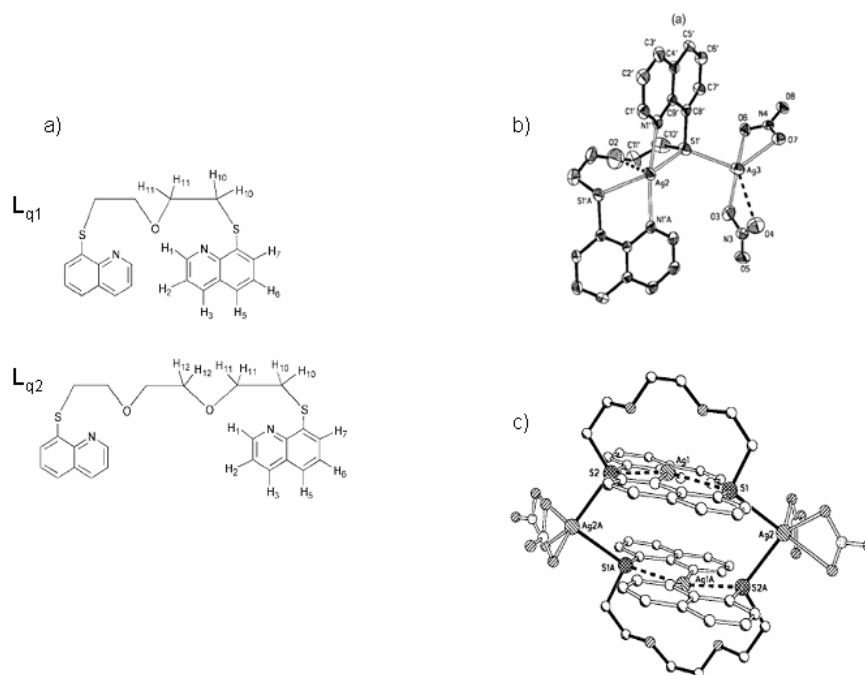
Figure 65. Some flexible ligands which generate zero-dimensional structures after coordination with silver salts

The interest on silver metallacycles has increased in the same proportion as some of their applications, as for example in the catalysis field. Silver metallacycles have been used not just in the epoxidation of unsaturated bonds, but also in other less typical procedures as the efficient catalysis on the aziridination reaction of unsaturated hydrocarbons developed by *Cui et al.* [300].

The presence of zero dimensional structures directed by different metal cations has been very commonly found by Hosseini's group in Strasbourg when semi rigid ligands have been used [146]. However, it is difficult to find discrete structures where flexible tectons are present, and the metal atom does not direct essentially this kind of arrangement.

We were surprised by the fact that when using diethylene glycol as spacer, almost only the formation of discrete structures was achieved, even when different solvents were used and the crystallization methods were varied in a large range. Just in one case infinite helical chains were formed and in the other an polycatenated network. However, both seem to be an exception and not the rule.

The general motif, when talking about "rings" in this chapter, is shown in Figure 66. Usually the ligand presents a "U"-shape conformation which allows it to coordinate two silver cations. A second ligand closes the loop to generate in principle a zero dimensional structure.

Silver Coordination Compounds with a Family of Ditopic Ligands of Varying Flexibility:
About Chains, Rings, Helices and Polycatenanes

76
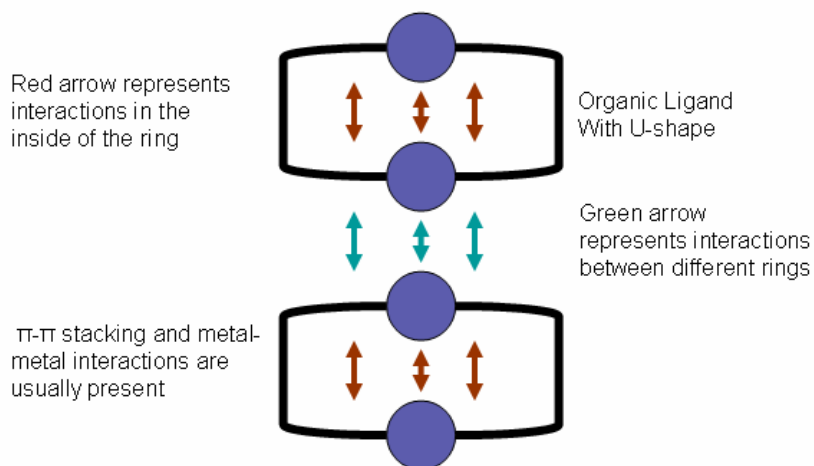
Figure 66. Schematic representation of ring like structures. The dimensionality is increased due to π-π stacking interactions, metal-metal contact and hydrogen bonds when present

The anion is linked generally directly to the metal atom perpendicular to the ring plane, and the coordination mode towards the metal ion can be mono or bidentate, depending on the counter ion used and the experimental conditions. "Intra" Ag–Ag or π–π contact refer exclusively to contacts in the ring. Whereas "inter"-ring contacts refers to distances and angles measured between different rings.

B - III.1 - {[Ag(L3)](ClO$_4$)}$_2$ (7) and network isomer (8).

In an "H"-shaped tube one solution of silver perchlorate in water and one solution of the ligand **L3** in THF were put in contact *via* THF as bridging solvent.

The complex {[Ag(**L3**)](ClO$_4$)}$_2$ (**7**) crystallizes in the triclinic space group P-1 (No. 2), with one ligand, one silver cation and one perchlorate counter ion contained in the asymmetric unit cell [164]. Every single silver cation presents a distorted T-like shape (Figure 67 a). The coordination sphere around the metal presents two nitrogen atoms belonging to the pyridine rings coordinating the silver cation (Ag(1)–N(1), 2.147(1) and Ag(1)–N(2)[#1], 2.152(9) Å) and one oxygen atom (Ag(1)–O(9), 2.935(8) Å) provided by the perchlorate counter ion. The second oxygen atom is too far apart to be coordinating the cation (Ag(1)–O(7)[#1], 3.907(9) Å) (Table B-III.36).

Silver Coordination Compounds with a Family of Ditopic Ligands of Varying Flexibility: About Chains, Rings, Helices and Polycatenanes

77
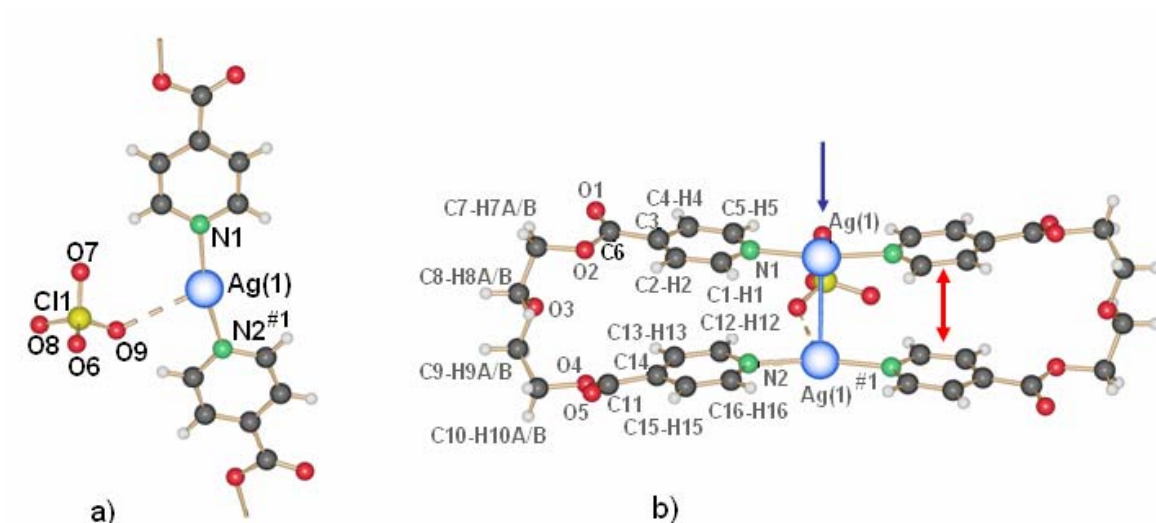
Figure 67. a) T-like coordination type. b) zero-dimensional structure formed due to the coordination between two ligands L3 and two cations (Note the "U"-shape of the ligand); the blue arrow signalizes the Ag(I)–Ag(I) contact, and the red π-π stacking interactions

A second counter ion has one oxygen atom pointing to the Ag^+, but it is less strongly bonded (Ag(1)–O(6), 3.448(7) Å).

The angle N(1)–Ag(1)–N(2)[#1] is bent from the ideal 180° to 167.8(1)°, which suggests a strong interaction between the cation and the counter ion.

In the pyridine ring, the carbonyl group attached in the para- position to the nitrogen atom remains almost in the same plane (torsion angle C2–C3–C6–O2, -9.1(4)°). The diethylene glycol used as spacer presents all its ethyl groups in a "gauche" (staggered) conformation.

Ag–Ag[#1] interactions are present in the motif, with distances of 3.146(8) Å between silver atoms in the same metallacycle, whereas between silver atoms of different metallacycles (5.095(1) Å), there is no metal-metal bond.

The metal-metal interaction act synergistically with the presence of π–π stacking, with centroids distances about 3.70 Å (Table B-III.35).

Exo π–π interactions are discarded due to the distances ring-centroid to ring-centroid (approximately 5.46 Å for the closest ring). Therefore, how could the way in which rings are stacked together parallel to each other in order to generate the final supramolecular array be explained?

Table B-III.35 π–π stacking present in complex **7**

π-π interaction	d_{R-R} (Å)	ρd_{R-R} (Å)	α	β
Intra π–π stacking interaction between aromatic rings of the same ligand.				
Ring (N1,C1,C2,C3,C4,C5)···Ring (N2,C12,C13,C14,C15,C16)[#2]	3.70	3.42	8.1	22.4
Inter π–π stacking interaction between aromatic rings of different ligands.				
Ring (N1,C1,C2,C3,C4,C5)···Ring (N2,C12,C13,C14,C15,C16)[#3]	5.45	2.64	57.1	61.0
Symmetry transformation used to generate equivalent atoms: #2 x, y, z #3 1+x, y, z				

The answer could be related to the formation of hydrogen bonds in the crystalline state [43, 45, 47, 48, 301, 302] (Table B-III.37). The ability of the perchlorate anion to generate hydrogen bonds when appropriate hydrogen atoms are present is remarkable [43, 45, 47, 48, 301-310]. Pyridine rings offer four potential hydrogen atoms that can be coordinated. These facts are reflected in the present motif, where seven potential hydrogen bonds are present. Almost all hydrogen bonds exist between the perchlorate anion and the hydrogen atoms attached to the pyridine ring.

Table B-III.36 Most important bond lengths [Å] and angles [°] present in complex **7**

Ag(1)–N(1)	2.148(4)	N(1)–Ag(1)–N(2)[#1]	167.9(1)
Ag(1)–N(2)[#1]	2.153(4)	N(1)–Ag(1)–Ag(1)[#1]	93.9(1)
Ag(1)–Ag(1)[#1]	3.147(1)	N(2)[#1]–Ag(1)–Ag(1)[#1]	92.4(1)
Ag(1)–O(ClO$_3$)	2.931(1), 3.445(4)	C–N–C	118.4(4), 118.1(4)
N–C	1.346(6), 1.341(7)		
Symmetry transformations used to generate equivalent atoms: #1 -x+2, -y+1, -z+2			

Table B-III.37 Hydrogen bond data [length (Å) and angle (°)] present in complex **7**

D-H···Acceptor	d (D–H)	d (H···A)	d (D···A)	Angle D-H···A
Intra ring hydrogen bonds between the anion and the hydrogen atoms of the pyridine ring.				
C1–H1···O7[#4]	0.94	2.28(9)	3.19(6)	160.2(8)
C5–H5···O6[#1]	0.94	2.53(0)	3.40(7)	154.4(2)
C12–H12···O9[#1]	0.94	2.31(7)	3.09(1)	140.4(9)
C16–H16···O6[#4]	0.94	2.46(6)	3.34(7)	155.3(9)
Exo hydrogen bond formed between the oxygen on the lateral chain and hydrogen from the pyridine ring.				
C4–H4···O3[#5]	0.94	2.45(6)	3.15(7)	131.3(0)
Exo hydrogen bonds formed between the anion and hydrogen atoms of the pyridine ring.				
C9–H9A···O8[#6]	0.98	2.57(6)	3.52(6)	164.1(1)
C10–H10A···O7[#5]	0.98	2.33(4)	3.22(7)	152.3(5)
Symmetry transformation used to generate equivalent atoms: #1 2-x,1-y,1-z, #4 x,y,1+z, #5 1-x,-y,1-z, #6 x,-1+y,z.				

Silver Coordination Compounds with a Family of Ditopic Ligands of Varying Flexibility: About Chains, Rings, Helices and Polycatenanes

79

After the generation of four hydrogen bonds by the perchlorate anion and hydrogen atoms of the pyridine ring, the resulting structure remains zero-dimensional. To increase the dimensionality the presence of three more hydrogen bonds is determining: two hydrogen bonds are formed between the counter ion and hydrogen atoms present in the diethylene glycol spacer (C9-H9A···O8[#6] and C10-H10A···O7[#5]), and another one between one oxygen atom of the lateral chain and one hydrogen atom localized in the pyridine ring of the next metallacycle close by (C4-H4···O3[#5]). These bonds bring the structure into a higher level of complexity, in this case into a 2-D more stabilized network system (Figure 68).
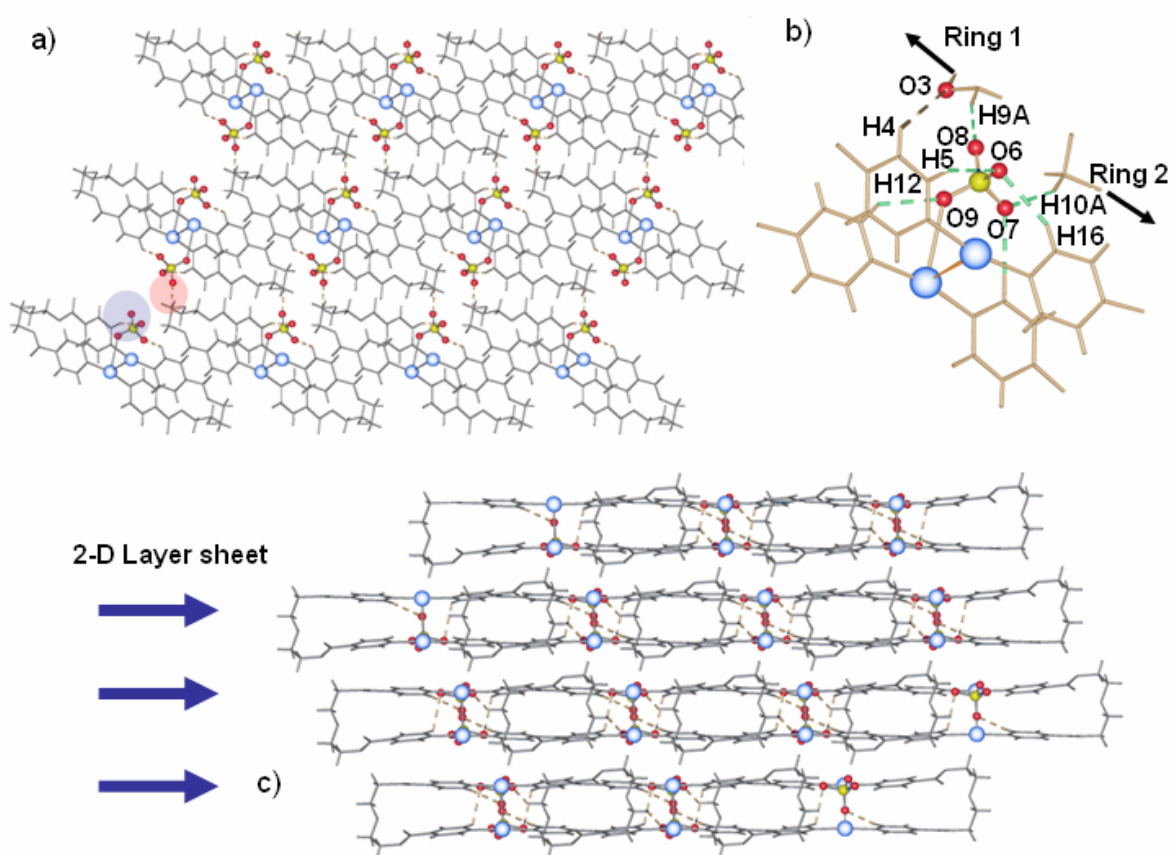
Figure 68. 2-D network generation through hydrogen bonds a) perchlorate anion as supramolecular linker; in blue intra hydrogen bonds, and the red zone corresponds to inter hydrogen bonds b) a zoom into the structure highlights how the counter ion links two different rings and an hydrogen bond between two ligands L3 belonging to two different metallacycles (O3···H4) c) sheet disposition in the supramolecular motif

TG measures show a melting point value at about 166 °C, followed by decomposition.

In the right hand side of the same "H"-shaped tube (ligand side) single crystals were collected and

measured. The new complex $\{[Ag(\mathbf{L3})_2](ClO_4)\}_n$ **(8)** crystallizes in the monoclinic group C2/c (No. 15), with one ligand, one cation and one counter ion in the asymmetric unit.

As with the case of the metallacycle **7**, in this complex the ligand possesses a "U"-shape and coordinates two silver cations. The cycle in **8** however is not closed, a second ligand coordinates one of the Ag^+ ions and a third cation to generate the starting point of a helical structure (Figure 69).
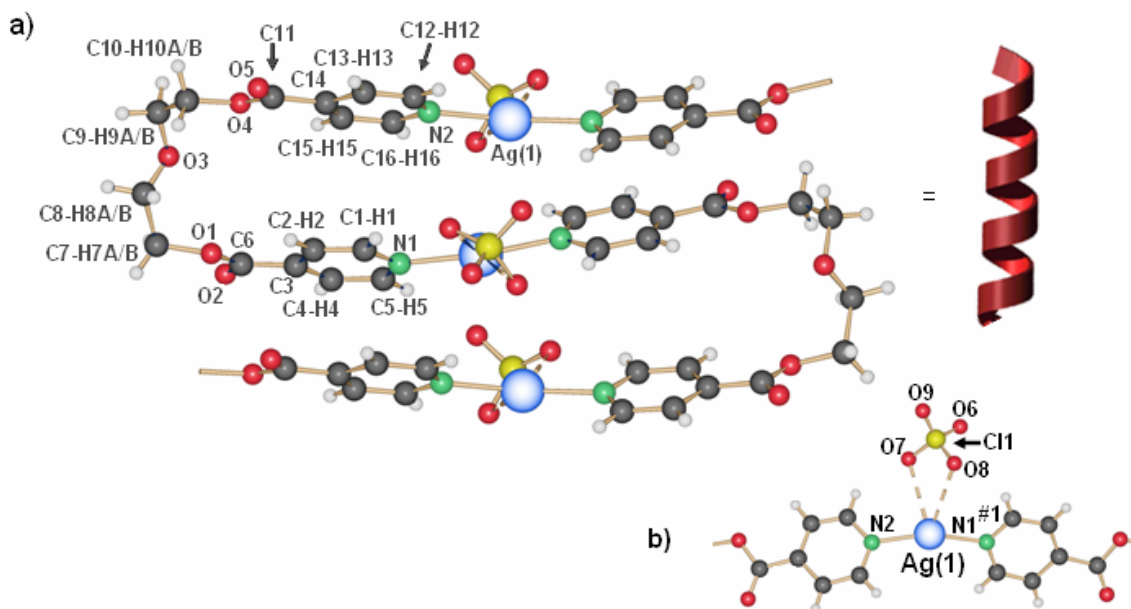
Figure 69. $\{[Ag(\mathbf{L3})_2](ClO_4)\}_n$ **(8) supramolecular motif a) Helices formation due to the coordination of one ligand to two Ag^+ metal atoms b) T-like shape coordination motif of the metal atom generated by two oxygen atoms of the counter ion and two nitrogen atoms from the pyridine ring**

The Ag(I) cation is coordinated by two nitrogen atoms of the pyridine ring (Ag(1)-N(1), 2.158(7) and Ag(1)-N(2)$^{\#1}$, 2.161(6) Å) and the counter ion in a bidentate fashion (distances Ag(1)–O(7), 2.942(8) and Ag(1)–O(8), 2.907(5) Å). The metal cation posseses a distorted tetrahedral geometry (Figure 69 b).

No metal-metal contacts are present between silver atoms (Ag–Ag$^{\#1}$, 3.7812(7) Å). The lateral diethylene glycol chain of each ligand shows torsion angles of 51.7(3) (O4–C10–C9–O3) and 64.9(2)° (O1–C7–C8–O3) in a gauche (staggered) conformation for both ethylene moieties.

Pyridine rings coordinating the same silver cation are twisted to an angle of 43.11°, which is quite distorted from the usual planar motif. Due to the geometry of the complex, we should expect the

Silver Coordination Compounds with a Family of Ditopic Ligands of Varying Flexibility: About Chains, Rings, Helices and Polycatenanes

81

presence of π–π stacking interactions between aromatic rings of different ligands. Distances between rings centroids, in contrast, are larger as those usually reported [56], see table B-III.38 for the values obtained.

Table B-III.38 π–π stacking present in complex **8**

π-π interaction	d_{R-R} (Å)	ρd_{R-R} (Å)	α	B
Intra π–π stacking interaction between aromatic rings of the same ligand.				
Ring (N1,C1,C2,C3,C4,C5)···Ring (N1,C1,C2,C3,C4,C5)[#2]	5.94	3.73	51.1	51.1
Inter π–π stacking interaction between aromatic rings of different ligands.				
(N1,C1,C2,C3,C4,C5)···Ring (N2,C12,C13,C14,C15,C16)[#3]	3.74	3.40	25.0	24.4
(N1,C1,C2,C3,C4,C5)···Ring (N2,C12,C13,C14,C15,C16)[#4]	4.78	3.25	48.7	47.2
Symmetry transformation used to generate equivalent atoms: #2 -x, 1-y, -z #3 x,-1+y,z #4 x,y,z				

From the supramolecular point of view, the helical motifs are stacked parallel to each other sustained by hydrogen bonds (Figure 70), The perchlorate counter ion forms three hydrogen bonds. However, these are in the helical array.
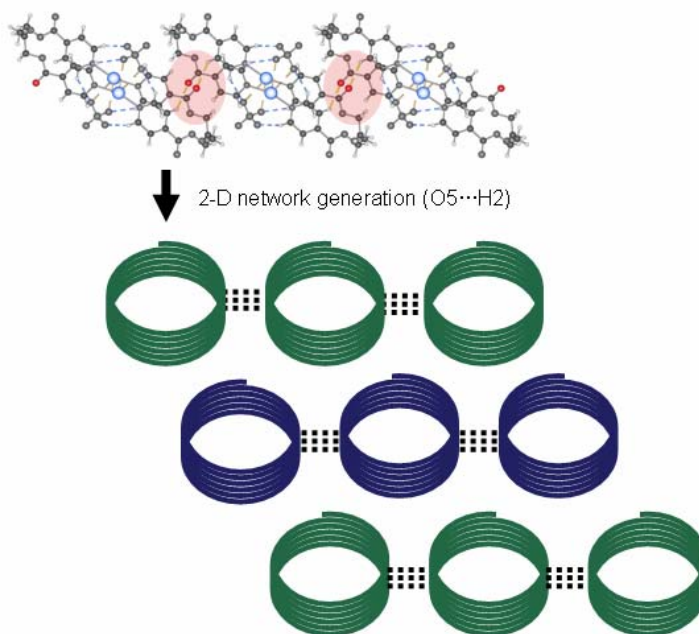
Figure 70. 2-D network generation through hydrogen bonds between the carbonyl group and hydrogen from the pyridine ring

Silver Coordination Compounds with a Family of Ditopic Ligands of Varying Flexibility: About Chains, Rings, Helices and Polycatenanes

82

The increase of dimensionality in the network occurs when one oxygen atom located at the carbonyl group of the isonicotinic groups coordinates one hydrogen atom from a pyridine ring located in the closest helical motif nearby.

Taking into account these hydrogen bonds, the overall motif changes from 1-D to 2-D. Here individual helices are attached together to generate alternating tubular surfaces, even when the empty space inside the helix is too small to embed a guest molecule.

Distance and angles are shown in Table B-III.39.

Table B-III.39 Most important bond lengths [Å] and angles [°]present in complex **8**

Ag(1)–N(1)	2.161(6)	N(1)–Ag(1)–N(2)[#1]	162.5(3)
Ag(1)–N(2)[#1]	2.158(7)		
Ag(1)–O(ClO3)	2.907(5), 2.942(8)	C–N–C	117.2(7)
N–C	1.320(1), 1.334(1)		
Symmetry transformations used to generate equivalent atoms: #1 1.5-x, 0.5+y, 1.5-z			

Table B-III.40 Hydrogen bond data [length (Å) and angle (°)] present in complex **8**

D-H···Acceptor	d (D–H)	d (H···A)	d (D···A)	Angle D-H···A
Intra ring hydrogen bonds between the anion and the pyridine hydrogen.				
C1–H1···O8[#5]	0.93	2.34(5)	3.13(1)	141.7(6)
C5–H5···O9[#3]	0.93	2.36(9)	3.25(2)	159.2(9)
C16–H16···O7	0.93	2.34(3)	3.13(1)	141.3(8)
Inter hydrogen bond formed between the oxygen on the lateral chain and the hydrogen from the pyridine ring.				
C2–H2···O5[#6]	0.93	2.52(8)	3.27(1)	136.7(9)
Symmetry transformation used to generate equivalent atoms: #5 1/2-x,-1/2+y,1/2-z, #6 1/2-x,3/2-y,-z, #3 x,-1+y,z.				

B - III.2 - Some comparison and difference between structures 7 and 8

Both structures crystallize in the same "H"-shaped tube where an aqueous solution of silver salt is put on one side, a THF solution of the ligand on the other, and both sides are connected via a mixture of both solvents or a new solvent.

We are in the presence of a dynamic system. This system is controlled by a concentration gradient in relation to the ligand and the silver salts, and a polarity gradient concerning the solvent mixture.

The slow diffusion of the ligand into the metal salt solution and vice versa yields the ring-forming compound **7** on the side of the silver salt, and the polymeric compound **8** in the ligand side, and the later is the major product obtained in this part of the "H"-shaped tube.

The concentration of the silver(I) salt drop from one side of the "H"-shaped tube to the side were the organic ligand was dissolved, the inverse phenomenon occurs concerning the concentration of the ligand **L3.** This concentration gradient may generated several species possesing different ratio **L3**:Ag(I). The formation of at least two of these species will be energetic favoured, and they may grow faster enough compare to the others. This could be claimed as an argument to explain the formation of the helix **8** and the metallacycle **7**.

The two structures share the same motif around the metal atom concerning the coordination motif: two nitrogen atoms belonging to the pyridine rings coordinate the cation almost in a linear fashion. The different coordination modes of the counter ion determines the angle formed by the pyridine rings in each case (N(1)-Ag(1)-N(2)$^{#1}$, 168.0(1)° for **7** and N(1)-Ag(1)-N(2)$^{#1}$, 162.5(1)° for **8**).

Concerning the polymeric structure, the perchlorate molecule coordinates in a strongly μ^2-pincer mode (Ag(1)–O(7), 2.942(8) and Ag(1)–O(8), 2.907(5) Å), whereas in the ring structure a monodentate perchlorate (Ag(1)–O(9), 2.935(8) Å) is present.

Regarding the counter ion position, it is noteworthy the enormous difference between the two structures. In **7,** the upper oxygen atoms of the counter ion form a plane parallel to the plane formed by the pyridine rings. At the same time, the oxygen atoms O(6), O(7) and O(9) are forming hydrogen bonds with the hydrogen atoms of those rings (O(9)–H(12), 2.308(6); O(7)–H(1), 2.294(1); O(6)–H(5), 2.53(8) and O(6)–H(16), 2.467(1) Å) (Figure 71).
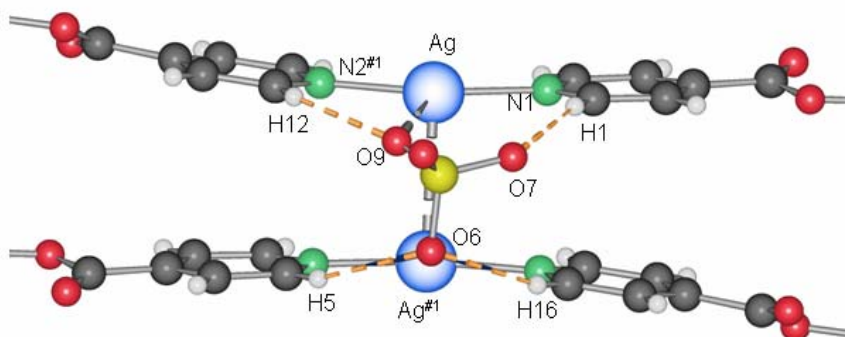
Figure 71. Schematic representation of the counter ion position within the metallacycle 7. H-bonds represented in oranger, bonds between metal atoms are three times fragmented; bond Ag$^+$–OClO$_3^-$ two times fragmented

Silver Coordination Compounds with a Family of Ditopic Ligands of Varying Flexibility:
About Chains, Rings, Helices and Polycatenanes

84

The counter ion fulfills almost all possibilities to form hydrogen bonds. Metal-metal and π–π contacts stabilize the overall array. The Ag–Ag[#1] contact (3.146(1) Å) influences the approach of aromatic rings. No other reason from solid state packing could explain why the silver atoms should come that close to each other.

In the case of complex **8,** the two pyridine rings are not parallel any more since they are twisted by about 43°. In this case, the counter ion is positioned in such a way that the number of hydrogen bonds is maximized (O(8)–H(1), 2.345(1); O(7)–H(16), 2.343(4) and O(9)–H(5), 2.369(4) Å), so the counter ion is twisted in contrast to the counter ion in **7** (Figure 72).
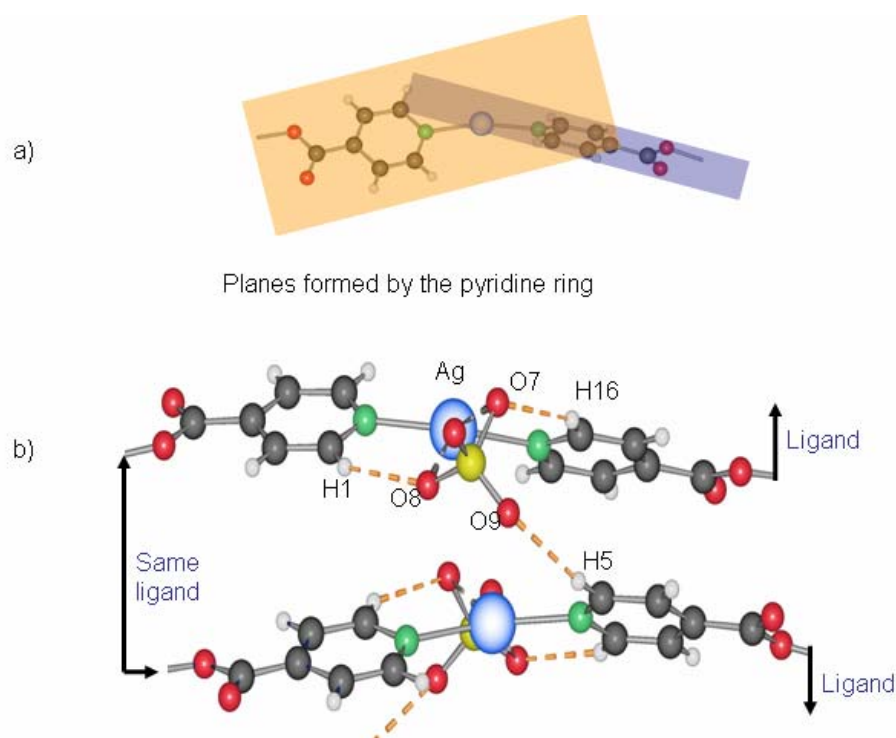
Figure 72. Positioning of perchlorate counter ion within the polymeric structure 8. Hydrogen bonds represented in orange color, oxygen O7 and O8 are coordinating the metal cation.

Shorter Ag–Ag contacts are present where the silver cation is bridged by anions in a monodentate rather than a bidentate fashion. This phenomenon was already observed in coordination polymers formed by pairs of one-dimensional chains, where silver is bridged by other anions such as NO_3^- [161, 162]. The presence of silver–silver contacts is often linked to interesting chemical-physical

properties [281, 311]. However, fluorescence measurements in **7** or **8** do not show remarkable differences in intensity shifts when compared to the ligand alone.

The perchlorate counter ion is non-coordinating in some crystalline motifs [312-314], but can exhibit as well several coordination modes: monodentate [271, 315], bidentate [271, 315], [316], linking different silver cations as monodentate [53] or combining at the same time both monodentate and bidentate coordination fashions over different metal cations [317-319].

The flexibility provided by the lateral chain is crucial for the existence of network isomers **7** and **8**. Torsion angle $CH_2–CH_2–O–CH_2$ values differ from **7** to **8**. For the metallacycle **7**, it is symmetrical in both sides of the ring (72.925(3)° and 175.33(2)°). In contrast, for the helical compound **8**, the torsion angle values are quite different for the ligands contained in the asymmetric unit (51.7(2)°, 177.8(9)° and 83.8(0)°). For this reason the cycle is never closed in complex **8**.

However, based on this difference in the torsion angle values it is difficult to asses if this is the cause or the consequence of the final supramolecular array.

Thermogravimetric curves of the two isomers are different. While **7** melts at 166° C, **8** does so at 152° C. In both cases the melting is followed by decomposition of the sample.

Establishing a direct relationship between crystal structure and melting point from TG/SDTA measurements is not a minor task, mostly due to the problems in reproducibility associated with this technique (grain size for example) [320-329]. Nevertheless, melting points found using TG/SDTA are useful to determine the presence of a specific complex between many others [326-329].

The syntheses of **7** and **8** could be achieved by the judicious choice of the solvent. Mass spectra show the presence of both isomers in solution at low concentration, but varying the solvent polarity and the equivalent proportion between the ligand and the silver salt, the equilibrium can be directed to the formation of the ring or the polymeric complex (Figure 73).
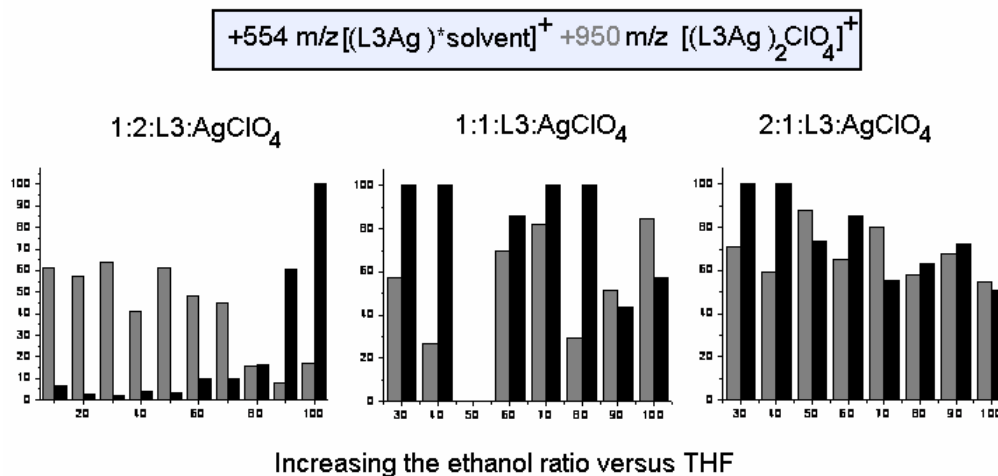
Figure 73. Mass spectra values with peaks at +554 (polymer) and +950 m/z (ring)

In order to verify the relation between concentration/solvent polarity and the formation of discrete or polymeric structures, the precipitation was tested under extreme conditions (only THF or EtOH and different proportion of silver/ligand). The results found tend to support this idea (Figure 74).
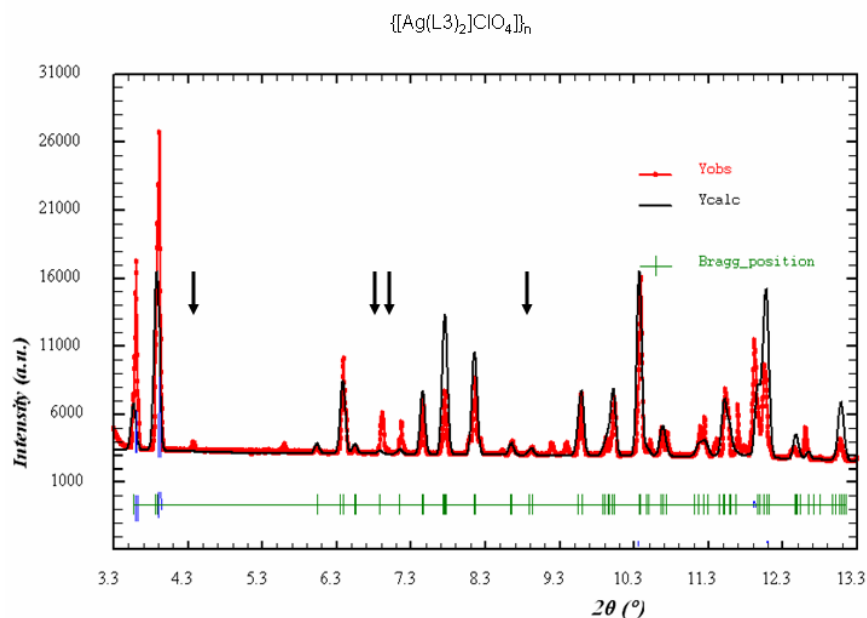
Figure 74. Powder x-ray spectra of complex 8. Observed (red crosses) and calculated (black lines) XRPD profiles of complex 8

The same results were obtained after analyzing the X-ray powder pattern of the precipitate formed after mixing two solutions containing the organic ligand and the silver perchlorate (1:2 equivalents)

in THF. Indexation of peaks with *Fullprof Suite* software followed by unit cell calculation with *McMaille* affords unit cell values close to the unit cell parameters of **7** (Table B-III.41).

Table B-III.41 Crystalline unit cell and unit cell indexed from powder spectra

Complexes		a (Å)	b (Å)	c (Å)	α (°)	β (°)	γ (°)
Crystal structure (1)	Triclinic	7.182(1)	12.076(2)	12.095(2)	112.58(3)	102.32(3)	96.64(3)
Powder-L1:AgClO$_4$:1:1 EtOH	Triclinic	13.0	12.2	7.2	80.3	92.9	120.4
Powder-L1:AgClO$_4$:1:2 THF	Triclinic	12.9	13.3	7.5	96.6	102.3	112.6

* X-ray powder measurements were performed at the synchrotron facilities in the "Paul Scherer" institute (Villigen PSI).

Interestingly, even when mass spectra results show the concomitant existence of both species in ethanol using a 1:1 ligand:silver salt equivalence, the main product obtained after precipitation is the metallacycle **7**.

Molecular boxes or rings with silver, as observed in **7,** are well described in the literature [115, 280, 285, 299, 312, 330, 331]. Single helical arrangements are highly interesting due to their inherent chirality [25, 132, 159, 221, 290, 297, 314, 318, 332-335], but it is rare to find examples where both isomers crystallize in a concomitant manner, one of them having an helical structure.

Reger et al. from the University of South Carolina (Columbia) reported the syntheses of two polymeric polymorphs from the same solvent combination using [(HC(3-Phpz)$_3$)Ag](BF$_4$) (pz = pyrazolyl). However, it is not clear from the description whether they crystallize simultaneously or in parallel assays [144]. Two polymeric network isomers out of the same solution at room temperature are described for a Cu(I) compound [336]. A hexamer and a zigzag structure, but not a helix, are observed for a Cu(II) compound [337]. For other M(II) metal ions, temperature, solvent and pressure dependent polymorphism has been observed [338-343]. It has been recently discussed over the fact that the anion tunes the secondary self-assembly, leading to rings, helices or chains [28]. This can be excluded in our case. Another theory of ring-opening polymerization also does not fit in our case, as the two crystallizations occur at the same time but independent one from the other [83, 344]. In fact, for the formation of complexes **7** and **8**, a concentration effect can be proposed. On the side with AgClO$_4$ in water, Ag cations are in excess with respect to the ligand **L3**, so that fragments of [Ag**L3**]$^+$ are formed as ligand diffuses towards this compartment of the "H"-shaped tube.

Silver Coordination Compounds with a Family of Ditopic Ligands of Varying Flexibility:
About Chains, Rings, Helices and Polycatenanes

88

In our polar solvents the dissociation of the possible soft species $[Ag_2L3]_2^+$ to yield $[Ag_2(L3)_2]_2^+$ and $[Ag]^+$ is probably entropically favored, leading to an anti-cooperative effect. To confirm this hypothesis, formation constants of the different species will have to be determined in different solvents. In one side of the "H"-shaped tube, ligand **L3** is in excess with respect to Ag^+, and fragments of the type $[Ag(L3)_2]^+$ can be formed, which would lead to the helical structure upon polymerization with other such fragments or $[Ag(L3)]^+$.

This is therefore, the first case of supramolecular isomerism induced by concentration effects, both isomers coexisting in the same solution, where a ring and a helical Ag (I) compound are formed.

After total diffusion, only the metallacycle, compound **7**, is found, so that compound **8** can be considered as the kinetic product, whereas the ring forming isomer **7** is the thermodynamically more stable product.

B - III.3 - {[Ag(L3)](NO₃)·2H₂O}₂ (9) and network isomers

The structure **9** crystallizes in the monoclinic space group $P2_1/n$ (No. 14). The asymmetric unit contains a silver cation coordinated by a ligand tecton, a nitrate anion and two water molecules. A C_2-centre of symmetry situated in the middle of the intra $Ag–Ag^{\#1}$ interaction generates a zero-dimensional structure (without taking into account the $Ag–Ag^{\#1}$ interaction) (Figure 75).
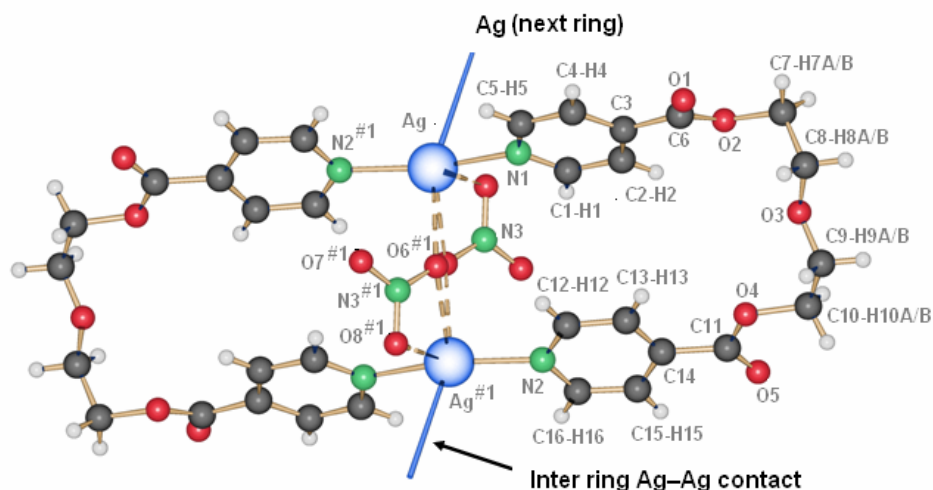
Figure 75. Metal–metal contact generating a two dimensional motif. Observe the bidentate and monodentate coordination type of the nitrate counter ion

As observed before, the organic ligand coordinates two cations, using the nitrogen atoms located at the pyridine rings with distances of Ag(1)–N(1) 2.195(4) and Ag(1)–N(2)[#2] 2.182(4) Å (Table B-III.42).

The nitrate counter ion is linked to one metal in a μ^2- fashion (Ag(1)–O(6), 2.742(8) and Ag(1)–O(7), 2.830(5) Å) and to the next silver in a monodentate manner with distance O(7)[#2]–Ag(1) of 2.764(5) Å. Thus, a distorted tetrahedral geometry on the metal atom is generated.

Table B-III.42 Most important bond lengths [Å] and angles [°] present in complex **9**

Ag(1)–N(1)	2.194(6)	N(1)–Ag(1)–N(2)[#1]	162.8(9)
Ag(1)–N(2)[#1]	2.181(5)	C–N–C	117.4(1)
Ag(1)–O(NO$_2$)	2.741(8), 2.830(5), 2.763(5)		
N–C	1.328(3), 1.335(3)		
Ag–Ag[#1]	3.320(6)		
Symmetry transformations used to generate equivalent atoms: #1 –x, -y, -z			

The pyridine rings of the ligand are stacked almost parallel (torsion angle between ring planes 11.9°). π–π stacking interactions between pyridine rings within the metallacycle are excluded due to the distance, however inter-metallacycle aromatic stacking interaction exists even if they are relatively weak (Table B-III.43).

Interestingly, one of the carbonyl groups attached to the pyridine ring is twisted respect to the plane of the aromatic ring, 16.8(2)° (C2–C3–C6–O2) compared with 4.5(2)° for the other carbonyl group (C13–C14–C11–O4).

Table B-III.43 π–π stacking present in complex **9**

π–π interaction	d_{R-R} (Å)	ρd_{R-R} (Å)	A	β
Intra π–π stacking interactions between aromatic rings of the same ligand.				
Ring (N1,C1,C2,C3,C4,C5)···Ring (N2,C12,C13,C14,C15,C16)[#2]	5.14	3.61	45.4	56.1
Inter π–π stacking interaction between aromatic rings of different ligands.				
Ring (N1,C1,C2,C3,C4,C5)···Ring (N2,C12,C13,C14,C15,C16)[#3]	3.76	3.37	26.4	21.1
Symmetry transformation used to generate equivalent atoms: #2 x, y, z #3 x, 1+y, z				

Finally, inter Ag–Ag[#1] contact affords a two dimensional motif based on rings stacked together by metal-metal contacts (see Figure 75 for more details).

Silver Coordination Compounds with a Family of Ditopic Ligands of Varying Flexibility: About Chains, Rings, Helices and Polycatenanes

90

Two water molecules are coordinated *via* hydrogen bonds to the oxygen atom O8 of the nitrate counter ion, which does not participate in the metal coordination and remains "free" pointing to the inside of the cavity formed by the metallacycles (looking alone the *b* axis). These molecules and the nitrates form a hydrogen bonding helical motif (Figure 76) of alternating helicity from one helix to the next.
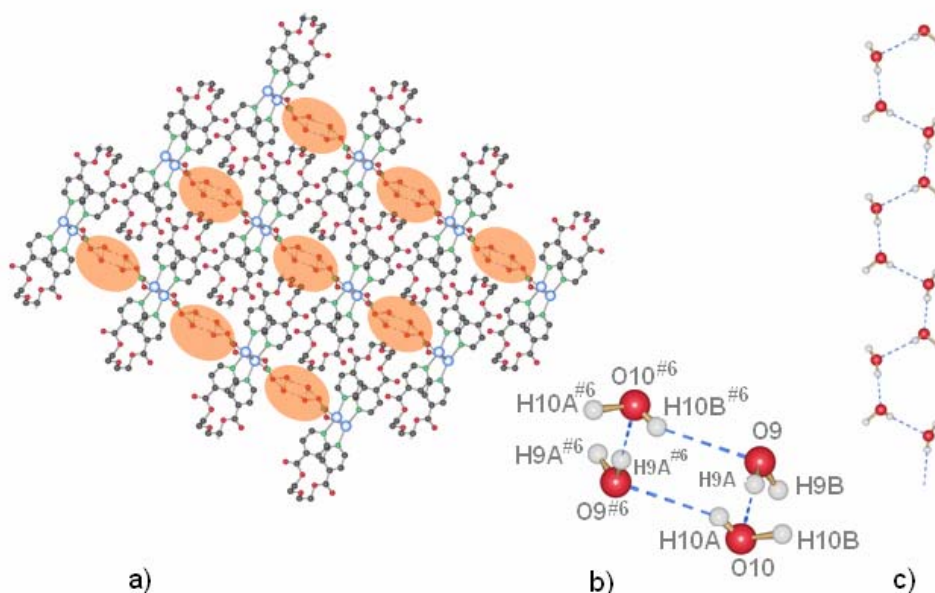
Figure 76. Water chains formed in the holes between rings of 9. The H$_2$O molecules joined by hydrogen bonds, are forming helices, these are anchored within the channels via hydrogen bonds to the nitrate counter ion.

Table B-III.44 Hydrogen bond data for **9** [length (Å) and angle (°)]

D-H···Acceptor	d (D–H)	d (H···A)	d (D···A)	Angle D-H···A
Hydrogen bonds between water molecules.				
O9–H9A···O10	0.97	2.01(8)	2.79(7)	178.0(7)
O10–H10A···O9$^{#4}$	0.97	2.17(8)	2.76(7)	157.0(9)
Hydrogen bonds formed between the nitrate oxygen atoms and the hydrogen atoms from water molecules.				
O9–H9A···O6	0.97	2.38(8)	3.08(7)	144.0(7)
O9–H9A···O8	0.97	2.21(8)	2.98(7)	159.0(7)
O10–H10A···O8$^{#5}$	0.97	1.99(1)	2.84(8)	150.0(1)
Hydrogen bond formed between the nitrate oxygen atoms and the hydrogen atoms from the closest pyridine ring.				
C12–H12···O7$^{#6}$	0.93	2.59(6)	3.39(6)	137
Symmetry transformation used to generate equivalent atoms: #4 x,-1+y,z, #5 1/2-x,-1/2+y,1/2-z, #6 1+x,-1+y,z.				

No other hydrogen bond is formed, so the structures remain as two dimensional interdigitated sheets. The aromatic rings are stacked together in an undulated fashion (see next chapter for detailed description), and the water molecules are directly responsible for this motif as will be shown.

The complex $\{[Ag(L3)](NO_3)\}_2$ **10** crystallizes in the side of the H-tube where the ligand was initially dissolved (THF). In this case, no water molecule was contained in the supramolecular motif which crystallizes in the monoclinic space group $P2_1/c$ (No. 14).

The asymmetric unit possess one Ag(I) cation, one nitrate and one organic ligand, both coordinating the silver atom. Distances Ag(1)–N are in the usual range (2.189(5), Ag(1)–N(1) Å and 2.180(5), Ag(1)–N(2)$^{\#1}$ Å) for this sort of coordination bond. The angle N(1)–Ag(1)–N(2)$^{\#2}$ is, however, quite distorted (149.1(4)°) mostly due to the strong interaction between the silver cation and the nitrate counter ion. Indeed the latter coordinates two silver ions of a same ring motif in an asymmetric μ^2-type, providing a trigonal bipyramidal geometry for the metal atom (Figure 77).
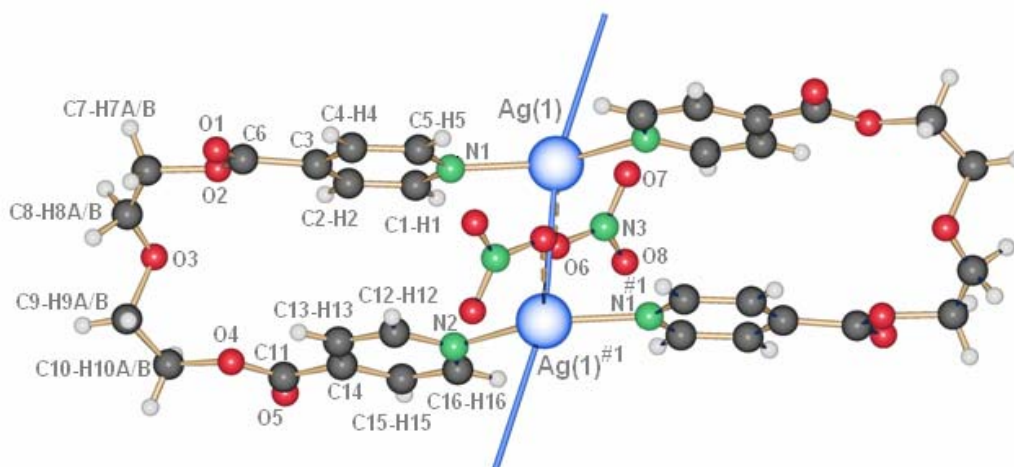
Figure 77. Schematic representation of the pentacoordinate silver cation. The Ag$^+$ on the top belongs to the next ring, whereas the Ag$^+$ on the bottom is linked by the same ligand forming a closed ring

Intra- and inter-ring metal-metal contacts are present (Table B-III.45). The structure is mono-dimensional viewed along the *b* axis. However, hydrogen bonds between parallel rings generate a 2-dimensional interdigitated array. This is substantially different from the interdigitation observed in **9**.

Silver Coordination Compounds with a Family of Ditopic Ligands of Varying Flexibility:
About Chains, Rings, Helices and Polycatenanes

92

Table B-III.45 Most important bond lengths [Å] and angles [°] present in complex **10**

Ag(1)–N(1)	2.184(6)	N(1)–Ag(1)–N(2)$^{\#1}$	149.1(4)
Ag(1)–N(2)$^{\#1}$	2.186(6)	N(1)–Ag(1)–Ag(1)$^{\#1}$	83.1(3)
Ag(1)–O(NO$_2$)	2.581(8), 2.737(6)	N(2)#1–Ag(1)–Ag(1)$^{\#1}$	101.8(3)
Ag(1)–Ag(1)$^{\#1}$	3.333(4)		
Ag(1)–Ag(1)$^{\#2}$	3.400(7)		

Symmetry transformations used to generate equivalent atoms: #1 -x,-y+1,-z #2 -1-x, 1-y, z

Table B-III.46 Hydrogen bond data for **10** [length (Å) and angle (°)]

D-H···Acceptor	d (D–H)	d (H···A)	d (D···A)	Angle D-H···A
Inter ring hydrogen bond formed between the oxygen atom on the lateral chain and the hydrogen atom from the pyridine ring.				
C13–H13···O5$^{\#3}$	0.93	2.52(2)	3.28(9)	138.7(1)

Symmetry transformation used to generate equivalent atoms: #3 1-x,1/2+y,1/2-z.

Considering the ligand, the carbonyl group remains in the same plane as the pyridine ring. Torsion angles in the lateral chain are 73.3(1)° (O3–C9–C10–O4) and 10.4(2)° (O2–C7–C8–O3), which implies an elongation on the diethylene spacer and a distortion of about 30.8° on the ring-ring stacking (Figure 78).
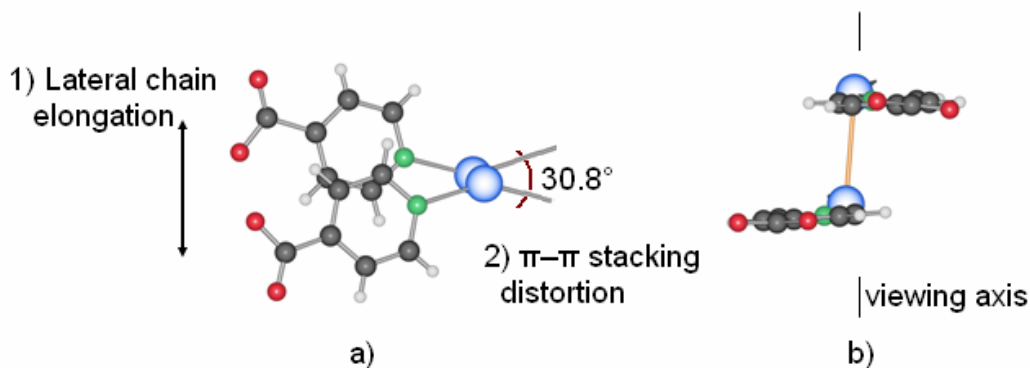
Figure 78. Influence of the torsion angles in the lateral chain over the π–π stacking system a) viewing along the a axis b) a view along the *c* axis

The metal-metal contact forces the pyridine ring to share a common axis which crosses the two silver cations. This is the reason why this distortion is more evident. The presence of π–π aromatic stacking interaction is excluded due to the distance (more than 4.0(7) Å between ring centroids).

The rings in the supramolecular motif are stacked parallel to each other (Figure 79) generating columns, as previously mentioned. They possess an undulated form along the *c* axis direction.
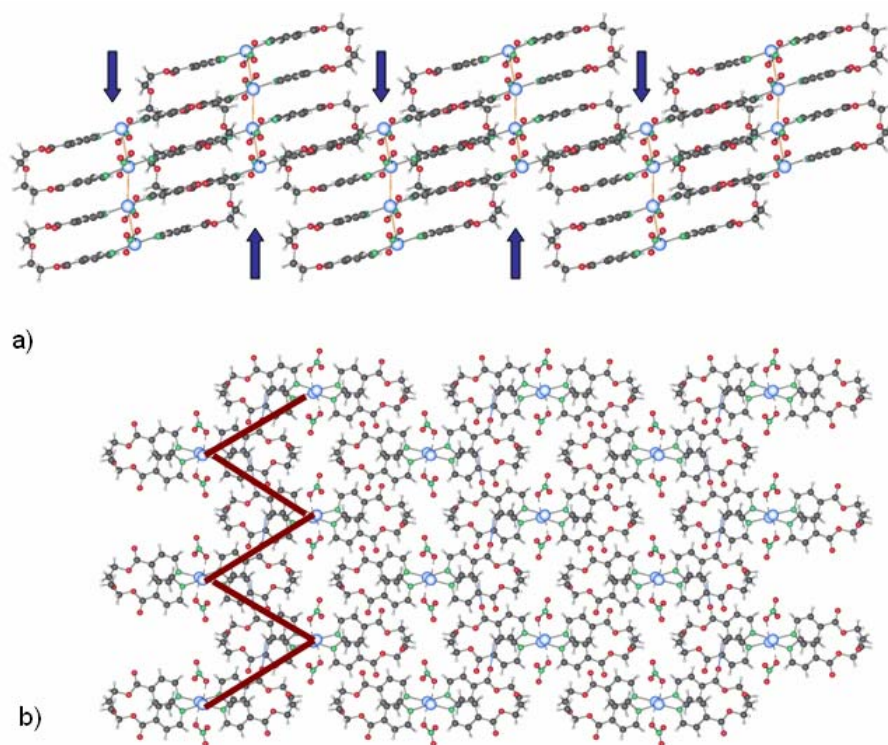
Figure 79. Schematic representation of the stacking of rings forming columns a) b axis view, blue arrows represent stacking direction, b) this view shows undulated interdigitation generating a 2-D framework (red line)

Single crystals grow when DMSO solutions of the organic ligand **L3** and silver nitrate were mixed together. The complex {[Ag(**L3**)](NO$_3$)}$_2$ **(11)** in the solid state crystallizes in the triclinic system group P-1 (No. 2). It contains a silver cation coordinated to a ligand and a nitrate counter ion similar to complex **10**.

In this case, the nitrate anions coordinates the silver cation in almost a quasi perfect symmetrical bidentate mode (Ag(1)–O(7), 2.658(8) Å and 2.653(3) Å, Ag(1)–O(6)). Every silver cation is linked by two pyridine rings to complete the tetrahedral motif around the metal atom (Table B-III.47). The angle N(1)–Ag(1)–N(2) is 151.5(2)° and the aromatic pyridine rings belonging to the same ligand are distorted by 28.5(2)° from the axis formed by the intra silver-silver contacts.

Silver Coordination Compounds with a Family of Ditopic Ligands of Varying Flexibility:
About Chains, Rings, Helices and Polycatenanes

94

Table B-III.47 Most important bond lengths [Å] and angles [°] present in complex **11**

Ag(1)–N(1)	2.189(4)	N(2)#1–Ag(1)–N(1)	151.5(1)
Ag(1)–N(2)[#1]	2.177(4)	C(1)–N(1)–Ag(1)	122.9(3)
Ag(1)–O	2.658(8), 2.653(3)		
Ag1–Ag1[#1]	3.434(1)		

Symmetry transformations used to generate equivalent atoms: #1 -x,-y+1,-z

Table B-III.48 Hydrogen bond [length (Å) and angle (°)] present in complex **11**

D–H···Acceptor	d (D–H)	d (H···A) Å	d (D···A) Å	Angle D–H···A
Inter ring hydrogen bonds formed between the oxygen atom on the lateral chain and the hydrogen atomfrom the pyridine ring.				
C2–H2···O5[#2]	0.93	2.37(0)	3.04(7)	129.5(8)
C12–H12···O1[#4]	0.93	2.43(5)	3.13(8)	132.1(2)
Hydrogen bond formed between the nitrate oxygen and the hydrogen atom from the closest pyridine ring.				
C5–H5···O7[#3]	0.93	2.50(4)	3.18(7)	129.4(9)

Symmetry transformation used to generate equivalent atoms: #2 -x,-y,1-z, #3 1-x,1-y,-z, #4 -x,1-y,1-z.

The carbonyl group remains in the plane of the aromatic ring (O1–C6–C3–C4, 3.8(5)° and O4–C11–C14–C13, 1.8(4)°) and points to the outer side(exo) of the surface containing the ring. The diethylene glycol spacer possesses a "gauche" type conformation with torsion angles of 46.1(4)° (O2–C7–C8–O3) and 79.4(3)° (O3–C9–C10–O4). The angle between the planes crossing the pyridine rings is 9.6(8)°, which shows a slight bending and asymmetry in the ring stacking. Indeed, π–π interactions are present, being stronger in the inter-ring region (Table B-III.49).

A found frequently in the solid state [56], the distance C1–H1···centroid (aromatic ring) is 3.18 Å (Figure 80), which suggests an interaction of type C–H···π. However, in the presence of this interaction, Ag–Ag and π···π stacking should act in a synergistic manner.
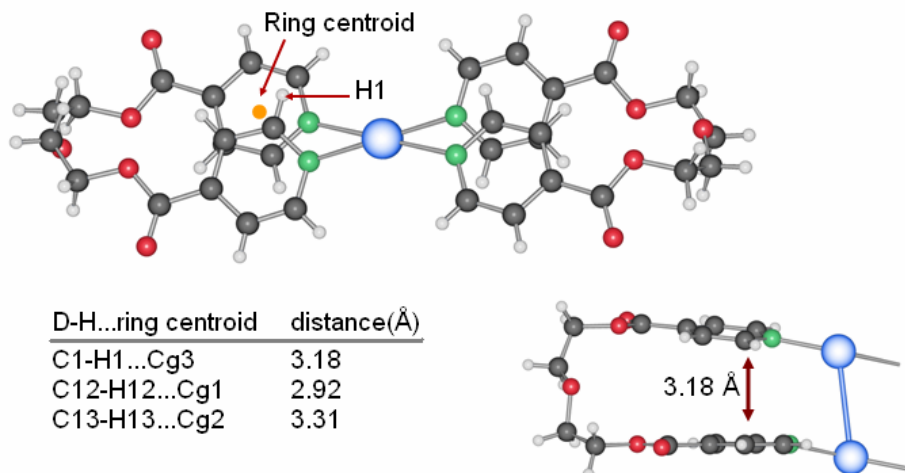
Figure 80. Schematic representation of potential C–H···π interaction with a distance of 3.18 Å. Ag-Ag contacts are represented in blue. The aromatic ring (up) is slightly bent to the plane formed by the ring on the bottom

Weak intra-ring Ag–Ag contacts are present, which are longer than the Ag–Ag contacts between the silver atoms from adjacent rings.

Table B-III.49 π–π stacking

π-π interaction	d_{R-R} (Å)	ρd_{R-R} (Å)	α	β
Intraπ–π stacking interactions between aromatic rings of the same ligand.				
Ring (N1,C1,C2,C3,C4,C5)···Ring (N2,C12,C13,C14,C15,C16)[#5]	4.11	3.94	49.87	16.44
Inter π–π stacking interactions between aromatic rings of different ligands.				
Ring (N1,C1,C2,C3,C4,C5)···Ring (N2,C12,C13,C14,C15,C16)[#5]	3.87	3.57	9.59	22.81
Symmetry transformation used to generate equivalent atoms: #5 1+x, y, z				

Hydrogen bonds between the oxygen atom of the carbonyl group and the hydrogen atom attached to the pyridine ring generate, in a first instance, a two dimensional network. The nitrate counter ion links one hydrogen atom of the ring below, and finally a three dimensional network results from the overall array (Figure 81).
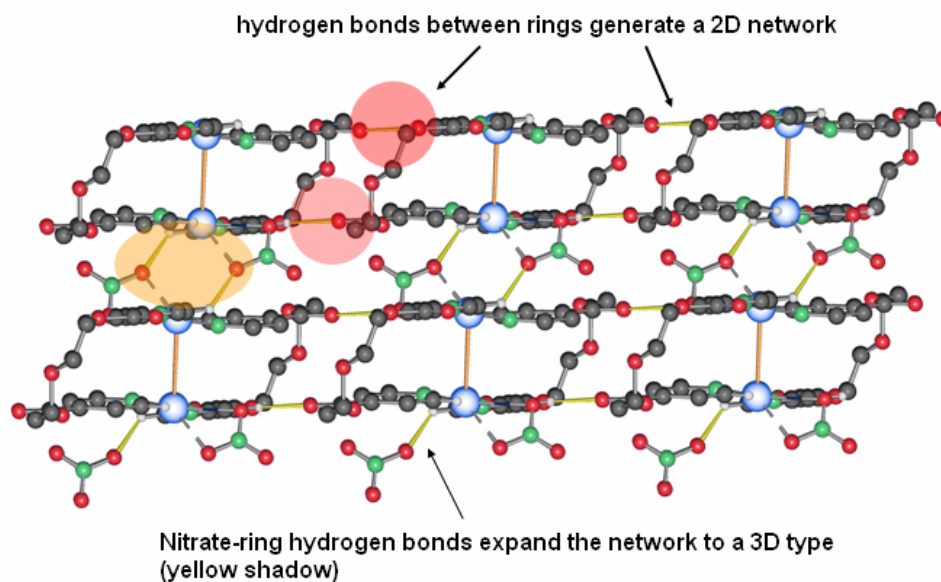
Figure 81. Expanded dimensionality due to hydrogen bonds. in this case silver-silver contacts are represented in orange

B - III.4 - Some comparison and difference between structures {[Ag(L3)]NO₃*H₂O}₂ (9), {[Ag(L3)]NO₃}₂ (10) and {[Ag(L3)]NO₃}₂ (11).

The complexes **9**, **10** and **11** possess the same crystal morphology and crystallize like prism type crystals. They can be considered network isomers, mostly because the water present in (**9**) does not affect the overall array. Indeed, after removing the water, the structure does not suffer any damage (Figure 82).
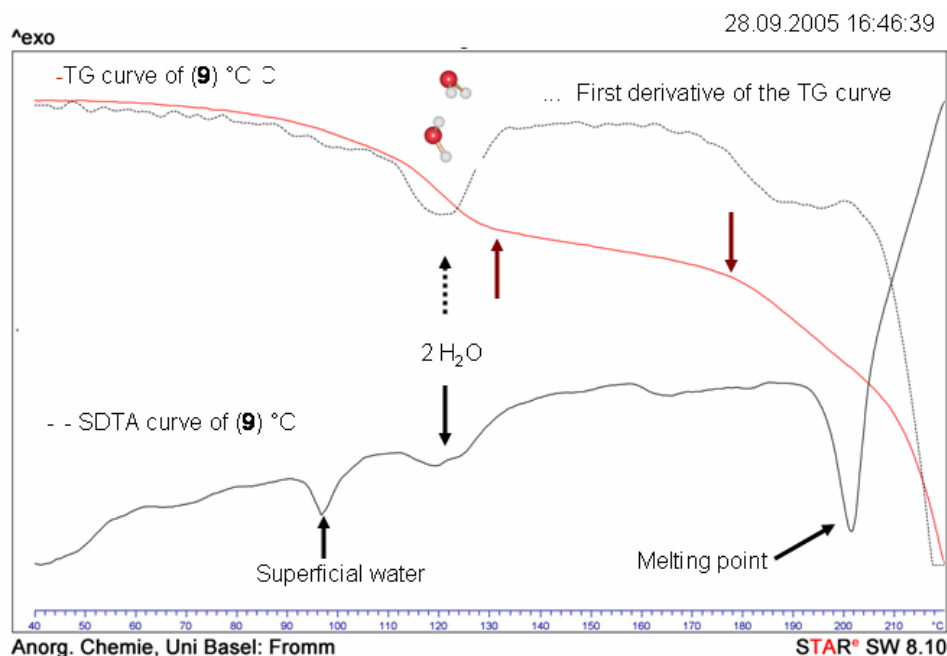
Figure 82. TG/SDTA spectra of complex 9. Note that after dehydration complex 9 evidences no loss of mass (red line)

The nitrate counter ions is coordinating in a different way in the three motifs: in **9** it does it in a μ^2–μ^1 fashion, coordinating two silver atoms from the same metallacycle (Ag(1)–O(6), 2.741(8) Å; 2.830(5) Å, Ag(1)–(O7) and Ag(1)–O(7) [#1], 2.763(5) Å). Weak exo–ring metal-metal contacts (Ag(1)–Ag(1)[#1], 3.320(6) Å) are present generating a distorted square planar pyramid.

The observable monodentate nitrate counter ion in **10** is unusual since NO₃⁻ more often bonds in a bidentate fashion. Only a few monodentate nitrate coordinating pattern have been reported so far [294], In **10,** the counter ion is asymmetrically coordinated to the silver atom in a μ^2– pincer mode (Ag(1)–O(7), 2.738(6) Å and 2.579(5) Å for Ag(1)–(O6)). This probably induces the approach of the

metal atoms (*endo-ring* Ag(1)–Ag(1)$^{#1}$, 3.334(7) Å and *exo-ring* Ag(1)–Ag(1), 3.399(7) Å). The nitrate molecules are slightly included in the region delimited by the metallacycle. Interestingly, this feature does not appear in the last complex **11**, since the counter ion is displaced from this area and occupies the space delimited by two different metallacycles. The nitrate coordinates the metal atom in a strongly symmetrical pincer fashion (Ag(1)–O(7), 2.658(8) Å and 2.653(6) Å for Ag(1)–(O6) Å) and weak Ag(1)–Ag(1)$^{#1}$ contacts are present in the metallacycle and between different rings (*endo* Ag(1)–Ag(1)$^{#1}$, 3.434(8) Å and *exo* Ag–Ag$^{#1}$, 3.684(9) Å) (Figure 83).
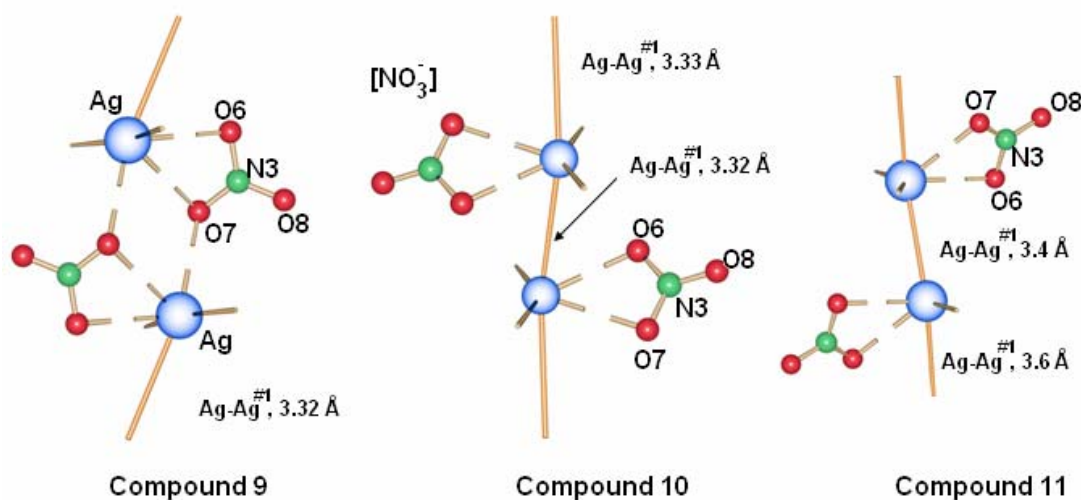
Figure 83. Schematic representation of the counter ion position in compounds 9, 10 and 11. Silver–silver contact represented in orange

When nitrate counter ions are used, the probability to find a water molecule within the crystalline structure is greatly increased, mainly due to the coordinating and H-bonding properties of this counter ion. In structure **9,** a helical array of water molecules was found. Water nanowires exist in nature and their existence is essential for life [345]. Other porous structures as those formed by calixarenes and their derivatives are suitable scaffolds for such arrays [346].

Since some time ago, it has been established that in particular conditions water tends to rearrange itself forming nanowires [347]. Single-walled carbon nanotubes have been used to direct the formation of this kind of arrays with interesting new applications [348]. Some other evidences suggest that water ordering structures may modulate proton conductance via a "proton wire" hydrogen bonding network; in particular, this ability to modulate water ordering with geometry

suggests a possible mechanism for a switchable nanoscale semiconductor [349]. In most cases, the water molecule nanowires do not possess external bonds except with water. In our case, the water helices are strongly supported by the nitrate counter ion as shown by TG/DSC measurements, which affords "boiling" temperatures of about 120° C (Figure 84). The interconversion between the hydrated and the dehydrated structure is not unusual and has been tested under thermal conditions for Zn(II) complexes [350]. In the case of **9,** the dehydration is an irreversible process. Water may play another role than just forming hydrogen bonds as it was shown in the synthesis of some Fe(II) compounds, which do not have water but have to be synthesized in water to obtain the correct properties [351].
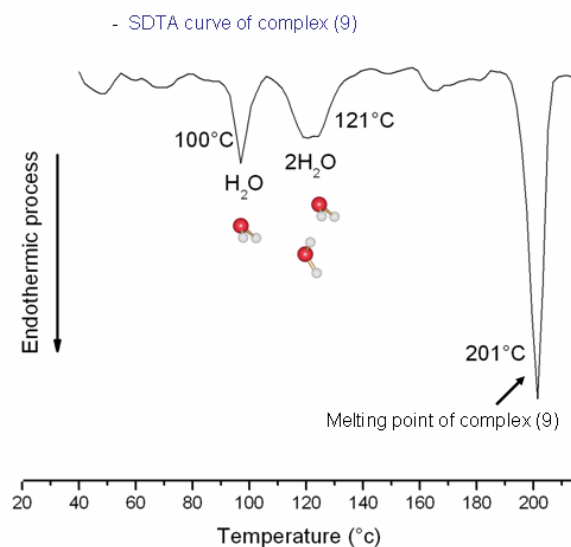
Figure 84. Differential scanning calorimetry of complex 9. Coordinating water is coming out at 121° C, which suggests a strong coordination with the nitrate counter ion

A reversible system containing water was reported by *Lou et al.* who found 1D left-handed helical water chains in an AABB fashion imbedded in chiral channels. The porous complex is dependent on water molecules, so when water is removed thermally the channel collapses [352]. In complex **9,** the thermal removing of water does not shows chemical decomposition (Figure 84).

Another important aspect to take into account is how the nitrate coordinative pattern modifies the positioning of the metallacycles. In **9,** the presence of the water helix in the cavity formed by the counter ion elongates the distance between parallel rings (Ag⋯Ag, 13.546(3) Å), so the presence of water conditiones in some way the final array. In **10,** this distance is 12.951(3) Å (Ag⋯Ag) and in **11** 12.156(2) Å (Ag⋯Ag). However, the distance between parallel silver atoms mostly depends on

whether the counter ion coordinates in a μ^1- or a μ^2- fashion; with the last mode occupying less volume and makes the structure more compact (Figure 85).
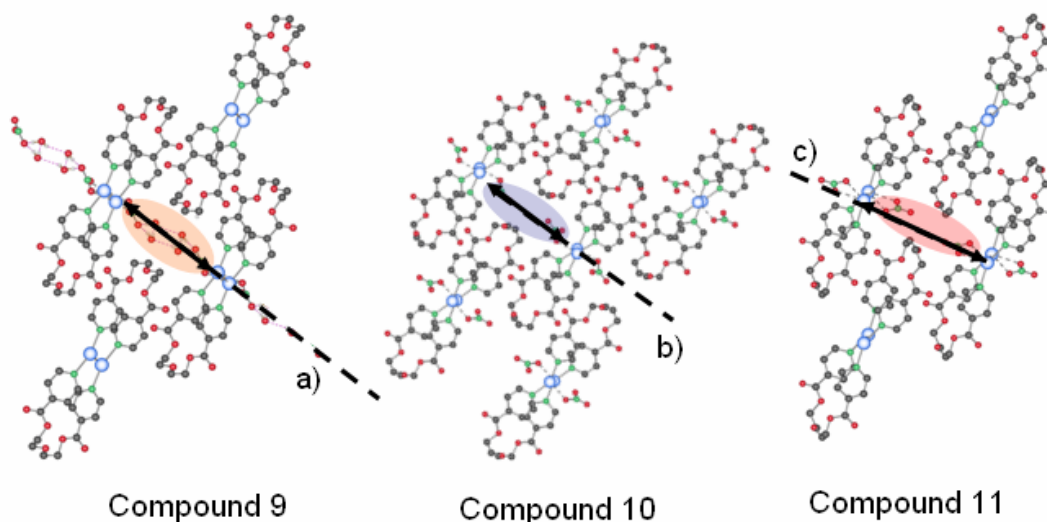
Figure 85. Controlling distance between parallel metal atoms by nitrate coordination pattern. Compound 9, distance a=13.546(3) Å, compound 10, distance b=12.951(3) Å and compound 11, distance c=12.156(2) Å

The structures **9** and **10** melt at different temperature, which allowed us to identify the three isomers not just when the samples were in the crystalline state, but also when polycrystalline or amorphous samples were obtained (Figure 86).
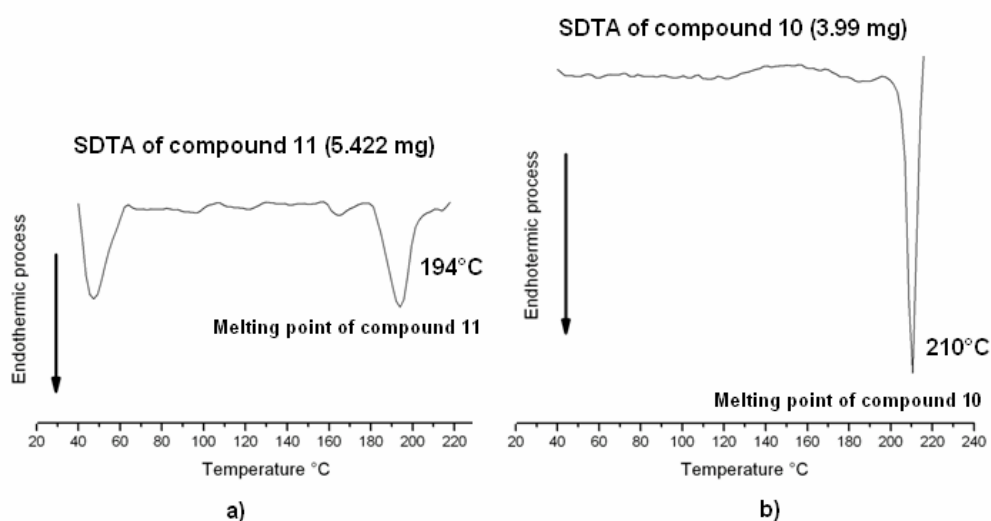
Figure 86. TG/SDTA curves of complex 10 and 11

Silver Coordination Compounds with a Family of Ditopic Ligands of Varying Flexibility:
About Chains, Rings, Helices and Polycatenanes

101

The disposition of the columns formed by the stacked rings differs as well in the three complexes; the presence of the water helix in **9** should be directly responsible of the twist of rings in parallel columns (Figure 87).
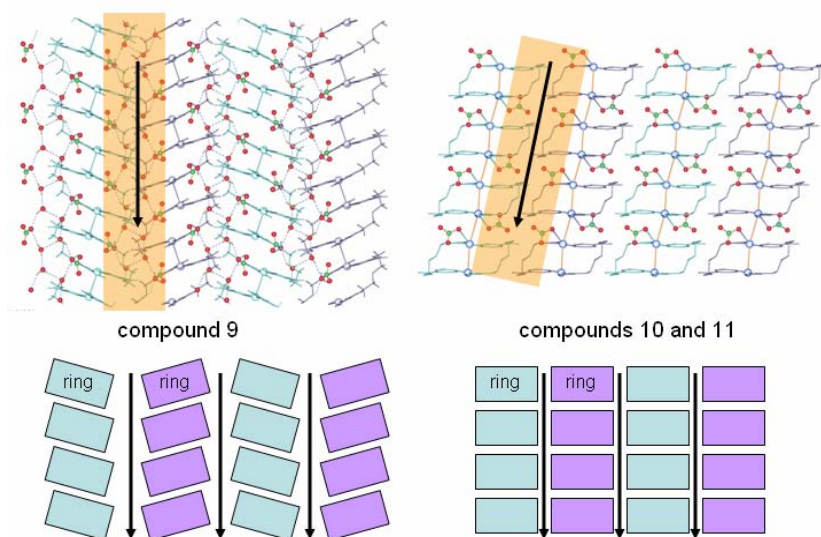
Figure 87. Schematic representation of column stacking in 9, 10 and 11. The last two complexes share the same motif; black arrows represent column direction in the crystalline state, position if counter ion and water in the case of 9 is represented in orange

Some essays to interchange NO_3^- counter ions with $SO_3CF_3^-$ were carried out without success. However, when single crystals of complex **11** were warmed (80°C) for a week and measured again, the structure obtained corresponded to **10**, where the nitrate counter ion is monodentate. Flexible coordinating ability of nitrate counter ion upon heating has been studied since 1996 [353]. In these complexes the process is time and temperature dependent; the conversion does not take place after four days and heating over 80°C destroys the crystalline structure. The use of TG/SDTA was not possible here due to time dependency.

Mass spectra show the presence of the metallacycle complex in solution ($\{[Ag(\mathbf{L3})]_2NO_3\}^+$, 910 m/z), but after increasing the concentration of ligand, new polymeric species appear and are dominant in the complexation process (Figure 88).

Silver Coordination Compounds with a Family of Ditopic Ligands of Varying Flexibility: About Chains, Rings, Helices and Polycatenanes

102
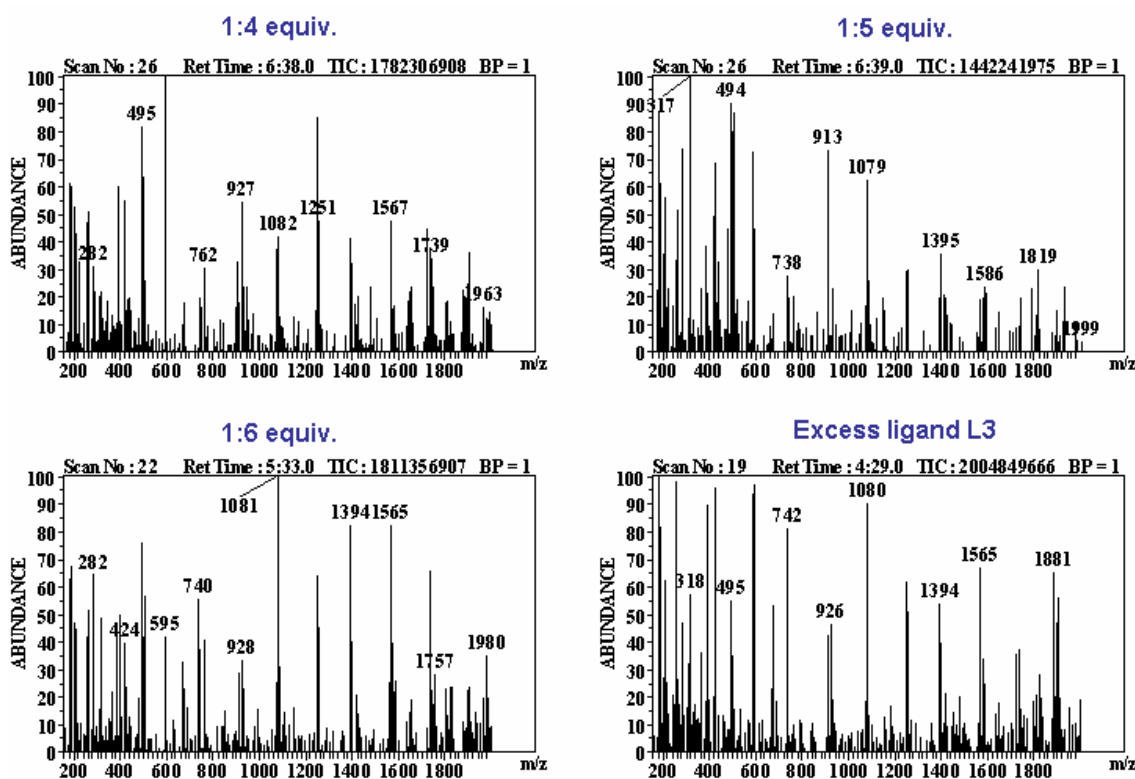
Figure 88. Mass spectra of a solution containing the organic tecton and silver nitrate. The first spectra was performed in a ligand L3:Silver nitrate 2:1 equivalent proportion; the concentration of ligand is gradually increased. Further spectra with higher equivalence of ligand show only presence of polymeric species

Even when concentration dependency has been used to direct the specific formation of polymorphs or crystals with desired chemical-physical properties, we were not able to crystallize other structures than **9**, **10** and **11.** The process seems to be entropically and thermodynamically controlled yielding only a ring when the system is allowed to be undisturbed forming crystals and when anions clamp together the Ag ions within the ring.

B - III.5 - {[Ag(L3)](PF$_6$) ·THF}$_2$ (12) and {[Ag(L3)](PF$_6$)}$_2$ (13)

In the silver salt containing side of the "H"-shaped tube with water as solvent for AgPF$_6$ and THF for **L3**, greenish monocrystals of {[Ag(**L3**)](PF$_6$)*THF}$_2$ **(12)** were collected and measured. The complex crystallizes in the triclinic space group P-1 (No. 2), with one molecule per unit cell.

As seen in previous complexes of this type, two ligands adopt a U-shape and coordinate two metal ions generating a cyclic structure (Figure 89).
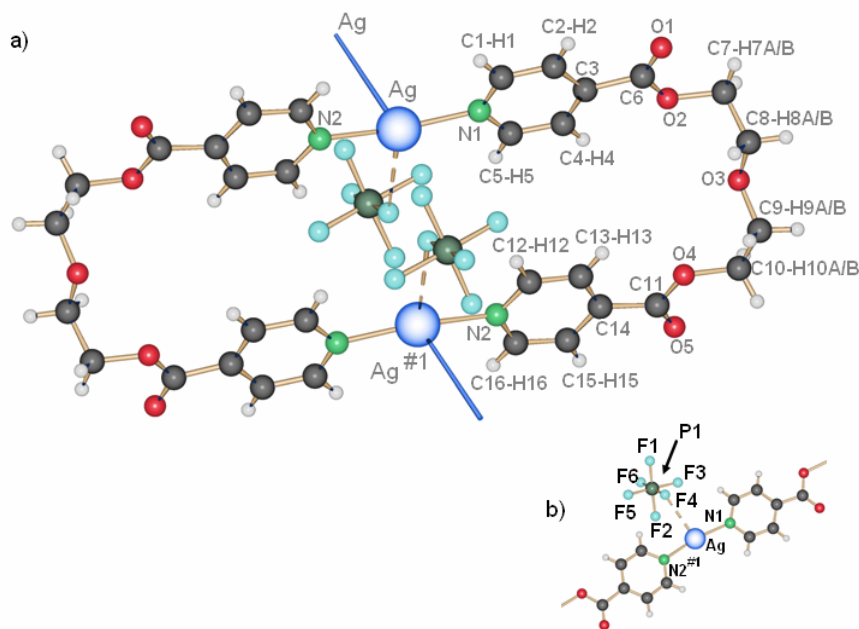
Figure 89. Metallacycle in complex 12. THF molecule was omitted for clarity reason

The nitrogen atom of the pyridine ring strongly coordinates the silver cation with Ag–N distances of 2.136(4) Å (Ag(1)–N(2)$^{\#1}$) and 2.143(4) Å (Ag(1)–N(1)). Less coordinating towards the metal atom are the hexafluorophosphate counter ions, which is determinant in the N(1)–Ag(1)–N(2)$^{\#1}$ angle of 169.3(2)°. The two PF$_6^-$ anions bridge two silver ions belonging to the same ring, Ag–F bonds being weak with 2.960(7) Å (Ag(1)–F(4)) and 3.092(5) Å (Ag(1)–F(1)$^{\#1}$) (Table B-III.50). Due to this arrangement, the Ag–Ag$^{\#1}$ distance within the ring is rather long with 5.213(1) Å, and π-stacking within the ring is thus excluded with pyridine rings offset by 5.12 Å to each other (Figure 90).

Silver Coordination Compounds with a Family of Ditopic Ligands of Varying Flexibility: About Chains, Rings, Helices and Polycatenanes

104
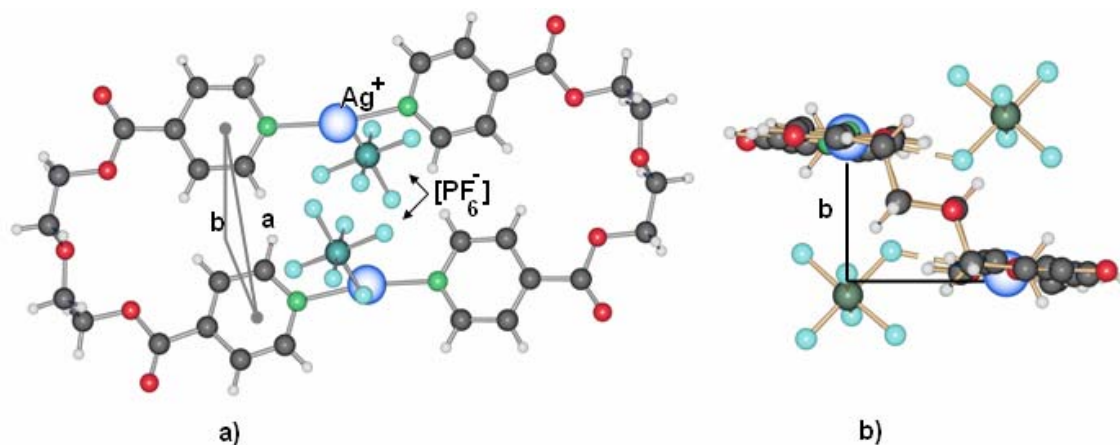
Figure 90. Stacking representation of pyridine ring in the complex 12. Rings and centroids are separated about 5.12 Å (represented as "a", "b" perpendicular from centroid to the plane containing the second aromatic ring)

The carbonyl group is coplanar to the aromatic ring (torsion angle C4–C3–C6–O2, 3.4(5)° and C13–C14–C11–O4, 4.8(8)°). All diethylene glycol moieties posses a "Gauche" (staggered) conformation with torsion angles of about 67.2(4)° (O2–C7–C8–O3) and -70.3(4)° (O3–C9–C10–O4).

Table B-III.50 Most important bond lengths [Å] and angles [°] present in complex **12**

Ag(1)–N(1)	2.143(4)	N(2)#1–Ag(1)–N(1)	169.3(2)
Ag(1)–N(2)[#1]	2.136(4)	C(1)–N(1)–Ag(1)	117.6(2)
Ag(1)–F(4)	2.960(7)		
Ag(1)–Ag(1)[#2]	3.459(1)		

Symmetry transformations used to generate equivalent atoms: #1 2-x, 1-y, 2-z #2 -1-x,1-y,2-z

The rings in **12** are arranged parallel to each other so that weak π-stacking between adjacent pyridine rings are possible (C5–C15[#2], 3.511(1) Å, N1–N2[#2], 3.529(1) Å).

The Ag–Ag contact is shortest between two rings with 3.459(1) Å. Taking into account the position of the Ag atoms, they form a zigzag line with Ag–Ag–Ag angles of 124.4(1)°.

Hydrogen bonds are present due to the interaction between the carbonyl group and the hydrogen atom located in the aromatic ring, which generate sheets formed of metallacycles (Figure 91).
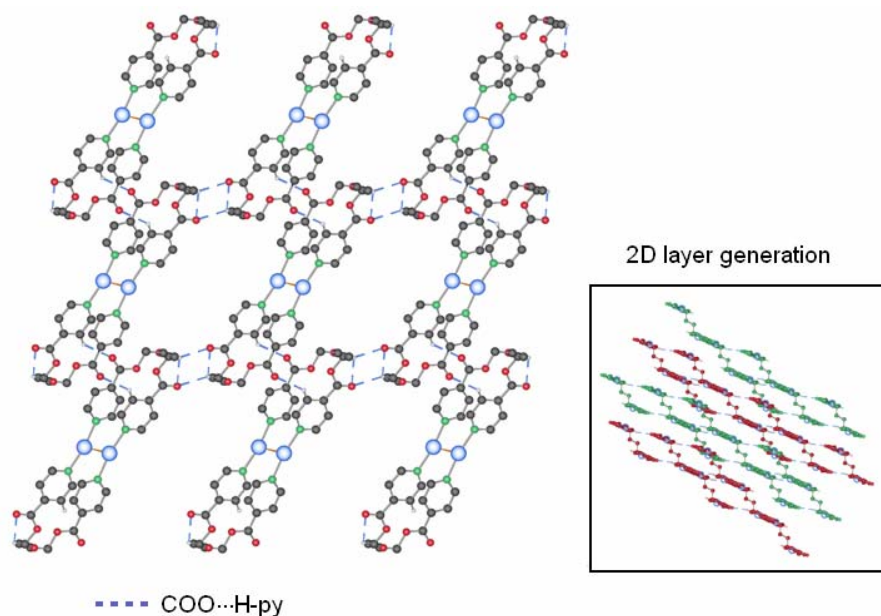
Figure 91. Hydrogen bonds (blue dashes) form two dimensional sheets. Left viewed through a axis; in the right side viewed from the [1.0 -17.4 -12.6] direction, sheets are differentiated by color. (THF molecules and counter ions are not showed for clarity reasons)

Table B-III.51 Hydrogen bond data for **12** [length (Å) and angle (°)]

D–H⋯Acceptor	d (D–H)	d (H⋯A)	d (D⋯A)	Angle D–H⋯A
Inter-ring hydrogen bonds formed between the oxygen atom on the lateral chain and hydrogen atom from the pyridine ring.				
C4–H4[#3]⋯O5	0.97	2.49(1)	3.22(6)	136.0(7)
C7–H7A[#4]⋯O1	0.97	2.55(4)	3.45(2)	154.0(4)
Symmetry transformation used to generate equivalent atoms: #3 1-x,-y,2-z, #4 -x,-y,1-z.				

Solvent molecules and the PF_6^- counter ion occupy the empty spaces in **12**. THF molecules are not coordinating the silver atoms in the metallacycle. TG and DTA measurements show a quantitative loss of THF at 230°C (Figure 92). Inter-metallacycle metal–metal contact finally generate a three dimensional supramolecular motif.
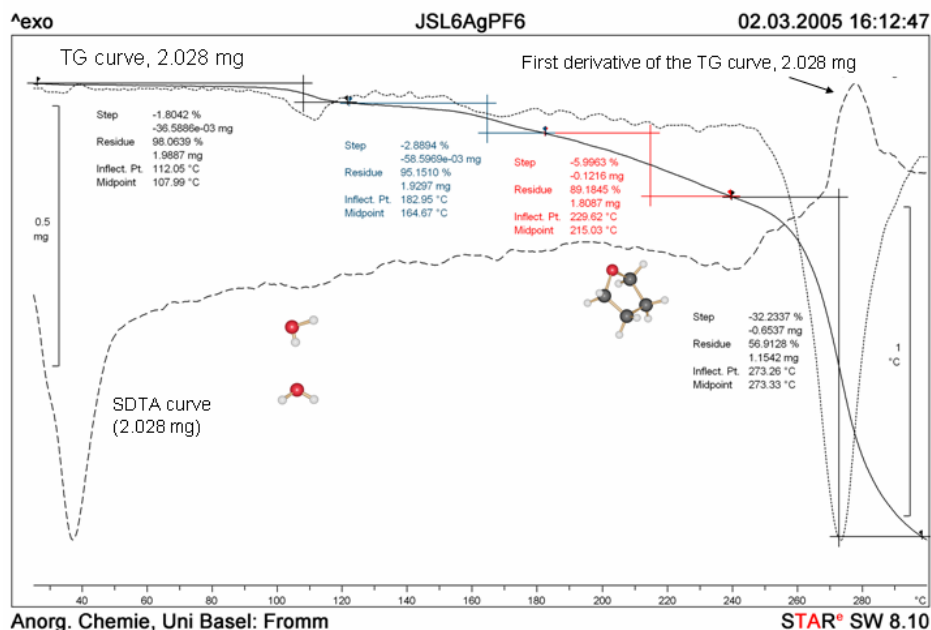
Figure 92. TG/SDTA curve of complex 12

When the mother liquor of **12** is allowed to stand for about two months, new crystals with the same morphology as **12**, but transparent rather than greenish and with a different ratio Ag:**L3**, can be observed. They correspond to a new complex {[Ag(**L3**)$_2$](PF$_6$)$_2$}$_2$, **(13).**

The complex **13** crystallizes in the orthorhombic system, space group Pbcn (No. 60), with two ligands, one silver cation and one counter ion in the asymmetric unit cell.

The basic motif of **13** consists of a chain of silver cations, which are coordinated in a distorted tetrahedral fashion by four nitrogen atoms of four different ligand molecules (Figure 93). The Ag(1)–N distances are longer than in the ring compounds with 2.287(3) to 2.381(3) Å, as expected for a coordination number of four for Ag$^+$. The N–Ag–N angles at the silver ion range from 103.5(8) to 118.2(1)°, the two larger angles being found within a metallacycle.

Silver Coordination Compounds with a Family of Ditopic Ligands of Varying Flexibility:
About Chains, Rings, Helices and Polycatenanes

107
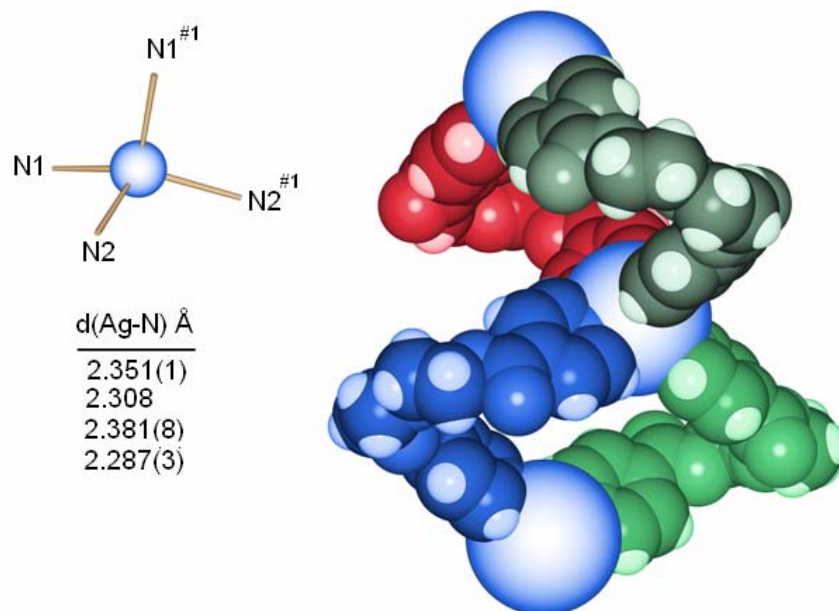
Figure 93. Distorted coordination sphere around the silver cation and metallacycle formation

Thus, within the chain, two silver ions are linked to each other by two ligands (Figure 93, right side), forming such a ring. Whereas one ligand possesses an all-gauche conformation with torsion angles at the ethyl groups of ca. 60°, the second ligand has one gauche arrangement and one ethyl group almost perfectly eclipsed with a torsion angle of only ca. 6.8° about the O8–C25–C26–O9 bonds. The angle between the plane formed by the carbonyl group and the plane formed by the aromatic ring differs for both carbonyl groups within the same ligand (18.69° and 3.81°; and 28.51° and 7.68° for the second one). The so formed [**L3**Ag]$_2$-metallacycle forms a cavity of the dimension of ca. 9.2 x 17.2 Å. This cavity is large enough to allow the insertion of two other ligand molecules, one from a neighbor chain below, the other from above. Another way to describe the topology can be considering the structure as parallel chains of one-dimensional polycatenanes, fused via the silver cations to yield the two-dimensional overall motif. The so formed entangled structure yields an unprecedented sort of chain mail motif which extends in a two-dimensional array (Figure 94).

Silver Coordination Compounds with a Family of Ditopic Ligands of Varying Flexibility: About Chains, Rings, Helices and Polycatenanes

108
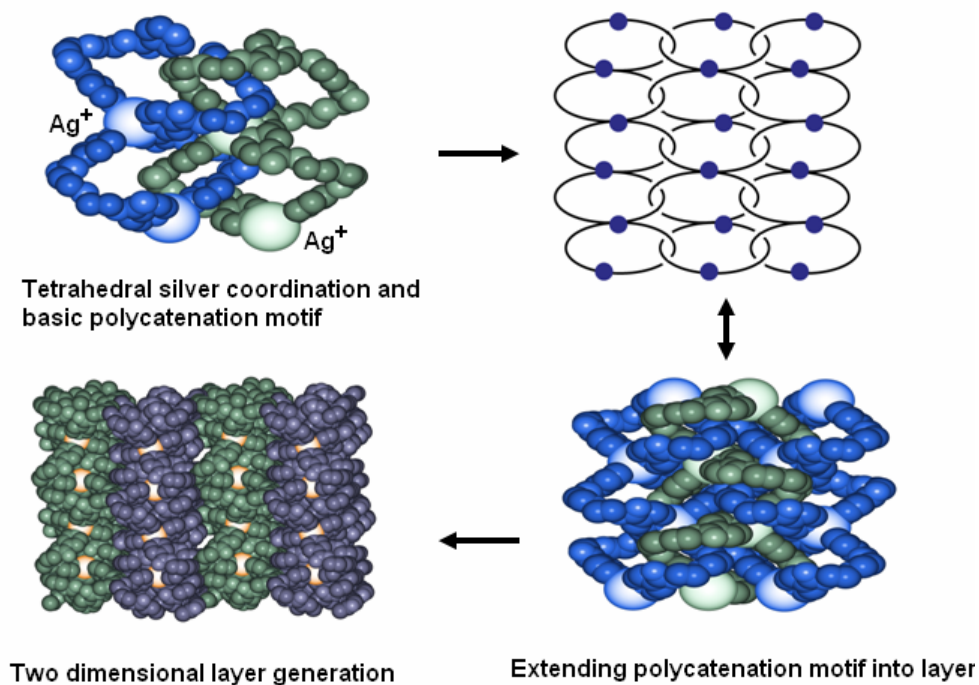
Figure 94. Schematic representation of the entanglement motif and sheet generation in 13

The polycatenation is stabilized as well through weak π-π interactions between aromatic rings belonging to a metallacycle and the crossing ligand, which generates the entanglement (Figure 95).
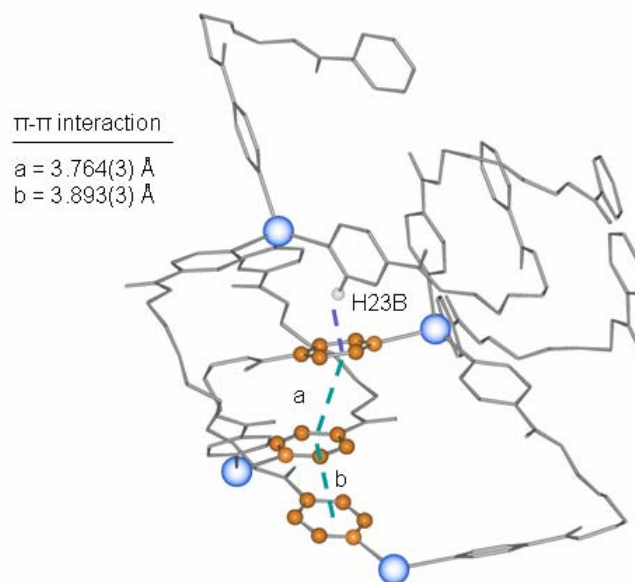
Figure 95. Weak π–π interactions stabilize the entanglement motif. C–H···π interactions are present to a distance about 2.95 Å

Silver Coordination Compounds with a Family of Ditopic Ligands of Varying Flexibility:
About Chains, Rings, Helices and Polycatenanes

109

The hexafluorophosphate counter ion is able to generate hydrogen bonds as well, but as with the case of **12,** these are between the fluor atoms and the hydrogen atom located in the closest pyridine ring.

B - III.6 - Some comparison and difference between structures {[Ag(L3)]PF$_6$·THF}$_2$ (12) and {[Ag(L3)]PF$_6$}$_2$ (13)

The most evident difference between **12** and **13** is the ligand to metal ratio, and thus the metal coordination sphere. Complex **12** retains the same motif as other metallacycles already studied in this chapter (**7**, **9**, **10** and **11)**. Two ligand molecules and two silver atoms generate a zero-dimensional structure with the hexafluorophosphate counter ion linking very weakly the metal atom (F$_5$P–F(4)···Ag, 2.960(1) Å), and more elongate F$_5$P–F(4)$^{\#1}$···Ag, 3.081(6), F$_5$P–F(1)$^{\#1}$···Ag, 3.092(1) Å). The counter ion is accommodated in the plane defined by parallel pyridine rings and is linked through hydrogen bonds with THF molecules. These solvent molecules are situated in channels perpendicular to the axis formed by the N(1)-Ag-N(2)$^{\#1}$ bond filling void space in the unit cell. The THF molecules are tightly attached in the crystalline motif, as TG/SDTA measurements evidence. In complex **13,** however, the metal cation is coordinated by four tectons instead of two. These are disposed in a tetrahedral fashion displacing the counter ion into the cavities formed in the crystal. Hexafluorophosphate is a weak coordinating counter ion with an increased ability to form multiple hydrogen bonds [354-357], providing a very rich structural chemistry. The Ag(1)–N distances are longer than those observed in **12** and range from 2.287(3) to 2.381(3) Å. The N–Ag–N angles at the silver ion range from 103.5(8) to 118.2(1)°. Thus, within the chain, two silver ions are linked to each other by two ligands.

Unexpectedly, the lower melting point value found was that of complex **13** (Figure 96). This fact could be explained by some constrains in the ligand geometry. Basically, the helical compound **8** and the polycatenated **13** share some aspects concerning distortion values of torsion angles in the diethylene glycol spacer (C9–O3–C8–C7, 137.5(2)° and C23–C24–O8–C25, 153.9(2)°), which differ from usual values found for the metallacycles.
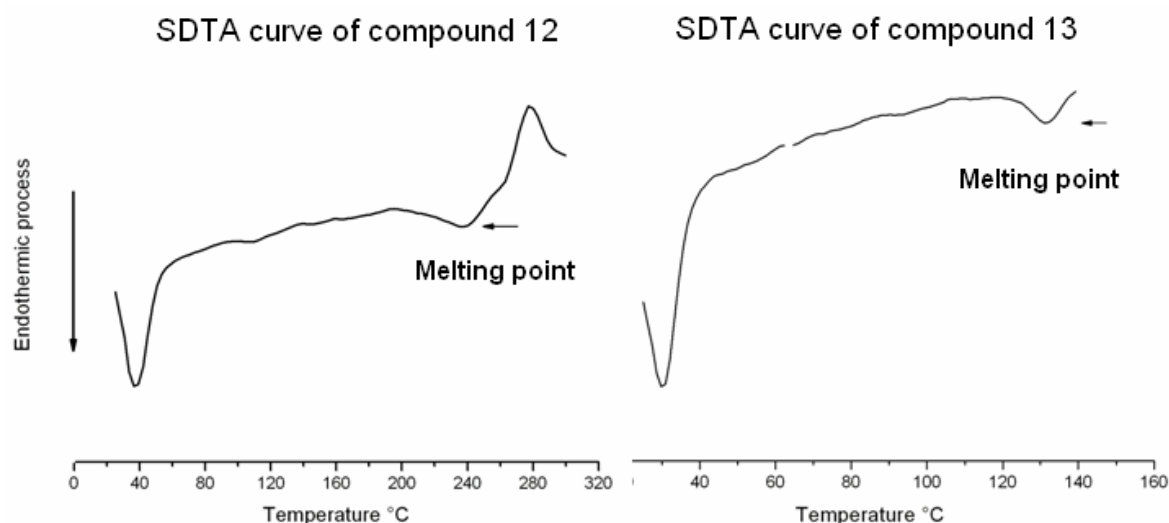
Figure 96. TG/SDTA curve of complexes 12 and 13

The interpenetrated structure **13** crystallizes in the side (H-tube) where the ligand was added in excess, after about 2 months of slow evaporation.

In entanglement phenomena in supramolecular chemistry [358], silver is a suitable metal ion used to generate interpenetrated structures [235, 239, 359, 360], especially with non- or weak coordinating counter ions like perchlorate and hexafluorophosphate [361-364], where the ligand has a decisive role.

Currently studies on these systems performed by Prof. Meuwly shows that the metallacycles without coordinating anions open up when the structures are optimized (at the DFT level). The fact that silver(I) is a labile ion, and consequently allow the ligands to go off and on in solution, suggest a possible mechanism for the formation of the polycatenanes compound **1**.

Bai et al. were able to transmit chirality through different metal cations generating in such a way new enantiomeric interpenetrated 3D nets. They were formed by chiral helical coordination silver(I) polymers using the ligand *N,N*-bis[1-(pyrazine-2-yl)ethylidene]benzil dihydrazone [365].

Analogous strategies increasing the type of nodes have used Ag(I) with other cations in order to generate structures with interesting structural designs [232, 366].

Entanglement is mostly related with the concentration of reactants, an equivalence relation ligand:metal of more than 2:1 is usually required to synthesize this kind of array. We have been conducting some experiments mixing solid $AgPF_6$ and the solid ligand **L3** in different proportions of equivalents and then heating up to the ligand melting temperature, cooling down and heating again

until over 220°C. The resulting SDTA curves obtained were especially interesting since changing the ratio of the ligand to silver(I) from 1:1 to more than 2:1 resulted in a final decomposition temperature similar to that of **12,** and **13** respectively (Figure 97).
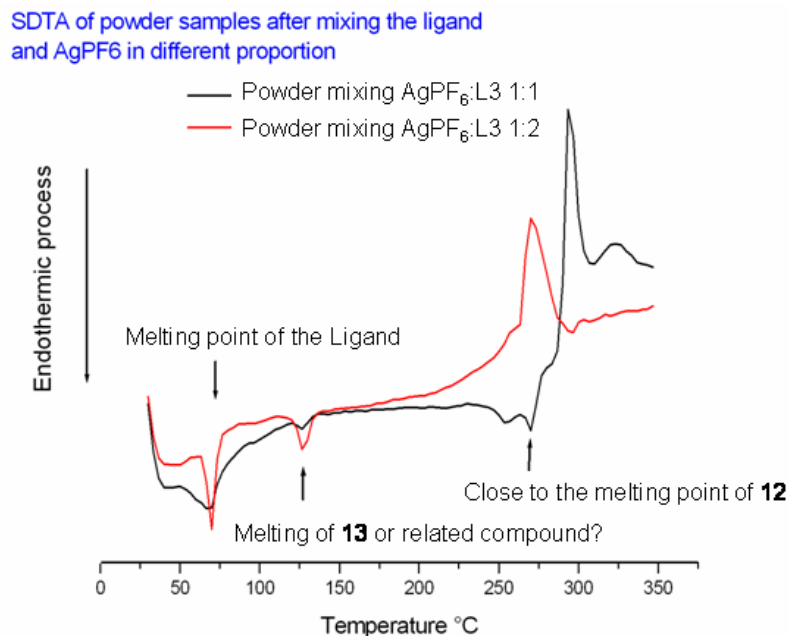
Figure 97. SDTA curve of mixing powder of ligand and silver hexafluorophosphate in different proportions

Even when the real presence of **12** or **13** (or related complexes) could be discussed based on the results obtained from TG/SDTA for powder mixing of ligand and the silver salts, the fact that we can confirm the presence of different complexes using the technique of solid state mixing, followed by heating and the use of liquid ligand as solvent is a tempting idea.

Another important difference between **12** and **13** is related to the empty space within the crystalline state. Whereas in **12** the percentage of filled space is about 70.3%, in **13** this is 68.3%, which means 58 Å^3 of available free volume for a solvent molecule (H$_2$O ~40 Å^3, small molecules like toluene ~100-300 Å^3) (Figure 98).
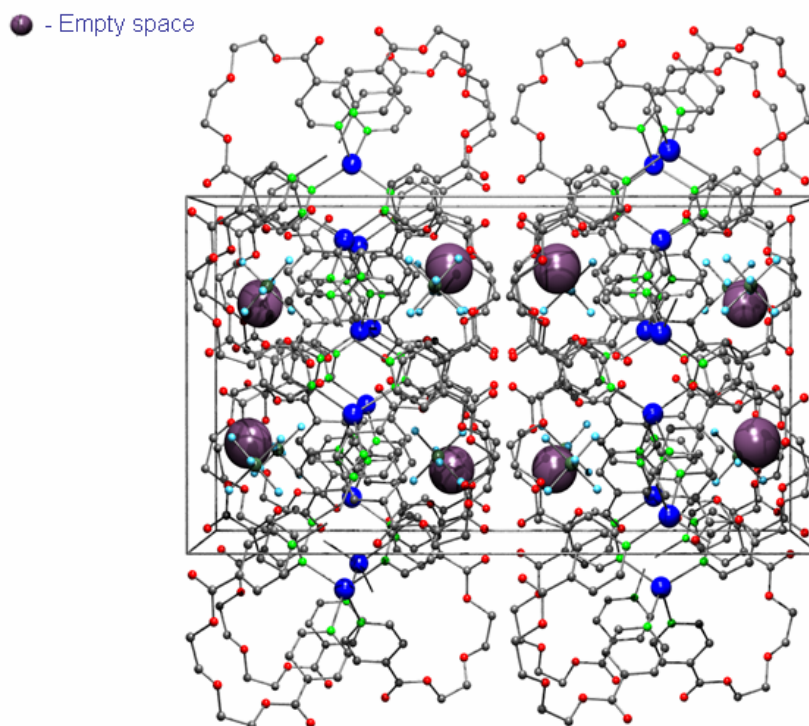
Figure 98. View along c axis of the crystal structure of complex 13. Empty space designed in dark spheres

Some confusion could arise from the use of words like "interpenetration" and "co-catenation". *Carlucci et al.* [367] described the interpenetration as a phenomenon that arises between components of the same dimensionality and results in no change of the overall dimensionality (1D → 1D, 2D → 2D and 3D → 3D); concatenation is present in all other cases as the one present here. Compound **13** belongs, according to this, to the class of polycatenated 1D motif which is linked parallel to give a 2D sheet, forming a new type of entanglement which should represent a missing link in polycatenation motifs.

The possible transformation of **12** into **13** at a temperature close to 200° C was investigated following this experiment: single crystals of complex **12** were subjected to a relatively slowly increase of temperature, until 200°C (10°C per minute). After this, the sample was subjected to an isothermal process for about 20 minutes and afterwards it was allowed to cool down until 30°C (20°C per minute). The X-ray powder spectra were recorded (Figure 99); the crystals retained their shape, but some loss in crystallinity was evident.

Powder spectra of a sample of **12** subjected to a thermic process
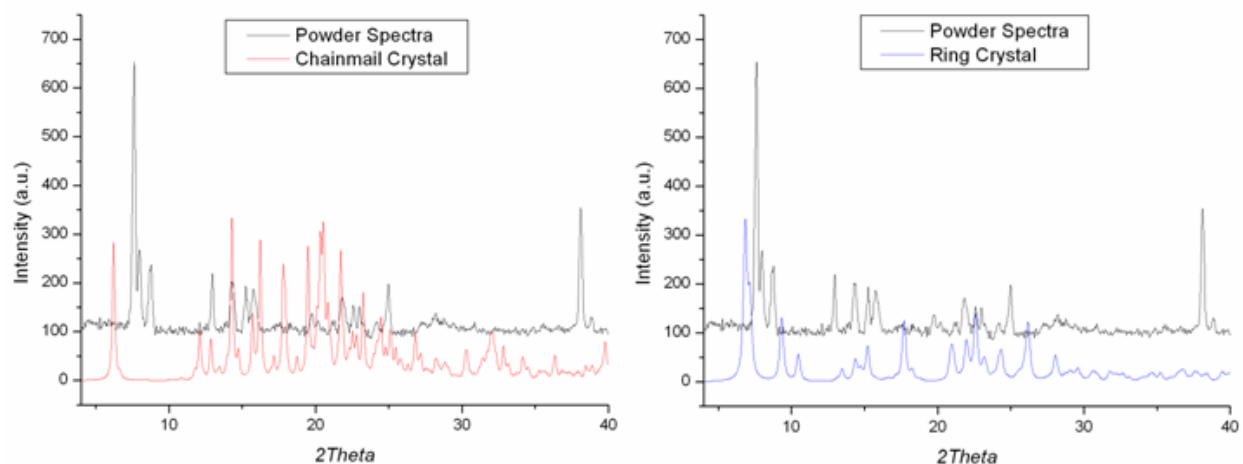
Figure 99. X-ray spectra comparison between a powder obtained after thermal treatment of crystals of 12 (black line) and the simulate powder spectra of crystal of 13 (red line) and 12 (blue line)

The thermal process was carried out under a nitrogen atmosphere. The results show a different powder pattern than both compounds **12** and **13**.

An analogue structure as **12** but using the ligand **L5** was synthesized and are described in page 152.

B - III.7 - {[Ag(L3)](SO$_3$CF$_3$)}$_2$ (14)

Complex **14** crystallizes in the monoclinic space group P2$_1$/c (No. 14), with one ligand and one counter ion coordinating a silver cation in the asymmetrical unit cell. The motif remains the same as before, the metallacycle is formed after two ligand molecules adopt a U-shape to coordinate two Ag$^+$ (Figure 100). Both pyridine rings remain almost at the same distances to the cation (Ag(1)–N(1), 2.160(4) Å and Ag(1)–N(2)$^{#1}$, 2.166(4) Å) (Table B-III.52).
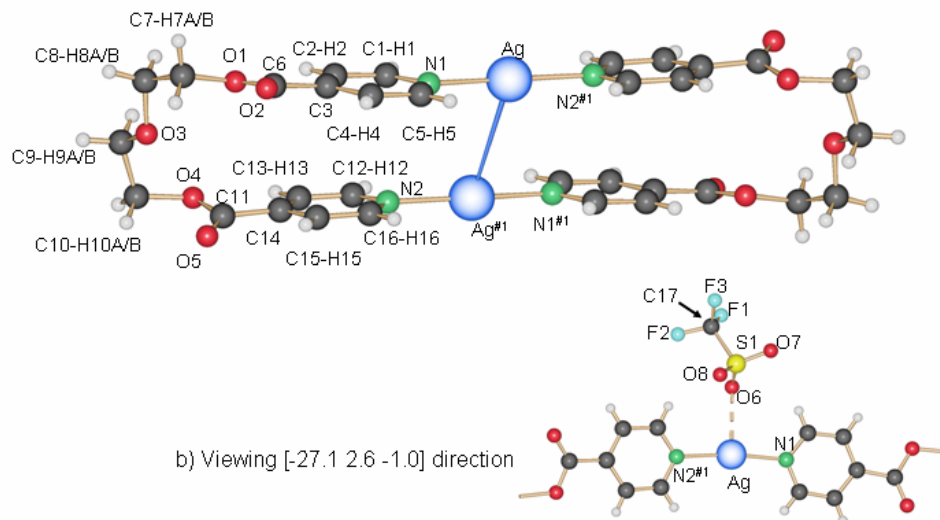
Figure 100. Metallacycle motif in complex 14.

One of the carbonyl groups is more twisted compared to the plane formed by the aromatic ring (13.6(4)° versus 7.9°); the intra-ring π-π stacking should be responsible for this phenomena.

Table B-III.52 Most important bond lengths [Å] and angles [°] present in complex **14**

Ag(1)–N(1)	2.161(3)	N(2)#1–Ag(1)–N(1)	172.1(1)
Ag(1)–N(2)#1	2.166(3)	C(1)–N(1)–Ag(1)	123.9(1)
Ag(1)–O	2.638(5)	Ag(1)–Ag(1)#1– Ag(1)#2	146.7(4)
Ag1–Ag1#1	3.576(8)		
Ag1–Ag1#2	3.832(9)		

Symmetry transformations used to generate equivalent atoms: #1 -x+1,-y+1,-z+1 #2 –x,-y+1,-z+1

All oxygen atoms in the lateral chain are in a gauche conformation mode (torsion angles O3–C9–C10–O4, 62.7(1)° and O2–C7–C8–O3, 68.1(1)°), with both carbonyl groups pointing to the same side of the metallacycle.

The counter ions are accommodated in the spaces formed by the four closest ring in a plane, and coordinate two different silver atoms from the two closest metallacycles (Figure 101).
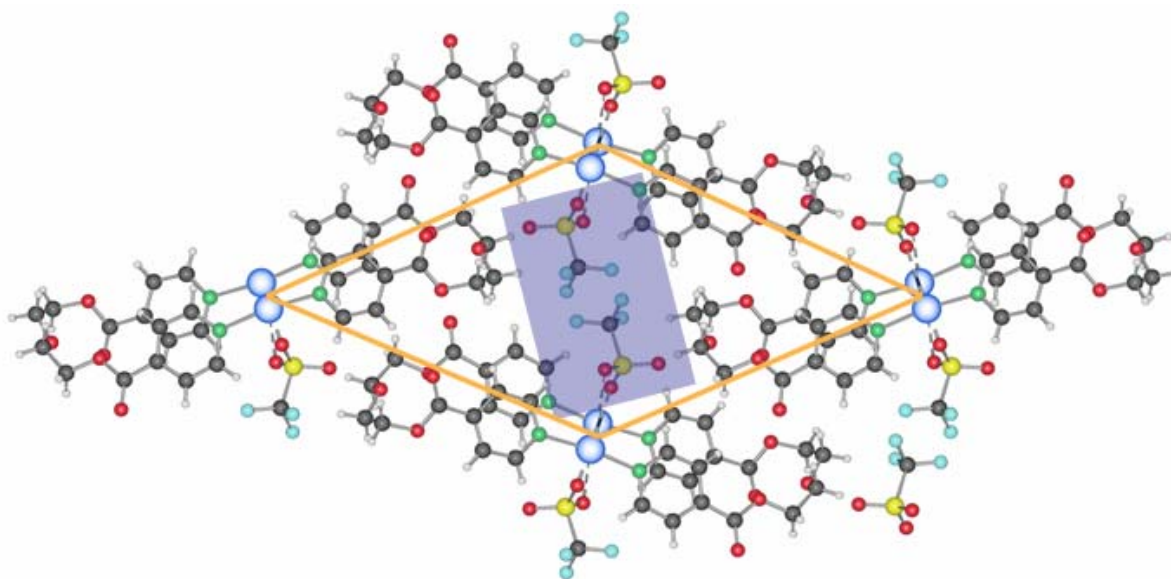
Figure 101. Schematic representation of position occupy by the counter ion in the motif (blue shadow). Triflate anion link silver from different metalla-cycle

The triflate anion coordinates the Ag(I) cation in a monodentate manner, and at the same time, using a second oxygen atom, it coordinates the silver ion located in the upper or lower ring (Figure 102).
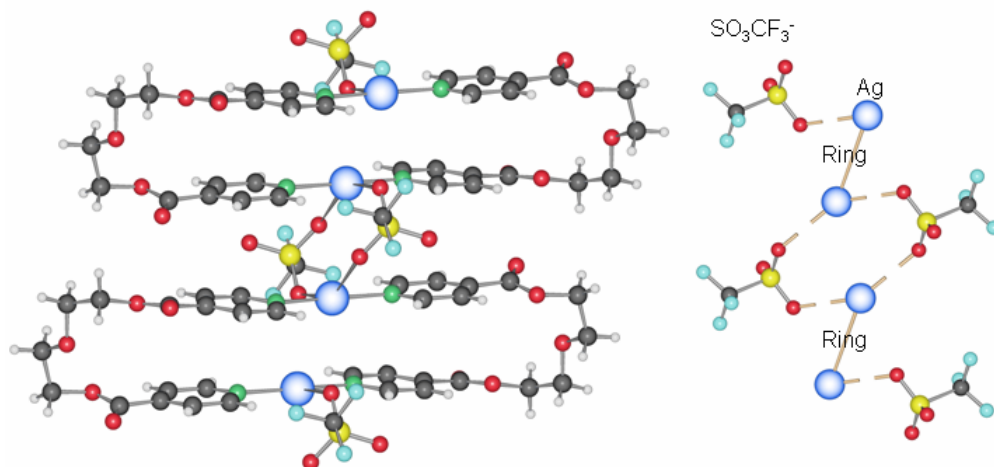
Figure 102. Counter ion position between metallacycles (left side). Right side showing bidentate coordination mode of the counter ion linking metallacycles

Due to the size of the triflate anion, the four rings surrounding two counter ions are not parallel any more, but slightly twisted (see next chapter). The linking mode of the $SO_3CF_3^-$ should be responsible

Silver Coordination Compounds with a Family of Ditopic Ligands of Varying Flexibility: About Chains, Rings, Helices and Polycatenanes

116

for the approach of the aromatic ring and indeed, attractive forces like π–π interaction stabilize the motif (Table B-III.53).

Table B-III.53 π–π stacking present in complex **14**

π–π interaction	d_{R-R} (Å)	ρd_{R-R} (Å)	α	β
Intra π–π stacking between aromatic rings of the same ligand.				
Ring (N1,C1,C2,C3,C4,C5)⋯Ring (N2,C12,C13,C14,C15,C16)[#1]	3.96	3.50	5.41	27.89
Inter π–π stacking between aromatic rings of different ligands.				
Ring (N1,C1,C2,C3,C4,C5)⋯Ring (N2,C12,C13,C14,C15,C16)[#2]	3.82	3.51	5.41	23.62
Symmetry transformation used to generate equivalent atoms: #1 1-x,1-y,1-z #2 2-x,1-y,1-z				

Table B-III.54 Hydrogen bond [length (Å) and angle (°)] present in complex **14**

D–H⋯Acceptor	d (D–H)	d (H⋯A)	d (D⋯A)	Angle D–H⋯A
Inter hydrogen bond formed between an oxygen of the triflate and an hydrogen located on the lateral chain of the ligand.				
C10–H10B⋯O7	0.97	2.54(0)	3.27(1)	132.2(3)
Symmetry transformation used to generate equivalent atoms: #1 -1+x,1/2-y,-1/2+z				

Taking advantage of the ability of their oxygen atom to form hydrogen bonds, the triflate counter ion links one hydrogen located in the lateral chain of a spatially close metallacycle to generate a three-dimensional network.

B - III.8 - General considerations about compounds 7, 8, 9, 10, 11, 12, 13 and 14.

The counter ions influence the crystalline solid state in some important aspects: (i) coordination mode concerning the metal cation, (ii) shape, and (iii) hydrogen bonding facility.

The use of different counter ions allows us to explore the impact of their supramolecular abilities forming bonds of different types and responding to the change in solvent polarity. We also learn how the ligand geometry affects the overall crystalline array.

The flexibility of the perchlorate counter ion is relevant for the number of hydrogen bonds (four for **7** and three for **8**), even if the structure has changed from a metallacycle to a helical array, changing so the coordination motif from μ^1- monodentate way to a μ^2- bidentate way in **8**. Variations in the coordination mode play a particular role in the stabilization of the crystalline network; both

phenomena seem to be related. The same effect is present in **9**, **10** and **11**: a change in the coordination mode of the nitrate counter ion is responsible for the change of the packing density (density values $\mu^1\mu^2$- (**9**) < μ^1- (**10**) < μ^2- (**11**)), and the potential presence of different metal Ag-Ag contacts (Table B-III.55).

Table B-III.55 Resume of distances and principal interactions in compounds **7-14**

Complex	Ag–N distance (Å)	Ag–Ag presence	π–π presence	Number H-bonds in the structure
7	2.148(4)–2.153(4)	3.147(8) Intra	3.70 Intra	7 (4 formed by the counter ion)
8	2.158(7)–2.161(6)	3.781(7) Inter	3.74 Inter	4 (3 formed by the counter ion)
9	2.181(5)–2.194(6)	3.320(6) Inter	3.83 Inter	6 (3 formed by the counter ion)
10	2.180(5)–2.189(5)	3.334(7) Intra 3.399(9) Inter	-	1
11	2.177(4)–2.189(4)	3.434(1) Intra 3.684(9) Intra	3.87 Inter	3 (1 formed by the counter ion)
12	2.136(4)–2.143(4)	3.459(1)	3.67 Inter	2
13	2.287(3)–2.381(3)	-	3.76 Inter 3.89 Inter	
14	2.161(3)–2.166(3)	3.576(8) Intra 3.832(9) Inter	3.96 Intra 3.83 Inter	1 formed by the counter ion)

Less-coordinating counter ions like hexafluorophosphate and trifluoromethanesulfonate are less coordinating over the silver ion, which may generate non-linear coordination geometries. At the same time these counter ions occupy more volume in the crystalline state and due the increase number of donor atoms the probabilities of forming hydrogen bonds increases, which results in the generation of amazing structural motifs like **13**.

The solvent influences the syntheses of almost all complexes. Solvent polarity directs the particular crystalline assembly of (i) compounds **7** and **8** by THF and ethanol, respectively, (ii) compounds **9**, **10** and **11** by THF/water in variable proportion and DMSO, (iii) compounds **12** and **13** have been obtained in THF/water whereas **12** was the exclusive product obtained in acetonitrile, and **14** was the main product in all attempted solvent combinations (Table B-III.56).

Different crystallization techniques were tested; the most common one was the solvent diffusion into a simple schlenk vessel or into a "H"-shaped tube through a filter, forcing the diffusion process to be slow.

Silver Coordination Compounds with a Family of Ditopic Ligands of Varying Flexibility: About Chains, Rings, Helices and Polycatenanes

118

Table B-III.56 Crystallization techniques and solvents used in the crystallization of compounds **7-14**

Compounds	Solvent or combination of solvents used	Crystallization techniques
7	THF, THF/water	Solvent diffusion, slow evaporation in TFH
8	THF/water, THF/Ethanol, Ethanol	Solvent diffusion, slow evaporation in THF/ethanol
9	THF/water	Solvent diffusion, slow evaporation
10	THF/water, Ethanol, THF/Ethanol	Solvent diffusion, slow evaporation in Ethanol
11	THF/water, DMSO	Solvent diffusion, slow evaporation in DMSO
12	THF/water, acetonitrile	Solvent diffusion, slow evaporation in all solvents
13	THF/water, acetone	Solvent diffusion, slow evaporation in acetone
14	THF/water, acetonitrile, acetone, ethanol	Solvent diffusion, slow evaporation in all solvents

Concentration is an important factor for compounds **7**, **8** and **12** and **13**, respectively. For these compounds a proportion ligand/silver salt >2, directs the syntheses to the helical chain **8** or the chainmail **13** in detriment of the metallacycle **7,** or **12** respectively. The other complexes remain the single products in the crystalline state, which does not prove that their polymeric arrays could not exist.

Mass spectra indicate actually the presence of some polymeric structures in solution. Crystals of these complexes remain stable under daylight for several months. This phenomenon has been reported in a recent publication [368].

Some silver complexes are generally weakly fluorescent at room temperature, with some exceptions [369-372] (measurements were performed at 77 K). Recently Janiak *et al*. identified the presence of new peaks around 495 nm and related them with weak Ag–Ag contacts in silver complexes [368].

When irradiated at a wavelength value correspondent to their maximum absorption value, the fluorescence curve of our compounds shows some qualitative differences compared with the spectrum of the ligand alone. This is interesting because all compounds differ in the nature of metal-metal contact. Whereas in **12** inter-ring Ag–Ag contacts are present, in **7** the closest distance between silver atoms is from the same metallacycle. In complex **11**, both kinds of contacts are present, inter- and intra- metallacycle silver–silver contacts (Figure 103). All these comparison are based on a qualitative point of view.
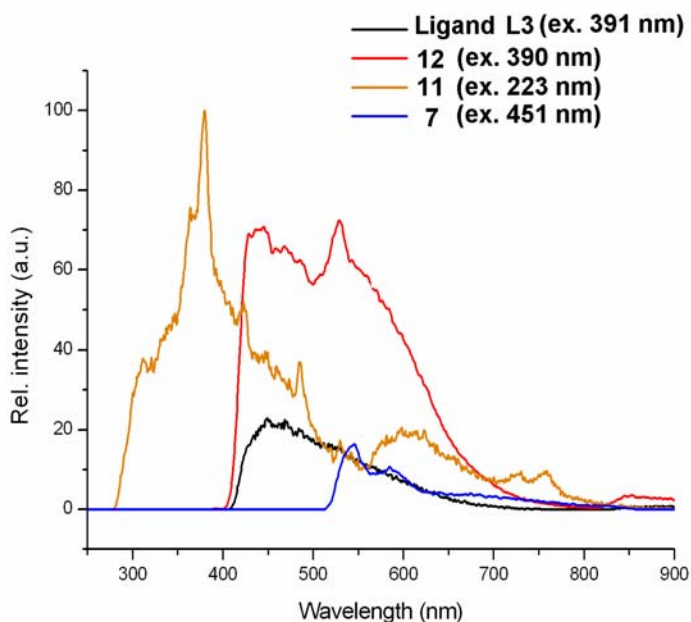
Figure 103. Solid state fluorescence in crystals of ligand L3 and 7, 11 and 12. The spectra were recorded at 77 K with 400 nm*min⁻¹ for the ligand and compound 6 and 60 nm*min⁻¹ for 7 and 11. (Some complexes were measured at different scan rate and no differences were found)

Even when the presence of weak fluorescence is usually assigned to LMCT processes, it is still quite difficult to establish a relationship between the results obtained here and the crystalline structure. Assigning the shape, intensity and location of peaks present in the curve for **11** to the presence of Ag–Ag nanowires in the crystalline state is an attractive point, but clearly it needs more experimental evidence.

Complementary measurements of fluorescence in solution should bring some clarity into this phenomenon.

DOSY-NMR analyses were performed with samples containing the ligand **L3** and $AgPF_6$ or $AgNO_3$ in different concentrations. THF-d8 was used as solvent, the NMR tubes containing the samples for the DOSY-NMR measures were prepared and sealed under argon atmosphere (Table B-III.57).

The potential formation of metallacycle in solution and the dependence of the concentration to form some specific species was envisaged at this point. The results obtained need be correlated by a theoretical model. Some differences above the limit of error were found for the ligand sample and the complexes samples. Same differences in the mobility through the solvent were found for the compounds when different concentrations are used.

Even if minimal, these differences could indicate the presence of a compound similar to the metallacycle in solution [373-375]. Some studies are being carried on in our group at this point to resolve this particular problem.

Table B-III.57 Hydrodynamic radii calculated based in DOSY-NMR experiments

	Solvent used, Temperature	DC (x 10^{-10} m^2/s) τ_1/τ_2 (ms)	Hydrodynamic radii (Å)
L3		3.018/3.081	3.63/3.55
L3AgNO$_3$ (1:1 equiv.)		2.381/2.385	4.60/4.59
L3AgNO$_3$ (2:1 equiv.)	DMSO-d6,	2.805/2.759	3.91/3.97
L3AgPF$_6$ (1:1 equiv.)	298 K	2.571/2.577	4.26/4.25
L3AgPF$_6$ (2:1 equiv.)		2.807/2.899	3.90/3.78

The radii calculated possess a ±3% error. Measure times $\tau 1$= 250 ms and $\tau 2$ = 500 ms.

B - III.9 - Theoretical calculations on metallacycles

Some DFT calculations using the B3LYP/6-311++G** method were performed on the ligand of the metallacycles. The goal was to estimate how much stabilization the ligand affords the general metallacycle motif.

After the silver cation and the nitrate anion were removed from the crystal structure of these compounds, the crystallographic coordinates of the organic tecton were unchanged and used without further optimization. The difference of total energy (Δ**E total**), energy due to π–π interactions (Δ**E ring**) and stabilization energy due to the diethylene glycol conformation (Δ**E τorsion**) were calculated using values obtained for the ligand **L3** as reference (Table B-III.58).

Table B-III.58 DFT calculation results for the ligand in the metallacycles

Compound	ΔE total	π–π (Å)	ΔE ring	$\tau_{torsion}$ (°)	ΔE τorsion
Ligand **L3**	-	5.801(6)	-	69.9(2), 62.6(6)	-
7 (ClO$_4^-$)	-28.63	3.704(5)	-19.96	52.7(1), 67.7(4)	-8.21
9 (NO$_3^-$)	+9.99	5.142(6)	-7.22	62.3(9), 50.8(2)	+16.46
10 (NO$_3^-$)	+20.07	4.082(9)	-5.12	73.2(9), 15.4(2)	+25.42
11 (NO$_3^-$)	+74.14	4.149(8)	+3.00	46.1(4), 79.3(6)	+68.72
12 (PF$_6^-$)	-6.03	5.775(8)	-7.62	67.2(5), 70.2(7)	+0.82
14 (SO$_3$CF$_3^-$)	-3.94	3.965(4)	-5.84	62.6(8), 68.0(9)	+1.41

All calculated energies are given in kcal/mol

Silver Coordination Compounds with a Family of Ditopic Ligands of Varying Flexibility: About Chains, Rings, Helices and Polycatenanes

121

This preliminary calculation shows interesting results. The **ΔE ring** may depend on the distance between the centroids of the rings and the way in which the pyridine rings are stacked together (Figure 104). Approaching the centroids of two aromatic rings may increase the repulsion between the aromatic electrons, this is proportional to the values founded for **ΔE ring**. This increase of energy is reaches a maximum at a distance about 4.14 Å (compound **11**) and then drops after 4.08 Å (-7.22 kcal/mol, compound **10**) and reaches a minimum at 3.70 Å (-19.96 kcal/mol, compound **7**).
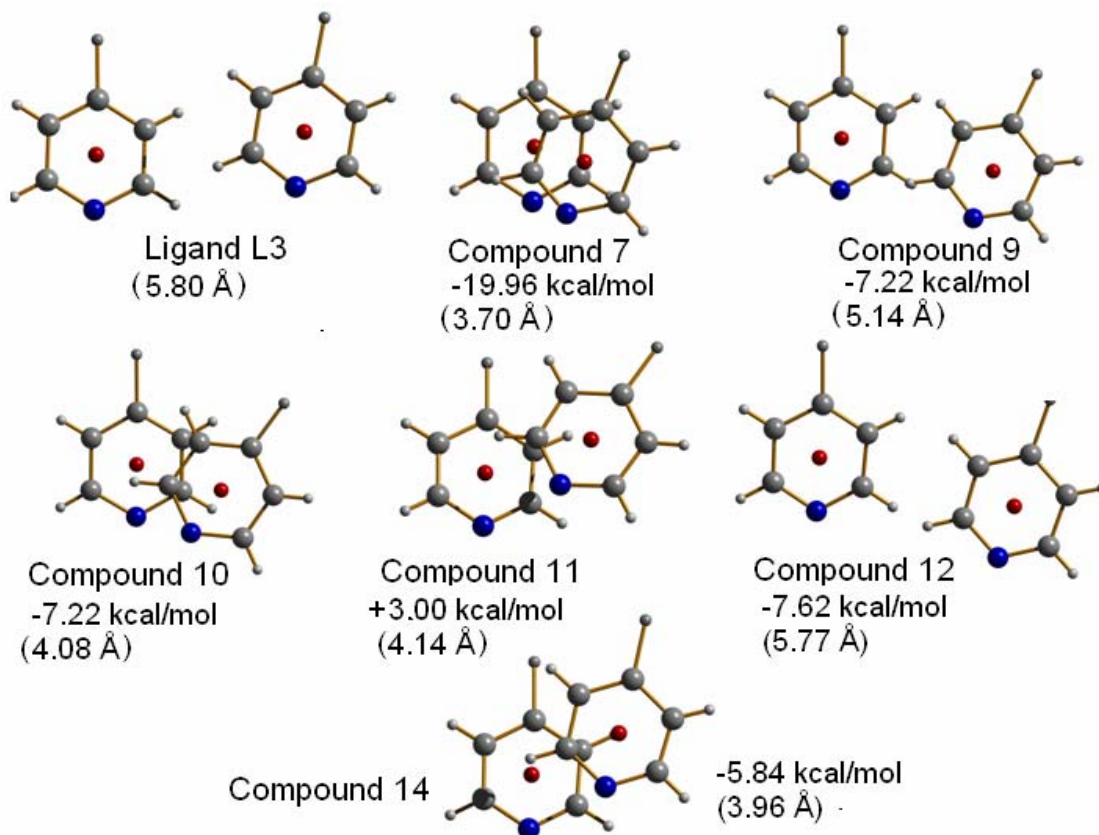
Figure 104. π–π stacking energies calculate using the B3LYP/6-311++G** (DFT) method, the values are given as the difference versus the energy of the π–π stacking in the ligand L3. The distances are calculated between ring centroids (red). For the calculation the carbonyl group was substituted for a hydrogen atom (light gray)

Concerning the diethylene glycol chain, the torsion angles of compounds **10** and **11**, are relatively constrained compared to the values founded in the organic ligand of other metallacycles. This fact could explain in part the energy difference, which may significantly destabilize the rings in both these compounds compared to the other metallacycles in this series.

The **ΔE total** is calculated without taking into account the ligand-silver(I) and silver(I)-counter ion interactions in the metallacycle (Table B-III.59), thus, this result concerns only the ligand part of the ring. Is noteworthy that the value of **ΔE total** is approximately equal to (**ΔE ring** + **ΔE τorsion**). That indicates that the substitution of the carbonyl group for a hydrogen atom, to calculate the stacking energy between aromatic rings, does not significantly effect the result of **ΔE ring**.

Table B-III.59 Supramolecular nteractions present in the metallacycles

Complexes	Ag–N (Å)	Ag–O/F (Å)	π–π (Å)	$\tau_{torsion}$ (°)	Ag–Ag (Å)
7 (ClO_4^-)	2.149(5)	2.930(8)	3.704(5) *intra*	52.7(1)	3.145(9) *intra*
	2.154(9)	3.453(0)	5.460(0) *inter*	67.7(4)	5.095(5) *inter*
9 (NO_3^-)	2.194(6)	2.741(6)	5.142(6) *intra*	62.3(9)	4.491(1) *intra*
	2.181(6)	2.830(2)	3.763(9) *inter*	50.8(2)	3.320(3) *inter*
10 (NO_3^-)	2.189(0)	2.738(8)	4.082(9) *intra*	73.2(9)	3.334(6) *intra*
	2.180(5)	2.579(2)	4.088(7) *inter*	15.4(2)	3.399(0) *inter*
11 (NO_3^-)	2.188(6)	2.653(2)	4.149(8) *intra*	46.1(4)	3.434(1) *intra*
	2.176(8)	2.658(1)	3.874(1) *inter*	79.3(6)	3.684(4) *inter*
12 (PF_6^-)	2.143(1)	2.960(4)	5.775(8) *intra*	67.2(5)	5.213(1) *intra*
	2.136(6)	3.018(3)	3.670(6) *inter*	70.2(7)	3.459(3) *inter*
14 ($SO_3CF_3^-$)	2.160(9)	2.638(6)	3.965(4) *intra*	62.6(8)	3.576(2) *intra*
	2.166(1)	3.243(9)	3.829(3) *inter*	68.0(9)	3.832(5) *inter*

Interestingly, when crystals of **11** are heated for a week at 80°C, the crystalline structure transforms into **10**, where the silver(I) cation is asymmetrically coordinated by the nitrate counter ion. This phenomenon agrees with the plausible gain in energy for the ligand when passing from **11** to **10** (about +54 kcal/mol, Table B-III.59). However, previous calculations on the metallacycles of **10** and **11,** without considering the counter ion, show the opposite result. In this case the metollacycle in **11** seems to be energetically more stable than the metallacycle in **10**. The theoretical effect of the counter ion in both structures is currently under investigation.

B - IV - L5 and L6 and their Ag (I) complexes. The helicate motif

Helical arrays belong intrinsically to the Nature. They take part in a role, not just important, but decisive for life. Structures as the DNA unquestionable play the key function in formation and development of all living species [376, 377].

Within the realm of supramolecular chemistry, the emulation of systems based on Nature examples has attracted researchers since the publication of Jean M.-Lehn *et al.* in 1987 of a system based in the 2,2'-bipy and Cu(I), which undergoes self-assembly generating dinuclear and trinuclear 'double-stranded helicates' [378] (Figure 105).
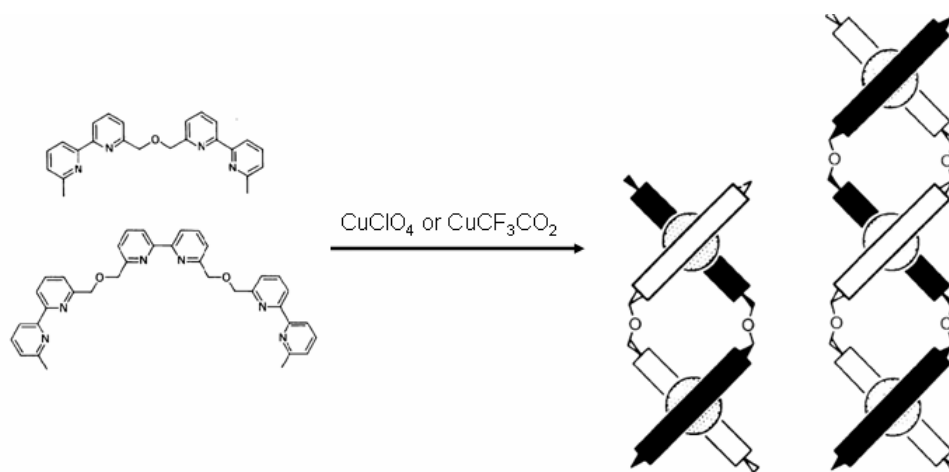
Figure 105. Helical complexes synthesized by Lehn et al. using bipy derivate ligands. This work presented for the first time concepts like self-assembly and cooperativity in supramolecular systems

The research on helicates is not exclusively based on their inherent structural beauty, but in the high degree of sophistication and effectiveness of these systems driving life processes. In most of the numerous examples of helical arrays found in the literature [19, 21, 298, 365, 379-390], two important distinctions should be made: i) helical arrays which exist in solution and eventually in the solid state [264, 297, 391-394] and ii) helical arrays found in the crystalline state but without experimental evidence of existing in solution, which suggests that their formation is strongly influenced by the crystallization process itself [2, 159, 221, 395, 396].

The generation of helices is a process which could be basically directed by the metal cation with or without the cooperative effect of the ligand used. Their synthesis have created the basis for concepts like 'cooperativity' and 'self-assembly'. The type of ligand employed is related to the coordination geometry of the metal cation. More rigid organic ligands are used to generate helical motifs with metals possessing a tetrahedral or octahedral geometry (Figure 106) [397-402].
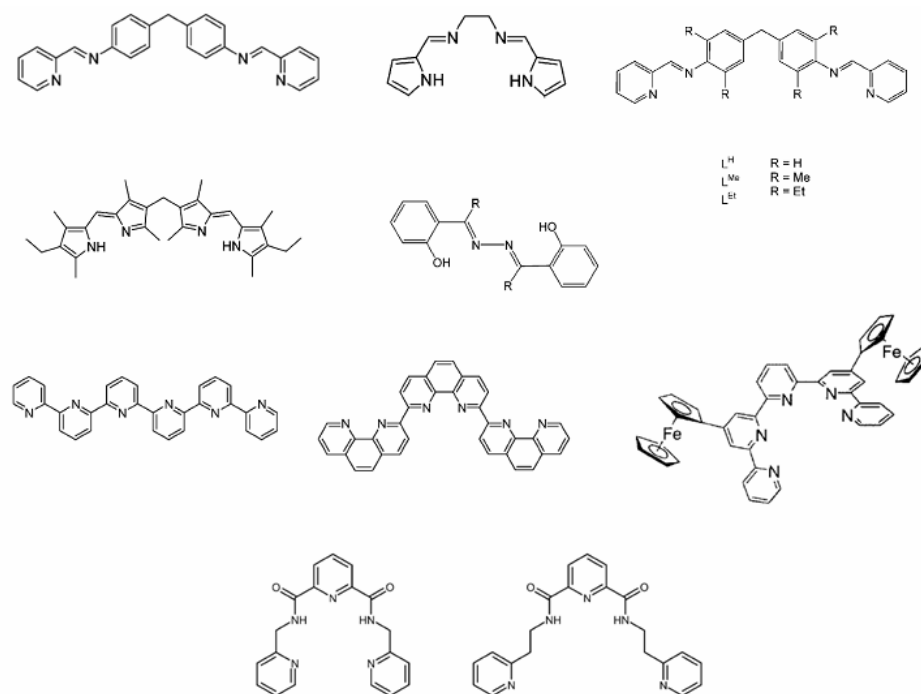
Figure 106. Rigid ligands used in the generation of helical supramolecular arrays

Flexible ligands are able to generate the helical motif through an efficient occupancy of the coordination sites of the silver cation by the ligand, but the experimental evidence of helicates formation remain delimited to the crystalline state [403-406]. Some reference to the formation of a silver complex in solution was published by Cai *et al*. [314], who found one and two strand helical complexes with silver. However, the presence of helicity in solution was not prove.

Concerning the topology, helical supramolecular complexes can be of *single-stranded* type, which are present usually when a metal cation with a linear coordination geometry is coordinated by shorter organic ligands with a "*twisting facility*" like pyradizine [332]. Some other examples have been recently reported [407, 408].

Double-stranded helicates are at the origin of supramolecular chemistry, and they are usually dependent on the coordination geometry of the metal (tetrahedral and/or octahedral) [19, 378, 379, 391, 409-411].

Increasing the coordination number of the metal cation when we move in the periodic table from the alkaline/alkaline earth metals to the lanthanides series implies the use of more ligands to fulfill the coordination sphere around the metal. *Triple-stranded helical* arrangements of ligands surrounding lanthanide cations are a common motif in this field of research. The helicate ligand is useful in this chemistry for several reasons: i) it acts as antenna for the transfer of energy to the metal cation ii) it wraps the metal cation avoiding the presence of solvent molecules, which can otherwise quench the luminescence properties of the complex and iii) the geometry of the ligand can control the distance between two metallic cations in the helicate affording new chemical-physical properties [387, 412].

Four-stranded helicates have been reported in the literature but their present is rare. A case where palladium and copper were used to generated this kind of arrangement has been reported for McMorran in 1998 [413]. Pentatopic ligands (**L$_5$**) have been synthetized to generate two supramolecular architectures with silver(I) ions, one of them a [4+5] grid $[Ag_{20}(\mathbf{L_5})_9]^{20+}$. The other structure is a quadruple-stranded helicate $[Ag_{10}(\mathbf{L_5})_4]^{10+}$ with four ligand strands binding to a total of 10 silver(I) ions. These ligands are wrapping around the metal ion [414].

In 1998, Saalfrank *et al* reported the first *hexa-stranded helicate* with six ligand strands wrapping around metaloxo clusters $[M_8O_2]^{12+}$ (M) Zn(II), Cd(II), Mn(II) [415].

Concerning the cation, the helical array could be *homometallic* or *heterometallic*. *Homometallic helicates* are in the base of supramolecular chemistry [378, 416]. However, the use of different metal cations to exploit the physical and chemical properties of both cations is the final goal of the actual research in this field [417].

It has been shown that flexible ditopic ligands with potential coordination sites in the spacer (oligooxygen donors or oligonitrogen donors) tend to adopt helical arrangements when they are combined with a suitable metal atom [159].

In this sense, silver salts constitute an excellent model due to their coordination properties [24, 117, 138, 418]. On the other side, ligand **L5** was conceived taking into account the necessary requirements to provide several possible contacts between the metal cation and the organic ligand through multiple potential coordination bonds.

Previous work released by Jouaiti *et al.* at the Louis Pasteur University in France, showed the implicit tendency of tectons like these to arrange itself in DNA type structures when combined with silver and non-coordinating ions like PF_6^- and BF_4^- [419].

The hexaethylene and tetraethylene glycol used by these authors as spacer between pyridines, provided enough binding sites and flexibility to fully coordinate the cation. The resulting structure is similar to a pseudo crown-ether array. The counter ion remains non- or less coordinating against the metal cation. In this work, the length of the tetraethylene glycol spacer was highlighted as determinant to generate the helical motif (Figure 107).
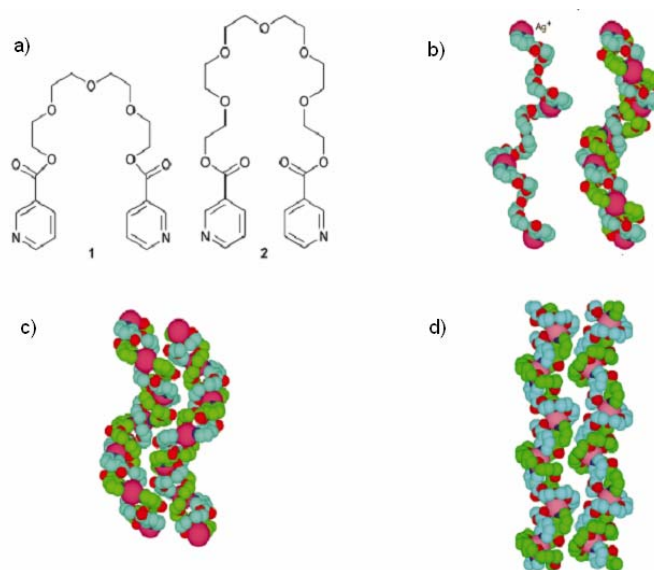
Figure 107. a) Ligands used in the generation of double stranded helices b) a portion of a single strand infinite helical coordination network through the bridging of consecutive tectons 1 by Ag^+ cations ($AgBF_4$) c) description of the conformation adopted by 1 in the crystalline phase d) a portion of the double helix formed between two single stranded helices generated upon self assembly between 2 and $AgPF_6$

B - IV.1 - Silver (I) complexes with ligands L5 and L6

Ligands **L5** and **L6** were synthesized envisaging flexibility. The triethylene glycol moity used as spacer may be important for the coordination of a second metal ion (Ca^{2+}, Ba^{2+}). The coordination compounds obtained using the ligands **L5** and **L6** with silver(I) salts and the network packing of these compounds are exposed in this part of the thesis.

Silver Coordination Compounds with a Family of Ditopic Ligands of Varying Flexibility: About Chains, Rings, Helices and Polycatenanes

127

B - IV.2 - {[Ag(L5)]SO$_3$CF$_3$}$_n$ coordination polymer (16)

Single crystals of medium quality were obtained after slow evaporation of a solution where the silver triflate and the organic ligand were dissolved. The crystals obtained were measured but the R$_1$ remains at about 12%. Crystals with optimal quality to be measured by X-ray diffraction of the same complex were isolated and measured after diffusion in a "H"-shaped tube in both sides.

The complex {[Ag(**L5**)SO$_3$CF$_3$]}$_n$ (**16**) crystallizes in the monoclinic space group P2$_1$/c (No.14) group, and could be described as two parallel helical chains composed by a repetitive motif of one silver coordinated by two ligands with distance Ag–N(1) of 2.168(4) Å and Ag–N(2) of 2.160(4) Å, forming an infinite one dimensional helical chain with a pitch of 17.860(3) Å (distance Ag1–Ag1') (Figure 108).
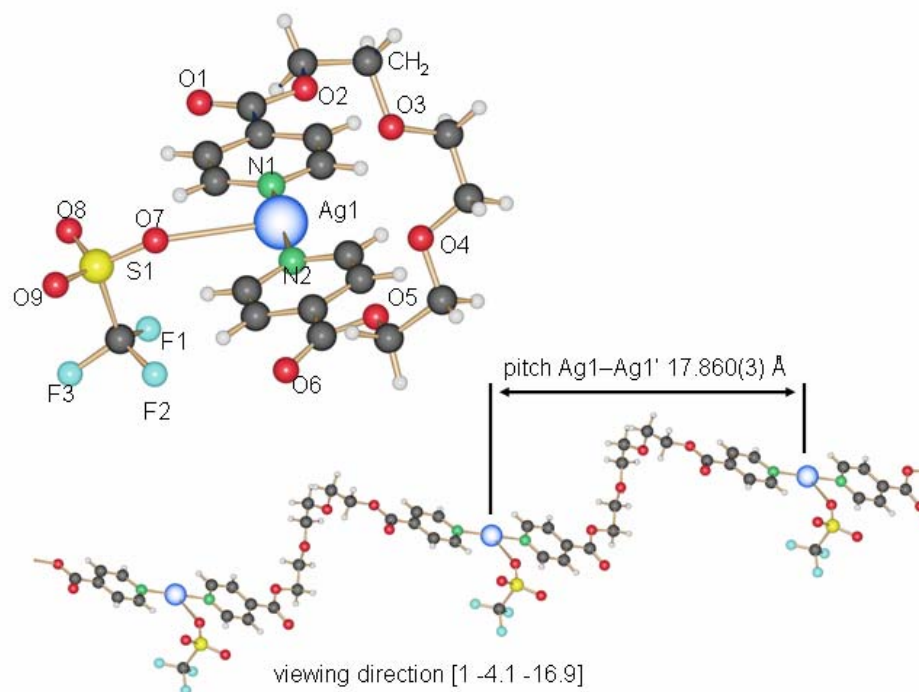
Figure 108. Infinite helical array in 16

The counter ion coordinates very weakly and in a mono-dentate way to the metal ion through the oxygen atom, Ag–O7 2.719(9) Å, (N1–Ag–N2 of 178.5(1)°). This metal cation is coordinated as

well by two oxygen atoms of the triethylene glycol moiety belonging to a parallel metallorganic polymer (Ag–O3, 3.136(7) and Ag–O4, 3.038(1) Å) (Figure 109).
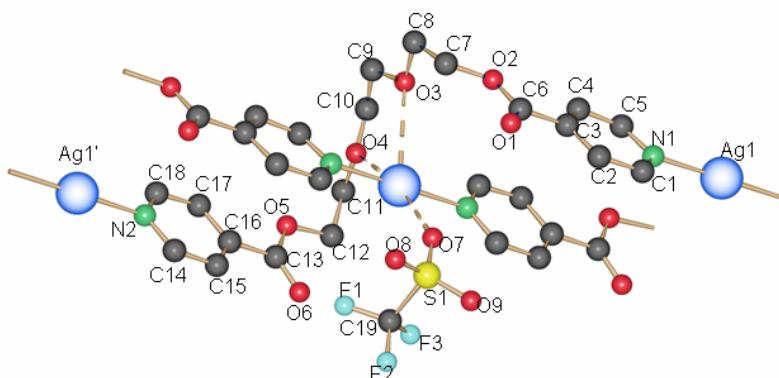
Figure 109. Double helical array generation in 16 after the coordination of the silver cation in one chain by the oxygen atoms of a second chain running in a parallel direction

The silver cation possesses a trigonal bi-pyramidal geometry (Table B-IV.60) in which both aromatic rings coordinating the metal atom are twisted by 9.68°.

Table B-IV.60 Most important Bond lengths [Å] and angles [°] present in complex **16**

Ag(1)–N(1)	2.168(4)	N(1)–Ag(1)–N(2)[#1]	178.5(1)
Ag(1)–N(2)[#1]	2.160(4)	N(1)–Ag(1)–O(7)	87.1(1)
Ag(1)–O7(SO$_2$CF$_3$)	2.720(9)	N(2)[#1]–Ag(1)–O(7)	94.0(1)
N–C	1.321(3), 1.341(4)	C–N–C	118.8(1)
Ag(1)–O(3)[#1]	3.037(1)		
Ag(1)–O(4)[#1]	3.145(7)		
Symmetry transformations used to generate equivalent atoms: #1 2+x, y, z			

One of the planes containing the carbonyl group is twisted compare to the plane of the aromatic ring, being the torsion angle C17–C16–C13–O5 10.7(3)°. The lateral chain elongates them to wrap the metal ion. Some π–π interaction exists within the double helice between rings of individual chains (Figure 110 a), and even when they are weak, their stabilizing effect in the helical motif should not be minimized (Table B-IV.61).
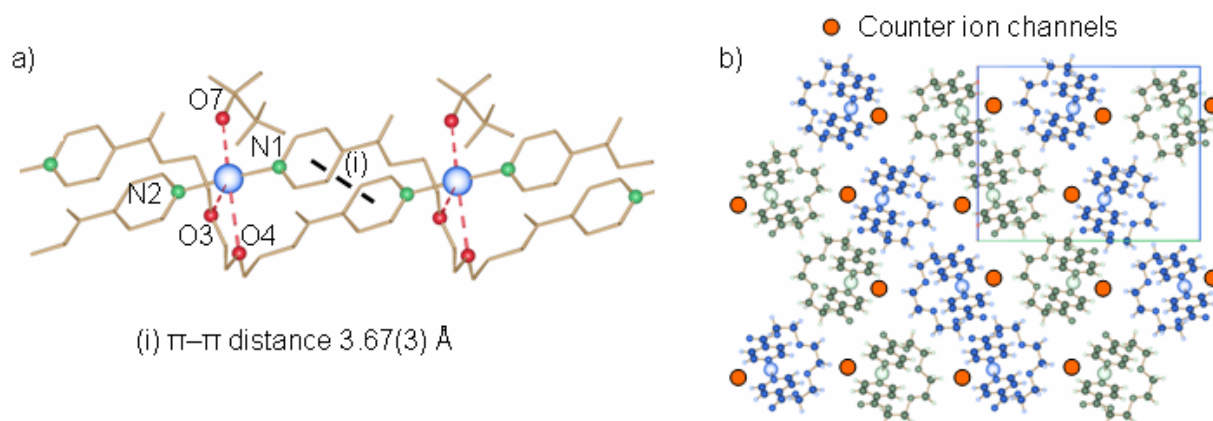
Figure 110. Counter ion position within the crystalline structure of complex 16

Four parallel double helices are contained in the unit cell, aligned in the (0 0 1) direction. These chains are packed with alternating opposite chirality. Distances between silver atoms of different chains with opposite chirality are 11.332(1) Å (blue-blue or green-green) and 17.071(4) Å between the more distant helices (blue-green) in the unit cell (Figure 110 b).

The counter ion plays an important role in the formation of hydrogen bond interactions in order to bring helices closer, and increases the stability and density in the crystalline packing. Examples have already been published how the counter ion, due to its coordination abilities, can exert a definitive role in the crystal package [332, 420].

The counter ion can distort in some cases the whole structure i) acting as bridging point between metal cations [183], and ii) in other cases approaching motifs that otherwise would be independent [389]. The $CF_3SO_3^-$ counter ion belongs to the anion type that can act poly-dentately as in **6**, or mono-dentately as in **5**.

In **16,** the oxygen atom (O7) of the $SO_3CF_3^-$ anion coordinates to the Ag cation, and forms hydrogen bonds with the hydrogen atoms H1 and H18 (C1–H1···O7, 2.48 Å and C18–H18···O7, 2.68 Å). Other hydrogen bonds are formed between the carbonyl group and a hydrogen atom of the pyridine group of the closest helical array (C2–H2···O1, 2.56 Å). A third double helical array forms hydrogen bonds through the counter ion (C4–H4···O8, 2.45 Å). At last one fluor atom coordinates a hydrogen atom of the lateral chain (C7A–H7B···F2, 2.71 Å).

Silver Coordination Compounds with a Family of Ditopic Ligands of Varying Flexibility:
About Chains, Rings, Helices and Polycatenanes

130

Table B-IV.61 π–π stacking present in complex **16**

π–π interaction	d$_{R-R}$ (Å)	ρd$_{R-R}$ (Å)	α	β
Inter chain π–π stacking between aromatic rings				
Ring (N1,C1,C2,C3,C4,C5)···Ring (N2,C18,C17,C16,C15,C14)[#1]	3.67	3.47	9.68	17.43
Symmetry transformation used to generate equivalent atoms: #1 1+x,y,z				

Table B-IV.62 Hydrogen bond [length (Å) and angle (°)] present in complex **16**

D–H···Acceptor	d (D–H)	d (H···A)	d (D···A)	Angle D–H···A
Intra chain hydrogen bonds between the anion and the pyridine ring hydrogen				
C1–H1···O7[#2]	0.93	2.48(0)	3.20(8)	134.4(6)
C18–H18···O7[#3]	0.93	2.68(4)	3.41(8)	136.4(2)
Inter chain hydrogen bonds between the anion and the pyridine ring hydrogen				
C2–H2···O1[#4]	0.93	2.52(2)	3.19(8)	126.4(2)
C4–H4···O8	0.93	2.45(3)	3.12(8)	128.9(1)
C9–H9B···O8[#5]	0.97	2.47(2)	3.43(1)	173.0(2)
Exo hydrogen bond formed between the anion hydrogen from the pyridine ring				
C7A–H7B···F2[#6]	0.97	2.71(0)	3.41(8)	128.7(1)
Symmetry transformation used to generate equivalent atoms: #2 x,1/2-y,-1/2+z , #3 -2+x, y, z #4 1-x,-y,-z, #4 -1+x,y,z #5 1-x, -y, -z				

B - IV.3 - {[Ag(L5)]PF$_6$}$_2$ metallacycle (17)

When a solution of silver hexafluorophosphate in water was allowed to diffuse through THF to a solution of THF containing the ligand, suitable crystals for X-ray analysis could be isolated and measured.

The compound **17** crystallizes in the triclinic space group P-1 (No. 2) with one silver cation, a ligand and one counter ion present in the asymmetric unit. Compound **17** exhibits the following structural motif: two ligands in U-shape coordinate two metal cations each, forming a metallacycle similar to compound **12**, but with **L5** instead of **L3** (Figure 111).

Silver Coordination Compounds with a Family of Ditopic Ligands of Varying Flexibility:
About Chains, Rings, Helices and Polycatenanes

131
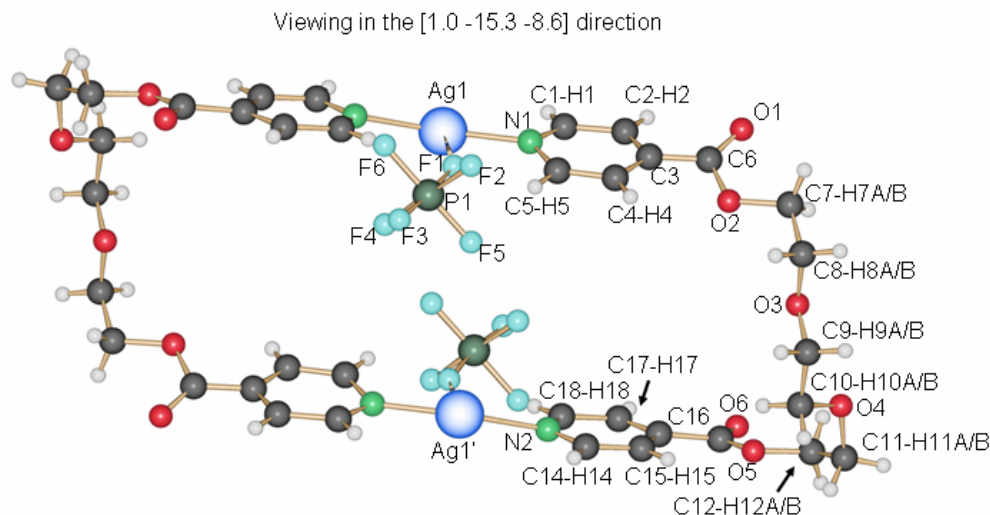
Figure 111. Metallacycle structure of 17

The nitrogen atoms of the aromatic rings coordinate the metal ion almost symmetrically with distances of Ag1–N1, 2.132(6) Å and Ag1–N2, 2.047(6) Å. The coordination environment of the metal ion is similar to that of **16,** where the oxygen atoms of the triethylene glycol moiety coordinate the silver cation with distances of Ag1–O3, 2.841(9) Å and more distant Ag1–O4, 3.243(1) Å (Figure 112).
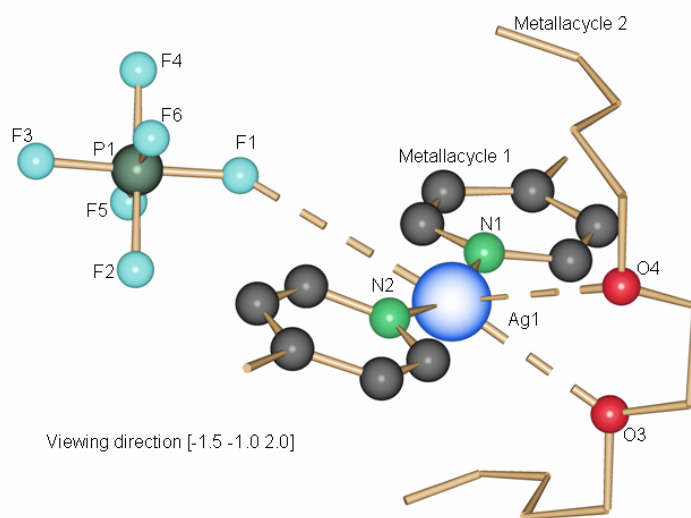
Figure 112. Coordination environment around the metal cation in complex 17. The PF$_6^-$ counter ion is weakly coordinating toward the Ag(I) cation

The counter ion coordinates extremely weak to the metal cation (F1–Ag1, 3.690(1) Å). The angle N1–Ag1–N2 of 163.0(2)° inclined in the direction of the oxygen atoms indicates a stronger

interaction with the triethylene glycol spacer than with the counter ion. The larger triethylene glycol spacer elongates the distance Ag1–Ag1$^{#1}$ to 6.802(1) Å compared with **9** (about 5.2 Å). The larger distance in the metallacycle is 18.112(5) Å (from ligand to ligand C9–C9$^{#1}$).

The pyridine rings coordinating the same metal cation are not parallel (12.7° twisting angle between both). Whereas the carbonyl group O5–C13–O6 remains in the plane formed by the aromatic ring (N2–C14–C15–C16–C17–C18), one carbonyl oxygen coordinates the silver cation of an adjacent metallacycle (O1–Ag1, 2.968(1) Å) and this carbonyl group O1–C6–O2 is twisted against the plane of the aromatic ring N1–C1–C2–C3–C4–C5 by 21.7(1)°.

Torsion angles O2–C7–C8–O3 (78.7(4)°), O3–C9–C10–O4 (63.3(4)°) are similar to **16**. However, O4–C11–C12–O5 (-70.0(5)°) turns the molecule to the metallacycle formation and avoids the stretching of the ligand **L5** to form an helical array like in **16**.

Table B-IV.63 Most important bond lengths [Å] and angles [°] present in complex **17**

Ag(1)–N(1)	2.132(6)	N(1)–Ag(1)–N(2)$^{#1}$	163.0(2)
Ag(1)–N(2)$^{#1}$	2.047(6)	N(1)–Ag(1)–F(5)	81.7(1)
Ag(1) –O(3)$^{#2}$	2.841(9)	N(1)–Ag(1)–O(3)$^{#1}$	89.4(2)
Ag(1) –O(4)$^{#2}$	3.243(1)	N(1)–Ag(1)–O(4)$^{#1}$	112.1(1)
Ag(1)–F5(PF$_6$)	3.690(1)	C–N–C	116.5(3)
N–C	1.302(4), 1.368(5)		

Symmetry transformations used to generate equivalent atoms: #1 -1–x, 1-y, -z #2 –x, 1-y, -z

Two different kinds of hydrogen bonds are present in the structure. The oxygen atoms of the lateral chain coordinate hydrogen atoms of the pyridine (C1–H1···O3, 2.58 Å and C14–H14···O4, 2.50 Å) approaching adjacent metallacycles together. More interestingly, the oxygen atom of the carbonyl group and the hydrogen atoms of the ethylene moiety are forming hydrogen bonds, but these bonds pass through the cavity formed by a metallacycle and joint separated metallacycles that otherwise would not be in contact (Figure 113).
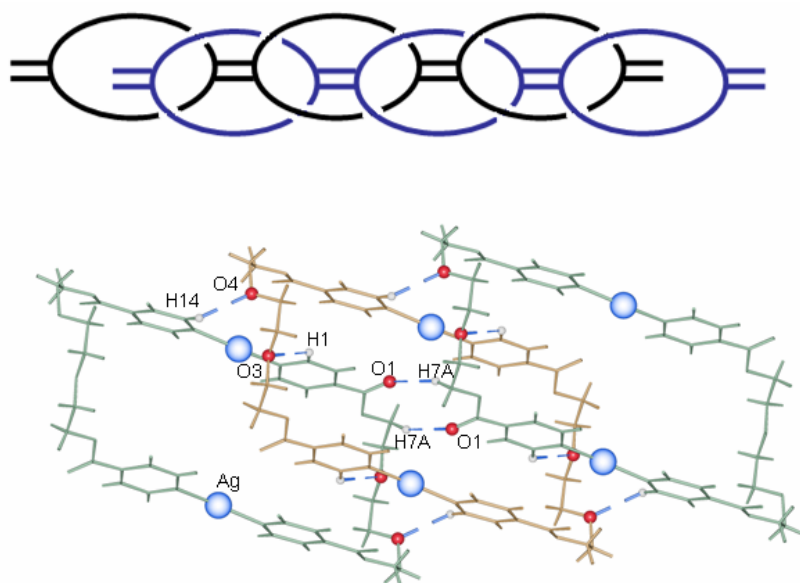
Figure 113. Hydrogen bonds generation within metallacycles. The bond O1···H7A–C7 links two different metallacycles which otherwise would not be in contact

Metallacycles are stacked together through interactions with hydrogen atoms of the lateral chain and the carbonyl group. A sum of other weak interactions like π–π interactions are present and sustain the crystalline array (Table B-IV.64), even if counted alone, they are too weak to be considered decisive from the stabilization point of view (Figure 114).

π–π interaction
a) 3.97(1) Å
b) 3.87(1) Å
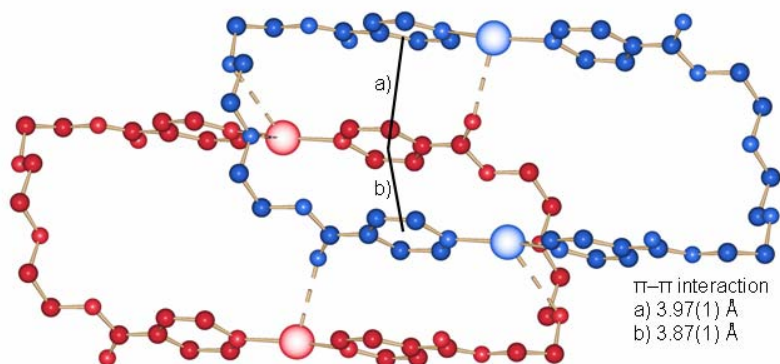
Figure 114. **Aromatic-aromatic interaction in complex 17. Oxygen atoms of the triethylene glycol chain and one carbonyl oxygen coordinate the silver cation**

Hexafluorophosphate is also able to form hydrogen bonds, but these are less directional. The PF_6^- anion forms hydrogen bonds with hydrogen atoms of the same metallacycle (C5–H5···F5, C18–H18···F6, C18–H18···F1, C1–H1···F3, C2–H2···F3 and C14–H14···F4), and with hydrogen atoms of

other metallacycles spatially close enough (C11–H11A···F6, C18–H18···F2, C9–H9B···F2, C7–H7B···F2, C7–H7B···F5 and C8–H8B···F4) (Table B-IV.65).

The counter ion is placed in between the sheet formed by macrocycle motifs joined by hydrogen bonds O···H. Due to the weakness of the hydrogen bonds formed by the hexafluorophosphate, these act more like a cement in the crystalline motif (Figure 115).
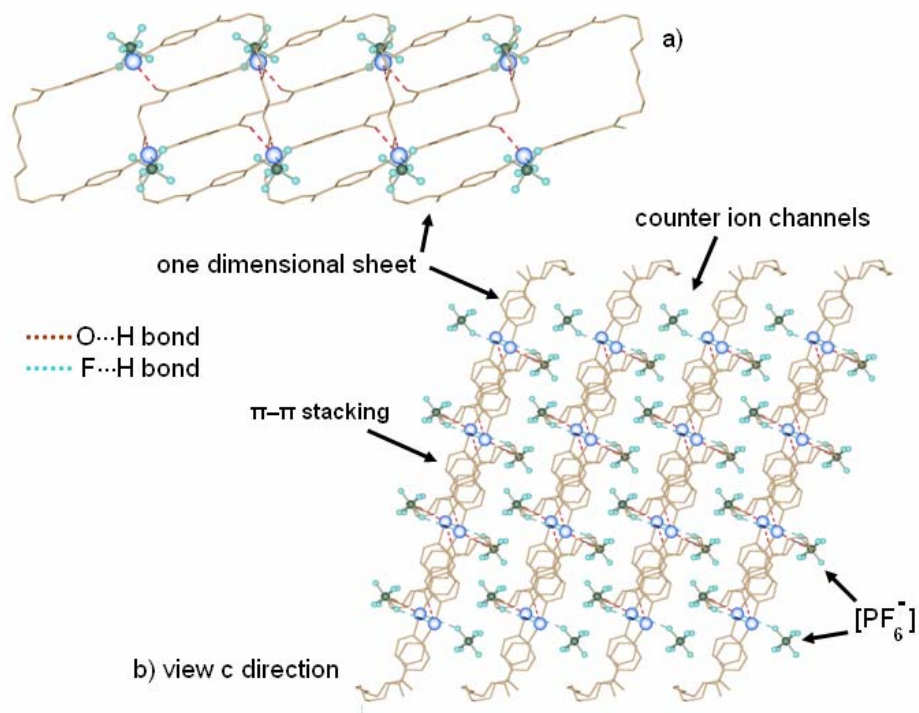
Figure 115. Position of the counter ion in the crystalline structure of complex 17

The crystalline motif remains compact with about 71.6 % of filled space even with the presence of metallacycles with a relative large cavity.

Table B-IV.64 π–π stacking present in complex **17**

π–π interaction	d_{R-R} (Å)	ρd_{R-R} (Å)	α	β
Intra π–π stacking between aromatic rings of the same ligand				
Ring (N1,C1,C2,C3,C4,C5)···Ring (N1,C1,C2,C3,C4,C5)[#3]	3.97	3.46	0.0	29.39
Inter π–π stacking between aromatic rings of different ligands				
Ring (N2,C18,C17,C16,C15,C14)···Ring (N1,C1,C2,C3,C4,C5)[#4]	3.87	3.29	11.25	21.75
Symmetry transformation used to generate equivalent atoms: #3 -x,1-y,1-z #4 -x,1-y,-z				

Table B-IV.65 Hydrogen bond [length (Å) and angle (°)] present in complex **17**

D–H⋯Acceptor	d (D–H)	d (H⋯A)	d (D⋯A)	Angle D–H⋯A
Inter metallacycle hydrogen bond between the anion and hydrogen atoms of the pyridine ring and lateral chain				
C11–H11A⋯F6[#3]	0.97	2.67(1)	3.38(1)	129.0(1)
C18–H18⋯F2[#6]	0.93	2.47(8)	3.23(1)	137.9(2)
C9–H9B⋯F2[#7]	0.97	2.78(0)	3.70(1)	158.1(2)
C7–H7B⋯F2[#3]	0.97	2.72(7)	3.30(1)	116.8(7)
C7–H7B⋯F5[#3]	0.97	2.59(1)	3.38(8)	138.0(2)
C8–H8B⋯F4[#8]	0.97	2.63(0)	3.56(7)	154.7(9)
Inter metallacycle hydrogen bond between oxygen atoms and hydrogen atoms of the pyridine ring and lateral chain				
C1–H1⋯O3[#3]	0.93	2.57(6)	3.30(3)	135.0(3)
C7–H7A⋯O1[#3]	0.97	2.55(0)	3.48(3)	159.7(7)
C14–H14⋯O4[#6]	0.93	2.50(1)	3.15(3)	127.1(0)
Intra metallacycle hydrogen bond between the anion and hydrogen atoms of the pyridine ring and lateral chain				
C5–H5⋯F5[#3]	0.93	2.55(1)	3.37(1)	147.7(2)
C18–H18⋯F6[#6]	0.93	2.49(2)	3.29(1)	143.0(8)
C18–H18⋯F1[#6]	0.93	2.46(7)	3.39(3)	167.6(7)
C1–H1⋯F3[#5]	0.93	2.26(0)	2.98(3)	133.0(3)
C2–H2⋯F3[#5]	0.93	2.68(1)	3.13(8)	110.0(1)
C14–H14⋯F4[#7]	0.93	2.54(0)	3.13(4)	121.7(1)

Symmetry transformation used to generate equivalent atoms: #5 1-x,-y,1-z #3 -x,1-y,1-z #6 -1+x,1+y,z #7 -1+x,y,z #8 x, 1+y, z.

B - IV.4 - {[Ag(L5)]NO₃}ₙ coordination polymer (18)

B - IV.4 - {[Ag(L5)]NO$_3$}$_n$ coordination polymer (18)

Single crystals of complex **18** formed after slow evaporation of a solution containing the ligand **L5** and silver nitrate, were isolated from the wall of the vessel.

The compound **18** {[Ag(**L5**)]NO$_3$}$_n$ crystallizes in the triclinic space group P-1 (No. 2). The asymmetrical unit contains a ligand, a silver cation coordinated by a nitrate counter ion and a water molecule. The motif is the same as that in **16**: two ligand molecules coordinate a cation using the nitrogen of the aromatic ring (Ag1–N1, 2.179(6) Å and Ag1–N2, 2.136(6) Å). The nitrate counter ion coordinates in a mono-dentate way to the silver cation with a distance of 2.929(8) Å (Ag–O) (Table B-IV.66). The coordination geometry of the metal ion is trigonal bipyramidal (Figure 116) and completed by the polyether O-atoms of a second chain.

Silver Coordination Compounds with a Family of Ditopic Ligands of Varying Flexibility: About Chains, Rings, Helices and Polycatenanes

136
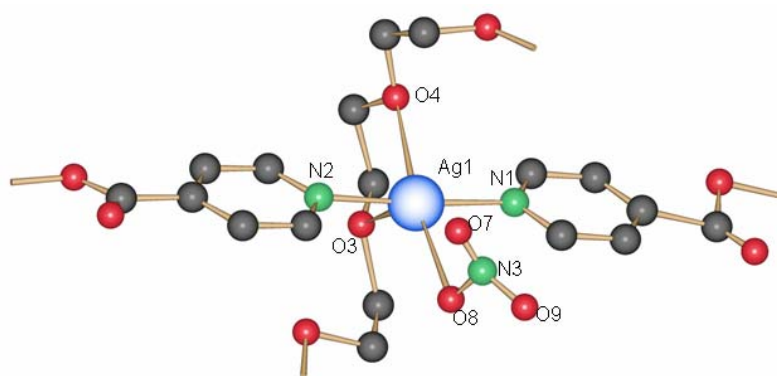
Figure 116. Coordination geometry around the metal cation in complex 18

Regarding the ligand, both carbonyl groups remain in the plane formed by the aromatic ring. Torsion angles are of the same sign and similar values O2–C7–C8–O3 (50.9(3)°), O3–C10–C11–O4 (59.9(3)°) and O4–C12–C13–O5 (75.0(3)°), which ensure the formation of the helicates.

An individual chain of type $\{-\mathbf{L5}-Ag\}_n$ through the oxygen atoms of the triethylene moiety coordinates the metal ion of a second one-dimensional motif. After wrapping, an infinite double helical array is formed (Ag1–O3$^{#2}$, 2.953(1) Å and Ag1–O4$^{#2}$, 2.948(7) Å) (Figure 117 a) and b)).
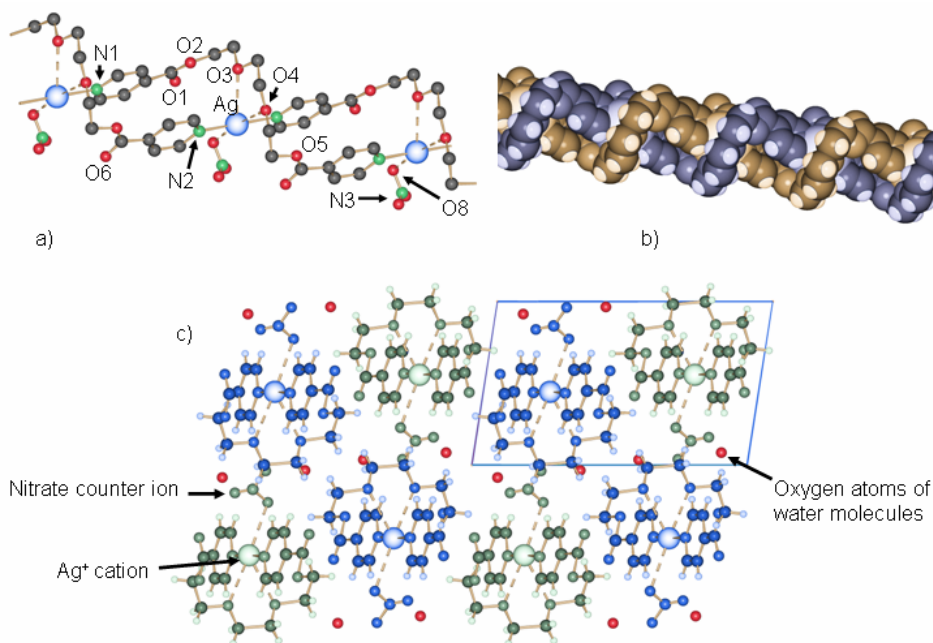
Figure 117. Double helical array generation in complex 18. Water molecules partially resolved are located in the spaces between helices

Double helices are aligned parallel and those with opposite chirality are packed together. Distances Ag–Ag[#5] are 9.266(1) Å between helices with the same chirality and 6.937(1) Å between Ag–Ag[#6] for helices with opposite chirality (Figure 117 c).

Weak π–π interactions are present between aromatic rings of different chains within the helical motif (Table B-IV.67). Other supramolecular interactions like hydrogen bonds exist between the nitrate counter ion and hydrogen atoms of the pyridine ring spatially close when both of them coordinate the same silver cation (C14–H14···O8[#4]). One oxygen atom of the triethylene glycol moiety after wrapping the metal cation coordinates also one hydrogen atom of the aromatic ring bonded to the same silver cation (C5–H5···O4[#2]). These two interactions exist within the same helical motif. The nitrate counter ion also coordinates a hydrogen atom located in the ethylene part of a ligand in a second helical motif (C7–H7A···O8[#4]) (Table B-IV.68). These helices linked by hydrogen bonds form two dimensional sheets in the crystalline array where water molecules occupy the empty space (Figure 118).
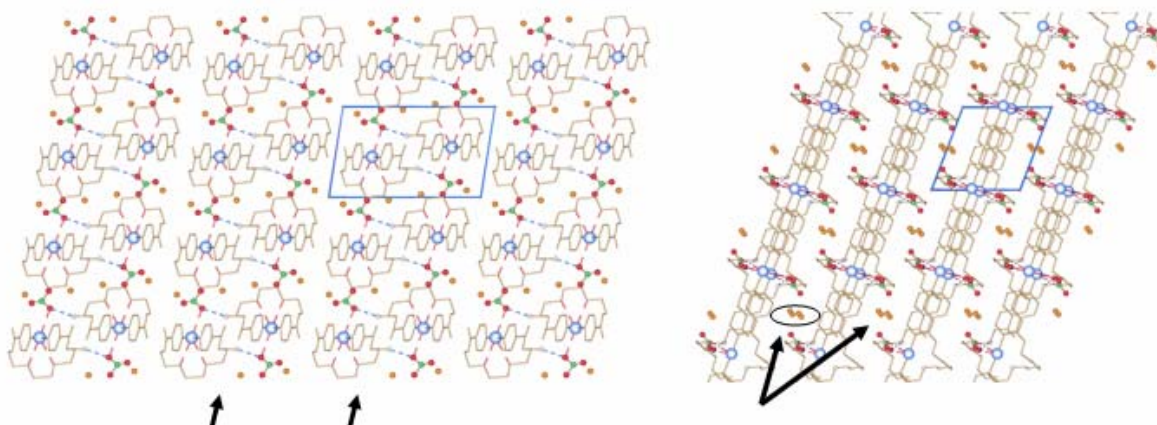
Figure 118. Two dimensional sheet formation through hydrogen bonds in complex 18, left side arrows shown layer direction, rigth side arrows showing water molecules in the crystalline structure

Due to the quality of the crystal measured, these two water molecules were not resolved good enough. The potential solvent volume is about 42 Å^3 per unit cell volume (1119.7 Å^3), which is equivalent to 3.8 % of the crystalline motif volume.

Silver Coordination Compounds with a Family of Ditopic Ligands of Varying Flexibility:
About Chains, Rings, Helices and Polycatenanes

138

Table B-IV.66 Most important bond lengths [Å] and angles [°] present in complex **18**

Ag(1)–N(1)	2.179(6)	N(1)–Ag(1)–N(2)$^{\#1}$	176.3(1)
Ag(1)–N(2)$^{\#1}$	2.136(6)	N(1)–Ag(1)–O8$^{\#1}$	92.4(1)
Ag(1)–O(NO$_2$)$^{\#1}$	2.929(8)	N(2)$^{\#1}$–Ag(1)–O(3)$^{\#2}$	90.3(1)
Ag(1)–O3$^{\#2}$	2.953(1)	C–N–C	119.1(3)
Ag(1)–O4$^{\#2}$	2.948(7)		
N–C	1.390(3)		

Symmetry transformations used to generate equivalent atoms: #1 2+x, y. z #2 1+x, y, z

Table B-IV.67 π–π stacking present in complex **18**

π –π interaction	d_{R-R} (Å)	ρd_{R-R} (Å)	α	β
Inter π–π stacking between aromatic rings of the same ligand				
Ring (N1,C1,C2,C3,C4,C5)···Ring (N2,C14,C15,C16,C17,C18)$^{\#3}$	3.80	3.46	3.42	23.48

Symmetry transformation used to generate equivalent atoms: #3 -1+x, y z

Table B-IV.68 Hydrogen bond [length (Å) and angle (°)] present in complex **18**

D–H···Acceptor	d (D–H) Å	d (H···A) Å	d (D···A) Å	Angle D–H···A (°)
Hydrogen bonds between the oxygen atom of the anion and lateral chain and hydrogen atoms of the pyridine ring of the same helicate				
C5–H5···O4$^{\#2}$	0.93	2.47(2)	3.18(2)	132.8(1)
C14–H14···O8$^{\#4}$	0.93	2.56(8)	3.32(3)	139.0(0)
Hydrogen bond between the oxygen of the anion and lateral chain and hydrogen atoms of the pyridine ring of different helicates				
C7–H7A···O8$^{\#4}$	0.98	2.49(0)	3.35(5)	146.1(0)

Symmetry transformation used to generate equivalent atoms: #2 1+x,y,z, #4 -1-x,1-y,1-z #5 x, y-1, z #6 –x, -1-y, -z

B - IV.5 - Some considerations about complex 16, 17 and 18

The pitch distances in the helices between the same silver atoms in **16** and **18** are approximately the same (8.95 Å), which is as expected when this value is controlled by the ligand geometry. The distances N–Ag vary depending on the coordination of the counter ion (Table B-IV.69). Both, **16** and **18**, share the same crystalline motif: double helicate 1D chains are stacked together to generate a 3D array via hydrogen bonds.

Table B-IV.69 Principal distances and interactions in compounds 16, 17 and 18

Complex	Ag–N distance (Å)	Ag–Ag presence	π–π presence	Number H-bonds in the structure
16	2.168(4)-2.160(4)	-	3.67(3)	6 *(5 formed by the counter ion)*
17	2.132(6)-2.047(6)	-	3.87(1)-3.97(1)	15 *(12 formed by the counter ion)*
18	2.179(6)-2.136(6)	-	3.80(9)	3 *(formed by the counter ion)*

The silver cation possesses in both cases a distorted trigonal bipyramidal geometry. Two nitrogen atoms are in the apical positions, whereas the trigonal plane is occupied by two oxygen atoms of the triethylene glycol moiety and one oxygen atom provided by the counter ion. Distances between the nitrogen atoms and the metal cation are essentially the same in all complexes (Table B-IV.69). In both complexes, the oxygen atoms coordinating the cation are disposed in a similar manner (Figure 119).

Complex	Distances (Å)	
16	N1 = 2.168(4)	X = 2.720(9)
	N2 = 2.160(4)	Y = 3.037(3)
		Z = 3.145(7)
17	N1 = 2.179(6)	X = 2.929(8)
	N2 = 2.136(6)	Y = 2.953(1)
		Z = 2.948(7)
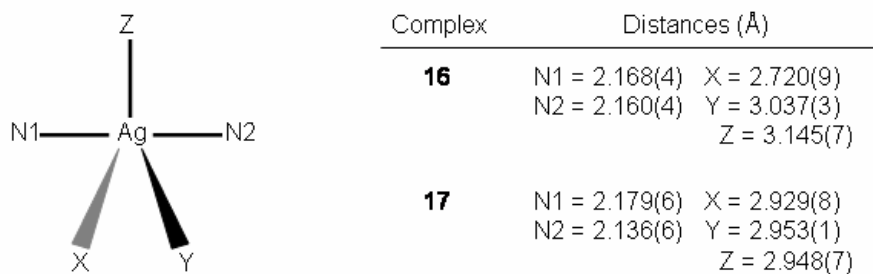
Figure 119. Bipyramidal geometry of the silver cation in complex 16 and 18.

The shape of the counter ion influences the distances between chains in **16** and **18**. The small nitrate counter ion provides a better packing of the chains compared with the triflate anion.

In complex **17,** the presence of a non-coordinating counter anion like PF_6^- avoids the generation of a third equatorial coordination site to form the trigonal base and consequently the double helical array. A third ligand is necessary to coordinate the silver cation. The most "*logical*" solution is that the silver(I) ion uses a close triethylene glycol chain of a second adjacent metallacycle to complete its coordination sphere.

Several crystallization attempts were performed with more or less degree of success. Solvent diffusion affords the crystals with better quality to be measured by X-ray diffraction (Table B-

IV.70). When crystals were obtained from different crystallization techniques, representative samples were picked and measured in order to verify the composition of batch material. The results showed the presence of a unique structure in all cases. The attempts to crystallize the complex $\{Ag(\mathbf{L5})ClO_4\}_n$ did not succeed. An amorphous product was obtained in all experiments.

Table B-IV.70 Combination of solvents and crystallization techniques employed in the synthesis of compounds **16**, **17** and **18**

Complex	Solvent or combination of solvents used	Crystallization techniques
16	Acetonitrile, THF/water	Solvent diffusion, slow evaporation in acetonitrile
17	THF/water, THF	Solvent diffusion, slow evaporation in THF
18	THF/water	Solvent diffusion

^{1}H-NMR and ^{13}C-NMR spectra were recorded but they did not show significant differences in comparison with the NMR spectra of the ligand **L5**.

However, the presence of metallacycle in solution has not been studied yet. Some experiments via ES-MS afforded contradictory results.

B - V - **Other complexes.**

Most of the complexes which will be now described were synthesized using the microwave technique (**15**, **19** and **20**). Other complexes were obtained after slow diffusion, but the final product was not well resolved by X-ray crystallography (**21**).

The complexes described here are interesting mostly from the topological point of view.

B - V.1 - {[Ag(L4)]PF$_6$}$_2$ metallacycle (15)

Complex **15** was crystallized by capillary solvent evaporation. Rod-like crystals appear on the wall and in the bottom of the vessel. The complex crystallizes in the triclinic space group P-1 (No. 2). One ligand shares the asymmetrical unit with a silver cation, one hexafluorophosphate anion and one solvent molecule (acetone) (Figure 120).
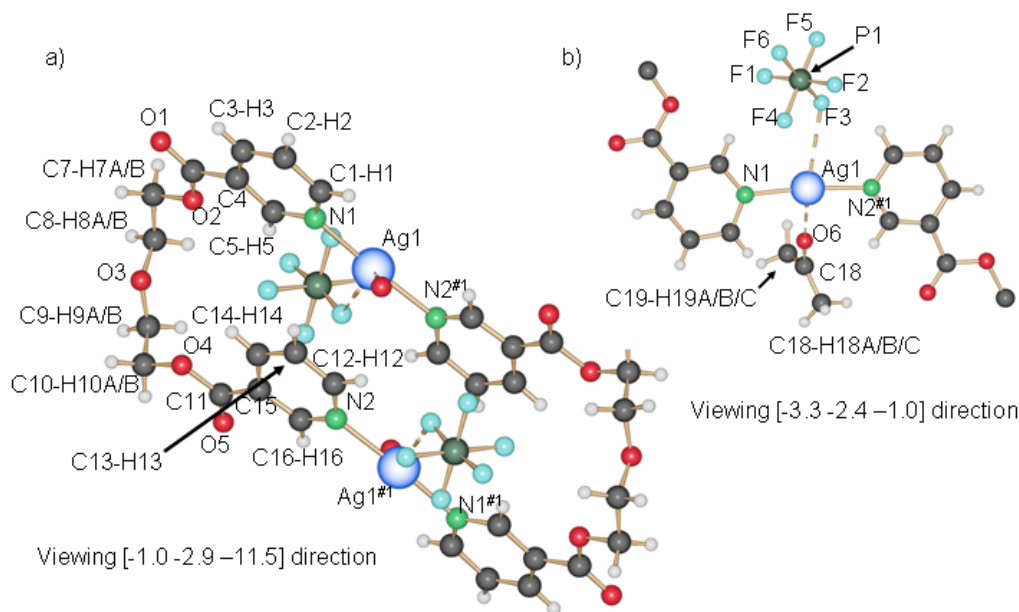
Figure 120. Zero-dimensional structurs of complex 15. The THF molecule is omitted for clarity reasons

An axis of symmetry generates in the unit cell a metallacycle motif in which two ligand molecules are coordinating two silver cations (Ag(1)–N(1), 2.135(6) Å and Ag(1)–N(2)$^{#1}$, 2.171(7) Å). The counter ion is weakly coordinated in a monodentate way to the silver ion (Ag(1)–F(3), 3.010(1) Å).

The second closest fluoro atom is located at 3.368(1) Å (Ag(1)–F(4)). The coordination sphere around the cation is completed with an acetone molecule which coordinates the metal ion at a distance of Ag(1)–O(6) 2.773(6) Å (Table B-V.71).

Within the ligand, both nitrogen atoms are pointing in the same direction. This is only possible if the aromatic ring has rotated around the C–COO bond in a different fashion for both pyridine rings. The nitrogen atom N(1) is in the opposite direction as the C=O(1) group, whereas N(2) in the next side of the ligand is directed in the same direction as the C=O(5) group. The carbonyl group remains in the plane formed by the aromatic rings. The ethylene moieties are in a gauche (staggered) conformation (O2–C7–C8–O3, 67.8(3)° and O3–C9–C10–O4, -64.7(4)°). Silver-silver distance within the metallacycle is 5.418(2) Å.

Weak π–π interactions support individual metallacycles contacts (Table B-V.72). These metallacycles are stacked forming columns where the solvent molecules and the counter ion are located (Figure 121).
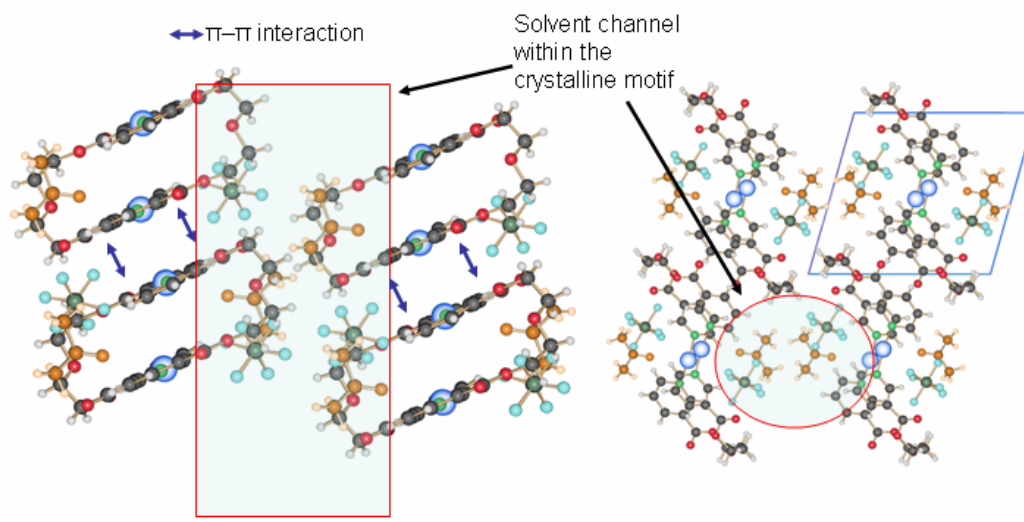
Figure 121. Solvent molecules within the crystalline structure of complex 15. The solvent and the counter ion are located in channel (left side, view *a* direction)

The hexafluorophosphate counter ion generates an intricate network of hydrogen bonds in the crystalline state. Fluoro atoms of the counter ion are involved in hydrogen bonds within the metallacycle (C5–H5···F1, C8–H8A···F1, C9–H9B···F1, C12–H12···F3, C5–H5···F4 and C8–H8A···F6) and in binding different metallacycles together (C1–H1[#6]···F2, C1–H1[#6]···F4 and C9–H9A···F5). The solvent provides some potential formation of hydrogen bonds with the counter ion

(C18–H18A$^{\#6}$···F6, C18–H18B···F2, C19–H19B···F6 and C18–H18C$^{\#1}$···F5) and the hydrogen atoms of the aromatic system (C16–H16$^{\#1}$···O6, C1–H1···O6, C12–H12···O6 and C13–H13···O6). Due to the positioning of the ligand, oxygen atoms like those of the carbonyl group are more exposed to form hydrogen bonds (C14–H14$^{\#3}$···O1, C13–H13$^{\#3}$···O1, C2–H2$^{\#3}$···O3, C9–H9A$^{\#4}$···O5 and C7–H7B$^{\#5}$···O5) (Table B-V.73).

Table B-V.71 Most important bond lengths [Å] and angles [°] present in complex **15**

Ag(1)–N(1)	2.135(6)	N(2)#1–Ag(1)–N(1)	174.1(2)
Ag(1)–N(2)$^{\#1}$	2.171(7)	C(1)–N(1)–Ag(1)	115.7(2)
Ag(1)–F	3.010(1)		
Ag(1)–O(6)	2.773(6)		

Symmetry transformations used to generate equivalent atoms: #1 2-x, 1-y, 1-z

Table B-V.72 π–π stacking present in complex **15**

π–π interaction	d$_{R-R}$ (Å)	ρd$_{R-R}$ (Å)	α	β
Inter π–π stacking between aromatic rings of the same ligand				
Ring (N1,C1,C2,C3,C4,C5)···Ring (N2,C12,C13,C14,C15,C16)$^{\#2}$	3.72	3.50	5.37	19.70

Symmetry transformation used to generate equivalent atoms: #2 1+x, y, z

Silver Coordination Compounds with a Family of Ditopic Ligands of Varying Flexibility: About Chains, Rings, Helices and Polycatenanes

144

Table B-V.73 Hydrogen bond [length (Å) and angle (°)] present in complex **15**

D–H⋯Acceptor	d (D–H)	d (H⋯A)	d (D⋯A)	Angle D–H⋯A
Inter hydrogen bonds formed between oxygen atoms of diethylene glycol moiety and hydrogen atoms located on the lateral chain and pyridine rings of the ligand.				
C14–H14[#3]⋯O1	0.93	2.74(8)	3.37(2)	125.2(3)
C13–H13[#3]⋯O1	0.93	2.83(0)	3.40(4)	120.9(3)
C2–H2[#3]⋯O3	0.93	2.56(6)	3.20(8)	126.8(2)
C9–H9A[#4]⋯O5	0.97	2.66(2)	3.29(8)	123.5(2)
C7–H7B[#5]⋯O5	0.97	2.58(0)	3.35(9)	137.3(3)
Hydrogen bonds formed between the counter ion and hydrogen atoms of the same metallacycle				
C5–H5⋯F1	0.93	2.44(2)	3.35(9)	168.6(2)
C8–H8A⋯F1	0.97	2.74(2)	3.44(2)	129.5(3)
C9–H9B⋯F1	0.97	2.76(1)	3.43(7)	127.3(3)
C12–H12⋯F3	0.93	2.34(8)	3.14(4)	143.3(3)
C5–H5⋯F4	0.93	2.56(1)	3.21(2)	127.3(2)
C8–H8A⋯F6	0.97	2.95(1)	3.92(0)	176.3(4)
Hydrogen bonds formed between the counter ion and hydrogen atoms of different metallacycle				
C1–H1[#6]⋯F2	0.93	2.58(0)	3.29(6)	134.2(2)
C1–H1[#6]⋯F4	0.93	2.67(0)	3.37(6)	133.1(3)
C9–H9A⋯F5	0.97	2.69(7)	3.46(1)	136.0(2)
C8–H8B[#7]⋯F6	0.97	2.92(0)	3.66(5)	134.4(2)
Hydrogen bonds formed between the oxygen atom of the acetone molecule and hydrogen atoms of the metallacycle				
C16–H16[#1]⋯O6	0.93	2.75(4)	3.32(5)	120.6(3)
C1–H1⋯O6	0.93	2.67(8)	3.25(0)	120.4(3)
C12–H12⋯O6	0.93	2.83(7)	3.38(2)	118.5(2)
C13–H13⋯O6	0.93	2.75(9)	3.29(8)	117.8(2)
Hydrogen bonds formed between the counter ion and hydrogen atoms of the acetone molecule				
C18–H18A[#6]⋯F6	0.97	2.91(6)	3.80(0)	153.5(3)
C18–H18B⋯F2	0.96	2.88(3)	3.73(0)	147.3(2)
C19–H19B⋯F6	0.97	2.81(2)	3.68(8)	152.2(3)
C18–H18C[#1]⋯F5	0.96	2.69(6)	3.55(3)	148.8(3)

Symmetry transformation used to generate equivalent atoms: #3 1-x, 2-y, 1-z #4 2-x, 2-y, -z #5 -1+x, y, z #6 1-x, 1-y, 1-z #7 1-x, 2-y, -z

Silver Coordination Compounds with a Family of Ditopic Ligands of Varying Flexibility: About Chains, Rings, Helices and Polycatenanes

145

B - V.2 - {[Cu(L4)₂](NO₃)₂} chelate complex (19)

Single blue crystals suitable for X-ray analysis of complex **19** were obtained after reacting in the microwave a THF solution containing the ligand **L4** and copper(II) nitrate. The complex crystallizes in the monoclinic space group $P2_1/c$ (No. 14).

The asymmetric unit contains one ligand coordinating a Cu(II) cation (N(1)–Cu(1) 2.051(6) Å, N(2)–Cu(1) 2.035(4) Å), and one nitrate counter ion (O(6)–Cu(1), 2.451(5) Å). A center of symmetry generates an octahedral Cu(II) coordinated by two chelating ligands and two counter ions (Figure 122).

Viewing [0.0 -1.0 1.2] direction
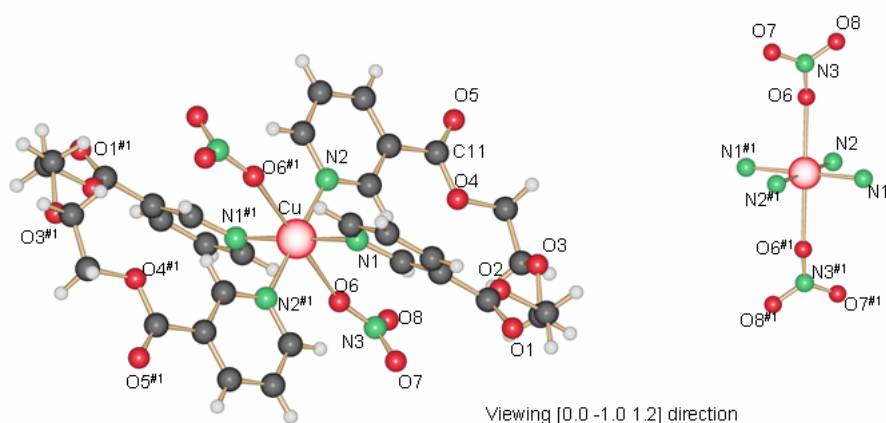
Figure 122. Zero dimensional structure formed by the coordination of the Cu(II) cation with two ligands and two nitrate counter ions

These molecules are stacked together in the crystalline state (Figure 123) sustained by hydrogen bonds between the oxygen atoms O(1), O(2) of the carbonyl group and hydrogen atoms located in the diethylene glycol spacer. Other hydrogen bonds are formed between the oxygen atoms of the counter ion and hydrogen atoms of the pyridine ring and the diethylene glycol chain of the closest ligands (Table B-V.74).
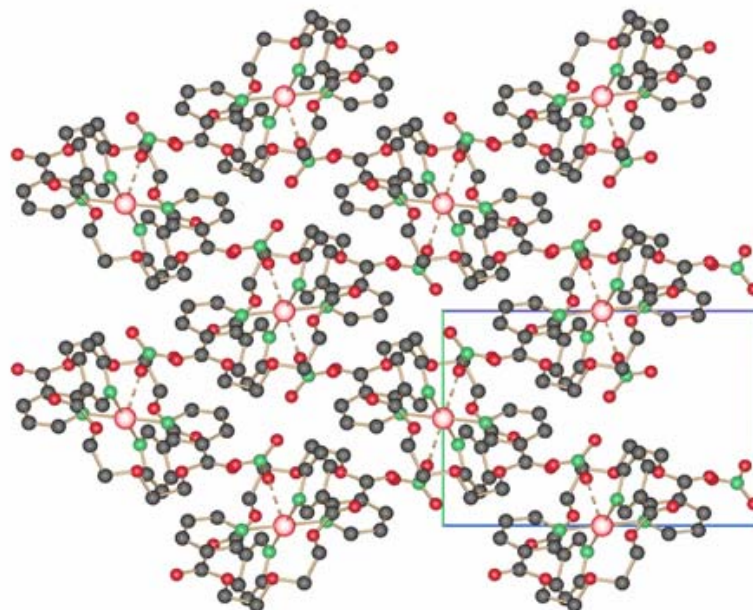
Figure 123. View through the "a" axis showing the stacking of the molecules in the crystalline state. Hydrogen atoms are omitted for clarity reasons. Molecules are linked together by hydrogen bonds

These hydrogen bonds form a three dimensional network. Other supramolecular forces like aromatic-aromatic interactions are discarded due to the distance 4.80 Å (centroid-centroid).

Within the ligand, one carbonyl group remains in the plane defined by the aromatic ring (O4–C11–C15–C16, 2.4(3)°), even if the next carbonyl group is slightly twisted (C5–C4–C6–O2, 30.4(2)°). This conformation allows the ligand to coordinate in a bidentate way the same Cu(II) cation. Both ethylene moieties are in a gauche (staggered) conformation.

Table B-V.74 Most important bond lengths [Å] and angles [°] present in complex 19

Cu(1)–N(1)	2.051(6)	N(2)–Cu(1)–N(1)	92.9(6)
Cu(1)–N(2)	2.035(4)	N(1)–Cu(1)–O(6)	91.8(7)
Cu(1)–O(6)	2.451(5)	C(1)–N(1)–Cu(1)	120.8(1)

Silver Coordination Compounds with a Family of Ditopic Ligands of Varying Flexibility: About Chains, Rings, Helices and Polycatenanes

147

Table B-V.75 Hydrogen bond data [length (Å) and angle (°)] present in complex **19**

D–H···Acceptor	d (D–H)	d (H···A)	d (D···A)	Angle D–H···A
Inter hydrogen bonds formed between the oxygen atom of diethylene glycol moiety and hydrogen atoms located on the lateral chain and pyridine rings of the ligand.				
C7–H7B[#1]···O2	0.97	2.81(5)	3.59(0)	138.1(1)
C10–H10A[#1]···O1	0.97	2.35(9)	3.26(8)	156.4(1)
C7–H7A[#2]···O1	0.97	2.91(4)	3.54(1)	123.8(1)
C3–H3[#2]···O1	0.93	2.88(5)	3.68(9)	146.3(1)
Hydrogen bonds formed between the counter ion and hydrogen atoms of the same complex				
C12–H12[#3]···O7	0.93	2.73(8)	3.64(7)	170.2(1)
C5–H5[#3]···O7	0.93	2.73(6)	3.43(1)	132.5(1)
C12–H12[#3]···O6	0.93	2.45(1)	3.08(0)	125.0(1)
C5–H5[#3]···O6	0.93	2.49(9)	3.12(1)	124.5(1)
C6–H16[#3]···O6	0.93	2.52(1)	3.11(0)	122.3(1)
C1–H1···O6	0.93	2.34(4)	3.02(2)	129.6(1)
Hydrogen bonds formed between the counter ion and hydrogen atoms of different complexes				
C13–H13[#4]···O8	0.93	2.76(3)	3.28(9)	116.9(1)
C14–H14[#4]···O8	0.93	2.58(3)	3.19(1)	124.0(1)
C1–H1[#5]···O8	0.93	2.80(3)	3.31(8)	116.2(1)
C13–H13[#5]···O8	0.93	2.87(4)	3.44(0)	120.9(6)

Symmetry transformation used to generate equivalent atoms: #1 3-x, 1-y, -z #2 x, 0.5-y, 0.5+z #3 2-x, 1-y, -z #4 2-x, 0.5+y, 0.5-z #5 x, 1.5-y, -0.5+z

B - V.3 - {[Cu(L4)]I}$_n$ coordination polymer (20)

When copper(I) iodide reacts with the ligand **L4** in THF, yellow crystals of {[Cu(**L4**)]I}$_n$ (**20**) suitable for X-ray were obtained in the reaction vessel. **20** crystallizes in the monoclinic space group P2$_1$/c (No. 14).

The asymmetrical unit contains one ligand, one copper cation and one iodide counter ion. In the unit cell, two ligands coordinate one tetrahedral Cu(II) cation. The next two positions in the tetrahedral coordination geometry are occupied by iodide counter ions (Figure 124).(Table B-V.76)
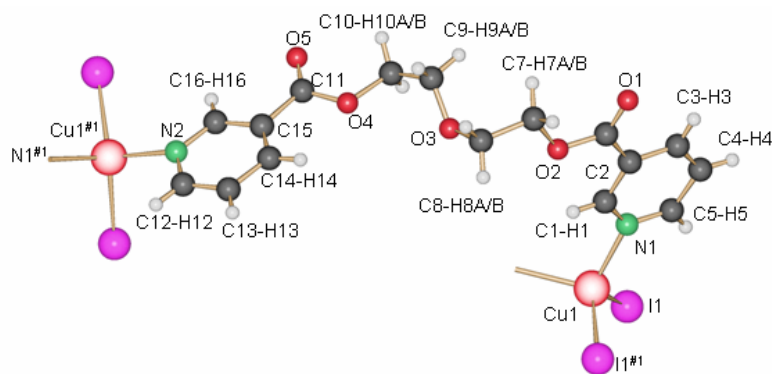
Figure 124. Tetrahedral coordination geometry of the copper (I) formed by two ligand molecules and two iodide counter ions

Concerning the ligand, the most remarkable difference between **19** and **20** is the extension of the ligand to coordinate two different metal cations in **20** rather than one in **19**. The ethylene glycol moieties are in a gauche (staggered) conformation, but the torsion angles possess different values O3–C9–C10–O4, -67.9(1)° and O2–C7–C8–O3, 70.5(1)° due to the stretched position of the ligand. Carbonyl groups remain in the plane formed by the atoms of the pyridine rings.

The iodide counter ions coordinating the copper (I) cation, link a second cation. This bond generates a chain $\{I–Cu–I–Cu\}_n$ along the *c* axis direction (Figure 125).
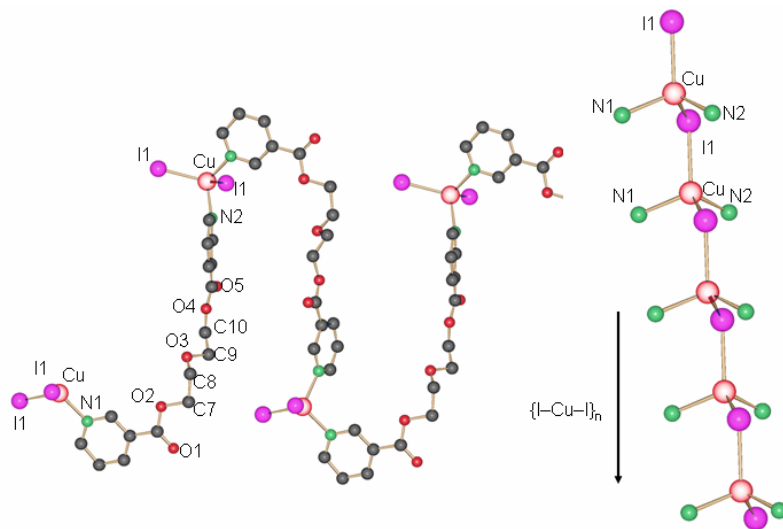
Figure 125. Schematic representation of the two dimensional motif in complex 20. 1D metal-organic chains are linked via I–Cu–I bonds running perpendicular to the chain direction (view c axis, link picture)

Silver Coordination Compounds with a Family of Ditopic Ligands of Varying Flexibility: About Chains, Rings, Helices and Polycatenanes

149

These two motifs complement each other to generate a supramolecular wall of 13.78(6) Å height from Cu(I)–Cu(I) cation and 20.69(9) Å from H(1)–H(4) hydrogen atoms, which is the longest distance in the motif.

Hydrogen bonds exist holding together these 2D motifs, generating thus a very robust supramolecular array.

Table B-V.76 Most important bond lengths [Å] and angles [°] present in complex **20**

Cu(1)–N(1)	2.089(3)	N(2)–Cu(1)–N(1)	106.4(5)
Cu(1)–N(2)[#1]	2.109(5)	N(1)–Cu(1)–I(1)	105.7(4)
Cu(1)–I(1)	2.612(8)	C(1)–N(1)–Cu(1)	118.0(4)
Symmetry transformations used to generate equivalent atoms: #1 –x, -0.5+y, 0.5-z			

Aromatic interactions are discarded due to the distance 4.80 Å (centroid-centroid).

Table B-V.77 Hydrogen bond [length (Å) and angle (°)] present in complex **20**

D–H···Acceptor	d (D–H)	d (H···A)	d (D···A)	Angle D–H···A
Inter hydrogen bonds formed between oxygen of carbonyl group and hydrogen atoms located on the pyridine rings of the ligand belonging to the next sheet.				
C4–H4[#2]···O1	0.93	2.37(7)	3.03(2)	127.3(1)
C5–H5[#2]···O1	0.93	2.70(2)	3.21(5)	115.5(6)
Hydrogen bonds formed between oxygen atoms and hydrogen atoms of the sheet				
C8–H8A[#3]···O2	0.97	2.86(1)	3.66(0)	140.2(8)
C8–H8A[#3]···O3	0.97	2.79(5)	3.71(0)	157.4(3)
C10–H10B[#4]···O3	0.97	2.56(1)	3.28(3)	131.2(8)
C13–H13···O5	0.93	2.41(9)	3.22(2)	144.5(7)
Symmetry transformation used to generate equivalent atoms: #2 1-x, -0.5+y, 0.5-z #3 x, -2.5+y, -0.5+z #4 x, 2.5-y, 0.5+z				

B - V.4 - {[Ag(L6)]NO$_3$}$_2$ metallacycle (21)

Crystals of {[Ag(**L6**)]NO$_3$}$_2$ (**21**) were obtained by slow evaporation at room temperature of a solution prepared by dissolving **L6** (50 mg, 0.12 mmol) and silver nitrate (21 mg, 0.12 mmol) in 8 mL of a mixture of methanol/acetonitrile 1:1.

Crystals for measurements were taken from the wall of the vessel. The crystals were of medium quality, but the structure could be resolved to a reasonable result. The complex **21** crystallizes in the monoclinic space group C2/c (No. 15).

The asymmetrical unit contain one ligand coordinated to a silver cation a nitrate (not resolved crystallographically), an inversion center generates a 2:2 (silver:ligand) metallacycle type complex. Due the poor quality of the crystal measured it was impossible to localized with confidence the counter ion. The silver atom has a distorted tetrahedral geometry (Figure 126).
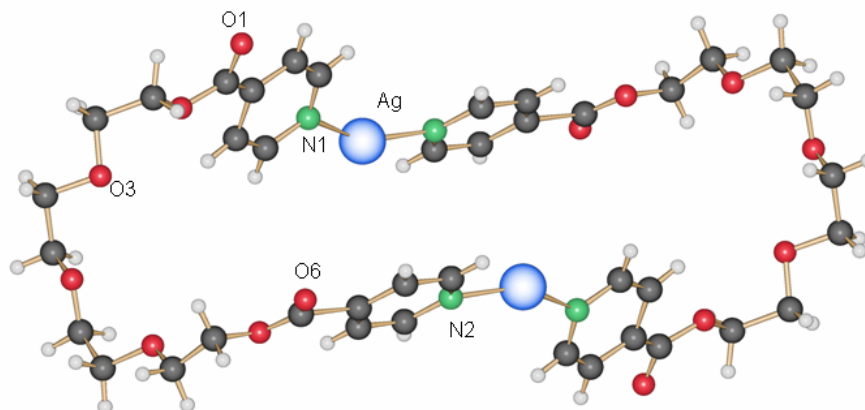
Figure 126. asymmetric unit cell view of complex 21

Distances Ag(I)–N are 2.230(5) and 2.079(4) Å (Ag(1)–N(1) and Ag(1)–N(2) respectively). A ligand of a ring parallel to the metallacycle wraps one of the metal cations of a ring, using the oxygen atoms of its tetraethylene glycol moiety (Ag(1)–O(3), 2.758(5) Å; Ag(1)–O(3), 2.558(1) Å and Ag(1)–O(5), 2.846(2) Å).

Ethylene glycol moiety in the lateral chain are disposed all in an staggered (gauche) conformation. The oxygen atoms are exposed into the interior of the cavity which allow the coordination to a neighbour silver cation of the next closest metallacycle.

The planes formed by the pyridine rings are twisted about 28°, the carbonyl groups are contained in these planes.

The ring has a cavity with dimensions 8.79(2) Å from silver to silver and 20.18(1) Å from the oxygen atom O(4) to O(4)[#1] within the ligand.

These metallacycles are stacked parallel via Ag–O and hydrogen bonds forming a two dimensional infinite sheet in the *b* direction (Figure 127).

Silver Coordination Compounds with a Family of Ditopic Ligands of Varying Flexibility:
About Chains, Rings, Helices and Polycatenanes

151

Viewing *b* direction
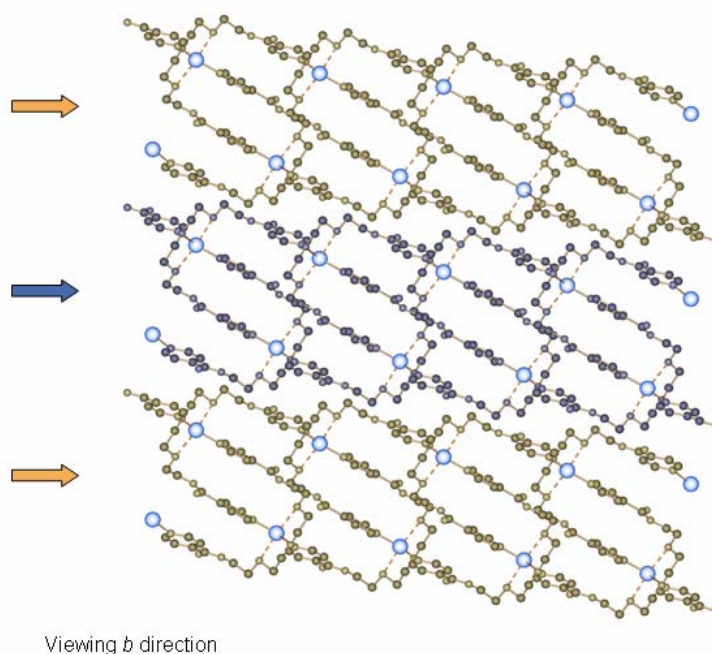
Figure 127. Two dimensional layer generation based on O–Ag bonds between metallacycles

An interesting fact concerning this complex is the cavity inside the metallacycle. This cavity should allow the compound to coordinate a second cation (Ca(II), Cd(II)) to form a double salt complex. Our group envisages the study and synthesis of these complexes in a near future.

The crystalline structure possesses a potential solvent area 1124.6 Å^3 (21.0%, 5355.0 Å^3), which is the larger so far than in the complexes here studied, in this volume some solvent molecule may be disordered.

Table B-V.78 Most important bond lengths [Å] and angles [°] present in complex **21**

Ag(1)–N(1)	2.230(5)	N(2)–Ag(1)–N(1)	149.0(8)
Ag(1)–N(2)$^{\#1}$	2.079(4)	N(1)–Ag(1)–O(6)	
Ag(1)–O$^{\#2}$	2.758(5) –O(3), 2.558(1) –O(4), 2.846(2) –O(5)	C(1)–N(1)–Ag(1)	

Symmetry transformations used to generate equivalent atoms: #1 1-x, 1-y, -z #2 0.5+x, 0.5+y, z

Aromatic interactions are discarded due to the distance 4.80 Å (centroid-centroid).

Silver Coordination Compounds with a Family of Ditopic Ligands of Varying Flexibility: About Chains, Rings, Helices and Polycatenanes

152

Table B-V.79 Hydrogen bond [length (Å) and angle (°)] present in complex **21**

D–H⋯Acceptor	d (D–H)	d (H⋯A)	d (D⋯A)	Angle D–H⋯A
Inter hydrogen bonds formed between oxygen of diethylene glycol moiety and hydrogen atoms located on the lateral chain and pyridine rings of the closest metallacycle.				
C10–H10A[#3]⋯O1	0.97	2.82(8)	3.72(3)	153.8(4)
C11–H11A[#4]⋯O1	0.97	2.81(6)	3.70(7)	153.0(7)
C10–H10A[#4]⋯O1	0.97	2.94(2)	3.40(4)	110.4(4)
C9–H9A[#5]⋯O1	0.97	2.66(8)	3.40(6)	133.2(1)
C13–H13A[#6]⋯O6	0.97	2.88(2)	3.44(9)	118.3(0)
C14–H14B[#6]⋯O6	0.97	2.57(7)	3.13(0)	118.6(2)
C14–H14A[#6]⋯O6	0.97	2.89(4)	3.13(0)	93.1(5)

Symmetry transformation used to generate equivalent atoms: #3 0.5+x, -0.5+y, z #4 1-x, 1-y, -z #5 0.5-x, -0.5+y, 0.5-z #6 –x, -y, -z #7

C - Conclusion

The results obtained and the conclusion this thesis brings are not conclusive, but some remarks and outlines could be presented.

This thesis reports the synthesis and characterization of six organic ligands (**L1-L6**) and the coordination network polymers formed between these ligands and Ag(I), Cu(I) and Cu(II) cations. The Figure 128 summarises the principal topologies found in the crystal structures of these complexes.

For the final crystal motif of this family of complexes was expected a high number of possible results. The reality shows something different. The number of structures we found seems to be rather quantized into a few types of networks motifs.

The synthesis of supramolecular arrays depends on various factors. The most important one is the interaction of the metal cation and the ligand. The interplay of all forces in the crystallization process will direct the overall array into the lower energetic minimum, although sometimes this is not achieved (presence of network isomerism). In this work three cases of network isomerism were found: i) the metallacycle **7** and helical array **8**, ii) the metallacycle **12** and the polycatenane **13**, and iii) the metallacycles **9**, **10** and **11**, from which **9** contains two molecules of water co-crystallized within the network. In the first case the formation of **7** or **8** may depend on the solvent and the gradient of concentration present in the H-tube, whereas in the second case the ratio ligand:Ag(I) and the counter ion may be a determining factor in the formation of the polycatenane. The combination of solvent used may also direct the formation of the complexes **9**, **10** and **11**.

Silver Coordination Compounds with a Family of Ditopic Ligands of Varying Flexibility:
About Chains, Rings, Helices and Polycatenanes

154

Figure 128. Principal topologies for Ag(I) compounds.

	X=ClO$_4^-$/L3	Compound 7
	X=NO$_3^-$/L3	Compound 9
	X=NO$_3^-$/L3	Compound 10
	X=NO$_3^-$/L3	Compound 11
0D	X=PF$_6^-$/L3	Compound 12
	X=SO$_3$CF$_3^-$/L3	Compound 14
	X=PF$_6^-$/L4	Compound 15
	X=PF$_6^-$/L5	Compound 17

Metallacylces

	X=SO$_3$CF$_3^-$/L2	Compound 6
1D	X=ClO$_4^-$/L3	Compound 8
	X=SO$_3$CF$_3^-$/L5	Compound 16
	X=NO$_3^-$/L5	Compound 18

Single helices

Double stranded helices

AgX

	X=NO$_3^-$/L1	Compound 1
	X=PF$_6^-$/L1	Compound 2
2D	X=NO$_3^-$/L2	Compound 4
	X=SO$_3$CF$_3^-$/L2	Compound 5
	X=PF$_6^-$/L3	Compound 13

Sheets

Polycatenane

Interpenetrated network

3D	X=SO$_3$CF$_3^-$/L1	Compound 3

A: Nitrogen atom (derived from the Isonicotinic or nicotinic acid)

L1, L2	n=1
L3, L4	n=2
L5	n=3
L6	n=4

C - I - Impact of the ligand structure in the crystalline motif

In order to modify the crystalline motif after coordination with the silver salts, different ligands with increasing lateral chain length (from ethylene to tetraethylene glycol) were used. It is noteworthy the change in the final crystalline motif of the ligands when the nitrogen atom position is moved within the pyridine ring. Even when we expect that this alteration will induce drastic modifications of the crystalline motif in the silver complexes, the motif found can be summarized as:

i)   **L1** and **L2** forms linear polymers (with the exception of **3**, where the compound effects interpenetration). These linear metal-organic polymers may be parallel stacked forming 2D layers like those in compounds **1**, **2**, **4** and **5**, or generate helices related by Ag–Ag and Ag–counter ion bond contacts like in **6.**

ii)   Ligands **L3** and **L4** form metallacycles in the crystalline state with [**L**:AgX]$_2$ stochiometry (X: NO$_3^-$, PF$_6^-$, ClO$_4^-$ and SO$_3$CF$_3^-$), two exceptions were found, **8** and **13**. In the compound **8**, where a helical array is the final motif the ligand **L3** retains the same conformation as in metallacycle **7**. In compound **13** the conformation of the ligand **L3** is slightly distorted, and may play an important role in the generation of the polycatenane structure.

iii)   **L5** and **L6** are the most flexible ligands. **L5** forming double-helical array in **16** and **18**, but a metallacycle in **17** with silver hexafluorophosphate. In the three cases, the ligand adopts the most suitable conformation to coordinate the silver(I) cation with all potential N– and O– donors. The metallacycle structure obtained in **21** was not expected, and clearly reveals in which a mysterious way nature works sometimes.

C - II - Impact of the counter ion in the crystalline motif

The counter ion may play an important role directing the final crystalline motif in the supramolecular array, not just due their coordination ability but for their intrinsic ease in forming hydrogen bonds which stabilize the crystalline packing.

Anions like NO$_3^-$ and ClO$_4^-$ are very flexible with their coordination modes with the metal cation. They form compounds of type (L–Ag–L) like in **1**, **4**, **7**, **8**, **9**, **10** and **11** and are directly responsible for the formation of different types of sheets, like in **1** and **4**.

The shape of the $SO_3CF_3^-$ counter ion could be responsible for the interpenetration phenomenon observed in compound **3**, and the shape and the poor coordination ability of the counter ion PF_6^- partially allow the formation of the polycatenane structure **13**, where the anion was displaced from the coordination sphere of the silver(I) cation.

If the PF_6^- counter ions are removed from the metallacycle structure in **12**, and the structure is allowed to search the conformation of the energetic minimum, the metallacycle elongates in the Ag–Ag direction, which suggest a mechanism path for the formation of the polycatenane in solution.

The coordination mode of the nitrate counter ion in **10** and **11** may also be responsible for the stability of the metallacycle and the variation in the inter- and intra-metallacycle Ag–Ag contacts in the crystal. Further calculations are carried out concerning the influence of the different counter ions in these compounds, and may bring insight to the energetic aspect directing the formation of particular motifs between other systems.

C - III - Impact of the solvent and the crystallization conditions in the crystalline motif

The importance of the solvent in the crystallization of different compounds has been outlined in a different part of this work. The solvent used may be responsible for the formation of compounds **7** or **8** (EtOH and THF), compounds **9**, **10** and **11** (water, EtOH and DMSO) and compounds **12** and **13** (Acetonitrile and acetone). The solvent may co-crystallize in the structure as in compounds **9**, **12**, **15** and **18**, in all cases remain non-coordinating with the metal cation

C - IV - General conclusion

Most of this work was related to the study of the complexation pattern in the crystalline state of a family of organic ligands and Ag(I) salts. The analysis of these compounds provided an insight into the weak supramolecular forces and other factors directing the formation of particular supramolecular arrays.

Some control may be gained over the final structure depending on the reaction conditions employed. It is noteworthy to say that this assertion is valid in principle for this particular family of organic ligands and silver(I) salts. An extension of this argument to a more general system may require the analysis of a considerable amount of empirical data.

C - V - Perspectives

The synthesis of these silver(I) metal-organic complexes is a further step in the preliminary work performed by Dr. Robin in our group. It allows the recognition of certain patterns in the generation of polymer networks, these compounds are now being investigated in our group for the functionalization of metal surfaces (gold and titanium), envisaging antibacterial properties for medical implants.

The coordination of an organic ligand of a second metal cation (like Ca(II), Sr(II) and Ba(II)) and silver(I) may lead to the generation of complexes with attractive NLO properties. Our group is now beginning to work in this line of research with some promising results.

An extension of the study of the coordination pattern of these ligands to other metal cations like Pt(II), Cu(I) and Cu(II) cations has been explored with some good results. The generation of Pt(II) frameworks and the study of their catalytic properties, and the study of Cu(I) network polymers and their potential long-range magnetic-ordering properties may in the future afford materials with physical applications.

From the point of view of crystal engineering these results will increase our understanding of the supramolecular forces involved in the generation of some crystal structures. Gaining insight into these factors may lead to a better control and prediction of the supramolecular processes that control the crystallization of a particular motifs between several other potential candidates.

Silver Coordination Compounds with a Family of Ditopic Ligands of Varying Flexibility:
About Chains, Rings, Helices and Polycatenanes

158

D - Experimental section

D - I - Materials

Ligands synthesized were used after purification (>98 % purity). Silver salts were purchased and used without further treatment.

Solvents were dried according to literature procedures. For reactions in the microwave the solvents were not dried.

D - II - Equipments, materials and methods

D - II.1 - Scanning differential thermoanalysis (SDTA) and Thermogravimetry (TG)

TG-thermograms were recorded with a TGA/SDTA 851e system (Mettler/Toledo, Switzerland) using the Mettler Toledo STAR^e Thermal analysis system software. Samples of approximately 3-7 mg (weight controlled to ± 0.1 μg using an internal ultramicrobalance) were weighted into light aluminium pans (20 μl). Dry nitrogen was used as purge gas (purge: 10 ml min^{-1}).

SDTA experiment were performed using a RTyp thermocouple (Pt-Pt/Rh 13%), recording temperatures fluctuation of ± 0.25 ^{0}C with a 0.005 ^{0}C resolution and the system was calibrated with Indium with a purity of 99.999% (156.6 ^{0}C, 28.4 ΔH_f), Au with a purity of 99.9 % (419.5 ^{0}C, 107.5 ΔH_f), Zn with a purity of 99.99% (660.3 ^{0}C, 397.0 ΔH_f) and Al with a purity of 99.99 % (1064.2 ^{0}C, 63.7 ΔH_f). The calculation of fusion enthalpy using the present method includes a 10% error.

D - II.2 - Infrared spectroscopy

Fourier transform infrared (FTIR) spectra were acquired on a Shimazu FTIR-8400S spectrometer equipped with Golden Gate ATR (attenuated total reflection) system at the University of Basle. Spectra were recorded over a range of 4000-400 cm^{-1} with a resolution of 0.01 cm^{-1} (16, number of scan). Abbreviations used are: s, strong; m, medium and w, weak.

D - II.3 - H^1-NMR, C^{13}-NMR and DOSY measurements

High resolution H^1 and C^{13}-NMR spectra were recorded in a Bruker AM 250 MHz, AV 400 MHz, Bruker DRX-500 MHz, Bruker Avance 600 MHz spectrometers. For DOSY experiments pulse

sequence was used to select spectra containing signals from the aromatic protons only, in order to evaluate the relaxation constant and their the diffusion coefficient.

Me$_4$Si was used as an internal standard. The following abbreviations are used; s: singlet, d: doublet, t: triplet, q: quartet, m: multiplet. Chemical shifts were determined with the solvent signal (CDCl3) at 7.26 ppm as referenz.

D - II.4 - Powder X-ray diffractometry (PXRD)

The X-ray diffraction patterns were obtained at the Paul Scherer Institute (PSI) using a line of the third-generation synchrotron light source (SLS). Samples were measured on sealed quartz capillary at 77 K. Other powder spectra were recorded using a STOE FR590 diffractometer. Data were analysis using the STOE WinXPOW package (version 2.12).

D - II.5 - Single crystal X-ray diffractometry (SCXRD)

Single crystals were mounted on a glass fiber and all geometric and intensity data were taken from this crystal. Data collection using Mo-Kα radiation (k = 0.71073 Å) was performed on a STOE IPDS-II diffractometer equipped with an Oxford Cryosystem open flow cryostat [421]. Absorption corrections were partially integrated in the data reduction procedure [422].

The structures were solved by direct methods (SHELXS) [423, 424] and refined using full-matrix least-squares on F^2 (SHELXL 97) [423, 424]. All heavy atoms could be refined anisotropically. Hydrogen atoms were introduced as fixed contributors when a residual electronic density was observed near their expected positions.

Crystallographic data for the structures **1**, **7** and **8** have been deposited with the Cambridge Crystallographic Data Center with the CCDC number 251188, 251189 and 238163 respectively. See See http://dx.doi.org/10.1039/b506389b for crystallographic data in CIF or other format. Copies of the data can be obtained free of charge on application to CCDC, 12 Union Road, Cambridge CB21EZ, UK (fax: (+44)1223-336-033; email: deposit@ccdc.cam.ac.uk).

D - II.6 - Elemental analysis

Elemental analyses were performed by Dr. W. Kirsch at the Microanalytical laboratory of the University of Basle.

Silver Coordination Compounds with a Family of Ditopic Ligands of Varying Flexibility:
About Chains, Rings, Helices and Polycatenanes

160

D - II.7 - Mass spectrometry (MS)

Electrospray mass spectra (ESI-MS) were recorded on a LCQ system (Finnigan MAT, USA) using acetonitrile, methanol, THF or a mixture DMSO/THF in different proportion as mobile phase.

D - II.8 - Fluorescence measurements

Luminescence curves were measured on a Perkin Elmer LS 50B at the University of Basle, excitation wavelength depend on the complex measured (223, 391 or 452 nm), split widths (em, ex) 5.0 nm, scan speed 2-10 nm S^{-1}.

Solid samples were measured in quartz capillaries at 77 K.

D - II.9 - Chromatography purification and analysis

Analytical thin sheet chromatography (TLC) was performed with Merck silica gel 60 F-254 plates. Column chromatography was performed using Merck silica gel 60.

D - II.10 - Representation of graphics

Crystals graphics were carried out using ORTEP [425], SCHAKAL [426-428], POV-RAY [429] and DIAMOND v3.0 software's [430].

Silver Coordination Compounds with a Family of Ditopic Ligands of Varying Flexibility: About Chains, Rings, Helices and Polycatenanes

161

D - III - Synthesis of ligands

Ligands were synthesized based on nicotinic and isonicotinic acid, and different poly-ethylene glycols (Figure 128). All products are commercially available and were purchased in *Acros Organics*. These compounds were used without further treatment.
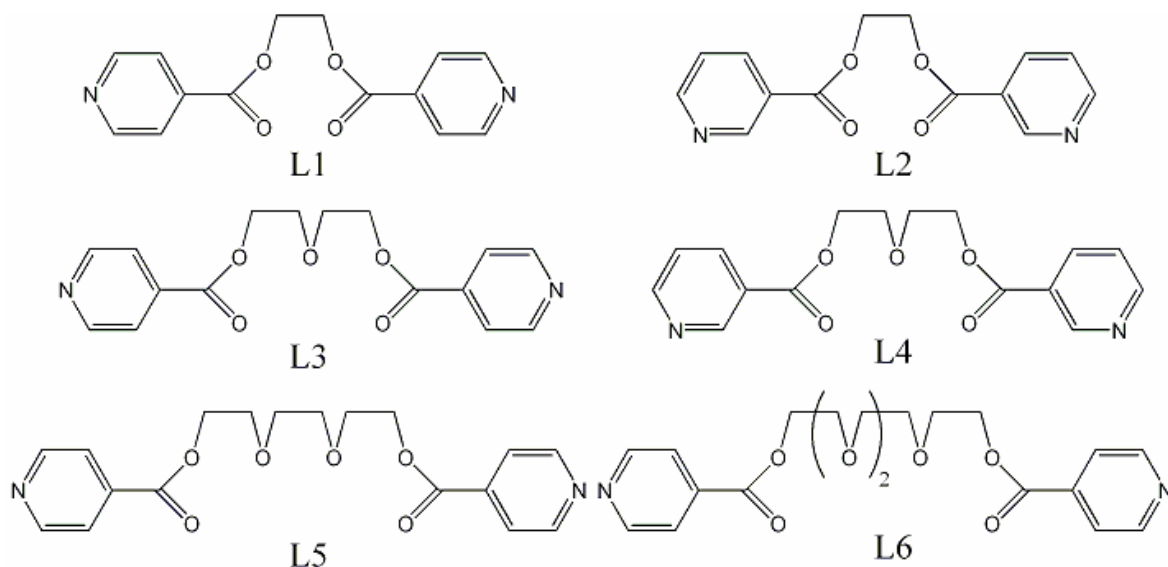
Figure 128. Ligands synthesized for the coordination of silver (I) salts

All experimental manipulations involving the use of 2-chloro-1,3 dimethylimidazolinium chloride as dehydrating agent were carried out under nitrogen using *Schlenk technique*.

Solvents were purchased from *Aldrich* and *Acros Organics* and dried when necessary before being used following literature procedures.

Multiple synthetic routes were tried for one ligand in order to find the best approach. Most synthetic routes required optimization processes for these specific ligands.

D - III.1 - Synthetic pathways

One pot synthesis was very effective for obtaining the shorter ligands (**L1** and **L2**). Dehydrating agent like 1,3-dimethyl-imidazolinium chloride (DMC) affords the best results, however it requires the use of Schlenk technique manipulation under $N_{2(g)}$ or $Ar_{(g)}$ (Figure 129).

Silver Coordination Compounds with a Family of Ditopic Ligands of Varying Flexibility: About Chains, Rings, Helices and Polycatenanes

162
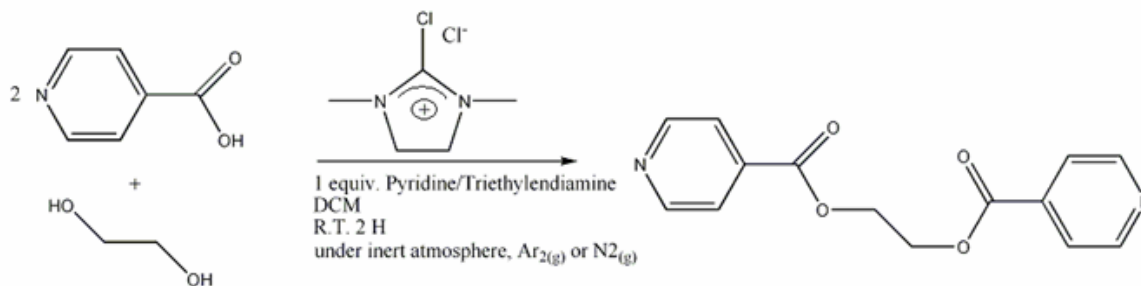
Figure 129. Synthetic route employed to synthesize L1 (same as for L2).

For this synthesis, it is necessary to manipulate the dehydrating agent in the glove box. The DMC is soluble in dichloromethane and is easily transferable to the vessel containing the acid and the alcohol. The solution changes the color from transparent to orange, and after two hours can be stopped.

If left in dichloromethane, the salts precipitate and the product can be isolated after a flash chromatographic column (n-hexane:ethyl acetate/ 2:1). The high yield (>96%) and purity leads to crystallization in the collection recipient. These crystals are suitable for X- ray measurements.

Synthesis of ligands with other polyethyleneglycol chains afford lower yields. Changing the temperature, or the equivalence of dehydrating agent to up to more than 3 times the acid, or changing the reaction time (until 24 hours) did not show any remarkable yield changes.

These ligands were synthesized using common procedures (Figure 130). Dicyclohexyl-carbodiimide (DCC) was used as dehydrating agent, but yields were lower as expected.
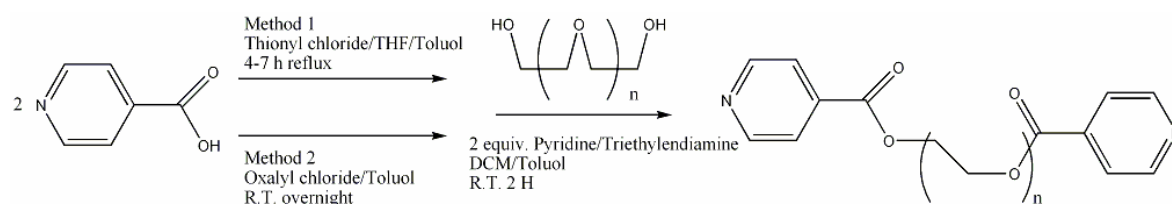
Figure 130. Other synthetic route to obtain the ligands derived from isonicotinic acid (L1, L3, L5 and L6) employed in the synthesis of supramolecular coordination polymers, same synthetic route was employed for ligands derived from the nicotinic acid (L2 and L4).

Using oxalyl chloride and subsequent transformation of the acyl chloride into the ester affords the best yield of the ligands **L3**, **L4**, **L5** and **L6**. The crude product was purified using silica gel chromatography (n-hexane:ethyl acetate for elution).

Single crystals for X- ray measurements were obtained with two different methods: i) solvent diffusion (usually n-hexane in a DCM solution containing the ligand) or ii) slow evaporation of a DCM:THF solution were the ligand was previously dissolved.

D - III.2 - Synthesis of ethane-1,2-diyl diisonicotinate (L1)

Isonicotinic acid (1.19 g, 9.66 mmol) was suspended in toluene and thionyl chloride (11.49 mL, 96.6 mmol) was added dropwise [431]. The reaction was refluxed for 3 hours and the solvent evaporated off. The yellow-white solid was dried under vacuum and used as such.

The acyl chloride was partially dissolved in 25 mL of dichloromethane and 5 mL pyridine; the solid was completely dissolved after 20 minutes at reflux. 4 mL ethylenglycol (4.06 mmol) were added slowly into the solution and the reaction was refluxed again for another 6 hours. Afterwards the organic phase was washed with 20 mL of a 5 % solution $NaCl_{(aq.)}$, 20 mL $NaHCO_{3(s)}$, and 20 mL water, dried with $MgSO_4$ and a yellow oil was obtained after evaporation of the solvent.

The resulting product was purified in a silica column, eluting with a 6:2 hexane/ethyl acetate mixture. The ligand crystallizes directly in the essay tubes as transparent needless.

Yield: 72%

NMR-^{13}C (CDCl$_3$): 165.1, 153.8, 137.3, 125.7, 123.5, 63.0, 45.2

NMR-^{1}H (CDCl$_3$): δ 9.2 (s, 2H), 8.7 (d, 2H), 8.3 (d, 2H), 7.4 (dd, 2H), 3.3 (t, 2), 2.9 (t, 2H)

IR: IR: ν(Ar-H) 3067.4s, ν(-HC-H) 2933.8 s, ν(C=O) 1721.9 s, ν (C=C) 1580.9 m, ν (ArC–C, C=N) 1423.6 s, ν (CO–O) 1273.7 s, ν (-C–O) 1100.7 s, δ(ArC–H) 1022.3 m, ν (ArC–H) 738.9 m

Elemental analysis: calculated: C 61.74, H 4.45, N 10.29%; found: C 59.79, H 4.48, N 9.81%.

Silver Coordination Compounds with a Family of Ditopic Ligands of Varying Flexibility: About Chains, Rings, Helices and Polycatenanes

164

D - III.3 - Synthesis of ethane-1,2-diyl dinicotinate (L2)

Into a three neck recipient containing a solution of 0.5 g (4.06 mmol) of nicotinic acid and 2.05 mL (2.03 mmol) of ethylene glycol in 20 mL of dichloromethane were added 10 mL of a dichloromethane solution where 0.686 g (4.06 mmol) of dimethylimidazolinium chloride[432] were dissolved.

5 minutes later 4.2 mL of dried triethylamine were added dropwise into the reaction mixture, which turned orange after some minutes. After refluxing for 2 hours, a white cake-like solid precipitated when cooling. More dichloromethane was added (15 mL) to dissolve the solid.

The reaction was followed by thin sheet chromatography. After 4 hours the reaction was stopped viewing that no more reactant was present. The solvent was evaporated and the solid dried under high vacuum.

The product was obtained pure after a flash chromatography. A mixture AcOEt:Hex:6:2 was used for elution.

Yield: 97 %

NRM-^{13}C (CDCl$_3$): 165.0, 150.8, 136.9, 122.9, 63.6, 45.2

NRM-^{1}H: δ 8.7 (t, 4H), 7.8 (t, 4H), 3.2 (t, 2H), 2.7(t, 2H)

IR: IR: ν(Ar-H) 3075.9s, ν(-HC-H) 2949.5 s, ν(C=O) 1714.5 s, ν (C=C) 1580.9 m, ν (ArC–C, C=N) 1431.1 s, ν (CO–O) 1273.7 s, ν (-C–O) 1124.5 s, δ(ArC–H) 1029.8 m, ν (ArC–H) 738.9 m

Elemental analysis: calculated: C 61.74, H 4.45, N 10.29%; found: C 59.97, H 4.36, N 9.93%.

D - III.4 - Synthesis of 2,2'-oxybis(ethane-2,1-diyl) diisonicotinate (L3)

5 g (0.040 mmol.) of nicotinic acid were suspended in 50 mL toluene in a two neck flask which was sealed with a CaCl$_2$ tube. 10 mL of oxalyl chloride [433] were added in the flask and the reaction was left overnight. The white solid was filtered off and dried under reduced pressure. Afterwards toluene was added and then 11.4 mL (0.08 mmol) of triethylamine and 1.94 mL (0.02 mmol) of ethylene glycol, and the solution was refluxed overnight.

Silver Coordination Compounds with a Family of Ditopic Ligands of Varying Flexibility: About Chains, Rings, Helices and Polycatenanes

165

20 mL of DCM were added after cooling and the organic solution was washed with 50 mL of a saturated aqueous solution of NaHCO$_3$, with 50 mL 5% NaCl and twice with 50 mL distilled water. The organic phase was dried with magnesium sulphate and evaporated under reduced pressure.

The ligand was obtained pure after a flash chromatography silica column. Hexane: ethyl acetate was used as eluting solvent in a 2:1 proportion. Recrystallization in DCM:Hexane:2:7 affords yellow crystals in form of cubes.

Yield: 75%

NRM-^{13}C (CDCl$_3$): 165.4, 151.0, 137.4, 123.2, 69.3, 64.9.

NRM-^{1}H: (300 MHz, CDCl$_3$) 6.92 (4H, d, H-py), 6.00 (4H, d, H-py), 2.61 (4H, t, O–CH2-), 1.97 (4H, t, -CH2-O).

IR: ν(Ar-H) 3042.7s, ν(-HC-H) 2953.2 s, ν(C=O) 1719.9 s, ν (C=C) 1562.6.4 m, ν (ArC–C, C=N) 1406 s, ν (CO–O) 1264 s, ν (-C–O) 1115.4 s, δ(ArC–H) 942.3 m, ν (ArC–H) 852.9 m

Elemental analysis: Calculated C 60.76, H 5.10, N 8.86; found: C 60.90, H 5.04, N 8.72%.

D - III.5 - Synthesis of 2,2'-oxybis(ethane-2,1-diyl) dinicotinate (L4)

The ligand was synthesized using the same procedures as before (III.3). 6 g of nicotinic acid (0.048 mmol) were used as starting material.

Yield: 75%

NRM-^{1}H: δ 9.24 (d, 2H), 8.80 (d, 2H), 8.28 (d, 2H), 7.39 (m, 2H), 4.56 (t, 4H), 3.91 (t, 4H)

IR: ν(Ar-H) 3056.2s, ν(-HC-H) 2906.3 s, ν(C=O) 1723.5 s, ν (C=C) 1546.3 m, ν (ArC–C, C=N) 1423.6 s, ν (CO–O) 1343.4 s, ν (-C–O) 1120.6 s, δ(ArC–H) 1104.2 m, ν (ArC–H) 750.0 m

Elemental analysis: Calculated C 60.76, H 5.10, N 8.86; found: C 60.7, H 5.08, N 8.81%.

Silver Coordination Compounds with a Family of Ditopic Ligands of Varying Flexibility: About Chains, Rings, Helices and Polycatenanes

166

D - III.6 - Synthesis of 2,2'-(ethane-1,2-diylbis(oxy))bis(ethane-2,1-diyl) dinicotinate (L5)

The same reaction as III.3 was used for the synthesis of this ligand. 4 g of nicotinic acid (0.032 mmol) and 2.17 mL of triethylene glycol (0.016 mmol) were used.

The same procedure as III.2 starting with 2 g of nicotinic acid (0.016 mmol) affords 85 % yield.

Yield: 75%

NMR-^{13}C (CDCl$_3$): 165.4, 150.9, 137.5, 123.2, 69.3, 64.9, 45.7

NMR-^{1}H: δ 8.74 (t, 4H), 7.80 (t, 4H), 4.51 (t, 4H), 3.86(t, 4H), 1.33 (m, 4H)

IR: ν(Ar-H) 3083.0 s, ν(-HC-H) 2957.7 s, ν(C=O) 1714.5 s, ν (C=C) 1588.5 m, ν (ArC–C, C=N) 1415.4 s, ν (CO–O) 1273.7 s, ν (-C–O) 1108.8 s, ν (ArC–H) 738.9 m

Elemental analysis: Calculated C 59.97, H 5.60, N 7.78; found: C 60.10, H 5.53, N 7.60%.

D - III.7 - Synthesis of 2,2'-(2,2'-oxybis(ethane-2,1-diyl) bis(oxy)) bis(ethane-2,1-diyl) diisonicotinate (L6)

The same reaction as III.3 was used for the synthesis of this ligand. 8 g of nicotinic acid (0.064 mmol) and 4.34 mL of triethylene glycol (0.032 mmol) were used were used.

Same procedure as II.1 starting from 4 g. isonicotinic acid (0.032 mmol) affords 60 % yield.

Yield: 75%

NMR-^{1}H: δ 9.13 (t, 4H), 8.23 (t, 4H), 4.49 (t, 4H), 3.91(t, 4H), 1.90 (m, 8H)

IR: ν(Ar-H) 3115.1 s, ν(-HC-H) 2987.2 s, ν(C=O) 1723.8 s, ν (C=C) 1534.2 m, ν (ArC–C, C=N) 1412.1 s, ν (CO–O) 1278.8 s, ν (-C–O) 1045.3 s, ν (ArC–H) 746.2 m

Elemental analysis: Calculated C 59.38, H 5.98, N 6.93; found: C 58.12, H 7.02, N 6.87%.

D - IV - Synthesis of silver complexes

D - IV.1 - Synthesis of $\{[Ag(L1)]NO_3\}_n$ (1) coordination polymer

In a "H"-shaped tube single crystals were isolated after diffusion through THF from of a solution of THF containing the **L1** (20 mg, 0.07 mmol) to a water solution containing the silver salt (12.4 mg, 0.07 mmol)

The same complex is obtained after slow evaporation of an acetonitrile solution in which the ligand and silver nitrate were dissolved. Different equivalents of ligand/silver salt (1:2, 2:1) do not alter the crystalline structure obtained.

Yields (**1**): 12 mg of **1** (0.028 mmol, 40 % calculated with respect to $AgNO_3$).

Elemental analysis: calculated: C 38.01, H 2.74, N 9.51%; found: C 41.02, H 3.89, N 8.18% (**1*** THF).

IR: ν(Ar-H) 3059.0 s, ν(-HC-H) 2965.2 s, ν(C=O) 1714.5 s, ν (C=C) 1588.4 m, ν (ArC–C, C=N) 1415.4 s, ν (NO_3) 1328-1242 s, ν (-C–O) 1029.8 s, ν (ArC–H) 738.9 m

D - IV.2 - Synthesis of two network isomer of $\{[Ag(L1)]PF_6\}_n$ (2) coordination polymer

Following the above procedure 30 mg **L1** (0.11 mmol) were dissolved in THF and 27.8 mg $AgPF_6$ (0.12 mmol) in the water side. Pale green crystals were picked from the wall of the "H"-shaped tube. Crystals formed in both sides of the "H"-shaped tube afford the same complex.

Other changes in the ratio ligand/silver salt (1:2 or 2:1) afford the same complex.

Yields (**2**): 40.2 mg of **2** (0.076 mmol, 64 % calculated with respect to $AgPF_6$).

Elemental analysis: calculated: C 32.0, H 2.30, N 5.34%; found: C 32.32, H 2.38, N 5.20%.

IR (cm^{-1}): ν(Ar-H) 3112.3 s, ν(-HC-H) 3986.6 s, ν(C=O) 1605.4 s, ν (ArC–C, C=N) 1447.9 m, ν (C–O) 1219.2 m, δ(ArC–H) 1072.3 m, ν (PF_6) 828.5 s, broad

Silver Coordination Compounds with a Family of Ditopic Ligands of Varying Flexibility:
About Chains, Rings, Helices and Polycatenanes

168

D - IV.3 - Synthesis of two network isomers of {[Ag(L1)]SO₃CF₃}ₙ (3) coordination polymer

A solution of silver triflate (20 mg, 0.07 mmol) and **L1** (21.25, 0.07 mmol) was refluxed in the microwave (580 W) for 4 minutes. The hot solution was filtered and the solution was left at room temperature for three days.

Single crystals of complex **3** were obtained in the wall and the bottom of the vessel after slow evaporation.

Same compound is obtained by diffusion in a "H"-shaped tube, but requires more than 20 days to crystallize.

Yields (**3**): 29.7 mg of **3** (0.056 mmol, 80 % calculated with respect to AgPF₆).

Elemental analysis: calculated: C 34.03, H 2.29, N 5.29%; found: C 34.5, H 2.3, N 5.27%

IR (cm⁻¹): ν(Ar-H) 3075.5 s, ν(-HC-H) 2957.7 s, ν(C=O) 1721.9 s, ν (C=C) 1604.1 m, ν (ArC–C, C=N) 1423.6 m, ν (SO₃CF₃) 1273.7 s, broad, ν (SO₃CF₃) 1108.8 s, broad, δ(ArC–H) 1072.3 m

D - IV.4 - Synthesis of {[Ag(L2)]NO₃}ₙ (4) coordination polymer

In an "H"-shaped tube silver nitrate (40 mg, 0.22 mmol) in water and **L2** (64 mg, 0.22 mmol) in THF were dissolved. Both sides were connected using THF (15 mL).

After two months transparent crystal suitable for X-ray diffraction were isolated from the wall of the vessel and measured.

Crystals picked from the bottom of both sides and the bridge wall afford the same complex.

The same complex is obtained when different proportions of silver nitrate/**L2** were tested (1:2, 2:1, 1:3 and 1:4).

Yields (**4**): 48.6 mg of **4** (0.11 mmol, 50 % calculated with respect to AgNO₃).

Elemental analysis: calculated: C 38.01, H 2.74, N 9.51%; found: C 35.15, H 3.37, N 8.79% (**4*** 2H₂O).

IR: ν(Ar-H) 3047.0 s, ν(-HC-H) 2917.6 s, ν(C=O) 1720.5 s, ν (C=C) 1553.4 m, ν (ArC–C, C=N) 1474.2 w, ν (NO₃) 1332-1210.2 s, ν (-C–O) 1119.0 s, ν (ArC–H) 692.5 m

D - IV.5 - Synthesis of two network isomers {[Ag(L2)]SO₃CF₃}ₙ (5) and {[Ag(L2)]SO₃CF₃}ₙ (6)

Silver triflate (20 mg, 0.07 mmol) was dissolved in water (5 mL), and the solution was connected with THF to a solution of THF (5 mL) containing **L2** (14.81 mg, 0.07 mmol). Single crystals were formed after some weeks on the bottom of both sides in the "H"-shaped tube.

The complex **5** was obtained in the side of the ligand, whereas complex **6** in the side of the silver salt.

Altering the ratio of silver salt: ligand affords always a mixture of both network isomers.

Yields (**5+6**): 22.6 mg of (**5+6**) (0.042 mmol, 60% calculated with respect to AgSO₃CF₃).

Elemental analysis (**5**): calculated: C 34.03, H 2.29, N 5.29%; found: C 34.0, H 2.22, N 5.2%.

IR (cm⁻¹): ν(Ar-H) 3102.2 s, ν(-HC-H) 2933.8 s, ν(C=O) 1723.9 s, ν (C=C) 1619.8 w, ν (ArC–C, C=N) 1431.1 m, ν (SO₃CF₃) 1260.0 s, broad, ν (SO₃CF₃) 1092-1039 s

Elemental analysis (**6**): calculated: C 34.03, H 2.29, N 5.29%; found: C 35.18, H 2.40, N 5.14%. (**6*THF**)

IR (cm⁻¹): ν(Ar-H) 3055.2 s, ν(-HC-H) 2918.7 s, ν(C=O) 1723.9 s, ν (C=C) 1557.1 w, ν (ArC–C, C=N) 1478.1 w, ν (SO₃CF₃) 1267.4 s, broad, ν (SO₃CF₃) 1123.5 s, broad.

D - IV.6 - Synthesis of two network isomers {[Ag(L3)]ClO₄}₂ (7) and {[Ag(L3)₂]ClO₄}ₙ (8)

In an "H"-shaped tube, 0.011 g (0.05 mmol) of AgClO₄ were dissolved in 5 ml of water and introduced into one side of the tube, whereas the other one was filled with 5 ml of a THF-solution containing 0.036 g (0.11 mmol) of **L3**. The two solutions were put in contact with each other via a 1 : 10 mixture of water and THF. Single crystals of **7** were collected on the silver salt side, whereas compound **8** formed on the other side of the "H"-shaped tube.

Yields (**7**): 9.3mg of **7** (0.018 mmol, 36% calculated respect to AgClO₄)

Silver Coordination Compounds with a Family of Ditopic Ligands of Varying Flexibility:
About Chains, Rings, Helices and Polycatenanes

170

Elemental analysis: calculated: C 36.70, H 3.08, N 5.35%; found: C 36.01, H 3.16, N 5.07%.

IR (KBr, cm21): IR: ν(Ar-H) 3092 s, ν(-HC-H) 2919 s, ν(C=O) 1718 s, ν (C=C) 1580 m, ν (ArC–C, C=N) 1449 w, ν (ClO$_4$) 1100-1050 s, ν (ArC–H) 810 m

Yields (**8**): 11.4 mg of **8** (0.022 mmol, 45% calculated with respect to AgClO$_4$).

Elemental analysis: calculated: C 36.70, H 3.08, N 5.35%; found: C 35.86, H 3.25, N 4.91%.

IR: ν(Ar-H) 3094 s, ν(-HC-H) 2953 s, ν(C=O) 1722 s, ν (C=C) 1560 m, ν (ArC–C, C=N) 1447 w, ν (ClO$_4$) 1100 s, ν (ArC–H) 812 m

D - IV.7 - Synthesis of {[Ag(L3)$_2$]ClO$_4$}$_n$ (8) coordination polymer

In an "H"-shaped tube, 0.017 g (0.05 mmol) of AgClO$_4$ were dissolved in 5 ml of water and introduced in one side of the tube, whereas the other one was filled with 5 ml of a THF-solution containing 0.036 g (0.11 mmol) of **L3**. The two solutions were put in contact with each other via a solution of ethanol. Single crystals of complex **8** were collected on both sides of the "H"-shaped tube.

Yields: 17.7 mg (0.034 mmol, 70% calculated with respect to AgClO4).

Elemental analysis: calculated: C 36.70, H 3.08, N 5.35%; found: C 35.86, H 3.25, N 4.91%.

IR: ν(Ar-H) 3094 s, ν(-HC-H) 2953 s, ν(C=O) 1722 s, ν (C=C) 1560 m, ν (ArC–C, C=N) 1447 w, ν (ClO$_4$) 1100 s, ν (ArC–H) 812 m

D - IV.8 - Synthesis of three network isomers of {[Ag(L3)]NO$_3$*2H$_2$O}$_2$ (9), {[Ag(L3)]NO$_3$}$_2$ (10) and {[Ag(L3)]NO$_3$}$_2$ (11)

Crystals suitable for single X-ray diffraction were grown after slow diffusion of 30 mg (0.094 mmol) of **L3** dissolved in THF (5 mL), through a mixture water:THF 1:5, until getting in contact with a solution of water (5 mL) containing 16.3 mg (0.094 mmol) of AgNO$_3$.

Crystals taken from the silver side afforded the complex **9** (hydrated). The crystals which grew in the ligand side showed the presence of complex **10**, where the absence of water was remarked.

60 mg of **L3** (0.18 mmol) were reacted with 32 mg of AgNO₃ (0.18 mmol) in 15 mL of DMSO. The solution was left in the dark for 1 month. Transparent single crystals suitable for X-ray diffraction were formed on the bottom. The crystals were filtered off and the complex **11** was measured. After another 45 days during a routine DSTA analysis the presence of a new network isomer (**?**) was detected and measured in the X-ray diffractometer, but the structure was so far impossible to be resolved.

Elemental analysis of this possible new structure afford similar values as for complex **11**.

Yields (**9**): 19.9 mg (0.037 mmol, 40% calculated with respect to AgNO₃).

Elemental analysis: calculated: C 36.78, H 3.86, N 8.05%; found: C 36.7, H 3.8, N 8.1 %.

IR: ν(Ar-H) 3067.4 s, ν(-HC-H) 2910.0 s, ν(C=O) 1721.9 s, ν (C=C) 1548.9 w, ν (ArC–C, C=N) 1423.6 w, ν (NO₃) 1375.9-1273.7 s, ν (-C–O) 1116.3 s, ν (ArC–H) 691.9 m

Yields (**10**): 13.8 mg (0.028 mmol, 30% calculated with respect to AgNO₃).

Elemental analysis: calculated: C 39.51, H 3.32, N 8.64%; found: C 38.7, H 3.3, N 8.60 %.

IR: ν(Ar-H) 3022.3 s, ν(-HC-H) 2919.2 s, ν(C=O) 1715.0 s, ν (ArC–C, C=N) 1412.1 w, ν (NO₃) 1362-1230.0 s, ν (-C–O) 1124.1 s, ν (ArC–H) 690.5 m

Yields (**11**): 56.8 mg (0.11 mmol, 65% calculated with respect to AgNO₃).

Elemental analysis: calculated: C 39.51, H 3.32, N 8.64%; found: C 39.5, H 3.30, N 8.62 %.

IR: ν(Ar-H) 3050.0 s, ν(-HC-H) 2925.2 s, ν(C=O) 1720.3 s, ν (ArC–C, C=N) 1414.0 w, ν (NO₃) 1373-1228.3 s, ν (-C–O) 1126.3 s, ν (ArC–H) 694.3 m

D - IV.9 - Synthesis of two network isomers of {[Ag(L3)PF₆[X]}₂ (X=THF) (12) and {[Ag(L3)₂PF₆}ₙ (13)

Single crystals of complex **12** suitable for X-ray diffraction were obtained from the wall of both sides of an "H"-shaped tube where 32 mg (0.12 mmol) of AgPF₆ dissolved in 4 mL water were left

to diffuse through 20 mL THF, until they got in contact with an organic solution (here THF or EtOH could be used with the same result) containing 40 mg (0.12 mmol) **L3**.

Usually such crystallization technique takes some time, until crystals are big enough. Increasing the concentration from reactants will accelerate the crystallization process. However, a concentration higher than 4.53 mmol/L will cause precipitation instead of crystallization in the "H"-shaped tube.

Following the same procedure, but using ethanol (15 mL) as linking solvent between the two solutions containing the ligand and the silver salt, afforded in the salt side rod-like crystals of complex **13** on the bottom and complex **12** on the wall.

Another way to crystallize the polymorph **13** was achieved after two days of slow evaporation of a solution were the ligand and the silver salt were mixed together in acetone and injected into capillar tubes for fusion point measurements.

Yields (**12**): 55.3 mg (0.08 mmol, 72% calculated with respect to AgPF$_6$).

Elemental analysis: calculated: C 43.4, H 3.6, N 6.3; found: C 43.59, H 3.8, N 6.19%.

IR (cm^{-1}): ν(Ar-H) 3105.4 s, ν(-HC-H) 2922.8 s, ν(C=O) 1733.4 s, ν (C=C) 1602.7 m, ν (ArC–C, C=N) 1411.8 m, ν (C–O) 1282.8 s, δ(ArC–H) 1056.6 m, ν (PF$_6$) 822.1 s, broad

Yields (**13**): 63.7 mg (0.07 mmol, 60% calculated with respect to AgPF$_6$).

Elemental analysis: calculated: C 43.39, H 3.64, N 6.33%; found: C 42.8, H 3.60, N 6.30%.

IR (cm^{-1}): ν(Ar-H) 3061.8 s, ν(-HC-H) 2947.9 s, ν(C=O) 1733.4 s, ν (C=C) 1602.7 m, ν (ArC–C, C=N) 1411.8 m, ν (CO–O) 1272.7 s, ν (-C–O) 1108.6 m, δ(ArC–H) 1056.6 m, ν (PF$_6$) 822.1 s, broad

D - IV.10 - Synthesis of {[Ag(L3)]SO$_3$CF$_3$}$_2$ (14) coordination metallacycle

12 mg (0.04 mmol) from a silver triflate were dissolved in 5 mL water. 14.81 mg (0.04 mmol) of the ligand were dissolved in THF; both solutions were connected using THF (EtOH affords the same result).

Single crystals are formed after some weeks on the wall and on the bottom of the "H"-shaped tube. Changing the equivalence between ligand and silver affords plenty of crystals, eventually in the frit as well. Measuring samples from all these sites gives the same structure here presented.

Slow evaporation, crystallization on capillary system and solvent diffusion afford always the same crystal structure.

Yields (**14**): 16.5 mg (0.02 mmol, 54% calculated with respect to AgSO$_3$CF$_3$).
Elemental analysis: calculated: C 35.6, H 2.81, N 4.89%; found: C 39.1, H 3.70, N 4.33% (**14***THF).
IR (cm^{-1}): ν(Ar-H) 3059.9 s, ν(-HC-H) 2918.2 s, ν(C=O) 1721.9 s, ν (C=C) 1557.0 w, ν (ArC–C, C=N) 1431.1 w, ν (SO$_3$CF$_3$) 1328.9-1281.9 s, broad, ν (SO$_3$CF$_3$) 1116.3 s, broad.

D - IV.11 - Synthesis of {[Ag(L4)]PF$_6$*C$_3$H$_6$O}$_2$ complex (15)

15 was prepared by refluxing for 1 min in the microwave a solution containing **L4** (88.0 mg, 0.27 mmol) and silver hexafluorophosphate (70 mg, 0.27 mmol) in 5 mL of acetone. Transparent crystals suitable for X-ray diffraction were obtained in the wall of the vessel by slow cooling of the THF solution after filtration.

Yields: 120 mg (0.19 mmol, 72% calculated with respect to AgPF$_6$).
Elemental analysis: calculated: C 36.3, H 3.54, N 4.47%; found: C 33.5, H 2.82, N 4.82% (**15**-Acetone).

D - IV.12 - Synthesis of {[Ag(L5)]SO$_3$CF$_3$}$_n$ (16)

Crystals of **16** were obtained by layering an acetonitrile solution of silver triflate (30 mg, 0.17 mmol, in 6 mL) onto a THF solution containing **L5** (64 mg, 0.17 mmol, in 15 mL). After 1 week of slow evaporation single crystals of medium quality were isolated and measured.
Slow diffusion of 20 mL THF linking 5 mL of a silver triflate solution in water and 5 mL of the ligand in THF in an "H"-shaped tube affords the same crystal structure after 45 days.

Yield: 50 mg (0.08 mmol, 48% calculated with respect to AgSO$_3$CF$_3$)
Anal. Calcd for: C 36.9, H 3.27, N 4.54%. Found: C 36.8, H 3.30, N 4.58%.
IR (cm^{-1}): ν(Ar-H) 3065.3 s, ν(-HC-H) 2948.4 s, ν(C=O) 1731.1 s, ν (C=C) 1543.9 w, ν (ArC–C, C=N) 1422.3 w, ν (SO$_3$CF$_3$) 1267.7 s, broad, ν (SO$_3$CF$_3$) 1102.6 s, broad, ν (ArC–H) 631.6 m.

D - IV.13 - Synthesis of {[Ag(L5)]PF₆}₂ (17) metallacycle

15 mg of **L5** (0.04 mmol) and 10.7 mg (0.04 mmol) of AgPF₆ were stirred in a CH₃CN solution (5 mL) in a dark place. 3 mL of EtOEt were layered over the filtered solution, affording single colorless crystals suitable for x-ray crystallography after slow evaporation in a few days.

The same complex can be obtained after a reaction in the microwave where a THF solution containing the ligand and the silver salt is irradiated for 4 minutes (580 W) and filtrated. Single crystals suitable for X-ray are obtained in the solution vessel.

Yield: 15.4 mg (0.02 mmol, 63% calculated with respect to AgPF₆)

Anal. Calcd for: C 35.24, H 3.29, N 4.57% Found: C 34.9, H 3.32, N 4.5%.

IR (cm⁻¹): ν(-HC-H) 2918.7 s, ν(C=O) 1716.5 s, ν (C=C) 1510.1 m, ν (ArC–C, C=N) 1462.4 m, ν (C–O) 1298.2 s, δ(ArC–H) 1054.5 m, ν (PF6) 636.2-530.5 s, broad

D - IV.14 - Synthesis of {[Ag(L5)]NO₃*(X)₂}ₙ (18) coordination polymer (X: H₂O)

A solution of THF containing 35.7 mg of the ligand **L5** (0.09 mmol) and 25 mg of AgNO₃ (0.09 mmol) were stirred together for an hour. Afterwards the solution was filtered using a 13 mm syringe filter (Puradisc ᵀᴹ, PTEF membrane (PTEF: Polytetrafluoroethylene)) and deposited in capillares. Single crystals of the complex suitable for x-ray diffraction were able to be collected the next day. Crystals of the same quality can be obtained after reacting in the microwave for 4 minutes (580 W) a solution of the ligand and the silver salt. After two days crystals are formed in the vessel where the filtrate was collected.

Yield: 19.1 mg (0.02 mmol, 48% calculated with respect to AgNO₃)

Anal. Calcd for: C 47.56, H 4.44, N 9.25% Found: C 45.2, H 5.1, N 9.1%.

IR: ν(Ar-H) 3098.7 s, ν(-HC-H) 2957.7 s, ν(C=O) 1730.1 s, ν (C=C) 1548.9 w, ν (ArC–C, C=N) 1407.2 w s, ν (NO₃) 1391.5-1187.2 s, ν (-C–O) 1116.3 s, ν (ArC–H) 691.0 m

Silver Coordination Compounds with a Family of Ditopic Ligands of Varying Flexibility: About Chains, Rings, Helices and Polycatenanes

175

D - V - Synthesis of Cu(I) and Cu(II) complexes

D - V.1 - Synthesis of {[Cu(L4)$_2$](NO$_3$)$_2$} chelate complex (19)

10 mL of a THF solution containing 40 mg (0.10 mmol) of anhydrous Cu(NO$_3$)$_2$ and 33.7 mg (0.10 mmol) of the ligand **L4** was refluxed for 2 min in the microwave (580 W). The clear solution was allowed to stand a room temperature for two days afterwards blue crystals suitable for X-ray diffraction were elevated form the wall of the vessel.

D - V.2 - {[Cu(L4)]I}$_n$ coordination polymer (20)

20 was prepared by refluxing for 1 min in the microwave a solution containing **L4** (50 mg, 0.16 mmol) and CuI (30 mg, 0.15 mmol) in 10 mL of THF. A yellow-orange precipitate was filtered off and the orange solution obtained was allowed stand a -20°C for three days. Small rod-like orange crystals were pick-up from the bottom of the vessel and measured by X-ray diffraction.

E - Crystallographic data

E - I - Crystal data and structure of Ligands

The crystal data and structure refinement for ethane-1,2-diyl diisonicotinate (**L1**) were reported in the PhD thesis of Dr. Robin [162].

Crystal data and structure refinement for Synthesis of ethane-1,2-diyl dinicotinate

Identification code	**L2**
Empirical formula	C28 H24 N4 O8
Formula weight	544.51
Temperature	293(2) K
Wavelength	0.71073 Å
Crystal system	Orthorhombic
Space group	$P2_12_12$
Unit cell dimensions	a = 4.0360(8) Å $\quad$ α = 90°.
	b = 21.310(4) Å $\quad$ β = 90°.
	c = 7.4260(15) Å $\quad$ γ = 90°.
Volume	638.7(2) Å^3
Z	1
Density (calculated)	1.416 Mg/m^3
Absorption coefficient	0.106 mm^{-1}
F(000)	284
Theta range for data collection	1.91 to 22.56°.
Index ranges	-4<=h<=4, -22<=k<=22, -7<=l<=7
Reflections collected	1726
Independent reflections	847 [R(int) = 0.0848]
Completeness to theta = 22.56°	99.4 %
Refinement method	Full-matrix least-squares on F^2
Data / restraints / parameters	847 / 0 / 98
Goodness-of-fit on F^2	0.956
Final R indices [I>2sigma(I)]	R1 = 0.0514, wR2 = 0.1256
R indices (all data)	R1 = 0.0989, wR2 = 0.1610
Absolute structure parameter	-7(5)

Silver Coordination Compounds with a Family of Ditopic Ligands of Varying Flexibility: About Chains, Rings, Helices and Polycatenanes

177

Extinction coefficient   0.056(14)

Largest diff. peak and hole   0.154 and -0.143 e.Å^{-3}

Table 2. Atomic coordinates (x 10^4) and equivalent isotropic displacement parameters (Å^{2}x 10^3) for **L2**. U(eq) is defined as one third of the trace of the orthogonalized U^{ij} tensor.

	x	y	z	U(eq)
N(1)	5397(13)	970(2)	728(7)	53(2)
C(1)	4005(14)	863(2)	2312(8)	41(2)
C(2)	3651(14)	1306(2)	3669(8)	34(2)
C(3)	4824(15)	1904(2)	3320(7)	40(2)
C(4)	6288(15)	2029(2)	1689(8)	42(2)
C(5)	6494(16)	1546(2)	467(9)	48(2)
C(6)	2044(14)	1162(2)	5419(8)	35(1)
O(1)	1154(12)	1552(2)	6483(6)	57(1)
O(2)	1712(10)	544(1)	5674(5)	39(1)
C(7)	23(16)	350(2)	7299(7)	38(1)

Table 3.   Bond lengths [Å] and angles [°] for **L2**.

N(1)-C(5)	1.318(7)	N(1)-C(1)	1.324(7)
C(1)-C(2)	1.388(7)	C(2)-C(3)	1.384(6)
C(2)-C(6)	1.484(7)	C(3)-C(4)	1.374(7)
C(4)-C(5)	1.374(7)	C(6)-O(1)	1.201(6)
C(6)-O(2)	1.339(5)	O(2)-C(7)	1.446(6)
C(7)-C(7)$^{\#1}$	1.490(9)		

C(5)-N(1)-C(1)	115.8(5)	N(1)-C(1)-C(2)	124.8(5)
C(3)-C(2)-C(1)	117.1(5)	C(3)-C(2)-C(6)	120.2(5)
C(1)-C(2)-C(6)	122.7(5)	C(4)-C(3)-C(2)	119.4(5)
C(5)-C(4)-C(3)	117.6(5)	N(1)-C(5)-C(4)	125.4(6)
O(1)-C(6)-O(2)	123.9(6)	O(1)-C(6)-C(2)	124.4(5)
O(2)-C(6)-C(2)	111.7(5)	C(6)-O(2)-C(7)	116.6(4)
O(2)-C(7)-C(7)$^{\#1}$	107.0(4)		

Symmetry transformations used to generate equivalent atoms:

#1 -x,-y,z

Table 4. Anisotropic displacement parameters ($Å^2$x 10^3)for ligand1. The anisotropic displacement factor exponent takes the form: $-2p^2[\,h^2a^{*2}U^{11} + ... + 2\,h\,k\,a^*\,b^*\,U^{12}\,]$

	U^{11}	U^{22}	U^{33}	U^{23}	U^{13}	U^{12}
N(1)	64(3)	51(3)	43(3)	-10(3)	15(3)	-12(3)
C(1)	43(4)	30(3)	50(4)	-3(3)	10(3)	-3(3)
C(2)	35(3)	32(3)	35(3)	-4(2)	-5(3)	-2(3)
C(3)	46(3)	31(3)	41(3)	-5(3)	-1(3)	-5(3)
C(4)	46(3)	34(3)	47(4)	6(3)	4(3)	-1(3)
C(5)	50(4)	47(4)	46(4)	4(3)	16(4)	-1(3)
C(6)	34(3)	29(3)	42(4)	-5(3)	0(3)	-4(3)
O(1)	86(3)	32(2)	53(3)	-3(2)	17(2)	0(2)
O(2)	50(2)	27(2)	38(2)	-4(2)	10(2)	-4(2)
C(7)	40(3)	45(3)	28(3)	-6(3)	5(3)	-9(3)

Table 5. Hydrogen coordinates (x 10^4) and isotropic displacement parameters ($Å^2$x 10^3) for **L2**.

	x	y	z	U(eq)
H(1)	3209	460	2533	22(12)
H(3)	4615	2218	4181	32(14)
H(4)	7109	2426	1423	42(15)
H(5)	7497	1632	-633	28(14)
H(7A)	-2218	514	7316	58(19)
H(7B)	1189	505	8351	35(14)

Table 6. Hydrogen bond data [length (Å) and angle (°)] for L2

D–H···Acceptor	d (D–H)	d (H···A)	d (D···A)	< D–H···A
C7–H7B···N1	0.97	2.64(1)	3.59(2)	167.7(8)
C3–H3···O1$^{\#2}$	0.93	2.73(8)	3.33(7)	123.0(7)

C4–H4···O1[#2]	0.93	2.70(3)	3.31(5)	124.0(7)
C5–H5···O1[#3]	0.93	2.60(6)	3.50(5)	162.8(9)

Symmetry transformation used to generate equivalent atoms: #2 0.5+x, 0.5-y, 1-z #3 1+x, y, -1+z

Crystal data and structure refinement for Synthesis of 2,2'-oxybis(ethane-2,1-diyl) diisonicotinate

Identification code	**L3**
Empirical formula	C16 H16 N2 O5
Formula weight	316.31
Temperature	293(2) K
Wavelength	0.71073 Å
Crystal system	Monoclinic
Space group	P2$_1$/n
Unit cell dimensions	a = 10.549(2) Å a= 90°.
	b = 11.675(2) Å b= 108.81(3)°.
	c = 13.039(3) Å g = 90°.
Volume	1520.1(5) Å^3
Z	4
Density (calculated)	1.382 Mg/m^3
Absorption coefficient	0.104 mm^{-1}
F(000)	664
Theta range for data collection	2.17 to 27.08°.
Index ranges	-13<=h<=13, -14<=k<=14, -15<=l<=16
Reflections collected	11782
Independent reflections	3327 [R(int) = 0.1410]
Completeness to theta = 27.08°	99.3 %
Refinement method	Full-matrix least-squares on F^2
Data / restraints / parameters	3327 / 0 / 186
Goodness-of-fit on F^2	1.134
Final R indices [I>2sigma(I)]	R1 = 0.0943, wR2 = 0.2063
R indices (all data)	R1 = 0.1875, wR2 = 0.2472
Largest diff. peak and hole	0.435 and -0.499 e.Å^{-3}

Table 2. Atomic coordinates (x 10^4) and equivalent isotropic displacement parameters (Å^2x 10^3) for **L3**. U(eq) is defined as one third of the trace of the orthogonalized U^{ij} tensor.

	x	y	z	U(eq)
N(1)	8790(3)	-2563(3)	6062(2)	54(1)
C(1)	8888(3)	-1590(2)	5478(3)	52(1)
C(2)	9750(3)	-1578(2)	4866(3)	43(1)
C(3)	10515(3)	-2540(2)	4838(2)	32(1)
C(4)	10418(3)	-3513(2)	5423(3)	43(1)
C(5)	9555(3)	-3525(2)	6034(3)	54(1)
C(6)	11443(5)	-2569(4)	4171(4)	37(1)
O(1)	11988(4)	-3430(3)	4018(3)	54(1)
O(2)	11576(3)	-1540(3)	3790(3)	40(1)
C(7)	12356(5)	-1467(5)	3059(4)	44(1)
C(8)	12042(4)	-337(4)	2501(4)	41(1)
O(3)	10658(3)	-321(3)	1887(3)	43(1)
C(9)	10198(4)	761(4)	1445(4)	36(1)
C(10)	8713(5)	704(4)	900(4)	41(1)
O(4)	7991(3)	588(3)	1670(3)	40(1)
O(5)	8031(3)	2498(3)	1873(3)	48(1)
C(11)	7685(4)	1570(4)	2082(4)	34(1)
N(2)	5361(3)	1085(3)	4201(2)	50(1)
C(12)	5942(3)	139(2)	3882(3)	49(1)
C(13)	6698(3)	279(2)	3193(3)	39(1)
C(14)	6873(3)	1365(2)	2823(2)	30(1)
C(15)	6293(3)	2311(2)	3142(3)	41(1)
C(16)	5537(3)	2171(2)	3832(3)	47(1)

Table 3. Bond lengths [Å] and angles [°] for **L3**.

N(1)-C(1)	1.3900	C(2)-C(3)	1.3900
N(1)-C(5)	1.3900	C(3)-C(4)	1.3900
C(1)-C(2)	1.3900	C(3)-C(6)	1.505(5)

Silver Coordination Compounds with a Family of Ditopic Ligands of Varying Flexibility: About Chains, Rings, Helices and Polycatenanes

181

C(4)-C(5)	1.3900	O(4)-C(11)	1.348(5)
C(6)-O(1)	1.206(5)	O(5)-C(11)	1.202(5)
C(6)-O(2)	1.325(6)	C(11)-C(14)	1.502(5)
O(2)-C(7)	1.448(6)	N(2)-C(12)	1.3900
C(7)-C(8)	1.491(7)	N(2)-C(16)	1.3900
C(8)-O(3)	1.421(5)	C(12)-C(13)	1.3900
O(3)-C(9)	1.408(5)	C(13)-C(14)	1.3900
C(9)-C(10)	1.499(6)	C(14)-C(15)	1.3900
C(10)-O(4)	1.450(6)	C(15)-C(16)	1.3900

C(1)-N(1)-C(5)	120.0	O(3)-C(9)-C(10)	108.9(4)
C(2)-C(1)-N(1)	120.0	O(4)-C(10)-C(9)	112.2(4)
C(3)-C(2)-C(1)	120.0	C(11)-O(4)-C(10)	116.3(4)
C(2)-C(3)-C(4)	120.0	O(5)-C(11)-O(4)	123.2(4)
C(2)-C(3)-C(6)	121.6(3)	O(5)-C(11)-C(14)	124.5(4)
C(4)-C(3)-C(6)	118.4(3)	O(4)-C(11)-C(14)	112.3(3)
C(3)-C(4)-C(5)	120.0	C(12)-N(2)-C(16)	120.0
C(4)-C(5)-N(1)	120.0	C(13)-C(12)-N(2)	120.0
O(1)-C(6)-O(2)	125.5(4)	C(12)-C(13)-C(14)	120.0
O(1)-C(6)-C(3)	123.2(4)	C(15)-C(14)-C(13)	120.0
O(2)-C(6)-C(3)	111.3(4)	C(15)-C(14)-C(11)	117.6(2)
C(6)-O(2)-C(7)	116.9(4)	C(13)-C(14)-C(11)	122.4(2)
O(2)-C(7)-C(8)	106.8(4)	C(16)-C(15)-C(14)	120.0
O(3)-C(8)-C(7)	108.2(4)	C(15)-C(16)-N(2)	120.0
C(9)-O(3)-C(8)	113.4(4)		

Table 4. Anisotropic displacement parameters (Å^2x 10^3) for **L3**. The anisotropic displacement factor exponent takes the form: $-2p^2[\,h^2a^{*2}U^{11} + ... + 2\,h\,k\,a^*\,b^*\,U^{12}\,]$

	U^{11}	U^{22}	U^{33}	U^{23}	U^{13}	U^{12}
N(1)	49(3)	73(3)	43(3)	3(2)	20(2)	1(2)
C(1)	55(3)	61(3)	47(3)	-6(3)	25(3)	10(3)
C(2)	50(3)	35(3)	49(3)	-6(2)	25(2)	6(2)
C(3)	28(2)	34(2)	34(2)	1(2)	10(2)	-1(2)

C(4)	38(3)	38(3)	55(3)	8(2)	17(2)	3(2)
C(5)	44(3)	63(4)	58(4)	15(3)	20(3)	4(3)
C(6)	37(2)	35(2)	37(3)	1(2)	13(2)	4(2)
O(1)	63(2)	39(2)	72(3)	6(2)	38(2)	20(2)
O(2)	48(2)	36(2)	49(2)	5(2)	31(2)	4(2)
C(7)	40(3)	52(3)	49(3)	3(3)	26(2)	3(2)
C(8)	33(2)	48(3)	50(3)	2(3)	24(2)	-1(2)
O(3)	35(2)	29(2)	65(2)	5(2)	16(2)	0(1)
C(9)	41(3)	33(2)	41(3)	1(2)	21(2)	-1(2)
C(10)	43(3)	43(3)	42(3)	2(2)	20(2)	4(2)
O(4)	40(2)	31(2)	56(2)	-2(2)	25(2)	1(1)
O(5)	56(2)	30(2)	65(2)	1(2)	29(2)	-5(2)
C(11)	33(2)	24(2)	41(3)	-2(2)	8(2)	3(2)
N(2)	48(2)	52(3)	51(3)	5(2)	18(2)	7(2)
C(12)	43(3)	42(3)	68(4)	8(3)	28(3)	2(2)
C(13)	42(3)	23(2)	55(3)	3(2)	18(2)	5(2)
C(14)	28(2)	27(2)	33(2)	-1(2)	5(2)	3(2)
C(15)	40(3)	34(3)	49(3)	0(2)	13(2)	5(2)
C(16)	60(3)	40(3)	44(3)	-1(2)	22(3)	12(2)

Table 5. Hydrogen coordinates (x 10^4) and isotropic displacement parameters (Å^2x 10^3) for **L3**.

	x	y	z	U(eq)
H(1)	8376	-946	5496	63
H(2)	9815	-927	4475	51
H(4)	10930	-4157	5404	52
H(5)	9490	-4176	6425	65
H(7A)	12119	-2085	2535	53
H(7B)	13304	-1520	3460	53
H(8A)	12245	277	3031	50
H(8B)	12577	-228	2028	50
H(9A)	10637	977	924	44
H(9B)	10409	1333	2015	44

H(10A)	8417	1394	475	50
H(10B)	8505	56	407	50
H(12)	5824	-588	4129	59
H(13)	7086	-354	2979	47
H(15)	6410	3038	2895	50
H(16)	5149	2804	4045	56

Table 5. Hydrogen bond data [length (Å) and angle (°)] for **L3**

D–H···Acceptor	d (D–H)	d (H···A)	d (D···A)	< D–H···A
C9–H9B···N1[#1]	0.97	2.77(6)	3.72(7)	167.5(1)
C10–H10A···N1[#2]	0.97	2.81(9)	3.64(0)	143.7(1)
C10–H10B···O1[#3]	0.97	2.75(6)	3.67(4)	158.8(1)
C9–H9A···O1[#4]	0.97	2.57(5)	3.34(9)	136.7(1)
C8–H8B···O1[#4]	0.97	2.62(4)	3.35(2)	132.1(1)

Symmetry transformation used to generate equivalent atoms: #1 2-x, -y, 1-z #2 1.5-x, -0.5+y, 0.5-z #3 0.5+x, -0.5+y, 0.5+z #4 2.5-x, -0.5+y, 0.5-z

Crystal data and structure refinement for Synthesis of 2,2'-oxybis(ethane-2,1-diyl) dinicotinate

Identification code	**L4**
Empirical formula	C18 H18 N2 O5
Formula weight	342.34
Temperature	293(2) K
Wavelength	0.71073 Å
Crystal system	Monoclinic
Space group	C_2/c
Unit cell dimensions	a = 13.521(3) Å a= 90°.
	b = 6.2159(12) Å b= 92.12(3)°.
	c = 17.712(4) Å g = 90°.
Volume	1487.6(5) Å^3
Z	2

Density (calculated)	0.764 Mg/m^3		
Absorption coefficient	0.056 mm^{-1}		
F(000)	360		
Theta range for data collection	3.02 to 27.08°.		
Index ranges	-16<=h<=17, 0<=k<=7, 0<=l<=22		
Reflections collected	1140		
Independent reflections	1140 [R(int) = 0.0000]		
Completeness to theta = 27.08°	69.6 %		
Refinement method	Full-matrix least-squares on F^2		
Data / restraints / parameters	1140 / 0 / 105		
Goodness-of-fit on F^2	1.169		
Final R indices [I>2sigma(I)]	R1 = 0.0725, wR2 = 0.1742		
R indices (all data)	R1 = 0.1233, wR2 = 0.2040		
Largest diff. peak and hole	0.174 and -0.172 e.Å^{-3}		

Table 2. Atomic coordinates (x 10^4) and equivalent isotropic displacement parameters (Å^{2}x 10^3) for **L4**. U(eq) is defined as one third of the trace of the orthogonalized U^{ij} tensor.

	x	y	z	U(eq)
N(1)	5959(3)	3050(6)	4040(2)	59(1)
C(1)	5936(3)	5088(7)	3797(3)	52(1)
C(2)	6115(3)	6825(7)	4251(3)	56(1)
C(3)	6323(3)	6487(6)	5008(3)	53(1)
C(4)	6347(3)	4405(6)	5287(2)	42(1)
C(5)	6166(3)	2763(7)	4775(3)	51(1)
C(6)	6554(3)	3977(6)	6096(3)	46(1)
O(1)	6829(3)	5343(5)	6541(2)	72(1)
O(2)	6401(2)	1929(4)	6271(2)	50(1)
C(7)	6632(3)	1237(8)	7046(3)	56(1)
C(8)	5808(3)	-170(6)	7296(3)	49(1)
O(3)	5000	1125(6)	7500	46(1)

Table 3.   Bond lengths [Å] and angles [°] for **L4**.

N(1)-C(5)	1.335(7)	C(6)-O(1)	1.209(6)
N(1)-C(1)	1.338(6)	C(6)-O(2)	1.329(5)
C(1)-C(2)	1.363(7)	O(2)-C(7)	1.460(5)
C(2)-C(3)	1.376(7)	C(7)-C(8)	1.497(6)
C(3)-C(4)	1.385(6)	C(8)-O(3)	1.414(4)
C(4)-C(5)	1.381(6)	O(3)-C(8)#1	1.414(4)
C(4)-C(6)	1.473(6)		

C(5)-N(1)-C(1)	116.2(4)	O(1)-C(6)-O(2)	124.6(5)
N(1)-C(1)-C(2)	124.0(5)	O(1)-C(6)-C(4)	123.4(4)
C(1)-C(2)-C(3)	118.7(4)	O(2)-C(6)-C(4)	112.0(4)
C(2)-C(3)-C(4)	119.4(4)	C(6)-O(2)-C(7)	118.2(4)
C(5)-C(4)-C(3)	117.1(5)	O(2)-C(7)-C(8)	108.4(4)
C(5)-C(4)-C(6)	121.8(4)	O(3)-C(8)-C(7)	109.5(3)
C(3)-C(4)-C(6)	121.1(4)	C(8)#1-O(3)-C(8)	110.6(4)
N(1)-C(5)-C(4)	124.6(4)		

Symmetry transformations used to generate equivalent atoms:

#1 -x+1,y,-z+3/2

Table 4. Anisotropic displacement parameters (Å^2x 10^3) for **L4**. The anisotropic displacement factor exponent takes the form: $-2p^2[\,h^2a*^2U^{11} + ... + 2\,h\,k\,a*\,b*\,U^{12}\,]$

	U^{11}	U^{22}	U^{33}	U^{23}	U^{13}	U^{12}
N(1)	84(2)	56(2)	39(2)	0(2)	1(2)	3(2)
C(1)	59(2)	60(2)	38(2)	7(2)	4(2)	-1(2)
C(2)	63(2)	48(2)	57(3)	12(2)	1(2)	1(2)
C(3)	62(2)	40(2)	57(3)	-1(2)	-2(2)	-3(2)
C(4)	42(2)	44(2)	40(2)	-2(2)	2(2)	1(2)
C(5)	73(2)	43(2)	37(2)	3(2)	-2(2)	1(2)
C(6)	47(2)	49(2)	41(3)	-7(2)	-4(2)	5(2)
O(1)	102(2)	61(2)	53(2)	-11(2)	-19(2)	3(2)
O(2)	62(2)	52(2)	37(2)	4(1)	1(1)	-5(1)

C(7)	52(2)	76(3)	39(3)	10(2)	-2(2)	5(2)
C(8)	60(2)	47(2)	41(2)	11(2)	8(2)	10(2)
O(3)	47(2)	42(2)	49(3)	0	8(2)	0

Table 5. Hydrogen coordinates (x 10^4) and isotropic displacement parameters (Å^2x 10^3) for **L4**.

	x	y	z	U(eq)
H(1)	5790	5335	3287	63
H(2)	6096	8211	4054	67
H(3)	6447	7646	5330	64
H(5)	6189	1359	4956	61
H(7A)	6701	2480	7375	67
H(7B)	7251	446	7068	67
H(8A)	5602	-1137	6890	59
H(8B)	6034	-1031	7726	59

Table 5. Hydrogen bond data [length (Å) and angle (°)] for L4

D–H···Acceptor	d (D–H)	d (H···A)	d (D···A)	< D–H···A
C1–H1···O3[#2]	0.93	2.79(5)	3.49(3)	132.6(8)
C8–H8A···O1[#3]	0.97	2.82(4)	3.40(7)	119.1(7)
C7–H7B···O1[#4]	0.97	2.71(7)	3.24(3)	114.4(5)
C8–H8A···N1[#5]	0.97	2.88(7)	3.75(4)	149.5(6)
C8–H8B···N1[#6]	0.97	2.64(4)	3.56(8)	158.2(1)

Symmetry transformation used to generate equivalent atoms: #2 1-x, 1-y, 1-z #3 x, 1+y, z #4 1.5-x, 1.5+y, 1.5-z #5 1-x, -y, -z #6 x, -y, -0.5+z

Crystal data and structure refinement for 2,2'-(ethane-1,2-diylbis(oxy))bis(ethane-2,1-diyl) dinicotinate

Identification code	**L5**
Empirical formula	C18 H20 N2 O6
Formula weight	360.36

Temperature	293(2) K	
Wavelength	0.71073 Å	
Crystal system	Triclinic	
Space group	P-1	
Unit cell dimensions	a = 5.9080(12) Å	a= 72.98(3)°.
	b = 7.1320(14) Å	b= 88.24(3)°.
	c = 10.807(2) Å	g = 78.97(3)°.
Volume	427.22(14) Å^3	
Z	1	
Density (calculated)	1.401 Mg/m^3	
Absorption coefficient	0.106 mm^{-1}	
F(000)	190	
Theta range for data collection	1.97 to 22.49°.	
Index ranges	-6<=h<=6, -7<=k<=7, 0<=l<=11	
Reflections collected	1112	
Independent reflections	1112 [R(int) = 0.0000]	
Completeness to theta = 22.49°	100.0 %	
Refinement method	Full-matrix least-squares on F^2	
Data / restraints / parameters	1112 / 0 / 129	
Goodness-of-fit on F^2	1.051	
Final R indices [I>2sigma(I)]	R1 = 0.1214, wR2 = 0.1868	
R indices (all data)	R1 = 0.3176, wR2 = 0.2867	
Extinction coefficient	0.026(13)	
Largest diff. peak and hole	0.288 and -0.288 e.Å^{-3}	

Table 2. Atomic coordinates (x 10^4) and equivalent isotropic displacement parameters (Å^{2}x 10^3) for **L5**. U(eq) is defined as one third of the trace of the orthogonalized U^{ij} tensor.

	x	y	z	U(eq)
N(1)	5490(30)	4350(20)	2665(12)	55(4)

C(1)	7210(30)	3210(20)	3420(14)	43(5)
C(2)	7090(30)	2140(20)	4734(16)	42(5)
C(3)	4940(30)	2332(18)	5262(13)	27(4)
C(4)	3100(30)	3477(19)	4478(13)	30(4)
C(5)	3390(30)	4450(20)	3203(16)	48(5)
C(6)	4590(30)	1210(20)	6642(13)	27(4)
O(1)	6228(17)	210(14)	7331(9)	43(3)
O(2)	2453(17)	1483(13)	6997(9)	36(3)
C(7)	2040(30)	400(20)	8295(13)	43(5)
C(8)	2480(30)	1450(20)	9262(12)	37(4)
O(3)	608(16)	3082(15)	9206(9)	39(3)
C(9)	1010(20)	4217(19)	10056(14)	32(4)

Table 3.   Bond lengths [Å] and angles [°] for **L5**.

N(1)-C(1)	1.304(19)	C(6)-O(1)	1.211(14)
N(1)-C(5)	1.352(18)	C(6)-O(2)	1.306(15)
C(1)-C(2)	1.41(2)	O(2)-C(7)	1.427(14)
C(2)-C(3)	1.376(18)	C(7)-C(8)	1.502(18)
C(3)-C(4)	1.370(16)	C(8)-O(3)	1.432(15)
C(3)-C(6)	1.500(17)	O(3)-C(9)	1.442(14)
C(4)-C(5)	1.371(18)	C(9)-C(9)[#1]	1.45(2)
C(1)-N(1)-C(5)	115.8(15)	O(1)-C(6)-O(2)	125.6(13)
N(1)-C(1)-C(2)	126.5(16)	O(1)-C(6)-C(3)	120.4(14)
C(3)-C(2)-C(1)	116.1(17)	O(2)-C(6)-C(3)	114.0(12)
C(4)-C(3)-C(2)	118.4(14)	C(6)-O(2)-C(7)	115.8(11)
C(4)-C(3)-C(6)	120.7(13)	O(2)-C(7)-C(8)	112.8(12)
C(2)-C(3)-C(6)	120.8(13)	O(3)-C(8)-C(7)	109.8(12)
C(5)-C(4)-C(3)	121.1(15)	C(8)-O(3)-C(9)	112.0(10)
N(1)-C(5)-C(4)	122.0(17)	O(3)-C(9)-C(9)[#1]	107.0(14)

Symmetry transformations used to generate equivalent atoms:

#1 -x,-y+1,-z+2

Table 4. Anisotropic displacement parameters ($\mathring{A}^2$x 10^3) for **L5**. The anisotropic displacement factor exponent takes the form: $-2p^2[\ h^2a*^2U^{11} + ... + 2\ h\ k\ a*\ b*\ U^{12}\ ]$

	U^{11}	U^{22}	U^{33}	U^{23}	U^{13}	U^{12}
N(1)	76(12)	74(12)	25(8)	-13(8)	-5(9)	-38(10)
C(1)	57(13)	70(13)	23(10)	-26(9)	31(10)	-45(10)
C(2)	48(12)	42(11)	52(12)	-34(10)	21(10)	-20(10)
C(3)	35(9)	5(8)	35(9)	-2(7)	-11(8)	5(7)
C(4)	34(10)	28(10)	33(10)	-12(8)	23(9)	-15(8)
C(5)	49(13)	48(12)	51(12)	-12(10)	5(11)	-20(10)
C(6)	34(10)	23(9)	19(9)	-1(7)	-13(8)	1(8)
O(1)	39(7)	49(8)	34(6)	1(5)	-3(6)	-9(6)
O(2)	41(7)	36(7)	29(7)	-8(5)	7(5)	-3(6)
C(7)	33(11)	53(13)	32(11)	-10(9)	12(8)	8(10)
C(8)	50(11)	28(9)	20(9)	1(7)	8(7)	6(8)
O(3)	36(7)	46(7)	32(6)	-13(5)	0(5)	7(5)
C(9)	44(11)	14(8)	41(10)	-13(8)	-1(8)	-6(7)

Table 5. Hydrogen coordinates (x 10^4) and isotropic displacement parameters ($\mathring{A}^2$x 10^3) for **L5**.

	x	y	z	U(eq)
H(1)	8659	3104	3068	0(30)
H(2)	8373	1374	5232	120(90)
H(4)	1634	3635	4812	0(30)
H(5)	2129	5187	2674	70(60)
H(7A)	3031	-902	8507	40(40)
H(7B)	458	218	8366	0(30)
H(8A)	2666	526	10128	0(30)
H(8B)	3877	1977	9046	0(30)
H(9A)	2372	4791	9797	20(30)
H(9B)	1253	3364	10939	70(50)

Silver Coordination Compounds with a Family of Ditopic Ligands of Varying Flexibility: About Chains, Rings, Helices and Polycatenanes

190

Table 6. Hydrogen bond data [length (Å) and angle (°)] for L5

D–H···Acceptor	d (D–H)	d (H···A)	d (D···A)	< D–H···A
C9–H9A···N1	0.96	2.80(1)	3.50(4)	129.4(2)
C7–H7B···O1[#3]	0.96	2.77(7)	3.65(9)	152.9(1)
C9–H9B···O1[#3]	0.96	2.85(1)	3.69(7)	146.6(2)
C9–H9B···O1[#3]	0.96	2.70(7)	3.56(9)	148.8(1)
C5–H5···O3[#4]	0.92	2.49(1)	3.40(1)	164.6(2)

Symmetry transformation used to generate equivalent atoms: #3 1-x, -y, 2-z #4 –x, 1-y, 1-z

Crystal data and structure refinement for 2,2'-(2,2'-oxybis(ethane-2,1-diyl) bis(oxy)) bis(ethane-2,1-diyl) diisonicotinate

Identification code	**L6**
Empirical formula	C20 H24 N2 O7
Formula weight	404.41
Temperature	293(2) K
Wavelength	0.71073 Å
Crystal system	Orthorhombic
Space group	Pbcn
Unit cell dimensions	a = 10.163(2) Å $\quad$ α = 90°.
	b = 8.7541(18) Å $\quad$ β = 90°.
	c = 22.081(4) Å $\quad$ γ = 90°.
Volume	1964.6(7) Å^3
Z	4
Density (calculated)	1.367 Mg/m^3
Absorption coefficient	0.104 mm^{-1}
F(000)	856
Theta range for data collection	1.84 to 29.54°.
Index ranges	-14<=h<=14, -12<=k<=12, -26<=l<=30
Reflections collected	17966
Independent reflections	2717 [R(int) = 0.0602]
Completeness to theta = 29.54°	98.7 %
Refinement method	Full-matrix least-squares on F^2

Silver Coordination Compounds with a Family of Ditopic Ligands of Varying Flexibility:
About Chains, Rings, Helices and Polycatenanes

191

Data / restraints / parameters	2717 / 0 / 134
Goodness-of-fit on F^2	1.522
Final R indices [I>2sigma(I)]	R1 = 0.0698, wR2 = 0.1744
R indices (all data)	R1 = 0.0769, wR2 = 0.1819
Largest diff. peak and hole	0.328 and -0.196 e.Å^{-3}

Table 2. Atomic coordinates (x 10^4) and equivalent isotropic displacement parameters (Å^{2}x 10^3) for **L6**. U(eq) is defined as one third of the trace of the orthogonalized U^{ij} tensor.

	x	y	z	U(eq)
N(1)	1046(1)	8226(2)	5289(1)	54(1)
C(1)	1699(1)	6914(2)	5351(1)	52(1)
C(2)	1184(1)	5609(2)	5613(1)	39(1)
C(3)	-91(1)	5663(1)	5833(1)	31(1)
C(4)	-784(1)	7023(2)	5775(1)	39(1)
C(5)	-181(1)	8253(2)	5501(1)	46(1)
C(6)	-733(1)	4337(1)	6137(1)	32(1)
O(1)	-1874(1)	4315(1)	6286(1)	45(1)
O(2)	111(1)	3196(1)	6229(1)	37(1)
C(7)	-386(1)	1937(2)	6586(1)	44(1)
C(8)	724(1)	832(1)	6680(1)	42(1)
O(3)	1714(1)	1529(1)	7031(1)	40(1)
C(9)	2750(1)	518(1)	7193(1)	35(1)
C(10)	3891(1)	1511(1)	7368(1)	39(1)
O(4)	5000	595(1)	7500	40(1)

Table 3. Bond lengths [Å] and angles [°] for **L6**.

N(1)-C(5)	1.332(2)	C(6)-O(1)	1.2052(14)
N(1)-C(1)	1.333(2)	C(6)-O(2)	1.3326(13)
C(1)-C(2)	1.384(2)	O(2)-C(7)	1.4463(15)
C(2)-C(3)	1.3845(16)	C(7)-C(8)	1.5003(17)
C(3)-C(4)	1.3883(16)	C(8)-O(3)	1.4090(15)
C(3)-C(6)	1.4924(16)	O(3)-C(9)	1.4214(13)
C(4)-C(5)	1.3786(19)	C(9)-C(10)	1.4994(16)

Silver Coordination Compounds with a Family of Ditopic Ligands of Varying Flexibility: About Chains, Rings, Helices and Polycatenanes

192

C(10)-O(4)	1.4142(13)	O(4)-C(10)#1	1.4142(13)

C(5)-N(1)-C(1)	116.47(12)	O(1)-C(6)-C(3)	123.78(11)
N(1)-C(1)-C(2)	124.43(13)	O(2)-C(6)-C(3)	111.73(10)
C(1)-C(2)-C(3)	118.17(12)	C(6)-O(2)-C(7)	115.40(9)
C(2)-C(3)-C(4)	118.17(11)	O(2)-C(7)-C(8)	107.69(10)
C(2)-C(3)-C(6)	122.70(10)	O(3)-C(8)-C(7)	109.52(11)
C(4)-C(3)-C(6)	119.11(11)	C(8)-O(3)-C(9)	113.47(9)
C(5)-C(4)-C(3)	118.96(12)	O(3)-C(9)-C(10)	106.03(9)
N(1)-C(5)-C(4)	123.79(13)	O(4)-C(10)-C(9)	109.91(9)
O(1)-C(6)-O(2)	124.48(11)	C(10)#1-O(4)-C(10)	110.91(12)

Symmetry transformations used to generate equivalent atoms:

#1 -x+1,y,-z+3/2

Table 4. Anisotropic displacement parameters ($Å^2$x 10^3) for **L6**. The anisotropic displacement factor exponent takes the form: $-2p^2[\,h^2a*^2U^{11} + ... + 2\,h\,k\,a*\,b*\,U^{12}\,]$

	U^{11}	U^{22}	U^{33}	U^{23}	U^{13}	U^{12}
N(1)	44(1)	49(1)	67(1)	16(1)	-3(1)	-11(1)
C(1)	36(1)	57(1)	62(2)	12(1)	12(1)	-4(1)
C(2)	30(1)	42(1)	46(1)	3(1)	6(1)	4(1)
C(3)	23(1)	35(1)	34(1)	1(1)	-5(1)	1(1)
C(4)	26(1)	39(1)	52(1)	3(1)	-5(1)	3(1)
C(5)	39(1)	36(1)	63(1)	8(1)	-11(1)	-1(1)
C(6)	22(1)	35(1)	39(1)	2(1)	-4(1)	1(1)
O(1)	22(1)	48(1)	66(1)	11(1)	1(1)	1(1)
O(2)	25(1)	36(1)	49(1)	9(1)	-1(1)	3(1)
C(7)	24(1)	41(1)	65(1)	18(1)	-5(1)	-3(1)
C(8)	30(1)	33(1)	63(1)	7(1)	-10(1)	-3(1)
O(3)	29(1)	37(1)	54(1)	-4(1)	-8(1)	8(1)
C(9)	25(1)	32(1)	48(1)	4(1)	-2(1)	3(1)
C(10)	27(1)	30(1)	58(1)	1(1)	-4(1)	3(1)
O(4)	21(1)	29(1)	69(2)	0	-6(1)	0

Table 5. Hydrogen coordinates (x 10^4) and isotropic displacement parameters (Å^2x 10^3) for **L6**.

	x	y	z	U(eq)
H(1)	2559	6874	5208	62
H(2)	1681	4720	5641	47
H(4)	-1641	7102	5919	47
H(5)	-658	9154	5462	55
H(7A)	-1107	1440	6376	52
H(7B)	-707	2305	6973	52
H(8A)	402	-74	6885	51
H(8B)	1081	525	6292	51
H(9A)	2982	-133	6854	42
H(9B)	2488	-123	7531	42
H(10A)	4097	2203	7038	46
H(10B)	3660	2117	7720	46

Table 6. Hydrogen bond data [length (Å) and angle (°)] for L6

D–H···Acceptor	d (D–H)	D (H···A)	d (D···A)	< D–H···A
C2–H2···N1[#2]	0.93	2.76(4)	3.57(6)	146.1(1)
C8–H8B···N1[#3]	0.97	2.99(4)	3.84(0)	146.7(9)
C5–H5···N1[#4]	0.93	2.85(4)	3.65(0)	143.7(1)
C7–H7A···O1[#5]	0.97	2.77(4)	3.66(8)	153.1(1)
C4–H4···O1[#5]	0.93	2.58(3)	3.31(1)	135.2(1)
C9–H9B···O1[#6]	0.97	2.73(5)	3.53(9)	140.5(9)
C9–H9A···O3[#2]	0.97	2.96(6)	3.55(2)	120.1(1)
C7–H7B···O3[#7]	0.97	2.51(4)	3.35(8)	144.7(9)

Symmetry transformation used to generate equivalent atoms: #2 0.5-x, 0.5+y, z #3 x, 1y, z #4 –x, 2-y, 1-z #5 -0.5-x, 0.5+y, z #6 -0.5+x, 0.5+y, 1.5-z #7 –x, y, 1.5-z

E - II - Crystal data and structure of Complexes

Crystal data and structure refinement for {[Ag(L1)]NO₃}ₙ (1)

Identification code	**1**
Empirical formula	C14 H12 Ag N3 O7
Formula weight	442.14
Temperature	293(2) K
Wavelength	0.71073 Å
Crystal system	Triclinic
Space group	P-1
Unit cell dimensions	a = 6.1668(12) Å α = 93.39(3)°.
	b = 8.9021(18) Å β = 100.00(3)°.
	c = 14.449(3) Å γ = 91.15(3)°.
Volume	779.4(3) Å³
Z	2
Density (calculated)	1.884 Mg/m³
Absorption coefficient	1.338 mm⁻¹
F(000)	440
Theta range for data collection	2.29 to 27.22°.
Index ranges	-7<=h<=7, -11<=k<=11, -17<=l<=16
Reflections collected	6157
Independent reflections	3188 [R(int) = 0.1345]
Completeness to theta = 27.22°	91.7 %
Refinement method	Full-matrix least-squares on F²
Data / restraints / parameters	3188 / 0 / 226
Goodness-of-fit on F²	0.951
Final R indices [I>2sigma(I)]	R1 = 0.0711, wR2 = 0.1065
R indices (all data)	R1 = 0.1863, wR2 = 0.1408
Largest diff. peak and hole	0.486 and -0.750 e.Å⁻³

Table 2. Atomic coordinates (x 10^4) and equivalent isotropic displacement parameters (Å²x 10^3) for **1**. U(eq) is defined as one third of the trace of the orthogonalized U^{ij} tensor.

_____

	x	y	z	U(eq)
Ag(1)	6223(2)	6422(1)	6104(1)	52(1)
N(1)	6980(13)	5118(9)	7354(7)	39(2)
C(1)	5531(16)	5084(12)	7955(8)	47(3)
C(2)	5997(16)	4405(11)	8804(8)	47(3)
C(3)	7969(15)	3690(10)	9031(7)	32(2)
C(4)	9428(18)	3690(12)	8400(8)	44(3)
C(5)	8852(19)	4442(12)	7584(9)	44(3)
C(6)	8436(19)	3013(12)	9981(8)	40(3)
O(1)	10313(11)	2265(8)	10088(5)	42(2)
O(2)	7267(12)	3151(9)	10556(6)	58(2)
C(7)	10773(15)	1549(12)	10991(8)	44(3)
C(8)	13020(16)	869(12)	11001(7)	47(3)
O(3)	13326(10)	152(8)	11878(5)	44(2)
O(4)	16510(12)	-802(8)	11561(6)	54(2)
C(9)	15173(18)	-614(11)	12082(8)	42(3)
N(2)	15766(14)	-2604(10)	14730(6)	45(2)
C(10)	13961(19)	-1827(14)	14398(10)	52(4)
C(11)	13708(19)	-1131(13)	13560(9)	49(3)
C(12)	15341(15)	-1245(10)	13033(7)	35(2)
C(13)	17218(17)	-2016(12)	13379(8)	48(3)
C(14)	17372(16)	-2702(12)	14204(8)	47(3)
O(6)	-165(12)	8245(10)	6640(7)	77(3)
N(3)	1432(17)	7497(11)	6505(7)	48(2)
O(5)	1145(14)	6272(10)	6067(7)	63(2)
O(7)	3355(12)	7974(8)	6841(6)	64(2)

Table 3.   Bond lengths [Å] and angles [°] for **1**.

Ag(1)-N(1)	2.191(8)	C(2)-C(3)	1.382(12)
Ag(1)-N(2)#1	2.189(9)	C(3)-C(4)	1.387(13)
N(1)-C(5)	1.313(12)	C(3)-C(6)	1.516(14)
N(1)-C(1)	1.350(13)	C(4)-C(5)	1.387(14)
C(1)-C(2)	1.388(14)	C(6)-O(2)	1.193(12)

C(6)-O(1)	1.337(12)	C(2)-C(3)-C(6)	117.2(10)
O(1)-C(7)	1.471(11)	C(3)-C(4)-C(5)	118.1(10)
C(7)-C(8)	1.521(13)	N(1)-C(5)-C(4)	124.1(11)
C(8)-O(3)	1.438(11)	O(2)-C(6)-O(1)	125.0(10)
O(3)-C(9)	1.337(11)	O(2)-C(6)-C(3)	123.6(10)
O(4)-C(9)	1.217(12)	O(1)-C(6)-C(3)	111.4(9)
C(9)-C(12)	1.503(14)	C(6)-O(1)-C(7)	112.7(8)
N(2)-C(10)	1.353(13)	O(1)-C(7)-C(8)	104.3(8)
N(2)-C(14)	1.350(13)	O(3)-C(8)-C(7)	101.3(7)
N(2)-Ag(1)#2	2.189(9)	C(9)-O(3)-C(8)	116.0(8)
C(10)-C(11)	1.379(14)	O(4)-C(9)-O(3)	124.7(10)
C(11)-C(12)	1.366(14)	O(4)-C(9)-C(12)	124.6(9)
C(12)-C(13)	1.390(12)	O(3)-C(9)-C(12)	110.6(10)
C(13)-C(14)	1.361(14)	C(10)-N(2)-C(14)	117.7(10)
O(6)-N(3)	1.237(10)	C(10)-N(2)-Ag(1)#2	122.4(8)
N(3)-O(5)	1.222(12)	C(14)-N(2)-Ag(1)#2	119.8(7)
N(3)-O(7)	1.256(11)	N(2)-C(10)-C(11)	123.1(10)
		C(10)-C(11)-C(12)	118.6(10)
N(1)-Ag(1)-N(2)#1	169.5(3)	C(11)-C(12)-C(13)	118.6(10)
C(5)-N(1)-C(1)	117.8(9)	C(11)-C(12)-C(9)	123.0(9)
C(5)-N(1)-Ag(1)	123.0(7)	C(13)-C(12)-C(9)	118.5(10)
C(1)-N(1)-Ag(1)	119.1(6)	C(14)-C(13)-C(12)	120.5(10)
N(1)-C(1)-C(2)	122.1(9)	N(2)-C(14)-C(13)	121.5(9)
C(3)-C(2)-C(1)	119.2(10)	O(6)-N(3)-O(5)	120.2(11)
C(4)-C(3)-C(2)	118.5(10)	O(6)-N(3)-O(7)	120.1(10)
C(4)-C(3)-C(6)	124.2(9)	O(5)-N(3)-O(7)	119.7(10)

Symmetry transformations used to generate equivalent atoms:

#1 x-1,y+1,z-1   #2 x+1,y-1,z+1

Table 4. Anisotropic displacement parameters ($Å^2$ x 10^3) for **1**. The anisotropic displacement factor exponent takes the form: $-2p^2[h^2a^{*2}U^{11} + ... + 2 h k a^* b^* U^{12}]$

	U^{11}	U^{22}	U^{33}	U^{23}	U^{13}	U^{12}

Ag(1)	55(1)	60(1)	43(1)	24(1)	5(1)	10(1)
N(1)	38(5)	47(5)	36(6)	18(4)	7(4)	22(4)
C(1)	36(6)	56(7)	49(8)	21(6)	0(5)	16(5)
C(2)	43(6)	52(7)	49(8)	16(5)	15(5)	15(5)
C(3)	36(6)	28(5)	32(7)	7(4)	1(4)	10(4)
C(4)	49(7)	49(7)	40(8)	19(5)	17(6)	7(5)
C(5)	56(7)	42(6)	37(8)	16(5)	13(5)	12(5)
C(6)	52(7)	35(6)	33(8)	2(5)	3(6)	4(5)
O(1)	45(4)	51(4)	33(5)	17(3)	6(3)	18(3)
O(2)	57(5)	75(6)	50(6)	26(4)	24(4)	20(4)
C(7)	46(7)	53(6)	31(7)	21(5)	-2(5)	17(5)
C(8)	63(7)	53(7)	28(7)	21(5)	10(5)	1(5)
O(3)	34(4)	58(5)	41(5)	20(4)	5(3)	10(3)
O(4)	58(5)	56(5)	53(6)	16(4)	14(4)	17(4)
C(9)	47(7)	34(6)	44(8)	7(5)	-2(5)	1(5)
N(2)	46(5)	49(6)	37(7)	5(4)	-6(4)	7(4)
C(10)	39(7)	67(8)	54(10)	7(7)	15(6)	9(6)
C(11)	52(8)	62(8)	35(9)	12(6)	9(6)	8(6)
C(12)	39(6)	37(6)	27(7)	12(4)	0(5)	5(4)
C(13)	48(6)	54(7)	51(9)	20(6)	24(5)	22(5)
C(14)	34(6)	55(7)	55(9)	15(6)	10(5)	7(5)
O(6)	41(5)	80(6)	107(8)	-18(5)	9(5)	15(4)
N(3)	66(7)	44(6)	36(7)	8(5)	10(5)	16(6)
O(5)	66(5)	52(5)	71(6)	-2(5)	14(4)	0(4)
O(7)	40(4)	57(5)	89(7)	-5(4)	-5(4)	2(4)

Table 5. Hydrogen coordinates (x 10^4) and isotropic displacement parameters (Å^2x 10^3) for **1**.

_____

	x	y	z	U(eq)

_____

H(1)	4177	5529	7794	56
H(2)	4993	4432	9216	56
H(4)	10756	3200	8522	53
H(5)	9856	4470	7173	53

_____

H(7A)	9664	775	11023	52
H(7B)	10812	2287	11515	52
H(8A)	13004	144	10471	56
H(8B)	14153	1639	10997	56
H(10)	12839	-1760	14752	63
H(11)	12453	-595	13358	59
H(13)	18378	-2062	13045	58
H(14)	18611	-3250	14411	57

Table 6. Hydrogen bond data [length (Å) and angle (°)] present in complex **1**

D-H···Acceptor	d (D–H)	d (H···A)	d (D···A)	< D-H···A
C5-H5···O5[#1]	0.93	2.56(2)	3.30(1)	137.5(9)
C8-H8B···O2[#1]	0.97	2.52(3)	3.45(1)	162.6(2)
C11-H11···O6[#2]	0.93	2.56(6)	3.41(1)	152.4(8)

Symmetry transformation used to generate equivalent atoms: #1 1+x,y,z, #2 -1-x,1-y,-z, #3 -x,1-y,-z.

Crystal data and structure refinement for {[Ag(L1)]PF$_6$}$_n$ (2)

Identification code	**2**
Empirical formula	C112 H96 Ag8 F48 N16 O32 P8
Formula weight	4200.77
Temperature	293(2) K
Wavelength	0.71073 Å
Crystal system	Monoclinic
Space group	C2/c
Unit cell dimensions	a = 35.290(8) Å $\alpha = 90°$.
	b = 10.453(2) Å $\beta = 101.43(3)°$.
	c = 9.3818(19) Å $\gamma = 90°$.
Volume	3392.2(12) Å^3
Z	1
Density (calculated)	2.056 Mg/m^3
Absorption coefficient	1.372 mm^{-1}
F(000)	2064
Theta range for data collection	2.92 to 24.96°.

Index ranges	-40<=h<=41, -12<=k<=12, -10<=l<=10
Reflections collected	3443
Independent reflections	1214 [R(int) = 0.0949]
Completeness to theta = 24.96°	40.8 %
Refinement method	Full-matrix least-squares on F^2
Data / restraints / parameters	1214 / 0 / 253
Goodness-of-fit on F^2	1.034
Final R indices [I>2sigma(I)]	R1 = 0.0447, wR2 = 0.0720
R indices (all data)	R1 = 0.0879, wR2 = 0.0834
Largest diff. peak and hole	0.287 and -0.274 e.$Å^{-3}$

Table 2. Atomic coordinates (x 10^4) and equivalent isotropic displacement parameters ($Å^2$x 10^3) for **2**. U(eq) is defined as one third of the trace of the orthogonalized U^{ij} tensor.

	x	y	z	U(eq)
Ag(1)	-1287(1)	381(1)	3679(1)	39(1)
N(1)	-1671(3)	1359(8)	1935(10)	31(2)
C(1)	-1691(3)	2618(12)	1855(13)	38(3)
C(2)	-1880(3)	3250(10)	610(12)	30(3)
C(3)	-2055(3)	2533(10)	-578(12)	23(3)
C(4)	-2041(3)	1216(10)	-497(11)	23(2)
C(5)	-1850(3)	649(10)	794(12)	30(3)
C(6)	-2244(3)	3211(12)	-1914(13)	30(3)
O(1)	-2357(2)	4302(7)	-1949(8)	43(2)
O(2)	-2313(3)	2426(7)	-3076(9)	35(3)
C(7)	-2509(3)	2992(12)	-4401(14)	31(3)
N(2)	-907(3)	-610(9)	5370(10)	29(2)
C(8)	-681(3)	65(11)	6452(11)	34(3)
C(9)	-465(3)	-482(11)	7677(11)	30(3)
C(10)	-471(3)	-1790(11)	7795(12)	28(3)
C(11)	-693(3)	-2500(10)	6725(12)	33(3)
C(12)	-904(3)	-1886(11)	5521(13)	34(3)
C(13)	-234(3)	-2395(10)	9138(13)	29(3)

C(14)	-11(5)	-4330(11)	10251(15)	58(5)
O(3)	-73(3)	-1801(7)	10187(11)	40(2)
O(4)	-227(2)	-3650(7)	8998(8)	39(2)
P(1)	-1236(1)	3428(3)	6320(4)	36(1)
F(1)	-1050(2)	2822(7)	5045(9)	54(2)
F(2)	-1357(3)	2029(7)	6734(10)	76(3)
F(3)	-1428(3)	3985(8)	7553(10)	89(4)
F(4)	-1122(2)	4786(6)	5902(10)	77(3)
F(5)	-834(3)	3235(10)	7381(10)	86(3)
F(6)	-1643(2)	3564(7)	5219(10)	67(3)

Table 3.   Bond lengths [Å] and angles [°] for **2**.

Ag(1)-N(2)	2.133(9)	C(8)-C(9)	1.372(13)
Ag(1)-N(1)	2.163(9)	C(9)-C(10)	1.372(14)
N(1)-C(1)	1.318(13)	C(10)-C(11)	1.365(15)
N(1)-C(5)	1.351(13)	C(10)-C(13)	1.507(15)
C(1)-C(2)	1.393(15)	C(11)-C(12)	1.381(15)
C(2)-C(3)	1.383(14)	C(13)-O(3)	1.206(14)
C(3)-C(4)	1.379(13)	C(13)-O(4)	1.320(11)
C(3)-C(6)	1.478(14)	C(14)-O(4)	1.453(14)
C(4)-C(5)	1.396(13)	C(14)-C(14)#2	1.48(2)
C(6)-O(1)	1.207(12)	P(1)-F(4)	1.547(7)
C(6)-O(2)	1.348(14)	P(1)-F(3)	1.565(9)
O(2)-C(7)	1.426(16)	P(1)-F(5)	1.577(9)
C(7)-C(7)#1	1.53(3)	P(1)-F(2)	1.593(8)
N(2)-C(12)	1.342(12)	P(1)-F(6)	1.601(9)
N(2)-C(8)	1.357(13)	P(1)-F(1)	1.605(8)
N(2)-Ag(1)-N(1)	178.9(4)	C(4)-C(3)-C(2)	119.4(9)
C(1)-N(1)-C(5)	119.5(9)	C(4)-C(3)-C(6)	122.1(10)
C(1)-N(1)-Ag(1)	122.2(7)	C(2)-C(3)-C(6)	118.5(10)
C(5)-N(1)-Ag(1)	117.6(7)	C(3)-C(4)-C(5)	118.5(9)
N(1)-C(1)-C(2)	122.1(11)	N(1)-C(5)-C(4)	121.6(9)
C(3)-C(2)-C(1)	118.8(10)	O(1)-C(6)-O(2)	123.2(11)

O(1)-C(6)-C(3)	124.6(11)	O(4)-C(14)-C(14)#2	104.9(15)
O(2)-C(6)-C(3)	111.9(10)	C(13)-O(4)-C(14)	115.1(9)
C(6)-O(2)-C(7)	115.6(9)	F(4)-P(1)-F(3)	91.1(5)
O(2)-C(7)-C(7)#1	106.1(12)	F(4)-P(1)-F(5)	91.7(5)
C(12)-N(2)-C(8)	116.6(10)	F(3)-P(1)-F(5)	92.8(6)
C(12)-N(2)-Ag(1)	123.5(8)	F(4)-P(1)-F(2)	179.4(6)
C(8)-N(2)-Ag(1)	119.6(7)	F(3)-P(1)-F(2)	89.1(5)
N(2)-C(8)-C(9)	123.8(11)	F(5)-P(1)-F(2)	88.8(5)
C(8)-C(9)-C(10)	117.9(11)	F(4)-P(1)-F(6)	90.1(4)
C(11)-C(10)-C(9)	119.9(11)	F(3)-P(1)-F(6)	88.8(5)
C(11)-C(10)-C(13)	122.0(10)	F(5)-P(1)-F(6)	177.6(5)
C(9)-C(10)-C(13)	118.1(10)	F(2)-P(1)-F(6)	89.4(5)
C(10)-C(11)-C(12)	119.1(10)	F(4)-P(1)-F(1)	90.5(5)
N(2)-C(12)-C(11)	122.7(11)	F(3)-P(1)-F(1)	178.1(5)
O(3)-C(13)-O(4)	125.3(11)	F(5)-P(1)-F(1)	88.3(5)
O(3)-C(13)-C(10)	124.0(11)	F(2)-P(1)-F(1)	89.3(4)
O(4)-C(13)-C(10)	110.7(9)	F(6)-P(1)-F(1)	90.1(5)

Symmetry transformations used to generate equivalent atoms:

#1 -x-1/2,-y+1/2,-z-1   #2 -x,-y-1,-z+2

Table 4. Anisotropic displacement parameters ($\mathring{A}^2$x 10^3) for **2**. The anisotropic displacement factor exponent takes the form: $-2p^2[\,h^2a^{*2}U^{11} + ... + 2\,h\,k\,a^*\,b^*\,U^{12}\,]$

	U^{11}	U^{22}	U^{33}	U^{23}	U^{13}	U^{12}
Ag(1)	41(1)	44(1)	27(1)	13(1)	-5(1)	7(1)
N(1)	37(6)	24(6)	28(5)	11(4)	0(5)	-1(4)
C(1)	24(7)	50(9)	35(7)	-5(6)	-9(6)	8(6)
C(2)	45(9)	12(5)	29(6)	3(5)	-4(6)	1(5)
C(3)	20(6)	19(6)	24(6)	4(5)	-4(5)	3(5)
C(4)	16(6)	29(6)	17(5)	-8(5)	-13(4)	1(5)
C(5)	32(6)	21(6)	32(6)	-6(5)	-3(5)	-5(5)
C(6)	29(8)	35(7)	25(6)	9(6)	7(6)	-5(6)
O(1)	65(6)	24(5)	32(5)	0(4)	-8(4)	12(4)
O(2)	59(8)	29(5)	14(4)	4(4)	1(5)	9(4)

C(7)	12(8)	55(9)	18(6)	-2(6)	-18(6)	-4(6)
N(2)	29(5)	32(5)	24(5)	7(4)	-2(4)	7(4)
C(8)	44(6)	20(5)	38(5)	9(8)	7(5)	5(7)
C(9)	31(6)	32(6)	26(5)	4(6)	1(5)	-7(6)
C(10)	24(7)	32(6)	30(7)	8(6)	6(5)	6(6)
C(11)	38(7)	26(6)	29(6)	8(5)	-6(6)	3(5)
C(12)	33(8)	34(7)	34(7)	-2(6)	10(6)	-8(6)
C(13)	38(7)	20(6)	26(6)	-2(5)	0(5)	4(5)
C(14)	76(9)	40(8)	45(12)	29(7)	-20(8)	20(8)
O(3)	49(8)	32(4)	32(5)	-8(4)	-14(4)	2(4)
O(4)	61(6)	20(4)	28(4)	8(4)	-13(4)	10(4)
P(1)	43(2)	29(2)	33(2)	-1(2)	-2(2)	0(2)
F(1)	60(6)	65(5)	38(5)	-9(4)	14(5)	5(4)
F(2)	92(7)	46(5)	90(8)	18(5)	19(6)	-9(5)
F(3)	116(10)	99(8)	57(6)	-26(5)	29(7)	32(6)
F(4)	98(6)	21(5)	109(7)	12(4)	11(5)	-9(4)
F(5)	65(7)	132(8)	46(6)	-11(6)	-22(5)	7(6)
F(6)	50(6)	81(6)	61(6)	-7(5)	-8(5)	11(5)

Table 5. Hydrogen coordinates (x 10^4) and isotropic displacement parameters ($Å^2$x 10^3) for **2**.

	x	y	z	U(eq)
H(1)	-1574	3098	2657	46
H(2)	-1889	4139	578	36
H(4)	-2157	716	-1283	28
H(5)	-1845	-238	871	35
H(7A)	-2383	3782	-4588	37
H(7B)	-2776	3178	-4354	37
H(8)	-673	950	6359	41
H(9)	-319	18	8403	36
H(11)	-703	-3386	6805	39
H(12)	-1050	-2378	4785	40

H(14A)	-144	-4288	11061	70
H(14B)	246	-3970	10551	70

Table 5. Hydrogen bond data for **2** [length (Å) and angle (°)]

D-H···Acceptor	d (D–H)	d (H···A)	d (D···A)	< D-H···A
C1-H1···F6[#1]	0.93	2.51(2)	3.27(1)	140.3(1)
C8-H8···F1[#2]	0.93	2.54(3)	3.32(1)	142.6(2)
C4-H4···O1[#3]	93	2.60(1)	3.49(1)	163.0(2)
C11-H11···F4[#2]	0.93	2.46(2)	3.23(1)	141.2(1)

Symmetry transformation used to generate equivalent atoms: #1 x,1-y,-1/2+z, #2 x,-y,-1/2+z, #3 1/2-x,-1/2+y,3/2-z

Crystal data and structure refinement for $\{[Ag(L1)]SO_3CF_3\}n$ (3)

Identification code	**3**
Empirical formula	C15 H12 Ag F3 N2 O7 S
Formula weight	529.20
Temperature	293(2) K
Wavelength	0.71073 Å
Crystal system	Monoclinic
Space group	$P2_1/c$
Unit cell dimensions	a = 8.9947(18) Å $\quad$ $\alpha = 90°$.
	b = 21.389(4) Å $\quad$ $\beta = 95.47(3)°$.
	c = 9.4895(19) Å $\quad$ $\gamma = 90°$.
Volume	1817.4(6) Å^3
Z	4
Density (calculated)	1.934 Mg/m^3
Absorption coefficient	1.297 mm^{-1}
F(000)	1048
Theta range for data collection	1.90 to 27.16°.
Index ranges	-11<=h<=11, -27<=k<=27, -12<=l<=12
Reflections collected	14456
Independent reflections	4008 [R(int) = 0.1077]
Completeness to theta = 27.16°	99.5 %
Refinement method	Full-matrix least-squares on F^2

Data / restraints / parameters	4008 / 0 / 262
Goodness-of-fit on F^2	1.038
Final R indices [I>2sigma(I)]	R1 = 0.0562, wR2 = 0.0959
R indices (all data)	R1 = 0.1132, wR2 = 0.1125
Largest diff. peak and hole	0.460 and -0.549 e.Å^{-3}

Table 2. Atomic coordinates (x 10^4) and equivalent isotropic displacement parameters (Å^{2}x 10^3) for **2**. U(eq) is defined as one third of the trace of the orthogonalized U^{ij} tensor.

	x	y	z	U(eq)
Ag(1)	5479(1)	7416(1)	215(1)	48(1)
N(1)	7002(5)	7842(2)	-1117(5)	38(1)
C(1)	7834(6)	7504(2)	-1933(6)	37(1)
C(2)	8651(7)	7765(2)	-2955(6)	37(1)
C(3)	8583(6)	8404(2)	-3128(6)	32(1)
C(4)	7743(7)	8757(2)	-2283(6)	38(1)
C(5)	6970(7)	8460(3)	-1293(6)	38(1)
C(6)	9456(7)	8701(3)	-4222(6)	39(1)
O(1)	10140(5)	8419(2)	-5043(5)	54(1)
O(2)	9375(5)	9322(2)	-4142(5)	48(1)
C(7)	10127(8)	9671(3)	-5177(7)	54(2)
N(1A)	3917(5)	7032(2)	1567(5)	39(1)
C(1A)	3788(7)	6415(3)	1685(7)	39(1)
C(2A)	2938(7)	6139(3)	2675(7)	40(1)
C(3A)	2195(6)	6521(3)	3545(6)	35(1)
C(4A)	2322(7)	7164(3)	3418(6)	38(1)
C(5A)	3183(6)	7393(3)	2413(6)	38(1)
C(6A)	1223(7)	6254(3)	4600(6)	39(1)
O(1A)	1007(5)	5646(2)	4378(5)	45(1)
O(2A)	718(5)	6552(2)	5493(5)	55(1)
C(7A)	88(7)	5321(3)	5313(7)	43(2)
S(1)	5822(2)	5984(1)	-2383(2)	50(1)
O(5)	5265(8)	6419(2)	-3470(6)	81(2)

Silver Coordination Compounds with a Family of Ditopic Ligands of Varying Flexibility:
About Chains, Rings, Helices and Polycatenanes

205

O(6)	7023(6)	5605(3)	-2762(7)	94(2)
O(7)	5958(7)	6233(2)	-973(5)	74(2)
C(18)	4295(11)	5448(4)	-2379(9)	70(2)
F(1)	3094(6)	5719(4)	-2044(8)	128(2)
F(2)	3993(8)	5173(3)	-3629(6)	116(2)
F(3)	4577(9)	4996(3)	-1471(7)	134(3)

Table 3.   Bond lengths [Å] and angles [°] for **3**.

Ag(1)-N(1)	2.152(4)	C(2A)-C(3A)	1.379(8)
Ag(1)-N(1A)	2.154(4)	C(3A)-C(4A)	1.387(8)
N(1)-C(5)	1.334(7)	C(3A)-C(6A)	1.502(7)
N(1)-C(1)	1.339(7)	C(4A)-C(5A)	1.374(7)
C(1)-C(2)	1.388(7)	C(6A)-O(2A)	1.185(7)
C(2)-C(3)	1.378(7)	C(6A)-O(1A)	1.329(7)
C(3)-C(4)	1.378(7)	O(1A)-C(7A)	1.447(6)
C(3)-C(6)	1.501(7)	C(7A)-C(7A)#2	1.498(12)
C(4)-C(5)	1.376(7)	S(1)-O(6)	1.424(5)
C(6)-O(1)	1.200(7)	S(1)-O(7)	1.434(5)
C(6)-O(2)	1.333(7)	S(1)-O(5)	1.442(5)
O(2)-C(7)	1.451(6)	S(1)-C(18)	1.791(8)
C(7)-C(7)#1	1.471(13)	C(18)-F(1)	1.292(10)
N(1A)-C(1A)	1.332(7)	C(18)-F(3)	1.304(9)
N(1A)-C(5A)	1.332(7)	C(18)-F(2)	1.329(9)
C(1A)-C(2A)	1.397(7)		
N(1)-Ag(1)-N(1A)	177.43(18)	C(5)-C(4)-C(3)	119.1(5)
C(5)-N(1)-C(1)	118.0(4)	N(1)-C(5)-C(4)	122.4(5)
C(5)-N(1)-Ag(1)	119.0(4)	O(1)-C(6)-O(2)	124.9(5)
C(1)-N(1)-Ag(1)	122.3(4)	O(1)-C(6)-C(3)	124.8(5)
N(1)-C(1)-C(2)	123.3(5)	O(2)-C(6)-C(3)	110.3(5)
C(3)-C(2)-C(1)	117.6(5)	C(6)-O(2)-C(7)	116.2(4)
C(2)-C(3)-C(4)	119.6(5)	O(2)-C(7)-C(7)#1	104.2(6)
C(2)-C(3)-C(6)	118.8(5)	C(1A)-N(1A)-C(5A)	118.1(5)
C(4)-C(3)-C(6)	121.5(5)	C(1A)-N(1A)-Ag(1)	119.7(4)

C(5A)-N(1A)-Ag(1)	121.8(4)	O(6)-S(1)-O(7)	116.6(4)
N(1A)-C(1A)-C(2A)	122.2(5)	O(6)-S(1)-O(5)	114.0(4)
C(3A)-C(2A)-C(1A)	118.7(5)	O(7)-S(1)-O(5)	114.9(3)
C(2A)-C(3A)-C(4A)	119.1(5)	O(6)-S(1)-C(18)	103.6(4)
C(2A)-C(3A)-C(6A)	121.4(5)	O(7)-S(1)-C(18)	103.5(3)
C(4A)-C(3A)-C(6A)	119.5(5)	O(5)-S(1)-C(18)	101.6(4)
C(5A)-C(4A)-C(3A)	118.0(5)	F(1)-C(18)-F(3)	106.6(8)
N(1A)-C(5A)-C(4A)	123.8(5)	F(1)-C(18)-F(2)	108.3(8)
O(2A)-C(6A)-O(1A)	125.4(5)	F(3)-C(18)-F(2)	105.8(7)
O(2A)-C(6A)-C(3A)	124.1(5)	F(1)-C(18)-S(1)	111.8(6)
O(1A)-C(6A)-C(3A)	110.5(5)	F(3)-C(18)-S(1)	112.1(7)
C(6A)-O(1A)-C(7A)	117.2(4)	F(2)-C(18)-S(1)	111.9(6)
O(1A)-C(7A)-C(7A)#2	104.0(6)		

Symmetry transformations used to generate equivalent atoms:

#1 -x+2,-y+2,-z-1   #2 -x,-y+1,-z+1

Table 4.   Anisotropic displacement parameters ($\text{Å}^2 \times 10^3$) for l2-agso3cf3. The anisotropic displacement factor exponent takes the form: $-2p^2[\, h^2a^{*2}U^{11} + ... + 2\,h\,k\,a^*\,b^*\,U^{12}\,]$

	U^{11}	U^{22}	U^{33}	U^{23}	U^{13}	U^{12}
Ag(1)	50(1)	52(1)	45(1)	16(1)	16(1)	-16(1)
N(1)	40(3)	38(3)	36(3)	10(2)	12(2)	-11(2)
C(1)	43(3)	26(3)	43(3)	3(2)	5(3)	-8(3)
C(2)	40(3)	29(3)	41(3)	1(2)	6(3)	-2(2)
C(3)	35(3)	31(3)	32(3)	9(2)	12(3)	-6(2)
C(4)	44(4)	31(3)	41(3)	2(2)	16(3)	-6(3)
C(5)	44(4)	33(3)	39(3)	2(2)	17(3)	-6(3)
C(6)	39(4)	42(3)	37(3)	3(3)	15(3)	-12(3)
O(1)	63(3)	52(2)	51(3)	-3(2)	33(3)	-8(2)
O(2)	64(3)	36(2)	48(3)	11(2)	29(2)	-10(2)
C(7)	71(5)	49(3)	48(4)	13(3)	33(4)	-16(3)
N(1A)	36(3)	40(3)	42(3)	8(2)	14(2)	-8(2)
C(1A)	39(3)	36(3)	46(4)	3(3)	17(3)	-11(3)

C(2A)	40(3)	33(3)	48(4)	6(3)	13(3)	-4(3)
C(3A)	35(3)	34(3)	36(3)	7(2)	5(3)	-5(2)
C(4A)	43(4)	34(3)	40(3)	1(2)	15(3)	1(3)
C(5A)	41(3)	29(3)	46(3)	12(3)	13(3)	-4(3)
C(6A)	43(4)	39(3)	36(3)	2(3)	11(3)	-7(3)
O(1A)	49(3)	40(2)	49(3)	8(2)	26(2)	-10(2)
O(2A)	63(3)	52(3)	55(3)	-6(2)	31(3)	-10(2)
C(7A)	46(4)	41(3)	45(4)	8(3)	25(3)	-10(3)
S(1)	56(1)	37(1)	60(1)	-7(1)	28(1)	-7(1)
O(5)	133(6)	46(3)	70(4)	21(3)	40(4)	11(3)
O(6)	54(3)	115(5)	115(5)	-24(4)	28(4)	23(3)
O(7)	107(5)	60(3)	59(3)	-16(2)	32(3)	-34(3)
C(18)	86(6)	65(5)	58(5)	8(4)	14(5)	-16(5)
F(1)	63(4)	184(6)	145(6)	-5(5)	49(4)	-18(4)
F(2)	144(6)	122(5)	79(4)	-18(3)	-7(4)	-71(4)
F(3)	211(8)	77(3)	106(5)	40(3)	-23(5)	-71(4)

Table 5.   Hydrogen coordinates (x 10^4) and isotropic displacement parameters ($Å^2$x 10^3) for **3**.

_____

	x	y	z	U(eq)

_____

H(1)	7866	7072	-1810	45
H(2)	9223	7518	-3502	44
H(4)	7699	9189	-2381	45
H(5)	6405	8700	-725	45
H(7A)	9702	9576	-6132	65
H(7B)	11186	9575	-5099	65
H(1A)	4280	6158	1088	47
H(2A)	2875	5706	2745	48
H(4A)	1840	7433	3996	46
H(5A)	3256	7824	2317	45
H(7C)	-874	5524	5331	51
H(7D)	576	5304	6269	51

Table 6. Hydrogen bond data for [length (Å) and angle (°)] present in complex **3**

D-H···Acceptor	d (D–H)	d (H···A)	d (D···A)	< D-H···A
C1A-H1A···O7	0.93	2.59(0)	3.35(6)	140.0(0)
C5-H5···O5#1	0.93	2.47(0)	3.22(2)	138.0(2)
C5A-H5A···O5#1	0.93	2.59(0)	3.31(3)	135.0(0)
C1A-H1A···F3#2	0.93	2.68(5)	3.37(0)	131.1(1)
C4-H4···F2#3	0.93	2.81(8)	3.55(1)	136.6(1)
C4-H4···F3#3	0.93	2.81(5)	3.50(7)	131.8(1)
C1A-H1A···F3#4	0.93	2.68(5)	3.37(0)	131.1(1)
C7A-H7D···F1	0.97	2.79(0)	3.60(1)	142.6(1)
C7-H7B···F1#5	0.97	2.71(0)	3.44(1)	132.6(1)

Symmetry transformation used to generate equivalent atoms: #1 x, 1.5-y, 0.5+z, #2 1-x, 1-y, z, #3 1-x, 0.5+y, -0.5-z #4 1-x, 1-y, -z #5 1+x, 1.5-y, -0.5+z #6 1-x, 1-y, -z

Crystal data and structure refinement for {[Ag(L2)]NO$_3$}$_n$ (4)

Identification code	**4**
Empirical formula	C14 H12 Ag N3 O7
Formula weight	442.14
Temperature	293(2) K
Wavelength	0.71073 Å
Crystal system	Orthorhombic
Space group	Pnma
Unit cell dimensions	a = 7.8952(16) Å $\quad$ α= 90°.
	b = 14.860(3) Å $\quad$ β= 90°.
	c = 13.177(3) Å $\quad$ γ = 90°.
Volume	1545.9(5) Å^3
Z	4
Density (calculated)	1.900 Mg/m^3
Absorption coefficient	1.349 mm^{-1}
F(000)	880
Theta range for data collection	2.07 to 27.12°.
Index ranges	-10<=h<=10, -19<=k<=18, -15<=l<=16

Reflections collected	11584
Independent reflections	1769 [R(int) = 0.0879]
Completeness to theta = 27.12°	99.5 %
Refinement method	Full-matrix least-squares on F^2
Data / restraints / parameters	1769 / 0 / 123
Goodness-of-fit on F^2	1.399
Final R indices [I>2sigma(I)]	R1 = 0.0703, wR2 = 0.1825
R indices (all data)	R1 = 0.1088, wR2 = 0.2128
Largest diff. peak and hole	0.610 and -1.016 e.Å^{-3}

Table 2. Atomic coordinates (x 10^4) and equivalent isotropic displacement parameters ($Å^2$x 10^3) for **4**. U(eq) is defined as one third of the trace of the orthogonalized U^{ij} tensor.

	x	y	z	U(eq)
Ag(1)	1874(1)	2500	3282(1)	101(2)
N(1)	1762(6)	3944(4)	3607(5)	87(2)
C(1)	287(7)	4381(4)	3544(5)	83(3)
C(2)	122(7)	5292(4)	3710(5)	82(3)
C(3)	1543(7)	5772(5)	4002(6)	90(3)
C(4)	3075(7)	5319(5)	4075(7)	98(3)
C(5)	3126(8)	4419(5)	3860(7)	95(3)
C(6)	-1533(7)	5717(5)	3601(6)	91(3)
O(1)	-2859(5)	5316(4)	3538(5)	109(3)
O(2)	-1424(6)	6597(4)	3529(7)	140(3)
C(7)	-2945(11)	7127(8)	3413(18)	254(14)
N(2)	1573(9)	2500	915(7)	87(3)
O(3)	398(9)	2500	1516(7)	119(3)
O(4)	1302(13)	2500	-15(8)	131(3)
O(5)	3026(8)	2500	1260(9)	119(3)

Table 3.   Bond lengths [Å] and angles [°] for **4**.

Ag(1)-N(1)	2.190(5)	N(1)-C(5)	1.330(8)
Ag(1)-N(1)#1	2.190(5)	N(1)-C(1)	1.336(7)

C(1)-C(2)	1.376(9)	C(1)-N(1)-Ag(1)	120.0(4)
C(2)-C(3)	1.385(8)	N(1)-C(1)-C(2)	123.4(5)
C(2)-C(6)	1.458(8)	C(1)-C(2)-C(3)	118.3(5)
C(3)-C(4)	1.388(9)	C(1)-C(2)-C(6)	119.7(5)
C(4)-C(5)	1.367(11)	C(3)-C(2)-C(6)	122.0(5)
C(6)-O(1)	1.207(7)	C(2)-C(3)-C(4)	118.4(6)
C(6)-O(2)	1.314(9)	C(5)-C(4)-C(3)	119.1(6)
O(2)-C(7)	1.444(10)	N(1)-C(5)-C(4)	123.2(6)
C(7)-C(7)#2	1.11(2)	O(1)-C(6)-O(2)	122.9(6)
N(2)-O(3)	1.220(11)	O(1)-C(6)-C(2)	124.8(6)
N(2)-O(5)	1.234(10)	O(2)-C(6)-C(2)	112.3(5)
N(2)-O(4)	1.243(13)	C(6)-O(2)-C(7)	119.7(6)
		C(7)#2-C(7)-O(2)	123.0(5)
N(1)-Ag(1)-N(1)#1	157.0(3)	O(3)-N(2)-O(5)	117.9(11)
C(5)-N(1)-C(1)	117.6(5)	O(3)-N(2)-O(4)	120.6(8)
C(5)-N(1)-Ag(1)	122.4(4)	O(5)-N(2)-O(4)	121.5(10)

Symmetry transformations used to generate equivalent atoms:

#1 x,-y+1/2,z   #2 x,-y+3/2,z

Table 4. Anisotropic displacement parameters (Å^2 x 10^3) for **4**. The anisotropic displacement factor exponent takes the form: $-2\pi^2[\,h^2a^{*2}U^{11} + ... + 2\,h\,k\,a^*\,b^*\,U^{12}\,]$

	U^{11}	U^{22}	U^{33}	U^{23}	U^{13}	U^{12}
Ag(1)	103(2)	73(2)	129(2)	0	-2(1)	0
N(1)	81(4)	72(3)	108(4)	1(2)	-7(2)	-1(2)
C(1)	68(3)	74(4)	106(5)	-2(3)	-1(3)	-5(2)
C(2)	71(3)	73(4)	101(4)	0(3)	5(3)	-4(2)
C(3)	74(4)	78(4)	116(5)	-1(3)	-1(3)	-6(2)
C(4)	71(4)	89(4)	135(6)	-4(4)	-10(3)	-10(3)
C(5)	78(4)	83(4)	123(6)	2(3)	-10(3)	3(3)
C(6)	68(4)	77(4)	128(6)	-10(3)	1(3)	-3(2)
O(1)	65(3)	95(4)	168(5)	-12(3)	-1(2)	-5(2)
O(2)	69(3)	77(4)	273(9)	-10(4)	-19(4)	1(2)
C(7)	75(5)	83(5)	600(40)	-41(10)	-63(9)	9(4)

	x	y	z	U(eq)
N(2)	73(5)	69(4)	117(7)	0	-6(4)	0

N(2)	73(5)	69(4)	117(7)	0	-6(4)	0
O(3)	72(4)	154(8)	131(6)	0	19(4)	0
O(4)	122(6)	143(7)	127(8)	0	-16(5)	0
O(5)	72(4)	125(6)	161(8)	0	-18(4)	0

Table 5. Hydrogen coordinates (x 10^4) and isotropic displacement parameters (Å^2x 10^3) for **4**.

	x	y	z	U(eq)
H(1)	-678	4054	3381	100
H(3)	1473	6384	4146	107
H(4)	4054	5623	4267	118
H(5)	4164	4125	3892	114
H(7A)	-3461	6941	2779	305
H(7B)	-3710	6941	3949	305

Table 6. Hydrogen bond data [length (Å) and angle (°)] present in complex **4**

D-H⋯Acceptor	d (D–H)	d (H⋯A)	d (D⋯A)	< D-H⋯A
C7-H7B⋯O4	0.97	2.60(1)	3.40(3)	141.2(0)
C1-H1⋯O5	0.93	2.57(2)	3.32(1)	139.1(2)

Crystal data and structure refinement for {[Ag(L2)]SO₃CF₃}ₙ (5)

Identification code	**5**
Empirical formula	C60 H48 Ag4 F12 N8 O28 S4
Formula weight	2116.82
Temperature	293(2) K
Wavelength	0.71073 Å
Crystal system	Monoclinic
Space group	P2₁/c
Unit cell dimensions	a = 15.483(3) Å α = 90°.
	b = 15.758(3) Å β = 90.59(3)°.

	c = 7.3972(15) Å	$\gamma = 90°$.
Volume	1804.7(6) Å^3	
Z	1	
Density (calculated)	1.948 Mg/m^3	
Absorption coefficient	1.306 mm^{-1}	
F(000)	1048	
Theta range for data collection	1.32 to 26.99°.	
Index ranges	-19<=h<=19, -20<=k<=20, -9<=l<=9	
Reflections collected	13685	
Independent reflections	3914 [R(int) = 0.2107]	
Completeness to theta = 26.99°	99.3 %	
Refinement method	Full-matrix least-squares on F^2	
Data / restraints / parameters	3914 / 0 / 271	
Goodness-of-fit on F^2	1.041	
Final R indices [I>2sigma(I)]	R1 = 0.1454, wR2 = 0.3864	
R indices (all data)	R1 = 0.1874, wR2 = 0.4249	
Extinction coefficient	0.041(6)	
Largest diff. peak and hole	2.070 and -1.279 e.Å^{-3}	

Table 2. Atomic coordinates (x 10^4) and equivalent isotropic displacement parameters (Å^{2}x 10^3) for **5**. U(eq) is defined as one third of the trace of the orthogonalized U^{ij} tensor.

	x	y	z	U(eq)
Ag(1)	2492(1)	8000(1)	1097(2)	73(1)
N(1)	1101(8)	8202(9)	1470(20)	66(4)
C(1)	798(12)	9005(11)	1490(30)	71(5)
C(2)	-25(11)	9179(12)	1990(30)	82(6)
C(3)	-592(11)	8541(13)	2410(30)	80(6)
C(4)	-301(10)	7692(11)	2300(30)	65(4)
C(5)	534(8)	7549(9)	1840(30)	59(4)
C(6)	-881(11)	6939(13)	2670(30)	69(5)
O(1)	-651(8)	6244(9)	2500(20)	90(5)
O(2)	-1628(8)	7172(8)	3330(20)	84(4)
C(7)	-2313(16)	6456(11)	3570(30)	86(6)

Silver Coordination Compounds with a Family of Ditopic Ligands of Varying Flexibility: About Chains, Rings, Helices and Polycatenanes

213

C(8)	-2863(13)	6744(13)	4860(30)	75(5)
O(3)	-3453(6)	7394(8)	4170(20)	75(4)
O(4)	-4348(8)	6361(8)	3020(20)	90(4)
C(9)	-4150(12)	7122(9)	3340(30)	73(5)
N(2)	-6145(9)	8240(8)	1670(20)	67(4)
C(10)	-5888(12)	9072(10)	1760(30)	71(5)
C(11)	-5070(11)	9282(11)	2460(30)	73(5)
C(12)	-4498(11)	8654(10)	3060(30)	67(4)
C(13)	-4736(10)	7835(9)	2830(20)	57(4)
C(14)	-5573(11)	7633(11)	2180(20)	64(4)
S(1)	2598(4)	5683(3)	2502(7)	78(2)
O(5)	2427(11)	6562(8)	2400(30)	103(5)
O(6)	3611(12)	5575(17)	1890(50)	222(19)
O(7)	2371(11)	5226(8)	4020(20)	97(5)
C(15)	2184(16)	5190(15)	590(50)	105(8)
F(1)	2406(12)	4345(9)	570(20)	126(6)
F(2)	1294(11)	5299(16)	770(40)	187(11)
F(3)	2486(10)	5492(14)	-990(20)	133(7)

Table 3.   Bond lengths [Å] and angles [°] for **5**.

Ag(1)-N(2)#1	2.182(14)	C(8)-O(3)	1.461(19)
Ag(1)-N(1)	2.197(13)	O(3)-C(9)	1.31(2)
Ag(1)-O(5)	2.466(13)	O(4)-C(9)	1.26(2)
N(1)-C(1)	1.35(2)	C(9)-C(13)	1.49(2)
N(1)-C(5)	1.380(18)	N(2)-C(14)	1.35(2)
C(1)-C(2)	1.36(2)	N(2)-C(10)	1.37(2)
C(2)-C(3)	1.37(2)	N(2)-Ag(1)#2	2.182(14)
C(3)-C(4)	1.42(3)	C(10)-C(11)	1.40(3)
C(4)-C(5)	1.36(2)	C(11)-C(12)	1.40(2)
C(4)-C(6)	1.52(2)	C(12)-C(13)	1.35(2)
C(6)-O(1)	1.16(2)	C(13)-C(14)	1.42(2)
C(6)-O(2)	1.31(2)	S(1)-O(7)	1.381(16)
O(2)-C(7)	1.56(2)	S(1)-O(5)	1.411(13)
C(7)-C(8)	1.36(3)	S(1)-O(6)	1.64(3)

S(1)-C(15)	1.73(3)	O(4)-C(9)-C(13)	121.8(16)
C(15)-F(3)	1.35(3)	O(3)-C(9)-C(13)	111.6(13)
C(15)-F(1)	1.37(3)	C(14)-N(2)-C(10)	118.3(15)
C(15)-F(2)	1.40(3)	C(14)-N(2)-Ag(1)#2	124.0(11)
		C(10)-N(2)-Ag(1)#2	117.0(11)
N(2)#1-Ag(1)-N(1)	154.0(6)	N(2)-C(10)-C(11)	120.2(16)
N(2)#1-Ag(1)-O(5)	97.3(5)	C(12)-C(11)-C(10)	121.2(16)
N(1)-Ag(1)-O(5)	92.3(5)	C(13)-C(12)-C(11)	117.7(16)
C(1)-N(1)-C(5)	118.3(13)	C(12)-C(13)-C(14)	120.4(15)
C(1)-N(1)-Ag(1)	118.6(11)	C(12)-C(13)-C(9)	121.6(15)
C(5)-N(1)-Ag(1)	122.9(10)	C(14)-C(13)-C(9)	117.9(14)
N(1)-C(1)-C(2)	121.3(16)	N(2)-C(14)-C(13)	121.9(15)
C(1)-C(2)-C(3)	121.2(17)	O(7)-S(1)-O(5)	120.3(11)
C(2)-C(3)-C(4)	118.3(15)	O(7)-S(1)-O(6)	114.8(13)
C(5)-C(4)-C(3)	118.4(15)	O(5)-S(1)-O(6)	105.4(12)
C(5)-C(4)-C(6)	118.9(15)	O(7)-S(1)-C(15)	109.5(12)
C(3)-C(4)-C(6)	122.7(15)	O(5)-S(1)-C(15)	109.3(12)
C(4)-C(5)-N(1)	122.3(14)	O(6)-S(1)-C(15)	94.4(16)
O(1)-C(6)-O(2)	125.2(17)	S(1)-O(5)-Ag(1)	156.0(12)
O(1)-C(6)-C(4)	122.5(16)	F(3)-C(15)-F(1)	104(2)
O(2)-C(6)-C(4)	112.0(16)	F(3)-C(15)-F(2)	113(2)
C(6)-O(2)-C(7)	116.3(16)	F(1)-C(15)-F(2)	112(2)
C(8)-C(7)-O(2)	105.7(16)	F(3)-C(15)-S(1)	114.8(18)
C(7)-C(8)-O(3)	112.5(18)	F(1)-C(15)-S(1)	110(2)
C(9)-O(3)-C(8)	116.4(14)	F(2)-C(15)-S(1)	103(2)
O(4)-C(9)-O(3)	126.6(15)		

Symmetry transformations used to generate equivalent atoms:

#1 x+1,y,z   #2 x-1,y,z

Table 4. Anisotropic displacement parameters ($\mathring{A}^2$x 10^3) for **5**. The anisotropic displacement factor exponent takes the form: $-2p^2[\ h^2a^{*2}U^{11} + ... + 2\ h\ k\ a^*\ b^*\ U^{12}\ ]$

	U^{11}	U^{22}	U^{33}	U^{23}	U^{13}	U^{12}
Ag(1)	47(1)	53(1)	118(2)	16(1)	-5(1)	-3(1)
N(1)	39(6)	58(7)	103(11)	23(7)	2(6)	2(5)
C(1)	63(10)	54(8)	97(14)	24(9)	-6(9)	-1(7)
C(2)	58(10)	56(9)	132(19)	30(10)	11(10)	5(7)
C(3)	49(9)	89(13)	102(15)	14(11)	18(9)	14(9)
C(4)	45(8)	68(9)	83(12)	29(9)	-5(7)	-3(7)
C(5)	36(7)	41(7)	101(13)	14(7)	0(7)	2(5)
C(6)	45(8)	82(12)	79(12)	19(9)	3(7)	2(8)
O(1)	54(7)	63(7)	154(15)	27(8)	21(7)	4(6)
O(2)	58(7)	58(7)	136(13)	41(7)	2(7)	-5(5)
C(7)	117(17)	42(8)	98(16)	-6(9)	-11(13)	-14(9)
C(8)	78(12)	71(10)	75(12)	6(9)	-27(9)	18(9)
O(3)	36(5)	59(6)	130(11)	30(7)	-19(6)	-10(5)
O(4)	71(8)	55(7)	143(13)	25(8)	-21(8)	-7(6)
C(9)	65(10)	40(7)	114(16)	21(8)	-5(9)	0(7)
N(2)	60(8)	46(6)	94(11)	15(7)	-16(7)	-4(6)
C(10)	80(12)	45(7)	89(13)	14(8)	-1(9)	-6(8)
C(11)	58(9)	60(9)	102(14)	14(9)	-8(9)	-6(7)
C(12)	66(10)	49(8)	85(12)	12(8)	-16(8)	-12(7)
C(13)	56(8)	50(8)	63(9)	15(6)	-11(7)	-8(6)
C(14)	63(9)	57(8)	72(11)	21(8)	4(8)	-6(7)
S(1)	114(4)	39(2)	81(3)	1(2)	-17(3)	4(2)
O(5)	119(12)	44(7)	146(16)	19(8)	-8(11)	9(7)
O(6)	81(12)	160(20)	420(50)	100(30)	-130(20)	-21(13)
O(7)	144(14)	51(7)	97(11)	8(7)	-10(10)	3(8)
C(15)	84(15)	67(12)	170(30)	-3(14)	-3(15)	-1(11)
F(1)	185(17)	71(8)	122(12)	-25(8)	-34(11)	13(9)
F(2)	92(11)	220(20)	250(30)	110(20)	36(13)	20(13)
F(3)	133(13)	185(19)	82(10)	38(10)	3(9)	14(11)

Silver Coordination Compounds with a Family of Ditopic Ligands of Varying Flexibility: About Chains, Rings, Helices and Polycatenanes

216

Table 5. Hydrogen coordinates (x 10^4) and isotropic displacement parameters ($Å^2$x 10^3) for **5**.

	x	y	z	U(eq)
H(1)	1154	9447	1127	210(160)
H(2)	-201	9742	2066	90(70)
H(3)	-1153	8667	2759	70(50)
H(5)	726	6991	1771	70(60)
H(7A)	-2622	6348	2451	130(100)
H(7B)	-2040	5933	3975	30(30)
H(8A)	-2521	6986	5835	60(50)
H(8B)	-3186	6271	5353	2000(4000)
H(10)	-6258	9499	1352	92
H(11)	-4905	9849	2519	95
H(12)	-3973	8794	3604	87
H(14)	-5736	7066	2097	83

Table 6. Hydrogen bond data for **5** [length (Å) and angle (°)]

D-H···Acceptor	d (D–H)	d (H···A)	d (D···A)	< D-H···A
C1-H1···O7#1	0.93	2.51(0)	3.29(2)	141.7(0)
C2-H2···F2#2	0.93	2.50(2)	3.12(0)	124.9(8)
C3-H3···F1#2	0.93	2.54(1)	3.43(3)	160.5(5)
C11-H11···O6#3	0.93	2.34(0)	3.07(1)	136.0(2)
C7-H7A···F1#4	0.97	2.52(1)	3.32(4)	140.3(0)
C7-H7B···O7#5	0.97	2.41(3)	3.19(0)	137.4(1)

Symmetry transformation used to generate equivalent atoms: #1 x,3/2-y,-1/2+z, #2 -x,1/2+y,1/2-z, #3 1-x,1/2+y,1/2-z, #4 -x,1-y,-z, #5 -x,1-y,1-z.

Crystal data and structure refinement for {[Ag(L2)]SO₃CF₃}ₙ (6)

Identification code	**6**
Empirical formula	C15 H12 Ag F3 N2 O7 S
Formula weight	529.20

Silver Coordination Compounds with a Family of Ditopic Ligands of Varying Flexibility: About Chains, Rings, Helices and Polycatenanes

217

Temperature	293(2) K	
Wavelength	0.71073 Å	
Crystal system	Monoclinic	
Space group	$P2_1/n$	
Unit cell dimensions	a = 8.3779(17) Å	$\alpha = 90°$.
	b = 22.502(5) Å	$\beta = 110.43(3)°$.
	c = 10.264(2) Å	$\gamma = 90°$.
Volume	1813.2(6) Å^3	
Z	4	
Density (calculated)	1.939 Mg/m^3	
Absorption coefficient	1.300 mm^{-1}	
F(000)	1048	
Theta range for data collection	2.75 to 27.13°.	
Index ranges	-10<=h<=9, 0<=k<=28, 0<=l<=13	
Reflections collected	3862	
Independent reflections	3862 [R(int) = 0.0000]	
Completeness to theta = 27.13°	96.4 %	
Refinement method	Full-matrix least-squares on F^2	
Data / restraints / parameters	3862 / 0 / 264	
Goodness-of-fit on F^2	1.065	
Final R indices [I>2sigma(I)]	R1 = 0.0819, wR2 = 0.2047	
R indices (all data)	R1 = 0.0858, wR2 = 0.2110	
Largest diff. peak and hole	2.792 and -2.571 e.Å^{-3}	

Table 2. Atomic coordinates (x 10^4) and equivalent isotropic displacement parameters (Å^{2}x 10^3) for **6**. U(eq) is defined as one third of the trace of the orthogonalized U^{ij} tensor.

	x	y	z	U(eq)
Ag(1)	3132(1)	282(1)	9362(1)	40(1)
N(1)	3468(5)	831(2)	7767(4)	32(1)
C(1)	2460(6)	769(2)	6430(5)	41(1)
C(2)	2565(7)	1131(2)	5388(5)	47(1)
C(3)	3749(6)	1585(2)	5703(5)	41(1)
C(4)	4813(5)	1651(2)	7092(4)	30(1)

Silver Coordination Compounds with a Family of Ditopic Ligands of Varying Flexibility: About Chains, Rings, Helices and Polycatenanes

218

C(5)	4631(5)	1272(2)	8081(4)	29(1)
C(6)	6178(5)	2108(2)	7550(4)	30(1)
O(1)	7088(5)	2180(2)	8733(3)	46(1)
O(2)	6292(4)	2418(1)	6476(3)	35(1)
C(7)	7623(6)	2859(2)	6824(5)	38(1)
C(8)	7598(6)	3134(2)	5498(5)	39(1)
O(3)	6206(4)	3559(1)	5047(3)	33(1)
O(4)	5504(5)	3259(2)	2828(4)	47(1)
C(9)	5310(5)	3579(2)	3694(4)	29(1)
N(2)	2580(5)	4852(2)	4055(4)	34(1)
C(10)	1888(6)	5018(2)	2707(6)	43(1)
C(11)	2200(8)	4724(3)	1657(6)	50(1)
C(12)	3307(6)	4248(2)	1969(5)	40(1)
C(13)	4070(5)	4083(2)	3352(4)	28(1)
C(14)	3661(5)	4393(2)	4356(4)	28(1)
S(1)	2807(2)	-947(1)	7274(1)	53(1)
O(5)	3884(5)	-846(2)	8678(4)	45(1)
O(6)	1355(10)	-610(3)	6804(12)	175(6)
O(7)	3703(14)	-987(6)	6361(7)	184(7)
C(15)	2009(7)	-1691(2)	7282(7)	56(2)
F(1)	3192(7)	-2074(2)	7855(8)	123(3)
F(2)	995(8)	-1700(3)	8020(7)	107(2)
F(3)	1065(6)	-1868(2)	6015(6)	97(2)

Table 3.   Bond lengths [Å] and angles [°] for **6**.

Ag(1)-N(2)#1	2.147(4)	C(4)-C(6)	1.487(6)
Ag(1)-N(1)	2.148(4)	C(6)-O(1)	1.198(5)
Ag(1)-Ag(1)#2	3.2019(11)	C(6)-O(2)	1.336(5)
N(1)-C(1)	1.344(6)	O(2)-C(7)	1.440(5)
N(1)-C(5)	1.348(5)	C(7)-C(8)	1.488(6)
C(1)-C(2)	1.371(7)	C(8)-O(3)	1.453(5)
C(2)-C(3)	1.380(7)	O(3)-C(9)	1.329(5)
C(3)-C(4)	1.401(6)	O(4)-C(9)	1.199(6)
C(4)-C(5)	1.375(6)	C(9)-C(13)	1.495(5)

N(2)-C(14)	1.337(5)	O(2)-C(6)-C(4)	111.7(3)
N(2)-C(10)	1.353(6)	C(6)-O(2)-C(7)	115.3(3)
N(2)-Ag(1)#3	2.147(4)	O(2)-C(7)-C(8)	107.3(4)
C(10)-C(11)	1.366(8)	O(3)-C(8)-C(7)	108.6(4)
C(11)-C(12)	1.379(7)	C(9)-O(3)-C(8)	116.9(4)
C(12)-C(13)	1.389(6)	O(4)-C(9)-O(3)	125.6(4)
C(13)-C(14)	1.382(6)	O(4)-C(9)-C(13)	123.0(4)
S(1)-O(6)	1.371(7)	O(3)-C(9)-C(13)	111.3(3)
S(1)-O(7)	1.394(8)	C(14)-N(2)-C(10)	117.7(4)
S(1)-O(5)	1.426(3)	C(14)-N(2)-Ag(1)#3	121.2(3)
S(1)-C(15)	1.803(6)	C(10)-N(2)-Ag(1)#3	121.0(3)
C(15)-F(1)	1.290(8)	N(2)-C(10)-C(11)	122.7(4)
C(15)-F(2)	1.321(9)	C(10)-C(11)-C(12)	119.5(5)
C(15)-F(3)	1.326(7)	C(11)-C(12)-C(13)	118.5(5)
		C(14)-C(13)-C(12)	118.8(4)
N(2)#1-Ag(1)-N(1)	168.99(14)	C(14)-C(13)-C(9)	122.7(4)
N(2)#1-Ag(1)-Ag(1)#2	90.14(11)	C(12)-C(13)-C(9)	118.5(4)
N(1)-Ag(1)-Ag(1)#2	99.80(10)	N(2)-C(14)-C(13)	122.8(4)
C(1)-N(1)-C(5)	117.7(4)	O(6)-S(1)-O(7)	114.8(9)
C(1)-N(1)-Ag(1)	121.0(3)	O(6)-S(1)-O(5)	116.0(5)
C(5)-N(1)-Ag(1)	121.2(3)	O(7)-S(1)-O(5)	113.0(4)
N(1)-C(1)-C(2)	123.1(4)	O(6)-S(1)-C(15)	103.3(4)
C(1)-C(2)-C(3)	119.5(4)	O(7)-S(1)-C(15)	103.3(5)
C(2)-C(3)-C(4)	117.8(4)	O(5)-S(1)-C(15)	104.4(3)
C(5)-C(4)-C(3)	119.3(4)	F(1)-C(15)-F(2)	105.9(7)
C(5)-C(4)-C(6)	117.8(4)	F(1)-C(15)-F(3)	110.3(6)
C(3)-C(4)-C(6)	122.8(4)	F(2)-C(15)-F(3)	105.9(6)
N(1)-C(5)-C(4)	122.5(4)	F(1)-C(15)-S(1)	113.3(5)
O(1)-C(6)-O(2)	124.2(4)	F(2)-C(15)-S(1)	109.3(4)
O(1)-C(6)-C(4)	124.1(4)	F(3)-C(15)-S(1)	111.8(5)

Symmetry transformations used to generate equivalent atoms:

#1 -x+1/2,y-1/2,-z+3/2   #2 -x+1,-y,-z+2   #3 -x+1/2,y+1/2,-z+3/2

Table 4. Anisotropic displacement parameters ($Å^2 x 10^3$)for **6**. The anisotropic displacement factor exponent takes the form: $-2p^2[h^2a*^2U^{11} + ... + 2 h k a* b* U^{12}]$

	U^{11}	U^{22}	U^{33}	U^{23}	U^{13}	U^{12}
Ag(1)	39(1)	25(1)	57(1)	10(1)	18(1)	-2(1)
N(1)	29(2)	21(2)	44(2)	5(1)	9(1)	-1(1)
C(1)	33(2)	27(2)	53(3)	1(2)	4(2)	-8(2)
C(2)	46(3)	39(2)	36(2)	5(2)	-8(2)	-7(2)
C(3)	39(2)	37(2)	35(2)	9(2)	-2(2)	-5(2)
C(4)	29(2)	23(2)	32(2)	5(1)	3(2)	4(1)
C(5)	29(2)	22(2)	35(2)	3(1)	10(2)	1(1)
C(6)	32(2)	20(2)	33(2)	5(1)	7(2)	1(1)
O(1)	52(2)	42(2)	34(2)	4(1)	2(1)	-17(2)
O(2)	34(2)	27(1)	37(2)	8(1)	4(1)	-5(1)
C(7)	29(2)	28(2)	48(2)	11(2)	3(2)	-4(2)
C(8)	31(2)	29(2)	57(3)	17(2)	14(2)	9(2)
O(3)	36(2)	23(1)	37(2)	6(1)	11(1)	9(1)
O(4)	46(2)	39(2)	53(2)	-11(2)	12(2)	11(2)
C(9)	29(2)	21(2)	36(2)	-1(1)	10(2)	-2(1)
N(2)	32(2)	21(2)	48(2)	2(2)	12(2)	2(2)
C(10)	37(2)	32(2)	57(3)	16(2)	14(2)	13(2)
C(11)	45(3)	61(4)	41(3)	22(2)	11(2)	17(2)
C(12)	36(2)	46(3)	36(2)	4(2)	10(2)	9(2)
C(13)	28(2)	21(2)	35(2)	1(1)	10(2)	-2(1)
C(14)	26(2)	20(2)	35(2)	1(1)	7(1)	0(1)
S(1)	58(1)	44(1)	39(1)	8(1)	-6(1)	-28(1)
O(5)	47(2)	37(2)	42(2)	-8(1)	5(2)	-9(2)
O(6)	94(5)	38(3)	265(11)	28(5)	-98(6)	-4(3)
O(7)	209(9)	300(14)	67(4)	-77(6)	79(5)	-208(11)
C(15)	39(3)	33(3)	83(4)	-22(3)	6(3)	-5(2)
F(1)	77(3)	44(2)	210(7)	-23(3)	3(4)	16(2)
F(2)	114(4)	81(4)	158(5)	-18(3)	87(4)	-48(3)
F(3)	69(3)	83(3)	116(4)	-53(3)	2(3)	-33(3)

Table 5. Hydrogen coordinates (x 10^4) and isotropic displacement parameters (Å^2x 10^3) for **6**.

	x	y	z	U(eq)
H(1)	1654	466	6201	49
H(2)	1844	1072	4476	56
H(3)	3837	1838	5015	49
H(5)	5336	1322	9002	35
H(7A)	8720	2674	7299	45
H(7B)	7426	3158	7430	45
H(8A)	8671	3334	5638	47
H(8B)	7441	2830	4795	47
H(10)	1170	5347	2487	51
H(11)	1670	4843	739	60
H(12)	3537	4042	1269	48
H(14)	4159	4276	5280	34

Table 6. Hydrogen bond data [length (Å) and angle (°)] present in complex **6**

D-H···Acceptor	d (D–H)	d (H···A)	d (D···A)	< D-H···A
C1-H1···O6[#1]	0.93	2.53(3)	3.29(8)	139.7(6)
C5-H5···O5[#2]	0.93	2.48(1)	3.26(2)	141.6(7)
C10-H10···O7[#3]	0.93	2.45(2)	3.34(7)	161.5(8)
C7-H7A···O4[#4]	0.97	2.52(4)	3.38(7)	148.1(4)

Symmetry transformation used to generate equivalent atoms: #1 1-x,-y,1-z, #2 x,y,1+z, #3 1/2-x,1/2+y,1/2-z, #4 0.5+x,0.5-y,0.5+z.

Crystal data and structure refinement for $\{[Ag(L3)]ClO_4\}_2$ (7)

Identification code	**7**
Empirical formula	C16 H16 Ag Cl N2 O9
Formula weight	523.63
Temperature	233(2) K
Wavelength	0.71073 Å

Crystal system	Triclinic	
Space group	P-1	
Unit cell dimensions	a = 7.1824(14) Å	α = 112.58(3)°.
	b = 12.077(2) Å	β = 102.32(3)°.
	c = 12.095(2) Å	γ = 96.64(3)°.
Volume	923.4(3) Å^3	
Z	2	
Density (calculated)	1.883 Mg/m^3	
Absorption coefficient	1.292 mm^{-1}	
F(000)	524	
Theta range for data collection	2.98 to 31.81°.	
Index ranges	-9<=h<=10, -17<=k<=17, -17<=l<=17	
Reflections collected	10734	
Independent reflections	5569 [R(int) = 0.0620]	
Completeness to theta = 31.81°	88.3 %	
Refinement method	Full-matrix least-squares on F^2	
Data / restraints / parameters	5569 / 0 / 262	
Goodness-of-fit on F^2	1.048	
Final R indices [I>2sigma(I)]	R1 = 0.0573, wR2 = 0.1582	
R indices (all data)	R1 = 0.0764, wR2 = 0.1798	
Largest diff. peak and hole	1.699 and -1.642 e.Å^{-3}	

Table 2. Atomic coordinates (x 10^4) and equivalent isotropic displacement parameters (Å^{2}x 10^3) for **7**. U(eq) is defined as one third of the trace of the orthogonalized U^{ij} tensor.

_____

	x	y	z	U(eq)
Ag(1)	8213(1)	5510(1)	9541(1)	56(1)
N(1)	6334(5)	3717(4)	8459(4)	39(1)
C(1)	5403(6)	3066(4)	8944(4)	37(1)
C(2)	4224(6)	1910(4)	8227(4)	32(1)
C(3)	3961(5)	1397(4)	6933(4)	29(1)
C(4)	4934(7)	2068(4)	6438(4)	37(1)
C(5)	6119(7)	3212(5)	7227(5)	41(1)

_____

Silver Coordination Compounds with a Family of Ditopic Ligands of Varying Flexibility: About Chains, Rings, Helices and Polycatenanes

223

C(6)	2664(6)	173(4)	6062(4)	34(1)
O(1)	2273(6)	-193(4)	4942(3)	52(1)
O(2)	2026(5)	-430(3)	6674(3)	38(1)
C(7)	844(7)	-1673(4)	5923(5)	42(1)
C(8)	1986(7)	-2570(4)	6171(5)	38(1)
O(3)	3591(5)	-2521(3)	5664(3)	37(1)
C(9)	4749(7)	-3380(4)	5726(5)	40(1)
C(10)	6000(8)	-3052(4)	7030(5)	42(1)
O(4)	7094(5)	-1792(3)	7528(3)	39(1)
O(5)	6116(8)	-1295(4)	9267(5)	63(1)
C(11)	6936(6)	-1010(4)	8612(4)	34(1)
C(12)	9573(6)	1852(4)	8543(5)	37(1)
C(13)	8560(6)	650(4)	8111(4)	32(1)
C(14)	7974(5)	275(4)	8960(4)	30(1)
C(15)	8371(7)	1118(4)	10190(4)	36(1)
C(16)	9402(7)	2299(4)	10548(5)	40(1)
N(2)	10026(6)	2664(3)	9743(4)	39(1)
Cl(1)	11441(2)	4671(1)	7247(1)	39(1)
O(6)	9691(6)	5071(4)	6898(4)	54(1)
O(7)	12956(8)	5733(5)	8088(4)	73(1)
O(8)	12053(8)	4111(7)	6166(6)	95(2)
O(9)	11100(11)	3895(8)	7797(10)	144(4)

Table 3. Bond lengths [Å] and angles [°] for **7**.

Ag(1)-N(1)	2.148(4)	C(6)-O(2)	1.330(5)
Ag(1)-N(2)#1	2.153(4)	O(2)-C(7)	1.459(5)
Ag(1)-Ag(1)#1	3.1473(12)	C(7)-C(8)	1.511(7)
N(1)-C(1)	1.346(6)	C(8)-O(3)	1.422(5)
N(1)-C(5)	1.341(7)	O(3)-C(9)	1.416(6)
C(1)-C(2)	1.379(6)	C(9)-C(10)	1.511(7)
C(2)-C(3)	1.405(6)	C(10)-O(4)	1.454(5)
C(3)-C(4)	1.387(5)	O(4)-C(11)	1.327(6)
C(3)-C(6)	1.494(6)	O(5)-C(11)	1.207(5)
C(4)-C(5)	1.383(7)	C(11)-C(14)	1.496(6)
C(6)-O(1)	1.207(6)	C(12)-N(2)	1.344(7)

C(12)-C(13)	1.386(5)	C(6)-O(2)-C(7)	116.9(4)
C(13)-C(14)	1.390(5)	O(2)-C(7)-C(8)	108.5(4)
C(14)-C(15)	1.386(6)	O(3)-C(8)-C(7)	106.5(3)
C(15)-C(16)	1.383(6)	C(9)-O(3)-C(8)	114.3(3)
C(16)-N(2)	1.346(7)	O(3)-C(9)-C(10)	113.3(4)
N(2)-Ag(1)#1	2.153(4)	O(4)-C(10)-C(9)	107.8(4)
Cl(1)-O(9)	1.369(5)	C(11)-O(4)-C(10)	117.2(4)
Cl(1)-O(8)	1.413(6)	O(5)-C(11)-O(4)	124.6(4)
Cl(1)-O(7)	1.438(5)	O(5)-C(11)-C(14)	123.4(4)
Cl(1)-O(6)	1.436(4)	O(4)-C(11)-C(14)	111.9(3)
		N(2)-C(12)-C(13)	123.1(4)
N(1)-Ag(1)-N(2)#1	167.97(16)	C(12)-C(13)-C(14)	118.2(4)
N(1)-Ag(1)-Ag(1)#1	93.92(11)	C(13)-C(14)-C(15)	119.2(4)
N(2)#1-Ag(1)-Ag(1)#1	92.43(11)	C(13)-C(14)-C(11)	123.0(4)
C(1)-N(1)-C(5)	118.4(4)	C(15)-C(14)-C(11)	117.8(4)
C(1)-N(1)-Ag(1)	124.1(3)	C(16)-C(15)-C(14)	118.9(4)
C(5)-N(1)-Ag(1)	117.5(3)	N(2)-C(16)-C(15)	122.5(5)
N(1)-C(1)-C(2)	122.8(4)	C(16)-N(2)-C(12)	118.1(4)
C(1)-C(2)-C(3)	118.6(4)	C(16)-N(2)-Ag(1)#1	118.3(3)
C(4)-C(3)-C(2)	118.4(4)	C(12)-N(2)-Ag(1)#1	123.6(3)
C(4)-C(3)-C(6)	118.4(4)	O(9)-Cl(1)-O(8)	112.6(6)
C(2)-C(3)-C(6)	123.2(3)	O(9)-Cl(1)-O(7)	110.9(5)
C(3)-C(4)-C(5)	119.3(4)	O(8)-Cl(1)-O(7)	106.7(4)
N(1)-C(5)-C(4)	122.5(4)	O(9)-Cl(1)-O(6)	109.9(4)
O(1)-C(6)-O(2)	125.9(4)	O(8)-Cl(1)-O(6)	108.0(3)
O(1)-C(6)-C(3)	122.4(4)	O(7)-Cl(1)-O(6)	108.7(3)
O(2)-C(6)-C(3)	111.8(4)		

Symmetry transformations used to generate equivalent atoms:

#1 -x+2,-y+1,-z+2

Silver Coordination Compounds with a Family of Ditopic Ligands of Varying Flexibility: About Chains, Rings, Helices and Polycatenanes

225

Table 4.   Anisotropic displacement parameters ($\text{Å}^2 \times 10^3$) for **7**. The anisotropic displacement factor exponent takes the form: $-2p^2[\,h^2a^{*2}U^{11} + ... + 2\,h\,k\,a^*\,b^*\,U^{12}\,]$

	U^{11}	U^{22}	U^{33}	U^{23}	U^{13}	U^{12}
Ag(1)	39(1)	27(1)	80(1)	14(1)	-1(1)	-2(1)
N(1)	34(2)	30(2)	46(2)	13(2)	3(2)	2(1)
C(1)	36(2)	35(2)	32(2)	9(2)	5(2)	4(2)
C(2)	32(2)	33(2)	33(2)	15(2)	10(1)	4(1)
C(3)	30(2)	26(2)	31(2)	11(2)	11(1)	6(1)
C(4)	40(2)	36(2)	36(2)	17(2)	12(2)	1(2)
C(5)	40(2)	36(2)	47(3)	20(2)	10(2)	-2(2)
C(6)	32(2)	30(2)	37(2)	11(2)	9(2)	5(1)
O(1)	65(2)	42(2)	34(2)	9(2)	9(2)	-5(2)
O(2)	43(2)	26(1)	41(2)	9(1)	16(1)	1(1)
C(7)	36(2)	26(2)	55(3)	10(2)	14(2)	0(2)
C(8)	45(2)	27(2)	42(2)	14(2)	19(2)	2(2)
O(3)	43(2)	35(2)	43(2)	20(2)	21(1)	9(1)
C(9)	47(2)	28(2)	41(2)	10(2)	13(2)	7(2)
C(10)	48(2)	28(2)	46(2)	17(2)	5(2)	-2(2)
O(4)	45(2)	30(1)	39(2)	13(1)	13(1)	-4(1)
O(5)	85(3)	45(2)	68(3)	23(2)	47(3)	1(2)
C(11)	36(2)	28(2)	39(2)	14(2)	13(2)	5(1)
C(12)	37(2)	29(2)	49(2)	19(2)	16(2)	5(1)
C(13)	36(2)	27(2)	35(2)	13(2)	13(2)	5(1)
C(14)	30(2)	26(2)	34(2)	13(2)	10(1)	6(1)
C(15)	44(2)	31(2)	31(2)	11(2)	12(2)	10(2)
C(16)	46(2)	31(2)	37(2)	9(2)	6(2)	11(2)
N(2)	35(2)	23(2)	48(2)	7(2)	5(2)	5(1)
Cl(1)	39(1)	31(1)	43(1)	14(1)	12(1)	2(1)
O(6)	50(2)	44(2)	63(2)	19(2)	12(2)	11(2)
O(7)	66(3)	66(3)	56(2)	17(2)	-3(2)	-20(2)
O(8)	64(3)	113(5)	74(3)	0(3)	25(3)	23(3)
O(9)	99(5)	152(6)	258(11)	180(8)	34(6)	2(4)

Table 5. Hydrogen coordinates (x 10^4) and isotropic displacement parameters ($Å^2$x 10^3) for **7**.

	x	y	z	U(eq)
H(1)	5563	3414	9809	44
H(2)	3609	1474	8597	39
H(4)	4790	1749	5575	44
H(5)	6800	3652	6887	50
H(7A)	534	-1846	5036	50
H(7B)	-385	-1755	6144	50
H(8A)	2451	-2336	7069	45
H(8B)	1164	-3402	5769	45
H(9A)	5598	-3433	5180	48
H(9B)	3891	-4192	5411	48
H(10A)	5175	-3128	7557	51
H(10B)	6898	-3608	7007	51
H(12)	9961	2111	7971	44
H(13)	8277	102	7266	39
H(15)	7948	891	10772	43
H(16)	9676	2867	11384	48

Table 6. Hydrogen bond data [length (Å) and angle (^{0})] present in complex **7**

D-H···Acceptor	d (D–H)	d (H···A)	d (D···A)	< D-H···A
C1-H1···O7[#4]	0.94	2.28(9)	3.19(6)	160.2(8)
C5-H5···O6[#1]	0.94	2.53(0)	3.40(7)	154.4(2)
C12-H12···O9[#1]	0.94	2.31(7)	3.09(1)	140.4(9)
C16-H16···O6[#4]	0.94	2.46(6)	3.34(7)	155.3(9)
C4-H4···O3[#5]	0.94	2.45(6)	3.15(7)	131.3(0)
C9-H9A···O8[#6]	0.98	2.57(6)	3.52(6)	164.1(1)
C10-H10A···O7[#5]	0.98	2.33(4)	3.22(7)	152.3(5)

Symmetry transformation used to generate equivalent atoms: #1 2-x,1-y,1-z, #4 x,y,1+z, #5 1-x,-y,1-z, #6 x,-1+y,z.

Silver Coordination Compounds with a Family of Ditopic Ligands of Varying Flexibility: About Chains, Rings, Helices and Polycatenanes

227

Crystal data and structure refinement for {[Ag(L3)₂]ClO₄}ₙ (8)

Identification code	**8**
Empirical formula	C16 H16 Ag Cl N2 O9
Formula weight	523.63
Temperature	293(2) K
Wavelength	0.71073 Å
Crystal system	Monoclinic
Space group	C2/c
Unit cell dimensions	a = 23.631(5) Å α = 90°.
	b = 7.1049(14) Å β = 117.12(3)°.
	c = 25.554(5) Å γ = 90°.
Volume	3818.7(13) Å^3
Z	8
Density (calculated)	1.822 Mg/m^3
Absorption coefficient	1.249 mm^{-1}
F(000)	2096
Theta range for data collection	1.79 to 27.20°.
Index ranges	-30<=h<=30, -9<=k<=8, -32<=l<=15
Reflections collected	7494
Independent reflections	4216 [R(int) = 0.1102]
Completeness to theta = 27.20°	99.1 %
Refinement method	Full-matrix least-squares on F^2
Data / restraints / parameters	4216 / 0 / 262
Goodness-of-fit on F^2	0.964
Final R indices [I>2sigma(I)]	R1 = 0.0785, wR2 = 0.1830
R indices (all data)	R1 = 0.1549, wR2 = 0.2241
Largest diff. peak and hole	1.142 and -1.127 e.Å^{-3}

Silver Coordination Compounds with a Family of Ditopic Ligands of Varying Flexibility:
About Chains, Rings, Helices and Polycatenanes

228

Table 2. Atomic coordinates (x 10^4) and equivalent isotropic displacement parameters (Å^2x 10^3) for **8**. U(eq) is defined as one third of the trace of the orthogonalized U^{ij} tensor.

	x	y	z	U(eq)
Ag(1)	7792(1)	6835(1)	7704(1)	71(1)
N(1)	8378(3)	7033(11)	8644(3)	51(2)
C(1)	8206(4)	6394(13)	9040(4)	55(2)
C(2)	8597(4)	6340(13)	9628(3)	49(2)
C(3)	9220(4)	6966(14)	9840(3)	50(2)
C(4)	9417(4)	7611(16)	9439(4)	64(3)
C(5)	8967(4)	7652(17)	8841(4)	66(3)
C(6)	9697(4)	6850(15)	10467(4)	59(2)
O(1)	9439(3)	6336(10)	10806(2)	61(2)
O(2)	10249(3)	7267(15)	10655(3)	93(3)
C(7)	9860(5)	5943(18)	11433(3)	72(3)
C(8)	9619(9)	3990(20)	11549(5)	140(8)
O(3)	9715(4)	2700(15)	11245(4)	96(3)
C(9)	9475(5)	1008(17)	11344(4)	75(3)
C(10)	8788(4)	533(18)	11006(4)	68(3)
O(4)	8610(3)	743(11)	10393(2)	63(2)
O(5)	7609(3)	74(14)	10175(3)	85(2)
C(11)	8007(4)	510(14)	10021(4)	57(2)
C(12)	7101(4)	740(18)	8390(4)	71(3)
C(13)	7240(4)	449(16)	8964(4)	64(2)
C(14)	7857(4)	841(14)	9403(4)	53(2)
C(15)	8295(4)	1500(13)	9234(4)	51(2)
C(16)	8113(4)	1772(14)	8644(4)	54(2)
N(2)	7522(3)	1392(12)	8223(3)	56(2)
Cl(1)	8725(1)	1286(5)	7397(1)	79(1)
O(6)	9100(6)	2173(18)	7186(6)	132(4)
O(7)	8553(6)	2800(20)	7697(5)	135(4)
O(8)	8168(4)	613(19)	6955(5)	137(4)
O(9)	9064(7)	0(40)	7792(9)	270(13)

Silver Coordination Compounds with a Family of Ditopic Ligands of Varying Flexibility: About Chains, Rings, Helices and Polycatenanes

229

Table 3. Bond lengths [Å] and angles [°] for **8**.

Ag(1)-N(2)#1	2.158(7)	C(5)-N(1)-C(1)	117.2(7)
Ag(1)-N(1)	2.161(6)	C(5)-N(1)-Ag(1)	118.5(6)
N(1)-C(5)	1.320(12)	C(1)-N(1)-Ag(1)	124.0(5)
N(1)-C(1)	1.334(11)	N(1)-C(1)-C(2)	124.1(8)
C(1)-C(2)	1.359(11)	C(1)-C(2)-C(3)	119.1(8)
C(2)-C(3)	1.392(11)	C(4)-C(3)-C(2)	118.1(7)
C(3)-C(4)	1.383(12)	C(4)-C(3)-C(6)	118.2(8)
C(3)-C(6)	1.481(11)	C(2)-C(3)-C(6)	123.5(7)
C(4)-C(5)	1.408(13)	C(3)-C(4)-C(5)	117.9(8)
C(6)-O(2)	1.204(11)	N(1)-C(5)-C(4)	123.4(8)
C(6)-O(1)	1.319(11)	O(2)-C(6)-O(1)	123.2(8)
O(1)-C(7)	1.478(9)	O(2)-C(6)-C(3)	124.7(8)
C(7)-C(8)	1.58(2)	O(1)-C(6)-C(3)	111.9(7)
C(8)-O(3)	1.288(16)	C(6)-O(1)-C(7)	118.7(7)
O(3)-C(9)	1.400(14)	O(1)-C(7)-C(8)	104.3(9)
C(9)-C(10)	1.489(14)	O(3)-C(8)-C(7)	109.6(10)
C(10)-O(4)	1.432(10)	C(8)-O(3)-C(9)	107.9(11)
O(4)-C(11)	1.313(10)	O(3)-C(9)-C(10)	120.9(10)
O(5)-C(11)	1.215(10)	O(4)-C(10)-C(9)	108.0(8)
C(11)-C(14)	1.472(12)	C(11)-O(4)-C(10)	117.4(7)
C(12)-N(2)	1.332(12)	O(5)-C(11)-O(4)	122.7(8)
C(12)-C(13)	1.365(13)	O(5)-C(11)-C(14)	123.1(8)
C(13)-C(14)	1.403(12)	O(4)-C(11)-C(14)	114.2(7)
C(14)-C(15)	1.373(12)	N(2)-C(12)-C(13)	123.3(9)
C(15)-C(16)	1.379(11)	C(12)-C(13)-C(14)	118.8(9)
C(16)-N(2)	1.346(11)	C(15)-C(14)-C(13)	118.3(8)
N(2)-Ag(1)#2	2.158(7)	C(15)-C(14)-C(11)	123.0(8)
Cl(1)-O(9)	1.323(14)	C(13)-C(14)-C(11)	118.7(8)
Cl(1)-O(8)	1.371(9)	C(14)-C(15)-C(16)	119.2(8)
Cl(1)-O(6)	1.383(9)	N(2)-C(16)-C(15)	122.6(8)
Cl(1)-O(7)	1.482(13)	C(12)-N(2)-C(16)	117.9(7)
		C(12)-N(2)-Ag(1)#2	118.0(6)
N(2)#1-Ag(1)-N(1)	162.5(3)	C(16)-N(2)-Ag(1)#2	124.1(6)

O(9)-Cl(1)-O(8)	114.1(12)	O(9)-Cl(1)-O(7)	108.7(14)
O(9)-Cl(1)-O(6)	109.8(10)	O(8)-Cl(1)-O(7)	107.1(7)
O(8)-Cl(1)-O(6)	112.5(8)	O(6)-Cl(1)-O(7)	104.2(7)

Symmetry transformations used to generate equivalent atoms:

#1 -x+3/2,y+1/2,-z+3/2   #2 -x+3/2,y-1/2,-z+3/2

Table 4. Anisotropic displacement parameters (Å^2x 10^3) for **8**. The anisotropic displacement factor exponent takes the form: $-2p^2[\,h^2a^{*2}U^{11} + ... + 2\,h\,k\,a^*\,b^*\,U^{12}\,]$

	U^{11}	U^{22}	U^{33}	U^{23}	U^{13}	U^{12}
Ag(1)	67(1)	86(1)	46(1)	-1(1)	15(1)	1(1)
N(1)	45(3)	58(5)	44(3)	-4(3)	15(3)	2(3)
C(1)	43(4)	56(6)	55(4)	-8(4)	13(3)	-7(4)
C(2)	43(4)	59(6)	46(4)	-8(4)	22(3)	-9(4)
C(3)	49(4)	58(5)	43(4)	-2(4)	21(3)	-1(4)
C(4)	44(4)	87(8)	63(5)	7(5)	25(4)	-10(4)
C(5)	51(5)	91(8)	57(5)	10(5)	26(4)	-1(5)
C(6)	52(5)	63(6)	53(4)	-3(5)	18(4)	-2(5)
O(1)	54(3)	78(5)	44(3)	10(3)	16(2)	-11(3)
O(2)	45(3)	160(9)	58(4)	3(4)	9(3)	-20(4)
C(7)	70(6)	87(8)	36(4)	-1(4)	3(4)	-10(6)
C(8)	245(18)	143(13)	83(7)	81(9)	119(11)	150(14)
O(3)	93(5)	107(7)	92(5)	19(5)	45(5)	8(5)
C(9)	81(7)	63(6)	58(5)	10(5)	12(5)	-25(6)
C(10)	62(5)	89(8)	53(5)	10(5)	26(4)	9(5)
O(4)	52(3)	85(5)	52(3)	0(3)	24(3)	-5(3)
O(5)	62(4)	130(8)	72(4)	7(5)	40(4)	-11(4)
C(11)	61(5)	60(6)	58(4)	3(4)	33(4)	-1(5)
C(12)	52(5)	92(8)	58(5)	-2(5)	15(4)	2(5)
C(13)	45(4)	79(7)	64(5)	2(5)	22(4)	0(5)
C(14)	49(4)	59(6)	56(4)	-4(4)	28(4)	2(4)
C(15)	46(4)	54(6)	54(4)	1(4)	25(3)	-3(4)
C(16)	52(4)	58(5)	55(4)	-1(4)	27(4)	3(4)

Silver Coordination Compounds with a Family of Ditopic Ligands of Varying Flexibility:
About Chains, Rings, Helices and Polycatenanes

231

N(2)	53(4)	66(5)	46(3)	6(3)	19(3)	7(4)
Cl(1)	50(1)	131(3)	48(1)	11(1)	15(1)	-11(1)
O(6)	159(9)	147(10)	156(9)	-30(8)	128(9)	-42(8)
O(7)	133(8)	198(13)	108(7)	-28(8)	84(7)	-29(9)
O(8)	71(5)	142(10)	138(8)	-43(8)	-3(5)	5(6)
O(9)	127(10)	340(30)	245(17)	220(20)	5(11)	24(14)

Table 5. Hydrogen coordinates (x 10^4) and isotropic displacement parameters ($Å^2$x 10^3) for **2**.

	x	y	z	U(eq)
H(1)	7792	5957	8906	66
H(2)	8449	5890	9886	59
H(4)	9833	8005	9560	77
H(5)	9091	8142	8572	79
H(7A)	9823	6918	11681	87
H(7B)	10300	5858	11507	87
H(8A)	9845	3685	11964	168
H(8B)	9169	4072	11440	168
H(9A)	9579	975	11757	90
H(9B)	9712	-4	11279	90
H(10A)	8714	-752	11089	82
H(10B)	8536	1367	11118	82
H(12)	6693	468	8101	85
H(13)	6931	0	9062	77
H(15)	8709	1760	9513	61
H(16)	8411	2235	8533	65

Table 6. Hydrogen bond data [length (Å) and angle (°)] present in complex **8**

D-H···Acceptor	d (D–H)	d (H···A)	d (D···A)	< D-H···A
C1-H1···O8[#5]	0.93	2.34(5)	3.13(1)	141.7(6)
C5-H5···O9[#3]	0.93	2.36(9)	3.25(2)	159.2(9)
C16-H16···O7	0.93	2.34(3)	3.13(1)	141.3(8)
C2-H2···O5[#6]	0.93	2.52(8)	3.27(1)	136.7(9)

Symmetry transformation used to generate equivalent atoms: #5 1/2-x,-1/2+y,1/2-z, #6 1/2-x,3/2-y,-z, #3 x,-1+y,z.

Silver Coordination Compounds with a Family of Ditopic Ligands of Varying Flexibility:
About Chains, Rings, Helices and Polycatenanes

232

Crystal data and structure refinement for {[Ag(L3)]NO₃*2H₂O}₂ (9)

Identification code	**9**
Empirical formula	C16 H20 Ag N3 O10
Formula weight	522.22
Temperature	293(2) K
Wavelength	0.71073 Å
Crystal system	Monoclinic
Space group	P2₁/n
Unit cell dimensions	a = 13.668(3) Å $\alpha = 90°$.
	b = 7.3268(15) Å $\beta = 94.86(3)°$.
	c = 20.232(4) Å $\gamma = 90°$.
Volume	2018.7(7) Å³
Z	4
Density (calculated)	1.718 Mg/m³
Absorption coefficient	1.058 mm⁻¹
F(000)	1056
Theta range for data collection	1.73 to 27.04°.
Index ranges	-17<=h<=17, -8<=k<=9, -25<=l<=25
Reflections collected	12538
Independent reflections	4277 [R(int) = 0.0844]
Completeness to theta = 27.04°	96.6 %
Refinement method	Full-matrix least-squares on F²
Data / restraints / parameters	4277 / 0 / 287
Goodness-of-fit on F²	1.037
Final R indices [I>2sigma(I)]	R1 = 0.0560, wR2 = 0.1319
R indices (all data)	R1 = 0.0730, wR2 = 0.1450
Largest diff. peak and hole	1.869 and -1.198 e.Å⁻³

Table 2. Atomic coordinates (x 10^4) and equivalent isotropic displacement parameters (Å^2x 10^3) for **9**. U(eq) is defined as one third of the trace of the orthogonalized U^{ij} tensor.

	x	y	z	U(eq)
Ag(1)	341(1)	2926(1)	257(1)	49(1)
N(1)	-903(3)	3321(5)	861(2)	39(1)
C(1)	-1834(3)	3040(7)	641(2)	42(1)
C(2)	-2618(3)	3332(6)	1028(2)	40(1)
C(3)	-2411(3)	3903(6)	1670(2)	35(1)
C(4)	-1448(3)	4159(8)	1908(3)	48(1)
C(5)	-720(3)	3867(8)	1486(2)	48(1)
C(6)	-3213(3)	4276(7)	2119(3)	45(1)
O(1)	-3070(3)	4400(8)	2705(2)	78(2)
O(2)	-4072(2)	4466(6)	1779(2)	52(1)
C(7)	-4942(4)	4693(9)	2144(3)	61(2)
C(8)	-5331(5)	2948(9)	2329(4)	80(2)
O(3)	-5462(4)	1760(8)	1782(4)	120(3)
C(9)	-5886(4)	162(11)	1833(4)	70(2)
C(10)	-5898(4)	-884(9)	1250(3)	62(2)
O(4)	-4890(2)	-1267(6)	1107(2)	54(1)
O(5)	-5467(3)	-2482(9)	154(3)	87(2)
C(11)	-4796(3)	-2051(7)	529(3)	47(1)
N(2)	-1822(3)	-2746(6)	64(2)	40(1)
C(12)	-2018(3)	-1910(7)	621(2)	40(1)
C(13)	-2964(3)	-1670(7)	806(2)	41(1)
C(14)	-3737(3)	-2304(6)	399(2)	37(1)
C(15)	-3543(4)	-3213(8)	-177(3)	50(1)
C(16)	-2581(4)	-3397(8)	-324(3)	50(1)
N(3)	-1002(3)	1560(6)	-977(2)	45(1)
O(6)	-928(4)	3207(6)	-863(3)	74(1)
O(7)	-319(3)	547(7)	-789(3)	93(2)
O(8)	-1750(3)	934(8)	-1266(3)	81(1)
O(9)	-2633(3)	4329(7)	-1871(2)	57(1)

Silver Coordination Compounds with a Family of Ditopic Ligands of Varying Flexibility: About Chains, Rings, Helices and Polycatenanes

234

O(10)	-1625(4)	-2390(7)	-1981(3)	60(1)

Table 3.   Bond lengths [Å] and angles [°] for **9**.

Ag(1)-N(2)#1	2.182(4)		
Ag(1)-N(1)	2.195(4)	N(2)#1-Ag(1)-N(1)	162.87(15)
Ag(1)-Ag(1)#2	3.3203(10)	N(2)#1-Ag(1)-Ag(1)#2	101.84(11)
N(1)-C(1)	1.329(6)	N(1)-Ag(1)-Ag(1)#2	80.98(10)
N(1)-C(5)	1.331(6)	C(1)-N(1)-C(5)	117.4(4)
C(1)-C(2)	1.394(6)	C(1)-N(1)-Ag(1)	124.0(3)
C(2)-C(3)	1.372(6)	C(5)-N(1)-Ag(1)	118.5(3)
C(3)-C(4)	1.375(6)	N(1)-C(1)-C(2)	123.3(5)
C(3)-C(6)	1.507(6)	C(3)-C(2)-C(1)	118.2(4)
C(4)-C(5)	1.380(6)	C(2)-C(3)-C(4)	119.1(4)
C(6)-O(1)	1.189(6)	C(2)-C(3)-C(6)	121.7(4)
C(6)-O(2)	1.318(6)	C(4)-C(3)-C(6)	119.3(4)
O(2)-C(7)	1.462(6)	C(3)-C(4)-C(5)	118.8(5)
C(7)-C(8)	1.446(9)	N(1)-C(5)-C(4)	123.2(4)
C(8)-O(3)	1.407(10)	O(1)-C(6)-O(2)	125.3(5)
O(3)-C(9)	1.314(9)	O(1)-C(6)-C(3)	123.2(5)
C(9)-C(10)	1.404(9)	O(2)-C(6)-C(3)	111.4(4)
C(10)-O(4)	1.459(5)	C(6)-O(2)-C(7)	118.3(4)
O(4)-C(11)	1.320(7)	C(8)-C(7)-O(2)	111.3(5)
O(5)-C(11)	1.183(7)	O(3)-C(8)-C(7)	111.7(6)
C(11)-C(14)	1.504(6)	C(9)-O(3)-C(8)	121.1(6)
N(2)-C(12)	1.329(6)	O(3)-C(9)-C(10)	113.2(6)
N(2)-C(16)	1.335(7)	C(9)-C(10)-O(4)	109.1(5)
N(2)-Ag(1)#1	2.182(4)	C(11)-O(4)-C(10)	115.1(4)
C(12)-C(13)	1.388(6)	O(5)-C(11)-O(4)	123.8(5)
C(13)-C(14)	1.365(7)	O(5)-C(11)-C(14)	124.1(5)
C(14)-C(15)	1.388(7)	O(4)-C(11)-C(14)	112.0(4)
C(15)-C(16)	1.379(7)	C(12)-N(2)-C(16)	117.5(4)
N(3)-O(8)	1.224(6)	C(12)-N(2)-Ag(1)#1	122.6(3)
N(3)-O(7)	1.227(6)	C(16)-N(2)-Ag(1)#1	119.8(3)
N(3)-O(6)	1.232(6)	N(2)-C(12)-C(13)	123.2(4)

C(14)-C(13)-C(12)	119.0(4)	N(2)-C(16)-C(15)	123.0(5)
C(13)-C(14)-C(15)	118.5(4)	O(8)-N(3)-O(7)	120.3(5)
C(13)-C(14)-C(11)	124.1(4)	O(8)-N(3)-O(6)	120.6(5)
C(15)-C(14)-C(11)	117.4(4)	O(7)-N(3)-O(6)	119.1(5)
C(16)-C(15)-C(14)	118.8(5)		

Symmetry transformations used to generate equivalent atoms:

#1 -x,-y,-z   #2 -x,-y+1,-z

Table 4. Anisotropic displacement parameters ($Å^2$x 10^3)for **9**. The anisotropic displacement factor exponent takes the form: $-2p^2[h^2a^{*2}U^{11} + ... + 2 h k a^* b^* U^{12}]$

	U^{11}	U^{22}	U^{33}	U^{23}	U^{13}	U^{12}
Ag(1)	41(1)	54(1)	56(1)	-5(1)	21(1)	2(1)
N(1)	35(2)	39(2)	43(2)	2(2)	8(2)	3(2)
C(1)	41(2)	45(3)	42(2)	-5(2)	8(2)	-6(2)
C(2)	33(2)	44(2)	43(2)	-2(2)	4(2)	-4(2)
C(3)	32(2)	40(2)	36(2)	2(2)	8(2)	-1(2)
C(4)	34(2)	67(3)	42(3)	-4(2)	2(2)	1(2)
C(5)	30(2)	71(3)	42(2)	-2(2)	-1(2)	5(2)
C(6)	37(2)	51(3)	47(3)	-4(2)	11(2)	-2(2)
O(1)	55(2)	134(5)	48(2)	-12(3)	14(2)	10(3)
O(2)	29(2)	67(2)	62(2)	-5(2)	12(2)	2(2)
C(7)	36(2)	65(4)	84(4)	-13(3)	22(3)	3(2)
C(8)	60(4)	64(4)	125(6)	6(4)	57(4)	13(3)
O(3)	99(4)	78(4)	197(7)	-45(4)	103(5)	-21(3)
C(9)	43(3)	90(5)	79(4)	-5(4)	15(3)	2(3)
C(10)	38(2)	63(4)	87(4)	18(3)	25(3)	9(2)
O(4)	31(2)	67(2)	67(2)	-3(2)	14(2)	2(2)
O(5)	37(2)	127(5)	95(4)	-29(3)	-8(2)	-3(2)
C(11)	35(2)	50(3)	57(3)	7(2)	5(2)	0(2)
N(2)	41(2)	42(2)	39(2)	-2(2)	16(2)	1(2)
C(12)	33(2)	44(3)	44(2)	-7(2)	6(2)	-2(2)
C(13)	36(2)	46(3)	42(2)	-7(2)	11(2)	0(2)

Silver Coordination Compounds with a Family of Ditopic Ligands of Varying Flexibility:
About Chains, Rings, Helices and Polycatenanes

236

C(14)	31(2)	40(2)	42(2)	8(2)	6(2)	-2(2)
C(15)	45(2)	63(3)	41(3)	-9(2)	0(2)	-6(2)
C(16)	52(3)	63(3)	37(2)	-8(2)	13(2)	-4(2)
N(3)	41(2)	51(2)	43(2)	5(2)	5(2)	1(2)
O(6)	97(3)	47(2)	76(3)	-4(2)	-3(3)	2(2)
O(7)	58(3)	66(3)	149(5)	32(3)	-24(3)	6(2)
O(8)	47(2)	86(3)	107(4)	-22(3)	-12(2)	-3(2)
O(9)	52(2)	56(2)	64(3)	6(2)	1(2)	3(2)
O(10)	56(2)	51(2)	73(3)	0(2)	-3(2)	7(2)

Table 5. Hydrogen coordinates (x 10^4) and isotropic displacement parameters (Å^2x 10^3) for **9**.

	x	y	z	U(eq)
H(1)	-1971	2629	208	51
H(2)	-3262	3145	855	48
H(4)	-1290	4522	2344	57
H(5)	-71	4062	1648	57
H(7A)	-4772	5408	2541	73
H(7B)	-5442	5354	1872	73
H(8A)	-4884	2394	2669	96
H(8B)	-5956	3133	2512	96
H(9A)	-6556	346	1943	84
H(9B)	-5541	-513	2194	84
H(10A)	-6235	-221	884	74
H(10B)	-6246	-2019	1307	74
H(12)	-1496	-1463	899	48
H(13)	-3070	-1087	1202	49
H(15)	-4053	-3690	-459	60
H(16)	-2455	-4002	-712	60
H(9A)	-2260(50)	3580(110)	-1690(40)	70(20)
H(9B)	2340(50)	4760(110)	1900(30)	70(20)
H(10A)	-1690(80)	-1590(160)	-1620(60)	130(40)
H(10B)	1910(60)	1960(120)	2190(40)	70(30)

Table 6. Hydrogen bond data for **9** [length (Å) and angle (°)].

D-H···Acceptor	d (D–H)	d (H···A)	d (D···A)	< D-H···A
O9–H9A···O10	0.97	2.01(8)	2.79(7)	178.0(7)
O10–H10A···O9[#4]	0.97	2.17(8)	2.76(7)	157.0(9)
O9–H9A···O6	0.97	2.38(8)	3.08(7)	144.0(7)
O9–H9A···O8	0.97	2.21(8)	2.98(7)	159.0(7)
O10–H10A···O8[#5]	0.97	1.99(1)	2.84(8)	150.0(1)
C12–H12···O7[#6]	0.93	2.59(6)	3.39(6)	137

Symmetry transformation used to generate equivalent atoms: #4 x,-1+y,z, #5 1/2-x,-1/2+y,1/2-z, #6 1+x,-1+y,z.

Crystal data and structure refinement for {[Ag(L3)]NO₃}₂ (10)

Identification code	**10**
Empirical formula	C64 H64 Ag4 N12 O32
Formula weight	1944.75
Temperature	293(2) K
Wavelength	0.71073 Å
Crystal system	Monoclinic
Space group	$P2_1/c$
Unit cell dimensions	a = 6.6811(13) Å $\alpha = 90°$.
	b = 12.263(3) Å $\beta = 94.74(3)°$.
	c = 22.585(4) Å $\gamma = 90°$.
Volume	1844.1(7) Å³
Z	1
Density (calculated)	1.751 Mg/m³
Absorption coefficient	1.144 mm⁻¹
F(000)	976
Theta range for data collection	1.81 to 27.15°.
Index ranges	-8<=h<=7, -15<=k<=15, -28<=l<=27
Reflections collected	13141
Independent reflections	3804 [R(int) = 0.2612]
Completeness to theta = 27.15°	93.0 %

Refinement method	Full-matrix least-squares on F^2
Data / restraints / parameters	3804 / 0 / 229
Goodness-of-fit on F^2	1.087
Final R indices [I>2sigma(I)]	R1 = 0.1270, wR2 = 0.2499
R indices (all data)	R1 = 0.2750, wR2 = 0.3144
Largest diff. peak and hole	0.799 and -1.224 e.Å^{-3}

Table 2. Atomic coordinates (x 10^4) and equivalent isotropic displacement parameters (Å^{2}x 10^3) for **10**. U(eq) is defined as one third of the trace of the orthogonalized U^{ij} tensor.

	x	y	z	U(eq)
Ag(1)	-2454(3)	5104(1)	74(1)	78(1)
N(1)	-1430(17)	5528(8)	989(3)	53(4)
C(1)	-1020(17)	4735(6)	1422(4)	52(4)
C(2)	-514(17)	5041(7)	2008(3)	55(4)
C(3)	-417(18)	6139(8)	2160(3)	57(5)
C(4)	-827(19)	6931(6)	1727(4)	53(4)
C(5)	-1333(18)	6626(7)	1141(4)	65(5)
C(6)	50(30)	6496(18)	2808(7)	62(5)
O(1)	340(20)	7426(12)	2921(5)	84(5)
O(2)	160(20)	5654(11)	3169(4)	80(4)
C(7)	790(50)	5930(20)	3791(9)	122(11)
C(8)	1950(90)	5120(20)	4028(12)	380(50)
O(3)	2730(40)	4317(19)	3831(8)	151(9)
C(9)	4950(60)	4530(30)	3936(9)	145(14)
C(10)	5740(40)	3700(20)	3595(8)	96(8)
O(4)	5370(30)	3977(11)	2962(5)	90(5)
O(5)	5250(30)	2274(13)	2679(6)	94(5)
C(11)	5170(30)	3225(16)	2562(8)	58(5)
N(2)	3608(19)	4374(9)	815(3)	70(5)
C(12)	3883(18)	5114(7)	1281(4)	53(4)
C(13)	4374(18)	4742(7)	1856(3)	53(4)
C(14)	4591(18)	3631(8)	1965(3)	48(4)
C(15)	4320(20)	2892(7)	1499(5)	72(6)

Silver Coordination Compounds with a Family of Ditopic Ligands of Varying Flexibility: About Chains, Rings, Helices and Polycatenanes

239

C(16)	3820(20)	3263(8)	924(4)	81(6)
N(3)	-1880(30)	2625(15)	-86(6)	79(6)
O(6)	-700(30)	3237(13)	229(6)	98(5)
O(7)	-3510(30)	3030(14)	-273(6)	104(6)
O(8)	-1310(30)	1722(14)	-196(6)	122(7)

Table 3. Bond lengths [Å] and angles [°] for **10**.

Ag(1)-N(1)	2.184(6)	C(14)-C(15)	1.3900
Ag(1)-N(2)#1	2.186(6)	C(15)-C(16)	1.3900
Ag(1)-O(6)	2.581(17)	N(3)-O(8)	1.20(2)
Ag(1)-Ag(1)#1	3.333(4)	N(3)-O(7)	1.24(2)
N(1)-C(1)	1.3900	N(3)-O(6)	1.262(19)
N(1)-C(5)	1.3900		
C(1)-C(2)	1.3900	N(1)-Ag(1)-N(2)#1	149.1(4)
C(2)-C(3)	1.3900	N(1)-Ag(1)-O(6)	88.9(4)
C(3)-C(4)	1.3900	N(2)#1-Ag(1)-O(6)	120.3(4)
C(3)-C(6)	1.534(18)	N(1)-Ag(1)-Ag(1)#1	83.1(3)
C(4)-C(5)	1.3900	N(2)#1-Ag(1)-Ag(1)#1	101.8(3)
C(6)-O(1)	1.18(2)	O(6)-Ag(1)-Ag(1)#1	60.5(4)
C(6)-O(2)	1.31(2)	C(1)-N(1)-C(5)	120.0
O(2)-C(7)	1.47(2)	C(1)-N(1)-Ag(1)	121.8(5)
C(7)-C(8)	1.35(3)	C(5)-N(1)-Ag(1)	118.0(5)
C(8)-O(3)	1.21(3)	N(1)-C(1)-C(2)	120.0
O(3)-C(9)	1.51(4)	C(1)-C(2)-C(3)	120.0
C(9)-C(10)	1.40(3)	C(4)-C(3)-C(2)	120.0
C(10)-O(4)	1.469(19)	C(4)-C(3)-C(6)	119.0(10)
O(4)-C(11)	1.29(2)	C(2)-C(3)-C(6)	121.0(10)
O(5)-C(11)	1.20(2)	C(3)-C(4)-C(5)	120.0
C(11)-C(14)	1.459(18)	C(4)-C(5)-N(1)	120.0
N(2)-C(12)	1.3900	O(1)-C(6)-O(2)	128.7(16)
N(2)-C(16)	1.3900	O(1)-C(6)-C(3)	119.9(15)
N(2)-Ag(1)#1	2.186(6)	O(2)-C(6)-C(3)	111.3(16)
C(12)-C(13)	1.3900	C(6)-O(2)-C(7)	113.9(16)
C(13)-C(14)	1.3900	C(8)-C(7)-O(2)	108.6(17)

O(3)-C(8)-C(7)	135(2)	N(2)-C(12)-C(13)	120.0
C(8)-O(3)-C(9)	104(3)	C(14)-C(13)-C(12)	120.0
C(10)-C(9)-O(3)	102(3)	C(13)-C(14)-C(15)	120.0
C(9)-C(10)-O(4)	109.4(19)	C(13)-C(14)-C(11)	121.0(10)
C(11)-O(4)-C(10)	121.2(16)	C(15)-C(14)-C(11)	119.0(10)
O(5)-C(11)-O(4)	122.8(17)	C(14)-C(15)-C(16)	120.0
O(5)-C(11)-C(14)	122.8(18)	C(15)-C(16)-N(2)	120.0
O(4)-C(11)-C(14)	114.0(15)	O(8)-N(3)-O(7)	125.6(17)
C(12)-N(2)-C(16)	120.0	O(8)-N(3)-O(6)	118(2)
C(12)-N(2)-Ag(1)#1	121.3(5)	O(7)-N(3)-O(6)	116.2(19)
C(16)-N(2)-Ag(1)#1	118.3(5)	N(3)-O(6)-Ag(1)	101.4(14)

Symmetry transformations used to generate equivalent atoms:

#1 -x,-y+1,-z

Table 4. Anisotropic displacement parameters (Å^2x 10^3) for **10**. The anisotropic displacement factor exponent takes the form: $-2p^2[\, h^2a^{*2}U^{11} + ... + 2\, h\, k\, a^*\, b^*\, U^{12}\,]$

	U^{11}	U^{22}	U^{33}	U^{23}	U^{13}	U^{12}
Ag(1)	85(1)	101(1)	47(1)	-2(1)	-1(1)	-6(1)
N(1)	38(10)	63(10)	62(7)	14(7)	20(6)	9(7)
C(1)	21(9)	72(13)	66(9)	-7(8)	16(6)	1(8)
C(2)	38(10)	68(12)	60(7)	5(10)	10(6)	-3(10)
C(3)	41(12)	66(13)	64(9)	-3(9)	13(8)	-14(9)
C(4)	50(12)	57(11)	51(8)	7(8)	-4(7)	2(8)
C(5)	43(13)	62(13)	91(13)	15(9)	15(9)	0(9)
C(6)	68(14)	61(13)	55(9)	15(9)	-13(8)	-10(10)
O(1)	115(14)	63(10)	71(8)	-4(7)	-13(7)	5(9)
O(2)	121(13)	71(9)	46(6)	-16(6)	-11(6)	31(8)
C(7)	190(30)	97(19)	72(12)	-44(12)	-33(15)	31(19)
C(8)	830(110)	130(30)	130(20)	-150(20)	-250(40)	300(50)
O(3)	150(20)	190(20)	101(12)	-16(12)	-58(13)	41(15)
C(9)	210(40)	170(30)	52(11)	-22(13)	-12(15)	110(30)
C(10)	110(20)	120(19)	57(10)	21(11)	-11(11)	-2(15)

O(4)	140(16)	54(9)	71(8)	8(7)	-17(8)	3(8)
O(5)	123(16)	69(10)	91(10)	9(8)	9(9)	16(9)
C(11)	53(13)	37(11)	85(12)	18(9)	12(9)	10(8)
N(2)	70(13)	93(13)	48(7)	17(7)	2(7)	-6(9)
C(12)	66(12)	52(10)	42(6)	-1(8)	2(6)	5(10)
C(13)	34(10)	63(12)	65(8)	-6(8)	17(7)	-7(8)
C(14)	25(10)	57(11)	64(9)	-3(8)	13(7)	-14(8)
C(15)	81(17)	70(13)	66(11)	-13(10)	11(10)	11(11)
C(16)	100(19)	81(16)	60(10)	-19(10)	2(10)	-14(13)
N(3)	140(20)	53(11)	39(7)	-14(7)	-2(9)	-40(11)
O(6)	109(14)	105(11)	78(8)	-12(8)	2(8)	-18(10)
O(7)	118(15)	118(14)	70(8)	3(8)	-26(9)	3(11)
O(8)	220(20)	69(11)	77(9)	0(8)	-26(10)	6(12)

Table 5. Hydrogen coordinates (x 10^4) and isotropic displacement parameters (Å^2x 10^3) for **10**.

	x	y	z	U(eq)
H(1)	-1084	4001	1320	63
H(2)	-240	4511	2298	66
H(4)	-763	7666	1829	64
H(5)	-1607	7156	851	78
H(7A)	1545	6611	3806	147
H(7B)	-373	6028	4014	147
H(8A)	3069	5499	4239	457
H(8B)	1172	4828	4336	457
H(9A)	5300	5245	3798	174
H(9B)	5408	4454	4353	174
H(10A)	5112	3012	3674	116
H(10B)	7174	3635	3699	116
H(12)	3738	5857	1208	64
H(13)	4558	5237	2168	64
H(15)	4461	2148	1572	86
H(16)	3641	2768	612	97

Table 6. Hydrogen bond data for **10** [length (Å) and angle (°)].

D-H···Acceptor	d (D–H)	d (H···A)	d (D···A)	< D-H···A
C13–H13···O5[#3]	0.93	2.52(2)	3.28(9)	138.7(1)

Symmetry transformation used to generate equivalent atoms: #3 1-x,1/2+y,1/2-z.

Crystal data and structure refinement for {[Ag(L3)]NO₃}₂ (11)

Identification code	**11**
Empirical formula	C16 H16 Ag N3 O8
Formula weight	486.19
Temperature	293(2) K
Wavelength	0.71073 Å
Crystal system	Triclinic
Space group	P-1
Unit cell dimensions	a = 6.9203(14) Å α = 63.18(3)°.
	b = 12.156(2) Å β = 87.13(3)°.
	c = 12.332(3) Å γ = 79.87(3)°.
Volume	910.9(3) Å^3
Z	2
Density (calculated)	1.773 Mg/m^3
Absorption coefficient	1.158 mm^{-1}
F(000)	488
Theta range for data collection	3.35 to 26.87°.
Index ranges	-6<=h<=8, -15<=k<=15, -15<=l<=15
Reflections collected	4389
Independent reflections	3074 [R(int) = 0.0446]
Completeness to theta = 26.87°	78.2 %
Refinement method	Full-matrix least-squares on F^2
Data / restraints / parameters	3074 / 0 / 253
Goodness-of-fit on F^2	1.048
Final R indices [I>2sigma(I)]	R1 = 0.0587, wR2 = 0.1600
R indices (all data)	R1 = 0.0623, wR2 = 0.1647
Largest diff. peak and hole	2.228 and -0.575 e.Å^{-3}

Table 2. Atomic coordinates (x 10^4) and equivalent isotropic displacement parameters ($Å^2$x 10^3) **11**. U(eq) is defined as one third of the trace of the orthogonalized U^{ij} tensor.

	x	y	z	U(eq)
Ag(1)	2428(1)	4824(1)	379(1)	54(1)
N(1)	2673(6)	4233(3)	2333(3)	40(1)
C(1)	2579(6)	3062(4)	3175(4)	38(1)
C(2)	2563(6)	2715(4)	4406(4)	37(1)
C(3)	2651(6)	3607(4)	4795(4)	38(1)
C(4)	2783(9)	4803(4)	3936(5)	54(1)
C(5)	2804(9)	5077(4)	2725(4)	52(1)
C(6)	2592(8)	3311(4)	6110(4)	47(1)
O(1)	2556(12)	4080(5)	6462(4)	100(2)
O(2)	2539(6)	2122(3)	6824(3)	49(1)
C(7)	2250(9)	1733(6)	8117(4)	56(1)
C(8)	324(11)	1462(9)	8428(6)	81(2)
O(3)	-391(8)	794(5)	8050(5)	79(1)
C(9)	-2530(10)	999(9)	7994(6)	78(2)
C(10)	-2897(9)	478(5)	7186(5)	60(1)
O(4)	-2677(6)	1370(3)	5947(3)	50(1)
O(5)	-2435(10)	-128(3)	5371(4)	92(2)
C(11)	-2464(7)	946(4)	5126(4)	44(1)
N(2)	-2012(6)	3731(3)	1496(3)	39(1)
C(16)	-1880(8)	2518(4)	1767(4)	45(1)
C(15)	-2009(7)	1606(4)	2923(4)	43(1)
C(14)	-2290(6)	1935(3)	3873(4)	34(1)
C(13)	-2402(6)	3182(4)	3605(4)	35(1)
C(12)	-2262(6)	4040(4)	2417(4)	38(1)
N(3)	4275(7)	2409(4)	267(4)	48(1)
O(6)	2645(8)	2490(5)	714(5)	80(1)
O(7)	4938(7)	3393(4)	-355(4)	72(1)
O(8)	5219(9)	1393(4)	445(5)	80(1)

Silver Coordination Compounds with a Family of Ditopic Ligands of Varying Flexibility: About Chains, Rings, Helices and Polycatenanes

244

Table 3. Bond lengths [Å] and angles [°] for **11**.

Ag(1)-N(2)#1	2.177(4)	C(9)-C(10)	1.453(9)
Ag(1)-N(1)	2.189(4)	C(10)-O(4)	1.440(6)
N(1)-C(5)	1.334(6)	O(4)-C(11)	1.320(6)
N(1)-C(1)	1.342(5)	O(5)-C(11)	1.196(6)
C(1)-C(2)	1.380(6)	C(11)-C(14)	1.484(6)
C(2)-C(3)	1.380(5)	N(2)-C(16)	1.343(6)
C(3)-C(4)	1.376(6)	N(2)-C(12)	1.344(5)
C(3)-C(6)	1.495(6)	N(2)-Ag(1)#1	2.177(4)
C(4)-C(5)	1.376(7)	C(16)-C(15)	1.365(7)
C(6)-O(1)	1.191(6)	C(15)-C(14)	1.394(5)
C(6)-O(2)	1.316(6)	C(14)-C(13)	1.387(5)
O(2)-C(7)	1.459(6)	C(13)-C(12)	1.374(6)
C(7)-C(8)	1.422(9)	N(3)-O(8)	1.219(6)
C(8)-O(3)	1.276(8)	N(3)-O(6)	1.239(7)
O(3)-C(9)	1.457(9)	N(3)-O(7)	1.249(6)
N(2)#1-Ag(1)-N(1)	151.54(13)	C(8)-O(3)-C(9)	114.2(6)
C(5)-N(1)-C(1)	117.5(4)	C(10)-C(9)-O(3)	101.5(6)
C(5)-N(1)-Ag(1)	119.5(3)	O(4)-C(10)-C(9)	109.3(5)
C(1)-N(1)-Ag(1)	122.9(3)	C(11)-O(4)-C(10)	117.1(4)
N(1)-C(1)-C(2)	122.9(4)	O(5)-C(11)-O(4)	123.0(5)
C(3)-C(2)-C(1)	118.9(4)	O(5)-C(11)-C(14)	123.6(4)
C(4)-C(3)-C(2)	118.4(4)	O(4)-C(11)-C(14)	113.3(4)
C(4)-C(3)-C(6)	119.5(4)	C(16)-N(2)-C(12)	117.6(4)
C(2)-C(3)-C(6)	122.0(4)	C(16)-N(2)-Ag(1)#1	120.9(3)
C(3)-C(4)-C(5)	119.4(4)	C(12)-N(2)-Ag(1)#1	120.3(3)
N(1)-C(5)-C(4)	122.9(4)	N(2)-C(16)-C(15)	123.0(4)
O(1)-C(6)-O(2)	124.2(4)	C(16)-C(15)-C(14)	119.2(4)
O(1)-C(6)-C(3)	123.2(4)	C(13)-C(14)-C(15)	118.3(4)
O(2)-C(6)-C(3)	112.6(3)	C(13)-C(14)-C(11)	122.6(4)
C(6)-O(2)-C(7)	118.2(4)	C(15)-C(14)-C(11)	119.1(3)
C(8)-C(7)-O(2)	110.5(4)	C(12)-C(13)-C(14)	118.8(4)
O(3)-C(8)-C(7)	120.4(7)	N(2)-C(12)-C(13)	123.2(4)

Silver Coordination Compounds with a Family of Ditopic Ligands of Varying Flexibility:

About Chains, Rings, Helices and Polycatenanes

| O(8)-N(3)-O(6) | 120.8(5) | O(6)-N(3)-O(7) | 118.3(5) |
| O(8)-N(3)-O(7) | 120.9(5) | | |

Symmetry transformations used to generate equivalent atoms:

#1 -x,-y+1,-z

Table 4.   Anisotropic displacement parameters ($Å^2$x 10^3) for **11**. The anisotropic displacement factor exponent takes the form: $-2p^2[h^2a^{*2}U^{11} + ... + 2 h k a^* b^* U^{12}]$

	U^{11}	U^{22}	U^{33}	U^{23}	U^{13}	U^{12}
Ag(1)	70(1)	53(1)	27(1)	-8(1)	2(1)	-6(1)
N(1)	46(2)	38(2)	31(2)	-11(2)	1(2)	-7(1)
C(1)	45(2)	38(2)	30(2)	-14(2)	-1(2)	-11(2)
C(2)	45(2)	33(2)	31(2)	-11(2)	-1(2)	-12(2)
C(3)	44(2)	39(2)	33(2)	-18(2)	4(2)	-11(2)
C(4)	85(3)	37(2)	43(3)	-19(2)	9(2)	-20(2)
C(5)	78(3)	35(2)	38(2)	-11(2)	11(2)	-15(2)
C(6)	61(3)	49(2)	35(2)	-21(2)	3(2)	-18(2)
O(1)	207(7)	66(3)	52(2)	-41(2)	18(3)	-49(4)
O(2)	67(2)	53(2)	30(2)	-18(1)	5(2)	-22(2)
C(7)	66(3)	69(3)	25(2)	-13(2)	-6(2)	-18(3)
C(8)	76(4)	136(6)	36(3)	-36(4)	11(3)	-45(4)
O(3)	86(3)	78(3)	69(3)	-32(3)	-6(3)	-6(3)
C(9)	68(4)	130(6)	34(3)	-29(4)	7(3)	-36(4)
C(10)	63(3)	59(3)	31(2)	-2(2)	9(2)	1(2)
O(4)	70(2)	43(2)	28(2)	-11(1)	6(2)	-7(2)
O(5)	186(7)	36(2)	52(3)	-13(2)	22(4)	-32(3)
C(11)	53(2)	36(2)	35(2)	-10(2)	-1(2)	-5(2)
N(2)	51(2)	37(2)	25(2)	-10(1)	0(2)	-3(2)
C(16)	60(3)	41(2)	37(2)	-23(2)	-1(2)	-1(2)
C(15)	58(2)	34(2)	40(2)	-20(2)	0(2)	-5(2)
C(14)	38(2)	31(2)	31(2)	-12(2)	-1(2)	-4(1)
C(13)	43(2)	34(2)	31(2)	-17(2)	-1(2)	-4(2)
C(12)	48(2)	32(2)	32(2)	-14(2)	-1(2)	-4(2)

N(3)	64(2)	47(2)	30(2)	-17(2)	0(2)	-6(2)
O(6)	87(3)	72(3)	83(3)	-36(3)	32(3)	-23(2)
O(7)	73(3)	61(2)	59(3)	-6(2)	8(2)	-19(2)
O(8)	111(4)	57(2)	71(3)	-35(2)	0(3)	2(2)

Table 5. Hydrogen coordinates (x 10^4) and isotropic displacement parameters ($Å^2$x 10^3) for **11**.

	x	y	z	U(eq)
H(1)	2522	2458	2917	45
H(2)	2493	1895	4963	44
H(4)	2858	5422	4173	64
H(5)	2915	5886	2155	63
H(7A)	3209	996	8589	67
H(7B)	2448	2395	8312	67
H(8A)	290	1055	9308	97
H(8B)	-565	2256	8147	97
H(9A)	-3056	558	8790	94
H(9B)	-3083	1882	7658	94
H(10A)	-1976	-291	7382	72
H(10B)	-4217	286	7290	72
H(16)	-1692	2289	1140	54
H(15)	-1911	776	3074	52
H(13)	-2568	3433	4219	42
H(12)	-2344	4876	2242	45

Table 6. Hydrogen bond [length (Å) and angle (°)] present in complex **11**

D–H···Acceptor	d (D–H)	d (H···A) Å	d (D···A) Å	< D–H···A
C2–H2···O5[#2]	0.93	2.37(0)	3.04(7)	129.5(8)
C12–H12···O1[#4]	0.93	2.43(5)	3.13(8)	132.1(2)
C5–H5···O7[#3]	0.93	2.50(4)	3.18(7)	129.4(9)
Symmetry transformation used to generate equivalent atoms: #2 -x,-y,1-z, #3 1-x,1-y,-z, #4 -x,1-y,1-z.				

Crystal data and structure refinement for {[Ag(L3)]PF$_6$*THF}$_2$ (12)

Identification code	**12**
Empirical formula	C20 H24 Ag F6 N2 O6 P
Formula weight	641.25
Temperature	293(2) K
Wavelength	0.71073 Å
Crystal system	Triclinic
Space group	P-1
Unit cell dimensions	a = 7.7161(15) Å α = 82.09(3)°.
	b = 12.970(3) Å β = 84.27(3)°.
	c = 13.037(3) Å γ = 72.81(3)°.
Volume	1232.2(4) Å^3
Z	2
Density (calculated)	1.728 Mg/m^3
Absorption coefficient	0.967 mm^{-1}
F(000)	644
Theta range for data collection	1.58 to 26.97°.
Index ranges	-9<=h<=9, -16<=k<=16, 0<=l<=16
Reflections collected	4974
Independent reflections	4974 [R(int) = 0.0000]
Completeness to theta = 26.97°	92.7 %
Refinement method	Full-matrix least-squares on F^2
Data / restraints / parameters	4974 / 0 / 322
Goodness-of-fit on F^2	1.067
Final R indices [I>2sigma(I)]	R1 = 0.0586, wR2 = 0.1460
R indices (all data)	R1 = 0.0845, wR2 = 0.1624
Largest diff. peak and hole	0.767 and -1.090 e.Å^{-3}

Table 2. Atomic coordinates (x 10^4) and equivalent isotropic displacement parameters (Å^2x 10^3) for **12**. U(eq) is defined as one third of the trace of the orthogonalized U^{ij} tensor.

	x	y	z	U(eq)
Ag(1)	6893(1)	5188(1)	9258(1)	59(1)
N(1)	7870(6)	3744(3)	8495(4)	51(1)
C(1)	7228(8)	3756(5)	7581(5)	62(2)
C(2)	7872(8)	2923(5)	6964(5)	57(1)
C(3)	9218(7)	2007(4)	7328(4)	44(1)
C(4)	9877(8)	1979(4)	8275(4)	50(1)
C(5)	9186(8)	2861(4)	8828(5)	51(1)
C(6)	9871(7)	1099(4)	6649(4)	47(1)
O(1)	9318(8)	1152(4)	5818(4)	80(1)
O(2)	11079(5)	254(3)	7102(3)	54(1)
C(7)	11944(8)	-646(5)	6488(5)	60(2)
C(8)	13832(9)	-628(5)	6166(5)	58(2)
O(3)	14851(5)	-875(3)	7050(3)	56(1)
C(9)	16685(8)	-854(5)	6835(5)	60(2)
C(10)	17501(7)	-940(4)	7833(5)	55(1)
O(4)	16650(5)	84(3)	8265(3)	53(1)
O(5)	18158(7)	-560(3)	9709(4)	74(1)
C(11)	17113(7)	147(4)	9202(4)	46(1)
N(2)	14331(6)	3244(3)	10241(4)	51(1)
C(12)	13920(8)	2969(4)	9361(5)	57(1)
C(13)	14741(8)	1981(4)	9003(5)	52(1)
C(14)	16070(7)	1236(4)	9566(4)	45(1)
C(15)	16508(8)	1487(5)	10483(5)	55(1)
C(16)	15598(8)	2498(4)	10796(4)	54(1)
O(6)	2598(12)	2345(6)	5647(7)	131(3)
C(17)	1516(13)	3289(9)	5118(10)	126(5)
C(18)	2678(16)	3915(11)	4525(11)	137(5)
C(19)	4343(14)	3505(7)	5124(9)	162(6)
C(20)	3986(14)	2706(7)	5904(9)	159(7)

Silver Coordination Compounds with a Family of Ditopic Ligands of Varying Flexibility: About Chains, Rings, Helices and Polycatenanes

249

P(1)	8825(2)	4012(1)	12099(1)	58(1)
F(1)	10928(6)	3576(4)	12305(4)	91(1)
F(2)	6757(6)	4449(4)	11837(5)	104(2)
F(3)	8981(8)	2927(4)	11622(7)	134(3)
F(4)	9333(8)	4535(6)	10994(5)	139(3)
F(5)	8695(10)	5082(5)	12494(8)	163(3)
F(6)	8350(11)	3458(8)	13146(6)	183(4)

Table 3. Bond lengths [Å] and angles [°] for **12**.

Ag(1)-N(2)#1	2.137(4)	C(11)-C(14)	1.517(6)
Ag(1)-N(1)	2.143(4)	N(2)-C(12)	1.340(8)
N(1)-C(1)	1.332(9)	N(2)-C(16)	1.344(8)
N(1)-C(5)	1.339(8)	N(2)-Ag(1)#1	2.137(4)
C(1)-C(2)	1.380(8)	C(12)-C(13)	1.374(7)
C(2)-C(3)	1.389(8)	C(13)-C(14)	1.376(8)
C(3)-C(4)	1.374(8)	C(14)-C(15)	1.381(8)
C(3)-C(6)	1.507(7)	C(15)-C(16)	1.387(7)
C(4)-C(5)	1.379(7)	O(6)-C(20)	1.375(12)
C(6)-O(1)	1.190(7)	O(6)-C(17)	1.396(12)
C(6)-O(2)	1.322(7)	C(17)-C(18)	1.476(14)
O(2)-C(7)	1.463(6)	C(18)-C(19)	1.492(14)
C(7)-C(8)	1.481(9)	C(19)-C(20)	1.4171
C(8)-O(3)	1.407(8)	P(1)-F(6)	1.517(6)
O(3)-C(9)	1.422(7)	P(1)-F(5)	1.518(6)
C(9)-C(10)	1.478(9)	P(1)-F(4)	1.570(6)
C(10)-O(4)	1.459(5)	P(1)-F(2)	1.582(5)
O(4)-C(11)	1.327(7)	P(1)-F(3)	1.583(5)
O(5)-C(11)	1.195(7)	P(1)-F(1)	1.590(5)
N(2)#1-Ag(1)-N(1)	169.3(2)	C(1)-C(2)-C(3)	118.5(6)
C(1)-N(1)-C(5)	117.3(5)	C(4)-C(3)-C(2)	118.6(5)
C(1)-N(1)-Ag(1)	117.6(4)	C(4)-C(3)-C(6)	123.9(5)
C(5)-N(1)-Ag(1)	124.8(4)	C(2)-C(3)-C(6)	117.4(5)
N(1)-C(1)-C(2)	123.4(5)	C(3)-C(4)-C(5)	119.0(5)

N(1)-C(5)-C(4)	123.2(6)	C(14)-C(15)-C(16)	118.2(5)
O(1)-C(6)-O(2)	125.6(5)	N(2)-C(16)-C(15)	123.0(5)
O(1)-C(6)-C(3)	122.8(5)	C(20)-O(6)-C(17)	101.1(9)
O(2)-C(6)-C(3)	111.6(5)	O(6)-C(17)-C(18)	109.8(9)
C(6)-O(2)-C(7)	117.1(4)	C(17)-C(18)-C(19)	100.4(9)
O(2)-C(7)-C(8)	108.9(5)	C(20)-C(19)-C(18)	105.5(6)
O(3)-C(8)-C(7)	109.0(5)	O(6)-C(20)-C(19)	110.7(6)
C(8)-O(3)-C(9)	113.9(5)	F(6)-P(1)-F(5)	95.2(6)
O(3)-C(9)-C(10)	108.2(5)	F(6)-P(1)-F(4)	177.4(6)
O(4)-C(10)-C(9)	106.7(5)	F(5)-P(1)-F(4)	87.4(5)
C(11)-O(4)-C(10)	116.2(4)	F(6)-P(1)-F(2)	91.8(4)
O(5)-C(11)-O(4)	125.4(5)	F(5)-P(1)-F(2)	90.1(3)
O(5)-C(11)-C(14)	124.3(5)	F(4)-P(1)-F(2)	88.5(3)
O(4)-C(11)-C(14)	110.3(4)	F(6)-P(1)-F(3)	88.1(5)
C(12)-N(2)-C(16)	117.3(4)	F(5)-P(1)-F(3)	176.7(5)
C(12)-N(2)-Ag(1)#1	122.3(4)	F(4)-P(1)-F(3)	89.3(5)
C(16)-N(2)-Ag(1)#1	120.3(4)	F(2)-P(1)-F(3)	89.6(3)
N(2)-C(12)-C(13)	123.4(6)	F(6)-P(1)-F(1)	90.6(4)
C(12)-C(13)-C(14)	118.7(6)	F(5)-P(1)-F(1)	90.8(3)
C(13)-C(14)-C(15)	119.4(5)	F(4)-P(1)-F(1)	89.1(3)
C(13)-C(14)-C(11)	122.3(5)	F(2)-P(1)-F(1)	177.3(3)
C(15)-C(14)-C(11)	118.3(5)	F(3)-P(1)-F(1)	89.4(3)

Symmetry transformations used to generate equivalent atoms:

#1 -x+2,-y+1,-z+2

Table 4.   Anisotropic displacement parameters ($Å^2$x 10^3) for **12**. The anisotropic displacement factor exponent takes the form: $-2p^2[h^2a^{*2}U^{11} + ... + 2 h k a^* b^* U^{12}]$

	U^{11}	U^{22}	U^{33}	U^{23}	U^{13}	U^{12}
Ag(1)	59(1)	45(1)	71(1)	-21(1)	11(1)	-10(1)
N(1)	48(2)	46(2)	54(3)	-13(2)	1(2)	-5(2)
C(1)	55(3)	51(3)	67(4)	-8(3)	-4(3)	7(2)
C(2)	58(3)	63(3)	42(3)	-7(2)	-9(3)	-2(3)

C(3)	42(2)	43(2)	43(3)	-6(2)	-1(2)	-8(2)
C(4)	51(3)	46(2)	47(3)	-10(2)	-8(2)	-2(2)
C(5)	57(3)	51(3)	45(3)	-14(2)	-8(3)	-8(2)
C(6)	53(3)	50(3)	39(3)	-10(2)	-4(2)	-12(2)
O(1)	103(4)	70(3)	59(3)	-24(2)	-33(3)	2(3)
O(2)	59(2)	50(2)	47(2)	-18(2)	-12(2)	1(2)
C(7)	64(3)	48(3)	64(4)	-27(3)	-14(3)	2(2)
C(8)	72(4)	58(3)	42(3)	-22(2)	6(3)	-10(3)
O(3)	55(2)	62(2)	48(2)	-11(2)	3(2)	-14(2)
C(9)	58(3)	60(3)	67(4)	-30(3)	18(3)	-20(3)
C(10)	47(3)	42(2)	74(4)	-21(2)	3(3)	-6(2)
O(4)	58(2)	40(2)	56(2)	-13(2)	-8(2)	0(2)
O(5)	84(3)	52(2)	70(3)	-9(2)	-27(3)	13(2)
C(11)	45(3)	39(2)	53(3)	-7(2)	-1(2)	-7(2)
N(2)	50(2)	43(2)	58(3)	-13(2)	2(2)	-8(2)
C(12)	58(3)	41(2)	65(4)	-4(2)	-17(3)	-2(2)
C(13)	56(3)	42(2)	55(3)	-4(2)	-14(3)	-6(2)
C(14)	46(2)	38(2)	46(3)	-3(2)	0(2)	-7(2)
C(15)	59(3)	51(3)	48(3)	-4(2)	-12(3)	-3(2)
C(16)	68(3)	51(3)	42(3)	-11(2)	-4(3)	-11(2)
O(6)	130(6)	101(5)	130(6)	13(4)	6(5)	-3(4)
C(17)	85(6)	121(8)	128(9)	51(7)	13(6)	6(5)
C(18)	119(8)	153(11)	132(10)	65(8)	-47(8)	-54(8)
C(19)	114(9)	174(13)	225(18)	-5(12)	-36(10)	-81(10)
C(20)	234(15)	64(5)	202(14)	19(7)	-165(13)	-46(7)
P(1)	56(1)	46(1)	66(1)	-5(1)	-7(1)	-6(1)
F(1)	66(2)	95(3)	108(4)	-7(3)	-25(2)	-13(2)
F(2)	53(2)	81(3)	171(5)	-22(3)	-17(3)	0(2)
F(3)	96(4)	82(3)	224(8)	-63(4)	-60(4)	14(3)
F(4)	90(4)	205(7)	97(4)	57(4)	-22(3)	-33(4)
F(5)	144(5)	104(4)	253(9)	-96(5)	-66(6)	0(4)
F(6)	147(6)	250(10)	124(6)	78(6)	4(5)	-65(6)

Silver Coordination Compounds with a Family of Ditopic Ligands of Varying Flexibility: About Chains, Rings, Helices and Polycatenanes

252

Table 5.   Hydrogen coordinates (x 10^4) and isotropic displacement parameters ($Å^2$x 10^3) for **12**.

	x	y	z	U(eq)
H(1)	6297	4358	7347	75
H(2)	7416	2974	6319	69
H(4)	10775	1375	8540	59
H(5)	9657	2842	9462	62
H(7A)	11270	-575	5880	72
H(7B)	11952	-1331	6897	72
H(8A)	14369	-1156	5681	70
H(8B)	13832	85	5824	70
H(9A)	16727	-182	6416	72
H(9B)	17357	-1456	6453	72
H(10A)	17273	-1541	8302	66
H(10B)	18804	-1059	7724	66
H(12)	13033	3473	8973	68
H(13)	14406	1819	8392	63
H(15)	17391	993	10881	66
H(16)	15877	2667	11418	65
H(17A)	699	3728	5611	152
H(17B)	788	3100	4649	152
H(18A)	2140	4691	4535	164
H(18B)	2928	3750	3812	164
H(19A)	5396	3191	4677	195
H(19B)	4567	4090	5432	195
H(20A)	5075	2099	5988	191
H(20B)	3657	3010	6559	191

Table 6. Hydrogen bond data for **12** [length (Å) and angle (°)]

D–H···Acceptor	d (D–H)	d (H···A)	d (D···A)	< D–H···A
C4–H4[#3]···O5	0.97	2.49(1)	3.22(6)	136.0(7)
C7–H7A[#4]···O1	0.97	2.55(4)	3.45(2)	154.0(4)
Symmetry transformation used to generate equivalent atoms: #3 1-x,-y,2-z, #4 -x,-y,1-z.				

Silver Coordination Compounds with a Family of Ditopic Ligands of Varying Flexibility:
About Chains, Rings, Helices and Polycatenanes

253

Crystal data and structure refinement for {[Ag(L3)₂]PF₆}ₙ (13)

Identification code	**13**
Empirical formula	C32 H32 Ag F6 N4 O10 P
Formula weight	885.46
Temperature	293(2) K
Wavelength	0.71073 Å
Crystal system	Orthorhombic
Space group	Pbcn
Unit cell dimensions	a = 28.389(6) Å $\alpha = 90°$.
	b = 15.020(3) Å $\beta = 90°$.
	c = 17.060(3) Å $\gamma = 90°$.
Volume	7274(3) Å^3
Z	8
Density (calculated)	1.617 Mg/m^3
Absorption coefficient	0.690 mm^{-1}
F(000)	3584
Theta range for data collection	1.43 to 27.19°.
Index ranges	-36<=h<=33, -19<=k<=19, -21<=l<=21
Reflections collected	56024
Independent reflections	8016 [R(int) = 0.1195]
Completeness to theta = 27.19°	99.0 %
Absorption correction	NUMERICAL
Refinement method	Full-matrix least-squares on F^2
Data / restraints / parameters	8016 / 0 / 488
Goodness-of-fit on F^2	1.032
Final R indices [I>2sigma(I)]	R1 = 0.0698, wR2 = 0.1840
R indices (all data)	R1 = 0.0971, wR2 = 0.2075
Extinction coefficient	0.0020(3)
Largest diff. peak and hole	0.765 and -0.935 e.Å^{-3}

Table 2. Atomic coordinates (x 10^4) and equivalent isotropic displacement parameters (Å^2x 10^3) for **13**. U(eq) is defined as one third of the trace of the orthogonalized U^{ij} tensor.

	x	y	z	U(eq)
Ag(1)	7433(1)	6178(1)	2216(1)	82(1)
N(1)	8096(2)	5349(2)	1997(2)	70(1)
C(1)	8193(2)	4590(3)	2360(3)	73(1)
C(2)	8612(2)	4128(3)	2238(3)	75(1)
C(3)	8939(2)	4477(3)	1729(3)	77(1)
C(4)	8839(2)	5266(3)	1359(4)	97(2)
C(5)	8421(2)	5669(3)	1506(4)	87(2)
C(6)	9390(2)	4030(4)	1509(5)	107(2)
O(1)	9699(2)	4391(4)	1150(6)	197(4)
O(2)	9389(1)	3180(3)	1687(3)	92(1)
C(7)	9808(2)	2690(5)	1415(5)	111(2)
C(8)	9701(2)	1764(5)	1480(6)	126(3)
O(3)	9341(2)	1483(3)	974(4)	141(2)
C(9)	9391(3)	706(4)	592(4)	112(2)
C(10)	8969(3)	333(4)	325(5)	123(3)
O(4)	8036(2)	384(3)	146(3)	115(2)
O(5)	8738(2)	921(2)	-222(2)	80(1)
C(11)	8271(2)	868(3)	-244(3)	75(1)
N(2)	7676(1)	2775(2)	-1817(2)	66(1)
C(12)	8144(2)	2708(3)	-1723(3)	66(1)
C(13)	8355(2)	2109(3)	-1229(3)	64(1)
C(14)	8068(2)	1525(3)	-815(3)	62(1)
C(15)	7588(2)	1584(3)	-906(3)	72(1)
C(16)	7408(2)	2214(3)	-1409(3)	75(1)
N(3)	7237(1)	7290(2)	1303(2)	65(1)
C(17)	7524(2)	7881(3)	960(3)	72(1)
C(18)	7369(2)	8512(3)	441(3)	72(1)
C(19)	6897(2)	8546(3)	259(3)	65(1)
C(20)	6596(2)	7933(3)	610(3)	61(1)

Silver Coordination Compounds with a Family of Ditopic Ligands of Varying Flexibility:
About Chains, Rings, Helices and Polycatenanes

255

C(21)	6779(2)	7331(3)	1123(3)	62(1)
C(22)	6724(2)	9196(3)	-330(3)	78(1)
O(6)	6973(2)	9669(2)	-722(3)	105(1)
O(7)	6258(2)	9160(3)	-393(3)	97(1)
C(23)	6063(3)	9693(4)	-1039(5)	124(3)
C(24)	5586(3)	9421(4)	-1163(5)	113(2)
O(8)	5542(2)	8535(3)	-1395(3)	125(2)
C(25)	5246(4)	8100(8)	-1312(14)	391(19)
C(26)	5121(2)	7213(4)	-1409(5)	110(2)
O(9)	5505(1)	6752(2)	-1812(3)	89(1)
O(10)	5159(2)	5480(3)	-1522(4)	128(2)
C(27)	5481(2)	5879(3)	-1794(3)	74(1)
N(4)	6745(2)	4589(2)	-2531(2)	71(1)
C(28)	6623(2)	5370(3)	-2847(3)	70(1)
C(29)	6215(2)	5819(3)	-2642(3)	67(1)
C(30)	5920(2)	5444(3)	-2098(2)	62(1)
C(31)	6039(2)	4623(3)	-1792(3)	83(1)
C(32)	6451(2)	4234(3)	-2022(4)	85(2)
P(1)	8918(1)	2493(1)	4852(1)	73(1)
F(1)	8541(1)	1736(2)	4709(3)	105(1)
F(2)	8512(1)	3207(2)	4891(2)	104(1)
F(3)	9294(1)	3246(2)	4980(3)	122(1)
F(4)	9327(1)	1783(2)	4805(3)	117(1)
F(5)	8875(2)	2355(3)	5761(2)	129(1)
F(6)	8950(2)	2631(3)	3926(2)	121(1)

Table 3.   Bond lengths [Å] and angles [°] for **13**.

Ag(1)-N(1)	2.287(4)	C(2)-C(3)	1.376(8)
Ag(1)-N(4)#1	2.308(4)	C(3)-C(4)	1.373(7)
Ag(1)-N(3)	2.351(4)	C(3)-C(6)	1.493(8)
Ag(1)-N(2)#1	2.382(4)	C(4)-C(5)	1.356(8)
N(1)-C(1)	1.326(6)	C(6)-O(1)	1.200(8)
N(1)-C(5)	1.336(7)	C(6)-O(2)	1.313(7)
C(1)-C(2)	1.393(7)	O(2)-C(7)	1.473(7)

C(7)-C(8)	1.429(9)	C(22)-O(7)	1.327(7)
C(8)-O(3)	1.404(8)	O(7)-C(23)	1.471(7)
O(3)-C(9)	1.344(7)	C(23)-C(24)	1.428(10)
C(9)-C(10)	1.398(10)	C(24)-O(8)	1.395(7)
C(10)-O(5)	1.443(6)	O(8)-C(25)	1.074(10)
O(4)-C(11)	1.190(6)	C(25)-C(26)	1.388(11)
O(5)-C(11)	1.329(7)	C(26)-O(9)	1.464(6)
C(11)-C(14)	1.500(7)	O(9)-C(27)	1.314(6)
N(2)-C(16)	1.332(6)	O(10)-C(27)	1.188(6)
N(2)-C(12)	1.341(6)	C(27)-C(30)	1.498(7)
N(2)-Ag(1)#2	2.382(4)	N(4)-C(32)	1.318(7)
C(12)-C(13)	1.370(6)	N(4)-C(28)	1.335(6)
C(13)-C(14)	1.389(6)	N(4)-Ag(1)#2	2.308(4)
C(14)-C(15)	1.375(7)	C(28)-C(29)	1.386(7)
C(15)-C(16)	1.377(7)	C(29)-C(30)	1.371(6)
N(3)-C(21)	1.337(6)	C(30)-C(31)	1.381(6)
N(3)-C(17)	1.339(6)	C(31)-C(32)	1.364(8)
C(17)-C(18)	1.369(7)	P(1)-F(5)	1.570(4)
C(18)-C(19)	1.376(7)	P(1)-F(3)	1.570(3)
C(19)-C(20)	1.392(6)	P(1)-F(2)	1.575(3)
C(19)-C(22)	1.485(7)	P(1)-F(1)	1.580(3)
C(20)-C(21)	1.363(6)	P(1)-F(4)	1.580(3)
C(22)-O(6)	1.204(6)	P(1)-F(6)	1.596(4)
N(1)-Ag(1)-N(4)#1	117.06(15)	C(4)-C(3)-C(2)	118.7(5)
N(1)-Ag(1)-N(3)	118.22(14)	C(4)-C(3)-C(6)	116.7(6)
N(4)#1-Ag(1)-N(3)	106.21(14)	C(2)-C(3)-C(6)	124.5(5)
N(1)-Ag(1)-N(2)#1	103.54(14)	C(5)-C(4)-C(3)	118.7(5)
N(4)#1-Ag(1)-N(2)#1	116.45(14)	N(1)-C(5)-C(4)	124.1(5)
N(3)-Ag(1)-N(2)#1	93.33(13)	O(1)-C(6)-O(2)	123.9(6)
C(1)-N(1)-C(5)	117.2(5)	O(1)-C(6)-C(3)	123.6(6)
C(1)-N(1)-Ag(1)	124.2(3)	O(2)-C(6)-C(3)	112.2(5)
C(5)-N(1)-Ag(1)	118.4(3)	C(6)-O(2)-C(7)	114.3(5)
N(1)-C(1)-C(2)	122.5(5)	C(8)-C(7)-O(2)	106.8(6)
C(3)-C(2)-C(1)	118.7(5)	O(3)-C(8)-C(7)	113.6(7)

C(9)-O(3)-C(8)	118.8(5)	C(25)-O(8)-C(24)	127.8(7)
O(3)-C(9)-C(10)	114.5(6)	O(8)-C(25)-C(26)	140.2(9)
C(9)-C(10)-O(5)	110.8(6)	C(25)-C(26)-O(9)	108.6(6)
C(11)-O(5)-C(10)	115.9(5)	C(27)-O(9)-C(26)	115.0(4)
O(4)-C(11)-O(5)	125.3(5)	O(10)-C(27)-O(9)	123.6(5)
O(4)-C(11)-C(14)	123.4(6)	O(10)-C(27)-C(30)	123.7(5)
O(5)-C(11)-C(14)	111.2(4)	O(9)-C(27)-C(30)	112.6(4)
C(16)-N(2)-C(12)	117.1(4)	C(32)-N(4)-C(28)	117.2(4)
C(16)-N(2)-Ag(1)#2	127.9(3)	C(32)-N(4)-Ag(1)#2	117.2(3)
C(12)-N(2)-Ag(1)#2	114.8(3)	C(28)-N(4)-Ag(1)#2	125.6(3)
N(2)-C(12)-C(13)	123.8(4)	N(4)-C(28)-C(29)	122.8(4)
C(12)-C(13)-C(14)	118.1(4)	C(30)-C(29)-C(28)	118.9(4)
C(15)-C(14)-C(13)	118.8(4)	C(29)-C(30)-C(31)	118.1(5)
C(15)-C(14)-C(11)	119.7(4)	C(29)-C(30)-C(27)	124.2(4)
C(13)-C(14)-C(11)	121.4(4)	C(31)-C(30)-C(27)	117.6(4)
C(14)-C(15)-C(16)	118.9(5)	C(32)-C(31)-C(30)	119.0(5)
N(2)-C(16)-C(15)	123.2(5)	N(4)-C(32)-C(31)	124.0(5)
C(21)-N(3)-C(17)	117.4(4)	F(5)-P(1)-F(3)	90.5(3)
C(21)-N(3)-Ag(1)	114.4(3)	F(5)-P(1)-F(2)	89.5(2)
C(17)-N(3)-Ag(1)	128.1(3)	F(3)-P(1)-F(2)	90.0(2)
N(3)-C(17)-C(18)	123.1(5)	F(5)-P(1)-F(1)	90.3(2)
C(17)-C(18)-C(19)	119.0(4)	F(3)-P(1)-F(1)	179.1(3)
C(18)-C(19)-C(20)	118.4(4)	F(2)-P(1)-F(1)	90.1(2)
C(18)-C(19)-C(22)	120.0(4)	F(5)-P(1)-F(4)	91.1(3)
C(20)-C(19)-C(22)	121.5(5)	F(3)-P(1)-F(4)	89.6(2)
C(21)-C(20)-C(19)	118.8(4)	F(2)-P(1)-F(4)	179.4(3)
N(3)-C(21)-C(20)	123.3(4)	F(1)-P(1)-F(4)	90.25(19)
O(6)-C(22)-O(7)	124.4(5)	F(5)-P(1)-F(6)	178.9(3)
O(6)-C(22)-C(19)	124.7(6)	F(3)-P(1)-F(6)	90.3(3)
O(7)-C(22)-C(19)	110.9(4)	F(2)-P(1)-F(6)	89.8(2)
C(22)-O(7)-C(23)	114.4(5)	F(1)-P(1)-F(6)	88.9(2)
C(24)-C(23)-O(7)	108.2(6)	F(4)-P(1)-F(6)	89.7(3)
O(8)-C(24)-C(23)	113.6(6)		

Symmetry transformations used to generate equivalent atoms:

#1 x,-y+1,z+1/2   #2 x,-y+1,z-1/2

Table 4.   Anisotropic displacement parameters ($Å^2$x 10^3) for **13**. The anisotropic displacement factor exponent takes the form: $-2p^2[h^2a*^2U^{11} + ... + 2 h k a* b* U^{12}]$

	U^{11}	U^{22}	U^{33}	U^{23}	U^{13}	U^{12}
Ag(1)	76(1)	67(1)	102(1)	1(1)	-11(1)	-3(1)
N(1)	89(3)	55(2)	67(2)	-1(2)	7(2)	4(2)
C(1)	93(3)	53(2)	73(3)	6(2)	16(2)	0(2)
C(2)	98(4)	50(2)	77(3)	-4(2)	-3(3)	5(2)
C(3)	79(3)	58(2)	93(4)	-15(2)	1(3)	-11(2)
C(4)	103(4)	66(3)	120(5)	10(3)	27(4)	-11(3)
C(5)	107(4)	58(3)	97(4)	18(3)	23(3)	2(3)
C(6)	79(4)	71(3)	170(7)	-14(4)	13(4)	-9(3)
O(1)	104(4)	120(4)	365(12)	20(6)	83(6)	-12(3)
O(2)	81(2)	84(2)	110(3)	-12(2)	-4(2)	15(2)
C(7)	78(3)	114(5)	140(6)	-21(4)	-8(4)	22(3)
C(8)	86(4)	98(5)	196(8)	-26(5)	-45(5)	29(3)
O(3)	112(3)	110(3)	202(6)	-71(4)	-76(4)	58(3)
C(9)	131(5)	88(4)	116(5)	-2(4)	-31(4)	49(4)
C(10)	182(8)	57(3)	128(6)	13(3)	-71(5)	16(4)
O(4)	150(4)	70(2)	124(4)	33(2)	-10(3)	-25(3)
O(5)	107(3)	59(2)	75(2)	6(2)	-19(2)	12(2)
C(11)	111(4)	43(2)	71(3)	-1(2)	-6(3)	-4(2)
N(2)	72(2)	54(2)	73(2)	-1(2)	-6(2)	0(2)
C(12)	74(3)	60(2)	63(3)	6(2)	5(2)	-1(2)
C(13)	68(2)	59(2)	65(3)	-1(2)	0(2)	6(2)
C(14)	83(3)	43(2)	60(2)	-6(2)	1(2)	-2(2)
C(15)	84(3)	54(2)	78(3)	1(2)	3(2)	-13(2)
C(16)	69(3)	63(3)	92(4)	-4(2)	-4(2)	-7(2)
N(3)	71(2)	54(2)	68(2)	0(2)	-3(2)	-6(2)
C(17)	68(3)	60(2)	90(3)	-4(2)	1(2)	-13(2)
C(18)	77(3)	56(2)	82(3)	2(2)	10(2)	-14(2)
C(19)	81(3)	44(2)	70(3)	-3(2)	7(2)	-5(2)
C(20)	64(2)	59(2)	60(2)	-2(2)	3(2)	-5(2)
C(21)	67(2)	56(2)	64(3)	2(2)	4(2)	-8(2)

C(22)	108(4)	48(2)	79(3)	0(2)	-6(3)	-7(2)
O(6)	140(4)	68(2)	108(3)	27(2)	-5(3)	-25(2)
O(7)	103(3)	71(2)	117(3)	28(2)	-13(2)	8(2)
C(23)	145(6)	64(3)	161(7)	38(4)	-42(5)	5(4)
C(24)	137(6)	64(3)	138(6)	1(3)	-27(5)	29(3)
O(8)	150(5)	68(2)	157(5)	-11(3)	49(4)	6(3)
C(25)	140(9)	165(10)	870(50)	-290(20)	207(18)	-66(8)
C(26)	65(3)	104(4)	160(7)	-46(4)	20(4)	4(3)
O(9)	64(2)	76(2)	127(3)	-23(2)	12(2)	3(2)
O(10)	93(3)	99(3)	192(5)	7(3)	53(3)	-12(2)
C(27)	68(3)	76(3)	77(3)	-2(2)	0(2)	-8(2)
N(4)	83(3)	55(2)	73(2)	0(2)	2(2)	9(2)
C(28)	80(3)	59(2)	71(3)	5(2)	13(2)	1(2)
C(29)	80(3)	56(2)	65(3)	4(2)	3(2)	5(2)
C(30)	71(2)	59(2)	56(2)	-3(2)	-1(2)	-5(2)
C(31)	97(4)	63(3)	90(4)	14(2)	21(3)	-5(2)
C(32)	104(4)	60(3)	91(4)	15(2)	11(3)	12(3)
P(1)	72(1)	55(1)	91(1)	-12(1)	0(1)	0(1)
F(1)	92(2)	75(2)	148(3)	-15(2)	0(2)	-19(2)
F(2)	94(2)	83(2)	136(3)	-17(2)	-5(2)	24(2)
F(3)	98(2)	84(2)	184(4)	-38(2)	-10(3)	-19(2)
F(4)	89(2)	80(2)	183(4)	-23(2)	-2(2)	23(2)
F(5)	155(4)	138(3)	95(3)	7(2)	-9(2)	18(3)
F(6)	151(3)	120(3)	91(3)	1(2)	15(2)	-13(3)

Table 5. Hydrogen coordinates (x 10^4) and isotropic displacement parameters (Å^2x 10^3) for **13**.

	x	y	z	U(eq)
H(1)	7973	4358	2708	88
H(2)	8669	3593	2496	90
H(4)	9054	5519	1013	116
H(5)	8357	6202	1250	105
H(7A)	9878	2843	875	133
H(7B)	10079	2838	1736	133

H(8A)	9983	1423	1369	152
H(8B)	9608	1636	2016	152
H(9A)	9544	284	939	134
H(9B)	9597	799	146	134
H(10A)	8763	222	768	147
H(10B)	9034	-232	72	147
H(12)	8336	3090	-2008	79
H(13)	8681	2093	-1174	77
H(15)	7388	1204	-633	87
H(16)	7083	2250	-1467	90
H(17)	7843	7863	1079	87
H(18)	7579	8911	214	86
H(20)	6275	7935	496	74
H(21)	6576	6927	1360	75
H(23A)	6073	10321	-906	148
H(23B)	6246	9601	-1512	148
H(24A)	5411	9508	-681	135
H(24B)	5447	9799	-1561	135
H(25A)	5001	8404	-1603	470
H(25B)	5169	8202	-765	470
H(26A)	4834	7171	-1715	132
H(26B)	5065	6940	-902	132
H(28)	6821	5622	-3221	84
H(29)	6143	6365	-2869	81
H(31)	5842	4340	-1434	100
H(32)	6528	3684	-1808	102

Table 6. Hydrogen bond [length (Å) and angle (°)] present in complex **13**

D–H···Acceptor	d (D–H)	d (H···A)	d (D···A)	< D–H···A
C5–H5···F2	0.93	2.52(0)	3.24(1)	134.0(0)
C9–H9A···O10	0.97	2.31(0)	3.23(2)	158.0(0)
C10–H10B···F4	0.97	2.52(0)	3.45(2)	162.0(0)
C15–H15···O6	0.93	2.59(0)	3.38(0)	142.0(0)
C18–H18···O4	0.93	2.57(0)	3.42(7)	154.0(0)
C24–H24B···O1	0.97	2.54(0)	3.08(6)	115.0(0)

Crystal data and structure refinement for {[Ag(L3)]SO₃CF₃}₂ (14)

Identification code	**14**
Empirical formula	C17 H16 Ag F3 N2 O8 S
Formula weight	764.33
Temperature	293(2) K
Wavelength	0.71073 Å
Crystal system	Monoclinic
Space group	P2₁/c
Unit cell dimensions	a = 7.0987(14) Å α = 90°.
	b = 26.081(5) Å β = 91.10(3)°.
	c = 11.121(2) Å γ = 90°.
Volume	2058.6(7) Å³
Z	3
Density (calculated)	1.850 Mg/m³
Absorption coefficient	1.156 mm⁻¹
F(000)	1144
Theta range for data collection	1.56 to 27.13°.
Index ranges	-9<=h<=8, -33<=k<=33, -14<=l<=14
Reflections collected	16323
Independent reflections	4528 [R(int) = 0.1144]
Completeness to theta = 27.13°	99.6 %
Refinement method	Full-matrix least-squares on F²
Data / restraints / parameters	4528 / 0 / 290
Goodness-of-fit on F²	1.069
Final R indices [I>2sigma(I)]	R1 = 0.0480, wR2 = 0.1201
R indices (all data)	R1 = 0.0631, wR2 = 0.1307
Extinction coefficient	0.0063(6)
Largest diff. peak and hole	1.014 and -0.870 e.Å⁻³

Crystal data and structure refinement for {[Ag(L3)]SO_3CF_3}$_2$ (14)

Identification code	**14**
Empirical formula	C17 H16 Ag F3 N2 O8 S
Formula weight	764.33
Temperature	293(2) K
Wavelength	0.71073 Å
Crystal system	Monoclinic
Space group	$P2_1/c$
Unit cell dimensions	a = 7.0987(14) Å $\alpha = 90°$.
	b = 26.081(5) Å $\beta = 91.10(3)°$.
	c = 11.121(2) Å $\gamma = 90°$.
Volume	2058.6(7) $Å^3$
Z	3
Density (calculated)	1.850 Mg/m^3
Absorption coefficient	1.156 mm^{-1}
F(000)	1144
Theta range for data collection	1.56 to 27.13°.
Index ranges	-9<=h<=8, -33<=k<=33, -14<=l<=14
Reflections collected	16323
Independent reflections	4528 [R(int) = 0.1144]
Completeness to theta = 27.13°	99.6 %
Refinement method	Full-matrix least-squares on F^2
Data / restraints / parameters	4528 / 0 / 290
Goodness-of-fit on F^2	1.069
Final R indices [I>2sigma(I)]	R1 = 0.0480, wR2 = 0.1201
R indices (all data)	R1 = 0.0631, wR2 = 0.1307
Extinction coefficient	0.0063(6)
Largest diff. peak and hole	1.014 and -0.870 e.$Å^{-3}$

Table 2. Atomic coordinates (x 10^4) and equivalent isotropic displacement parameters ($Å^2$x 10^3) for **14**. U(eq) is defined as one third of the trace of the orthogonalized U^{ij} tensor.

	x	y	z	U(eq)
Ag(1)	2608(1)	4945(1)	5459(1)	50(1)
N(1)	3191(5)	5690(1)	6231(3)	38(1)
C(1)	3441(5)	6115(1)	5583(3)	37(1)
C(2)	3719(5)	6597(1)	6096(3)	36(1)
C(3)	3769(5)	6635(1)	7340(3)	34(1)
C(4)	3532(6)	6194(2)	8018(3)	41(1)
C(5)	3259(7)	5730(2)	7435(3)	46(1)
C(6)	3994(5)	7135(1)	7987(3)	35(1)
O(1)	3817(5)	7183(1)	9048(2)	54(1)
O(2)	4397(4)	7511(1)	7236(2)	38(1)
C(7)	4462(6)	8020(1)	7750(3)	39(1)
C(8)	5240(5)	8373(2)	6828(3)	39(1)
O(3)	7152(4)	8244(1)	6667(2)	39(1)
C(9)	7976(6)	8478(2)	5655(3)	42(1)
C(10)	9818(6)	8219(2)	5467(4)	49(1)
O(4)	9482(4)	7684(1)	5201(2)	44(1)
O(5)	10126(4)	7448(1)	7125(3)	53(1)
C(11)	9599(5)	7355(2)	6105(3)	39(1)
N(2)	8066(5)	5835(1)	5068(3)	40(1)
C(12)	8369(6)	6191(1)	4232(3)	38(1)
C(13)	8833(5)	6690(2)	4509(3)	37(1)
C(14)	9036(5)	6828(1)	5719(3)	34(1)
C(15)	8725(6)	6457(2)	6581(3)	42(1)
C(16)	8262(6)	5968(2)	6237(3)	43(1)
S(1)	1805(2)	5432(1)	2485(1)	42(1)
O(6)	3319(6)	5255(2)	3255(3)	76(1)
O(7)	1671(5)	5979(1)	2419(3)	57(1)
O(8)	77(5)	5167(2)	2629(4)	71(1)
C(17)	2582(8)	5241(2)	1014(4)	57(1)
F(1)	4267(5)	5421(2)	793(3)	94(1)

Silver Coordination Compounds with a Family of Ditopic Ligands of Varying Flexibility: About Chains, Rings, Helices and Polycatenanes

263

F(2)	2642(6)	4734(1)	917(3)	86(1)
F(3)	1443(7)	5419(2)	154(3)	105(1)

Table 3.   Bond lengths [Å] and angles [°] for **14**.

Ag(1)-N(1)	2.161(3)	O(4)-C(11)	1.324(5)
Ag(1)-N(2)#1	2.166(3)	O(5)-C(11)	1.212(5)
N(1)-C(1)	1.336(5)	C(11)-C(14)	1.491(5)
N(1)-C(5)	1.343(5)	N(2)-C(12)	1.335(5)
C(1)-C(2)	1.391(5)	N(2)-C(16)	1.351(5)
C(2)-C(3)	1.388(5)	N(2)-Ag(1)#1	2.166(3)
C(3)-C(4)	1.387(5)	C(12)-C(13)	1.376(5)
C(3)-C(6)	1.495(5)	C(13)-C(14)	1.398(5)
C(4)-C(5)	1.386(6)	C(14)-C(15)	1.384(5)
C(6)-O(1)	1.195(4)	C(15)-C(16)	1.369(6)
C(6)-O(2)	1.325(4)	S(1)-O(8)	1.419(4)
O(2)-C(7)	1.445(4)	S(1)-O(7)	1.433(3)
C(7)-C(8)	1.492(5)	S(1)-O(6)	1.437(4)
C(8)-O(3)	1.413(4)	S(1)-C(17)	1.807(4)
O(3)-C(9)	1.416(4)	C(17)-F(1)	1.313(6)
C(9)-C(10)	1.490(6)	C(17)-F(3)	1.325(7)
C(10)-O(4)	1.444(5)	C(17)-F(2)	1.327(6)
N(1)-Ag(1)-N(2)#1	172.16(12)	O(1)-C(6)-C(3)	123.6(3)
C(1)-N(1)-C(5)	118.1(3)	O(2)-C(6)-C(3)	111.4(3)
C(1)-N(1)-Ag(1)	124.0(2)	C(6)-O(2)-C(7)	115.9(3)
C(5)-N(1)-Ag(1)	117.9(3)	O(2)-C(7)-C(8)	107.7(3)
N(1)-C(1)-C(2)	123.2(3)	O(3)-C(8)-C(7)	108.0(3)
C(3)-C(2)-C(1)	118.4(3)	C(8)-O(3)-C(9)	114.2(3)
C(4)-C(3)-C(2)	118.7(3)	O(3)-C(9)-C(10)	107.0(3)
C(4)-C(3)-C(6)	118.3(3)	O(4)-C(10)-C(9)	108.9(3)
C(2)-C(3)-C(6)	123.0(3)	C(11)-O(4)-C(10)	117.6(3)
C(5)-C(4)-C(3)	119.2(3)	O(5)-C(11)-O(4)	126.4(4)
N(1)-C(5)-C(4)	122.4(4)	O(5)-C(11)-C(14)	122.1(4)
O(1)-C(6)-O(2)	125.0(4)	O(4)-C(11)-C(14)	111.5(3)

C(12)-N(2)-C(16)	118.4(3)	O(8)-S(1)-O(6)	114.5(3)
C(12)-N(2)-Ag(1)#1	120.2(2)	O(7)-S(1)-O(6)	113.4(2)
C(16)-N(2)-Ag(1)#1	121.4(3)	O(8)-S(1)-C(17)	104.3(2)
N(2)-C(12)-C(13)	122.9(3)	O(7)-S(1)-C(17)	104.4(2)
C(12)-C(13)-C(14)	118.7(3)	O(6)-S(1)-C(17)	102.3(3)
C(15)-C(14)-C(13)	118.1(3)	F(1)-C(17)-F(3)	106.5(4)
C(15)-C(14)-C(11)	119.4(3)	F(1)-C(17)-F(2)	108.1(4)
C(13)-C(14)-C(11)	122.5(3)	F(3)-C(17)-F(2)	108.2(4)
C(16)-C(15)-C(14)	119.9(3)	F(1)-C(17)-S(1)	111.5(3)
N(2)-C(16)-C(15)	122.0(4)	F(3)-C(17)-S(1)	111.3(4)
O(8)-S(1)-O(7)	115.8(2)	F(2)-C(17)-S(1)	111.1(3)

Symmetry transformations used to generate equivalent atoms:

#1 -x+1,-y+1,-z+1

Table 4. Anisotropic displacement parameters (Å^2 x 10^3) for **14**. The anisotropic displacement factor exponent takes the form: $-2p^2[h^2a^{*2}U^{11} + ... + 2 h k a^* b^* U^{12}]$

	U^{11}	U^{22}	U^{33}	U^{23}	U^{13}	U^{12}
Ag(1)	70(1)	28(1)	51(1)	-5(1)	0(1)	-4(1)
N(1)	47(2)	27(1)	41(2)	-5(1)	0(1)	-4(1)
C(1)	47(2)	31(2)	34(2)	0(1)	3(1)	-3(2)
C(2)	42(2)	30(2)	35(2)	5(1)	-1(1)	2(2)
C(3)	39(2)	31(2)	32(2)	0(1)	0(1)	-1(1)
C(4)	57(2)	35(2)	33(2)	5(1)	-1(2)	-6(2)
C(5)	65(3)	34(2)	39(2)	3(2)	1(2)	-5(2)
C(6)	40(2)	34(2)	32(2)	0(1)	-2(1)	-3(2)
O(1)	88(2)	44(2)	30(1)	-1(1)	-1(1)	-7(2)
O(2)	53(2)	29(1)	33(1)	-3(1)	4(1)	-7(1)
C(7)	46(2)	32(2)	40(2)	-10(2)	3(2)	-3(2)
C(8)	39(2)	30(2)	48(2)	-3(2)	-3(2)	0(2)
O(3)	39(1)	40(1)	40(1)	4(1)	2(1)	2(1)
C(9)	52(2)	30(2)	45(2)	3(2)	3(2)	-5(2)
C(10)	55(2)	34(2)	60(2)	-9(2)	14(2)	-14(2)

O(4)	57(2)	30(1)	46(1)	-5(1)	7(1)	-4(1)
O(5)	60(2)	44(2)	53(2)	-13(1)	-18(1)	6(1)
C(11)	36(2)	35(2)	46(2)	-9(2)	-1(2)	4(2)
N(2)	52(2)	28(2)	40(2)	-5(1)	-1(1)	1(1)
C(12)	47(2)	32(2)	35(2)	-4(1)	-1(1)	2(2)
C(13)	41(2)	33(2)	35(2)	-1(1)	-2(1)	3(2)
C(14)	31(2)	32(2)	40(2)	-6(1)	-4(1)	5(1)
C(15)	49(2)	43(2)	34(2)	-5(2)	-1(2)	7(2)
C(16)	56(2)	36(2)	37(2)	3(2)	-2(2)	1(2)
S(1)	57(1)	30(1)	39(1)	1(1)	9(1)	-1(1)
O(6)	105(3)	68(2)	54(2)	7(2)	-21(2)	18(2)
O(7)	64(2)	26(1)	81(2)	2(1)	14(2)	1(1)
O(8)	78(2)	54(2)	84(2)	-8(2)	38(2)	-19(2)
C(17)	74(3)	49(3)	49(2)	-8(2)	11(2)	-10(2)
F(1)	95(2)	91(3)	98(2)	-31(2)	54(2)	-29(2)
F(2)	118(3)	58(2)	84(2)	-30(2)	29(2)	-9(2)
F(3)	154(4)	118(4)	44(2)	14(2)	-15(2)	-23(3)

Table 5. Hydrogen coordinates (x 10^4) and isotropic displacement parameters (Å^2x 10^3) for **14**.

_____

	x	y	z	U(eq)
H(1)	3429	6088	4749	44
H(2)	3868	6885	5616	43
H(4)	3557	6210	8853	50
H(5)	3118	5435	7894	55
H(7A)	5259	8022	8468	47
H(7B)	3207	8129	7968	47
H(8A)	4541	8336	6074	47
H(8B)	5135	8726	7094	47
H(9A)	8164	8841	5798	51
H(9B)	7163	8437	4950	51
H(10A)	10466	8379	4806	59
H(10B)	10606	8250	6186	59

H(12)	8261	6098	3426	46
H(13)	9009	6930	3904	44
H(15)	8830	6539	7393	50
H(16)	8077	5721	6825	52

Table 6. Hydrogen bond [length (Å) and angle (°)] present in complex **14**

D–H···Acceptor	d (D–H)	d (H···A)	d (D···A)	< D–H···A
C10–H10B···O7	0.97	2.54(0)	3.27(1)	132.2(3)

Crystal data and structure refinement for {[Ag(L4)]PF$_6$}$_2$ (15)

Identification code	**15**
Empirical formula	C19 H22 Ag F6 N2 O6 P
Formula weight	627.23
Temperature	293(2) K
Wavelength	0.71073 Å
Crystal system	Triclinic
Space group	P-1
Unit cell dimensions	a = 8.7377(17) Å $\quad$ a= 73.97(3)°.
	b = 11.459(2) Å $\quad$ b= 82.82(3)°.
	c = 12.530(3) Å $\quad$ g = 87.37(3)°.
Volume	1196.2(4) Å^3
Z	2
Density (calculated)	1.741 Mg/m^3
Absorption coefficient	0.994 mm^{-1}
F(000)	628
Theta range for data collection	1.70 to 27.07°.
Index ranges	-11<=h<=10, -14<=k<=14, -16<=l<=15
Reflections collected	9465
Independent reflections	4845 [R(int) = 0.1081]
Completeness to theta = 27.07°	92.3 %
Refinement method	Full-matrix least-squares on F^2
Data / restraints / parameters	4845 / 0 / 306

Goodness-of-fit on F^2 1.028

Final R indices [I>2sigma(I)]   R1 = 0.1204, wR2 = 0.3075

R indices (all data)   R1 = 0.2090, wR2 = 0.3695

Largest diff. peak and hole   2.516 and -1.059 e.Å^{-3}

Table 2. Atomic coordinates (x 10^4) and equivalent isotropic displacement parameters (Å^{2}x 10^3) for **15**. U(eq) is defined as one third of the trace of the orthogonalized U^{ij} tensor.

	x	y	z	U(eq)
Ag(1)	6903(2)	5344(1)	5268(1)	61(1)
N(1)	5322(10)	6788(7)	5401(8)	58(4)
C(1)	4479(11)	6657(7)	6443(7)	50(4)
C(2)	3429(12)	7554(9)	6615(7)	66(5)
C(3)	3223(10)	8583(8)	5744(8)	61(4)
C(4)	4066(10)	8714(6)	4702(7)	43(3)
C(5)	5116(10)	7817(8)	4530(6)	51(4)
C(6)	3850(20)	9803(12)	3734(18)	64(5)
O(1)	2926(14)	10598(10)	3836(11)	70(3)
O(2)	4748(16)	9793(10)	2816(10)	68(3)
C(7)	4580(20)	10772(15)	1815(15)	73(5)
C(8)	5980(30)	10720(17)	1027(16)	83(6)
O(3)	7260(14)	11044(12)	1482(10)	73(4)
C(9)	8700(30)	10850(20)	879(19)	128(13)
C(10)	9890(30)	10950(19)	1520(30)	142(15)
O(4)	9898(13)	10017(11)	2597(13)	88(5)
O(5)	11682(15)	8980(13)	1747(14)	101(6)
C(11)	10820(20)	9048(14)	2540(20)	80(7)
N(2)	11571(15)	6214(10)	4690(11)	52(3)
C(12)	10481(19)	6274(14)	5523(15)	61(5)
C(13)	9500(20)	7228(14)	5510(16)	66(5)
C(14)	9570(20)	8151(17)	4504(19)	78(6)
C(15)	10659(16)	8109(12)	3632(14)	54(4)
C(16)	11595(19)	7086(11)	3753(15)	55(4)
P(1)	7414(8)	6708(4)	1836(4)	75(2)

F(1)	7563(19)	7925(12)	2214(15)	125(5)
F(2)	7230(30)	5512(13)	1505(12)	174(10)
F(3)	8310(30)	6109(18)	2864(16)	186(10)
F(4)	5920(30)	6390(20)	2650(20)	195(11)
F(5)	8920(30)	7020(20)	1024(16)	188(10)
F(6)	6710(40)	7400(20)	770(20)	227(14)
O(6)	7460(18)	5142(16)	7443(10)	96(5)
C(17)	7610(30)	4970(20)	8401(16)	97(8)
C(18)	7160(50)	3960(30)	9260(20)	184(19)
C(19)	8580(90)	5910(40)	8670(30)	310(40)

Table 3.   Bond lengths [Å] and angles [°] for **15**.

Ag(1)-N(1)	2.135(7)	N(2)-Ag(1)#1	2.171(12)
Ag(1)-N(2)#1	2.171(12)	C(12)-C(13)	1.35(2)
N(1)-C(1)	1.3900	C(13)-C(14)	1.40(2)
N(1)-C(5)	1.3900	C(14)-C(15)	1.37(3)
C(1)-C(2)	1.3900	C(15)-C(16)	1.38(2)
C(2)-C(3)	1.3900	P(1)-F(6)	1.535(17)
C(3)-C(4)	1.3900	P(1)-F(4)	1.55(2)
C(4)-C(5)	1.3900	P(1)-F(5)	1.55(2)
C(4)-C(6)	1.505(16)	P(1)-F(2)	1.558(14)
C(6)-O(1)	1.21(2)	P(1)-F(3)	1.566(16)
C(6)-O(2)	1.31(2)	P(1)-F(1)	1.608(14)
O(2)-C(7)	1.451(17)	O(6)-C(17)	1.18(2)
C(7)-C(8)	1.48(3)	C(17)-C(18)	1.38(4)
C(8)-O(3)	1.42(3)	C(17)-C(19)	1.53(6)
O(3)-C(9)	1.42(2)		
C(9)-C(10)	1.42(5)	N(1)-Ag(1)-N(2)#1	174.1(4)
C(10)-O(4)	1.47(2)	C(1)-N(1)-C(5)	120.0
O(4)-C(11)	1.35(2)	C(1)-N(1)-Ag(1)	115.7(5)
O(5)-C(11)	1.19(3)	C(5)-N(1)-Ag(1)	124.3(5)
C(11)-C(15)	1.49(2)	C(2)-C(1)-N(1)	120.0
N(2)-C(16)	1.313(18)	C(1)-C(2)-C(3)	120.0
N(2)-C(12)	1.34(2)	C(4)-C(3)-C(2)	120.0

C(3)-C(4)-C(5)	120.0	C(14)-C(15)-C(16)	117.5(14)
C(3)-C(4)-C(6)	121.5(10)	C(14)-C(15)-C(11)	124.1(14)
C(5)-C(4)-C(6)	118.5(10)	C(16)-C(15)-C(11)	118.3(17)
C(4)-C(5)-N(1)	120.0	N(2)-C(16)-C(15)	123.2(17)
O(1)-C(6)-O(2)	125.4(16)	F(6)-P(1)-F(4)	99.6(18)
O(1)-C(6)-C(4)	121.0(19)	F(6)-P(1)-F(5)	81.0(16)
O(2)-C(6)-C(4)	113.6(13)	F(4)-P(1)-F(5)	179.3(17)
C(6)-O(2)-C(7)	118.3(13)	F(6)-P(1)-F(2)	88.4(12)
O(2)-C(7)-C(8)	106.3(13)	F(4)-P(1)-F(2)	88.2(11)
O(3)-C(8)-C(7)	107.5(17)	F(5)-P(1)-F(2)	91.6(11)
C(9)-O(3)-C(8)	112(2)	F(6)-P(1)-F(3)	172.8(17)
C(10)-C(9)-O(3)	108(2)	F(4)-P(1)-F(3)	86.6(15)
C(9)-C(10)-O(4)	116(2)	F(5)-P(1)-F(3)	92.8(15)
C(11)-O(4)-C(10)	113.5(17)	F(2)-P(1)-F(3)	95.6(12)
O(5)-C(11)-O(4)	125.1(15)	F(6)-P(1)-F(1)	92.5(11)
O(5)-C(11)-C(15)	124.7(14)	F(4)-P(1)-F(1)	90.0(10)
O(4)-C(11)-C(15)	110.1(18)	F(5)-P(1)-F(1)	90.3(11)
C(16)-N(2)-C(12)	117.6(13)	F(2)-P(1)-F(1)	178.1(10)
C(16)-N(2)-Ag(1)#1	118.5(12)	F(3)-P(1)-F(1)	83.7(10)
C(12)-N(2)-Ag(1)#1	123.5(9)	O(6)-C(17)-C(18)	127(3)
N(2)-C(12)-C(13)	124.6(14)	O(6)-C(17)-C(19)	116(3)
C(12)-C(13)-C(14)	116.1(18)	C(18)-C(17)-C(19)	117(3)
C(15)-C(14)-C(13)	120.5(16)		

Symmetry transformations used to generate equivalent atoms:

#1 -x+2,-y+1,-z+1

Table 4. Anisotropic displacement parameters ($\mathring{A}^2$x 10^3)for **15**. The anisotropic displacement factor exponent takes the form: $-2p^2[\ h^2a^{*2}U^{11} + ... + 2\ h\ k\ a^*\ b^*\ U^{12}\ ]$

	U^{11}	U^{22}	U^{33}	U^{23}	U^{13}	U^{12}
Ag(1)	80(1)	36(1)	65(1)	-5(1)	-25(1)	17(1)
N(1)	65(9)	41(6)	67(9)	-7(6)	-25(7)	9(6)
C(1)	37(8)	42(7)	65(10)	-5(7)	-3(7)	-8(6)

Silver Coordination Compounds with a Family of Ditopic Ligands of Varying Flexibility: About Chains, Rings, Helices and Polycatenanes

270

C(2)	78(12)	66(10)	43(8)	0(8)	0(8)	8(9)
C(3)	48(9)	50(8)	79(12)	-8(8)	-8(8)	0(7)
C(4)	44(8)	39(6)	42(7)	2(6)	-17(6)	-16(6)
C(5)	63(10)	35(6)	56(9)	-15(6)	-17(7)	13(6)
C(6)	74(11)	27(6)	104(15)	-18(8)	-55(11)	5(7)
O(1)	74(8)	52(6)	76(8)	-7(6)	-16(6)	25(6)
O(2)	111(10)	45(6)	46(6)	-11(5)	-7(6)	23(6)
C(7)	93(14)	48(8)	69(11)	5(8)	-21(10)	13(9)
C(8)	119(18)	59(10)	58(11)	0(9)	-13(11)	40(11)
O(3)	64(8)	83(8)	51(6)	5(6)	6(6)	31(6)
C(9)	130(20)	100(16)	81(14)	52(13)	50(15)	82(16)
C(10)	92(17)	67(12)	180(30)	69(16)	70(18)	48(12)
O(4)	46(7)	66(7)	118(11)	27(7)	1(7)	21(5)
O(5)	52(8)	88(10)	111(11)	42(9)	21(8)	17(7)
C(11)	40(9)	47(8)	118(17)	34(10)	0(10)	13(7)
N(2)	55(8)	34(5)	63(8)	0(5)	-23(7)	9(5)
C(12)	53(9)	52(8)	61(10)	18(8)	-22(8)	-7(7)
C(13)	61(10)	48(8)	75(11)	10(8)	-16(9)	3(7)
C(14)	60(12)	60(10)	101(15)	2(10)	-18(11)	7(8)
C(15)	28(7)	38(7)	77(11)	18(7)	-15(7)	-4(5)
C(16)	60(9)	28(6)	76(10)	-4(7)	-28(8)	0(6)
P(1)	133(5)	43(2)	44(2)	-7(2)	-14(3)	14(2)
F(1)	152(13)	80(8)	170(15)	-71(10)	-36(11)	10(8)
F(2)	360(30)	69(8)	87(9)	-48(8)	79(14)	-55(13)
F(3)	300(30)	132(14)	124(14)	-22(11)	-103(16)	100(16)
F(4)	190(20)	210(20)	230(20)	-150(20)	78(18)	-81(18)
F(5)	270(30)	164(18)	119(13)	-50(13)	82(16)	-73(18)
F(6)	380(40)	166(19)	170(20)	-36(16)	-180(20)	40(20)
O(6)	108(11)	133(13)	42(7)	-14(8)	-14(7)	15(10)
C(17)	150(20)	89(15)	47(11)	-21(11)	-14(12)	47(15)
C(18)	280(50)	160(30)	57(15)	32(18)	0(20)	70(30)
C(19)	700(140)	140(40)	100(30)	-50(30)	-70(50)	-20(60)

Silver Coordination Compounds with a Family of Ditopic Ligands of Varying Flexibility: About Chains, Rings, Helices and Polycatenanes

271

Table 5.   Hydrogen coordinates (x 10^4) and isotropic displacement parameters ($Å^2$x 10^3) for **15**.

	x	y	z	U(eq)
H(1)	4617	5968	7026	60
H(2)	2865	7467	7312	80
H(3)	2520	9184	5859	73
H(5)	5680	7904	3833	61
H(7A)	4510	11549	1987	88
H(7B)	3665	10665	1493	88
H(8A)	6129	9907	936	99
H(8B)	5875	11280	301	99
H(9A)	8725	10053	753	153
H(9B)	8829	11454	159	153
H(10A)	9805	11742	1662	170
H(10B)	10873	10914	1074	170
H(12)	10387	5614	6155	73
H(13)	8822	7268	6133	79
H(14)	8872	8797	4430	93
H(16)	12275	7012	3142	66
H(18A)	6381	3538	9040	276
H(18B)	6758	4199	9915	276
H(18C)	8037	3427	9419	276
H(19A)	9261	5507	9205	460
H(19B)	7905	6455	8985	460
H(19C)	9167	6371	8002	460

Table 6. Hydrogen bond [length (Å) and angle (°)] present in complex **15**

D–H···Acceptor	d (D–H)	d (H···A)	d (D···A)	< D–H···A
C14–H14[#3]···O1	0.93	2.74(8)	3.37(2)	125.2(3)
C13–H13[#3]···O1	0.93	2.83(0)	3.40(4)	120.9(3)
C2–H2[#3]···O3	0.93	2.56(6)	3.20(8)	126.8(2)
C9–H9A[#4]···O5	0.97	2.66(2)	3.29(8)	123.5(2)
C7–H7B[#5]···O5	0.97	2.58(0)	3.35(9)	137.3(3)

C5–H5···F1	0.93	2.44(2)	3.35(9)	168.6(2)
C8–H8A···F1	0.97	2.74(2)	3.44(2)	129.5(3)
C9–H9B···F1	0.97	2.76(1)	3.43(7)	127.3(3)
C12–H12···F3	0.93	2.34(8)	3.14(4)	143.3(3)
C5–H5···F4	0.93	2.56(1)	3.21(2)	127.3(2)
C8–H8A···F6	0.97	2.95(1)	3.92(0)	176.3(4)
C1–H1[#6]···F2	0.93	2.58(0)	3.29(6)	134.2(2)
C1–H1[#6]···F4	0.93	2.67(0)	3.37(6)	133.1(3)
C9–H9A···F5	0.97	2.69(7)	3.46(1)	136.0(2)
C8–H8B[#7]···F6	0.97	2.92(0)	3.66(5)	134.4(2)
C16–H16[#1]···O6	0.93	2.75(4)	3.32(5)	120.6(3)
C1–H1···O6	0.93	2.67(8)	3.25(0)	120.4(3)
C12–H12···O6	0.93	2.83(7)	3.38(2)	118.5(2)
C13–H13···O6	0.93	2.75(9)	3.29(8)	117.8(2)
C18–H18A[#6]···F6	0.97	2.91(6)	3.80(0)	153.5(3)
C18–H18B···F2	0.96	2.88(3)	3.73(0)	147.3(2)
C19–H19B···F6	0.97	2.81(2)	3.68(8)	152.2(3)
C18–H18C[#1]···F5	0.96	2.69(6)	3.55(3)	148.8(3)

Symmetry transformation used to generate equivalent atoms: #3 1-x, 2-y, 1-z #4 2-x, 2-y, -z #5 -1+x, y, z
#6 1-x, 1-y, 1-z #7 1-x, 2-y, -z

Crystal data and structure refinement for {[Ag(L5)]SO$_3$CF$_3$}$_n$ (16)

Identification code	**16**
Empirical formula	C76 H80 Ag4 F12 N8 O36 S4
Formula weight	2469.24
Temperature	293(2) K
Wavelength	0.71073 Å
Crystal system	Monoclinic
Space group	P2$_1$/c
Unit cell dimensions	a = 8.9301(18) Å $\quad$ α = 90°.
	b = 14.200(3) Å $\quad$ β = 116.14(2)°.
	c = 20.264(6) Å $\quad$ γ = 90°.
Volume	2306.8(10) Å^3
Z	1

Density (calculated)	1.777 Mg/m^3
Absorption coefficient	1.042 mm^{-1}
F(000)	1240
Theta range for data collection	1.82 to 27.13°.
Index ranges	-10<=h<=11, -18<=k<=18, -25<=l<=23
Reflections collected	18213
Independent reflections	4843 [R(int) = 0.1170]
Completeness to theta = 27.13°	94.7 %
Refinement method	Full-matrix least-squares on F^2
Data / restraints / parameters	4843 / 0 / 316
Goodness-of-fit on F^2	1.039
Final R indices [I>2sigma(I)]	R1 = 0.0746, wR2 = 0.1617
R indices (all data)	R1 = 0.1328, wR2 = 0.1901
Largest diff. peak and hole	1.282 and -1.109 e.Å^{-3}

Table 2. Atomic coordinates (x 10^4) and equivalent isotropic displacement parameters (Å^{2}x 10^3) for **16**. U(eq) is defined as one third of the trace of the orthogonalized U^{ij} tensor.

	x	y	z	U(eq)
Ag(1)	11116(1)	2610(1)	699(1)	59(1)
N(2)	-6751(5)	3162(3)	589(3)	49(1)
C(18)	-6756(6)	3227(4)	-70(3)	49(1)
C(17)	-5411(7)	3604(4)	-158(3)	52(1)
C(16)	-4055(6)	3924(3)	455(3)	46(1)
C(15)	-4056(7)	3867(4)	1131(3)	52(1)
C(14)	-5426(7)	3470(4)	1172(3)	56(2)
C(13)	-2605(7)	4335(4)	356(3)	52(2)
O(6)	-2622(5)	4396(3)	-252(3)	76(1)
O(5)	-1390(5)	4610(3)	980(3)	65(1)
C(12)	96(7)	4982(5)	952(4)	72(2)
C(11)	1482(9)	5012(5)	1715(5)	87(3)
O(4)	1809(6)	4031(3)	1993(3)	88(2)
C(10)	3156(10)	3921(6)	2661(4)	87(3)
C(9)	3330(8)	2971(5)	2898(4)	73(2)

Silver Coordination Compounds with a Family of Ditopic Ligands of Varying Flexibility: About Chains, Rings, Helices and Polycatenanes

274

O(3)	3296(5)	2375(3)	2338(2)	62(1)
C(8)	3712(8)	1454(5)	2587(4)	69(2)
C(7)	3670(6)	883(5)	1963(3)	64(2)
O(2)	5021(4)	1202(3)	1810(2)	54(1)
O(1)	3977(6)	407(4)	760(3)	90(2)
C(6)	4994(6)	918(4)	1177(3)	47(1)
N(1)	9019(5)	2037(3)	836(2)	44(1)
C(1)	7767(6)	1596(4)	301(3)	50(1)
C(2)	6459(6)	1213(4)	403(3)	49(1)
C(3)	6426(6)	1316(3)	1073(3)	39(1)
C(4)	7726(6)	1767(4)	1630(3)	46(1)
C(5)	9010(6)	2118(4)	1494(3)	50(1)
S(1)	9047(2)	1958(1)	-1459(1)	54(1)
O(7)	9281(6)	2343(4)	-771(3)	86(2)
O(8)	9925(6)	2488(3)	-1782(3)	81(1)
O(9)	7395(6)	1678(4)	-1939(3)	97(2)
C(19)	10210(9)	871(5)	-1186(5)	82(2)
F(1)	11814(5)	1022(3)	-852(3)	109(2)
F(2)	9724(7)	346(3)	-779(3)	125(2)
F(3)	9936(7)	352(4)	-1771(4)	148(2)

Table 3. Bond lengths [Å] and angles [°] for **16**.

Ag(1)-N(2)#1	2.161(4)	O(5)-C(12)	1.452(8)
Ag(1)-N(1)	2.168(4)	C(12)-C(11)	1.496(10)
Ag(1)-O(7)	2.720(5)	C(11)-O(4)	1.482(9)
N(2)-C(14)	1.325(7)	O(4)-C(10)	1.367(9)
N(2)-C(18)	1.336(8)	C(10)-C(9)	1.418(11)
N(2)-Ag(1)#2	2.161(4)	C(9)-O(3)	1.405(8)
C(18)-C(17)	1.396(8)	O(3)-C(8)	1.393(8)
C(17)-C(16)	1.375(7)	C(8)-C(7)	1.490(9)
C(16)-C(15)	1.373(9)	C(7)-O(2)	1.444(7)
C(16)-C(13)	1.511(8)	O(2)-C(6)	1.336(7)
C(15)-C(14)	1.382(8)	O(1)-C(6)	1.178(6)
C(13)-O(6)	1.228(8)	C(6)-C(3)	1.495(7)
C(13)-O(5)	1.311(7)	N(1)-C(1)	1.322(6)

N(1)-C(5)	1.341(7)	S(1)-O(7)	1.426(5)
C(1)-C(2)	1.385(8)	S(1)-O(8)	1.436(5)
C(2)-C(3)	1.377(8)	S(1)-C(19)	1.807(7)
C(3)-C(4)	1.371(7)	C(19)-F(1)	1.304(8)
C(4)-C(5)	1.386(8)	C(19)-F(2)	1.318(10)
S(1)-O(9)	1.420(5)	C(19)-F(3)	1.323(10)
N(2)#1-Ag(1)-N(1)	178.51(16)	O(1)-C(6)-O(2)	123.8(6)
N(2)#1-Ag(1)-O(7)	94.03(17)	O(1)-C(6)-C(3)	124.7(6)
N(1)-Ag(1)-O(7)	87.12(16)	O(2)-C(6)-C(3)	111.5(4)
C(14)-N(2)-C(18)	118.5(5)	C(1)-N(1)-C(5)	118.8(5)
C(14)-N(2)-Ag(1)#2	120.6(4)	C(1)-N(1)-Ag(1)	122.6(4)
C(18)-N(2)-Ag(1)#2	120.9(3)	C(5)-N(1)-Ag(1)	118.5(3)
N(2)-C(18)-C(17)	122.0(5)	N(1)-C(1)-C(2)	121.9(5)
C(16)-C(17)-C(18)	118.5(6)	C(3)-C(2)-C(1)	119.4(5)
C(15)-C(16)-C(17)	119.6(5)	C(4)-C(3)-C(2)	118.9(5)
C(15)-C(16)-C(13)	122.2(5)	C(4)-C(3)-C(6)	121.8(5)
C(17)-C(16)-C(13)	118.2(5)	C(2)-C(3)-C(6)	119.3(4)
C(16)-C(15)-C(14)	118.3(5)	C(3)-C(4)-C(5)	118.6(5)
N(2)-C(14)-C(15)	123.2(6)	N(1)-C(5)-C(4)	122.3(5)
O(6)-C(13)-O(5)	125.8(5)	O(9)-S(1)-O(7)	115.9(4)
O(6)-C(13)-C(16)	121.8(5)	O(9)-S(1)-O(8)	116.5(3)
O(5)-C(13)-C(16)	112.4(5)	O(7)-S(1)-O(8)	111.8(3)
C(13)-O(5)-C(12)	116.9(6)	O(9)-S(1)-C(19)	104.7(3)
O(5)-C(12)-C(11)	108.9(7)	O(7)-S(1)-C(19)	102.2(4)
O(4)-C(11)-C(12)	107.4(5)	O(8)-S(1)-C(19)	103.4(3)
C(10)-O(4)-C(11)	115.0(6)	S(1)-O(7)-Ag(1)	152.0(3)
O(4)-C(10)-C(9)	111.2(6)	F(1)-C(19)-F(2)	110.9(7)
O(3)-C(9)-C(10)	109.8(6)	F(1)-C(19)-F(3)	106.5(7)
C(8)-O(3)-C(9)	111.4(5)	F(2)-C(19)-F(3)	105.3(6)
O(3)-C(8)-C(7)	107.5(5)	F(1)-C(19)-S(1)	111.7(5)
O(2)-C(7)-C(8)	107.5(5)	F(2)-C(19)-S(1)	111.8(6)
C(6)-O(2)-C(7)	116.6(4)	F(3)-C(19)-S(1)	110.3(6)

Symmetry transformations used to generate equivalent atoms:

#1 x+2,y,z   #2 x-2,y,z

Table 4. Anisotropic displacement parameters ($Å^2$x 10^3) for **16**. The anisotropic displacement factor exponent takes the form: $-2p^2[\, h^2a^{*2}U^{11} + ... + 2\, h\, k\, a^*\, b^*\, U^{12}\,]$

	U^{11}	U^{22}	U^{33}	U^{23}	U^{13}	U^{12}
Ag(1)	54(1)	54(1)	84(1)	11(1)	46(1)	-1(1)
N(2)	56(2)	38(2)	66(2)	4(2)	39(2)	0(2)
C(18)	51(2)	39(3)	66(3)	-2(2)	34(2)	-7(2)
C(17)	64(3)	42(3)	60(3)	4(2)	38(2)	-2(2)
C(16)	43(2)	38(2)	63(3)	5(2)	28(2)	-1(2)
C(15)	54(3)	54(3)	55(3)	-3(2)	30(2)	-8(2)
C(14)	57(3)	52(3)	63(3)	-1(3)	30(2)	-11(2)
C(13)	54(3)	44(3)	64(3)	5(2)	31(2)	-4(2)
O(6)	72(2)	77(3)	100(3)	9(2)	57(2)	-5(2)
O(5)	47(2)	59(2)	86(3)	13(2)	27(2)	-7(2)
C(12)	58(3)	58(4)	105(5)	7(3)	41(3)	-10(3)
C(11)	72(4)	76(4)	103(5)	-37(4)	31(4)	-17(3)
O(4)	74(3)	65(3)	117(4)	0(3)	35(3)	16(2)
C(10)	73(4)	117(6)	63(4)	-34(4)	22(4)	-26(4)
C(9)	54(3)	104(5)	56(4)	-13(3)	21(3)	7(3)
O(3)	66(2)	83(3)	49(2)	-13(2)	36(2)	-15(2)
C(8)	67(3)	94(5)	59(3)	25(3)	39(3)	19(3)
C(7)	64(2)	70(4)	86(3)	14(3)	58(2)	-2(3)
O(2)	49(2)	64(2)	59(2)	-3(2)	34(2)	-8(2)
O(1)	90(2)	107(3)	92(3)	-38(2)	58(2)	-56(2)
C(6)	48(2)	44(3)	54(3)	-5(2)	28(2)	-10(2)
N(1)	45(2)	46(2)	50(2)	2(2)	28(2)	-4(2)
C(1)	57(2)	59(3)	45(2)	-3(2)	32(2)	-3(2)
C(2)	58(2)	52(3)	49(3)	-12(2)	35(2)	-17(2)
C(3)	38(2)	40(2)	42(2)	1(2)	20(2)	-3(2)
C(4)	48(2)	48(3)	44(3)	-3(2)	23(2)	-5(2)
C(5)	40(2)	67(3)	44(3)	-3(2)	20(2)	-11(2)
S(1)	50(1)	68(1)	47(1)	11(1)	25(1)	2(1)
O(7)	103(3)	107(4)	65(2)	-7(2)	52(2)	-3(3)
O(8)	80(2)	91(3)	81(3)	39(2)	45(2)	7(2)

Silver Coordination Compounds with a Family of Ditopic Ligands of Varying Flexibility:
About Chains, Rings, Helices and Polycatenanes

277

O(9)	43(2)	123(4)	98(4)	5(3)	7(3)	-4(3)
C(19)	73(4)	62(4)	115(5)	8(4)	46(4)	-6(3)
F(1)	58(2)	92(3)	159(5)	37(3)	30(3)	13(2)
F(2)	129(3)	81(3)	171(4)	54(3)	72(3)	-3(3)
F(3)	134(4)	105(3)	205(5)	-70(3)	75(4)	4(3)

Table 5. Hydrogen coordinates (x 10^4) and isotropic displacement parameters ($Å^2$x 10^3) for **16**.

_____

	x	y	z	U(eq)

_____

H(18)	-7683	3015	-482	59
H(17)	-5432	3638	-620	62
H(15)	-3159	4090	1550	62
H(14)	-5417	3416	1631	67
H(12A)	-122	5610	743	86
H(12B)	409	4583	644	86
H(11A)	2476	5282	1711	104
H(11B)	1164	5397	2029	104
H(10A)	3024	4320	3020	105
H(10B)	4158	4118	2625	105
H(9A)	4376	2892	3335	87
H(9B)	2429	2806	3021	87
H(8A)	2919	1208	2751	83
H(8B)	4816	1434	2997	83
H(7A)	3806	220	2092	77
H(7B)	2611	966	1533	77
H(1)	7765	1542	-157	60
H(2)	5610	889	24	58
H(4)	7746	1836	2090	55
H(5)	9898	2421	1872	60

Table 5. Hydrogen bond [length (Å) and angle (°)] present in complex 16

D–H···Acceptor	d (D–H)	d (H···A)	d (D···A)	< D–H···A
C1–H1···O7[#2]	0.93	2.48(0)	3.20(8)	134.4(6)
C18–H18···O7[#3]	0.93	2.68(4)	3.41(8)	136.4(2)
C2–H2···O1[#4]	0.93	2.52(2)	3.19(8)	126.4(2)
C4–H4···O8	0.93	2.45(3)	3.12(8)	128.9(1)
C9–H9B···O8[#5]	0.97	2.47(2)	3.43(1)	173.0(2)
C7A–H7B···F2[#6]	0.97	2.71(0)	3.41(8)	128.7(1)

Symmetry transformation used to generate equivalent atoms: #2 x,1/2-y,-1/2+z, #3 -2+x, y, z #4 1-x,-y,-z, #4 -1+x,y,z #5 1-x, -y, -z

Crystal data and structure refinement for {[Ag(L5)]PF$_6$}$_2$ (17)

Identification code	**17**
Empirical formula	C36 H40 Ag2 F12 N4 O12 P2
Formula weight	1226.40
Temperature	293(2) K
Wavelength	0.71073 Å
Crystal system	Triclinic
Space group	P-1
Unit cell dimensions	a = 8.7123(17) Å α = 75.58(3)°.
	b = 9.806(2) Å β = 79.75(3)°.
	c = 14.257(3) Å γ = 72.75(3)°.
Volume	1119.4(4) Å^3
Z	1
Density (calculated)	1.819 Mg/m^3
Absorption coefficient	1.060 mm^{-1}
F(000)	612
Theta range for data collection	1.48 to 27.09°.
Index ranges	-10<=h<=11, -11<=k<=12, 0<=l<=18
Reflections collected	4537
Independent reflections	4537 [R(int) = 0.0000]
Completeness to theta = 27.09°	92.0 %
Refinement method	Full-matrix least-squares on F^2

Silver Coordination Compounds with a Family of Ditopic Ligands of Varying Flexibility:
About Chains, Rings, Helices and Polycatenanes

279

Data / restraints / parameters	4537 / 0 / 307
Goodness-of-fit on F^2	0.846
Final R indices [I>2sigma(I)]	R1 = 0.1101, wR2 = 0.2143
R indices (all data)	R1 = 0.3207, wR2 = 0.3006
Largest diff. peak and hole	0.825 and -1.389 e.$Å^{-3}$

Table 2. Atomic coordinates (x 10^4) and equivalent isotropic displacement parameters ($Å^2$x 10^3) for **17**. U(eq) is defined as one third of the trace of the orthogonalized U^{ij} tensor.

	x	y	z	U(eq)
Ag(1)	-4470(2)	4190(3)	7399(1)	73(1)
N(1)	-2370(30)	4850(20)	6802(12)	75(6)
C(1)	-930(30)	3850(30)	6743(11)	56(6)
C(2)	570(30)	4240(30)	6359(12)	58(6)
C(3)	540(20)	5670(20)	5957(11)	38(5)
C(4)	-920(30)	6680(30)	5913(10)	53(6)
C(5)	-2310(20)	6230(30)	6314(12)	55(6)
C(6)	2070(30)	5950(30)	5601(13)	49(6)
O(1)	3379(19)	5257(16)	5850(8)	64(4)
O(2)	1940(16)	7234(16)	4926(8)	57(4)
C(7)	3410(30)	7710(20)	4573(12)	58(6)
C(8)	3000(30)	9090(20)	3818(11)	68(7)
O(3)	2915(16)	8658(14)	2916(7)	56(4)
C(9)	2470(30)	9960(20)	2194(13)	62(6)
C(10)	2310(30)	9550(30)	1269(11)	72(7)
O(4)	3801(19)	8739(18)	924(9)	71(5)
C(11)	3900(30)	8390(30)	-43(11)	70(7)
C(12)	3640(30)	6990(30)	74(12)	68(7)
O(5)	2730(20)	4530(20)	638(11)	92(6)
O(6)	2044(16)	6927(17)	416(8)	56(4)
C(13)	1680(30)	5760(40)	668(13)	57(7)
N(2)	-3150(30)	5880(20)	1839(13)	86(9)
C(14)	-2680(30)	7070(30)	1472(12)	61(7)
C(15)	-1110(30)	7040(30)	1116(14)	62(7)

C(16)	0(30)	5710(30)	1103(11)	50(6)
C(17)	-540(30)	4530(20)	1453(11)	59(7)
C(18)	-2150(30)	4590(30)	1825(14)	71(9)
P(1)	7426(9)	500(9)	2964(4)	67(2)
F(1)	6040(20)	1850(20)	2774(17)	184(10)
F(2)	8330(20)	1390(20)	3333(9)	134(7)
F(3)	8880(30)	-790(20)	3060(20)	215(12)
F(4)	6550(30)	-390(30)	2587(14)	201(12)
F(5)	6580(30)	50(30)	3966(11)	190(11)
F(6)	8260(20)	1050(20)	1917(8)	134(7)

Table 3.   Bond lengths [Å] and angles [°] for **17**.

Ag(1)-N(2)#1	2.18(3)	C(11)-C(12)	1.42(3)
Ag(1)-N(1)	2.09(2)	C(12)-O(6)	1.40(2)
N(1)-C(1)	1.35(3)	O(5)-C(13)	1.28(3)
N(1)-C(5)	1.37(3)	O(6)-C(13)	1.23(3)
C(1)-C(2)	1.45(3)	C(13)-C(16)	1.49(3)
C(2)-C(3)	1.37(3)	N(2)-C(14)	1.31(3)
C(3)-C(4)	1.36(3)	N(2)-C(18)	1.30(3)
C(3)-C(6)	1.42(3)	N(2)-Ag(1)#1	2.18(3)
C(4)-C(5)	1.39(2)	C(14)-C(15)	1.36(3)
C(6)-O(1)	1.20(2)	C(15)-C(16)	1.38(3)
C(6)-O(2)	1.37(2)	C(16)-C(17)	1.33(2)
O(2)-C(7)	1.46(2)	C(17)-C(18)	1.40(3)
C(7)-C(8)	1.50(3)	P(1)-F(5)	1.512(16)
C(8)-O(3)	1.47(2)	P(1)-F(1)	1.51(2)
O(3)-C(9)	1.42(2)	P(1)-F(3)	1.50(2)
C(9)-C(10)	1.51(2)	P(1)-F(2)	1.562(15)
C(10)-O(4)	1.39(2)	P(1)-F(4)	1.548(16)
O(4)-C(11)	1.48(2)	P(1)-F(6)	1.580(13)
N(2)#1-Ag(1)-N(1)	162.8(9)	C(5)-N(1)-Ag(1)	125.6(18)
C(1)-N(1)-C(5)	113(2)	N(1)-C(1)-C(2)	123(2)
C(1)-N(1)-Ag(1)	120.2(16)	C(3)-C(2)-C(1)	120(2)

Silver Coordination Compounds with a Family of Ditopic Ligands of Varying Flexibility:
About Chains, Rings, Helices and Polycatenanes

281

C(4)-C(3)-C(2)	118.3(19)	C(18)-N(2)-Ag(1)#1	113.6(16)
C(4)-C(3)-C(6)	126(2)	N(2)-C(14)-C(15)	122(3)
C(2)-C(3)-C(6)	116(2)	C(16)-C(15)-C(14)	119(2)
C(5)-C(4)-C(3)	119(2)	C(17)-C(16)-C(15)	116(2)
C(4)-C(5)-N(1)	126(2)	C(17)-C(16)-C(13)	127(3)
O(1)-C(6)-O(2)	119(2)	C(15)-C(16)-C(13)	116(2)
O(1)-C(6)-C(3)	129(2)	C(16)-C(17)-C(18)	123(2)
O(2)-C(6)-C(3)	112(2)	N(2)-C(18)-C(17)	117(2)
C(6)-O(2)-C(7)	117.0(17)	F(5)-P(1)-F(1)	89.4(14)
O(2)-C(7)-C(8)	107.7(17)	F(5)-P(1)-F(3)	95.9(15)
O(3)-C(8)-C(7)	106.4(16)	F(1)-P(1)-F(3)	174.7(14)
C(9)-O(3)-C(8)	107.5(14)	F(5)-P(1)-F(2)	93.1(9)
O(3)-C(9)-C(10)	109.0(17)	F(1)-P(1)-F(2)	89.4(12)
O(4)-C(10)-C(9)	108.7(17)	F(3)-P(1)-F(2)	90.0(13)
C(10)-O(4)-C(11)	116.0(15)	F(5)-P(1)-F(4)	87.6(10)
C(12)-C(11)-O(4)	109.9(15)	F(1)-P(1)-F(4)	90.9(14)
C(11)-C(12)-O(6)	115(2)	F(3)-P(1)-F(4)	89.6(14)
C(13)-O(6)-C(12)	122(2)	F(2)-P(1)-F(4)	179.2(9)
O(6)-C(13)-O(5)	122(2)	F(5)-P(1)-F(6)	177.0(14)
O(6)-C(13)-C(16)	120(3)	F(1)-P(1)-F(6)	87.8(11)
O(5)-C(13)-C(16)	117(2)	F(3)-P(1)-F(6)	86.9(13)
C(14)-N(2)-C(18)	121(3)	F(2)-P(1)-F(6)	85.7(8)
C(14)-N(2)-Ag(1)#1	125(2)	F(4)-P(1)-F(6)	93.6(9)

Symmetry transformations used to generate equivalent atoms:

#1 -x-1,-y+1,-z+1

Table 4. Anisotropic displacement parameters ($Å^2$x 10^3) for **17**. The anisotropic displacement factor exponent takes the form: $-2p^2[\ h^2a^{*2}U^{11} + ... + 2\ h\ k\ a^*\ b^*\ U^{12}\ ]$

	U^{11}	U^{22}	U^{33}	U^{23}	U^{13}	U^{12}
Ag(1)	71(1)	112(2)	44(1)	-21(1)	2(1)	-37(1)
N(1)	107(19)	48(16)	73(12)	-8(11)	-59(12)	-3(15)
C(1)	100(20)	45(17)	26(9)	-14(9)	-23(11)	-13(17)

C(2)	60(16)	80(20)	36(10)	-35(12)	-7(10)	-3(15)
C(3)	35(13)	39(16)	35(9)	-10(9)	-7(8)	-1(13)
C(4)	55(14)	74(19)	23(8)	-4(9)	0(8)	-15(15)
C(5)	26(11)	67(19)	44(10)	-7(11)	0(8)	23(13)
C(6)	55(16)	43(17)	44(11)	-33(11)	-12(11)	19(14)
O(1)	75(11)	63(12)	40(7)	-1(7)	-4(7)	-6(10)
O(2)	73(10)	73(12)	32(6)	-17(7)	-1(6)	-28(9)
C(7)	68(15)	62(17)	46(10)	-13(11)	-16(10)	-16(14)
C(8)	106(19)	68(18)	35(9)	4(10)	1(10)	-49(16)
O(3)	92(11)	37(9)	36(6)	-4(6)	-17(6)	-10(9)
C(9)	63(16)	59(18)	64(12)	-20(12)	-6(11)	-11(15)
C(10)	81(18)	90(20)	26(9)	4(10)	-24(10)	9(17)
O(4)	71(11)	88(14)	56(8)	-26(8)	-16(7)	-8(11)
C(11)	77(16)	110(20)	28(9)	-21(11)	2(9)	-38(17)
C(12)	93(19)	80(20)	32(9)	-12(11)	7(10)	-38(17)
O(5)	54(11)	132(19)	86(11)	-46(11)	5(9)	-4(13)
O(6)	50(10)	70(12)	55(7)	-17(7)	17(6)	-36(10)
C(13)	34(14)	100(20)	43(10)	-14(13)	-6(9)	-24(16)
N(2)	160(20)	38(14)	75(12)	31(12)	-93(15)	-33(17)
C(14)	100(20)	41(17)	39(10)	-1(10)	-37(11)	-1(16)
C(15)	54(16)	80(20)	64(13)	13(13)	-29(11)	-38(17)
C(16)	60(15)	64(19)	22(8)	-4(10)	-25(9)	-4(15)
C(17)	140(20)	4(12)	31(9)	14(8)	-40(12)	-20(14)
C(18)	90(20)	80(20)	65(13)	15(14)	-12(13)	-80(20)
P(1)	69(5)	68(6)	67(4)	-28(3)	-9(3)	-12(5)
F(1)	83(13)	140(20)	270(20)	-14(18)	7(14)	27(14)
F(2)	177(17)	187(19)	80(9)	-55(10)	23(9)	-112(16)
F(3)	130(19)	84(17)	370(30)	-9(19)	-50(20)	39(16)
F(4)	200(20)	320(30)	189(17)	-200(20)	73(15)	-160(20)
F(5)	310(30)	250(30)	76(10)	-29(12)	23(13)	-190(20)
F(6)	154(15)	210(20)	57(7)	-57(10)	15(8)	-74(15)

Table 5.   Hydrogen coordinates (x 10^4) and isotropic displacement parameters ($Å^2$x 10^3) for **17**.

	x	y	z	U(eq)
H(1)	-899	2867	6958	67
H(2)	1552	3526	6385	70
H(4)	-983	7650	5619	63
H(5)	-3292	6939	6247	66
H(7A)	4232	6964	4289	69
H(7B)	3833	7881	5107	69
H(8A)	1964	9723	4022	81
H(8B)	3819	9616	3717	81
H(9A)	3297	10484	2070	74
H(9B)	1458	10584	2421	74
H(10A)	1519	8988	1400	87
H(10B)	1934	10431	784	87
H(11A)	3096	9128	-419	84
H(11B)	4961	8403	-396	84
H(12A)	4353	6296	525	81
H(12B)	3932	6699	-549	81
H(14)	-3433	7975	1455	73
H(15)	-799	7902	884	74
H(17)	181	3617	1449	71
H(18)	-2505	3746	2054	85

Table 6. Hydrogen bond [length (Å) and angle (°)] present in complex **17**

D–H···Acceptor	d (D–H)	d (H···A)	d (D···A)	< D–H···A
C11–H11A···F6[#3]	0.97	2.67(1)	3.38(1)	129.0(1)
C18–H18···F2[#6]	0.93	2.47(8)	3.23(1)	137.9(2)
C9–H9B···F2[#7]	0.97	2.78(0)	3.70(1)	158.1(2)
C7–H7B···F2[#3]	0.97	2.72(7)	3.30(1)	116.8(7)
C7–H7B···F5[#3]	0.97	2.59(1)	3.38(8)	138.0(2)
C8–H8B···F4[#8]	0.97	2.63(0)	3.56(7)	154.7(9)
C1–H1···O3[#3]	0.93	2.57(6)	3.30(3)	135.0(3)

C7–H7A···O1#3	0.97	2.55(0)	3.48(3)	159.7(7)
C14–H14···O4#6	0.93	2.50(1)	3.15(3)	127.1(0)
C5–H5···F5#3	0.93	2.55(1)	3.37(1)	147.7(2)
C18–H18···F6#6	0.93	2.49(2)	3.29(1)	143.0(8)
C18–H18···F1#6	0.93	2.46(7)	3.39(3)	167.6(7)
C1–H1···F3#5	0.93	2.26(0)	2.98(3)	133.0(3)
C2–H2···F3#5	0.93	2.68(1)	3.13(8)	110.0(1)
C14–H14···F4#7	0.93	2.54(0)	3.13(4)	121.7(1)

Symmetry transformation used to generate equivalent atoms: #5 1-x,-y,1-z #3 -x,1-y,1-z #6 -1+x,1+y,z #7 -1+x,y,z #8 x, 1+y, z.

Crystal data and structure refinement for {[Ag(L5)]NO₃}ₙ (18)

Identification code	**18**
Empirical formula	C18 H22 Ag N3 O10
Formula weight	548.26
Temperature	293(2) K
Wavelength	0.71073 Å
Crystal system	Monoclinic
Space group	P-1
Unit cell dimensions	a = 9.2026(18) Å a= 78.32(3)°.
	b = 9.2967(19) Å b= 80.75(3)°.
	c = 14.494(3) Å g = 67.82(3)°.
Volume	1119.7(4) Å^3
Z	2
Density (calculated)	1.626 Mg/m^3
Absorption coefficient	0.958 mm^{-1}
F(000)	556
Theta range for data collection	1.44 to 27.04°.
Index ranges	-11<=h<=11, -11<=k<=11, -18<=l<=0
Reflections collected	4869
Independent reflections	4869 [R(int) = 0.0000]
Completeness to theta = 27.04°	99.3 %
Refinement method	Full-matrix least-squares on F^2

Data / restraints / parameters	4869 / 0 / 298		
Goodness-of-fit on F^2	0.642		
Final R indices [I>2sigma(I)]	R1 = 0.1084, wR2 = 0.2297		
R indices (all data)	R1 = 0.4660, wR2 = 0.4721		
Largest diff. peak and hole	0.809 and -0.685 e.Å^{-3}		

Table 2. Atomic coordinates (x 10^4) and equivalent isotropic displacement parameters ($Å^2$x 10^3) for **18**. U(eq) is defined as one third of the trace of the orthogonalized U^{ij} tensor.

	x	y	z	U(eq)
Ag(1)	177(3)	4479(3)	2423(2)	49(1)
N(1)	-2160(20)	4420(20)	2986(14)	45(6)
C(1)	-3260(30)	5830(50)	3150(20)	87(14)
C(2)	-4880(40)	5890(20)	3587(16)	160(8)
C(3)	-5130(30)	4600(30)	3760(30)	98(13)
C(4)	-4010(20)	3090(20)	3564(16)	43(5)
C(5)	-2530(30)	3180(30)	3163(18)	51(7)
C(6)	-6900(20)	4620(40)	4365(16)	68(10)
O(1)	-7800(20)	5800(30)	4497(15)	89(9)
C(7)	-8490(20)	3190(20)	4850(20)	107(7)
C(8)	-8600(30)	1710(40)	4830(40)	180(20)
O(2)	-6941(19)	3150(20)	4306(18)	85(8)
O(3)	-8326(19)	1470(20)	3644(14)	58(6)
C(9)	-8600(50)	170(40)	3620(20)	95(13)
C(10)	-8230(30)	-60(30)	2490(30)	129(19)
O(4)	-9330(20)	1370(20)	1955(12)	71(7)
C(11)	-9190(40)	1280(40)	990(30)	87(12)
C(12)	-10190(30)	2830(40)	533(18)	79(9)
O(5)	-11702(16)	2958(18)	767(9)	45(4)
O(6)	-12630(20)	5530(30)	504(14)	95(6)
C(13)	-12880(30)	4360(30)	783(14)	39(7)
N(2)	-17530(30)	4480(30)	1809(14)	104(8)
C(14)	-17250(30)	5840(20)	1624(13)	48(7)
C(15)	-15800(40)	5900(120)	1390(50)	350(50)

C(16)	-14690(20)	4590(20)	1104(13)	127(4)
C(17)	-14790(30)	2950(40)	1350(20)	77(12)
C(18)	-16430(30)	3230(50)	1790(30)	221(16)
N(3)	-21510(30)	8570(20)	2250(30)	125(15)
O(7)	-21020(40)	8330(50)	1554(15)	257(17)
O(8)	-20670(30)	7680(30)	2780(30)	160(15)
O(9)	-22520(50)	9640(30)	2510(40)	370(30)
O(10)	5350(30)	9240(30)	1000(20)	124(11)
O(11)	4990(60)	9650(50)	3980(30)	270(20)

Table 3. Bond lengths [Å] and angles [°] for **18**.

Ag(1)-N(2)#1	2.16(2)	O(4)-C(11)	1.41(4)
Ag(1)-N(1)	2.19(2)	C(11)-C(12)	1.47(4)
N(1)-C(5)	1.29(3)	C(12)-O(5)	1.35(3)
N(1)-C(1)	1.36(4)	O(5)-C(13)	1.35(3)
C(1)-C(2)	1.50(4)	O(6)-C(13)	1.17(3)
C(2)-C(3)	1.27(4)	C(13)-C(16)	1.59(3)
C(3)-C(4)	1.45(3)	N(2)-C(18)	1.22(4)
C(3)-C(6)	1.72(3)	N(2)-C(14)	1.36(3)
C(4)-C(5)	1.42(3)	N(2)-Ag(1)#2	2.16(2)
C(6)-O(1)	1.13(3)	C(14)-C(15)	1.34(5)
C(6)-O(2)	1.40(4)	C(15)-C(16)	1.36(8)
C(7)-C(8)	1.42(4)	C(16)-C(17)	1.53(4)
C(7)-O(2)	1.50(3)	C(17)-C(18)	1.48(4)
C(8)-O(3)	1.75(6)	N(3)-O(8)	1.15(4)
O(3)-C(9)	1.34(4)	N(3)-O(7)	1.07(4)
C(9)-C(10)	1.66(5)	N(3)-O(9)	1.15(4)
C(10)-O(4)	1.49(3)		

N(2)#1-Ag(1)-N(1)	176.9(10)	C(3)-C(2)-C(1)	117(3)
C(5)-N(1)-C(1)	120(2)	C(2)-C(3)-C(4)	126(3)
C(5)-N(1)-Ag(1)	125.2(15)	C(2)-C(3)-C(6)	117(2)
C(1)-N(1)-Ag(1)	115(2)	C(4)-C(3)-C(6)	116(2)
N(1)-C(1)-C(2)	119(3)	C(5)-C(4)-C(3)	111(2)

N(1)-C(5)-C(4)	127(2)	O(6)-C(13)-C(16)	115(2)
O(1)-C(6)-O(2)	136(2)	O(5)-C(13)-C(16)	124.6(19)
O(1)-C(6)-C(3)	117(3)	C(18)-N(2)-C(14)	120(3)
O(2)-C(6)-C(3)	104(2)	C(18)-N(2)-Ag(1)#2	119(2)
C(8)-C(7)-O(2)	105(2)	C(14)-N(2)-Ag(1)#2	119.3(18)
C(7)-C(8)-O(3)	107(3)	N(2)-C(14)-C(15)	123(5)
C(6)-O(2)-C(7)	102.5(16)	C(14)-C(15)-C(16)	116(8)
C(9)-O(3)-C(8)	107(2)	C(15)-C(16)-C(13)	125(4)
O(3)-C(9)-C(10)	105(2)	C(15)-C(16)-C(17)	124(4)
O(4)-C(10)-C(9)	107(2)	C(13)-C(16)-C(17)	107.4(16)
C(11)-O(4)-C(10)	112(2)	C(18)-C(17)-C(16)	104(3)
O(4)-C(11)-C(12)	106(2)	N(2)-C(18)-C(17)	128(4)
O(5)-C(12)-C(11)	108(3)	O(8)-N(3)-O(7)	108(3)
C(13)-O(5)-C(12)	122(2)	O(8)-N(3)-O(9)	119(5)
O(6)-C(13)-O(5)	120(2)	O(7)-N(3)-O(9)	132(4)

Symmetry transformations used to generate equivalent atoms:

#1 x+2,y,z   #2 x-2,y,z

Table 4.   Anisotropic displacement parameters ($\mathring{A}^2$x 10^3) for **18**. The anisotropic displacement factor exponent takes the form: $-2p^2[h^2a^{*2}U^{11} + ... + 2 h k a^* b^* U^{12}]$

	U^{11}	U^{22}	U^{33}	U^{23}	U^{13}	U^{12}
Ag(1)	33(1)	75(1)	47(1)	-20(1)	13(1)	-30(1)
N(1)	37(10)	50(11)	48(11)	-43(9)	7(9)	-1(10)
C(1)	43(16)	140(30)	48(19)	10(20)	8(15)	-13(19)
C(2)	330(20)	57(7)	133(10)	-102(7)	-140(13)	-16(14)
C(3)	0(10)	34(14)	230(40)	-75(19)	-11(16)	59(10)
C(4)	64(9)	44(8)	62(14)	-38(9)	18(10)	-60(7)
C(5)	30(11)	78(17)	55(15)	-37(13)	11(11)	-24(11)
C(6)	0(7)	120(20)	44(12)	59(13)	-51(8)	8(11)
O(1)	41(11)	119(19)	65(14)	-2(13)	-32(10)	21(13)
C(7)	36(7)	70(7)	280(20)	-147(9)	-13(12)	-32(7)
C(8)	0(10)	100(30)	450(70)	-100(30)	-80(20)	27(14)

O(2)	44(8)	39(10)	170(20)	9(12)	19(12)	-35(7)
O(3)	38(9)	38(10)	89(14)	-17(10)	4(10)	-7(8)
C(9)	140(30)	80(20)	63(18)	-56(15)	-34(19)	0(20)
C(10)	74(12)	1(9)	340(60)	-6(18)	-50(20)	-40(9)
O(4)	59(12)	88(14)	43(10)	-37(10)	19(9)	4(11)
C(11)	60(17)	80(20)	130(30)	-50(20)	32(19)	-30(16)
C(12)	44(11)	200(30)	27(13)	-34(15)	2(11)	-74(14)
O(5)	84(7)	92(9)	0(6)	7(6)	-7(6)	-83(6)
O(6)	121(12)	179(15)	52(12)	-56(11)	27(10)	-122(11)
C(13)	79(15)	36(13)	5(10)	-1(9)	19(10)	-34(11)
N(2)	97(13)	187(18)	35(10)	117(11)	-61(10)	-105(12)
C(14)	81(15)	3(7)	27(9)	75(7)	-37(10)	-3(9)
C(15)	0(12)	810(140)	220(60)	-140(70)	40(20)	-100(30)
C(16)	314(7)	235(7)	0(9)	8(7)	-24(8)	-295(5)
C(17)	0(10)	100(20)	90(20)	0(20)	23(13)	15(13)
C(18)	99(10)	180(30)	380(30)	190(20)	-236(13)	-87(16)
N(3)	56(14)	0(9)	260(40)	79(16)	0(20)	-1(10)
O(7)	190(20)	620(50)	57(11)	-199(18)	88(13)	-220(30)
O(8)	104(12)	102(14)	310(40)	-30(20)	30(20)	-100(10)
O(9)	200(40)	36(15)	630(80)	170(30)	120(50)	60(20)
O(10)	96(15)	150(20)	150(20)	-14(18)	-34(17)	-60(15)
O(11)	420(50)	320(40)	130(30)	-30(30)	70(30)	-250(30)

Table 5. Hydrogen coordinates (x 10^4) and isotropic displacement parameters ($\mathring{A}^2$x 10^3) for **18**.

_____

	x	y	z	U(eq)
H(1)	-3016	6737	3003	104
H(2)	-5657	6826	3723	192
H(4)	-4236	2166	3687	51
H(5)	-1751	2254	3012	61
H(7A)	-8503	3339	5501	128
H(7B)	-9355	4047	4562	128

_____

Silver Coordination Compounds with a Family of Ditopic Ligands of Varying Flexibility:

About Chains, Rings, Helices and Polycatenanes

H(8A)	-9621	1697	5114	217
H(8B)	-7792	874	5184	217
H(9A)	-9687	292	3841	114
H(9B)	-7912	-729	4007	114
H(10A)	-7143	-169	2271	155
H(10B)	-8398	-987	2404	155
H(11A)	-9542	465	893	104
H(11B)	-8100	1040	721	104
H(12A)	-9990	3653	748	95
H(12B)	-9951	2923	-149	95
H(14)	-18102	6781	1660	58
H(15)	-15578	6781	1429	424
H(17)	-14013	1990	1246	92
H(18)	-16646	2334	2084	265

Table 6. Hydrogen bond [length (Å) and angle (°)] present in complex **18**

D–H···Acceptor	d (D–H) Å	d (H···A) Å	d (D···A) Å	< D–H···A (°)
C5–H5···O4[#2]	0.93	2.47(2)	3.18(2)	132.8(1)
C14–H14···O8[#4]	0.93	2.56(8)	3.32(3)	139.0(0)
C7–H7A···O8[#4]	0.98	2.49(0)	3.35(5)	146.1(0)

Symmetry transformation used to generate equivalent atoms: #2 1+x,y,z, #4 -1-x,1-y,1-z #5 x, y-1, z #6 –x, -1-y, -z

Crystal data and structure refinement for {[Ag(L6)]NO₃}₂ (21)

Identification code	**21**
Empirical formula	C160 H192 Ag8 N24 O80
Formula weight	4594.34
Temperature	293(2) K
Wavelength	0.71073 Å
Crystal system	Monoclinic
Space group	C2/c
Unit cell dimensions	a = 18.478(7) Å a= 90°.

Silver Coordination Compounds with a Family of Ditopic Ligands of Varying Flexibility:
About Chains, Rings, Helices and Polycatenanes

290

	b = 10.603(2) Å	b= 96.22(4)°.
	c = 27.494(5) Å	g = 90°.
Volume	5355(2) Å^3	
Z	1	
Density (calculated)	1.425 Mg/m^3	
Absorption coefficient	0.805 mm^{-1}	
F(000)	2336	
Crystal size	? x ? x ? mm^3	
Theta range for data collection	1.49 to 29.64°.	
Index ranges	-25<=h<=25, -14<=k<=14, -38<=l<=0	
Reflections collected	14389	
Independent reflections	7432 [R(int) = 0.3441]	
Completeness to theta = 29.64°	98.2 %	
Refinement method	Full-matrix least-squares on F^2	
Data / restraints / parameters	7432 / 0 / 283	
Goodness-of-fit on F^2	1.082	
Final R indices [I>2sigma(I)]	R1 = 0.2049, wR2 = 0.3651	
R indices (all data)	R1 = 0.4565, wR2 = 0.4657	
Largest diff. peak and hole	2.065 and -0.865 e.Å^{-3}	

Table 2. Atomic coordinates (x 10^4) and equivalent isotropic displacement parameters (Å^{2}x 10^3) for **21**. U(eq) is defined as one third of the trace of the orthogonalized U^{ij} tensor.

	x	y	z	U(eq)
Ag(1)	5874(1)	7262(2)	1273(1)	71(1)
N(1)	5129(8)	5875(12)	1589(7)	74(7)
C(1)	5413(6)	4680(15)	1695(8)	105(12)
C(2)	4968(8)	3729(11)	1843(8)	89(10)
C(3)	4238(8)	3971(12)	1884(7)	48(6)
C(4)	3953(7)	5166(14)	1779(7)	61(8)
C(5)	4399(9)	6118(10)	1631(6)	83(10)
C(6)	3760(15)	2950(30)	2002(10)	78(9)
O(1)	3993(11)	1852(19)	2057(9)	110(9)

Silver Coordination Compounds with a Family of Ditopic Ligands of Varying Flexibility:
About Chains, Rings, Helices and Polycatenanes

291

O(2)	3095(8)	3247(15)	2092(7)	76(6)
C(7)	2621(13)	2260(30)	2211(10)	79(8)
C(8)	1999(14)	2930(30)	2387(13)	103(12)
O(3)	1568(8)	3525(16)	2082(7)	62(5)
C(9)	1003(14)	4080(20)	2287(11)	73(8)
C(10)	610(17)	5010(30)	1941(12)	89(11)
O(4)	290(9)	4317(16)	1544(8)	72(6)
C(11)	29(17)	5160(30)	1164(13)	101(12)
C(12)	-407(15)	4460(30)	737(13)	89(10)
O(5)	56(10)	3550(18)	518(8)	99(7)
C(13)	-380(17)	2850(30)	107(8)	119(14)
C(14)	150(30)	1770(30)	-7(11)	150(20)
O(6)	926(11)	150(20)	-438(8)	101(7)
O(7)	781(9)	2132(17)	-205(7)	76(5)
C(15)	1139(17)	1200(30)	-414(11)	77(9)
N(2)	3148(7)	2299(18)	-947(6)	92(7)
C(16)	2704(9)	3225(13)	-779(7)	82(10)
C(17)	2053(8)	2891(14)	-603(7)	74(8)
C(18)	1846(8)	1632(16)	-595(7)	79(9)
C(19)	2290(10)	706(12)	-763(8)	81(9)
C(20)	2941(9)	1040(15)	-939(7)	111(13)
N(3)	7091(14)	2943(15)	1227(7)	43(6)
O(8)	7840(30)	2500(50)	1240(19)	380(40)
O(9)	6590(30)	2530(40)	1209(19)	280(30)
O(10)	7177(15)	3950(40)	1430(11)	182(14)

Table 3.   Bond lengths [Å] and angles [°] for **21**.

Ag(1)-N(2)#1	2.154(11)	C(2)-C(3)	1.3900
Ag(1)-N(1)	2.253(11)	C(3)-C(4)	1.3900
Ag(1)-O(4)#2	2.577(16)	C(3)-C(6)	1.46(3)
N(1)-C(1)	1.3900	C(4)-C(5)	1.3900
N(1)-C(5)	1.3900	C(6)-O(1)	1.24(3)
C(1)-C(2)	1.3900	C(6)-O(2)	1.32(3)

Silver Coordination Compounds with a Family of Ditopic Ligands of Varying Flexibility:
About Chains, Rings, Helices and Polycatenanes

292

O(2)-C(7)	1.42(3)	C(3)-C(2)-C(1)	120.0
C(7)-C(8)	1.47(3)	C(2)-C(3)-C(4)	120.0
C(8)-O(3)	1.26(3)	C(2)-C(3)-C(6)	119.9(15)
O(3)-C(9)	1.37(3)	C(4)-C(3)-C(6)	120.0(15)
C(9)-C(10)	1.50(4)	C(5)-C(4)-C(3)	120.0
C(10)-O(4)	1.39(3)	C(4)-C(5)-N(1)	120.0
O(4)-C(11)	1.42(4)	O(1)-C(6)-O(2)	121(3)
O(4)-Ag(1)#3	2.577(16)	O(1)-C(6)-C(3)	121(2)
C(11)-C(12)	1.55(4)	O(2)-C(6)-C(3)	118(2)
C(12)-O(5)	1.46(3)	C(6)-O(2)-C(7)	118(2)
O(5)-C(13)	1.51(3)	O(2)-C(7)-C(8)	104(2)
C(13)-C(14)	1.56(5)	O(3)-C(8)-C(7)	119(3)
C(14)-O(7)	1.40(4)	C(8)-O(3)-C(9)	113(2)
O(6)-C(15)	1.18(3)	O(3)-C(9)-C(10)	111(2)
O(7)-C(15)	1.35(3)	O(4)-C(10)-C(9)	107(2)
C(15)-C(18)	1.52(3)	C(10)-O(4)-C(11)	109(2)
N(2)-C(16)	1.3900	C(10)-O(4)-Ag(1)#3	121.0(18)
N(2)-C(20)	1.3900	C(11)-O(4)-Ag(1)#3	116.2(16)
N(2)-Ag(1)#1	2.154(11)	O(4)-C(11)-C(12)	111(2)
C(16)-C(17)	1.3900	O(5)-C(12)-C(11)	111(2)
C(17)-C(18)	1.3900	C(12)-O(5)-C(13)	110(2)
C(18)-C(19)	1.3900	O(5)-C(13)-C(14)	103(3)
C(19)-C(20)	1.3900	O(7)-C(14)-C(13)	116(2)
N(3)-O(9)	1.02(5)	C(15)-O(7)-C(14)	116(2)
N(3)-O(10)	1.21(4)	O(6)-C(15)-O(7)	122(3)
N(3)-O(8)	1.45(5)	O(6)-C(15)-C(18)	124(3)
		O(7)-C(15)-C(18)	113(2)
N(2)#1-Ag(1)-N(1)	151.4(7)	C(16)-N(2)-C(20)	120.0
N(2)#1-Ag(1)-O(4)#2	109.5(6)	C(16)-N(2)-Ag(1)#1	122.5(10)
N(1)-Ag(1)-O(4)#2	98.5(6)	C(20)-N(2)-Ag(1)#1	117.3(9)
C(1)-N(1)-C(5)	120.0	N(2)-C(16)-C(17)	120.0
C(1)-N(1)-Ag(1)	116.2(8)	C(16)-C(17)-C(18)	120.0
C(5)-N(1)-Ag(1)	123.4(8)	C(19)-C(18)-C(17)	120.0
N(1)-C(1)-C(2)	120.0	C(19)-C(18)-C(15)	117.2(15)

C(17)-C(18)-C(15)	122.8(15)	O(9)-N(3)-O(10)	118(3)
C(20)-C(19)-C(18)	120.0	O(9)-N(3)-O(8)	136(4)
C(19)-C(20)-N(2)	120.0	O(10)-N(3)-O(8)	101(3)

Symmetry transformations used to generate equivalent atoms:

#1 -x+1,-y+1,-z   #2 x+1/2,y+1/2,z   #3 x-1/2,y-1/2,z

Table 4.   Anisotropic displacement parameters ($Å^2$ x 10^3) for **21**. The anisotropic displacement factor exponent takes the form: $-2p^2[h^2 a^{*2} U^{11} + ... + 2 h k a^* b^* U^{12}]$

	U^{11}	U^{22}	U^{33}	U^{23}	U^{13}	U^{12}
Ag(1)	66(1)	56(1)	96(2)	-1(2)	26(1)	-9(1)
N(1)	81(17)	32(12)	110(20)	-3(12)	6(15)	-11(11)
C(1)	100(20)	47(18)	170(40)	30(20)	10(20)	26(17)
C(2)	90(20)	57(17)	120(30)	35(18)	40(20)	14(16)
C(3)	39(13)	27(12)	80(19)	-10(11)	25(12)	-11(9)
C(4)	69(17)	36(14)	80(20)	11(13)	31(15)	-13(12)
C(5)	100(20)	58(18)	80(20)	-42(16)	-19(18)	43(17)
C(6)	66(18)	100(30)	60(20)	35(17)	-19(14)	18(17)
O(1)	86(15)	73(15)	180(30)	34(15)	59(15)	33(11)
O(2)	31(9)	60(11)	137(18)	43(11)	15(10)	12(8)
C(7)	72(17)	85(19)	80(20)	12(19)	13(15)	18(18)
C(8)	37(15)	110(30)	160(30)	-60(30)	-1(18)	-19(17)
O(3)	33(9)	77(12)	74(13)	22(10)	-3(9)	24(8)
C(9)	65(18)	47(16)	100(20)	-1(16)	-18(17)	8(13)
C(10)	110(20)	90(20)	80(20)	-50(20)	40(20)	-40(20)
O(4)	61(12)	51(11)	106(17)	6(12)	19(11)	29(9)
C(11)	90(20)	80(20)	130(30)	-70(20)	-20(20)	11(18)
C(12)	70(20)	65(19)	130(30)	30(20)	20(20)	21(16)
O(5)	81(13)	86(14)	140(20)	9(14)	54(14)	29(11)
C(13)	190(30)	140(30)	26(13)	-102(16)	18(15)	-130(30)
C(14)	340(60)	80(20)	42(19)	-36(17)	80(30)	-90(30)
O(6)	100(16)	73(15)	130(20)	-27(14)	28(14)	-18(12)

O(7)	77(11)	68(11)	87(13)	-16(11)	29(10)	-48(10)
C(15)	110(20)	44(16)	70(20)	-30(15)	-11(17)	-3(17)
N(2)	94(16)	72(16)	112(19)	-28(16)	15(14)	-50(15)
C(16)	100(20)	44(15)	110(30)	-14(16)	60(20)	-13(15)
C(17)	58(15)	63(17)	110(20)	-1(18)	38(15)	1(14)
C(18)	80(19)	77(19)	80(20)	13(17)	0(16)	-56(16)
C(19)	100(20)	38(15)	110(20)	-13(15)	39(19)	33(15)
C(20)	90(20)	160(40)	100(30)	-10(20)	70(20)	0(20)
N(3)	106(18)	0(8)	29(10)	-7(7)	33(11)	7(9)
O(8)	340(60)	320(60)	430(70)	-320(60)	-190(50)	90(50)
O(9)	380(70)	190(40)	290(50)	-100(40)	170(50)	-80(40)
O(10)	130(20)	300(40)	100(20)	90(30)	-67(18)	20(30)

Table 5. Hydrogen coordinates (x 10^4) and isotropic displacement parameters (Å^2x 10^3) for **21**.

_____

	x	y	z	U(eq)

_____

H(1)	5902	4518	1667	126
H(2)	5159	2929	1913	106
H(4)	3465	5328	1807	74
H(5)	4208	6917	1561	99
H(7A)	2859	1718	2464	95
H(7B)	2465	1754	1925	95
H(8A)	1715	2312	2545	124
H(8B)	2193	3519	2637	124
H(9A)	1189	4507	2586	87
H(9B)	666	3432	2370	87
H(10A)	241	5448	2100	106
H(10B)	948	5620	1835	106
H(11A)	438	5596	1045	121
H(11B)	-280	5794	1293	121
H(12A)	-813	4018	856	107
H(12B)	-601	5057	490	107

Silver Coordination Compounds with a Family of Ditopic Ligands of Varying Flexibility: About Chains, Rings, Helices and Polycatenanes

295

H(13A)	-497	3390	-175	143
H(13B)	-827	2515	211	143
H(14A)	288	1308	293	180
H(14B)	-117	1188	-234	180
H(16)	2842	4068	-784	99
H(17)	1756	3511	-491	89
H(19)	2152	-137	-758	98
H(20)	3239	420	-1051	134

Table 6. Hydrogen bond data [length (Å) and angle (°)] present in complex **21**

D–H···Acceptor	d (D–H)	d (H···A)	d (D···A)	Angle D–H···A
C10–H10A[#3]···O1	0.97	2.82(8)	3.72(3)	153.8(4)
C11–H11A[#4]···O1	0.97	2.81(6)	3.70(7)	153.0(7)
C10–H10A[#4]···O1	0.97	2.94(2)	3.40(4)	110.4(4)
C9–H9A[#5]···O1	0.97	2.66(8)	3.40(6)	133.2(1)
C13–H13A[#6]···O6	0.97	2.88(2)	3.44(9)	118.3(0)
C14–H14B[#6]···O6	0.97	2.57(7)	3.13(0)	118.6(2)
C14–H14A[#6]···O6	0.97	2.89(4)	3.13(0)	93.1(5)

Symmetry transformation used to generate equivalent atoms: #3 0.5+x, -0.5+y, z #4 1-x, 1-y, -z #5 0.5-x, -0.5+y, 0.5-z #6 –x, -y, -z #7

E - III - Crystal data and structure refinement for Cu(I) and Cu(II) complexes

Crystal data and structure refinement for {[Cu(L6)₂](NO3)₂} (19)

Identification code	**19**
Empirical formula	C16 H16 Cu0.50 N3 O8
Formula weight	410.09
Temperature	293(2) K
Wavelength	0.71073 Å
Crystal system	Monoclinic
Space group	P2$_1$/c
Unit cell dimensions	a = 13.336(3) Å a= 90°.

	b = 13.906(3) Å	b= 99.91(3)°.
	c = 9.5234(19) Å	g = 90°.
Volume	1739.8(6) Å^3	
Z	4	
Density (calculated)	1.566 Mg/m^3	
Absorption coefficient	0.713 mm^{-1}	
F(000)	846	
Theta range for data collection	1.55 to 27.22°.	
Index ranges	-16<=h<=17, -17<=k<=17, -12<=l<=12	
Reflections collected	13648	
Independent reflections	3822 [R(int) = 0.0986]	
Completeness to theta = 27.22°	98.4 %	
Refinement method	Full-matrix least-squares on F^2	
Data / restraints / parameters	3822 / 0 / 250	
Goodness-of-fit on F^2	1.025	
Final R indices [I>2sigma(I)]	R1 = 0.0451, wR2 = 0.1249	
R indices (all data)	R1 = 0.0516, wR2 = 0.1313	
Largest diff. peak and hole	0.363 and -0.619 e.Å^{-3}	

Table 2. Atomic coordinates (x 10^4) and equivalent isotropic displacement parameters (Å^{2}x 10^3) for **19**. U(eq) is defined as one third of the trace of the orthogonalized U^{ij} tensor.

	x	y	z	U(eq)
Cu(1)	10000	5000	0	33(1)
N(1)	11329(1)	4528(1)	1218(2)	34(1)
C(1)	11371(2)	4322(2)	2610(2)	40(1)
C(2)	12178(2)	3845(2)	3400(3)	51(1)
C(3)	12972(2)	3555(2)	2756(3)	48(1)
C(4)	12960(2)	3793(2)	1339(2)	38(1)
C(5)	12126(2)	4284(2)	618(2)	37(1)
C(6)	13793(2)	3487(2)	589(2)	40(1)
O(1)	14305(1)	2775(1)	888(2)	53(1)
O(2)	13895(1)	4091(1)	-454(2)	45(1)

Silver Coordination Compounds with a Family of Ditopic Ligands of Varying Flexibility: About Chains, Rings, Helices and Polycatenanes

297

C(7)	14700(2)	3899(2)	-1260(3)	53(1)
C(8)	14413(2)	4370(2)	-2672(3)	59(1)
O(3)	14377(1)	5375(1)	-2467(2)	51(1)
C(9)	13912(2)	5873(2)	-3697(3)	56(1)
C(10)	13656(2)	6862(2)	-3280(3)	49(1)
O(4)	12823(1)	6776(1)	-2494(2)	46(1)
O(5)	12780(2)	8379(1)	-2286(3)	71(1)
C(11)	12472(2)	7594(2)	-2046(2)	43(1)
N(2)	10566(1)	6342(1)	-212(2)	36(1)
C(12)	10166(2)	7100(2)	377(2)	41(1)
C(13)	10482(2)	8025(2)	213(3)	46(1)
C(14)	11230(2)	8199(2)	-583(2)	44(1)
C(15)	11649(2)	7422(2)	-1199(2)	38(1)
C(16)	11294(2)	6508(1)	-988(2)	36(1)
N(3)	8839(2)	5756(1)	3013(2)	41(1)
O(6)	9438(1)	5503(2)	2207(2)	55(1)
O(7)	8418(2)	6535(2)	2831(3)	90(1)
O(8)	8715(3)	5228(2)	3988(3)	101(1)

Table 3.   Bond lengths [Å] and angles [°] for **19**.

Cu(1)-N(2)	2.0353(17)	O(2)-C(7)	1.448(3)
Cu(1)-N(2)#1	2.0353(17)	C(7)-C(8)	1.486(4)
Cu(1)-N(1)#1	2.0515(18)	C(8)-O(3)	1.413(3)
Cu(1)-N(1)	2.0515(18)	O(3)-C(9)	1.410(3)
N(1)-C(5)	1.334(3)	C(9)-C(10)	1.487(4)
N(1)-C(1)	1.348(3)	C(10)-O(4)	1.448(3)
C(1)-C(2)	1.374(3)	O(4)-C(11)	1.327(3)
C(2)-C(3)	1.372(4)	O(5)-C(11)	1.202(3)
C(3)-C(4)	1.387(3)	C(11)-C(15)	1.489(3)
C(4)-C(5)	1.382(3)	N(2)-C(16)	1.338(3)
C(4)-C(6)	1.483(3)	N(2)-C(12)	1.347(3)
C(6)-O(1)	1.208(3)	C(12)-C(13)	1.371(3)
C(6)-O(2)	1.325(3)	C(13)-C(14)	1.375(3)

C(14)-C(15)	1.390(3)	N(3)-O(7)	1.219(3)
C(15)-C(16)	1.383(3)	N(3)-O(6)	1.249(2)
N(3)-O(8)	1.218(3)		

N(2)-Cu(1)-N(2)#1	180.00(10)	O(3)-C(8)-C(7)	108.7(2)
N(2)-Cu(1)-N(1)#1	87.13(7)	C(9)-O(3)-C(8)	113.1(2)
N(2)#1-Cu(1)-N(1)#1	92.87(7)	O(3)-C(9)-C(10)	108.7(2)
N(2)-Cu(1)-N(1)	92.87(7)	O(4)-C(10)-C(9)	107.1(2)
N(2)#1-Cu(1)-N(1)	87.13(7)	C(11)-O(4)-C(10)	116.14(18)
N(1)#1-Cu(1)-N(1)	180.00(9)	O(5)-C(11)-O(4)	124.5(2)
C(5)-N(1)-C(1)	117.71(17)	O(5)-C(11)-C(15)	123.8(2)
C(5)-N(1)-Cu(1)	120.94(13)	O(4)-C(11)-C(15)	111.77(18)
C(1)-N(1)-Cu(1)	120.63(14)	C(16)-N(2)-C(12)	118.13(18)
N(1)-C(1)-C(2)	122.5(2)	C(16)-N(2)-Cu(1)	122.04(14)
C(3)-C(2)-C(1)	119.3(2)	C(12)-N(2)-Cu(1)	119.74(14)
C(2)-C(3)-C(4)	119.0(2)	N(2)-C(12)-C(13)	122.4(2)
C(5)-C(4)-C(3)	118.3(2)	C(12)-C(13)-C(14)	119.6(2)
C(5)-C(4)-C(6)	120.55(19)	C(13)-C(14)-C(15)	118.6(2)
C(3)-C(4)-C(6)	121.1(2)	C(16)-C(15)-C(14)	118.7(2)
N(1)-C(5)-C(4)	123.07(19)	C(16)-C(15)-C(11)	121.86(19)
O(1)-C(6)-O(2)	124.8(2)	C(14)-C(15)-C(11)	119.4(2)
O(1)-C(6)-C(4)	124.1(2)	N(2)-C(16)-C(15)	122.56(19)
O(2)-C(6)-C(4)	111.13(17)	O(8)-N(3)-O(7)	121.6(3)
C(6)-O(2)-C(7)	117.41(17)	O(8)-N(3)-O(6)	118.9(2)
O(2)-C(7)-C(8)	107.4(2)	O(7)-N(3)-O(6)	119.4(2)

Symmetry transformations used to generate equivalent atoms:

#1 -x+2,-y+1,-z

Table 4. Anisotropic displacement parameters ($\mathring{A}^2$x 10^3) for **19**. The anisotropic displacement factor exponent takes the form: $-2p^2[\,h^2a*^2U^{11} + ... + 2\,h\,k\,a*\,b*\,U^{12}\,]$

	U^{11}	U^{22}	U^{33}	U^{23}	U^{13}	U^{12}
Cu(1)	29(1)	36(1)	37(1)	4(1)	11(1)	0(1)
N(1)	33(1)	37(1)	34(1)	3(1)	8(1)	0(1)
C(1)	45(1)	41(1)	35(1)	2(1)	13(1)	1(1)
C(2)	59(1)	56(1)	37(1)	8(1)	10(1)	7(1)
C(3)	51(1)	51(1)	40(1)	8(1)	4(1)	12(1)
C(4)	37(1)	36(1)	39(1)	0(1)	5(1)	1(1)
C(5)	32(1)	45(1)	34(1)	2(1)	8(1)	2(1)
C(6)	37(1)	38(1)	44(1)	-4(1)	4(1)	2(1)
O(1)	50(1)	44(1)	65(1)	4(1)	10(1)	14(1)
O(2)	42(1)	46(1)	52(1)	2(1)	20(1)	11(1)
C(7)	48(1)	46(1)	70(2)	-7(1)	29(1)	7(1)
C(8)	72(2)	55(1)	58(2)	-13(1)	35(1)	-2(1)
O(3)	54(1)	53(1)	49(1)	-2(1)	13(1)	1(1)
C(9)	50(1)	81(2)	41(1)	1(1)	17(1)	2(1)
C(10)	37(1)	66(2)	47(1)	15(1)	14(1)	-4(1)
O(4)	40(1)	46(1)	55(1)	4(1)	21(1)	-6(1)
O(5)	83(1)	48(1)	91(2)	8(1)	41(1)	-16(1)
C(11)	44(1)	43(1)	41(1)	5(1)	7(1)	-8(1)
N(2)	35(1)	37(1)	36(1)	2(1)	10(1)	0(1)
C(12)	43(1)	43(1)	38(1)	-1(1)	10(1)	5(1)
C(13)	53(1)	41(1)	45(1)	-2(1)	9(1)	9(1)
C(14)	53(1)	33(1)	46(1)	1(1)	5(1)	1(1)
C(15)	40(1)	37(1)	35(1)	2(1)	4(1)	-2(1)
C(16)	36(1)	35(1)	37(1)	-1(1)	8(1)	-2(1)
N(3)	45(1)	42(1)	39(1)	-7(1)	12(1)	0(1)
O(6)	50(1)	75(1)	43(1)	-9(1)	19(1)	4(1)
O(7)	96(2)	73(1)	99(2)	-9(1)	7(1)	44(1)
O(8)	167(3)	75(2)	80(2)	13(1)	72(2)	-16(2)

Silver Coordination Compounds with a Family of Ditopic Ligands of Varying Flexibility:
About Chains, Rings, Helices and Polycatenanes

300

Table 5. Hydrogen coordinates (x 10^4) and isotropic displacement parameters (Å^2x 10^3) for **19**.

	x	y	z	U(eq)
H(1)	10833	4510	3052	48
H(2)	12187	3721	4361	61
H(3)	13509	3204	3261	57
H(5)	12120	4451	-329	44
H(7A)	14776	3211	-1378	63
H(7B)	15340	4155	-764	63
H(8A)	14910	4217	-3272	70
H(8B)	13753	4139	-3139	70
H(9A)	13298	5540	-4135	67
H(9B)	14371	5903	-4382	67
H(10A)	14241	7156	-2689	59
H(10B)	13457	7257	-4120	59
H(12)	9658	6992	916	49
H(13)	10192	8532	638	56
H(14)	11451	8822	-708	53
H(16)	11573	5989	-1402	43

Table 6. Hydrogen bond data [length (Å) and angle (°)] present in complex **19**

D–H···Acceptor	d (D–H)	d (H···A)	d (D···A)	< D–H···A
C7–H7B$^{\#1}$···O2	0.97	2.81(5)	3.59(0)	138.1(1)
C10–H10A$^{\#1}$···O1	0.97	2.35(9)	3.26(8)	156.4(1)
C7–H7A$^{\#2}$···O1	0.97	2.91(4)	3.54(1)	123.8(1)
C3–H3$^{\#2}$···O1	0.93	2.88(5)	3.68(9)	146.3(1)
C12–H12$^{\#3}$···O7	0.93	2.73(8)	3.64(7)	170.2(1)
C5–H5$^{\#3}$···O7	0.93	2.73(6)	3.43(1)	132.5(1)
C12–H12$^{\#3}$···O6	0.93	2.45(1)	3.08(0)	125.0(1)
C5–H5$^{\#3}$···O6	0.93	2.49(9)	3.12(1)	124.5(1)
C6–H16$^{\#3}$···O6	0.93	2.52(1)	3.11(0)	122.3(1)
C1–H1···O6	0.93	2.34(4)	3.02(2)	129.6(1)
C13–H13$^{\#4}$···O8	0.93	2.76(3)	3.28(9)	116.9(1)

Silver Coordination Compounds with a Family of Ditopic Ligands of Varying Flexibility: About Chains, Rings, Helices and Polycatenanes

301

C14–H14$^{\#4}$···O8	0.93	2.58(3)	3.19(1)	124.0(1)
C1–H1$^{\#5}$···O8	0.93	2.80(3)	3.31(8)	116.2(1)
C13–H13$^{\#5}$···O8	0.93	2.87(4)	3.44(0)	120.9(6)

Symmetry transformation used to generate equivalent atoms: #1 3-x, 1-y, -z #2 x, 0.5-y, 0.5+z #3 2-x, 1-y, -z #4 2-x, 0.5+y, 0.5-z #5 x, 1.5-y, -0.5+z

Crystal data and structure refinement for $\{[Cu(L4)]I\}_n$ (20)

Identification code	**20**
Empirical formula	C21.33 H21.33 Cu1.33 I1.33 N2.67 O6.67
Formula weight	675.66
Temperature	293(2) K
Wavelength	0.71073 Å
Crystal system	Monoclinic
Space group	P2$_1$/c
Unit cell dimensions	a = 19.125(4) Å a= 90°.
	b = 13.073(3) Å b= 99.57(3)°.
	c = 7.2767(15) Å g = 90°.
Volume	1794.0(6) Å^3
Z	3
Density (calculated)	1.876 Mg/m^3
Absorption coefficient	2.967 mm^{-1}
F(000)	992
Theta range for data collection	2.16 to 27.17°.
Index ranges	-20<=h<=24, -16<=k<=13, -9<=l<=7
Reflections collected	5708
Independent reflections	3428 [R(int) = 0.1445]
Completeness to theta = 27.17°	86.0 %
Refinement method	Full-matrix least-squares on F^2
Data / restraints / parameters	3428 / 0 / 226
Goodness-of-fit on F^2	0.920
Final R indices [I>2sigma(I)]	R1 = 0.0818, wR2 = 0.1738
R indices (all data)	R1 = 0.1969, wR2 = 0.2331
Largest diff. peak and hole	0.905 and -1.218 e.Å^{-3}

Table 2. Atomic coordinates (x 10^4) and equivalent isotropic displacement parameters (Å^{2}x 10^3) for **20**. U(eq) is

defined as one third of the trace of the orthogonalized U^{ij} tensor.

	x	y	z	U(eq)
Cu(1)	3085(1)	8281(2)	4530(3)	43(1)
I(1)	3273(1)	8528(1)	8142(2)	40(1)
N(1)	3744(7)	9352(10)	3550(20)	36(3)
C(1)	3589(8)	10345(11)	3690(20)	32(4)
C(2)	4056(8)	11077(12)	3210(20)	35(4)
C(3)	4681(10)	10793(14)	2600(30)	51(6)
C(4)	4839(10)	9770(14)	2460(30)	47(5)
C(5)	4324(10)	9055(13)	2970(20)	39(4)
C(6)	3901(9)	12204(11)	3310(30)	39(5)
O(1)	4310(8)	12850(10)	2950(30)	68(5)
O(2)	3245(6)	12373(8)	3712(18)	41(3)
C(7)	3076(10)	13479(13)	3660(30)	48(5)
C(8)	2347(10)	13561(15)	4190(30)	49(5)
O(3)	1813(7)	13175(9)	2740(20)	51(4)
C(9)	1626(10)	13822(16)	1190(30)	58(6)
C(10)	970(9)	13460(20)	10(30)	63(6)
O(4)	390(7)	13609(13)	1090(20)	68(4)
O(5)	-382(9)	13597(17)	-1540(20)	88(6)
C(11)	-270(10)	13647(15)	100(30)	46(5)
N(2)	-2034(9)	13710(11)	1564(19)	47(4)
C(12)	-1876(11)	13895(14)	3380(30)	49(5)
C(13)	-1188(12)	14020(20)	4280(30)	69(7)
C(14)	-634(10)	13957(16)	3230(30)	58(6)
C(15)	-804(10)	13754(12)	1390(20)	40(5)
C(16)	-1504(10)	13623(15)	530(20)	47(5)

Table 3.   Bond lengths [Å] and angles [°] for **20**.

Cu(1)-N(1)	2.089(15)	I(1)-Cu(1)#3	2.620(3)
Cu(1)-N(2)#1	2.110(15)	N(1)-C(5)	1.31(2)
Cu(1)-I(1)	2.613(3)	N(1)-C(1)	1.34(2)
Cu(1)-I(1)#2	2.620(3)	C(1)-C(2)	1.39(2)

Silver Coordination Compounds with a Family of Ditopic Ligands of Varying Flexibility:
About Chains, Rings, Helices and Polycatenanes

303

C(2)-C(3)	1.39(3)	C(10)-O(4)	1.47(3)
C(2)-C(6)	1.51(2)	O(4)-C(11)	1.35(2)
C(3)-C(4)	1.38(3)	O(5)-C(11)	1.18(2)
C(4)-C(5)	1.45(3)	C(11)-C(15)	1.51(3)
C(6)-O(1)	1.21(2)	N(2)-C(12)	1.33(2)
C(6)-O(2)	1.35(2)	N(2)-C(16)	1.36(3)
O(2)-C(7)	1.481(19)	N(2)-Cu(1)#4	2.110(15)
C(7)-C(8)	1.51(3)	C(12)-C(13)	1.38(3)
C(8)-O(3)	1.43(2)	C(13)-C(14)	1.41(3)
O(3)-C(9)	1.41(2)	C(14)-C(15)	1.35(3)
C(9)-C(10)	1.48(2)	C(15)-C(16)	1.39(2)
N(1)-Cu(1)-N(2)#1	106.5(6)	C(6)-O(2)-C(7)	111.1(13)
N(1)-Cu(1)-I(1)	105.7(4)	O(2)-C(7)-C(8)	105.6(15)
N(2)#1-Cu(1)-I(1)	108.0(5)	O(3)-C(8)-C(7)	111.4(16)
N(1)-Cu(1)-I(1)#2	110.1(4)	C(9)-O(3)-C(8)	115.5(15)
N(2)#1-Cu(1)-I(1)#2	106.1(4)	O(3)-C(9)-C(10)	110.5(18)
I(1)-Cu(1)-I(1)#2	119.68(8)	O(4)-C(10)-C(9)	107.0(17)
Cu(1)-I(1)-Cu(1)#3	105.73(6)	C(11)-O(4)-C(10)	116.1(15)
C(5)-N(1)-C(1)	121.5(16)	O(5)-C(11)-O(4)	123(2)
C(5)-N(1)-Cu(1)	120.2(11)	O(5)-C(11)-C(15)	127.7(17)
C(1)-N(1)-Cu(1)	118.0(13)	O(4)-C(11)-C(15)	109.8(16)
N(1)-C(1)-C(2)	119.3(17)	C(12)-N(2)-C(16)	119.8(16)
C(1)-C(2)-C(3)	121.0(16)	C(12)-N(2)-Cu(1)#4	118.0(15)
C(1)-C(2)-C(6)	121.5(17)	C(16)-N(2)-Cu(1)#4	121.2(10)
C(3)-C(2)-C(6)	117.5(15)	N(2)-C(12)-C(13)	122(2)
C(4)-C(3)-C(2)	119.5(19)	C(12)-C(13)-C(14)	119.0(19)
C(3)-C(4)-C(5)	116.0(19)	C(15)-C(14)-C(13)	118.0(16)
N(1)-C(5)-C(4)	122.6(15)	C(14)-C(15)-C(16)	122(2)
O(1)-C(6)-O(2)	126.1(15)	C(14)-C(15)-C(11)	124.2(16)
O(1)-C(6)-C(2)	122.2(18)	C(16)-C(15)-C(11)	114.0(15)
O(2)-C(6)-C(2)	111.5(13)	N(2)-C(16)-C(15)	119.3(16)

Symmetry transformations used to generate equivalent atoms:

#1 -x,y-1/2,-z+1/2   #2 x,-y+3/2,z-1/2   #3 x,-y+3/2,z+1/2   #4 -x,y+1/2,-z+1/2

Table 4. Anisotropic displacement parameters (Å^2x 10^3) for **20**. The anisotropic displacement factor exponent takes the form: $-2p^2[\ h^2a^{*2}U^{11} + ... + 2\ h\ k\ a^*\ b^*\ U^{12}\ ]$

	U^{11}	U^{22}	U^{33}	U^{23}	U^{13}	U^{12}
Cu(1)	43(1)	39(1)	47(1)	1(1)	9(1)	0(1)
I(1)	46(1)	36(1)	38(1)	-1(1)	9(1)	-2(1)
N(1)	32(7)	33(7)	44(8)	-4(6)	10(7)	1(6)
C(1)	24(7)	30(8)	41(9)	-1(6)	-2(7)	4(7)
C(2)	19(7)	43(9)	42(9)	4(7)	1(7)	-19(7)
C(3)	32(9)	47(10)	69(13)	13(9)	-8(10)	-1(8)
C(4)	37(9)	59(12)	44(9)	1(8)	1(9)	20(9)
C(5)	57(12)	34(9)	28(8)	-4(6)	11(8)	5(8)
C(6)	30(9)	14(7)	70(12)	4(7)	3(9)	-10(6)
O(1)	48(8)	40(8)	124(14)	-10(8)	36(9)	-4(6)
O(2)	32(6)	26(5)	61(7)	3(5)	1(6)	4(5)
C(7)	49(10)	29(8)	67(11)	8(9)	9(9)	10(8)
C(8)	44(10)	47(10)	61(11)	-9(10)	21(9)	24(10)
O(3)	37(7)	51(7)	64(8)	23(6)	3(7)	6(6)
C(9)	36(10)	63(13)	78(14)	15(10)	19(11)	-7(9)
C(10)	21(8)	130(20)	45(10)	-1(13)	12(8)	6(12)
O(4)	39(7)	100(11)	61(8)	8(9)	-3(7)	6(9)
O(5)	57(10)	165(18)	41(7)	19(10)	5(8)	15(12)
C(11)	37(10)	48(11)	55(11)	1(9)	15(9)	17(9)
N(2)	59(10)	45(9)	33(7)	-11(6)	-6(8)	2(7)
C(12)	42(11)	57(11)	52(11)	-2(8)	19(10)	1(8)
C(13)	53(14)	113(19)	37(10)	2(11)	-8(11)	24(13)
C(14)	27(9)	80(14)	60(13)	-20(10)	-13(10)	7(9)
C(15)	41(10)	35(9)	37(8)	4(7)	-12(9)	-2(7)
C(16)	46(10)	52(10)	42(9)	-11(9)	4(9)	5(10)

Silver Coordination Compounds with a Family of Ditopic Ligands of Varying Flexibility: About Chains, Rings, Helices and Polycatenanes

305

Table 5. Hydrogen coordinates (x 10^4) and isotropic displacement parameters (Å^2x 10^3) for **20**.

	x	y	z	U(eq)
H(1)	3174	10543	4098	39
H(3)	4990	11290	2294	61
H(4)	5252	9551	2066	57
H(5)	4408	8358	2880	47
H(7A)	3076	13754	2421	58
H(7B)	3421	13852	4537	58
H(8A)	2337	13179	5326	59
H(8B)	2247	14272	4426	59
H(9A)	2008	13835	465	69
H(9B)	1557	14513	1614	69
H(10A)	879	13848	-1138	76
H(10B)	1012	12743	-290	76
H(12)	-2242	13943	4076	59
H(13)	-1090	14136	5553	83
H(14)	-165	14056	3783	69
H(16)	-1609	13477	-737	56

Table 6. Hydrogen bond [length (Å) and angle (°)] present in complex **20**

D–H···Acceptor	d (D–H)	d (H···A)	d (D···A)	< D–H···A
C4–H4$^{\#2}$···O1	0.93	2.37(7)	3.03(2)	127.3(1)
C5–H5$^{\#2}$···O1	0.93	2.70(2)	3.21(5)	115.5(6)
C8–H8A$^{\#3}$···O2	0.97	2.86(1)	3.66(0)	140.2(8)
C8–H8A$^{\#3}$···O3	0.97	2.79(5)	3.71(0)	157.4(3)
C10–H10B$^{\#4}$···O3	0.97	2.56(1)	3.28(3)	131.2(8)
C13–H13···O5	0.93	2.41(9)	3.22(2)	144.5(7)

Symmetry transformation used to generate equivalent atoms: #2 1-x, -0.5+y, 0.5-z #3 x, -2.5+y, -0.5+z #4 x, 2.5-y, 0.5+z

Bibliography

1. Fromm, K.M., Gueneau, E.D., Robin, A.Y., Maudez, W., Sague, J. and Bergougnant, R., *Zeitschrift fuer Anorganische und Allgemeine Chemie.* 2005. **631**(10): p. 1725-1740.
2. Fromm, K.M., Doimeadios, J.L.S. and Robin, A.Y., *Chemical Communications (Cambridge, United Kingdom).* 2005(36): p. 4548-4550.
3. Robin, A.Y., Sague, J.L. and Fromm, K.M., *CrystEngComm.* 2006. **8**(5): p. 403-416.
4. Sague, J.L. and Fromm, K.M., *Crystal Growth & Design.* 2006. **6**(7): p. 1566-1568.
5. Lehn, J.M. and Montavon, F., *Tetrahedron Letters.* 1972(44): p. 4557-60.
6. Lehn, J.M. and Stubbs, M.E., *Journal of the American Chemical Society.* 1974. **96**(12): p. 4011-12.
7. Lehn, J.M., *Neurosciences Research Program bulletin.* 1976. **14**(2): p. 133-7.
8. Dietrich, B., Lehn, J.M. and Sauvage, J.P., *Tetrahedron Letters.* 1969(34): p. 2889-92.
9. Dietrich, B., Lehn, J.M. and Sauvage, J.P., *Journal of the Chemical Society, Chemical Communications.* 1973(1): p. 15-16.
10. Behr, J.P. and Lehn, J.M., *Journal of the American Chemical Society.* 1973. **95**(18): p. 6108-10.
11. Behr, J.P., Girodeau, J.M., Hayward, R.C., Lehn, J.M. and Sauvage, J.P., *Helvetica Chimica Acta.* 1980. **63**(7): p. 2096-111.
12. Cheney, J., Lehn, J.M., Sauvage, J.P. and Stubbs, M.E., *Journal of the Chemical Society, Chemical Communications.* 1972(19): p. 1100-1.
13. Dietrich, B., Lehn, J.M. and Sauvage, J.P., *Tetrahedron.* 1973. **29**(11): p. 1647-58.
14. Lehn, J.M. and Sauvage, J.P., *Journal of the American Chemical Society.* 1975. **97**(23): p. 6700-7.
15. Cheney, J. and Lehn, J.M., *Journal of the Chemical Society, Chemical Communications.* 1972(8): p. 487-9.
16. Constable, E.C., *Progress in Inorganic Chemistry.* 1994. **42**: p. 67-138.
17. Constable, E.C., Edwards, A.J., Marcos, M.D., Raithby, P.R., Martinez-Manez, R. and Tendero, M.J.L., *Inorganica Chimica Acta.* 1994. **224**(1-2): p. 11-14.
18. Constable, E., *Chemistry & Industry (London, United Kingdom).* 1994(2): p. 56-9.
19. Lehn, J.M. and Rigault, A., *Angewandte Chemie.* 1988. **100**(8): p. 1121-2.
20. Lehn, J.M., *Angewandte Chemie.* 1990. **102**(11): p. 1347-62 (See also Angew Chem , Int Ed Engl , 1990, 29(11), 1304-19).
21. Garrett, T.M., Koert, U., Lehn, J.M., Rigault, A., Meyer, D. and Fischer, J., *Journal of the Chemical Society, Chemical Communications.* 1990(7): p. 557-8.
22. Lehn, J.M., *Supramolecular Chemistry: Concepts and Perspectives*. 1995. approx 262 pp.
23. Lehn, J.M., *Org. Chem.: Its Lang. Its State of the Art.* 1993: p. 77-89.
24. Brooks, N.R., Blake, A.J., Champness, N.R., Cunningham, J.W., Hubberstey, P., Teat, S.J., Wilson, C. and Schroeder, M., *Journal of the Chemical Society, Dalton Transactions.* 2001(17): p. 2530-2538.

25. Withersby, M.A., Blake, A.J., Champness, N.R., Hubberstey, P., Li, W.-S. and Schroder, M., *Angewandte Chemie, International Edition in English.* 1997. **36**(21): p. 2327-2329.

26. Long, D.-L., Hill, R.J., Blake, A.J., Champness, N.R., Hubberstey, P., Wilson, C. and Schroeder, M., *Chemistry--A European Journal.* 2005. **11**(5): p. 1384-1391.

27. Khlobystov, A.N., Champness, N.R., Roberts, C.J., Tendler, S.J.B., Thompson, C. and Schroeder, M., *CrystEngComm.* 2002. **4**: p. 426-431.

28. Kim, H.-J., Zin, W.-C. and Lee, M., *Journal of the American Chemical Society.* 2004. **126**(22): p. 7009-7014.

29. Ren, Y.-P., Kong, X.-J., Long, L.-S., Huang, R.-B. and Zheng, L.-S., *Crystal Growth & Design.* 2006. **6**(2): p. 572-576.

30. Elliott, E.L., Hernandez, G.A., Linden, A. and Siegel, J.S., *Organic & Biomolecular Chemistry.* 2005. **3**(3): p. 407-413.

31. Steel, P.J. and Sumby, C.J., *Inorganic Chemistry Communications.* 2002. **5**(5): p. 323-327.

32. Burchell, T.J., Eisler, D.J. and Puddephatt, R.J., *Crystal Growth & Design.* p. ACS ASAP.

33. Silva, R.M., Smith, M.D. and Gardinier, J.R., *Inorganic Chemistry.* 2006. **45**(5): p. 2132-2142.

34. Taylor, R. and Kennard, O., *Journal of the American Chemical Society.* 1982. **104**(19): p. 5063-70.

35. Aakeroy, C.B. and Seddon, K.R., *Chemical Society Reviews.* 1993. **22**(6): p. 397-407.

36. Barnes, A.J., *Journal of Molecular Structure.* 2004. **704**(1-3): p. 3-9.

37. Beatty, A.M., *CrystEngComm.* 2001: p. Paper No 51, No pp given, Paper No 51.

38. Bernstein, J., Davis, R.E., Shimoni, L. and Chang, N.-L., *Angewandte Chemie, International Edition in English.* 1995. **34**(15): p. 1555-73.

39. Brammer, L., *Perspectives in Supramolecular Chemistry.* 2003. **7**(Crystal Design): p. 1-75.

40. Burrows, A.D., *Structure and Bonding (Berlin, Germany).* 2004. **108**(Supramolecular Assembly via Hydrogen Bonds I): p. 55-96.

41. Desiraju, G.R., *Chemical Communications (Cambridge, United Kingdom).* 2005(24): p. 2995-3001.

42. Hobza, P. and Havlas, Z., *Chemical Reviews (Washington, D. C.).* 2000. **100**(11): p. 4253-4264.

43. Jeffrey, G.A., *Journal of Molecular Structure.* 1999. **485-486**: p. 293-298.

44. King, G.S.D., *Intermol. Forces.* 1991: p. 451-8.

45. Steiner, T., *Crystallography Reviews.* 1996. **6**(1): p. 1-51.

46. Sarkhel, S. and Desiraju, G.R., *Proteins: Structure, Function, and Bioinformatics.* 2003. **54**(2): p. 247-259.

47. Steiner, T., *Chemical Communications (Cambridge).* 1997(8): p. 727-734.

48. Steiner, T., *Crystallography Reviews.* 2003. **9**(2-3): p. 177-228.

49. Videnova-Adrabinska, V.G., *Prace Naukowe Instytutu Chemii Nieorganicznej i Metalurgii Pierwiastkow Rzadkich Politechniki Wroclawskiej.* 1994. **65**: p. 250 PP.

50. Wahl, M.C. and Sundaralingam, M., *Trends in Biochemical Sciences.* 1997. **22**(3): p. 97-102.

51. Yang, H., Wang, C. and Wang, B., *Huaxue Yu Nianhe.* 2003(4): p. 186-189.

52. Mascal, M., Kerdelhue, J.-L., Blake, A.J., Cooke, P.A., Mortimer, R.J. and Teat, S.J., *European Journal of Inorganic Chemistry.* 2000(3): p. 485-490.

53. Munakata, M., Zhong, J.C., Kuroda-Sowa, T., Maekawa, M., Suenaga, Y., Kasahara, M. and Konaka, H., *Inorganic Chemistry.* 2001. **40**(27): p. 7087-7090.

54.   Hunter, C.A. and Sanders, J.K.M., *Journal of the American Chemical Society.* 1990. **112**(14): p. 5525-34.
55.   Aakeroy, C.B., Evans, T.A. and Seddon, K.R., *NATO ASI Series, Series C: Mathematical and Physical Sciences.* 1997. **499**(Modular Chemistry): p. 153-162.
56.   Janiak, C., *Dalton.* 2000(21): p. 3885-3896.
57.   Singh, K., Long, J.R. and Stavropoulos, P., *Journal of the American Chemical Society.* 1997. **119**(12): p. 2942-2943.
58.   Tong, M.-L., Chen, X.-M., Ye, B.-H. and Ji, L.-N., *Angewandte Chemie, International Edition.* 1999. **38**(15): p. 2237-2240.
59.   Pyykko, P. and Mendizabal, F., *Chemistry--A European Journal.* 1997. **3**(9): p. 1458-1465.
60.   Pyykko, P., Runeberg, N. and Mendizabal, F., *Chemistry--A European Journal.* 1997. **3**(9): p. 1451-1457.
61.   Fernandez, E.J., Laguna, A., Lopez-De-Luzuriaga, J.M., Monge, M., Pyykko, P. and Runeberg, N., *European Journal of Inorganic Chemistry.* 2002(3): p. 750-753.
62.   Doll, K., Pyykko, P. and Stoll, H., *Journal of Chemical Physics.* 1998. **109**(6): p. 2339-2345.
63.   Andrews, L.J. and Keefer, R.M., *Journal of the American Chemical Society.* 1949. **71**: p. 3644-7.
64.   Andrews, L.J. and Keefer, R.M., *Journal of the American Chemical Society.* 1950. **72**: p. 5034-7.
65.   Ferey, G. and Cheetham, A.K., *Science (Washington, D. C.).* 1999. **283**(5405): p. 1125-1126.
66.   Gravereau, P., Garnier, E. and Hardy, A., *Acta Crystallographica, Section B: Structural Crystallography and Crystal Chemistry.* 1979. **B35**(12): p. 2843-8.
67.   Moulton, B. and Zaworotko, M.J., *Chemical Reviews (Washington, D. C.).* 2001. **101**(6): p. 1629-1658.
68.   Zaworotko, M.J., *Angewandte Chemie, International Edition.* 2000. **39**(17): p. 3052-3054.
69.   Eddaoudi, M., Moler, D.B., Li, H., Chen, B., Reineke, T.M., O'Keeffe, M. and Yaghi, O.M., *Accounts of Chemical Research.* 2001. **34**(4): p. 319-330.
70.   Kim, J., Chen, B., Reineke, T.M., Li, H., Eddaoudi, M., Moler, D.B., O'Keeffe, M. and Yaghi, O.M., *Journal of the American Chemical Society.* 2001. **123**(34): p. 8239-8247.
71.   Zaworotko, M.J., *Nature (London).* 1999. **402**(6759): p. 242-243.
72.   Janiak, C., *Angewandte Chemie, International Edition in English.* 1997. **36**(13/14): p. 1431-1434.
73.   Hoskins, B.F. and Robson, R., *Journal of the American Chemical Society.* 1989. **111**(15): p. 5962-4.
74.   Hoskins, B.F. and Robson, R., *Journal of the American Chemical Society.* 1990. **112**(4): p. 1546-54.
75.   Abrahams, B.F., Hoskins, B.F., Michall, D.M. and Robson, R., *Nature (London, United Kingdom).* 1994. **369**(6483): p. 727-9.
76.   Abrahams, B.F., Hardie, M.J., Hoskins, B.F., Robson, R. and Sutherland, E.E., *Journal of the Chemical Society, Chemical Communications.* 1994(9): p. 1049-50.
77.   Venkataraman, D., Gardner, G.B., Lee, S. and Moore, J.S., *Journal of the American Chemical Society.* 1995. **117**(46): p. 11600-1.
78.   Yaghi, O.M., Li, G. and Li, H., *Nature (London).* 1995. **378**(6558): p. 703-6.
79.   Yaghi, O.M. and Li, H., *Journal of the American Chemical Society.* 1995. **117**(41): p. 10401-2.

80. Subramanian, S. and Zaworotko, M.J., *Angewandte Chemie, International Edition in English.* 1995. **34**(19): p. 2127-9.

81. James, S.L., *Chemical Society Reviews.* 2003. **32**(5): p. 276-288.

82. Kepert, C.J., *Chemical Communications (Cambridge, United Kingdom).* 2006(7): p. 695-700.

83. Lozano, E., Nieuwenhuyzen, M. and James, S.L., *Chemistry (Weinheim an der Bergstrasse, Germany).* 2001. **7**(12): p. 2644-51.

84. Yaghi, O.M. and Li, H., *Journal of the American Chemical Society.* 1996. **118**(1): p. 295-6.

85. Yaghi, O.M., Li, H. and Groy, T.L., *Inorganic Chemistry.* 1997. **36**(20): p. 4292-4293.

86. Gable, R.W., Hoskins, B.F. and Robson, R., *Journal of the Chemical Society, Chemical Communications.* 1990(10): p. 762-3.

87. Biradha, K., Domasevitch, K.V., Moulton, B., Seward, C. and Zaworotko, M.J., *Chemical Communications (Cambridge).* 1999(14): p. 1327-1328.

88. MacGillivray, L.R., Subramanian, S. and Zaworotko, M.J., *Journal of the Chemical Society, Chemical Communications.* 1994(11): p. 1325-6.

89. Carlucci, L., Ciani, G., Proserpio, D.M. and Sironi, A., *Journal of the Chemical Society, Chemical Communications.* 1994(24): p. 2755-6.

90. Blake, A.J., Champness, N.R., Khlobystov, A.N., Lemenovskii, D.A., Li, W.-S. and Schroder, M., *Chemical Communications (Cambridge).* 1997(15): p. 1339-1340.

91. Blake, A.J., Champness, N.R., Hubberstey, P., Li, W.-S., Withersby, M.A. and Schroder, M., *Coordination Chemistry Reviews.* 1999. **183**: p. 117-138.

92. Xu, X., Nieuwenhuyzen, M. and James, S.L., *Angewandte Chemie, International Edition.* 2002. **41**(5): p. 764-767.

93. Uemura, K., Kitagawa, S., Kondo, M., Fukui, K., Kitaura, R., Chang, H.-C. and Mizutani, T., *Chemistry--A European Journal.* 2002. **8**(16): p. 3586-3600.

94. Carlucci, L., Ciani, G., Moret, M., Proserpio, D.M. and Rizzato, S., *Angewandte Chemie, International Edition.* 2000. **39**(8): p. 1506-1510.

95. Tabares, L.C., Navarro, J.A.R. and Salas, J.M., *Journal of the American Chemical Society.* 2001. **123**(3): p. 383-387.

96. Uemura, K., Kitagawa, S., Fukui, K. and Saito, K., *Journal of the American Chemical Society.* 2004. **126**(12): p. 3817-3828.

97. Maspoch, D., Ruiz-Molina, D., Wurst, K., Domingo, N., Cavallini, M., Biscarini, F., Tejada, J., Rovira, C. and Veciana, J., *Nature Materials.* 2003. **2**(3): p. 190-195.

98. Jung, O.-S., Kim, Y.J., Lee, Y.-A., Park, J.K. and Chae, H.K., *Journal of the American Chemical Society.* 2000. **122**(41): p. 9921-9925.

99. Muthu, S., Yip, J.H.K. and Vittal, J.J., *Journal of the Chemical Society, Dalton Transactions.* 2002(24): p. 4561-4568.

100. Kitaura, R., Fujimoto, K., Noro, S.-i., Kondo, M. and Kitagawa, S., *Angewandte Chemie, International Edition.* 2002. **41**(1): p. 133-135.

101. Kitaura, R., Seki, K., Akiyama, G. and Kitagawa, S., *Angewandte Chemie, International Edition.* 2003. **42**(4): p. 428-431.

102. Kepert, C.J., Prior, T.J. and Rosseinsky, M.J., *Journal of the American Chemical Society.* 2000. **122**(21): p. 5158-5168.

103. Makinen, S.K., Melcer, N.J., Parvez, M. and Shimizu, G.K., *Chemistry (Weinheim an der Bergstrasse, Germany).* 2001. **7**(23): p. 5176-82.

104.   Biradha, K. and Fujita, M., *Angewandte Chemie, International Edition.* 2002. **41**(18): p. 3392-3395.

105.   Alberti, G., Murcia-Mascaros, S. and Vivani, R., *Journal of the American Chemical Society.* 1998. **120**(36): p. 9291-9295.

106.   Serre, C., Millange, F., Thouvenot, C., Nogues, M., Marsolier, G., Loueer, D. and Ferey, G., *Journal of the American Chemical Society.* 2002. **124**(45): p. 13519-13526.

107.   Lu, J.Y. and Babb, A.M., *Chemical Communications (Cambridge, United Kingdom).* 2002(13): p. 1340-1341.

108.   Edgar, M., Mitchell, R., Slawin, A.M.Z., Lightfoot, P. and Wright, P.A., *Chemistry--A European Journal.* 2001. **7**(23): p. 5168-5175.

109.   Cai, J., Zhou, J.-S. and Lin, M.-L., *Journal of Materials Chemistry.* 2003. **13**(7): p. 1806-1811.

110.   Takamizawa, S., Nakata, E.-i., Yokoyama, H., Mochizuki, K. and Mori, W., *Angewandte Chemie, International Edition.* 2003. **42**(36): p. 4331-4334.

111.   Yildirim, T. and Hartman, M.R., *Physical Review Letters.* 2005. **95**(21): p. 215504/1-215504/4.

112.   Rosseinsky, M.J., *Microporous and Mesoporous Materials.* 2004. **73**(1-2): p. 15-30.

113.   Fletcher, A.J., Thomas, K.M. and Rosseinsky, M.J., *Journal of Solid State Chemistry.* 2005. **178**(8): p. 2491-2510.

114.   Kitagawa, S. and Uemura, K., *Chemical Society Reviews.* 2005. **34**(2): p. 109-119.

115.   Cortez, S.M. and Raptis, R.G., *Coordination Chemistry Reviews.* 1997. **162**: p. 495-538.

116.   Cortez, S.M. and Raptis, R.G., *Coordination Chemistry Reviews.* 1998. **169**: p. 363-426.

117.   Khlobystov, A.N., Blake, A.J., Champness, N.R., Lemenovskii, D.A., Majouga, A.G., Zyk, N.V. and Schroder, M., *Coordination Chemistry Reviews.* 2001. **222**: p. 155-192.

118.   Feazell, R.P., Carson, C.E. and Klausmeyer, K.K., *Inorganic Chemistry.* 2006. **45**(6): p. 2627-2634.

119.   Schultheiss, N., Powell, D.R. and Bosch, E., *Inorganic Chemistry.* 2003. **42**(26): p. 8886-8890.

120.   Lozano, E., Nieuwenhuyzen, M. and James, S.L., *Chemistry--A European Journal.* 2001. **7**(12): p. 2644-2651.

121.   Sampanthar, J.T. and Vittal, J.J., *Crystal Engineering.* 2000. **3**(2): p. 117-133.

122.   Suenaga, Y., Kuroda-Sowa, T., Maekawa, M. and Munakata, M., *Acta Crystallographica, Section C: Crystal Structure Communications.* 1999. **C55**(10): p. 1623-1625.

123.   Feazell Rodney, P., Carson Cody, E. and Klausmeyer Kevin, K., *Inorganic chemistry.* 2006. **45**(2): p. 935-44.

124.   Schultheiss, N., Powell Douglas, R. and Bosch, E., *Inorganic chemistry.* 2003. **42**(26): p. 8886-90.

125.   Suenaga, Y., Kuroda-Sowa, T., Maekawa, M. and Munakata, M., *Dalton.* 2000(20): p. 3620-3623.

126.   Silva Rosalice, M., Smith Mark, D. and Gardinier James, R., *Inorganic chemistry.* 2006. **45**(5): p. 2132-42.

127.   Ozin, G.A., Mattar, S.M. and McIntosh, D.F., *Journal of the American Chemical Society.* 1984. **106**(25): p. 7765-76.

128.   Mak, T.C.W., Ho, W.C. and Huang, N.Z., *Journal of Organometallic Chemistry.* 1983. **251**(3): p. 413-21.

129.   Aly, A.A.M., Neugebauer, D., Orama, O., Schubert, U. and Schmidbaur, H., *Angewandte Chemie.* 1978. **90**(2): p. 125-6.

130.   Hanton, L.R. and Young, A.G., *Crystal Growth & Design.* 2006. **6**(4): p. 833-835.

131. Chowdhury, S., Drew, M.G.B. and Datta, D., *New Journal of Chemistry.* 2003. **27**(5): p. 831-835.
132. Blake, A.J., Champness, N.R., Cooke, P.A., Nicolson, J.E.B. and Wilson, C., *Dalton.* 2000(21): p. 3811-3819.
133. Xie, Y.-B. and Bu, X.-H., *Journal of Cluster Science.* 2004. **14**(4): p. 471-482.
134. Jenkins, H.D.B., Roobottom, H.K., Passmore, J. and Glasser, L., *Inorganic Chemistry.* 1999. **38**(16): p. 3609-3620.
135. Krossing, I. and Raabe, I., *Chemistry--A European Journal.* 2004. **10**(20): p. 5017-5030.
136. Awaleh, M.O., Badia, A. and Brisse, F., *Crystal Growth & Design.* 2005. **5**(5): p. 1897-1906.
137. Feazell, R.P., Carson, C.E. and Klausmeyer, K.K., *Inorganic Chemistry.* 2006. **45**(2): p. 935-944.
138. Oxtoby, N.S., Blake, A.J., Champness, N.R. and Wilson, C., *Proceedings of the National Academy of Sciences of the United States of America.* 2002. **99**(8): p. 4905-4910.
139. Sague, J.L., *Journal.* 2006(Issue).
140. Brandys, M.-C. and Puddephatt, R.J., *Chemical Communications (Cambridge, United Kingdom).* 2001(16): p. 1508-1509.
141. Venkataraman, D., Lee, S., Moore, J.S., Zhang, P., Hirsch, K.A., Gardner, G.B., Covey, A.C. and Prentice, C.L., *Chemistry of Materials.* 1996. **8**(8): p. 2030-2040.
142. Awaleh Mohamed, O., Badia, A. and Brisse, F., *Inorganic chemistry.* 2005. **44**(22): p. 7833-45.
143. Bu, X.-H., Xie, Y.-B., Li, J.-R. and Zhang, R.-H., *Inorganic Chemistry.* 2003. **42**(23): p. 7422-7430.
144. Reger, D.L., Semeniuc, R.F. and Smith, M.D., *European Journal of Inorganic Chemistry.* 2003(18): p. 3480-3494.
145. Constable, E.C., Housecroft, D.F.C.E. and Kulke, T., *Chemical Communications (Cambridge).* 1998(23): p. 2659-2660.
146. Pocic, D., *Journal.* 2005(Issue): p. 226.
147. Song, L.-C., Zhang, W.-X. and Hu, Q.-M., *Chinese Journal of Chemistry.* 2002. **20**(11): p. 1421-1429.
148. Song, L.-C., Zhang, W.-X., Wang, J.-Y. and Hu, Q.-M., *Transition Metal Chemistry (Dordrecht, Netherlands).* 2002. **27**(5): p. 526-531.
149. Zhang, H., Wang, X., Zhang, K. and Teo, B.K., *Coordination Chemistry Reviews.* 1999. **183**: p. 157-195.
150. Zhang, H., Wang, X. and Teo, B.K., *Journal of the American Chemical Society.* 1996. **118**(47): p. 11813-11821.
151. Yao, Z.Q., Liu, P., Yan, R.Z., Liu, L.Y., Liu, X.H. and Wang, W.C., *Thin Solid Films.* 1992. **210-211**(1-2): p. 208-10.
152. Yuan, Q. and Liu, B., *Bulletin of the Korean Chemical Society.* 2005. **26**(10): p. 1575-1578.
153. Liu, B. and Yuan, Q., *Inorganic Chemistry Communications.* 2005. **8**(11): p. 1022-1024.
154. Yan, Z.-Q., *Jiegou Huaxue.* 2005. **24**(3): p. 315-318.
155. Cova, B., Briceno, A. and Atencio, R., *New Journal of Chemistry.* 2001. **25**(12): p. 1516-1519.
156. Burrows, A.D., Mahon, M.F. and Palmer, M.T., *Journal of the Chemical Society, Dalton Transactions: Inorganic Chemistry.* 1998(12): p. 1941-1942.
157. Luo, C., Zhang, Y., Zeng, X., Zeng, Y. and Wang, Y., *Journal of Colloid and Interface Science.* 2005. **288**(2): p. 444-448.

Silver Coordination Compounds with a Family of Ditopic Ligands of Varying Flexibility: About Chains, Rings, Helices and Polycatenanes

312

158. Mallick, K., Witcomb, M.J. and Scurrell, M.S., *Materials Chemistry and Physics.* 2005. **90**(2-3): p. 221-224.

159. Jouaiti, A., Hosseini, M.W. and Kyritsakas, N., *Chemical Communications (Cambridge, United Kingdom).* 2003(4): p. 472-473.

160. van Veggel, F.C.J.M., Verboom, W. and Reinhoud, D.N., *Chemical reviews.* 1994. **94**(2): p. 279-299.

161. Robin, A.Y., Meuwly, M., Fromm, K.M., Goesmann, H. and Bernardinelli, G., *CrystEngComm.* 2004. **6**: p. 336-343.

162. Robin, A., *Journal.* 2005(Issue): p. 248.

163. Robin, A.Y., Fromm, K.M., Goesmann, H. and Bernardinelli, G., *CrystEngComm.* 2003. **5**: p. 405-410.

164. Fromm Katharina, M., Doimeadios Jorge, L.S. and Robin Adeline, Y., *Chemical communications (Cambridge, England).* 2005(36): p. 4548-50.

165. Moret, M., Campione, M., Borghesi, A., Miozzo, L., Sassella, A., Trabattoni, S., Lotz, B. and Thierry, A., *Journal of Materials Chemistry.* 2005. **15**(25): p. 2444-2449.

166. Kuleshova, L.N., Antipin, M.Y., Khrustalev, V.N., Gusev, D.V., Grintselev-Knyazev, G.V. and Bobrikova, E.S., *Crystallography Reports (Translation of Kristallografiya).* 2003. **48**(4): p. 594-601.

167. Bombicz, P., Czugler, M., Tellgren, R. and Kalman, A., *Angewandte Chemie, International Edition.* 2003. **42**(17): p. 1957-1960.

168. Kuleshova, L.N. and Antipin, M.Y., *Crystallography Reports (Translation of Kristallografiya).* 2002. **47**(2): p. 268-280.

169. Gavezzotti, A., *Synlett.* 2002(2): p. 201-214.

170. Fraxedas, J., Caro, J., Santiso, J., Figueras, A., Gorostiza, P. and Sanz, F., *Physica Status Solidi B: Basic Research.* 1999. **215**(1): p. 859-863.

171. Nangia, A. and Desiraju, G.R., *Chemical Communications (Cambridge).* 1999(7): p. 605-606.

172. Gavezzotti, A. and Filippini, G., *Journal of the American Chemical Society.* 1995. **117**(49): p. 12299-305.

173. Day, G.M., Chisholm, J., Shan, N., Motherwell, W.D.S. and Jones, W., *Crystal Growth & Design.* 2004. **4**(6): p. 1327-1340.

174. Shi, X.-F., Xing, Z.-Y., Wu, L. and Zhang, W.-Q., *Inorganica Chimica Acta.* 2006. **359**(2): p. 603-608.

175. Hamamci, S., Yilmaz, V.T. and Harrison, W.T.A., *Structural Chemistry.* 2005. **16**(4): p. 379-383.

176. Senel, E., Yilmaz, V.T. and Harrison, W.T.A., *Zeitschrift fuer Naturforschung, B: Chemical Sciences.* 2005. **60**(6): p. 659-662.

177. Jiang, Z.-H., *Abstracts of Papers, 228th ACS National Meeting, Philadelphia, PA, United States, August 22-26, 2004.* 2004: p. INOR-146.

178. Wang, R., Hong, M., Su, W., Cao, R., Zhao, Y. and Weng, J., *Australian Journal of Chemistry.* 2003. **56**(11): p. 1167-1171.

179. Rarig, R.S. and Zubieta, J., *Inorganica Chimica Acta.* 2001. **319**(1,2): p. 235-239.

180. Robinson, F. and Zaworotko, M.J., *Journal of the Chemical Society, Chemical Communications.* 1995(23): p. 2413-14.

181. Vranka, R.G. and Amma, E.L., *Inorg. Chem.* 1966. **5**(6): p. 1020-5.

182. Munakata, M., Kitagawa, S., Ujimaru, N., Nakamura, M., Maekawa, M. and Matsuda, H., *Inorganic Chemistry.* 1993. **32**(6): p. 826-32.

183. Blake, A.J., Baum, G., Champness, N.R., Chung, S.S.M., Cooke, P.A., Fenske, D., Khlobystov, A.N., Lemenovskii, D.A., Li, W.-S. and Schroder, M., *Dalton.* 2000(23): p. 4285-4291.

184. Gimeno, M.C., Jones, P.G., Laguna, A. and Sarroca, C., *Zeitschrift fuer Naturforschung, B: Chemical Sciences.* 2004. **59**(11/12): p. 1365-1371.

185. Wen, M., Munakata, M., Suenaga, Y., Kuroda-Sowa, T., Maekawa, M. and Yan, S.G., *Inorganica Chimica Acta.* 2001. **322**(1,2): p. 133-137.

186. Tong, M.-L., Chen, X.-M., Ye, B.-H. and Ng, S.W., *Inorganic Chemistry.* 1998. **37**(20): p. 5278-5281.

187. Thebault, F., Barnett, S.A., Blake, A.J., Wilson, C., Champness, N.R. and Schroeder, M., *Inorganic Chemistry.* p. ACS ASAP.

188. Kitagawa, S., Matsuyama, S., Munakata, M. and Emori, T., *Journal of the Chemical Society, Dalton Transactions: Inorganic Chemistry (1972-1999).* 1991(11): p. 2869-74.

189. Richardson, C. and Steel, P.J., *Inorganic Chemistry Communications.* 1998. **1**(7): p. 260-262.

190. Bond, A.D. and McKenzie, C.J., *Acta Crystallographica, Section C: Crystal Structure Communications.* 2005. **C61**(12): p. m519-m522.

191. Mao, H., Zhang, C., Li, G., Zhang, H., Hou, H., Li, L., Wu, Q., Zhu, Y. and Wang, E., *Dalton Transactions.* 2004(22): p. 3918-3925.

192. Noro, S.-I., Kitagawa, S., Yamashita, M. and Wada, T., *CrystEngComm.* 2002. **4**: p. 162-164.

193. Dietzel Pascal, D.C., Blom, R. and Fjellvag, H., *Dalton transactions (Cambridge, England : 2003).* 2006(4): p. 586-93.

194. Goforth, A.M., Gerth, K., Smith, M.D., Shotwell, S., Bunz, U.H.F. and zur Loye, H.-C., *Solid State Sciences.* 2005. **7**(9): p. 1083-1095.

195. Kitamura, M. and Nakano, K., *Journal.* 2005(Issue): p. 6 pp.

196. Meng, X., Xiao, B., Fan, Y., Hou, H. and Li, G., *Inorganica Chimica Acta.* 2004. **357**(5): p. 1471-1477.

197. Knaust, J.M., Lopez, S. and Keller, S.W., *Inorganica Chimica Acta.* 2001. **324**(1,2): p. 81-89.

198. Li, L., Yang, H., Song, Y., Hou, H. and Fan, Y., *Inorganica Chimica Acta.* 2006. **359**(7): p. 2135-2140.

199. Wang, X., Qin, C., Wang, E. and Xu, L., *Journal of Molecular Structure.* 2005. **737**(1): p. 49-54.

200. Lang, H., del Villar, A. and Walfort, B., *Inorganic Chemistry Communications.* 2004. **7**(5): p. 694-697.

201. Liu, Y., Dou, J., Zhu, L., Sun, D. and Zheng, P., *Indian Journal of Chemistry, Section A: Inorganic, Bio-inorganic, Physical, Theoretical & Analytical Chemistry.* 2000. **39A**(9): p. 983-984.

202. Netto, A.V.G., Frem, R.C.G. and Mauro, A.E., *Polyhedron.* 2005. **24**(9): p. 1086-1092.

203. Hasik, M., Bernasik, A., Adamczyk, A., Malata, G., Kowalski, K. and Camra, J., *European Polymer Journal.* 2003. **39**(8): p. 1669-1678.

204. Liu, X.-Y., Zhu, H.-L. and Fun, H.-K., *Synthesis and Reactivity in Inorganic, Metal-Organic, and Nano-Metal Chemistry.* 2005. **35**(2): p. 149-154.

205. Li, M.-X., Cheung, K.-K. and Mayr, A., *Journal of Solid State Chemistry.* 2000. **152**(1): p. 247-252.

Silver Coordination Compounds with a Family of Ditopic Ligands of Varying Flexibility:
About Chains, Rings, Helices and Polycatenanes

314

206. Drexler, H.-J., Grotjahn, M., Kleinpeter, E. and Holdt, H.-J., *Inorganica Chimica Acta.* 1999. **285**(2): p. 305-308.

207. Vallina, A.T. and Stoeckli-Evans, H., *Polyhedron.* 2002. **21**(12-13): p. 1177-1187.

208. Mueller, A., Boegge, H. and Koeniger-Ahlborn, E., *Zeitschrift fuer Naturforschung, Teil B: Anorganische Chemie, Organische Chemie.* 1979. **34B**(12): p. 1698-702.

209. Schnebeck, R.-D., Freisinger, E. and Lippert, B., *European Journal of Inorganic Chemistry.* 2000(6): p. 1193-1200.

210. Loi, M., Hosseini, M.W., Jouaiti, A., De Cian, A. and Fischer, J., *European Journal of Inorganic Chemistry.* 1999(11): p. 1981-1985.

211. Withersby, M.A., Blake, A.J., Champness, N.R., Cooke, P.A., Hubberstey, P., Li, W.-S. and Schroder, M., *Crystal Engineering.* 1999. **2**(2/3): p. 123-136.

212. Kuang, S.-M., Zhang, Z.-Z., Wang, Q.-G. and Mak, T.C.W., *Chemical Communications (Cambridge).* 1998(5): p. 581-582.

213. Reger, D.L., Brown, K.J., Gardinier, J.R. and Smith, M.D., *Organometallics.* 2003. **22**(24): p. 4973-4983.

214. Braunstein, P., Frison, C., Oberbeckmann-Winter, N., Morise, X., Messaoudi, A., Benard, M., Rohmer, M.-M. and Welter, R., *Angewandte Chemie, International Edition.* 2004. **43**(45): p. 6120-6125.

215. Baenziger, N.C. and Struss, A.W., *Inorganic Chemistry.* 1976. **15**(8): p. 1807-9.

216. Capacchi, L.C., Fava Gasparri, G., Ferrari, M. and Nardelli, M., *Chemical Communications (London).* 1968. **No. 15**: p. 910-11.

217. Dong, Y.-B., Layland, R.C., Smith, M.D., Pschirer, N.G., Bunz, U.H.F. and Zur Loye, H.-C., *Inorganic Chemistry.* 1999. **38**(13): p. 3056-3060.

218. Rochon, F.D., Andruh, M. and Melanson, R., *Canadian Journal of Chemistry.* 1998. **76**(11): p. 1564-1570.

219. Begley, M.J., Hubberstey, P. and Stroud, J., *Journal of the Chemical Society, Dalton Transactions: Inorganic Chemistry.* 1996(11): p. 2323-2328.

220. Carlucci, L., Ciani, G. and Proserpio, D.M., *Chemical Communications (Cambridge).* 1999(5): p. 449-450.

221. Carlucci, L., Ciani, G., v. Gundenberg, D.W. and Proserpio, D.M., *Inorganic Chemistry.* 1997. **36**(18): p. 3812-3813.

222. Smith, G., Cloutt, B.A., Lynch, D.E., Byriel, K.A. and Kennard, C.H.L., *Inorganic Chemistry.* 1998. **37**(13): p. 3236-3242.

223. Smith, G., Reddy, A.N., Byriel, K.A. and Kennard, C.H.L., *Polyhedron.* 1994. **13**(15/16): p. 2425-30.

224. Whang, D. and Kim, K., *Journal of the American Chemical Society.* 1997. **119**(2): p. 451-452.

225. Kleina, C., Graf, E., Hosseini, M.W., De Cian, A. and Fischer, J., *Chemical Communications (Cambridge).* 2000(3): p. 239-240.

226. Fujita, M., Kwon, Y.J., Sasaki, O., Yamaguchi, K. and Ogura, K., *Journal of the American Chemical Society.* 1995. **117**(27): p. 7287-8.

227. Hoskins, B.F., Robson, R. and Slizys, D.A., *Journal of the American Chemical Society.* 1997. **119**(12): p. 2952-2953.

228. Konnert, J. and Britton, D., *Inorg. Chem.* 1966. **5**(7): p. 1193-6.

229. Batten, S.R., Hoskins, B.F. and Robson, R., *New Journal of Chemistry.* 1998. **22**(2): p. 173-175.

230.   Soma, T. and Iwamoto, T., *Chemistry Letters.* 1994(4): p. 821-4.
231.   Gable, R.W., Hoskins, B.F. and Robson, R., *Journal of the Chemical Society, Chemical Communications.* 1990(23): p. 1677-8.
232.   Carlucci, L., Ciani, G., Proserpio, D.M. and Sironi, A., *Chemical Communications (Cambridge).* 1996(11): p. 1393-1394.
233.   Abrahams, B.F., Batten, S.R., Hamit, H., Hoskins, B.F. and Robson, R., *Chemical Communications (Cambridge).* 1996(11): p. 1313-1314.
234.   Withersby, M.A., Blake, A.J., Champness, N.R., Cooke, P.A., Hubberstey, P. and Schroder, M., *New Journal of Chemistry.* 1999. **23**(6): p. 573-575.
235.   Fan, J., Sun, W.-Y., Okamura, T.-A., Tang, W.-X. and Ueyama, N., *Inorganica Chimica Acta.* 2004. **357**(8): p. 2385-2389.
236.   Fu, Z.-Y., Wu, X.-T., Dai, J.-C., Wu, L.-M., Cui, C.-P. and Hu, S.-M., *Chemical Communications (Cambridge, United Kingdom).* 2001(18): p. 1856-1857.
237.   Batten, S.R., *CrystEngComm.* 2001: p. No pp given, Paper No 18.
238.   Carlucci, L., Ciani, G. and Proserpio, D.M., *New Journal of Chemistry.* 1998. **22**(12): p. 1319-1321.
239.   Aakeroy, C.B., Beatty, A.M. and Helfrich, B.A., *Journal of the Chemical Society, Dalton Transactions: Inorganic Chemistry.* 1998(12): p. 1943-1946.
240.   Batten, S.R., Hoskins, B.F., Robson, R., Moubaraki, B. and Murray, K.S., *Chemical Communications (Cambridge).* 2000(13): p. 1095-1096.
241.   Wu, H.-P., Janiak, C., Uehlin, L., Klufers, P. and Mayer, P., *Chemical Communications (Cambridge).* 1998(23): p. 2637-2638.
242.   Carlucci, L., Ciani, G., Proserpio, D.M. and Rizzato, S., *CrystEngComm.* 2002. **4**: p. 413-425.
243.   Carlucci, L., Ciani, G., Proserpio, D.M. and Rizzato, S., *CrystEngComm.* 2002. **4**: p. 121-129.
244.   Carlucci, L., Ciani, G., Proserpio Davide, M. and Rizzato, S., *Chemistry (Weinheim an der Bergstrasse, Germany).* 2002. **8**(7): p. 1520-7.
245.   Carlucci, L., Ciani, G., Proserpio, D.M. and Rizzato, S., *Dalton.* 2000(21): p. 3821-3828.
246.   Carlucci, L., Ciani, G. and Proserpio, D.M., *Journal of the Chemical Society, Dalton Transactions: Inorganic Chemistry.* 1999(11): p. 1799-1804.
247.   Grosshans, P., Jouaiti, A., Bulach, V., Planeix, J.-M., Hosseini, M.W. and Kyritsakas, N., *European Journal of Inorganic Chemistry.* 2004(3): p. 453-458.
248.   Morris, K.F., Stilbs, P. and Johnson, C.S., Jr., *Analytical Chemistry.* 1994. **66**(2): p. 211-15.
249.   Tashiro, M., Fujimoto, T., Suzuki, T., Furihata, K., Machinami, T. and Yoshimura, E., *Journal of Inorganic Biochemistry.* 2006. **100**(2): p. 201-205.
250.   Gostan, T., Tramesel, D., Brun, E., Prigent, Y. and Delsuc, M.-A., *Spectra Analyse.* 2004. **33**(240): p. 26-32.
251.   Yu, X., Cai, S. and Chen, Z., *Spectrochimica Acta, Part A: Molecular and Biomolecular Spectroscopy.* 2004. **60A**(1-2): p. 391-396.
252.   Huo, R., Wehrens, R., Van Duynhoven, J. and Buydens, L.M.C., *Analytica Chimica Acta.* 2003. **490**(1-2): p. 231-251.
253.   Johnston, M.R. and Latter, M.J., *Journal of Porphyrins and Phthalocyanines.* 2002. **6**(11 & 12): p. 757-762.
254.   Viel, S., Mannina, L. and Segre, A., *Tetrahedron Letters.* 2002. **43**(14): p. 2515-2519.
255.   Morris, K.F., Dixon, A., Cutak, B. and Larive, C.K., *Book of Abstracts, 218th ACS National Meeting, New Orleans, Aug. 22-26.* 1999: p. ANYL-068.

256. Jerschow, A. and Mueller, N., *Macromolecules.* 1998. **31**(19): p. 6573-6578.

257. Barjat, H., Morris, G.A., Smart, S., Swanson, A.G. and Williams, S.C.R., *Journal of Magnetic Resonance, Series B.* 1995. **108**(2): p. 170-2.

258. Leschke, M., Rheinwald, G. and Lang, H., *Zeitschrift fuer Anorganische und Allgemeine Chemie.* 2002. **628**(11): p. 2470-2477.

259. Danil de Namor, A.F., Piro, O.E., Pulcha Salazar, L.E., Aguilar-Cornejo, A.F., Al-Rawi, N., Castellano, E.E. and Sueros Velarde, F.J., *Journal of the Chemical Society, Faraday Transactions.* 1998. **94**(20): p. 3097-3104.

260. Park, B.I., Lee, J.W., Lee, Y.-A., Hong, J. and Jung, O.-S., *Bulletin of the Chemical Society of Japan.* 2005. **78**(9): p. 1624-1628.

261. Custer, P.D., Garrison, J.C., Tessier, C.A. and Youngs, W.J., *Journal of the American Chemical Society.* 2005. **127**(16): p. 5738-5739.

262. Tan, H.-Y., Zhang, H.-X., Ou, H.-D. and Kang, B.-S., *Inorganica Chimica Acta.* 2004. **357**(3): p. 869-874.

263. Jung, O.-S., Kim, Y.J., Lee, Y.-A., Park, K.-M. and Lee, S.S., *Inorganic Chemistry.* 2003. **42**(3): p. 844-850.

264. Bachechi, F., Burini, A., Galassi, R., Pietroni, B.R. and Tesei, D., *European Journal of Inorganic Chemistry.* 2002(8): p. 2086-2093.

265. Chen, X.-D. and Mak, T.C.W., *Journal of Molecular Structure.* 2005. **743**(1-3): p. 1-6.

266. Dong, Y.-B., Cheng, J.-Y., Ma, J.-P., Huang, R.-Q. and Smith, M.D., *Crystal Growth & Design.* 2005. **5**(2): p. 585-591.

267. Dong, Y.-B., Xu, H.-X., Ma, J.-P. and Huang, R.-Q., *Inorganic Chemistry.* 2006. **45**(8): p. 3325-3343.

268. Rais, D., Mingos, D.M.P., Vilar, R., White, A.J.P. and Williams, D.J., *Journal of Organometallic Chemistry.* 2002. **652**(1-2): p. 87-93.

269. Rais, D., Yau, J., Mingos, M.P., Vilar, R., White, A.J.P. and Williams, D.J., *Angewandte Chemie, International Edition.* 2001. **40**(18): p. 3464-3467.

270. Qin, S., Lu, S., Ke, Y., Li, J., Wu, X. and Du, W., *Solid State Sciences.* 2004. **6**(7): p. 753-755.

271. Bowmaker, G.A., Effendy, Nitiatmodjo, M., Skelton, B.W. and White, A.H., *Inorganica Chimica Acta.* 2005. **358**(14): p. 4327-4341.

272. Schultheiss, N., Barnes, C.L. and Bosch, E., *Crystal Growth & Design.* 2003. **3**(4): p. 573-580.

273. van Eijck, B.P., Mooij, W.T.M. and Kroon, J., *Journal of Physical Chemistry B.* 2001. **105**(43): p. 10573-10578.

274. Beyer, T., Day, G.M. and Price, S.L., *Journal of the American Chemical Society.* 2001. **123**(21): p. 5086-5094.

275. Van Eijck, B.P. and Kroon, J., *Acta Crystallographica, Section B: Structural Science.* 2000. **B56**(3): p. 535-542.

276. Gavezzotti, A., *Accounts of Chemical Research.* 1994. **27**(10): p. 309-14.

277. Mochida, T., Okazawa, K. and Horikoshi, R., *Dalton Transactions.* 2006(5): p. 693-704.

278. Awaleh, M.O., Badia, A. and Brisse, F., *Inorganic Chemistry.* 2005. **44**(22): p. 7833-7845.

279. Blake, A.J., Champness, N.R., Cooke, P.A. and Nicolson, J.E.B., *Chemical Communications (Cambridge).* 2000(8): p. 665-666.

280. Bu, X.-H., Liu, H., Du, M., Wong, K.M.-C., Yam, V.W.-W. and Shionoya, M., *Inorganic Chemistry.* 2001. **40**(17): p. 4143-4149.

281.   Lee, J.W., Kim, E.A., Kim, Y.J., Lee, Y.-A., Pak, Y. and Jung, O.-S., *Inorganic Chemistry.* 2005. **44**(9): p. 3151-3155.

282.   Pretsch, T. and Hartl, H., *Inorganica Chimica Acta.* 2005. **358**(4): p. 1179-1185.

283.   Zhang, G., Yang, G., Chen, Q. and Ma, J.S., *Crystal Growth & Design.* 2005. **5**(2): p. 661-666.

284.   Reger, D.L., Gardinier, J.R. and Smith, M.D., *Inorganic Chemistry.* 2004. **43**(13): p. 3825-3832.

285.   Bhogala, B.R., Thallapally, P.K. and Nangia, A., *Crystal Growth & Design.* 2004. **4**(2): p. 215-218.

286.   Fan, C., Ma, C., Chen, C., Chen, F. and Liu, Q., *Inorganic Chemistry Communications.* 2003. **6**(5): p. 491-494.

287.   Zheng, S.-L., Zhang, J.-P., Wong, W.-T. and Chen, X.-M., *Journal of the American Chemical Society.* 2003. **125**(23): p. 6882-6883.

288.   Cheng, J.-Y., Dong, Y.-B., Huang, R.-Q. and Smith, M.D., *Inorganica Chimica Acta.* 2005. **358**(4): p. 891-902.

289.   Dong, Y.-B., Cheng, J.-Y., Huang, R.-Q., Smith, M.D. and Zur Loye, H.-C., *Inorganic Chemistry.* 2003. **42**(18): p. 5699-5706.

290.   Beauchamp, D.A. and Loeb, S.J., *Chemical Communications (Cambridge, United Kingdom).* 2002(21): p. 2484-2485.

291.   Jung, O.-S., Lee, Y.-A., Kim, Y.J. and Hong, J., *Crystal Growth & Design.* 2002. **2**(6): p. 497-499.

292.   Majumdar, P., Kamar, K.K., Goswami, S. and Castineiras, A., *Chemical Communications (Cambridge, United Kingdom).* 2001(14): p. 1292-1293.

293.   Braga, D., Polito, M., Bracaccini, M., D'Addario, D., Tagliavini, E., Proserpio, D.M. and Grepioni, F., *Chemical Communications (Cambridge, United Kingdom).* 2002(10): p. 1080-1081.

294.   Sommerer, S.O., Westcott, B.L., Jircitano, A.J. and Abboud, K.A., *Inorganica Chimica Acta.* 1995. **238**(1-2): p. 149-53.

295.   Sengupta, P., Zhang, H. and Son, D.Y., *Inorganic Chemistry.* 2004. **43**(6): p. 1828-1830.

296.   Hartshorn, C.M. and Steel, P.J., *Inorganic Chemistry.* 1996. **35**(23): p. 6902-6903.

297.   Suzuki, T., Kotsuki, H., Isobe, K., Moriya, N., Nakagawa, Y. and Ochi, M., *Inorganic Chemistry.* 1995. **34**(3): p. 530-1.

298.   He, C., Duan, C.-y., Fang, C.-j. and Meng, Q.-j., *Dalton.* 2000(14): p. 2419-2424.

299.   Su, C.-Y., Liao, S., Zhu, H.-L., Kang, B.-S., Chen, X.-M. and Liu, H.-Q., *Dalton.* 2000(13): p. 1985-1993.

300.   Cui, Y. and He, C., *Journal of the American Chemical Society.* 2003. **125**(52): p. 16202-16203.

301.   Steiner, T., *Angewandte Chemie, International Edition.* 2002. **41**(1): p. 48-76.

302.   Jeffrey, G.A., Maluszynska, H. and Mitra, J., *International Journal of Biological Macromolecules.* 1985. **7**(6): p. 336-48.

303.   Carlucci, L., Ciani, G., Proserpio, D.M. and Sironi, A., *Journal of the Chemical Society, Dalton Transactions: Inorganic Chemistry.* 1997(11): p. 1801-1803.

304.   Barnett, S.A., Blake, A.J., Champness, N.R. and Wilson, C., *Journal of Supramolecular Chemistry.* 2003. **2**(1-3): p. 17-20.

305.   Felix, O., Hosseini, M.W. and De Cian, A., *Solid State Sciences.* 2001. **3**(7): p. 789-793.

306.   Ferlay, S., Bulach, V., Felix, O., Hosseini, M.W., Planeix, J.-M. and Kyritsakas, N., *CrystEngComm.* 2002. **4**: p. 447-453.

307. Ferlay, S., Felix, O., Hosseini, M.W., Planeix, J.-M. and Kyritsakas, N., *Chemical Communications (Cambridge, United Kingdom)*. 2002(7): p. 702-703.

308. Grosshans, P., Jouaiti, A., Bulach, V., Planeix, J.-M., Hosseini, M.W. and Nicoud, J.-F., *CrystEngComm*. 2003. **5**: p. 414-416.

309. Hosseini, M.W., Tsiourvas, D., Planeix, J.-M., Sideratou, Z., Thomas, N. and Paleos, C.M., *Collection of Czechoslovak Chemical Communications*. 2004. **69**(5): p. 1161-1168.

310. Jaunky, W., Hosseini, M.W., Planeix, J.M., De Cian, A., Kyritsakas, N. and Fischer, J., *Chemical Communications (Cambridge)*. 1999(22): p. 2313-2314.

311. Fei, B.-L., Sun, W.-Y., Okamura, T.-a., Tang, W.-X. and Ueyama, N., *New Journal of Chemistry*. 2001. **25**(2): p. 210-212.

312. Zhu, H.-F., Kong, L.-Y., Okamura, T.-a., Fan, J., Sun, W.-Y. and Ueyama, N., *European Journal of Inorganic Chemistry*. 2004(7): p. 1465-1473.

313. Horikoshi, R., Mochida, T., Maki, N., Yamada, S. and Moriyama, H., *Journal of the Chemical Society, Dalton Transactions*. 2002(1): p. 28-33.

314. Cai, Y.-P., Zhang, H.-X., Xu, A.-W., Su, C.-Y., Chen, C.-L., Liu, H.-Q., Zhang, L. and Kang, B.-S., *Journal of the Chemical Society, Dalton Transactions*. 2001(16): p. 2429-2434.

315. Yamazaki, S., Deeming, A.J., Speel, D.M., Hibbs, D.E., Hursthouse, M.B. and Malik, K.M.A., *Chemical Communications (Cambridge)*. 1997(2): p. 177-178.

316. Liu, S.Q., Kuroda-Sowa, T., Konaka, H., Suenaga, Y., Maekawa, M., Mizutani, T., Ning, G.L. and Munakata, M., *Inorganic Chemistry*. 2005. **44**(4): p. 1031-1036.

317. Haftbaradaran, F., Draper, N.D., Leznoff, D.B. and Williams, V.E., *Dalton Transactions*. 2003(11): p. 2105-2106.

318. Hong, M., Su, W., Cao, R., Fujita, M. and Lu, J., *Chemistry--A European Journal*. 2000. **6**(3): p. 427-431.

319. Ara, I., Fornies, J., Gomez, J., Lalinde, E., Merino, R.I. and Moreno, M.T., *Inorganic Chemistry Communications*. 1999. **2**(2): p. 62-65.

320. Zielenkiewicz, W., Margas, E. and Editors, *Theory of Calorimetry*. 2002. No pp given.

321. Cheng, S.Z.D. and Editor, *Handbook of Thermal Analysis and Calorimetry Volume 3: Applications to Polymers and Plastics*. 2002. 828 pp.

322. Haines, P.J. and Editor, *Principles of Thermal Analysis and Calorimetry*. 2002. 220 pp.

323. Kemp, R.B. and Editor, *Handbook of Thermal Analysis and Calorimetry, Volume 4: from Macromolecules to Man*. 1999. 1032 pp.

324. Suga, H., *Journal of Thermal Analysis and Calorimetry*. 2005. **80**(1): p. 49-55.

325. Cebe, P., *Journal of Polymer Science, Part B: Polymer Physics*. 2005. **43**(6): p. 629-636.

326. Giron, D., *Pharmaceutical Science & Technology Today*. 1998. **1**(6): p. 262-268.

327. Johari, G.P., *Thermochimica Acta*. 1995. **266**: p. 31-47.

328. Giron, D., *Thermochimica Acta*. 1995. **248**: p. 1-59.

329. Snider Daniel, A., Addicks, W. and Owens, W., *Advanced drug delivery reviews*. 2004. **56**(3): p. 391-5.

330. Akdas, H., Graf, E., Hosseini, M.W., De Cian, A. and Harrowfield, J.M., *Chemical Communications (Cambridge)*. 2000(22): p. 2219-2220.

331. Kariuki, N.N., Luo, J., Hassan, S.A., Lim, I.I.S., Wang, L. and Zhong, C.J., *Chemistry of Materials*. p. ACS ASAP.

332. Carlucci, L., Ciani, G., Proserpio, D.M. and Sironi, A., *Inorganic Chemistry*. 1998. **37**(22): p. 5941-5943.

333. Kaes, C., Hosseini, M.W., Rickard, C.E.F., Skelton, B.W. and White, A.H., *Angewandte Chemie, International Edition.* 1998. **37**(7): p. 920-922.

334. Carlucci, L., Ciani, G., Proserpio, D.M. and Rizzato, S., *New Journal of Chemistry.* 2003. **27**(3): p. 483-489.

335. Blake, A.J., Champness, N.R., Chung, S.S.M., Li, W.-S. and Schroder, M., *Chemical Communications (Cambridge).* 1997(17): p. 1675-1676.

336. Masaoka, S., Tanaka, D., Nakanishi, Y. and Kitagawa, S., *Angewandte Chemie, International Edition.* 2004. **43**(19): p. 2530-2534.

337. Abourahma, H., Moulton, B., Kravtsov, V. and Zaworotko, M.J., *Journal of the American Chemical Society.* 2002. **124**(34): p. 9990-9991.

338. Lee, I.S., Shin, D.M. and Chung, Y.K., *Chemistry--A European Journal.* 2004. **10**(13): p. 3158-3165.

339. Braga, D., Polito, M., D'Addario, D. and Grepioni, F., *Crystal Growth & Design.* 2004. **4**(6): p. 1109-1112.

340. Soldatov, D.V., Diamente, P.R., Ratcliffe, C.I. and Ripmeester, J.A., *Inorganic Chemistry.* 2001. **40**(22): p. 5660-5667.

341. Soldatov, D.V., Henegouwen, A.T., Enright, G.D., Ratcliffe, C.I. and Ripmeester, J.A., *Inorganic Chemistry.* 2001. **40**(7): p. 1626-1636.

342. Soldatov, D.V., Henegouwen, A.T., Enright, G.D., Ratcliffe, C.I. and Ripmeester, J.A., *Inorganic chemistry.* 2001. **40**(7): p. 1626-36.

343. Tynan, E., Jensen, P., Kelly Niamh, R., Kruger Paul, E., Lees Anthea, C., Moubaraki, B. and Murray Keith, S., *Dalton Trans.* 2004(21): p. 3440-7.

344. Yue Nancy, L.S., Jennings Michael, C. and Puddephatt Richard, J., *Chemical communications (Cambridge, England).* 2005(38): p. 4792-4.

345. Pomes, R. and Roux, B., *Biophysical Journal.* 2002. **82**(5): p. 2304-2316.

346. Liu, Y., Guo, D.-S. and Zhang, H.-Y., *Journal of Molecular Structure.* 2005. **734**(1-3): p. 241-245.

347. Jensen, M.O., Rothlisberger, U. and Rovira, C., *Biophysical Journal.* 2005. **89**(3): p. 1744-1759.

348. Mann David, J. and Halls Mathew, D., *Physical review letters.* 2003. **90**(19): p. 195503.

349. Mashl, R.J., Joseph, S., Aluru, N.R. and Jakobsson, E., *Nano Letters.* 2003. **3**(5): p. 589-592.

350. Vittal, J.J. and Yang, X., *Crystal Growth & Design.* 2002. **2**(4): p. 259-262.

351. Roubeau, O., Haasnoot, J.G., Codjovi, E., Varret, F. and Reedijk, J., *Chemistry of Materials.* 2002. **14**(6): p. 2559-2566.

352. Lou, B., Jiang, F., Yuan, D., Wu, B. and Hong, M., *European Journal of Inorganic Chemistry.* 2005(16): p. 3214-3216.

353. Katrusiak, A. and Szafranski, M., *Journal of Molecular Structure.* 1996. **378**(3): p. 205-223.

354. Dong, Y.-B., Zhao, X., Huang, R.-Q., Smith, M.D. and Zur Loye, H.-C., *Inorganic Chemistry.* 2004. **43**(18): p. 5603-5612.

355. Colquhoun, H.M., Stoddart, J.F. and Williams, D.J., *Journal of the Chemical Society, Chemical Communications.* 1981(16): p. 849-50.

356. Ashworth, T.V., Nolte, M.J. and Singleton, E., *Journal of Organometallic Chemistry.* 1977. **139**(2): p. C73-C76.

357. Maud, J.M., Stoddart, J.F. and Williams, D.J., *Acta Crystallographica, Section C: Crystal Structure Communications.* 1985. **C41**(1): p. 137-40.

358. Batten, S.R. and Robson, R., *Angewandte Chemie, International Edition.* 1998. **37**(11): p. 1461-1494.
359. Fan, J., Zhu, H.-F., Okamura, T.-a., Sun, W.-Y., Tang, W.-X. and Ueyama, N., *Chemistry--A European Journal.* 2003. **9**(19): p. 4724-4731.
360. Bu, W.-M., Ye, L. and Fan, Y.-G., *Chemistry Letters.* 2000(2): p. 152-153.
361. Ni, Z. and Vittal, J.J., *Crystal Growth & Design.* 2001. **1**(3): p. 195-197.
362. Klein, C., Graf, E., Wais Hosseini, M. and De Cian, A., *New Journal of Chemistry.* 2001. **25**(2): p. 207-209.
363. Ino, I., Zhong, J.C., Munakata, M., Kuroda-Sowa, T., Maekawa, M., Suenaga, Y. and Kitamori, Y., *Inorganic Chemistry.* 2000. **39**(19): p. 4273-4279.
364. Carlucci, L., Ciani, G., Proserpio, D.M. and Rizzato, S., *Chemistry--A European Journal.* 2002. **8**(7): p. 1519-1526.
365. Bai, Y., Duan, C.-Y., Cai, P., Dang, D.-B. and Meng, Q.-J., *Dalton Transactions.* 2005(16): p. 2678-2680.
366. Chippindale, A.M., Cheyne, S.M. and Hibble, S.J., *Angewandte Chemie, International Edition.* 2005. **44**(48): p. 7942-7946.
367. Carlucci, L., Ciani, G. and Proserpio, D.M., *Coordination Chemistry Reviews.* 2003. **246**(1-2): p. 247-289.
368. Dorn, T., Fromm Katharina, M. and Christoph, J., *Australian Journal of Chemistry.* 2006. **59**(1): p. 22-25.
369. Liu, Z., Liu, P., Chen, Y., Wang, J. and Huang, M., *New Journal of Chemistry.* 2005. **29**(3): p. 474-478.
370. Wu, T., Li, D., Feng, X.-L. and Cai, J.-W., *Inorganic Chemistry Communications.* 2003. **6**(7): p. 886-890.
371. Corni, S. and Tomasi, J., *Journal of Chemical Physics.* 2003. **118**(14): p. 6481-6494.
372. Astilean, S. and Barnes, W.L., *Applied Physics B: Lasers and Optics.* 2002. **75**(4-5): p. 591-594.
373. Ahn, S., Kim, E.-H. and Lee, C., *Bulletin of the Korean Chemical Society.* 2005. **26**(2): p. 331-333.
374. Jacobson, M.A., Keresztes, I. and Williard, P.G., *Journal of the American Chemical Society.* 2005. **127**(13): p. 4965-4975.
375. Gambs, C., Dickerson, T.J., Mahajan, S., Pasternack, L.B. and Janda, K.D., *Journal of Organic Chemistry.* 2003. **68**(9): p. 3673-3678.
376. Watson, J.D., *A Passion for DNA: Genes, Genomes, and Society.* 2000. 250 pp.
377. Watson, J.D. and Editor, *Discovering the Double Helix: History of Science; Biotechnology.* 2001. No pp given.
378. Lehn, J.M., Rigault, A., Siegel, J., Harrowfield, J., Chevrier, B. and Moras, D., *Proceedings of the National Academy of Sciences of the United States of America.* 1987. **84**(9): p. 2565-9.
379. Constable, E.C., Walker, J.V., Tocher, D.A. and Daniels, M.A.M., *Journal of the Chemical Society, Chemical Communications.* 1992(10): p. 768-71.
380. Constable, E.C. and Chotalia, R., *Journal of the Chemical Society, Chemical Communications.* 1992(1): p. 64-6.
381. Constable, E.C., Hannon, M.J. and Tocher, D.A., *Journal of the Chemical Society, Dalton Transactions: Inorganic Chemistry (1972-1999).* 1993(12): p. 1883-90.

382. Constable, E.C., Heirtzler, F.R., Neuburger, M. and Zehnder, M., *Supramolecular Chemistry.* 1995. **5**(3): p. 197-200.

383. Constable, E.C., Edwards, A.J., Raithby, P.R., Smith, D.R., Walker, J.V. and Whall, L., *Chemical Communications (Cambridge).* 1996(22): p. 2551-2552.

384. Constable, E.C., Heirtzler, F.R., Neuburger, M. and Zehnder, M., *Chemical Communications (Cambridge).* 1996(8): p. 933-934.

385. Constable, E.C., *Comprehensive Supramolecular Chemistry.* 1996. **9**: p. 213-252.

386. Constable, E.C. and Rees, D.G.F., *New Journal of Chemistry.* 1997. **21**(3): p. 369-376.

387. Piguet, C., Bernardinelli, G. and Hopfgartner, G., *Chemical Reviews (Washington, D. C.).* 1997. **97**(6): p. 2005-2062.

388. Bowyer, P.K., Porter, K.A., Rae, A.D., Willis, A.C. and Wild, S.B., *Chemical Communications (Cambridge).* 1998(10): p. 1153-1154.

389. Sailaja, S. and Rajasekharan, M.V., *Inorganic Chemistry.* 2003. **42**(18): p. 5675-5684.

390. Albrecht, M., *Chemical Reviews (Washington, D. C.).* 2001. **101**(11): p. 3457-3497.

391. Constable, E.C., Chotalia, R. and Tocher, D.A., *Journal of the Chemical Society, Chemical Communications.* 1992(10): p. 771-3.

392. Constable, e.C., Daniels, M.A.M., Drew, M.G.B., Tocher, D.A., Walker, J.V. and Wood, P.D., *Journal of the Chemical Society, Dalton Transactions: Inorganic Chemistry (1972-1999).* 1993(13): p. 1947-58.

393. Constable, E.C., Edwards, A.J., Hannon, M.J. and Raithby, P.R., *Journal of the Chemical Society, Chemical Communications.* 1994(17): p. 1991-2.

394. Constable, E.C., Neuburger, M., Smith, D.R. and Zehnder, M., *Chemical Communications (Cambridge).* 1996(16): p. 1917-1918.

395. Hirsch, K.A., Wilson, S.R. and Moore, J.S., *Chemical Communications (Cambridge).* 1998(1): p. 13-14.

396. Hester, C.A., Baughman, R.G. and Collier, H.L., *Polyhedron.* 1997. **16**(16): p. 2893-2895.

397. Reid, S.D., Blake, A.J., Wilson, C. and Love, J.B., *Inorganic Chemistry.* 2006. **45**(2): p. 636-643.

398. Sreerama, S.G. and Pal, S., *Inorganic Chemistry.* 2005. **44**(18): p. 6299-6307.

399. Zong, R. and Thummel, R.P., *Inorganic Chemistry.* 2005. **44**(17): p. 5984-5986.

400. Alcock, N.W., Clarkson, G., Glover, P.B., Lawrance, G.A., Moore, P. and Napitupulu, M., *Dalton Transactions.* 2005(3): p. 518-527.

401. Hou, L. and Li, D., *Inorganic Chemistry Communications.* 2005. **8**(1): p. 128-130.

402. Childs, L.J., Pascu, M., Clarke, A.J., Alcock, N.W. and Hannon, M.J., *Chemistry--A European Journal.* 2004. **10**(17): p. 4291-4300.

403. Zang, S., Su, Y., Li, Y., Ni, Z. and Meng, Q., *Inorganic Chemistry.* 2006. **45**(1): p. 174-180.

404. Yi, L., Yang, X., Lu, T. and Cheng, P., *Crystal Growth & Design.* 2005. **5**(3): p. 1215-1219.

405. Erxleben, A., *Inorganica Chimica Acta.* 2003. **348**: p. 107-114.

406. Wang, R.-H., Hong, M.-C., Su, W.-P., Liang, Y.-C., Cao, R., Zhao, Y.-J. and Weng, J.-B., *Inorganica Chimica Acta.* 2001. **323**(1,2): p. 139-146.

407. Sun, D., Cao, R., Sun, Y., Bi, W., Li, X., Hong, M. and Zhao, Y., *European Journal of Inorganic Chemistry.* 2003(1): p. 38-41.

408. Kawano, T., Du, C.-X., Araki, T. and Ueda, I., *Inorganic Chemistry Communications.* 2003. **6**(2): p. 165-167.

Silver Coordination Compounds with a Family of Ditopic Ligands of Varying Flexibility: About Chains, Rings, Helices and Polycatenanes

322

409. Constable, E.C., Hannon, M.J., Martin, A., Raithby, P.R. and Tocher, D.A., *Polyhedron.* 1992. **11**(22): p. 2967-71.
410. Constable, E.C., Elder, S.M. and Tocher, D.A., *Polyhedron.* 1992. **11**(11): p. 1337-42.
411. Constable, E.C. and Walker, J.V., *Journal of the Chemical Society, Chemical Communications.* 1992(12): p. 884-6.
412. Piguet, C., Bernardinelli, G., Bocquet, B., Quattropani, A. and Williams, A.F., *Journal of the American Chemical Society.* 1992. **114**(19): p. 7440-51.
413. McMorran, D.A. and Steel, P.J., *Angewandte Chemie, International Edition.* 1998. **37**(23): p. 3295-3297.
414. Baxter, P.N.W., Lehn, J.-M., Baum, G. and Fenske, D., *Chemistry--A European Journal.* 2000. **6**(24): p. 4510-4517.
415. Saalfrank, R.W., Loew, N., Trummer, S., Sheldrick, G.M., Teichert, M. and Stalke, D., *European Journal of Inorganic Chemistry.* 1998(5): p. 559-563.
416. Floquet, S., Ouali, N., Bocquet, B., Bernardinelli, G., Imbert, D., Bunzli, J.-C.G., Hopfgartner, G. and Piguet, C., *Chemistry--A European Journal.* 2003. **9**(8): p. 1860-1875.
417. Andre, N., Jensen, T.B., Scopelliti, R., Imbert, D., Elhabiri, M., Hopfgartner, G., Piguet, C. and Buenzli, J.-C.G., *Inorganic Chemistry.* 2004. **43**(2): p. 515-529.
418. Blake, A.J., Champness, N.R., Crew, M. and Parsons, S., *New Journal of Chemistry.* 1999. **23**(1): p. 13-15.
419. Jouaiti, A., Hosseini Mir, W. and Kyritsakas, N., *Chemical communications (Cambridge, England).* 2003(4): p. 472-3.
420. Fei, B.-L., Sun, W.-Y., Yu, K.-B. and Tang, W.-X., *Dalton.* 2000(5): p. 805-811.
421. Cosier, J. and Glazer, A.M., *Journal of Applied Crystallography.* 1986. **19**(2): p. 105-7.
422. Blanc, E., Schwarzenbach, D. and Flack, H.D., *Journal of Applied Crystallography.* 1991. **24**(6): p. 1035-41.
423. Sheldrick, G.M., *Crystallogr. Comput.: Data Collect., Struct. Determ., Proteins, Databases, Pap. Int. Summer Sch., 9th.* 1985: p. 184-9.
424. Sheldrick, G.M., *Comput. Crystallogr., Proc. Int. Summer Sch.* 1978: p. 34-42.
425. Farrugia, L.J., *Journal of Applied Crystallography.* 1997. **30**(5, Pt. 1): p. 565.
426. Keller, E., *GIT Fachzeitschrift fuer das Laboratorium.* 1995. **39**(3): p. 232-4, 237-8.
427. Keller, E., *Chemie in Unserer Zeit.* 1986. **20**(6): p. 178-81.
428. Keller, E., *Chemie in Unserer Zeit.* 1980. **14**(2): p. 56-60.
429. Cason, C.T., F. Nathan, K and Ron, P, *Journal.* 2003(Issue).
430. Bergerhoff, G., Berndt, M. and Brandenburg, K., *Journal of Research of the National Institute of Standards and Technology.* 1996. **101**(3): p. 221-225.
431. Nishimura, T., Maeda, Y., Kakiuchi, N. and Uemura, S., *Perkin 1.* 2000(24): p. 4301-4305.
432. Isobe, T. and Ishikawa, T., *Journal of Organic Chemistry.* 1999. **64**(19): p. 6984-6988.
433. Adams, R. and Ulich, L.H., *Journal of the American Chemical Society.* 1920. **42**: p. 599-611.

F - Appendices

I. Abbreviations

DMC   2-Chloro-1,3 dimethyl imidazolinium chloride
DMF   Dimethylformamide
DMSO   Dimethylsulfoxide
THF   Tetrahydrofuran
EtOH   Ethanol
DCM   Dichloromethane
MeOH   Methanol
ESI/MS   Electrospray Ionization Mass Spectrometry
FT-IR   Fourier Tranformed Infrared
IR   Infrared
NMR   Nuclear Magnetic Resonance
SDTA   Scanning Differential Thermal Analysis
TGA   Thermal Gravimetric Analysis
D–H⋯Acceptor   Distance betweem the donor atom (D) and the acceptor atom (A)
d (D–H)   Distance between the donor atom (D) and the hydrogen atom (H)
d (H⋯A)   Distance betweem the hydrogen atom (H) and the acceptor atom (A)
Angle D–H⋯A   Angle formed between the donor atom (D), the hydrogen atom (H) and the acceptor atom (A)
d_{R-R} (Å)   Distance between aromatic rings
ρd_{R-R} (Å)   Distance between the centroids of aromatic rings
α   Dihedral angle between the planes of the aromatic rings
β   Angle between the planes of the aromatic rings

IR assignations

ν   Stretching vibration
δ   Out of plane vibration
s   Strong
m   Medium
w   Weak

^{1}H-NMR assignations

s   Singulet   **t**   Triplet
d   Doublet   **m**   Multiplet

Concomitant crystallization of two polymorphs—a ring and a helix: concentration effect on supramolecular isomerism

Katharina M. Fromm,* Jorge L. Sagué Doimeadios and Adeline Y. Robin

For the first time in Ag coordination chemistry, two supramolecular isomers, a ring and a helix, are isolated from the same mother liquor as a result of concentration effects.

During the past years, there has been considerable interest in the supramolecular architectures that can possibly be obtained by the combination of organic building blocks with transition metal ions.[1] In this context, it has been shown that coordination polymers constructed from rigid organic ligands show parallels with some standard inorganic compounds such as i.e. graphite, diamond or wurtzite.[2] However, with more flexible building blocks, the structures become less predictable.[3] When considering likely transition metal geometries, some predictions can be made, as to whether for instance a one- or two-dimensional compound is expected. But weaker supramolecular forces such as hydrogen bonding, π-interactions, or the coordination ability of the counter anions as well as the presence of solvent molecules are all able to strongly influence the final framework,[1,4] making polymorphism and pseudo-polymorphism more probable. Polymorphism is a phenomenon observed throughout all branches of chemistry as soon as a solid crystalline compound has the possibility to adopt at least two different arrangements in the solid state.[5] One example of polymorphism can be supramolecular isomerism in which the packing is insofar different, as for instance coordination polymers versus monomers can be obtained.[6] Different polymorphs may have very different physical and chemical properties, and are therefore interesting study objects. Supramolecular crystal engineering is a related attractive research field with the aim of exerting more control over the solid state structures.[7,8]

So far, our group has been interested in the design of predictable low-dimensional polymers containing alkaline earth metal ions.[9–12] With a view to oxide materials, we now aim at single source precursors containing all metal ions necessary for the desired product. In order to synthesize mixed metal compounds, a series of ligands derived from pyridine was designed, possessing two different coordination sites encoded for two types of metal ions (Scheme 1). We here report on two compounds obtained with the ligand L for $n = 2$ and $AgClO_4$. These two compounds are important because they are the first examples in silver coordination chemistry, yielding two polymorphs (a ring and a helix) as a function of concentration in the same reaction sample. It is reasonable to expect such phenomena in future studies owing to the weakness of the forces implied in the structure formation, both structures being apparently of similar energy.

Universität Basel, Departement Chemie, Spitalstrasse 51, Basel, CH-4056, Switzerland. E-mail: katharina.fromm@unibas.ch; Fax: 41 61 2671021; Tel: 41 61 2671004
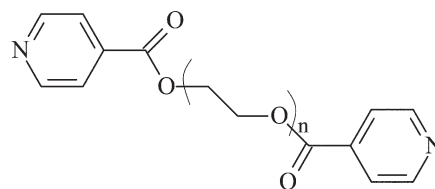
Scheme 1 Ligand designed for accepting two different metal ions.

Single crystals of both compounds are obtained in an H-tube,† with an aqueous solution of silver salt on one side, a THF solution of ligand on the other side, both connected via a mixture of both solvents. Slow diffusion of the ligand into the metal salt solution and vice versa yields the ring-forming compound $[Ag(L)]ClO_4$, **1**, which was obtained on the side of the silver salt. **1** crystallizes in the triclinic space group $P\bar{1}$ (no. 2)[13] with half of a molecule per asymmetric unit. In a molecule, two metal ions are bridged by two ligands L to form an oval-shaped ring (Fig. 1a). The shortest contact across the loop is the Ag–Ag contact of 3.146(1) Å, the longest is between opposite hydrogen atoms in C_2H_4-groups at ca. 20 Å (Fig. 1b). Interestingly, the short Ag–Ag contact is not bridged by anions in a pincer fashion as observed in coordination polymers formed by pairs of one-dimensional chains where silver is
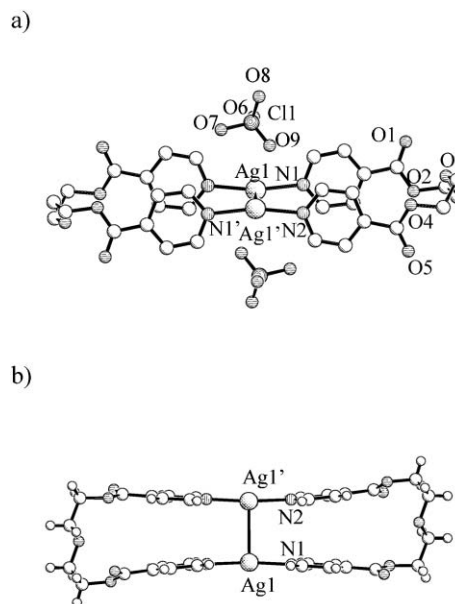
Fig. 1 a) View of the molecular structure of **1**, H-atoms omitted for clarity; b) top-view of **1**, showing Ag–Ag closest contacts; anions omitted for clarity (symmetry operation (') −x, −y, −z).

bridged by other anions such as NO_3^-.[14] Among the Ag–O contacts that can be considered as weak interactions between the cation and the perchlorate anion, the shortest is Ag1–O9 [2.931(1) Å]. The Ag1–N distances [2.150(6) (N1) and 2.155(6) Å (N2')] are almost identical, and the angle N1–Ag1–N2' [167.8(2)°] is far from linear due to the deformation resulting from Ag–Ag contacts. There is no obvious reason from solid state packing why the silver atoms should come that close to each other if it were not for metal–metal interactions. The rings are arranged in a parallel fashion with the empty space in between filled with the perchlorate anions. Some of the oxygen atoms of the latter are weakly bonded to the hydrogen atoms of the ligand L, the shortest bond being O7···H1' (2.28 Å).

On the ligand side of the H-tube, single crystals of the same composition [Ag(L)]ClO$_4$, **2** are found. However, the unit cell dimensions are different in length and angles, **2** crystallizing in the monoclinic space group $C2/c$ (no. 15).[13] Instead of forming molecular units in a ring-form, the loops (with two ligand molecules per two silver cations) in **1** open up to yield a single stranded helix where three ligand molecules are coordinated to two silver cations (Fig. 2). The chain thus obtained, ···L–Ag–L–Ag–L···, has the ligand again in a U-shaped conformation, all-*gauche*, similar to the ring described above for **1**. The silver ions are distributed along a zig-zag chain in the direction of the *b*-axis, with shortest Ag1–Ag1' distances of 3.781(2) Å, excluding metal–metal interactions. The Ag1–N distances in **2** are 2.158(7) and 2.161(6) Å for N2 and N1, respectively. The two pyridine rings within one ligand are at their shortest distance [4.39(1) Å] measured from N1 to N2, thus excluding π-stacking. The N–N distance through space between two different ligands is 3.59(1) Å with the centers of these pyridine rings 3.742(6) Å apart, and almost completely offset by 3.4 Å, excluding efficient π–π interactions. The height of one full turn of the helix, measured from Ag1 to the next Ag1 in the chain, is 7.104 Å, corresponding to the *b*-parameter of the unit cell.

Whereas molecular boxes or rings as observed in **1** are well described,[15] single helical arrangements remain quite rare, even though they are highly interesting due to their inherent chirality.[8,16] Even rarer are examples for concomitant polymorphs, one of them having a helical structure. The compound [{HC(3-Phpz)$_3$}Ag](BF$_4$) (pz = pyrazolyl) yields two polymeric polymorphs from the same solvent combination, but it is not clear
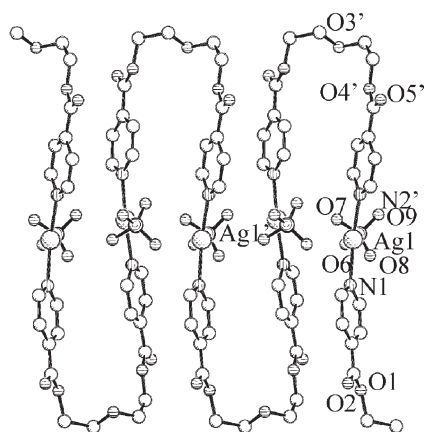
from the description whether they crystallize simultaneously or in parallel assays.[17] Two polymeric polymorphs out of the same solution at room temperature are described for a Cu(I) compound.[18] A hexamer and a zig-zag-structure, but not a helix, are observed for a Cu(II) compound.[19] For other M(II) metal ions, temperature, solvent and pressure dependent polymorphism has been observed.[20] It has been discussed recently that the anion tunes the secondary self-assembly, leading to rings, helices or chains.[21] This can be excluded in our case. Another theory of ring-opening polymerization also does not fit in our case as both crystals occur at the same time.[22] In fact, in this case, a concentration effect can be proposed. On the side with AgClO$_4$ in water, Ag cations are in excess with respect to ligand L, so that fragments of [AgL]$^+$ are formed as ligand diffuses towards this compartment of the H-tube. In our polar solvents, the dissociation of the possible soft species [Ag$_2$L]$^{2+}$ to yield [Ag$_2$L$_2$]$^{2+}$ and [Ag]$^+$ is probably entropically favored, leading to an anti-cooperative effect. To confirm this hypothesis, formation constants of the different species will have to be determined in different solvents. On the other side, ligand L is in excess with respect to Ag$^+$, and fragments of the type [Ag(L)$_2$]$^+$ can be formed, which would lead to the helical structure upon polymerization with other such fragments or [Ag(L)]$^+$. The presence of such species in varying ratios as a function of time and concentration could be confirmed by electrospray mass spectrometry.

This is therefore the first case of supramolecular isomerism induced by concentration effects, both polymorphs coexisting in the same solution, where a ring and a helical Ag(I) compound are formed. After total diffusion, only the ring, compound **1**, is found, so that compound **2** can be considered as a kinetic product, whereas the ring forming isomer **1** is the thermodynamically more stable product. With other anions as counter ions, only the ring isomer has been obtained and observed so far, but this will be the subject of another publication.[23]

Notes and references

Fig. 2 Side-view of one helical single-strand structure of **2**, H-atoms omitted for clarity (symmetry operation (') −x + 0.5, y + 0.5, −z + 0.5).

1 S. R. Batten and R. Robson, *Angew. Chem. Int. Ed.*, 1998, **37**, 1460; A. J. Blake, N. R. Champness, P. Hubberstey, W.-S. Li, M. Schröder and M. A. Withersby, *Coord. Chem. Rev.*, 1999, **183**, 117; A. N. Khlobystov, A. J. Blake, N. R. Champness, D. A. Lemenovskii, A. G. Majouga, N. V. Zyk and M. Schroder, *Coord. Chem. Rev.*, 2001, **222**, 155–192.

2 G. R. Desiraju (Editor), *The Crystal as a Supramolecular Entity*, Wiley, New York, 1995 and refs. therein; R. Robson, B. F. Abrahams,

S. R. Batten, R. W. Gable, B. F. Hoskins and J. Liu, in *Supramolecular Architecture*, American Chemical Society, Washington, DC, 1992, ch. 19, p. 256.

3 L. R. Hanton and K. Lee, *J. Chem. Soc., Dalton Trans.*, 2000, 1161; N. Hong, W. Su, R. Cao, M. Fujita and J. Lu, *Chem. Eur. J.*, 2000, **6**, 427; L. Carlucci, D. M. Proserpio and S. Rizzato, *Chem. Eur. J.*, 2002, **8**, 1520 and refs. therein.

4 S. A. Barnett, A. J. Blake, N. R. Champness and C. Wilson, *Chem. Commun.*, 2002, 1640 and refs. therein.

5 J. Bernstein, R. J. Davey and J.-O. Henck, *Angew. Chem. Int. Ed.*, 1999, **38**, 3440–3461.

6 M. Schröder and N. R. Champness, in *Encyclopedia of Supramolecular Chemistry*, ed. J. L. Atwood and J. W. Steed, Dekker, New York, 2004, pp. 1420–1426; D. Braga, L. Brammer and N. R. Champness, *CrystEngComm*, 2005, **7**, 1–19.

7 J. Bernstein, in *Supramolecular Engineering of Synthetic Metallic Materials*, Kluwer Academic Publishers, Dordrecht, The Netherlands, 1999, pp. 23–40.

8 B. Moulton and M. J. Zaworotko, *Chem. Rev.*, 2001, **101**, 1629–1658.

9 K. M. Fromm, G. Bernardinelli, H. Goesmann, M.-J. Mayor-Lopez and J. Weber, *Z. Anorg. Allg. Chem.*, 2000, **626**, 1685–1691.

10 K. M. Fromm, G. Bernardinelli and H. Goesmann, *Polyhedron*, 2000, **19**, 1783–1789.

11 K. M. Fromm, *Chem. Eur. J.*, 2001, **7**, 2236–2244.

12 K. M. Fromm and H. Goesmann, *Acta Crystallogr., Sect. C*, 2000, **56**, 1179–1180.

13 Single crystal data for **1**: $AgC_{16}H_{16}ClN_2O_9$, $M = 523.63$ g mol^{-1}, triclinic, space group $P\bar{1}$ (No. 2), $a = 7.190(1)$, $b = 12.074(2)$, $c = 12.078(2)$ Å, $\alpha = 112.54(3)$, $\beta = 102.27(3)$, $\gamma = 96.68(3)^\circ$, $V = 923.3(3)$ Å^3, $Z = 2$, $T = 240(2)$ K, $\rho = 1.883$ Mg m^{-3}, $\mu(MoK_\alpha) = 1.292$ mm^{-1}, $F(000) = 524$, 10734 reflections of which 5569 unique and 4391 observed, 278 parameters refined, GooF = 1.013, $R1 = 0.0568$, $wR2 = 0.1508$ for $I > 2\sigma(I)$ and $R1 = 0.0759$, $wR2 = 0.1732$ for all data. Single crystal data for **2**: $AgC_{16}H_{16}ClN_2O_9$, $M = 523.63$ g mol^{-1}, monoclinic, space group $C2/c$ (No. 15), $a = 23.631(5)$, $b = 7.104(1)$, $c = 25.554(5)$ Å, $\beta = 117.12(3)^\circ$, $V = 3818.7(1)$ Å^3, $Z = 8$, $T = 240(2)$ K, $\rho = 1.822$ Mg m^{-3}, $\mu(Mo_{K\alpha}) = 1.249$ mm^{-1}, $F(000) = 2096$, 7494 reflections of which 4216 unique and 2037 observed, 262 parameters refined, GooF = 0.971, $R1 = 0.0785$, $wR2 = 0.188$ for $I > 2\sigma(I)$ and $R1 = 0.1549$, $wR2 = 0.2220$ for all data. The intensities from the single crystals of **1** and **2** were measured on a STOE IPDS-II diffractometer, equipped with monochromated MoK$_\alpha$ radiation, at 240K. The structures were solved by direct methods and refined by full matrix least-squares on F^2 with the SHELX-97 package.[24] All heavy atoms were refined anisotropically. The positions of the hydrogen atoms could be calculated using riding models for all carbon atoms. CCDC 251188 (**1**) and 251189 (**2**). See http://dx.doi.org/10.1039/b506389b for crystallographic data in CIF or other electronic format.

14 K. M. Fromm, A. Robin, M. Meuwly, H. Goesmann and G. Bernardinelli, *CrystEngComm*, 2004, **6**, 336–343.

15 Rings: O.-S. Jung, Y.-A. Lee, Y. J. Kim and J. Hong, *Cryst. Growth Des.*, 2002, **2**, 497–499; O.-S. Jung, Y. J. Kim, Y.-A. Lee, S. W. Kang and S. N. Choi, *Cryst. Growth Des.*, 2004, **4**, 1, 23–24; M.-C. Brandys and R. J. Puddephatt, *Chem. Commun.*, 2001, 1508–1509; D. Braga, M. Polito, M. Bracaccini, D. D'Addario, E. Tagliavini, D. M. Proserpio and F. Grepioni, *Chem. Commun.*, 2002, 1080–1081; E. Lindner, R. Zong, K. Eichele, U. Weisser and M. Ströbele, *Eur. J. Inorg. Chem.*,

2003, 705–712; P. L. Caradoc-Davies and L. R. Hanton, *Dalton Trans.*, 2003, 1754–1758; J. C. Garrison, R. S. Simons, J. M. Talley, C. Wesdemiotis, C. A. Tessier and W. J. Youngs, *Organometallics*, 2001, **20**, 1276–1278; D. Braga, M. Polito, D. D'Addario, E. Tagliavini, D. M. Proserpio, F. Grepioni and J. W. Steed, *Organometallics*, 2003, **22**, 4532–4538; C. M. Hartshorn and P. J. Steel, *Inorg. Chem.*, 1996, **35**, 6902–6903; S. Chowdhury, M. G. B. Drew and D. Datta, *New. J. Chem.*, 2003, **27**, 831–835; T. Suzuki, H. Kotsuki, K. Isobe, N. Moriya, Y. Nakagawa and M. Ochi, *Inorg. Chem.*, 1995, **34**, 530–531.

16 Helices: P. L. Caradoc-Davies and L. R. Hanton, *Chem. Commun.*, 2001, 1098–1099; S. Sailaja and M. V. Rajasekharan, *Inorg. Chem.*, 2000, **39**, 4586–4590; Y.-B. Dong, J.-Y. Cheng, J.-P. Ma, H.-Y. Wang, R.-Q. Huang, D.-S. Guo and M. D. Smith, *Solid State Sciences*, 2003, **5**, 1177–1186; S. Qin, S. Lu, Y. Ke, J. Li, X. Wu and W. Du, *Solid State Sciences*, 2004, **6**, 753–755; C.-D. Wu, H. L. Ngo and W. Lin, *Chem. Commun.*, 2004, 1588–1589; S. P. Anthony and T. P. Radhakrishnan, *Chem. Commun.*, 2004, 1058–1059; Y.-T. Fu, V. M. Lynch and R. J. Lagow, *Chem. Commun.*, 2004, 1068–1069; J.-H. Yang, S.-L. Zheng, X.-L. Wu and X.-M. Chen, *Cryst. Growth Des.*, 2004, **4**, 831–836; A. Erxleben, *Inorg. Chim. Acta*, 2003, **348**, 107–114; A. J. Blake, N. R. Champness, P. A. Cooke, J. E. B. Nicolson and C. Wilson, *J. Chem. Soc., Dalton Trans.*, 2000, 3811–3819; F. Tuna, J. Hamblin, G. Clarkson, W. Errington, N. W. Alcock and M. J. Hannon, *Chem. Eur. J.*, 2002, **8**, 21, 4957–4964; G. Dong, H. Cheng, D. Chun-Ying, Q. Chun-Qi and M. Qing-Jin, *New J. Chem.*, 2002, **26**, 796–802; Y.-P. Cai, H.-X. Zhang, A.-W. Xu, C.-Y. Su, C.-L. Chen, H.-Q. Liu, L. Zhang and B.-S. Kang, *J. Chem. Soc. Dalton Trans.*, 2001, 2429–2434; Y. Kang, S. S. Lee, K.-M. Park, S. H. Lee, S. O. Kang and J. Ko, *Inorg. Chem.*, 2001, **40**, 7027–7031; A. Jouaiti, M. W. Hosseini and N. Kyritsakas, *Chem. Commun.*, 2003, 472–473; B. Schmaltz, A. Jouaiti, M. W. Hosseini and A. De Cian, *Chem. Commun.*, 2001, 1242–1243; M. J. Hannon, C. L. Painting, E. A. Plummer, L. J. Childs and N. W. Alcock, *Chem. Eur. J.*, 2002, **8**, 2225–2238; K.-M. Park, D. Whang, E. Lee, J. Heo and K. Kim, *Chem. Eur. J.*, 2002, **8**, 498–508; D. Whang, J. Heo, C.-A. Kim and K. Kim, *Chem. Commun.*, 1997, 2361–2362.

17 D. L. Reger, R. F. Semeniuc and M. D. Smith, *Eur. J. Inorg. Chem.*, 2003, 3480–3494.

18 S. Masoaka, D. Tanaka, Y. Nakanishi and S. Kitagawa, *Angew. Chem. Int. Ed.*, 2004, **43**, 2530–2534.

19 H. Abourahma, B. Moulton, V. Kravtsov and M. J. Zaworotko, *J. Am. Chem. Soc.*, 2002, **124**, 9990–9991.

20 I. S. Lee, D. M. Shin and Y. K. Chung, *Chem. Eur. J.*, 2004, **10**, 3158–3165; D. Braga, M. Polito, D. D'Addario and F. Grepioni, *Cryst. Growth Des.*, 2004, **4**, 1109–1112; D. V. Soldatov, G. D. Enright, J. A. Ripmeester, J. Lipkowski and E. A. Ukraintseva, *J. Supramol. Chem.*, 2001, **1**, 245–251; E. Tynan, P. Jensen, N. R. Kelly, P. E. Kruger, A. C. Lees, B. Moubaraki and K. S. Murray, *Dalton Trans.*, 2004, 3440–3447.

21 H.-J. Kim, W.-C. Zin and M. Lee, *J. Am. Chem. Soc.*, 2004, **126**, 7009–7014.

22 E. Lozano, M. Nieuwenhuyzen and S. L. James, *Chem. Eur. J.*, 2001, **7**, 2644–2651.

23 J. L. Sague Doimeadios, A. Y. Robin and K. M. Fromm, unpublished results.

24 G. M. Sheldrick, SHELX-99, *Program for Crystal Structure Refinement*, University of Göttingen, Germany, 1999.

The First Two-Dimensional Polycatenane: A New Type of Robust Network Obtained by Ag-Connected One-Dimensional Polycatenanes

Jorge L. Sagué and Katharina M. Fromm*

University of Basel, Department of Chemistry, Spitalstrasse 51, CH-4056 Basel, Switzerland

ABSTRACT: The two-dimensional structure described here is the first example of a coordination polymer structure consisting of one-dimensional polycatenanes fused via silver ions. It can be derived from simple rings consisting of two silver ions and two ligand molecules.

In the past decade, metal–organic frameworks (MOFs) have turned out to be a fascinating pool for structure design, synthesis, and applications in numerous fields such as catalysis, magnetism, luminescence, or gas storage.[1] By judicious choice of the building units, (i) the ligand concerning rigidity, form, and donor functions and (ii) the metal ion with its capacity to accept coordination by a given number of ligands, low-dimensional frameworks can be designed and constructed.[2] However, polymorphism and supramolecular isomerism occur more frequently the more flexible both building blocks are.[3] Porous frameworks with large empty spaces are a big challenge as interpenetration can occur.[4]

We are interested in using a flexible system with a metal ion such as Ag$^+$ and a multitopic ligand Ln ($n = 1, 2 ...$) (Scheme 1) with N- and O-donor atoms to synthesize adaptable MOFs, which are able to link a second metal ion type. With the shorter ligand L1, $n = 1$, a number of one-dimensional (1D) structural motifs could be characterized,[5–7] whereas with L2, a zero-dimensional metallacycle with two Ag$^+$ ions and two L2 molecules, as well as a 1D helix, could be reported.[8] Whereas with this ligand type Ln and Ag$^+$, only coordination numbers of two for Ag$^+$ with respect to the nitrogen atoms of Ln were reported so far;[6–9] we now report a new type of network derived from the polycatenation of a 1D chain of fused metallacycles in which Ag$^+$ has a coordination number of four with respect to L2. The obtained structure is an unprecedented example of linked polycatenane chains to give a very robust two-dimensional (2D) network of high density.

Results and Discussion. The reaction of L2 with AgClO$_4$ in the ratio 1:1 yields the 2:2 metallacycle or a 1D helix as a supramolecular isomer.[8] With AgPF$_6$, exo-linked 2:2 metallacycles of the composition [Ag(L2)]$_2$(PF$_6$)$_2$·THF (**1**) (THF = tetrahydrofuran) are obtained. The ratio L2/Ag$^+$ of 2:1 yields, after a long reaction time of over two months, a very dense and highly catenated structure of composition [Ag(L2)$_2$](PF$_6$) (**2**) representing a missing link in polycatenation motifs.

1 crystallizes in the triclinic space group $P\bar{1}$ (No. 2),[15] with one molecule per unit cell. Two ligands L2 adopt a U-shape and coordinate to two metal ions to yield a cyclic structure, with Ag–N distances of 2.136(4) and 2.143(4) Å, and an N1–Ag–N2 angle of 169.31(19)° (Figure 1). The two PF$_6^-$ anions bridge two silver ions belonging to the same ring; the Ag–F bonds are weak with distances of 2.960(7) and 3.092(5) Å. Because of this arrangement, the Ag–Ag distance within the ring is rather long at 5.213(13) Å, and π-stacking within the ring is thus excluded with pyridine rings offset from each other by 5.1218 Å.

The rings in **1** are arranged parallel to each other so that weak π-stacking between adjacent pyridine rings are possible (C5–C15′ 3.511(11) Å, N1–N2′ 3.529(11) Å. The Ag–Ag contact is the shortest between two rings with a distance of 3.4591(10) Å. Taking into account the positions of the Ag atoms, they form a zigzag line

with Ag–Ag–Ag angles of 124.4(1)°. The chains of rings are arranged in parallel to form sheets, between which the THF molecules are found, not coordinating to the rings in any way. Thermogravimetric and differential thermal analysis measurements show a quantitative loss of THF between 160 and 230 °C. **1** differs from the literature known ClO$_4$ analogue insofar as the ring in **1** has no intraring Ag–Ag contact, but an inter-ring one, the opposite of which is true in the perchlorate compound.[8] Solvent-containing structures such as **1** are usually not the thermodynamically most stable compounds, but so far the THF-free ring compound could only be generated by heating of **1** and not by crystallization from solvent. Qualitative powder spectra following the elimination of THF show peaks different from **1** and **2**, indicating a new structure (ESI[17]). However, if the mother liquor of **1** is allowed to stand for two months, new crystals can be observed, corresponding to the compound [Ag(L2)$_2$](PF$_6$) (**2**).

The basic motif of **2** consists of a chain of silver cations,[16] which are coordinated in a distorted tetrahedral fashion by four nitrogen atoms of four different ligand molecules (Figure 2). The Ag1–N distances are longer than in **1** and range from 2.287(3) to 2.381(3) Å, as expected for a coordination number of four for Ag$^+$.[10] The

Scheme 1. Ligand Series Ln, $n = 1, 2, ...$
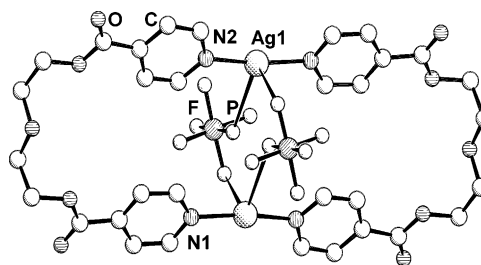
Figure 1. Molecular structure of **1**; hydrogen atoms and THF are not shown for clarity.
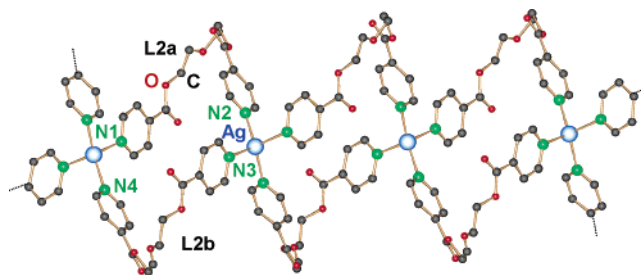
Figure 2. Simple chain motif of **2** showing the 1D structure of Ag-fused metalla-cycles; hydrogen atoms and anions are omitted for clarity.

* To whom correspondence should be addressed. Prof. Dr. Katharina M. Fromm, University of Basel, Dept of Chemistry, Spitalstrasse 51, CH-4056 Basel, Switzerland. Phone: +41 61 261004. E-mail: Katharina.Fromm@unibas.ch.
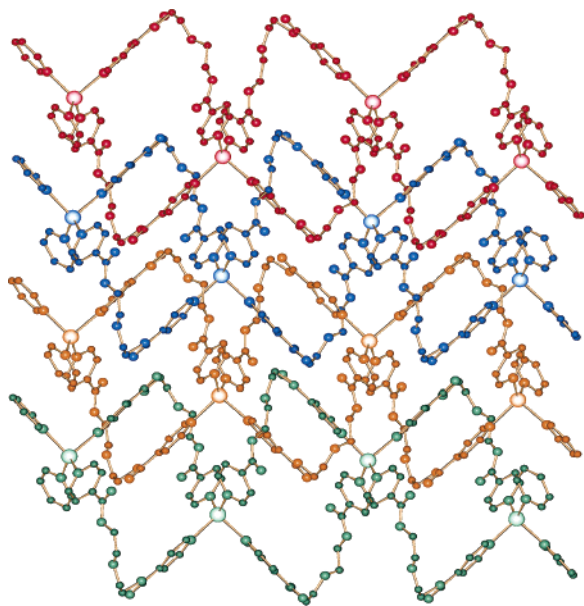
Figure 3. Interpenetration of 1D chains to yield 2D polycatenanes **2**; hydrogen atoms and anions are omitted for clarity.

N−Ag−N angles at the silver ion range from 103.53(8) to 118.2-(1)°, the two larger angles being found within a metallacycle. Thus, within the chain, two silver ions are linked to each other by two ligands, L2a (labeled from N1 to N2) and L2b (from N3 to N4), forming such a ring (Figure 2). Whereas L2a possesses an all-gauche conformation with torsion angles at the ethyl groups of ca. 60°, L2b has one gauche arrangement and one ethyl group almost perfectly eclipsed with a torsion angle of only ca. 6.8° about the O8−C25−C26−O9 bonds. The so-formed [L2Ag]$_2$-metalla-cycle forms a cavity of the dimension of ca. 9.2 × 17.2 Å. This cavity is large enough to allow the insertion of two other ligand molecules, one from a neighbor chain below and the other from above (Figure 3). Another way to describe the topology can be to consider the structure as parallel chains of 1D polycatenates, fused via the silver cations to yield the 2D overall motif. The so-formed entangled structure yields an unprecedented structure that is vaguely reminiscent of a chain mail motif, but with linked rings instead of separated ones, extending in a 2D array.

Organic- and metal-mediated synthesis of organic and metal-containing catenanes and more complicated knots has been well-established now;[11] however, coordination catenanes are rarer. Quantitative self-assembly of a coordination [2]catenane has been described by Fujita with Pd^{2+} and Pt^{2+},[12] showing that simple rings and [2]catenane are in equilibrium, which can be influenced by the concentration of the participating species. The mechanism to obtain such a [2]catenane is proposed as a reversible ring formation and reopening processes during which interpenetration can occur. Whereas this process was shown to be rapid, the formation of the polycatenane **2** seems to be a more complicated, slower process since the only product first observed is **1**, while **2** forms only after a long period with L2 in excess. Indeed, entropically, a high order has to be established in **2**, leading to a very dense structure with only 0.8% of free space, as compared to 10% in **1** (without THF). Fujita showed also that one or the other species of his compounds can be obtained in high yield depending on the polarity of solvent. This can also be applied to our system, since crystals of **1** were obtained in more aqueous medium, while **2** crystallized from the compartment containing a high concentration of THF or ethanol. Another example to be mentioned in this context is the system observed by Puddephatt et al. where a U-shaped diacetylide (L) forms rings with two gold ions of the type [LAu$_2$(dppe)] (dppe = diphenylphosphine ethane), which can entangle or not. Au−Au contacts can lead to a 1D chain of the simple rings without catenation.[13]

Polycatenation has been observed in coordination polymer networks, however, not with the topology observed in **2**, and usually involving larger ring species, such as (4,4) or (6,3) nets.[14] Here, **2** is the parallel catenation of ribbons of rings.

In summary, we have synthesized the first chain mail topology of a coordination compound via polycatenation of 1D chains of [Ag$_2$(L2)$_2$]-rings connected by Ag$^+$-nodes.

Experimental Section. Synthesis of 1. In an H-tube, 4 mg (0.015 mmol) of AgPF$_6$ dissolved in 4 mL of water were allowed to diffuse through 25 mL of THF to an organic solution of 4 mL of THF or EtOH containing 5 mg (0.015 mmol) of L2. Single crystals of **1** suitable for single-crystal X-ray analysis were obtained growing on the wall of the glass recipient in a yield of 46% with respect to Ag$^+$. Higher concentrations of reactants cause precipitation instead of crystallization.

Elemental Analysis. Calculated for **1**, [AgC$_{16}$H$_{16}$N$_2$O$_5$]PF$_6$·THF: C 37.5, H 3.8, N 4.4; found: C 37.1, H 3.7, N 4.3%.

IR (KBr, cm^{-1}). ν(Ar−H) 3061.8 s, ν(−HC−H) 2947.9 s, ν(C=O) 1733.4 s, ν (C=C) 1602.7 m, ν (ArC−C, C=N) 1411.8 m, ν (CO−O) 1272.7 s, ν (−C−O) 1108.6 m, δ(ArC−H) 1056.6 m, ν (PF$_6$) 822.1 s, broad

Melting Point. 242 °C (decomposition)

Synthesis of 2. Following the same procedure as for **1**, but using ethanol as linking solvent between the two solutions containing the ligand and the silver salt, afforded rodlike crystals of **2** in the bottom of the salt-containing part of the H-tube and crystals of **1** growing on the walls. Another way to crystallize **2** purely was achieved after 2 days of slow evaporation from a solution in which the ligand and the silver salt were mixed together in acetone. Yield: 20% with respect to Ag$^+$.

Elemental Analysis. Calculated: C 43.4, H 3.6, N 6.3%; found: C 43.6, H 3.8, N 6.2%.

IR (cm^{-1}). ν(Ar−H) 3105.4 s, ν(−HC−H) 2922.8 s, ν(C=O) 1733.4 s, ν (C=C) 1602.7 m, ν (ArC−C, C=N) 1411.8 m, ν (C−O) 1282.8 s, δ(ArC−H) 1056.6 m, ν (PF$_6$) 822.1 s, broad.

Melting Point. 130 °C (decomposition).

References

(1) Dobrawa, R.; Wuerthner, F. *J. Polym. Science, Part A: Polymer Chem.* **2005**, *43*, 4981−4995. Journal issue "Reticular Chemistry: Design, Synthesis, Properties and Applications of Metal-Organic Polyhedra and Frameworks," Yaghi, O. M., Ed. *J. Solid State Chem.* **2005**, *178*, 2409−2574, and references therein. Real, J. A.; Gaspar, A. B.; Munoz, M. C. *Dalton Trans.* **2005**, *12*, 2062−2079. Maspoch, D.; Ruiz-Molina, D.; Veciana, J. *J. Mater. Chem.* **2004**, *14*, 2713−2723. Andres, P. R.; Schubert, U. S. *Adv. Mater.* **2004**, *16*, 1043−1068. Millward, A. R.; Yaghi, O. M. *J. Am. Chem. Soc.* **2005**, *127*, 17998−17999. Rowsell, J. L. C.; Spencer, E. C.; Eckert, J.; Howard, J. A. K.; Yaghi, O. M. *Science* **2005**, *309*, 1350−1354. Sudik, A. C.; Millward, A. R.; Ockwig, N. W.; Cote, A. P.; Kim, J.; Yaghi, O. M. *J. Am. Chem. Soc.* **2005**, *127*, 7110−7118.

(2) James, S. L. *Chem. Soc. Rev.* **2003**, *32*, 276−288. Constable, E. C. *Compreh. Coord. Chem. II* **2004**, *7*, 263−302. Kitagawa, S.; Noro, S. *Compreh. Coord. Chem. II* **2004**, *7*, 231−261. Robinson, F.; Zaworotko, M. J. *Chem. Commun.* **1995**, 2413. Roesky, H. W.; Andruh, M. *Coord. Chem. Rev.* **2003**, *236*, 91. Blake, A. J.; Champness, N. R.; Hubberstey, P.; Li, W.-S.; Withersby, M. A.; Schroder, M. *Coord. Chem. Rev.* **1999**, *183*, 117. Khlobystov, A. N.; Blake, A. J.; Champness, N. R.; Lemenovskii, D. A.; Majouga, A. G.; Zyk, N. V.; Schroder, M. *Coord. Chem. Rev.* **2001**, *222*, 155. Cote, A. P.; Shimizu, G. K. H. *Coord. Chem. Rev.* **2003**, *245*, 49. Cote, A. P.; Ferguson, M. J.; Khan, K. A.; Enright, G. D.; Kulynych, A. D.; Dalrymple, S. A.; Shimizu, G. K. H. *Inorg. Chem.* **2002**, *41*, 287. Withersby, M. A.; Blake, A. J.; Champness, N. R.; Cooke, P. A.; Hubberstey, P.; Li, W.-S.; Schroder, M. *Cryst. Eng. Comm.* **1999**, *2*, 123. Reger, D. L.; Semeniuc, R. F.; Rassolov, V.; Smith, M. D. *Inorg. Chem.* **2004**, *43*, 537. Carlucci, L.; Ciani, G.; Proserpio, D. M.; Rizzato, S. *CrystEngComm* **2002**, *4*, 413. Pocic, D.; Planeix, J.-M.; Kyritsakas, N.; Jouaiti, A.; Hosseini, M. W. *CrystEngComm* **2005**, *7*, 624−628.

(3) Moulton, B.; Zaworotko, M. J. *Chem. Rev.* **2001**, *101*, 1629−1658. Ring, D. J.; Aragoni, M. C.; Champness, N. R.; Wilson, C. *CrystEngComm* **2005**, *7*, 621−623, Gale, P. A.; Light, M. E.; Quesada, R. *Chem. Commun.* 2005, 5864−5866. Aitipamula, S.; Nangia, A. *Chem. Eur. J.* **2005**, *11*, 6727−6742;

(4) Delgado-Friedrichs, O.; Foster, M. D.; O'Keeffe, M.; Proserpio, D. M.; Treacy, M. M. J.; Yaghi, O. M. *J. Solid State Chem.* **2005**, *178*, 2533−2554.

(5) Fromm, K. M.; Gueneau, E. D.; Robin, A. Y.; Maudez, W.; Sague, J.; Bergougnant, R. *Z. Anorg. Allg. Chem.* **2005**, *631*, 1725−1740.

(6) Robin, A. Y.; Meuwly, M.; Fromm, K. M.; Goesmann, H.; Bernardinelli, G. *CrystEngComm* **2004**, *6*, 336−343.

(7) Robin, A. Y.; Fromm, K. M.; Goesmann, H.; Bernardinelli, G. *CrystEngComm* **2003**, *5*, 405−410.

(8) Fromm, K. M.; Sague Doimeadios, J. L.; Robin, A. Y. *Chem. Commun.* **2005**, 4548−4550.

(9) Jouaiti, A.; Hosseini, M. W.; Kyritsakas, N. *Chem. Commun.* **2003**, 472−473.

(10) Dyason, J. C.; Healy, P. C.; Engelhardt, L. M.; White, A. H. *Aust. J. Chem.* **1985**, *38(9)*, 1325−1328. Nilsson, K.; Oskarsson, A. *Acta Chem. Scand., Series A: Phys. and Inorg. Chem.* **1982**, *A36*, 605−610.

(11) Carlucci, L.; Ciani, G.; Proserpio, D. M. *Coord. Chem. Rev.* **2003**, *246*, 247−289. Lukin, O.; Voegtle, F. *Macrocyclic Chem.* **2005**, 15−36; *Molecular Catenanes, Rotaxanes, and Knots*; Sauvage, J.-P.; Dietrich-Buchecker, C., Eds.; Wiley-VCH: Weinheim, Germany, 1999 and references therein. Collin, J.-P.; Sauvage, J.-P. *Chem. Lett.* **2005**, *34*, 742−747; Menon, S. K.; Guha, T. B.; Agrawal, Y. K. *Rev. Inorg. Chem.* **2004**, *24*, 97−133. Batten, S. R. Interpenetration, In *Encyclopedia of Supramolecular Chemistry*; Atwood, J. L., Steed, J. W., Eds.; Marcel Dekker: New York, 2004; pp 735−741.

(12) Fujita, M. In *Molecular Catenanes, Rotaxanes, and Knots*; Sauvage, J.-P., Dietrich-Buchecker, C., Eds.; Wiley-VCH: New York, 1999; pp 57−76.

(13) Mohr, F.; Jennings, M. C.; Puddephat, R. J. *Eur. J. Inorg. Chem.* **2003**, 217−223 and therein.

(14) Baburin, I. A.; Blatov, V. A.; Carlucci, L.; Ciani, G.; Proserpio, D. M. *J. Solid State Chem.* **2005**, *178*, 2471−2493; Blatov, V. A.; Carlucci, L.; Ciani, G.; Proserpio, D. M. *CrystEngComm* **2004**, *6*, 377−395.

(15) Crystallographic data for **1**: AgC$_{20}$H$_{24}$N$_2$O$_6$PF$_6$, M = 641.25 g mol^{-1}, triclinic, space group $P\bar{1}$ (No. 2), a = 7.701(1), b = 12.961(3), c = 13.021(3) Å, α = 94.55(3), β = 95.85(3), γ = 107.23(3)°, V = 1226.7(4) Å^3, Z = 2, T = 240(2) K, ρ = 1.736 Mg m^{-3}, μ(Mo Kα) = 0.971 mm^{-1}, $F(000)$ = 644, 4984 reflections of which 4984 unique and 4984 observed, 325 parameters refined, GOF = 0.931, R1 = 0.0602, wR2 = 0.1342 for $I > 2\sigma(I)$ and R1 = 0.1157, wR2 = 0.1584 for all data.

(16) Crystallographic data for **2**: AgC$_{32}$H$_{32}$N$_4$O$_{10}$PF$_6$, M = 885.46 g mol^{-1}, orthorhombic, space group *Pbcn* (No. 60), a = 28.388(8), b = 15.020(1), c = 17.059(6) Å, V = 7274(3) Å^3, Z = 8, T = 153(2) K, ρ = 1.617 Mg m^{-3}, μ(Mo Kα) = 0.690 mm^{-1}, $F(000)$ = 3584, 56 024 reflections of which 21 906 unique and 4391 observed, 488 parameters refined, GOF = 1.032, R1 = 0.0698, wR2 = 0.1840 for $I > 2\sigma(I)$ and R1 = 0.0971, wR2 = 0.2075 for all data.

(17) The single crystals of **1** and **2** were measured on a STOE IPDS-II diffractometer, equipped with monochromated MoKα radiation, at 240 K (1) and 153 K (2). The structures were solved with direct methods and refined by full matrix least-squares on F^2 with the SHELX-97 package. All heavy atoms were refined anisotropically. The positions of the hydrogen atoms could be calculated using riding models for all carbon atoms. Crystallographic data for the structures reported here have been deposited with the Cambridge Crystallographic Data Centre as supplementary publications no. CCDC-295448 (1) and CCDC-295449 (2). Copies of the data can be obtained free of charge on application to CCDC, 12 Union Road, Cambridge CB21EZ, UK (fax: (+44)1223-336-033; e-mail: deposit@ccdc.cam.ac.uk).

On the coordination behaviour of NO_3^- in coordination compounds with Ag^+
Part 1. Solubility effect on the formation of coordination polymer networks between $AgNO_3$ and L (L = ethanediyl bis(isonicotinate)) as a function of solvent

Adeline Y. Robin, Jorge L. Sagué and Katharina M. Fromm*

The influence of the solubility of $AgNO_3$ in three solvent systems is studied for the reaction between $AgNO_3$ and the ligand **L** (= ethanediyl bis(isonicotinate)). Three solid state structures are obtained, differing in the relative ratio Ag : **L** in the first case, and in polymorphism in the second. The Ag–$O(NO_3^-)$ distance correlates strongly with the solubility of $AgNO_3$ in the used solvent. Solution studies prove indeed the existence of close ion contact pairs in the less good solvents, where as ion solvation is observed in good solvents for $AgNO_3$. The three different structures are compared to two solvated structures in which H_2O demonstrates coordination to the nitrate anion *via* H-bonding.

Introduction

During the last fifteen years the number of publications concerning coordination polymer networks has dramatically increased from 100 articles per year to 1000 in 2004 as shown in recent reviews on the subject.[1–3] The numerous literature contributions in the field of coordination polymers are due to several points: (i) incorporating metal ions in supramolecular networks permits the control of the metal atom positions in the materials, giving them some desired properties. The types of metal ions and distances between them can be chosen so that stable functional solid materials can be tuned; (ii) the variety of "nodes and linkers" offers to the chemists infinite possibilities for building new species with intriguing properties, architectures and topologies.[4–7] Moreover, the studies of crystals become much easier thanks to the technological improvements in the field of X-ray measurements and computational resolution techniques.

A large amount of coordination polymer networks involve bipyridyl (*N*-donors) ligands. They include pyrazine[8–10] and its derivatives,[11–14] 4,4′-bipyridine[15–22] and longer bridged bipyridyl ligands[23–41] as linkers with a large diversity of the metal centers as nodes. The coordination polymers derived from Ag^I with N-donor ligands are well-known for making simple 1-D motifs when the metal ion reacts with a bipyridine-type ligand.[42,43] Ag^I prefers mostly a linear geometry with respect to the coordination of N-donor ligands in these cases. Nevertheless, as the coordination sphere of Ag^I is very flexible,[15,21,32,38,45–53] it can adopt coordination numbers between two and six, the geometry changing from linear to octahedral. The coordination geometries of Ag^I are often

distorted owing to the inherent lack of ligand field stabilization effects. This flexibility of the Ag^I ion is used to investigate the role played by the weak interactions during the crystal formation. The lability of the silver-donor atom bonds allows furthermore building complexes, so that the process of coordination polymer formation is reversible.

All building blocks included in one coordination polymer have particular interactions with the solvents, according to their polarity, hydrophilic/hydrophobic groups, *etc*.... The solvent can have a role as coordinating molecules[54] or template molecules.[55] It is assumed that the differences in size and shape of the used solvents affect the self-assembly and result in the formation of different 2-D frameworks.[55]

The work on coordination polymers in our group follows the synthesis of homo- and mixed compounds of group 1 and 2 metals with the aim to synthesise new precursors for CVD and sol-gel techniques used for oxide materials.[56–65] In order to obtain better performing and single source precursors, mixed metal compounds containing transition metal, as well as group 1 and 2 metal ions began to be investigated. The formation of coordination polymers is thus an efficient way to get a good distribution of the metals within the materials.

With regard to the field of coordination polymers formed with group 11 elements, the ligand ethanediyl bis(isonicotinate), **L**, was chosen[66,67] because it (i) is flexible (structurally adaptive), (ii) contains different functional groups allowing coordination of two different metal ions, and (iii) can be prepared easily, which makes potential applications possible. **L** can adopt two main conformations, *gauche* or *anti*, due to the free rotation around the ethyl group C–C bond. Obviously, different conformations of the ligand in the coordination polymers can drastically change the resulting framework architecture. Several ligands with the same flexibility have already been used.[50,68,69] In most cases, only one conformation

University of Basel, Department of Chemistry, Spitalstrasse 51, CH-4056, Basel, Switzerland. E-mail: katharina.fromm@unibas.ch; Fax: +41 (0)61|267 1021; Tel: +41 (0)61|267 1004
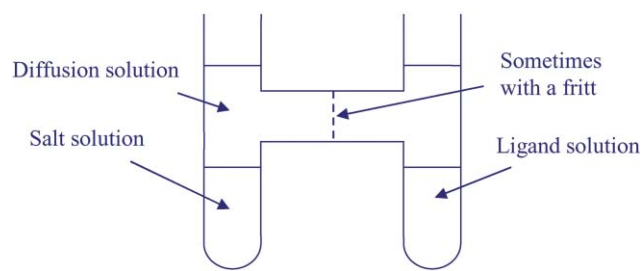
Scheme 1 "H-shaped" tube.
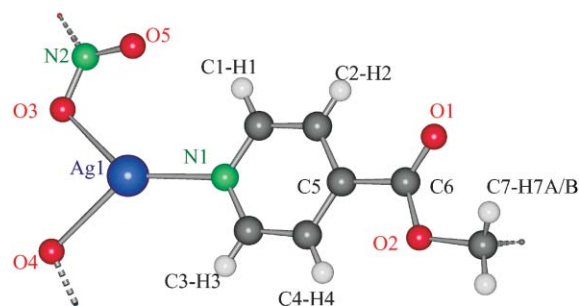
Fig. 1 Asymmetric unit of 1.

per framework is observed. As we have already reported on pseudo-polymorphism of **L** with CuCl and AgNO₃, we here wish to report the effect of solubility on the formation of coordination polymer networks of **L** with AgNO₃.

Results and discussion

Crystals of {[Ag₂(NO₃)₂(**L**)]}ₙ, **1**, grow in a "H-shaped" tube (Scheme 1). With the proportion **L** : Ag = 1 : 1, **L** dissolved in THF and silver nitrate in ethanol, are put each in one arm of the tube, the solutions are frozen by immersion of the tube in liquid nitrogen and finally the diffusion solvent (THF) is added. The slow diffusion can take place in order to yield high quality crystals of **1** at the interface EtOH/THF. Unfortunately, the yield is not high and only few crystals grow in each batch. The results of performed reactions in order to get more of **1** in higher quantity are resumed in Table 1. Only the first two reactions gave **1**, but always in very low yield.

Compound **1** crystallizes in the monoclinic space group C2/c (no.15).[70] There are eight asymmetric units consisting of one silver atom, one nitrate anion and half of a ligand molecule in each unit cell (Fig. 1).

There are thus two silver atoms for one ligand molecule. Each silver atom is coordinated with one ligand molecule, and the distance Ag–N is with 2.226(7) Å in the same range than in comparable silver coordination compounds.[10,36,42,43,67] It is also linked to two oxygen atoms of two different nitrate anions, O3 and O4, the distances Ag–O are 2.354(5) and 2.390(7) Å long. (Table 2) This corresponds to short Ag–O(NO₃) distances showing a strong coordination bond between cation and anions (Fig. 2b). These Ag–O distances belong to the shortest ones known in the literature.[54,71,72] The Ag–O(NO₃) distances are usually found from 2.3 to 2.6 Å, as the nitrate anion is a moderate good coordinating counter anion.[42,43] The nitrate anions of **1** act as bridging ligands between two silver cations, two oxygen atoms of each anion bridging two adjacent metal ions. This leaves the third oxygen atom, O5, uncoordinated within this chain.

Table 2 Most important bond lengths (Å) and angles (°) in 1

Ag–N	2.226(7)	O–Ag–N	138.2(3), 135.3(2)
Ag–O(O₂N)	2.354(5), 2.390(7) 2.72(1)	O–Ag–O	84.6(2)
C–N	1.334(8), 1.35(1)	C–N–C	118.6(6)

The angle sum around the silver cation arises to *ca.* 358°, showing the quasi-trigonal planar arrangement of closest ligands around the metal ion. Ligand molecules, silver atoms and nitrate anions are organized so that a neutral 2-D motif appears. This motif is called "fishbone"-like layer (Fig. 2a). It is evident from Fig. 2 that the motif is constituted by AgNO₃-chains (in the *c* direction), which are linked through the ligand molecules. The ligand molecules are running in symmetric directions on both sides of the silver nitrate chain, explaining the "fishbone" name.

The conformation of the ligand is *anti* as in the free ligand.[66] The pyridine planes within a ligand molecule are parallel as there is an inversion center in the middle of the C7–C7#1 bond, the two planes being separated by 0.46(5) Å. The plane containing the pyridine ring and the plane containing the adjacent ester group form an angle of 10.1(8)° to each other. One hydrogen bond is found between the oxygen atom O1 and the hydrogen atom H7B within a ligand molecule (Table 3).

This intra-ligand hydrogen bond can appear as the ligand is highly distorted with a O2–C7–C7#1 angle of 77(3)° (Fig. 3). The position of O2 is disordered: this atom position is disordered and was split into two positions with 50% occupancy, O2A and O2B in the crystallographic data. In spite of this distortion, the distance Ag–Ag is 17.76 Å long, corresponding to the same Ag–Ag distance observed in other coordination polymers with the *anti*-conformation of **L**.[66,67] The distortion is compensated by *ca.* 0.04 Å longer O–C bonds compared to these literature compounds.

Some other weak interactions can be observed within the layer (Fig. 4, Table 3): (i) hydrogen bonds are observed between two parallel ligand molecules (highlighted in yellow in

Table 1 Experiments and products of reaction **L** + AgNO₃ (1:1) with ethanol

Ligand	AgNO₃	Experiment	Diffusion solvent	Product	Concentration/mol L⁻¹
THF	EtOH	"H-shaped" tube	THF	**1**	3.10⁻³
THF	EtOH	"H-shaped" tube	THF	**1**	1,5.10⁻³
THF	EtOH	"H-shaped" tube	THF	"{Ag**L**NO₃}"	6.10⁻³
EtOH	EtOH	"H-shaped" tube	EtOH	{[Ag(**L**)](NO₃)}ₙ[58]	3.10⁻³
EtOH	H₂O	"H-shaped" tube	EtOH	{[Ag(**L**)](NO₃)(H₂O)₂}ₙ[58]	3.10⁻³
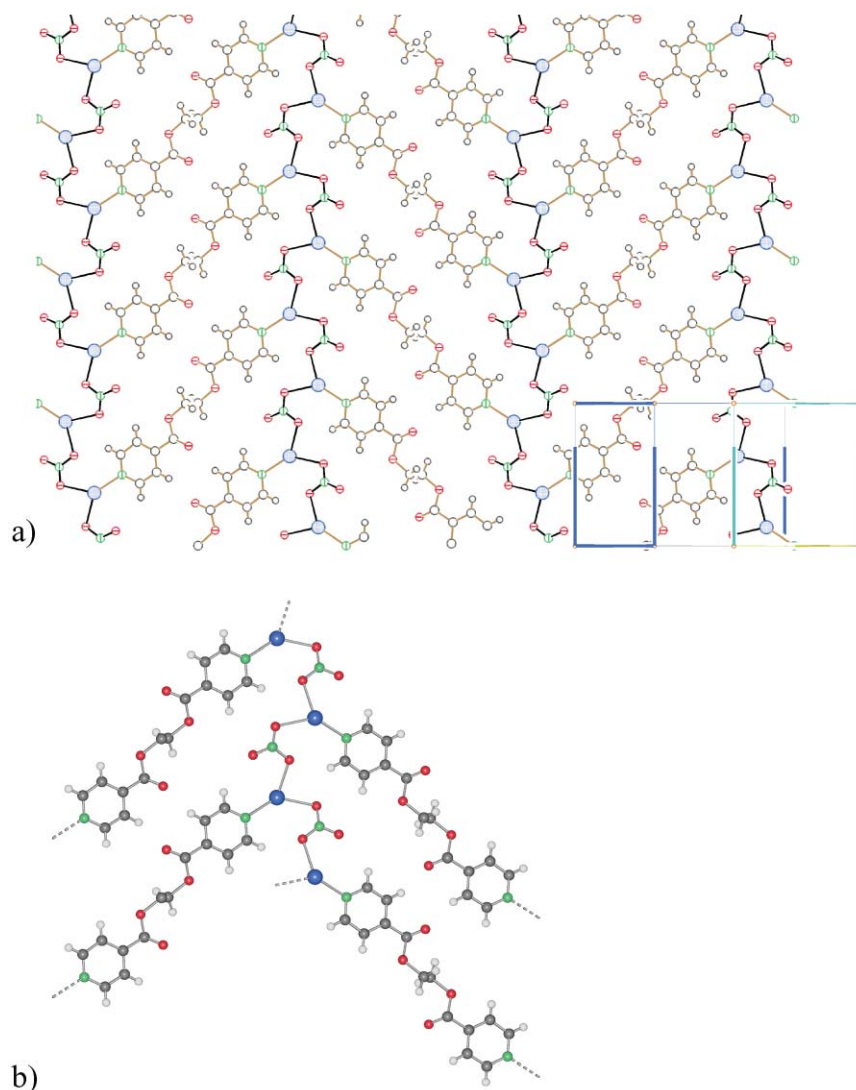
Fig. 2 (a) The two-dimensional 'fishbone' motif in **1**; (b) detail around the silver atoms.

Fig. 4), and (ii) the nitrate anions are involved in hydrogen bonding to the surrounding pyridyl hydrogen atoms, ranging from 2.46 to 2.89 Å (highlighted in blue in Fig. 4).

The so formed layers are stacked parallel to each other to form the overall 3-D structure (Fig. 5a). The layers are rather flat; however, the silver atoms don't exactly lie in the mean plane of the layers. If one considers the three atoms around one silver atom (N1, O3 and O4), the sum of the three angles

Table 3 Hydrogen bond data for **1** [lengths (Å) and angles (°)]

D–H···A	D(D–H)	d(H···A)	d(D···A)	Angle D–H···A
Intra-ligand				
C7–H7B···O1[#1]	0.97	2.37	2.98(3)	120.6
Intra-sheet hydrogen bonding interactions				
C2–H2···O1[#2]	0.93	2.38	3.27(1)	161.2
C3–H3···O3[#3]	0.93	2.49	3.29(1)	143.7
C3–H3···O4[#3]	0.93	2.46	3.167(9)	132.9
C4–H4···O4[#3]	0.93	2.89	3.37(1)	113.0
C1–H1···O5	0.93	2.80	3.55(1)	137.8

[a] Symmetry transformations used to generate equivalent atoms: #1 −x, −y − 1, −z; #2 −x, −y, −z; #3 −x + 1/2, y−1/2, −z + 3/2.

(O3–Ag–N1, N1–Ag–O4, O4–Ag–O3) is smaller than 360° (358°) indicating a weak deformation from the trigonal planar coordination sphere of the silver atom. Indeed the silver atoms are coordinated perpendicular to the layer plane by the O5-atom of a nitrate anion of the next sheet, at a distance of 2.72(1) Å. This distance Ag–O5 is much longer than Ag–O3 and Ag–O4 but is in the range of those of weak coordinating nitrate anions.

Furthermore, there is a weak metal–ring interaction on the other side of the silver atom (Fig. 5b, Table 4). Whereas the literature reports mainly η^2-interactions between aromatic rings and silver ions, we observe a distorted η^3-binding between pyridine and Ag$^+$. The strongest contacts are found between Ag and C5 with 3.39(1) Å, the distances Ag–C4 and

Fig. 3 Top view of the ligand in **1** with the distortion.
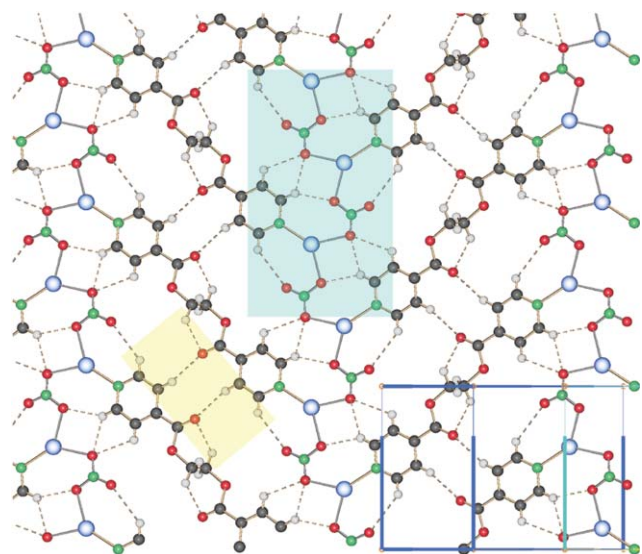
Fig. 4 Intra-sheet interactions in **1**: hydrogen bonds between ligand molecules in yellow and hydrogen bonds involving the nitrate counter anions in blue.

Ag–C2 being 3.56(1) and 3.59(1) Å, respectively (Fig. 5b).[73–77] The remaining distances Ag–ring are longer than 3.85 Å. No other interactions are found between two adjacent layers except these interactions involving the silver atoms.

The arrangement of the main structure made of …–Ag–NO$_3$–Ag–NO$_3$–… chains, is probably due to the poor solubility of AgNO$_3$ in ethanol, which is unable to dissolve the silver nitrate contacts completely. This can be confirmed experimentally by two methods, solution IR and ES-MS, both of which show that NO$_3^-$ exists associated to the silver cations in solution and the gas phase. Indeed, the IR-bands at 1327 and 1412 cm^{-1} can be attributed to coordinating anion.[78] The fragments observed in ES-MS at 431.9 m/z confirm the presence of species of the type [Ag$_2$(NO$_3$)$_2$(EtOH)$_2$]$^+$.

To our knowledge, this is the first example of 2-D neutral silver coordination polymer, with a trigonal planar coordination of silver {AgO$_2$N} and this motif. Some

Table 4 Ag···pyridine ring interactions lengths (Å) and angles (°) in **1**.

	d_{M-R}[b]	pd_{M-R}[c]	β[d]
Ring (N1, C1, C2, C3, C4, C5) ···Ag1$^{\#1\ a}$	3.472	3.357	14.77

^{a} Symmetry transformations used to generate equivalent atoms: #1 x, $-y$, $z + 1/2$. ^{b} d_{M-R}, distance metal-geometrical center of the ring. ^{c} pd_{M-R}, perpendicular distance of the metal on the ring. ^{d} β, shift angle.

[–Ag–(NO$_3$)–]$_n$ are found in the compound {[Ag(1,4-bis(phenylthio)butane)(NO$_3$)]}$_n$,[54] in which the Ag^I center is tetrahedrally coordinated to two S atoms from the ligand and two O atoms from nitrate anions. The structure may be described as [–Ag–(NO$_3$)–]$_n$ linked *via* the ligands as in **1**, but with a different coordination environment for the silver ion and longer silver-nitrate distances (2.452(6) and 2.557(6) Å).

The synthesis of silver coordination polymers using silver nitrate and **L** was also performed in acetonitrile. The solutions of **L** and silver nitrate, each dissolved in acetonitrile, are mixed, stirred and then left at room temperature ($C = 5 \times 10^{-3}$ mol L^{-1}). Self-assembly between silver ions and **L** occurs in darkness giving colourless single crystals of {[Ag(L)]NO$_3$}$_n$, **2**, suitable for X-ray diffraction. The quantity of crystals was not sufficient to perform other analyses on this sample. However the reaction of **L** and AgNO$_3$ in dichloromethane gives a white polycrystalline precipitate. Its powder X-ray spectrum was compared to the calculated one (from single crystal data) showing that the precipitate is isostructural and thus identical with **2**. This precipitate was therefore used for the further characterizations.

Compound **2** crystallizes in the triclinic space group $P\bar{1}$ (no.2).[70] The asymmetric unit is composed of one ligand molecule, one silver atom and one nitrate anion (Fig. 6) and there are two of such moieties in the unit cell. The most important bond lengths and angles are listed in Table 5.

In this case, the silver atoms are coordinated by two different ligands through their nitrogen atoms. The ligand molecules thus act as connectors between the silver atoms, the final motif being a charged one-dimensional, also called polyelectrolyte chain (Fig. 7). The distances Ag–N are 2.183(4)
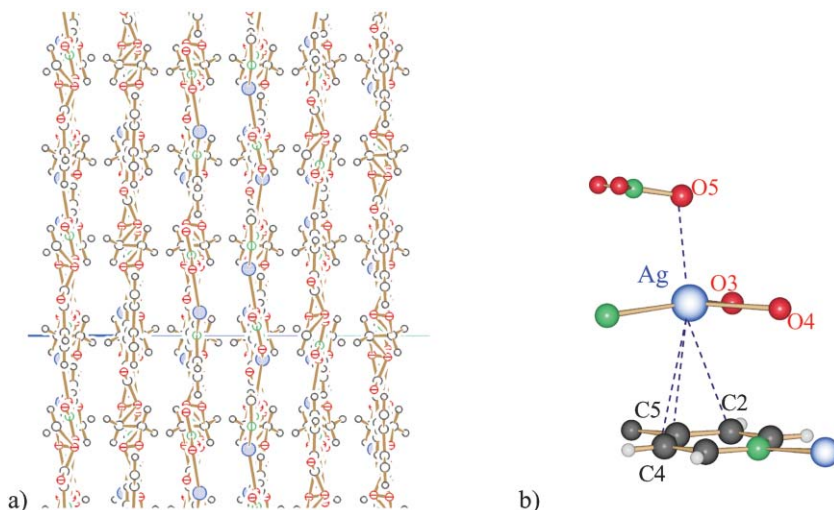
Fig. 5 (a) Three-dimensional structure of **1** in the direction (11 0 10); (b) coordination environment around silver atoms in **1**.
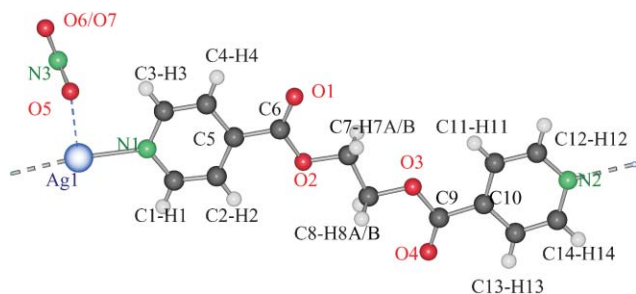
Fig. 6 Asymmetric unit in **2**.

Table 5 Most important bond lengths (Å) and angles (°) in **2**

Ag–Ag	4.017(2)		
Ag–N	2.183(4), 2.189(4)	N–Ag–N	169.8(2)
Ag–O(O$_2$NO)	2.599(5), 2.703(7)		
	3.044(4), 3.122(4)		
C–N	1.342(5), 1.343(7)	C–N–C	117.5(4)
	1.352(6), 1.347(5)		116.6(4)

and 2.189(4) Å long, and the N–Ag–N angle is with 169.8(2)° quite deviated from linear.

The linearity in the chain is due to the *anti*-conformation adopted by the ligand molecules. The ligand molecules alternating with the silver atoms have all the same direction and are oriented in the same direction "up-to-down" (Fig. 7). The distance Ag–Ag within the chain is thus 17.66 Å long as in **1** and similar compounds where the same ligand is in *anti* conformation.[66,67] The coordination sphere of the silver atoms is completed by interactions with the nitrate anions. All three nitrate oxygen atoms, O5, O6 and O7, are linked to silver atoms, so that the nitrate anions act as linkers in-between the chains (Fig. 8). The silver–oxygen distances range from 2.599(5) to 3.122(4) Å. These distances in **2** are by 0.25 Å longer on average than in **1** and smaller than in other
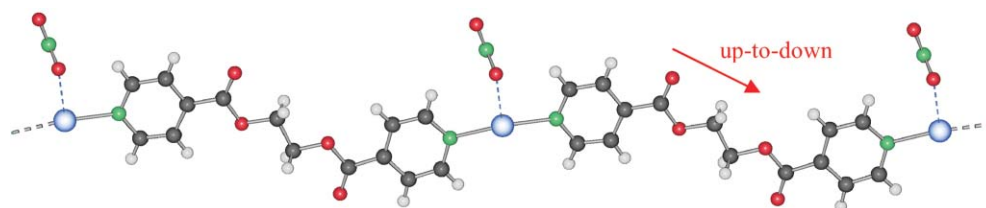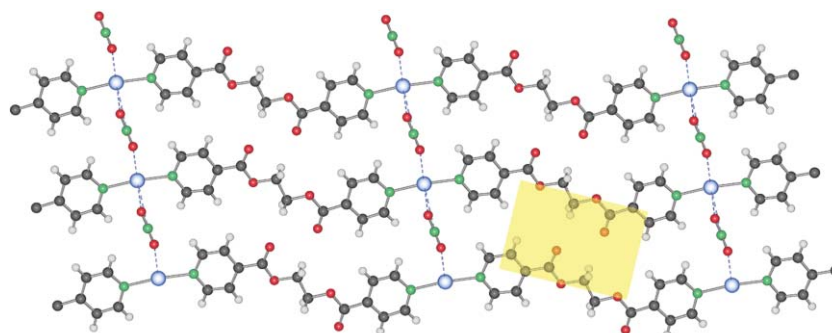
comparable compounds.[10,36,42,43,67] The N–Ag–N deviation from linearity is due to the strong Ag1–O5 interactions (2.599(5) Å). Hydrogen bonds (C8–H8B···O1) allow the alignment of the chains and thus the formation of an overall neutral layer. The shortest distance between the silver atoms in the layer is 6.159(1) Å.

As shown on Fig. 9a, the chains are ordered in the direction (−12 10 22) with a slight inclination of the molecular mean plane compared to this direction, the counter anions lying only on one side of the chains. Indeed the coordination of the nitrate molecules is not distributed homogeneously around the silver atoms but they are found only on one side (Fig. 9b). In the 3-D structure of **2**, the layers stack parallel and alternate their orientations: the nitrate anions are pointing in one direction, and in the next layer they are pointing in the opposite one (Fig. 9c).

Two types of inter-sheet areas are thus created: in the first one the anions are embedded, and in the next one the chains are simply parallel to each other, as described in Fig. 10b.

As there are two types of inter-sheets, there are various complementary interactions between the layers (Fig. 10a). In the "empty" inter-sheets, the layers interact *via* π-stacking (Table 6) between the rings N1, C1…C5 and N2, C10…C14 with a center-to-center distance of 3.82 Å and an offset of 1.5 Å. The silver–silver distances are 4.017(2) Å long and are not the shortest contact between two chains. Pairs of chains similar to literature compounds appear (see below),[67] but in contrast to the latter, the counter ion role is different, there are no short Ag–Ag contacts, and only the π-stacking remains. The much shorter Ag–Ag distances of the literature compounds must apparently be supported by the nitrate anions, which is not the case here.

The overall arrangement is strengthened with hydrogen bonds between the ligand molecules of two close layers, and between the nitrate anions and neighboring ligand molecules

Fig. 7 The linear motif in **2**.

Fig. 8 Alignment of the chains in **2** with the nitrate as linkers and the hydrogen bond region highlighted in yellow.
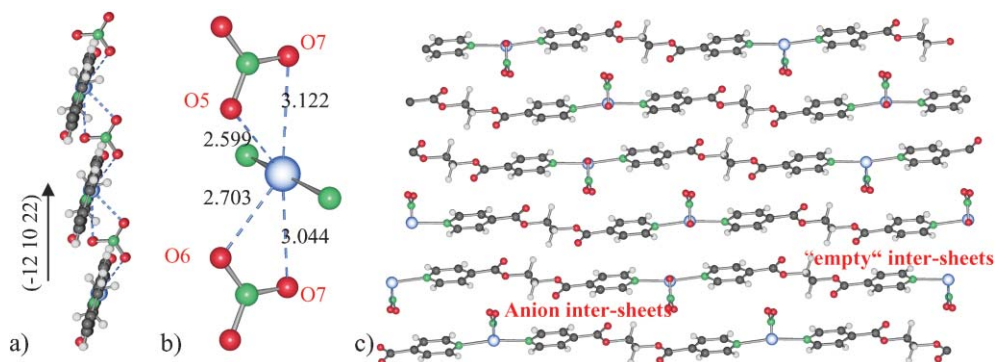
Fig. 9 (a) Organisation of the chains and the nitrate anions within a layer; (b) coordination of silver; (c) stacking of the layers in the structure of **2**.
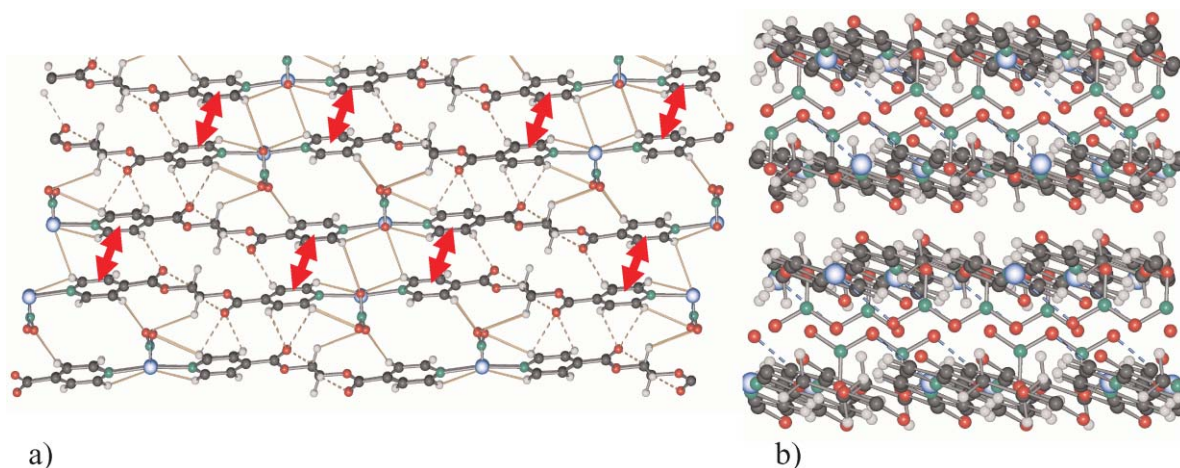
Fig. 10 (a) 3-D structure of **2** with the inter-sheets interactions (red arrows: π-stacking in the empty inter-sheets; dashed lines: hydrogen bonds between ligands; full lines: hydrogen bonding involving the nitrate anions). (b) View of the stacked layers in **2**.

Table 6 Ring interactions lengths (Å) and angles (°) in **2**.

π–π interactions	d_{R-R} [b]	pd_{R-R} [c]	β [d]	α [e]
Ring (N1, C1, C2, C3, C4, C5) ···Ring (N2, C10, C11, C12, C13, C14)[#1 a]	3.82	3.49	24.0	2.1

[a] Symmetry transformations used to generate equivalent atoms: #1 $-x + 2$, $-y + 1$, $-z + 1$. [b] d_{R-R}, distance between the two geometrical centers of the rings. [c] pd_{R-R}, perpendicular distance of the geometrical center of one ring on the other. [d] β, shift angle. [e] α, inclination angle between the two rings.

(Fig. 10a). These interactions take place in the two kinds of inter-sheet layers (Table 7).

Coordination polymer synthesis based on **L** and AgNO$_3$ and crystallization were also attempted from a THF/water mixture. Compound **3** is obtained purely by crystallisation from an **L**/AgNO$_3$ mixture in THF/water after slow evaporation of the solution. Elementary analysis for **3** shows a composition: Ag : NO$_3$: L of 1 : 1 : 1, as for **2**. {[Ag(**L**)]NO$_3$}$_n$, **3**, crystallizes in the monoclinic space group $P2_1/n$ (no.14).[67] There are four asymmetric units per unit cell, made of one ligand molecule, one silver atom and one nitrate anion (Fig. 11). The pyridine rings coordinate to the silver ions creating a 1-D motif: a chain with alternating silver ions and ligand molecules –Ag–**L**–Ag–**L**–, the silver atoms being coordinated by two nitrogen atoms of two different ligand molecules (Fig. 12). This compound has been described previously in another context together with two pseudo-polymorphs of **3**, {[Ag(**L**)](NO$_3$)(H$_2$O)}$_n$, **4**, and

Table 7 Hydrogen bond data for **2** [lengths (Å) and angles (°)]

D–H···A	d(D–H)	d(H···A)	d(D···A)	Angle D–H···A
Inter-chains interactions				
C8–H8B···O1[#1]	0.97	2.64	3.580(7)	163.4
Intra-sheets hydrogen interactions				
C11–H11···O1[#2]	0.93	2.79	3.648(7)	153.2
C13–H13···O3[#3]	0.93	2.63	3.195(7)	119.3
C14–H14···O4[#3]	0.93	2.85	3.316(6)	112.3
C7–H7A···O4[#4]	0.97	2.50	3.436(7)	161.9
Hydrogen bonds involving nitrate anions				
C1–H1···O7[#4]	0.93	2.65	3.403(7)	138.9
C12–H12···O7[#4]	0.93	2.58	3.309(8)	135.3
C1–H1···O7[#5]	0.93	2.80	3.38(1)	121.3
C4–H4···O6[#3]	0.93	2.53	3.390(8)	154.7
C8–H8A···O6[#3]	0.97	2.83	3.494(7)	126.5
C14–H14···O5	0.93	2.65	3.308(9)	128.3

[a] Symmetry transformations used to generate equivalent atoms: #1 $x + 1$, y, z; #2 $-x$, $-y + 2$, $-z + 2$; #3 $-x + 2$, $-y + 1$, $z + 1$; #4 $x - 1$, y, z; #5 $-x + 1$, $-y + 2$, $-z + 2$.
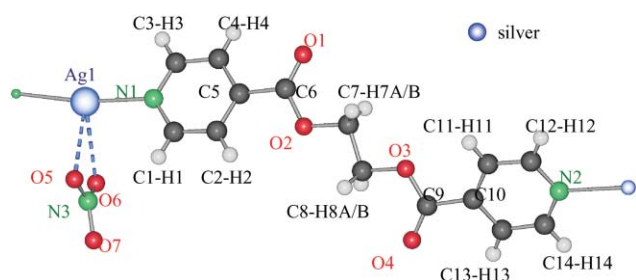
Fig. 11 Asymmetric unit in **3** (colour codes given for all following figures).

$\{[Ag(\mathbf{L})](NO_3)(H_2O)_2\}_n$, **5**.[67] Due to the relevance of these structures in the discussion here, their main structural features will briefly be highlighted in the following (Table 8, Fig. 11–16).

The conformation of the ligand within the coordination polymer of **3** is the *anti* one, the same as in the crystalline ligand alone[66] and as in compounds **1** and **2**. In contrast to **2**, the chains of **3** have an undulating form because the direction of the ligand molecules changes after each silver cation, going alternately "up-to-down" and then "down-to-up" as shown in Fig. 12.

The Ag–N distances of **3** are 2.232(2) and 2.239(2) Å long and the angle N–Ag–N is 170.25(9)°. This non-180° angle at the silver cation is due to the asymmetric coordination of the nitrate anion. Each nitrate anion is connected with two silver atoms and each silver atom with two nitrate anions (Fig. 13b):

Table 8 Most important bond lengths (Å) and angles (°) in **3**, **4**, and **5**.

3			
Ag–N	2.232(2), 2.239(2)	N–Ag–N	170.25(9)
Ag–O(O₂NO)	2.669(2), 2.724(2)	O–Ag–O	47.05(6)
	2.800 (3)		149.70(7), 103.32(6)
C–N	1.337(3), 1.343(4)	C–N–C	117.7(2)
	1.340(3), 1.335(4)		117.7(2)
4			
Ag–Ag	3.136(1)		
Ag–N	2.171(4), 2.189(4)	N–Ag–N	161.1(2)
Ag–O(O₂NO)	2.671(8), 2.874(5)		
C–N	1.357(6), 1.359(6)	C–N–C	117.1(4)
	1.350(6), 1.332(7)		117.2(4)
O(H2)–O(H2)	2.77(1), 2.81(1)		
O(H2)–O(O₂NO)	3.329(9), 3.243(9)		
5			
Ag–Ag	3.4079(6)		
Ag–N	2.150(2), 2.154(2)	N–Ag–N	173.2(8)
Ag–O(O₂NO)	2.704(2), 2.892(2)		
C–N	1.343(3), 1.347(3)	C–N–C	117.7(2)
	1.345(3), 1.350(3)		118.1(2)
O(H2)–O(H2)	2.761(3), 2.779(4)		
O(H2)–O(O₂NO)	2.827(3), 3.196(3)		
	2.974(3), 3.503(3)		

the nitrate anions act as bidentate linkers between the silvers atoms, perpendicular to the chain propagation direction ···–Ag–**L**–Ag–**L**–··· (Fig. 13a). Each silver ion reaches thus a coordination number of five: the two nitrogen atoms occupy the axial positions of the distorted trigonal bipyramid, whereas three nitrate oxygen atoms occupy the equatorial ones. One of the nitrate anions is coordinated to the silver in an anisobidentate way with Ag–O distances of 2.669(2) and

Fig. 12 Chain motif in **3**.

Fig. 13 (a) The nitrate anions act as linkers between the chains in **3**; other interactions between two chains in **3** (C–H⋯π: red arrow; H-bonds: yellow); (b) coordination sphere of the silver atom in **3**.
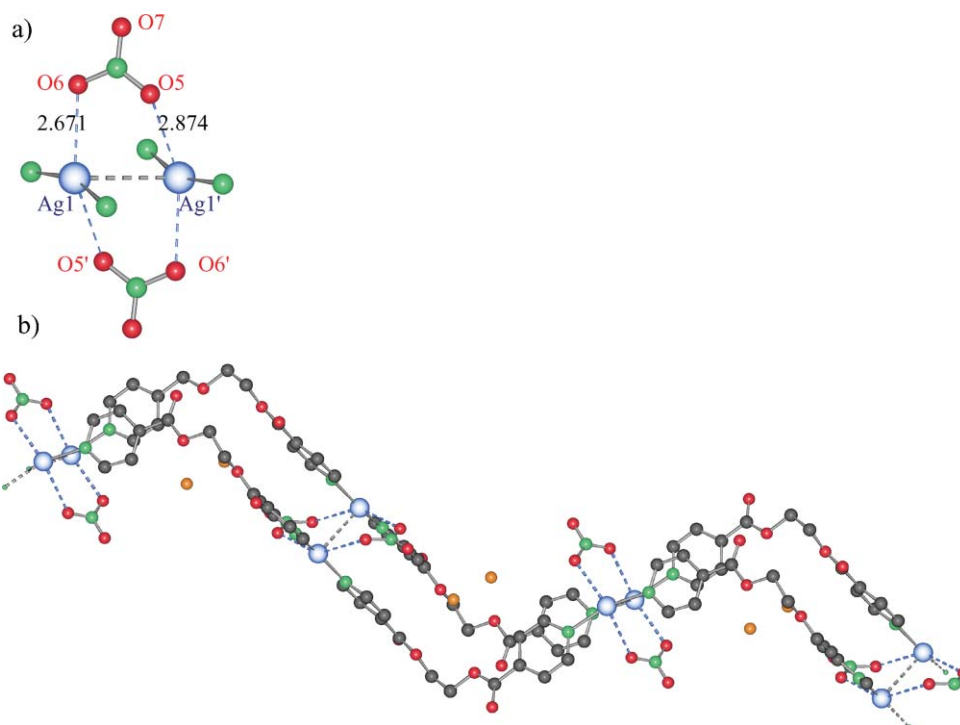
Fig. 14 (a) The silver environment in **4**; (b) leading to the formation of a pair of chains (hydrogen atoms omitted for clarity).

2.724(2) Å and the other nitrate anion is coordinated to the same silver atom in a monodentate way with silver–oxygen distances of 2.800(3) Å. The longer Ag–O distances in **3** as compared to **1** and **2** indicate a weaker coordinating effect. The delocalized charge allows generally a bridging or chelating action of the nitrate anion. The interaction Ag–O in **3** is however strong enough to deform the N–Ag–N angle (170.2°) to the side of the bidentate coordination (Fig. 13b).

Another coordination polymer based on silver nitrate and the rigid ligand 1,2-bis(4-pyridyl)ethane (bpe) affords a similar sheet with bridging nitrate between the linear chains. However the coordination geometry of the Ag[I] nodes is slightly different with a {AgN$_2$O$_2$} unit instead of a {AgN$_2$O$_3$} silver coordination sphere in **3**.[35]

Weak interactions between the close packed chains appear. (i) Hydrogen bonding occurs between the –C=O groups of one
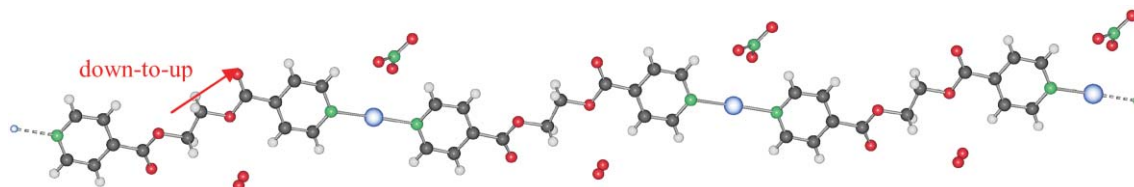
Fig. 15 The chain motif in **5**.
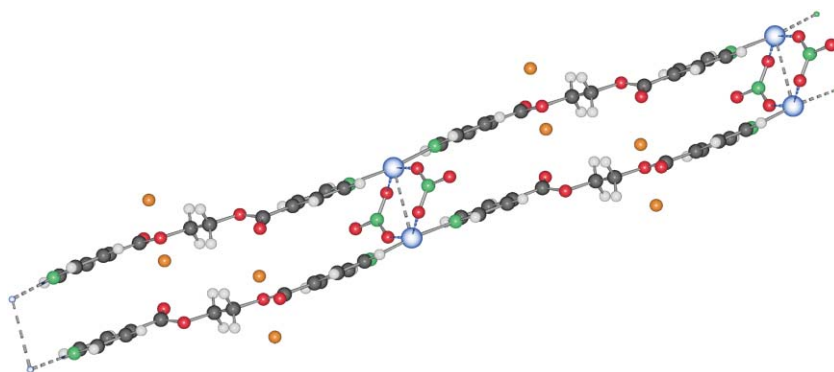
Fig. 16 Organisation of the chains in **5** with the fourth-coordinated silver atoms and the nitrate bridging anions.

chain and the CH_2 moieties of the parallel ones with H···O contacts of 2.57 and 2.75 Å. (ii) The two closest pyridine rings seem to be tilted in order to generate C–H···π interactions, also called "face-to-edge" interactions.[79] They occur between the tilted pyridine ring and the H1 atom of the next of pyridine group at 3.33 Å, offset by 0.47 Å. This interaction explains the bending within the ligand molecules: the pyridine planes are tilted with an angle of 50.25(7)°, and the planes containing the pyridine group and those of the corresponding ester function form angles of 16.5(3) and 20.9(2)°. The chains have thus a "bow-shaped" form if regarded along the propagation direction and the so-made sheets are not flat but undulating. Additionally to the already described interactions between the chains, other interactions complete the overall structure. (i) Hydrogen bonding occurs between close ligand molecules (C11–H1···O4 and C12–H12···O4) and between the nitrate anions and pyridine hydrogen atoms or ethyl hydrogen atoms. (ii) weak π-stacking of rings at a distance of 3.62 Å and offset by 1.61 Å is also observed. The closest distances between to silver atoms are 8.02(3) Å, so that no silver–silver contacts can be discussed.

Compound **4**, {[Ag(**L**)](NO$_3$)(H$_2$O)}$_n$, has an asymmetric unit formed of one silver atom, one ligand molecule, one nitrate counter anion and one water molecule. As before, the silver cation is coordinated by two different ligands through their nitrogen atoms leading to a 1-D chain. In contrast to **1**, **2**, and **3**, the ligand adopts the *gauche*-conformation with a torsion angle between its two pyridine planes of 81.8(1)° giving to the strand an undulating zig-zag structure. The distance between two silver atoms within a chain is 13.974(4) Å long, and thus shorter as in **1**, **2** and **3** in accordance with the strong bending of the ligand. It is however longer than in a comparable copper compound (9.167(7) Å), which presents the same ligand conformation, but with a more important bending of **L**.[66] The distances Ag–N in **4** are shorter than in the chains of **3**. Also, the N–Ag–N angle is smaller than in **3**. These differences are due to the different environment around the silver ions in the two structures. Indeed the coordination number of the silver cation in **4** is four with two nitrogen atoms and two oxygen atoms of the nitrate anions. Furthermore Ag–Ag interactions are observed at a distance of 3.136(1) Å (Fig. 14b). These contacts are the shortest distances between the two close chains which stack almost perfectly parallel giving pairs of chains. The arrangement in pairs is possible because the nitrate anions act as bridging linkers between the chains capping the silver–silver contacts (Fig. 14a). The distances Ag–O are longer than in **3** (on average, by 0.04 Å) indicating a weaker coordination to the metal ions. Another difference with **3** is that the third oxygen atom O7 of the nitrate anion is not involved in coordination bonding to another silver atom, but in H-bonding to the water molecule present in the structure.

Compound **5**, {[Ag(**L**)](NO$_3$)(H$_2$O)$_2$}$_n$, has one ligand molecule, one silver ion, one nitrate anion and two water molecules per asymmetric unit. The motif of **5** is a 1-D chain in which silver atoms and ligand molecules alternate, the silver ion being coordinated with two nitrogen atoms of two different ligand molecules, similar to the ones observed in **2** (Fig. 15).

The ligand molecules are in the *anti*-conformation as in **1**, **2** and **3**. The coordination environment of silver in **5** is similar to the one in **4**. However the angle N–Ag–N is larger, the distances Ag–N shorter and the Ag–Ag distance longer than in **4**. This is due to a decrease of coordination by the nitrate anions towards the cations. Indeed, the Ag–O(NO$_3$) distances are longer on average in **5** than in **4** and the other compounds.[67] The chains are also organized in pairs of chains as in **4** with the nitrate anions acting as pincers between the chains (Fig. 16).

Compound **2** is a structural supramolecular isomer of **3** (same Ag–ligand–nitrate system), showing apparently the same arrangement: 1-D chains, and nitrate anions in-between the chains. But paradoxically, the structure of **2** is closer to the structure of **5**. Both 1-D motifs are similar, the apparition of pairs of chains with π-stacking within the pairs, the parallel stacking of the pairs of chains with other π-stacking and the overall parallel stacking in order to build the 3-D network are also very similar (Fig. 17). It seems that the presence of water molecules in **5** increased the separation between the layers, the structural changes in **5** and **2** may be compared to the swelling of clays in case of water infiltration.

It can be thus assumed that the interactions nitrate–water molecules are responsible for the structural differences in **2** and **5**. However, the cell parameters for **5** and **2** do not show any correlation which means that more than simple water elimination is necessary to explain the transformation of one into the other.

In order to get information on the existence of coordination polymers or oligomers in solution, electrospray-ionization mass spectroscopy was performed. For instance, with a solution of compound Ag(**L**)NO$_3$, **2**, in CH$_3$CN at a concentration of 0.5 mg mL^{-1}, no other species were detected other than [Ag(CH$_3$CN)]$^+$ and [Ag(CH$_3$CN)$_2$]$^+$ (149 and 190 *m/z* respectively). Acetonitrile can easily coordinate to silver ions and the main species in solution are silver–acetonitrile complexes. Nevertheless, if we use a solvent mixture of CH$_3$CN and CH$_2$Cl$_2$ at a ratio 10 : 1, peaks are found at well identifiable *m/z* with a good isotopic resolution: 273.2, [**L**H]$^+$, 379.1, [**L**Ag]$^+$; 549.9 [**L**Ag$_2$(NO$_3$)]$^+$; 650.9 [**L**$_2$Ag]$^+$; 718.6 [**L**Ag$_3$(NO$_3$)$_2$]$^+$; 821.7 [**L**$_2$Ag$_2$(NO$_3$)]$^+$; 990 [**L**$_2$Ag$_3$(NO$_3$)$_2$]$^+$; 1161.3 [**L**$_2$Ag$_4$(NO$_3$)$_3$]$^+$; 1262.2 [**L**$_3$Ag$_3$(NO$_3$)$_2$]$^+$; 1432.6 [**L**$_3$Ag$_4$(NO$_3$)$_3$]$^+$ *m/z*.

Other electrospray ionization mass spectroscopy studies were performed in CH$_3$CN/CH$_2$Cl$_2$ in order to follow the evolution of the distribution of the above species in solution as a function of time and ligand to metal proportion. Solutions with M$_2$**L**, M**L**, M**L**$_2$ proportions were prepared and measured just after mixing **L** and AgNO$_3$, and after 24 h. The results are shown in Table 9.

Almost all species were found in each solution and at all times. For each solution, the main species are found whatever the reaction time: the distribution of the compounds in the solution is similar at $t = 0$ and $t = 24$ h. In the solution M$_2$**L**, the main species is [**L**Ag$_2$(NO$_3$)]$^+$ and species containing more Ag than **L** are favored; in the solution M**L**, a more important variety of species is observed; in the solution M**L**$_2$, only compounds [**L**$_2$Ag]$^+$ and [**L**$_2$Ag$_2$(NO$_3$)]$^+$ are mainly found.
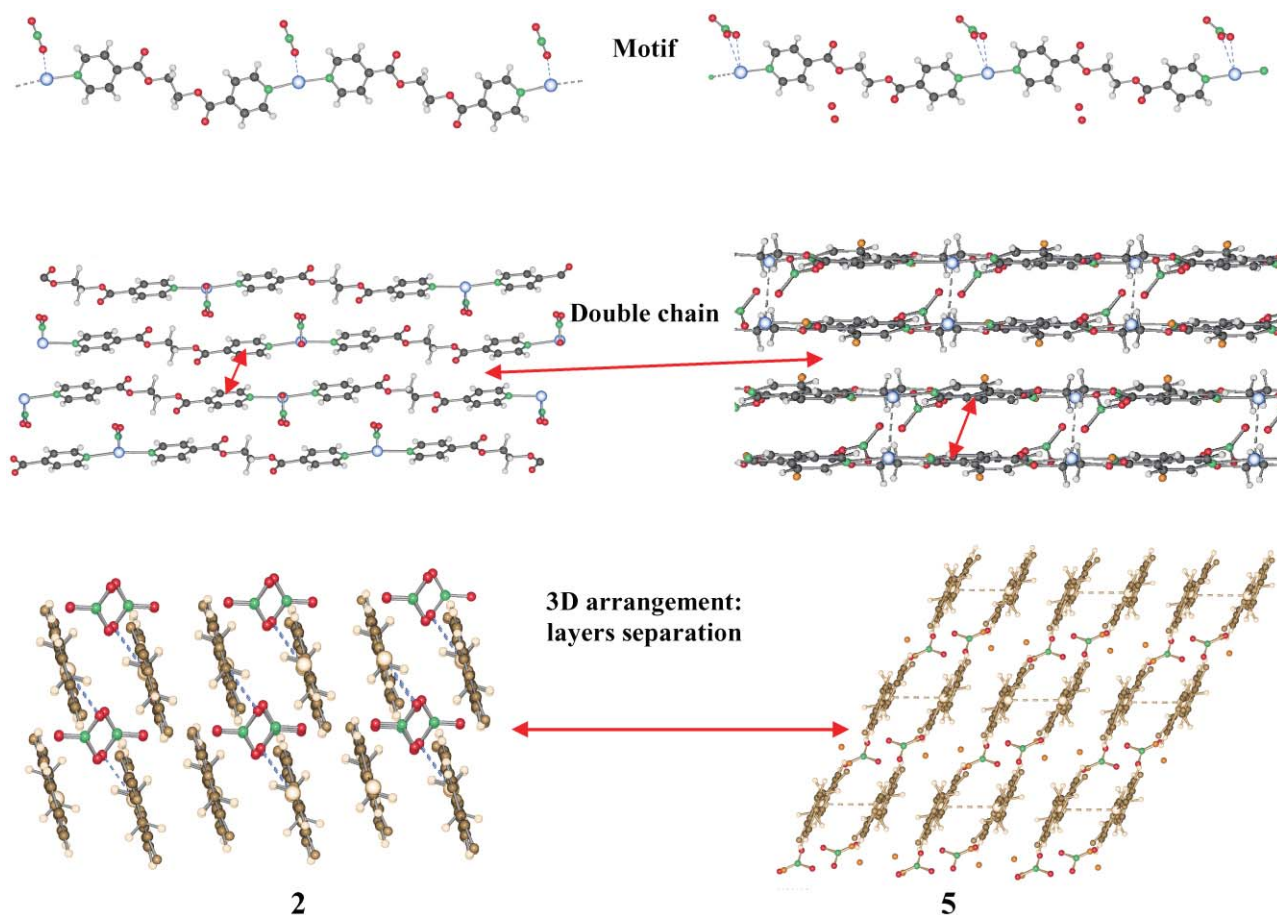
Fig. 17 Structural comparisons between **2** and **5**.

These results indicate that in all cases oligomeric fragments of coordination polymers are formed. This is in agreement with the fact that only the compound $\{[Ag(\mathbf{L})]NO_3\}_n$ is obtained by changing the metal to ligand stoichiometry for the reaction. Indeed the fact that many species are present indicates a fast complexation exchange. Additionally, acetonitrile is in concurrence with the pyridine groups of the ligand for the complexation of silver. The peaks corresponding to $[Ag(CH_3CN)]^+$ and $[Ag(CH_3CN)_2]^+$ (149 and 190 m/z, respectively) are in fact found in the mass spectra.

Table 9 Resume of the detected peaks (the main peaks are presented with the relative abundance ratio (%)) for the three tested solutions at 0 and 24H.

	M_2L		ML		ML_2	
	0	24 H	0	24 H	0	24 H
$[LH]^+$	ø	ø	√(2%)	ø	√(6%)	√(11%)
$[LAg]^+$	√(11%)	√(7%)	√(3%)	ø	√(1%)	√(4%)
$[LAg_2(NO_3)]^+$	√**(100%)**	√**(100%)**	√**(34%)**	√**(37%)**	√(18%)	√(26%)
$[L_2Ag]^+$	ø	ø	√(9%)	√(19%)	√(18%)	√**(69%)**
$[LAg_3(NO_3)_2]^+$	√**(52%)**	√**(69%)**	√(14%)	√**(37%)**	√(2%)	√(5%)
$[L_2Ag_2(NO_3)]^+$	√**(80%)**	√**(31%)**	√**(100%)**	√**(100%)**	√**(100%)**	√**(100%)**
$[L_2Ag_3(NO_3)_2]^+$	√**(45%)**	√(24%)	√**(30%)**	√**(60%)**	√(12%)	√(19%)
$[L_2Ag_4(NO_3)_3]^+$	√**(62%)**	√**(36%)**	√(18%)	√**(60%)**	√(5%)	√(7%)
$[L_3Ag_3(NO_3)_2]^+$	ø	ø	√(2%)	√(10%)	√(3%)	√(3%)
$[L_3Ag_4(NO_3)_3]^+$	√(18%)	√(8%)	√(7%)	√**(30%)**	√(3%)	√(4%)

Whereas measurements of UV-spectra of the above compounds in solution gave not enough information to calculate formation constants of the various species, a general increase of luminescence at 409 nm is observed in the solid state for all compounds, irradiating at 234 nm (Chart 1).

Solvent influence

It has been stated that the 1-D silver coordination polymer motifs including linear ligands with a poor delocalized π-system and moderately coordinating counter anions (such as nitrate) tend to arrange themselves parallel in the structure and that the coulombic repulsion between the Ag^I centers cannot be compensated by a strong face-to-face ligand stacking or by the coordination of the counter-anions to silver.[43] So, what is the behaviour of **L** in the AgNO₃ coordination polymers when diverse solvent conditions are applied?

It is worthy of noting that silver nitrate has a different solubility in the used crystallization solvents, allowing more or less good solvation of the ions. The comparison of the average silver–nitrate distances in the solid as a function of the solubility of the silver salt in the different solvents are shown on Chart 2.

IR-measurements in solution as well as ES-MS investigations prove the existence of close AgNO₃-aggregates, where
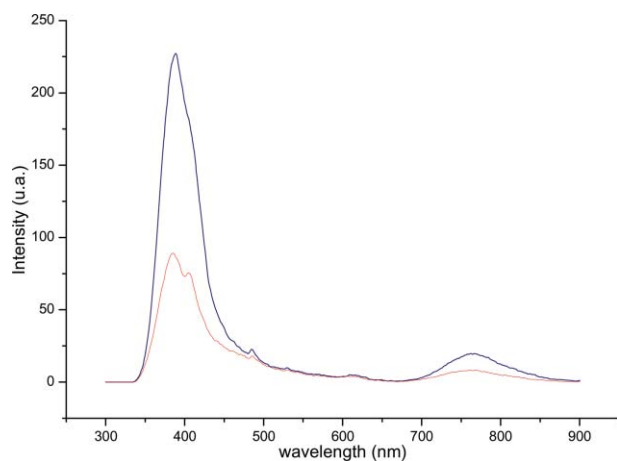
Chart 1 Emission spectra of **5** (blue) and **L** (red) (excitation wavelength: 234 nm).

nitrate is coordinated to the metal ion and even is likely to act as bridging ligand.[78] There is thus a link between these Ag–O(NO$_3$) distances and the solubility of silver nitrate in the mother liquor. The worst solvent for silver nitrate in this series is ethanol and the best is water. This bad solubility of AgNO$_3$ in ethanol can explain the short distances Ag–O(NO$_3$) in the solid state in **1**, and also the existence of the silver nitrate chains. On the other hand, the good solubility of AgNO$_3$ in water prevents Ag and nitrate to be so close. According to these results, it can be said that the solubility seems to be a major parameter for the crystallization. To the best of the authors' knowledge, this dependence has never been outlined in the literature by showing the variance of distances as a function of solubility.

However the importance of the solvent choice is known, without being clearly studied. The solvents are usually classified in two categories: the coordinating and the non coordinating ones. In compounds **4** or **5**, the solvent molecules co-crystallize without being cation coordinating solvents. It is the weak solvation of the anions by the solvent that remains, resulting in longer Ag–anion distances.

In the literature, numerous examples of silver coordination polymers with solvent molecules in the first coordination
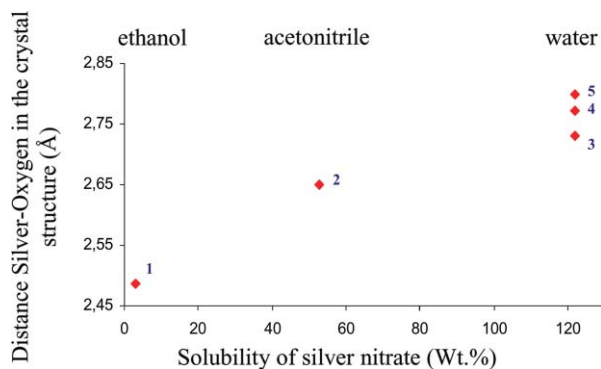
Chart 2 Average distances Ag–O(NO3) in compounds **1 to 5** as a function of the AgNO3 solubility.

sphere can be found. The coordinated solvent molecules are water,[37,39,68,80] acetonitrile[41,81–87] or methanol.[54] Water molecules can be directly coordinated to silver ions even in the presence of nitrate as counter anion. In {[Ag(1,3-bis(2-pyridylethynyl)-2-methyl-benzene)(NO$_3$)(H$_2$O)]}$_n$, there are two crystallographically and chemically different silver ions: both have a distorted tetrahedral coordination sphere containing two ligand nitrogen atoms in addition with either an anisobidentate nitrate anion or a monodentate nitrate anion and a water molecule.[37] This compound grows from a mixture of a solution of ligand in acetone and a solution of silver nitrate in water, illustrating the possible competition in coordination between the water molecules and the nitrate anions.

Acetonitrile has a favorable affinity toward silver ions in solution, and is also more easily involved in the coordination sphere of silver in the resulting coordination polymer structure. Reger *et al.* state that if compounds are crystallized from the coordinating solvent acetonitrile, the anions have less effect on the structure.[84] For instance, the silver ion has a {AgN(pyridyl)$_2$N(acetonitrile)O(nitrate)$_2$} coordination sphere in the compound {[Ag(2,2′,3″-tripyridylamine)(NO$_3$)(CH$_3$CN)]}$_n$.[86] When crystals grow from the mixture **L**/AgNO$_3$ in acetonitrile, we do not observe the formation of such compounds in the solid state. Crystals of **2** do not contain any acetonitrile molecules.

The used solvents are not the unique important factor but also the crystallization techniques have to be carefully studied. The "H-shaped" tubes allow slow diffusion of the reagents, and mostly the crystals are of better quality than if obtained by direct mixing. The drawbacks of this technique are the weak concentration and the non-homogeneous conditions depending on the localization in the tube. Indeed the crystallization can occur in one or the other arm, on the fritt if present, at the solvent/air interface, in the curved part, *etc*…, where the concentration and the ratio metal to ligand can be locally different. However, we always get pure phases during the direct mixing: **3** crystallizes in a THF/water solution of **L** and AgNO$_3$; **2** is obtained in a solution of both reagents in acetonitrile. The comparison between the diffusion techniques and the direct self-assembly methods is made by Champness and Schröder.[88] Contrary to our studies, their recommended method is the diffusion technique because they obtained mixtures of products with direct methods.

Another solvent influence in the formation of coordination polymers based on flexible organic ligand is the correlation between the presence of inclusion solvent molecules in the structures and the conformation of the ligand. In **4**, the presence of water molecules coincides with the *gauche*-conformation. The *gauche* conformation of **L** is also observed in a related copper coordination polymer in the presence of THF as co-crystallizing solvent.[66] However, in **5**, water molecules co-crystallize and the ligand adopts the *anti*-conformation. In all other products, the ligand adopts the *anti*-conformation as in free **L**. It can be concluded that the presence of non-coordinating co-crystallized solvent molecules may induce the change of conformation of the ligands in the crystallographic structures from *anti* to *gauche*. This confirms previous findings.[69]

Conclusions

The nitrate anion is very flexible in its bridging mode and strength. It is therefore able to act as bridging ligand between two silver atoms as in **3** or **2** in which it links several chains together. It also shows its ability to support a metal–metal contact in **4** and **5**. Its coordination strength can be tuned by the number of hydrogen bonds in which it can be involved, with for instance water molecules. Thus, the Ag–O(nitrate) distances increase with the number of co-crystallizing solvent. Solvation of the cations and anions of $AgNO_3$ also plays a role in final Ag–NO_3 distances in the products' crystal structure. The influence of the solvent has been outlined with different compounds. A solvent contribution can here be distinguished: the different solvation of the reagents by the solvent in the crystallization process. In some cases, the interactions between solvent molecules and reagents remain in the solid state, like in **1** and **2**, and in other cases, solvent molecules co-crystallize, as in **4**, and **5**.

Experimental

The synthesis of **L** has been reported previously.[66] Synthesis of **3**, **4** and **5** have been described elsewhere.[67]

$\{[Ag_2(NO_3)_2(L)]\}_n$ (1)

A solution of **L** (20 mg, 0.07 mmol) in THF (5 mL) is introduced in one arm of an "H-shaped" tube, a solution of $AgNO_3$ (12 mg, 0.07 mmol) in ethanol (5 mL) in the other one (molar ratio 1 : 1). The solutions are frozen in liquid nitrogen and THF is then layered into the tube in order to bridge the two reagent solutions. There is a fritt in the linking part of the tube. The slow diffusion occurs through the THF layer and the fritt. Crystals of **1** appear after several months at the interface EtOH/THF. After using some single crystals for X-ray diffraction, the product is collected. Yield: 4 mg (11%). This quantity was not sufficient to perform a satisfying elementary analysis.

$\{(Ag(L)](NO_3)\}_n$ 2

Reaction A: Crystals of **2** are obtained at room temperature from a solution of **L** (13.6 mg, 0.05 mmol) and silver nitrate (8.5 mg, 0.05 mmol) in acetonitrile (10 mL) (molar ratio 1 :1). The crystals grow on the glass walls of the beaker at the solution surface after slow evaporation of the solution. The colorless crystals are suitable for single crystal X-rays diffraction and allow the resolution of the crystallographic structure. Not enough crystals were collected in order to make further investigations on this sample.

Reaction B: A polycrystalline white powder is obtained from a mixture of **L** (60 mg, 0.22 mmol) and $AgNO_3$ (37.5 mg, 0.22 mmol) in CH_2Cl_2 (a large volume as $AgNO_3$ is less well soluble in CH_2Cl_2) (molar ratio 1 : 1). The powder X-ray spectrum of the compound shows that this polycrystalline precipitate has the same structure than **2**. It is worth noting that if the molar ratio is changed, the same product is obtained. Yield: 79 mg (81 %). Analysis calculated for [Ag(**L**)NO$_3$]: C 38.03, H 2.74, N 9.50; found C 37.26, H 2.64, N 9.4%. A certain amount of dichloromethane is adsorbed on the sample. IR (GB, cm^{-1}): ν(C=O) 1726 s, ν(C=C) 1612 w, ν(ArC–C, C=N) 1412 w, ν(NO$_3$) 1380–1330 s, ν(C–O) 1272 s, δ(ArC–H) 985, 992 (split) m, ν(ArC–H) 825 m. UV-Vis (CH$_3$CN): absorption at 212 and 273 nm. ESI/MS (CH$_3$CN/CH$_2$Cl$_2$ 10/1, m/z): 273.2, [**L**H]$^+$; 379.1, [**L**Ag]$^+$; 549.9, [**L**Ag$_2$(NO$_3$)]$^+$; 650.9, [**L**$_2$Ag]$^+$; 718.6, [**L**Ag$_3$(NO$_3$)$_2$]$^+$; 821.7, [**L**$_2$Ag$_2$(NO$_3$)]$^+$; 990, [**L**$_2$Ag$_3$(NO$_3$)$_2$]$^+$; 1161.3, [**L**$_2$Ag$_4$(NO$_3$)$_3$]$^+$; 1262.2, [**L**$_3$Ag$_3$(NO$_3$)$_2$]$^+$; 1432.6, [**L**$_3$Ag$_4$(NO$_3$)$_3$]$^+$. FAB (fast atom bombardment) mass spectroscopy (m/z): [**L**H]$^+$, [**L**Ag]$^+$, [**L**Ag$_2$NO$_3$]$^+$ and [**L**$_2$Ag]$^+$ at, respectively, 273, 379, 550 and 651.

References

1 C. Janiak, *Dalton Trans.*, 2003, 2781.
2 S. L. James, *Chem. Soc. Rev.*, 2003, **32**, 276.
3 A. Y. Robin and K. M. Fromm, *Coord. Chem. Rev.*, 2006 in the press.
4 Examples for porous coordination polymer compounds: S. Kitagawa, R. Kitaura and S. I. Noro, *Angew. Chem., Int. Ed.*, 2004, **116**, 2388; M. Eddaoudi, J. Kim, D. Vodak, A. Sudik, J. Wachter, M. O'Keeffe and O. M. Yaghi, *Poc. Natl. Acad. Sci. U. S. A.*, 2002, **99**, 4900.
5 Examples for luminescent coordination polymer compounds: S.-L. Zheng and X.-M. Chen, *Aust. J. Chem.*, 2004, **57**, 703.
6 Examples for magnetic coordination polymer compounds: D. Maspoch, D. Rioz-Molina and J. Veciana, *J. Mater. Chem.*, 2004, **14**, 2713; S. R. Batten and K. S. Murray, *Coord. Chem. Rev.*, 2003, **246**, 103.
7 Examples for polycatenated, polythreaded coordination polymer compounds: L. Carlucci, G. Ciani and D. Proserpio, *Coord. Chem. Rev.*, 2003, **246**, 247.
8 K. T. Holman, H. H. Hammud, S. Isber and M. Tabbal, *Polyhedron*, 2005, **24**, 2, 221–228.
9 S. Kawata, S. Kitagawa, H. Kumagai, S. Iwabuchi and M. Katada, *Inorg. Chim. Acta*, 1998, **267**, 1, 143–145.
10 R. G. Vranka and E. L. Amma, *Inorg. Chem.*, 1966, **5**, 6, 1020–1025.
11 J. L. Manson, T. Lancaster, L. C. Chapon, S. J. Blundell, J. A. Schlueter, M. L. Brooks, F. L. Pratt, C. L. Nygren and J. S. Qualls, *Inorg. Chem.*, 2005, **44**, 4, 989–995.
12 B. M. Wells, C. P. Landee, M. M. Turnbull, F. F. Awwadi and B. Twamley, *J. Mol. Catal. A*, 2005, **228**, 1–2, 117–123.
13 L. C. Tabares, J. A. R. Navarro and J. M. Salas, *J. Am. Chem. Soc.*, 2001, **123**, 3, 383–387.
14 C. Naether and I. Jess, *Eur. J. Inorg. Chem.*, 2004, 14, 2868–2876.
15 O. M. Yaghi and H. Li, *J. Am. Chem. Soc.*, 1996, **118**, 1, 295–296.
16 S. R. Batten, J. C. Jeffery and M. D. Ward, *Inorg. Chim. Acta*, 1999, **292**, 2, 231–237.
17 S. D. Huang, R.-G. Xiong, J. Han and B. R. Weiner, *Inorg. Chim. Acta*, 1999, **294**, 1, 95–98.
18 H. Hou, Y. Wei, Y. Fan, C. Du, Y. Zhu, Y. Song, Y. Niu and X. Xin, *Inorg. Chim. Acta*, 2001, **319**, 1,2, 212–218.
19 S. Noro, S. Kitagawa, M. Kondo and K. Seki, *Angew. Chem., Int. Ed. Engl.*, 2000, **39**, 12, 2082–2084.
20 M. Du and X.-J. Zhao, *Inorg. Chem. Commun.*, 2004, **7**, 9, 1056–1060.
21 F. Robinson and M. J. Zaworotko, *Chem. Commun.*, 1995, 23, 2413–2414.
22 H. W. Roesky and M. Andruh, *Coord. Chem. Rev.*, 2003, **236**, 1–2, 91–119.
23 Y.-B. Dong, R. C. Layland, M. D. Smith, N. G. Pschirer, U. H. F. Bunz and H.-C. Zur Loye, *Inorg. Chem.*, 1999, **38**, 13, 3056–3060.

24 H. Zhu, C. Huang, W. Huang and S. Gou, *Inorg. Chem. Commun.*, 2004, **7**, 10, 1095–1099.

25 R. Wang, L. Han, L. Xu, Y. Gong, Y. Zhou, M. Hong and A. S. C. Chan, *Eur. J. Inorg. Chem.*, 2004, **18**, 3751–3763.

26 R. Horikoshi and M. Mikuriya, *Cryst. Growth Des.*, 2005, **5**, 1, 223–230.

27 L. Carlucci, G. Ciani, D. W. v. Gundenberg and D. M. Proserpio, *Inorg. Chem.*, 1997, **36**, 18, 3812–3813.

28 X.-M. Ouyang, B.-L. Fei, T.-a. Okamura, H.-W. Bu, W.-Y. Sun, W.-X. Tang and N. Ueyama, *Eur. J. Inorg. Chem.*, 2003, **4**, 618–627.

29 M. Du, X.-H. Bu, Y.-M. Guo, H. Liu, S. R. Batten, J. Ribas and T. C. W. Mak, *Inorg. Chem.*, 2002, **41**, 19, 4904–4908.

30 B.-L. Fei, W.-Y. Sun, T.-a. Okamura, W.-X. Tang and N. Ueyama, *New J. Chem.*, 2001, **25**, 2, 210–212.

31 R. Horikoshi, T. Mochida, N. Maki, S. Yamada and H. Moriyama, *Dalton Trans.*, 2002, **1**, 28–33.

32 G. K. Patra and I. Goldberg, *Dalton Trans.*, 2002, **6**, 1051–1057.

33 L.-C. Song, W.-X. Zhang, J.-Y. Wang and Q.-M. Hu, *Transition Met. Chem.*, 2002, **27**, 5, 526–531.

34 A. J. Blake, N. R. Brooks, N. R. Champness, L. R. Hanton, P. Hubberstey and M. Schroder, *Pure Appl. Chem.*, 1998, **70**, 12, 2351–2357.

35 R. L. LaDuca, Jr., R. S. Rarig, Jr., P. J. Zapf and J. Zubieta, *Solid State Sci.*, 2000, **2**, 1, 39–45.

36 M.-L. Tong, X.-M. Chen, B.-H. Ye and S. W. Ng, *Inorg. Chem.*, 1998, **37**, 20, 5278–5281.

37 T. Kawano, C.-X. Du, T. Araki and I. Ueda, *Inorg. Chem. Commun.*, 2003, **6**, 2, 165–167.

38 A. J. Blake, G. Baum, N. R. Champness, S. S. M. Chung, P. A. Cooke, D. Fenske, A. N. Khlobystov, D. A. Lemenovskii, W.-S. Li and M. Schroder, *Dalton Trans.*, 2000, **23**, 4285–4291.

39 S. Muthu, J. H. K. Yip and J. J. Vittal, *Dalton Trans.*, 2001, **24**, 3577–3584.

40 M.-L. Tong, Y.-M. Wu, J. Ru, X.-M. Chen, H.-C. Chang and S. Kitagawa, *Inorg. Chem.*, 2002, **41**, 19, 4846–4848.

41 A. J. Blake, N. R. Champness, P. A. Cooke and J. E. B. Nicolson, *Chem. Commun.*, 2000, **8**, 665–666.

42 A. J. Blake, N. R. Champness, P. Hubberstey, W.-S. Li, M. A. Withersby and M. Schroder, *Coord. Chem. Rev.*, 1999, **183**, 117–138.

43 A. N. Khlobystov, A. J. Blake, N. R. Champness, D. A. Lemenovskii, A. G. Majouga, N. V. Zyk and M. Schroder, *Coord. Chem. Rev.*, 2001, **222**, 155–192.

44 L. Carlucci, G. Ciani, D. M. Proserpio and A. Sironi, *Chem. Commun.*, 1994, **24**, 2755–2756.

45 J. H. Liao, P. L. Chen and C. C. Hsu, *J. Phys. Chem. Solids*, 2001, **62**, 9–10, 1629–1642.

46 W. Bi, D. Sun, R. Cao and M. Hong, *Acta Crystallogr., Sect. E*, 2002, **E58**, 7, m324–m325.

47 M. Hong, W. Su, R. Cao, M. Fujita and J. Lu, *Chem.-Eur. J.*, 2000, **6**, 3, 427–431.

48 L. Carlucci, G. Ciani, D. M. Proserpio and S. Rizzato, *CrystEngComm*, 2002, **4**, 121–129.

49 L. Carlucci, G. Ciani and D. M. Proserpio, *Chem. Commun.*, 1999, **5**, 449–450.

50 Y.-B. Dong, H.-Y. Wang, J.-P. Ma, R.-Q. Huang and M. D. Smith, *Cryst. Growth Des.*, 2005, **5**, 2, 789–800.

51 Y.-B. Dong, X. Zhao, R.-Q. Huang, M. D. Smith and H.-C. Zur Loye, *Inorg. Chem.*, 2004, **43**, 18, 5603–5612.

52 H.-P. Wu, C. Janiak, G. Rheinwald and H. Lang, *J. Chem. Soc., Dalton Trans.*, 1999, 183.

53 C. Janiak, L. Uehlin, H.-P. Wu, P. Klüfers, H. Piotrowski and T. G. Scharmann, *J. Chem. Soc., Dalton Trans.*, 1999, 3121.

54 X.-H. Bu, W. Chen, W.-F. Hou, M. Du, R.-H. Zhang and F. Brisse, *Inorg. Chem.*, 2002, **41**, 13, 3477–3482.

55 X.-H. Bu, Y.-B. Xie, J.-R. Li and R.-H. Zhang, *Inorg. Chem.*, 2003, **42**, 23, 7422–7430.

56 K. M. Fromm, E. D. Gueneau, G. Bernardinelli, H. Goesmann, J. Weber, M. J. Mayor-Lopez, P. Boulet and H. Chermette, *J. Am. Chem. Soc.*, 2003, **125**, 12, 3593–3604.

57 K. M. Fromm, *CrystEngComm*, 2002, **4**, 318–322.

58 M. Mayor, M. Buschel, K. M. Fromm, J.-M. Lehn and J. Daub, *Chem.-Eur. J.*, 2001, **7**, 6, 1266–1272.

59 K. M. Fromm, E. D. Gueneau and H. Goesmann, *Chem. Commun.*, 2000, **22**, 2187–2188.

60 K. M. Fromm and H. Goesmann, *Acta Crystallogr., Sect. C*, 2000, **C56**, 10, 1179–1180.

61 K. M. Fromm, H. Goesmann and G. Bernardinelli, *Polyhedron*, 2000, **19**, 15, 1783–1789.

62 K. M. Fromm, G. Bernardinelli, M. J. Mayor-Lopez and H. Goesmann, *Z. Anorg. Allg. Chem.*, 2000, **626**, 7, 1685–1691.

63 K. M. Fromm, *Chem. Commun.*, 1999, **17**, 1659–1660.

64 K. M. Fromm, *Angew. Chem., Int. Ed. Engl.*, 1998, **36**, 24, 2799–2801.

65 K. Fromm and G. Bernardinelli, *Z. Anorg. Allg. Chem.*, 2001, **627**, 7, 1626–1630.

66 A. Y. Robin, K. M. Fromm, H. Goesmann and G. Bernardinelli, *CrystEngComm*, 2003, **5**, 405–410.

67 A. Y. Robin, M. Meuwly, K. M. Fromm, H. Goesmann and G. Bernardinelli, *CrystEngComm*, 2004, **6**, 336–343.

68 M. Sarkar and K. Biradha, *CrystEngComm*, 2004, **6**, 310–314.

69 B. Li, X. Zhu, J. Zhou, Y. Peng and Y. Zhang, *Polyhedron*, 2004, **23**, 18, 3133–3141.

70 Single crystal data for **1**: $C_7H_6N_2O_5Ag$, $M = 306.1$ g mol^{-1}, monoclinic, space group $C2/c$ (No. 15), $a = 20.976(7)$, $b = 9.346(2)$, $c = 9.903(3)$ Å, $\beta = 106.98(2)°$, $V = 1856.7(9)$ Å^3, $Z = 8$, $T = 240(2)$ K, μ(Mo Ka) = 2.174 mm^{-1}, 1972 reflections of which 1452 unique and 1452 observed, 147 parameters refined, R(int) = $\sigma|F_o^2 - F_o^2(\text{mean})|/S[F_o^2] = 0.0777$, $R1 = \sigma||F_o| - |F_c|| / \sigma|F_o| = 0.0733$, $wR2 = \{\sigma[w(F_o^2 - F_c^2)^2] / \sigma[w(F_o^2)^2]\}^{1/2} = 0.1742$ for $I > 2\sigma$ and $R1 = 0.0854$, $wR2 = 0.1885$ for all data. Single crystal data for **2**: $C_{14}H_{12}N_3O_7Ag$, $M = 442.14$ g mol^{-1}, triclinic, space group $P\bar{1}$ (No. 2), $a = 6.159(1)$, $b = 8.895(3)$, $c = 14.439(3)$ Å, $\alpha = 93.15(2)$, $\beta = 99.90(2)$, $\gamma = 91.43(2)°$, $V = 777.6(4)$ Å^3, $Z = 2$, $T = 293(2)$ K, μ(Mo Ka) = 1.341 mm^{-1}, 1565 reflections of which 1494 unique and 1494 observed, 226 parameters refined, R(int) = 0.0213, $R1 = 0.0312$, $wR2 = 0.0686$ for $I > 2\sigma$ and $R1 = 0.0408$, $wR2 = 0.0732$ for all data. Crystals **1**, and **2** were measured on a STOE IPDS diffractometer with monochromated graphite Mo Ka radiation, $\lambda = 0.71073$ Å, an Oxford Cryosystems open flow cryostat,[89] with an absorption correction by analytical integration.[90] The structures were solved with direct methods and refined by full-matrix least-squares on F^2 with the SHELX-99 package.[91] All heavy atoms could be refined anisotropically. Crystallographic data for the structures reported here **1**, and **2** have been deposited with the Cambridge Crystallographic Data Cente. CCDC reference numbers 285368 and 285369. For crystallographic data in CIF or other electronic format see DOI: 10.1039/b517191a. Copies of the data can be obtained free of charge on application to CCDC, 12 Union Road, Cambridge CB21EZ, UK (fax: (+44)1223-336-033; e-mail: deposit@ccdc.cam.ac.uk).

71 L. Yang, X. Shan, Q. Chen, Z. Wang and J. S. Ma, *Eur. J. Inorg. Chem.*, 2004, **7**, 1474–1477.

72 G. Zhang, G. Yang, Q. Chen and J. S. Ma, *Cryst. Growth Des.*, 2005, **5**, 2, 661–666.

73 D. Kim, S. Hu, P. Tarakeshwar, K. S. Kim and J. M. Lisy, *J. Phys. Chem. A*, 2003, **107**, 8, 1228–1238.

74 E. L. Elliott, G. A. Hernandez, A. Linden and J. S. Siegel, *Org. Biomol. Chem.*, 2005, **3**, 3, 407–413.

75 D. L. Reger, J. R. Gardinier and M. D. Smith, *Inorg. Chem.*, 2004, **43**, 13, 3825–3832.

76 E. Bosch and C. L. Barnes, *Inorg. Chem.*, 2002, **41**, 9, 2543–2547.

77 M. Mascal, J.-L. Kerdelhue, A. J. Blake, P. A. Cooke, R. J. Mortimer and S. J. Teat, *Eur. J. Inorg. Chem.*, 2000, **3**, 485–490.

78 C. Mabillard, *Thesis n°505* EPFL (Ecole Polytechnique fédérale de Lausanne)1983.

79 C. Janiak, *Dalton Trans.*, 2000, **21**, 3885–3896.

80 S. Q. Liu, T. Kuroda-Sowa, H. Konaka, Y. Suenaga, M. Maekawa, T. Mizutani, G. L. Ning and M. Munakata, *Inorg. Chem.*, 2005, **44**, 4, 1031–1036.

81 N. S. Oxtoby, A. J. Blake, N. R. Champness and C. Wilson, *Proc. Natl. Acad. Sci. U. S. A.*, 2002, **99**, 8, 4905–4910.

82 J. J. M. Amoore, C. A. Black, L. R. Hanton and M. D. Spicer, *Cryst. Growth Des.*, 2005, **5**, 3, 1255–1261.

83 S. Muthu, Z. Ni and J. J. Vittal, *Inorg. Chim. Acta*, 2005, **358**, 3, 595–605.

84 D. L. Reger, R. F. Semeniuc, V. Rassolov and M. D. Smith, *Inorg. Chem.*, 2004, **43**, 2, 537–554.

85 S.-L. Zheng, M.-L. Tong, S.-D. Tan, Y. Wang, J.-X. Shi, Y.-X. Tong, H. K. Lee and X.-M. Chen, *Organometallics*, 2001, **20**, 25, 5319–5325.

86 C. Seward, J. Chan, D. Song and S. Wang, *Inorg. Chem.*, 2003, **42**, 4, 1112–1120.

87 M. A. Withersby, A. J. Blake, N. R. Champness, P. A. Cooke, P. Hubberstey, W.-S. Li and M. Schroder, *Cryst. Eng.*, 1999, **2**, 2/3, 123–136.

88 D.-L. Long, A. J. Blake, N. R. Champness, C. Wilson and M. Schroder, *Chem.-Eur. J.*, 2002, **8**, 9, 2026–2033.

89 J. Cosier and A. M. Glazer, *J. Appl. Crystallogr.*, 1986, **19**, 105.

90 E. Blanc, D. Schwarzenbach and H. D. Flack, *J. Appl. Crystallogr.*, 1991, **24**, 1035.

91 G. M. Sheldrick, SHELX-99, *Program for Crystal Structure Refinement*, University of Göttingen, Göttingen, 1999.

Forschungsbericht – Research Report

Recent Advances in the Chemistry of "Clusters" and Coordination Polymers of Alkali, Alkaline Earth Metal and Group 11 Compounds

Katharina M. Fromm*, Estelle D. Gueneau, Adeline Y. Robin, William Maudez, Jorge Sague, and Rémi Bergougnant

Basel/Switzerland, University, Department of Chemistry

Abstract. This contribution gives an overview on the different subjects treated in our group. One of our fundamental interests lies in the synthesis and study of low-dimensional polymer and molecular solid state structures. We have chosen several synthetic approaches in order to obtain such compounds.

Firstly, the concept of cutting out structural fragments from a solid state structure of a binary compound will be explained on behalf of BaI_2. Oxygen donor ligands, used as chemical scissors on BaI_2, allow obtaining three-, two-, one- and zero-dimensional derived compounds depending on their size and concentration. Thus, a structural genealogy tree for BaI_2 can be established. This method, transferred to alkali halides using crown ethers and calix[n]arenes as delimiting ligands, leads us to the subject of one-dimensional ionic channels.

A second chapter deals with the supramolecular approach for the synthesis of different dimensional polymer structures derived from alkaline earth metal iodides, and based on the combination of metal ion coordination with hydrogen bonding between the cationic complexes and their anions. Under certain circumstances, rules can be established for the prediction of the dimensionality of a given compound, thus contributing to the fundamental problem of structure prediction in crystal engineering.

A third part describes a fundamentally new synthetic pathway for generating pure alkaline earth metal cage compounds as well as alkali and alkaline earth mixed metal clusters. In a first step, different molecular precursors, such as solvated alkaline earth metal halides are investigated as a function of the ligand size and reactivity. They are then reacted with some alkali metal compound in order to partially eliminate alkali halide and to form the clusters. The so obtained unique structures of ligand stabilized metal halide, hydroxide and/or alkoxide and aryloxide aggregates are of interest as potential precursors for oxide materials. Approaches to two synthetic methods of the latter, sol-gel and (MO)-CVD, are investigated with our compounds.

In order to generate single source precursors for oxide materials, we started to investigate transition metal ions, especially Cu and Ag, using multitopic ligands. This has led us into the fundamental problematic of "crystal engineering" and solid state structure prediction and we found ourselves confronted to numerous interesting cases of polymorphism and pseudo-polymorphism. Weak interactions, such as π-stacking, H-bonding and metal-metal interactions, and solvent, counter ion and concentration effects seem to play important roles in the construction of such low-dimensional structures.

Finally, the physical properties of some of our compounds are described qualitatively in order to show the wide spectrum of possibilities and potential applications for the chemistry in this field.

Keywords: Alkali metals; Alkaline earth metals; Coordination polymers; Clusters; Cage compounds; Structural investigations; Structure prediction

Introduction

We got interested in the non-aqueous chemistry of alkali and alkaline earth metal elements for several reasons: i) the chemistry of alkali and alkaline earth metal compounds in water can best be described as ionic whereas not much was known about their behaviour in organic solvents; ii) alkali and alkaline earth metal clusters – in the sense of aggregates or cage compounds – were observed as by-products in metallation reactions in organic chemistry which encouraged us to make such compounds on purpose; iii) we wanted to know whether there is an analogy in the clusters of group 1 and 2, and transition metal clusters, i. e. of group 11; iv) concerning the "covalent" polymers, the principle of cutting out structural fragments from a solid state structure with chemical scissors was to be tested; v) single source precursors for the chemical vapour deposition or sol-gel technique in the synthesis of oxide materials are scarce; and vi) we wanted to contribute to the problem of structure prediction in the case of supramolecular coordination polymers. Applications for such alkali and alkaline earth metal compounds can be found in many fields, such as metallation reactions and superbases in organic chemistry, biomineralization and biomimetics as far as biology is con-

* Prof. Dr. K. M. Fromm
University of Basel
Department of Chemistry
Spitalstrasse 31
CH-4056 Basel
Tel. : +41 61 267 1004
Fax: +41 61 267 1021
E-mail: katharina.fromm@unibas.ch
www.unibas.ch

Curriculum vitae of the principal author

Katharina M. Fromm, born in Germany and raised in France, Germany and USA, studied chemistry at the University of Karlsruhe, Germany, and the EHICS (Ecole des Hautes Etudes des Industries Chimiques de Strasbourg) in Strasbourg, France, with an Erasmus stipend. Back at the University of Karlsruhe, she started her thesis, supported by a Landesgraduierten-grant, in the group of Prof. Dr. E. Hey-Hawkins (currently at the University of Leipzig). In 1994, she received her Ph.D. from the University of Karlsruhe with a preparative work on the "Synthesis of new mono-cyclopentadienyl substituted Phosphido-Complexes of Mo, Nb and Ta". A postdoctoral stipend from the Deutsche Forschungsgemeinschaft (DFG) allowed her to start her own independent research on alkaline earth metal halides in the group of Prof. Dr. J. Strähle at the University of Tübingen. During a postdoctoral stay in the group of Prof. Dr. J.-M. Lehn at the University of Strasbourg, France, she got introduced to supramolecular chemistry. Postdocs in the groups of Prof. Dr. D. Fenske and Prof. Dr. R. Ahlrichs in Karlsruhe completed her training in cluster and theoretical chemistry, before she moved to the University of Geneva, Switzerland, where she started her habilitation in the group of Prof. Dr. A. F. Williams in 1998. Her research interests focused on alkali and alkaline earth metal compounds in non-aqueous solvents. After her habilitation in 2002, she was offered an Emmy-Noether-Programm, Phase II, by the DFG, a C3-position at the University of Erlangen, Germany, and a research professorship (Förderprofessur) from the Swiss National Science Foundation at the University of Basel, Switzerland, which she accepted in May 2003. Since then, her group is steadily growing, maintaining research interests in group 1 and 2 chemistry, and, furthermore, in ion transport channels, and group 11 coordination networks.

cerned, or precursors for superconductors or other oxide materials required for physical applications. For the latter, thin films of such materials are currently in the focus of research, and therefore we aimed at the synthesis of precursors for thin film synthesis methods such as the sol-gel or chemical vapour deposition (CVD) technique.

This article will review the different research subjects in our group, starting with the inorganic "covalent" polymers, the approach of alkali metal ions with crown ethers and calix[n]arenes to build channels, followed by the supramolecular coordination polymers of alkaline earth metal ions, a survey of our cluster compounds, and ending with Cu^I, and Ag^I coordination polymers before concluding about the properties and some potential applications.

Results and Discussion

1 Inorganic "covalent" polymers

The aim of this part of the project consists in the principle of cutting out structural fragments from a three-dimensional compound, using chemical scissors and by maintaining parts of the initial structure [1, 2]. In order to make a choice on which "bonds" to "cut", these bonds need to be different for instance in strength, and the most obvious parameter to look at is thus the bond lengths. A good starting material is for instance BaI$_2$, which possesses a PbCl$_2$-type structure in the solid state, with the alkaline earth me-

tal ion surrounded by nine iodide ions in form of a distorted, tri-capped trigonal prism (Fig. 1a). This leads to very different Ba−I distances, seven of which are comprised between 3.3 and 3.6 Å, and the other two are approximately 4.1 Å long. The idea is to use chemical scissors in order to "cut" along the longest bonds in the structure and to, successively, cut out structural fragments. Indeed, with H$_2$O acting as chemical scissor on BaI$_2$, the three-dimensional compound [BaI$_2$(μ$_2$-H$_2$O)$_2$] (**1**) can be isolated (Fig. 1b). Compared to BaI$_2$, the longest Ba−I-contacts are cut, the trigonal prism of iodide around the cation is maintained, whereas the three capping anions are replaced by four μ$_2$-bridging water molecules. The remaining Ba−I contacts are six of the shorter ones and are found between 3.3 and 3.6 Å. Upon substitution of one of the two bridging water molecules by a sterically more demanding oxygen donor ligand like acetone (CH$_3$)$_2$CO to yield [BaI$_2$(μ$_2$-H$_2$O){(CH$_3$)$_2$CO}] (**2**), a two-dimensional structure is obtained with the acetone ligand in a terminal position (Fig. 1c). In fact, the bulky CH$_3$-groups allow separation of the layers from each other. Still, the trigonal prismatic arrangement of the six iodide ions around barium is maintained [1].

Using a sterically even more demanding donor ligand like THF, two derivatives of BaI$_2$ can be obtained depending on the quantity of "chemical scissors" used. With three THF-molecules per BaI$_2$ unit, a one-dimensional polymer [BaI$_2$(thf)$_3$] (**3**), is obtained, in which only four Ba−I bonds are maintained to yield a zig-zag chain motif (Fig. 1d). The

remaining coordination sites on the cation are filled with the bulky THF-ligands to lead to the coordination number of seven for barium. Two more Ba−I bonds can be cut by adding more THF to yield the zero-dimensional [BaI$_2$(thf)$_5$] (**4**), in form of a pentagonal bipyramid with the anions in axial positions (Fig. 1e). The Ba−I bonds become shorter as their number per cation as well as its coordination number decreases to reach 3.374 Å, which is consistent if not shorter than the sum of ionic Shannon radii [1 and therein].

Figure 2 Excerpt of the one-dimensional structure of **5**

Figure 1 Structural genealogy tree for compounds derived from BaI$_2$

It was thus possible to establish a structural genealogy tree for BaI$_2$ which could also be transferred to SrI$_2$ and Ba(OTf)$_2$ (OTf = CF$_3$SO$_3^-$) [3]. Whereas the structures for the corresponding SrI$_2$-derivatives are similar to the presented BaI$_2$-adducts, other structures are obtained for barium triflate. Using THF as scissor on this starting material leads to the resulting compound which is a one-dimensional THF-adduct of Ba(OTf)$_2$, [{[Ba(OTf)$_2$(thf)$_3$]$_2$[Ba(OTf)$_2$(thf)$_2$]}$_{1/\infty}$ (**5**). The asymmetric unit is complicated to describe: it consists of two barium atoms Ba1 and Ba2 with a different coordination sphere each, two THF-molecules and six triflate ligands for the former, three THF-ligands and five triflate anions for the latter. The coordination sphere of Ba1 is filled by eight oxygen atoms in form of a square antiprism. It is coordinated by six triflate anions, of which four are μ$_3$- and two are μ$_2$-bridging ligands, as well as two terminal THF-molecules (Fig. 2). For Ba2, the coordination sphere is different with five triflate anions, four of them μ$_3$-bridging and one μ$_2$-bridging, and three terminal THF-ligands. The coordination sphere is quasi the same as for Ba1, a distorted square antiprism [3].

The crystal structure of Ba(OTf)$_2$ has not been investigated yet to our knowledge, but the IR-spectra seem to indicate tridentate triflate ligands corresponding to a similar structure of the compound as for other M(OTf)$_2$ compounds, M = Ni, Co, Zn, Cd [4]. Many of such triflates have a layered structure and thus a two-dimensional array. The one-dimensional compound **5** can therefore be considered as excerpt of such a structure. Furthermore, the literature known complex [{Ba(OTf)$_2$}$_4$(py)$_{14}$].py [5] can be considered as an excerpt from the crystal structure of **5**, regarding the structural part containing barium cations and triflate anions. [3] Pyridine seems to be a stronger chemical scissor than THF in this context.

We are now investigating other binary compounds, also of transition metals and lanthanides, in which very different bond lengths are observed to proceed similarly. This is insofar of interest as such low-dimensional compounds possess an intrinsic anisotropy, which can be fundamental for the expression of their physical properties.

As alkali metal iodides present the same M−I bonds in all directions, crown ethers were used to apply our strategy of cutting out fragments from a solid state structure. So far, this lead to the isolation of molecular species [Na⊂(DB18C6)I(L)], L = THF, (**6**), 1, 3-dioxolane, (**7**), in which the sodium cations are coordinated in an asymmetric fashion (Fig. 3a and 3b) [6].

Using larger crown ethers such as DB24C8 yields [Na⊂(DB24C8)]I (**8**), in which the cation is completely wrapped up by the ligand, leading to charge separation, and the iodide is no longer coordinated to the cation (Fig. 3c). Channels containing for instance one-dimensional NaI in DB18C8 could not be isolated so far. However, using protons as pseudo-alkali metal ion, and working with HI, I$_2$ and DB18C6 in THF and water as solvent mixture, a high yield of dark red needle-like single crystals of the composition [(H$_3$O)⊂(DB18C6)(H$_2$O)][(H$_2$O)⊂(DB18C6)(H$_2$O)]I$_3$ (**9**), (Fig. 4) is obtained [7, 8]. Its structure consists of almost perfectly stacked crown ether ligands, each coordinating to oxygen atoms in their centre. These central oxygen atoms are linked to each other via other bridging oxygen atoms. Hydrogen atoms could not be located in the solid state structure. However, the ligands in one of the two channels are more distorted than in the other, forming the less well packed channel. Attributing this distortion to a strong influence such as provoked by a positive charge, we concluded that this channel carried the positive charges

a)

b)

c)
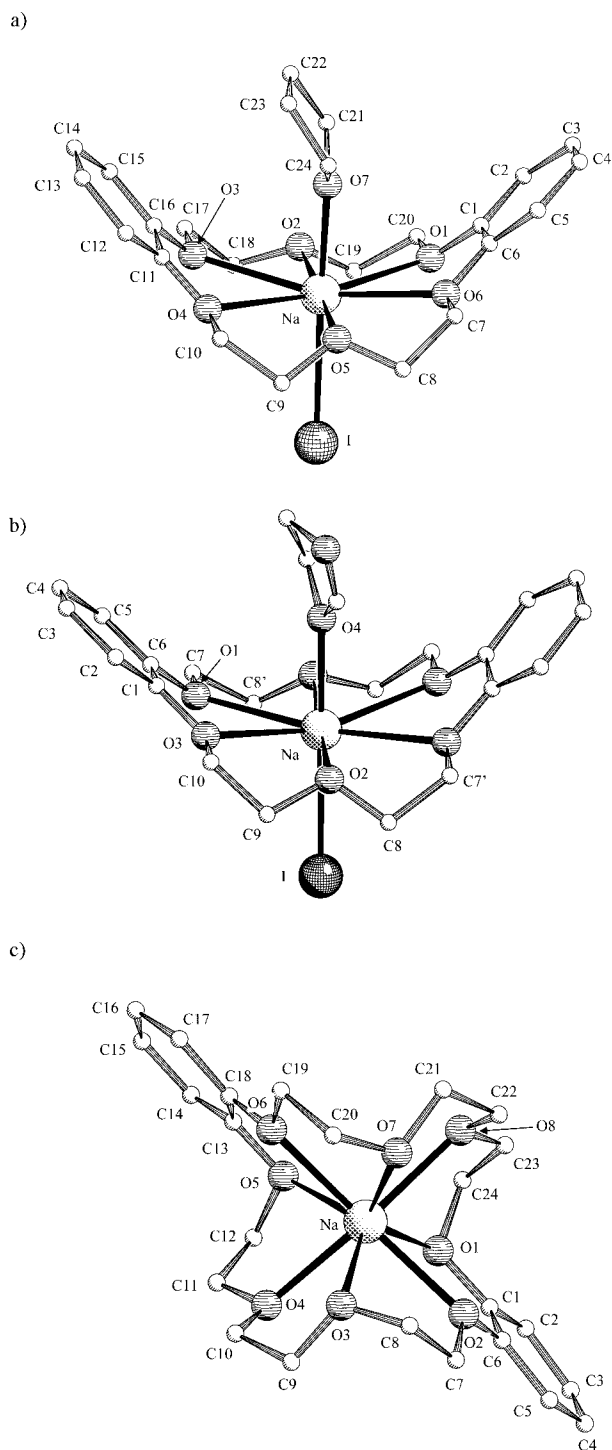
Figure 3 Molecular structure in the solid state of **6** (a), **7** (b) and **8** (c)

Figure 4 Side-view of the one-dimensional strands formed in **9**

and could therefore be considered as the [(H$_3$O)⊂(DB18C6)(H$_2$O)] part of the structure. It is only the second solid state structure known in literature in which the di-benzo crown ether molecules are stacked in such a fashion [9], and it is the first time to have one-dimensional water and acid isolated in such channels [7].

Other potential channel-formers are calix[n]arenes, which have been presented in earlier research reports in the context with transition metals [10]. We are interested in the alkali metallated species of these calix[n]arenes, as they are often used as intermediates in solution for the generation of transition metal derivatives. Little is known about the structures of such intermediate species, and the very few examples that have been isolated to date show interesting structural motifs. The low number of examples in the literature is probably due to the fact that these compounds do not easily crystallize, they are fragile towards hydrolysis, and their structure seems to be very much dependent on the presence, size and quantity of further donor ligands, stabilising the lithiated or otherwise metalated compound [11]. Single crystal structures containing these ligands are always a challenge insofar as calix[n]arenes can have different conformations. While working with tert-butyl-calix[4]arenes, we always observed the cone structure in the solid state so far. In a first step, complete metallation of the latter was achieved with each, LiO^{t}Bu and KO^{t}Bu in THF.

When calix[4]arene is treated with LiO^{t}Bu in THF at room temperature, colourless single crystals of [Li$_8$(calix[4]-arene-4H)$_2$(thf)$_8$]·6THF (**10**) are obtained [11]. The molecular unit of **10** consists of two face-sharing Li$_4$O$_4$-heterocubanes with an inversion centre in the geometrical middle of the central Li2-O3-Li2′-O3′-ring (Fig. 5a). Half of the oxygen atoms O2, O3 and O4 stem from the first calixarene, the other three O2′, O3′ and O4′ from the second calixarene ligand. Four lithium atoms, Li1, Li2 and their symmetry equivalents, lie between the two calixarene molecules, whereas Li3 points into the cavity of the deprotonated ligand and is bonded *endo*. It finds its tetrahedral coordination sphere completed by the oxygen atom O5 of a THF molecule fitting into the cavity of the calixarene, introducing itself from the larger side of the conical ligand featuring the *tert*-butyl groups. Li4 is bonded *exo* to only one oxygen atom of a calixarene ligand, and is further coordinated by three terminally bonded THF molecules linked via O6, O7 and O8. Two oxygen atoms of the calixarene ligand, O2 and

O4, act as μ_3-bridging ligands on three lithium atoms of the heterocubane system. One oxygen atom, O3, can be considered as μ_4-bridging donor atom with three short Li−O bonds. This arrangement gives a coordination number of four to all six lithium atoms in the di-heterocubane unit. Weak interactions of Li3 with the carbon atoms at the basis of three aromatic rings, C17, C28 and C39, can additionally be discussed.
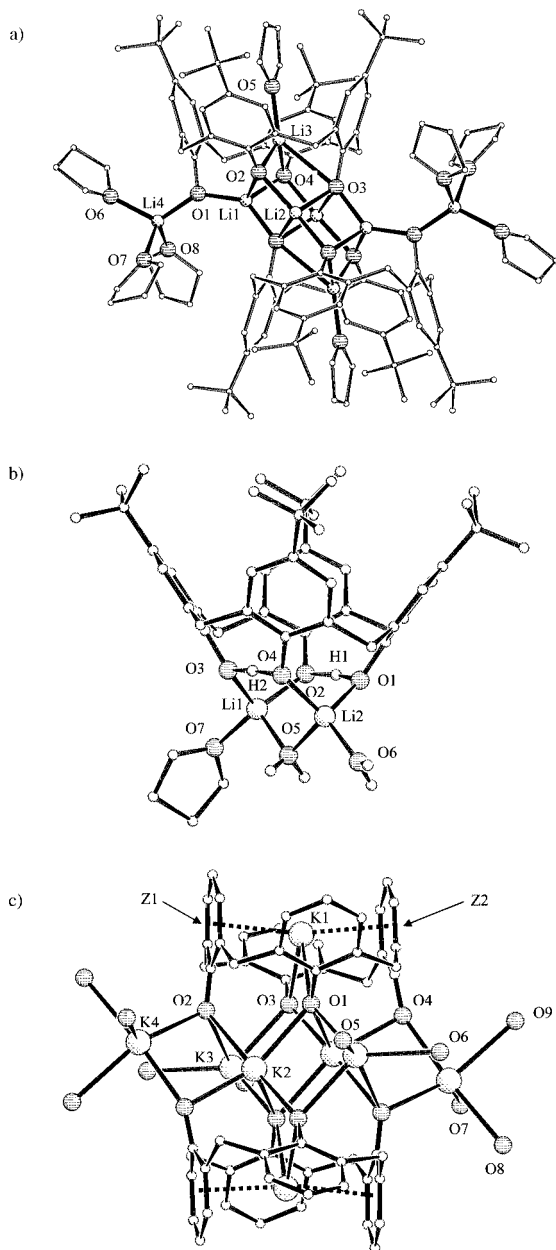
Figure 5 Structures of the cluster molecules of **10** (a), **11** (b), and **12** (c)

The literature known compound $[(L^1)_2Li_8(HMPA)_4]$ (L^1 = *p-tert*-butylcalix[4]arene) forms a fully lithiated calix[4]arene species in which also a dimeric structure is observed [11]. The lithium skeleton of $[(L^1)_2Li_8(HMPA)_4]$ can be described as two edge-sharing square pyramids, one oriented pointing upwards, the other downwards. The apical lithium ions of $[(L^1)_2Li_8(HMPA)_4]$, bonded *endo* to the calixarene, possess only a coordination number of three, as the solvent and ligand HMPA is too large to enter the upper rim cavity of the calixarene. Thus, the size of the ligand, on one hand the smaller THF and on the other larger HMPA, determines the overall structure of the alkali metal cluster formed by the lithiated calixarene in this case.

Further studies concerning the ability of calix[4]arenes L^1 to form monomeric lithiated derivatives, and the reactivity of **10** towards hydrolysis, lead to the formation of a partially hydrolysed compound identified as the monomeric species $[Li_2(L^1-2H)(H_2O)(\mu-H_2O)(thf)]\cdot3THF$ (**11**) [11]. The crystal structure of **11** is quite remarkable because partial hydrolysis of the fully deprotonated and lithiated dimeric compound **10** could also have lead to the formation of dimeric species such as those already known in the literature for the zinc derivative of L^1, $[Zn_2(L^1-2H)_2]$ [12]. The molecular unit of **11** consists of a twice deprotonated *p-tert*-butylcalix[4]arene (Fig. 5b). Two remaining lithium atoms Li1 and Li2 still bind to the "lower rim" of the calixarene cavity. The coordination sphere of Li1 is completed with the oxygen atom O7 of a THF molecule and the oxygen atom O5 of a water molecule. The latter is a μ_2-bridging ligand and connects also to Li2, whose coordination sphere is completed by the oxygen O6 of a second water molecule in terminal position. This leads to a near-tetrahedral geometry for the lithium ions. In d_8-THF solution, the ^{7}Li spectrum is composed of two broad signals indicating the non-equivalence of both lithium atoms in **11**. The ^{1}H-NMR spectrum of **11** exhibits a pair of doublets in the −CH$_2$ region (δ 3.1 to 4.3 ppm), indicative of the cone conformation for the calixarene in THF solution. In the case of calix[4]arene, this cone-shape is usually retained upon metallation, indicating that the solid state structure is maintained in solution. In the solid state, the two remaining phenolic protons H1 and H2 could be localized in the structure, and form intramolecular hydrogen bonds between O1 and O2, and O3 and O4 respectively.

In order to complete our family of calixarenes complexes with larger alkali metal ions, in a similar synthetic pathway, reaction of *p-tert*-butylcalix[4]arene L^1 with KO^{t}Bu in THF affords colourless single crystals of the new dimeric metallocalixarene specie $[K_4(L^1-4H)(THF)_5]_2\cdot1THF$ (**12**) [11]. In a similar way to the lithiated compound **10**, molecular units of **12** comprise two fully deprotonated *p-tert*-butylcalix[4]arene tetraanions fused at the lower rim by six bridging potassium cations arranged in a "sandwich" way between the two calixarenes moieties. The cavity of each calixarene is further filled with a fourth type of potassium ions, as in the previously described dimeric compound **10**, but no THF is *endo* coordinated to the potassium ion (Fig. 5c). Due to the larger ionic radius and the softer character of potassium compared to lithium, compounds **10** and **12** are not isostructural. The cluster core of **10** consists of two fused hetero-cubanes and one lithium ion linked on each side whereas in the potassium compound **12**, the hetero-

cubane structure is not maintained, and the outer cation K4 is linked differently. The potassium ion K1 in **12**, which is bonded *endo* to the calixarene, is much more pushed upward into the calixarene cavity than Li3 in **10**. Thus, the core structure in **12** consists of two fused open hetero-cubanes. The K1 ion is complexed by two oxygen atoms of the calixarene ligand, reaching a valence bond sum of 0.4, indicating that further coordination must exist. Indeed, to complete its coordination sphere, strong π-donation occurs from the two phenyl rings linked to O2 and O4 toward the cation K1 as well as from C1 and C20, basal carbon atoms of the phenyl rings linked to O1 and O3, respectively. The centres of the phenyl rings Z1 (C8-C13), and Z2 (C22-C27), are at distances of 2.799 Å for Z1 and 2.780 Å for Z2 of K1. This is by 0.05 Å shorter than the equivalent distances reported for theoretical calculations of $[K(C_6H_6)_2]^+$ [13]. In the solid state, only longer K^+-Aryl(centroid) (Aryl = aromatic six-ring) distances have been reported. Even in the cyclopentadienyl compound KCp, in which the potassium ion is sandwiched between two Cp-rings of a zigzag-chain-structure and interacts with two more Cp-rings of the neighbour chain, the K−Cp(centroid) distances are still longer than in **12** [11].

The strong interactions of two phenyl rings with the potassium ion K1 in **12**, compared to the weak ones with Li3 in **10**, can be a model for the high selectivity of potassium channels in living organisms. These interactions were shown to belong to cation−π interactions in general, and to be very strong for **12**. In detail, the selectivity of the benzene ring in the gas phase was shown to be highest for Li^+ and lowest for Rb^+, whereas in aqueous media, K^+ is always preferred leading to the formation of a sandwich compound. Similar interactions were attributed to the potassium selective channels of *Drosophila* [11 and therein].

In a next step, we tested larger calixarene ligands in order to have more than one metal ion present in the cavity of the ligand. The larger the calixarene ligand, the more possibilities there are for the formation of different conformers, making these compounds difficult to crystallize. Such compounds can be obtained from a two-phase system, in our case where K_2CO_3 is dissolved in water in the lower phase, and p-tertbutyl-calix[8]arene is suspended in THF in the upper phase. In such systems, the ligand usually arranges itself at the interface with the polar OH-groups towards the polar solvent, whereas the rest of the molecule remains in the apolar phase. Colorless crystals of [K(calix[8]arene-H)(thf)$_4$(H$_2$O)$_7$] (**13**) are formed at the interface of both phases after a period of ca. two days [14]. The asymmetric unit consists of one singly deprotonated calix[8]arene ligand, one potassium cation, and seven water molecules (Fig. 6a). The metal ion is bonded to one side of the calixarene ligand, where it is coordinated by O7 and O8. The coordination sphere of the potassium cation is completed by three oxygen atoms of water molecules, O9, O9′ and O10, as well as by one oxygen atom O11 of a THF molecule to yield a distorted octahedral environment for the cation. The oxygen atom O10 is positioned over the center of the cavity

in the calixarene ligand on the same side of the ligand as the potassium ion. It forms a hydrogen bonding contact through the cavity of the macrocycle, and to the oxygen atom O15 of a water molecule on the opposite side of the organic ligand. The latter is involved in further hydrogen bonding to the water molecules of O16, O17, and O16′. The four water molecules O15, O16, O17 and O18 form, together with their symmetry equivalents, a distorted cubane structure. The *C2*-symmetry of the (H$_2$O)$_8$-cubane however, and its coordination by four THF-ligands to O16, O16′, O18 and O18′ allow only one distribution of the protons. Twelve of the sixteen H-atoms bridge the edges of the cubane, whereas the remaining four are directed towards the THF-ligands. Thus, at least one proton of O10 has to point towards O15 in order to maintain the H-bonding system. To the best of our knowledge, this is the first water cubane structure with *C2*-symmetry isolated in the solid state.
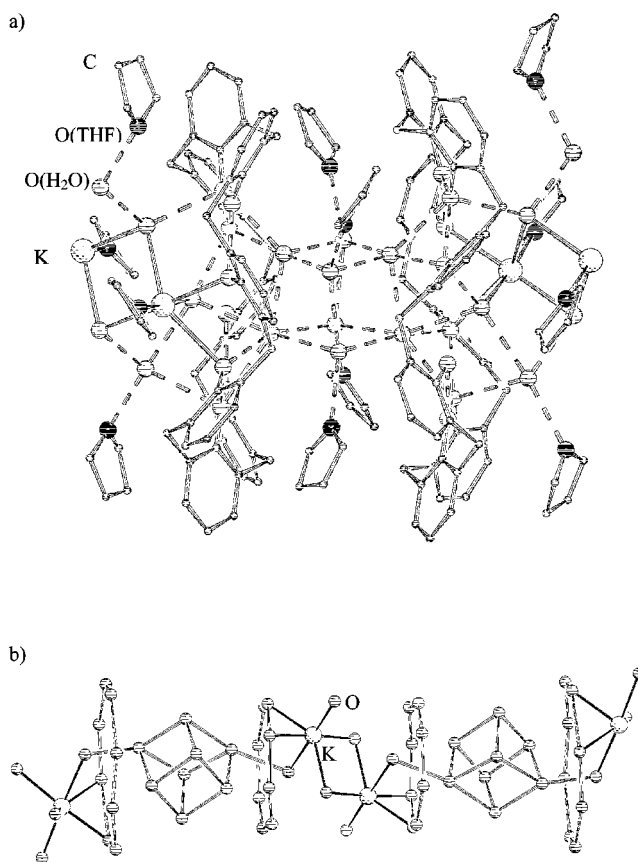
Figure 6 Side-view of the one-dimensional strands formed in **13** (a) and simplified core structure of the channel, C- and H-atoms omitted (b).

All in all, a one-dimensional system is obtained. The calix[8]arene can be considered as rings (or pearls) on a hydrogen-bonding chain between the water cubane cluster and the potassium dimer unit (Fig. 6b). Furthermore, there are three more THF ligands, and one additional water molecule in the asymmetric unit. The water molecule, O21, bridges the two water ligands O9 and O10. Two of the

THF-molecules and their symmetry equivalents are H-bonded to O16 and O18 as well as their symmetry equivalents and thus coordinate around the water cluster; the third one is linked to the bridging water molecule O21, and all of these ligands act as terminal ligands. Thus, the THF ligands and the calix[8]arene ligands form together a channel system with the non-polar part of the molecules pointing outward, the polar oxygen donors pointing inward the channel. The inside of the channel is filled with water molecules and potassium ions. We are now investigating such channels on a larger scale as models for biological ionic channels and try to test their ionic conductivity. Other alkali cations as well as other sizes of calixarenes are currently under investigation in our group.

2 Supramolecular inorganic polymers

This part focuses on the formation of different dimensional polymer structures obtained by the combination of two binding modes: firstly the metal ion coordination, and secondly the hydrogen bonds. The aim of this project is to contribute to the field of structure prediction, or, at least, the prediction of the dimensionality of a compound in the solid state. In the group, we are interested in cationic complexes of alkaline earth metal ions with at least one water molecule in the coordination sphere of the cation, using this water ligand as hydrogen bonding partner for spherical anions such as iodide [15−18]. In collaboration with other groups, we also deal with designed ligands which carry information to coordinate a transition metal on one hand and H-bond acceptors and donors on the other hand, and which are able to build up two-dimensional structures in the solid state, combining metal ion coordination with an H-bonding system [19].

Some first experiments lead to the conclusion, that it is only possible to predict interactions between complex cations, the counter ions and solvent molecules under very restricted conditions. For instance, the compound of the general formula trans-$[Ca(L)_4(H_2O)_2]I_2$ doesn't form similar solid state structures even when ligands L of similar size, and the same donor atoms are used, which are not involved in H-bonding [15]. Thus, the compound in which L = THF, **14**, forms a two-dimensional network via hydrogen bonds, whereas for L = ethyl acetate ($CH_3COOC_2H_5$), **15**, one-dimensional chains are observed (Fig. 7a and b).

These together with other results [16] lead us to fix several rules under which at least the dimensionality of a compound can be predicted. The following conditions are required in the case of structures of supramolecular polymers of alkaline earth metal iodides: i) the cations form complexes charged 2+ with inert polyether ligands and H-bonding water molecules, ii) the counterions, charged 1−, are the only H-bond acceptors, here two iodide ions per complex cation, iii) the water ligands, if several, are arranged in vicinal positions, iv) only the water molecules are involved in hydrogen bonding, and v) each hydrogen atom of water molecules forms a single hydrogen bond to iodide
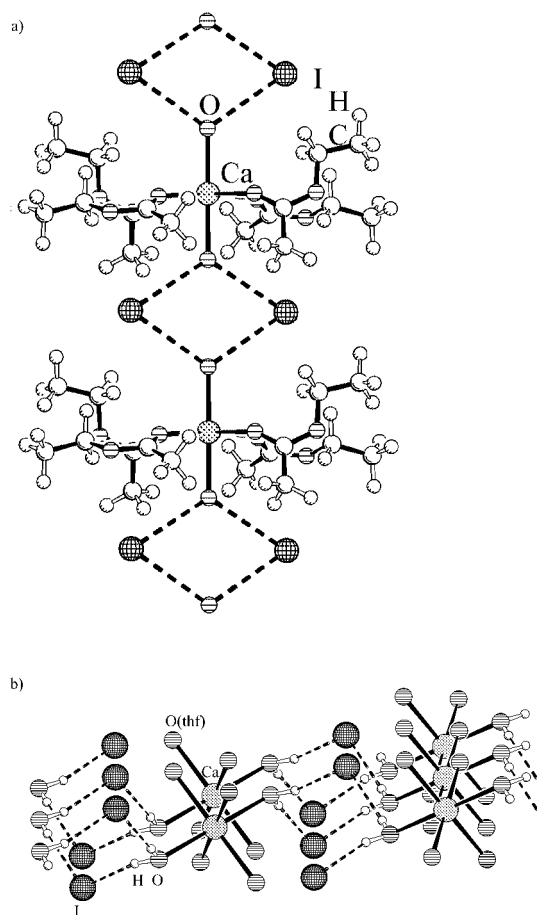
Figure 7 Excerpts of the solid state structures of **14** (a) and **15** (b)

ions, excluding that two hydrogen atoms of the same water molecule bind to the same iodide ion [17]. So, the only variable is the bridging functionality of iodide ion and the number of water ligands per cationic complex. It was found that under these conditions, the number of water molecules coordinated to the alkaline earth metal cation, directs the dimensionality of the final compound. Thus, a compound with one water molecule, like $[Ba(triglyme)_2(H_2O)]I_2$ (**16**) has a zero-dimensional structure, one with two water molecules forms a one-dimensional chain, i. e. $[Ca(diglyme)_2(H_2O)_2]I_2$ (**17**), three water molecules present will give a two-dimensional double-layer as in $[Ba(diglyme)_2(H_2O)_3]I_2$ (**18**) and four water molecules bonded to the cation will lead to a three-dimensional compound, i. e. $[Ca(triglyme)(H_2O)_4]I_2$ or $[Ca(dme)_2(H_2O)_4]I_2$, (**19**) and (**20**), respectively (Fig. 8 a, b, c and d, for **16**, **17**, **18** and **20** respectively). [17] Isostructural compounds to **17** and **20** have been obtained with Sr instead of Ca. [20]

In the case where four water ligands are bonded to the alkaline earth metal cation, even the compound in which the anions are directly linked to the cation can form such a three-dimensional structure, as has been shown for $[Ba(OH)I(H_2O)_4]$ (**21**) (Fig. 9) [18].

a)

b)

c)

d)
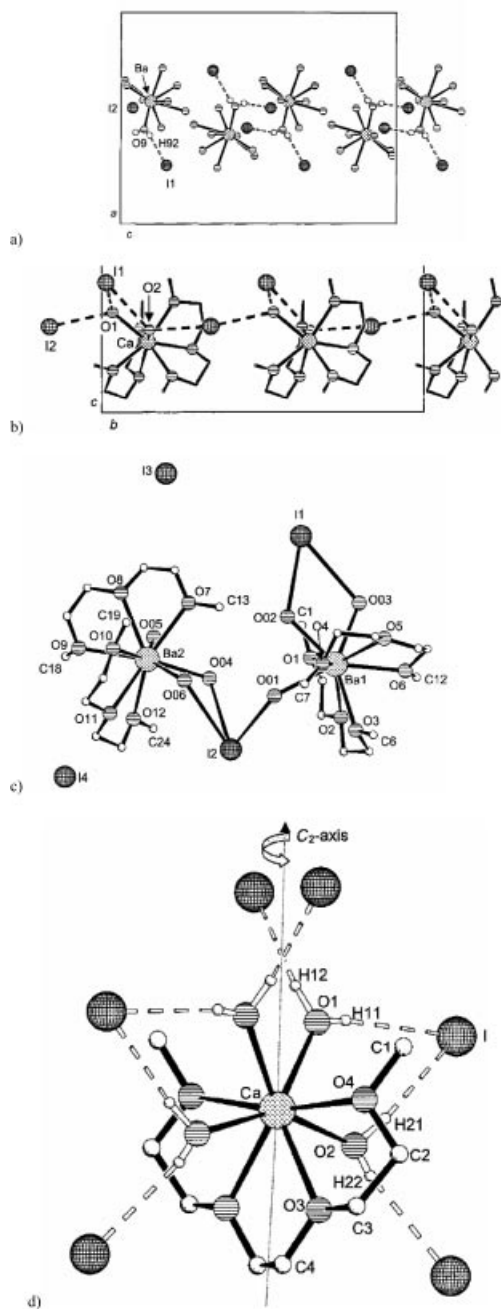
Figure 8 Networks on the solid state structures of **16**(a), **17**(b), **18**(c), **19**(d); for **20**, the triglyme ligand in **19** can be replaced by two DME-molecules

We are now investigating how this concept can be generalized to other metal ions, ligands and anions in order to contribute to this important field of fundamental research.

3 Clusters of alkali and alkaline earth metals

Looking for an analogy to transition metal clusters (in this case, clusters are defined as aggregates without necessarily presenting metal-metal bonds), the following general reaction scheme 1 for obtaining alkaline earth metal clusters was applied:
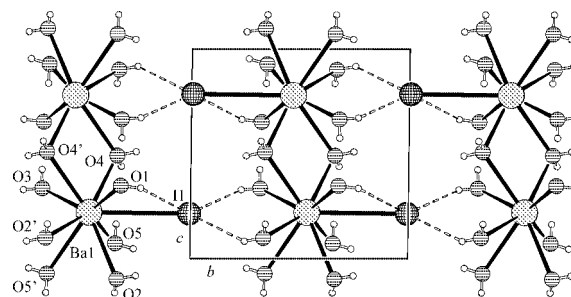
Figure 9 Excerpt of the solid state structure of **21**

$$n\,MX_2 + n\,{}^nBuLi + n\,LiOR \xrightarrow[+ \text{Ligand L}]{-\{[LiX][{}^nBuLi]\}_n} [(L)_mM_nX_n(OR)_n],$$
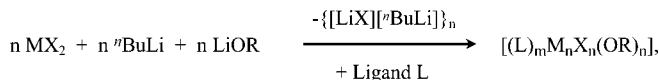
Scheme 1 Reaction scheme 1 for the generation of new alkaline earth metal cluster compounds

with MX_2 being an alkaline earth metal iodide, LiOR being either the hydroxide or LiO^{t}Bu, and L an oxygen donor ligand like THF or some polyether. [21, 22]

In a first step, our interest focuses on the investigation of potential starting compounds of the type $[MI_2(L)_x]$, as such adducts are formed in the cases where L is also used as solvent. In water as solvent, ion separation takes place and a typical ionic behaviour of the alkaline earth halides is observed. In organic solvents such as THF or polyethers (L = DME, diglyme), the M−I contacts remain mostly intact, and the alkaline earth halide is dissolved forming adducts $[MI_2(L)_x]$ where x depends on the size of the cation and the size and flexibility of the ligand L, similar to the ones observed for lanthanide cations, their coordination chemistry being very similar. [23] As described in the first part of this paper, the zero-dimensional structures $[MI_2(thf)_5]$, M = Ba and Sr, **4** and **22** respectively, were found to have a trans arrangement of the anions in a distorted pentagonal bipyramidal arrangement of ligands around the cation, as expected from the VSEPR model, due to maximum repulsion of the negative charges. This is also observed for $[CaI_2(thf)_4]$ (**23**) a literature known compound which we also crystallised, but in a different space group [21, 24]. As the cation is smaller than Sr and Ba, the coordination number is reduced from seven to six (Fig. 10) [21, 25].

When SrI_2 is dissolved and re-crystallized from freshly dried and distilled diglyme ($CH_3OC_2H_4OC_2H_4OCH_3$), only the compound cis-$[SrI_2(diglyme)_2]$ (**24**) is obtained [25−27]. Two independent molecules are found in the asymmetric unit, and both molecules consist of a strontium cation to which two diglyme ligands and two anions are directly linked (Fig. 11). In contrast to **22**, the I−Sr−I angles are with ca. 91.5° much smaller and close to a right angle. Together with the oxygen donor ligands, the coordination sphere of the cation can now be described as severely distorted square antiprismatic. The coordination number of eight for the strontium cation is common. Generally, the

a)

b)

c)
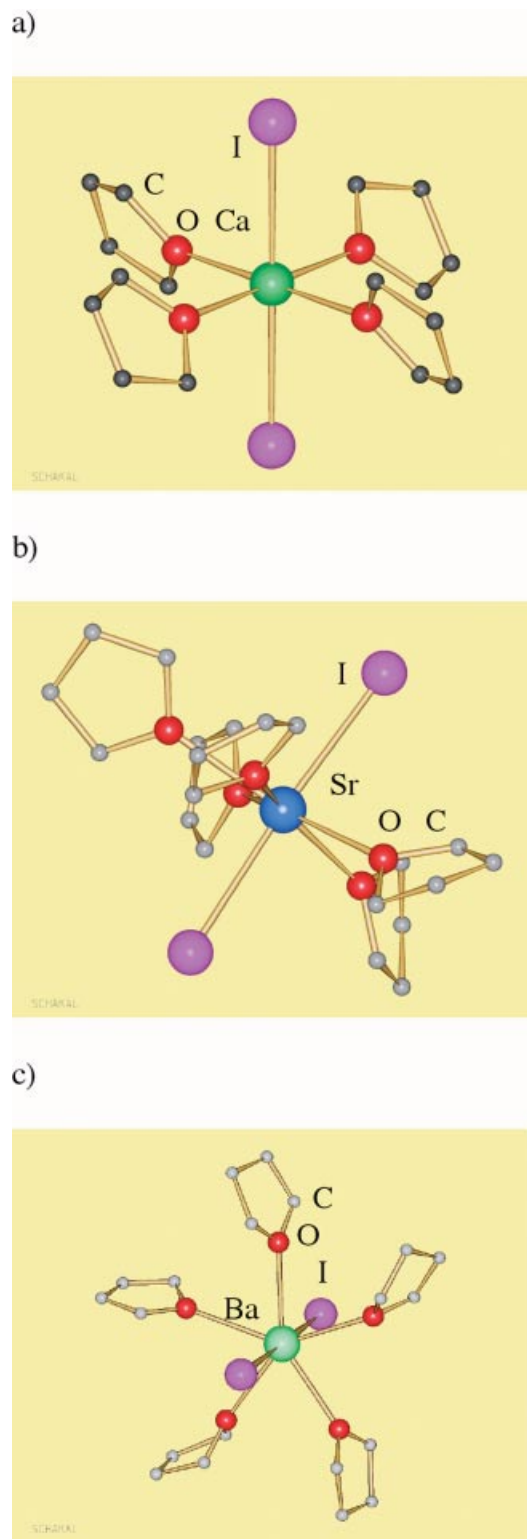
Figure 10 Comparison of the molecular structures of **23** (a), **22** (b) and **4** (c)

strontium cation usually behaves similar to the barium ion rather than calcium as far as coordination numbers are concerned. The most intriguing fact about this structure is that both anions occupy vicinal positions. In general, to obtain

such structures with the anions in cis-position, a sterically important ligand, which shields one side of the cation, such as slightly too small crown ethers, is required. And then, the X−M−X angles are usually much larger, the M−X bonds are longer than in **24**, and the anions are involved in H-bonding to build up a polymer structure. **24** is therefore the first example of a polar molecular alkaline earth metal iodide precursor. The strongly bent I−Sr−I feature in this structure reminds of the alkaline earth metal halides, especially the heavier ones with strontium, barium and iodide as counter ions, in the gas phase. Indeed, experimental as well as theoretical data show bent structures for the molecules in the gas phase [21, 28]. So, **24** could be compared to a gas phase species stabilized by oxygen donor ligands. The bent structure reminds also of the cyclopentadienyl derivatives of the alkaline earth metals. They have bent structures as well. However, in the solid state, they form polymers via contacts to neighbouring units [27].

Figure 11 The two independent molecules in **24**

a)

b)

Figure 12 Independent molecules of **25** (a), and molecular structure of **26**, when three DME molecules of **25** are replaced by two diglyme ligands (b)
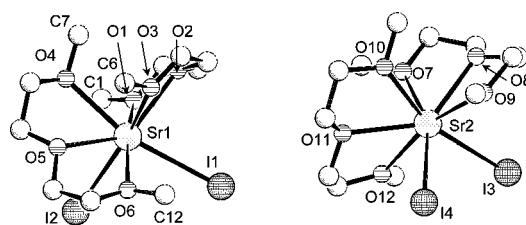
The second compound, [CaI(dme)$_3$]I(**25**), presented here, was obtained when crystallizing CaI$_2$ from freshly dried and distilled DME [27]. **25** is built up from two independent cationic molecules A and B per asymmetric unit, each consisting of a calcium cation, Ca1 and Ca2, to which one iodide ion and three DME-ligands are bonded terminally, respectively via both oxygen atoms each, and two separate iodides as counter ions (Fig. 12a). Thus, the cation reaches coordination number of seven. The coordination can roughly be described as a distorted pentagonal bipyramid with one iodide ion and an oxygen atom in axial positions. A similar compound can be obtained replacing the three DME-ligands of **2** by two, larger diglyme molecules. The number of oxygen atoms then remains identical, and so does their arrangement around the cation. The compound which is then obtained can be written as [CaI(diglyme)$_2$]I (**26**) (Fig. 12b). We have shown before (compounds **19** and **20**) that small polyether molecules (such as DME) can easily be replaced by larger ones (diglyme or triglyme for instance) as long as the number of oxygen atoms remains constant, without significant changes in the structure. The cations [CaI(dme)$_3$]$^+$ and [CaI(diglyme)$_2$]$^+$ of **25** and **26** possess a strong dipole moment along the Ca−I bond vector, as can be seen from figure 12. Such polar species are scarce: in the literature, only one example with calcium and iodide was described so far to our knowledge, [CaI(thf)$_5$]$^+$, in which the cation possesses coordination number of six, the counter ion being an extremely bulky phosphonium diylide [29].

In order to determine the space needed for different ethereal ligands, other adducts with differently sized polyethers as well as mixtures of ligands are currently under investigation. Among the presented starting materials, the THF-adducts were used so far in order to obtain cluster compounds as described in the reaction scheme 1. The results are presented in the next paragraphs [20, 30].

Using CaI$_2$ under the conditions given in reaction scheme 1, we were able to isolate the largest Ca-cluster so far, Li[Ca$_7$I$_6$(μ_3-OH)$_8$(thf)$_{12}$]$_2$(μ_2-I)(THF)$_n$ (**27**) with a unique structure of two double-hetero-cubanes linked together via hydrogen bonds to a central iodide ion, yielding a dumb-bell-shaped cluster of fourteen calcium ions (Fig. 13a) [30]. The cluster is made up of OH-bridged Ca$_3$-triangles, put together to build tetrahedra which are fused via one Ca-cation. This central cation has a coordination sphere of six OH-groups in a nearly octahedral environment. Two THF-ligands and one iodide ion are terminally bonded to the other six Ca-cations, which have their quasi octahedral coordination sphere completed by three OH-groups. One of these OH-groups binds to an iodide ion in order to bridge to the second Ca$_7$-cluster unit, build up in a mirror fashion to the first. One counter cation is needed and can be found as a Li-ion, coordinated by four THF-ligands.

When SrI$_2$ is used as starting material in a reaction scheme 1, [Sr$_3$I$_3$(μ_3-OH)$_2$(thf)$_9$]I (**28**) is obtained (Fig. 13b) [21]. Here, three metal ions are arranged in a perfect tri-

angle, its edges being bridged by iodide. The three cations are also "glued" by two μ_3-bridging OH-groups, one above, the second below the plane spanned by the cations. Each Sr-cation carries furthermore three THF-ligands to complete its coordination sphere to a distorted pentagonal bipyramid. It is interesting how the I−Sr−I angle varies from [SrI$_2$(thf)$_5$], (**22**), with ca. 176° to 172° in **28**. This triangular arrangement seems to be a fundamental unit for the construction of higher aggregates, since most of the alkaline earth metal clusters form polyhedra or sheet structures in which triangles of alkaline earth metal ions are fused together.
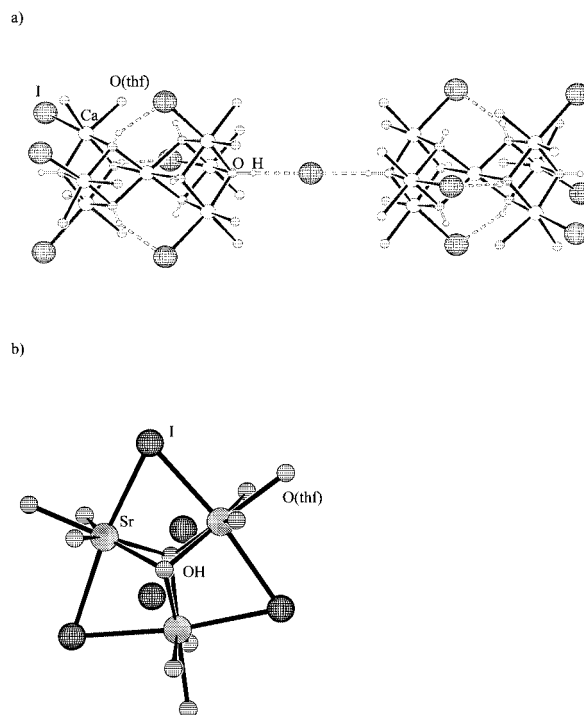
Figure 13 Cluster molecules of **27** (a) and **28** (b)

These two purely alkaline earth metal clusters **27** and **28** are not volatile, and can thus not be used as CVD (Chemical Vapor Deposition) precursors. However, they form extremely stable sols in THF upon hydrolysis with, in the case of the calcium compound, a particle size of ca. 1000 nm and a particle composition of Ca(OH)$_2$(H$_2$O)$_n$ which can be used to synthesize thin films of halide-free CaO. [21]

In order to introduce volatility, we aimed to replace LiOH by LiO^{t}Bu which is for itself volatile. To our surprise, the solid state structure of LiO^{t}Bu was unknown when we got interested in the compound, even though that other analytical methods and some single crystal data of bad quality were pointing to a hexameric structure. We were able, simultaneously but independently to another research group, [21, 31], to crystallize LiO^{t}Bu in order to obtain a satisfactory structure. The compound [LiO^{t}Bu]$_6$ (**29**) forms in principle hexamers, two independent molecules being found in the unit cell. The oxygen atoms are arranged in a distorted octahedral arrangement, with eight triangular

faces to be capped by six lithium cations. Due to this fact, the cations are disordered over all possible places which made structure solution quite difficult as the molecules are also highly symmetric. Nevertheless, the most probable structure can be described as a hexagonal anti-prism of O and Li atoms (Fig. 14a), confirming the literature discussion. [21, 32, 33]
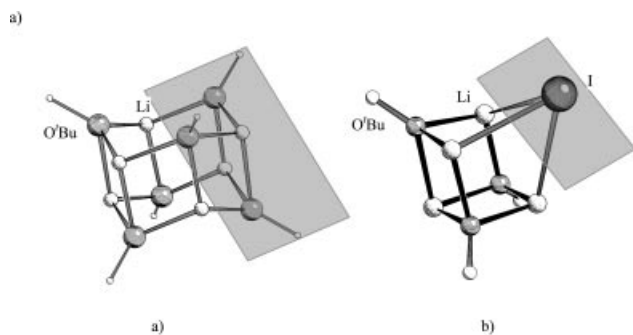

Figure 14 Structural relationship between the molecular structures of **29** (a) and **30** (b)

Under the above reaction conditions (scheme 1) and with CaI_2 as starting material, a pure lithium cluster $[Li_4(\mu_3\text{-}O^tBu)_3(thf)_4I]$ (**30**) with a distorted hetero-cubane structure was obtained (Fig. 14b). [32] Structurally, it can be related to the starting material **29** as shown in figure 14, replacing formally a $[Li_2(O^tBu)_3]^-$ unit by I^-. With this compound, we were for the first time able to isolate and structurally characterize the lithium compound produced along the reaction as secondary product. As can be seen from its composition, the iodide ion has been partially stripped off the alkaline earth starting product, and so there must also be a new calcium compound to be discovered. Recently, it was possible to characterize the latter. Instead of yielding a pure Ca-compound, a mixed metal cluster is obtained. The compound $[ICa(O^tBu)_4(Li\{thf\})_4(OH)]$ (**31**) consists of a calcium cation to which an iodide ion and four O^tBu-groups are bonded, the former in a terminal fashion (Fig. 15 a). [34] Four lithium cations are linked to the O^tBu-groups as well, the oxygen and lithium atoms forming a distorted square anti-prism. The open square face formed by the alkali metal ions is bridged by an OH-group. In order to complete the tetrahedral coordination sphere around each lithium cation, each is terminally coordinated by one THF ligand. The whole cluster has thus a spherical overall shape with mainly organic, apolar ligands pointing to the outside and shielding the cluster core. This is in principle a favourable structure for volatile compounds as intermolecular forces are expected to be weak. In analogy, the compounds $[IM(O^tBu)_4\{Li(thf)\}_4(OH)]$, M = Sr (**32**), [21], Ba (**33**), [35], were isolated (Fig. 15 b and c).

Comparing the structures of the three related compounds **31**, **32**, **33**, it can be seen that the cluster core is more and more flattened the smaller the cation, and, vice versa, the M−OH bond gets longer with increasing cation size. For compound **33**, solution and solid state analysis
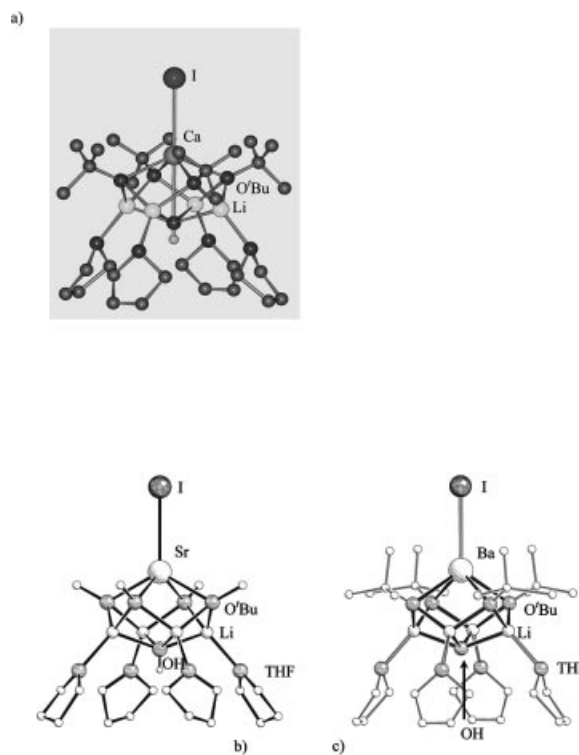
Figure 15 Comparison of the cluster structures of **31** (a), **32** (b) and **33** (c)

were found to be congruent as far as ^6Li and ^{13}C NMR is concerned. The ^{1}H-NMR of a solution of **33** in d_8-THF shows a temperature dependency of the signal for the OH-proton, indicating interactions of H-bonding nature in the cavity formed by the THF-molecules of the cluster (Fig. 16). It also turns out to be volatile, and therefore, deposition tests were carried out. Partially crystalline product was deposited on $SrTiO_3$, and after thermal treatment at 600 °C, halide-free BaO is formed on the surface, as identified by Auger electron spectroscopy. As an ingredient for high temperature superconductors, compounds **31**, **32** and **33** could possibly be a new solution in the generation of halide free, quantitatively deposited oxides.
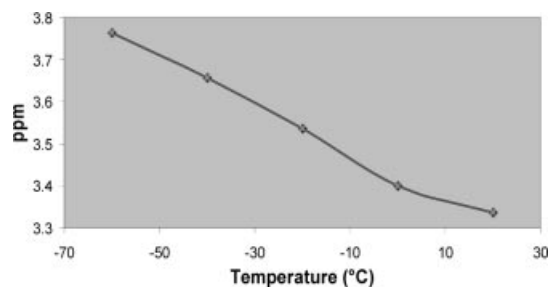

Figure 16 Temperature dependency of the OH-proton shift in ^{1}H-NMR of **33**

With the aim to make single source precursors for oxide materials, containing several metal ions within one compound, we started to investigate multitopic ligands and

their ability to coordinate to group 11 and group 1 or 2 metal ions. While studying group 11 metal ions, Cu^I, Cu^{II} and Ag^I, the problem of polymorphism and pseudo-polymorphism with such compounds came into the focus of our interest. Some of the results obtained in this context will be presented in the next chapter.

4 Coordination polymers and supramolecular structures of group 11 metal ions

In a first step, a ditopic ligand was chosen, built from pyridine and glycol units, thus being able to coordinate a "soft" cation via the nitrogen atoms, and a hard cation via the oxygen atoms. The chosen ligand is shown in scheme 2, and it has the advantages of being easily accessible, and of being easily modified in the position of the nitrogen atoms as well as in the middle part by choosing longer spacers such as diethylene glycol derivatives [36].
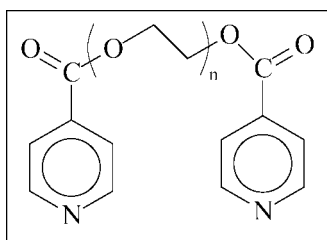
Scheme 2 Representation of the ligand family used in our coordination chemistry, for n = 1 → L = **34**

This ligand L, **34**, has a flexible backbone and might thus lead to coordination polymers with different conformations of ligand. The ligand alone crystallizes in its anti conformation, stacking the molecules parallel to each other and with hydrogen bonds stabilizing the network (Fig. 17). This can be represented as an S-shape, whereas the gauche conformation, the second stable structure of the ligand, is furthermore represented as U-shape. Their energies differ weakly by 0.8 kcal/mol [36].
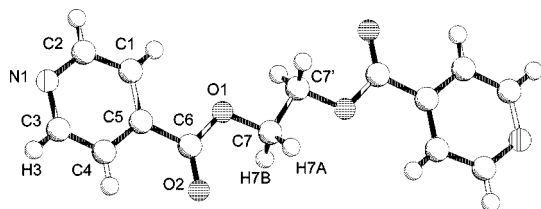
Figure 17 Molecular structure of the ligand L, **34**, showing its anti conformation

When **34** is reacted with CuCl in a mixture of solvents THF/CH$_3$CN, red single crystals of the composition [CuCl(L)](THF)$_{0.5}$ (**35**) are obtained [36]. A one-dimensional compound is found by repeating units of copper atoms which are, two by two, alternatingly bridged by two chloride anions and two ligands in gauche conformation, respectively (Figure 18a). Each copper cation is therefore

coordinated by two N-atoms of two different ligand molecules and two chloride ions. The Cu−Cl bonds are very asymmetric with 2.3255(9) and 2.546(1) Å, indicating that the Cu(μ-Cl)$_2$Cu unit could be interpreted as a dimer of two Cu−Cl fragments. The so-formed chains are stacked on top of each other so that the cavities in the centre of the Cu(μ-L)$_2$Cu rings form channels in which the disordered solvent molecules are located. The THF molecules are not in the same plane as the copper atoms and the two ligand molecules, but are placed in between the chains. Apparently, the presence of the THF molecules keeps the chains apart from each other, and prevents π-stacking in **35**.
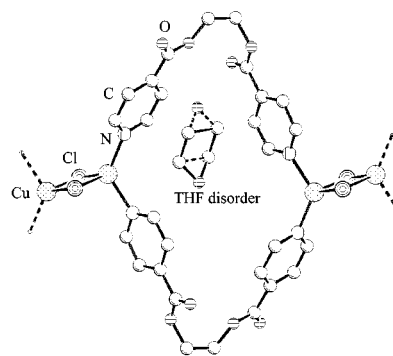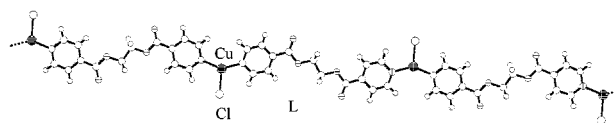

Figure 18 One-dimensional structures of **35** (a) and **36** (b)

After several days in the mother liquor, the crystals of **35** transform into yellow species of which single crystals were measured to be [CuCl(L)] (**36**) [36]. In contrast to **35**, compound **36** forms one-dimensional chains of copper atoms linked via the ligand, the latter coordinating through the nitrogen donor atoms (Fig. 18b). The copper ion, having a trigonal planar arrangement of ligands (angle sum = 360°), is coordinated by two nitrogen atoms of two different ligands and a chloride ion. The conformation of the ligand in **36** is anti and thus the same as in the free ligand **34**. **36** can be directly obtained when the reaction is carried out in pure CH$_3$CN as solvent.

Apparently, the presence of THF as solvent in the structure also influences on the conformation of the ligand. **35** slowly transforms into **36** when the crystals remain in the mother liquor, giving rise to the assumption that **36** is the thermodynamic more stable product obtained by diffusion of THF out of the structure and following reorganisation. Even though the transformation relies on severe rearrange-

ments in solution, one can propose a possible mechanism for it. Structurally speaking, one has to formally cut the longer Cu−L bond first (Scheme 3). The ligand would then bend over to the other side and displace a chloride ion at the next copper atom in order to adopt a stretched out anti conformation. One Cu−Cl bond at each copper atom is thus formally cut, and the structure of **35** could be transformed into compound **36**.
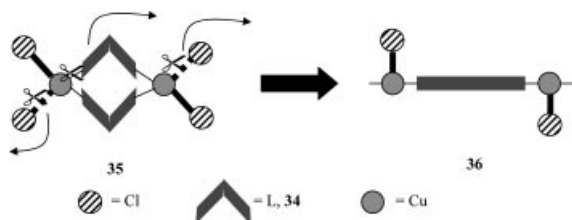
Scheme 3 Possible mechanism of transformation of **35** to **36**

Pseudo-polymorphs and real polymorphs can also be observed when L, **34**, is reacted with AgNO₃. Single crystals of the Ag-compounds are obtained in H-formed tubes, dissolving the silver salt in a polar solvent in one compartment, dissolving the ligand L in THF in the other compartment, and layering both with a mixture of solvents in order to bring both compartments into contact. Slow diffusion leads then to reaction and the formation of crystalline material. Only the results obtained when the silver salt is dissolved in H_2O will be reported here, but other results are numerous and currently under final investigation in our group [37].

When AgNO₃ is dissolved in water and mixed with a solution of L in THF, colourless single crystals of {[Ag(L)](NO₃)} (**37**) are obtained [37]. The structure consists firstly of one-dimensional chains of undulating Ag-L-Ag-L-motifs, the pyridine rings coordinating to the metal ions via the nitrogen atoms (Fig. 19a), and the ligand adopts the anti conformation. Each metal ion reaches a coordination number of five, with two nitrogen atoms in axial and three oxygen atoms of two nitrate anions in equatorial positions of a distorted trigonal bipyramid. Apart from the anions which act as bridging ligands between two silver ions of adjacent chains, other forces hold the chains parallel to each other: hydrogen bonding occurs as well as π-stacking.

Under similar conditions, the second compound {[Ag(L)](NO₃)(H₂O)} (**38**) is obtained via the diffusion technique [37]. The asymmetric unit is formed of one silver atom, one ligand molecule, a nitrate counter ion and one water molecule. Again, one-dimensional chains are formed by coordination of the pyridine rings of the ligand L to two different metal ions (Figure 19b). In contrast to **37**, the ligand L now adopts a gauche conformation, giving the strands an undulating zig-zag structure. The coordination number of the silver ion by O- and N-atoms has decreased from five in **37** to four in **38**. The second reason is the Ag-Ag interaction observed in **38**, with a Ag−Ag distance of 3.136(1) Å, leading to pairs of almost perfectly parallel chains. The metal-metal contacts in **38** are the shortest dis-
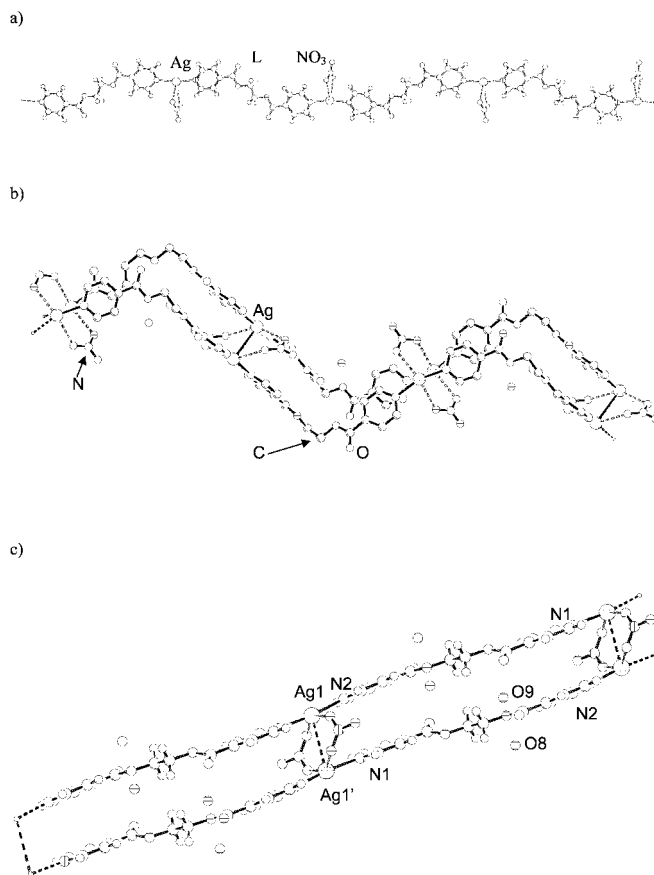

Figure 19 Solid state structures of **37** (a), **38** (b) and **39** (c)

tances between two parallel chains. Other forces contribute furthermore to the double chain formation: π-π interactions and two bridging NO₃³⁻ anions which coordinate only via two oxygen atoms as compared to **37**.

Under the same reaction conditions, colourless single crystals of {[Ag(L)](NO₃)(H₂O)₂} (**39**) are obtained in low yield only [37]. Again, a one-dimensional chain structure, alternating Ag-ions and ligand molecules, is obtained (Fig. 19c), in which the ligand molecules coordinate to two metal cations via the nitrogen atoms of the pyridine rings and possess anti conformation. Two chains form pairs by parallel arrangement via an inversion centre, allowing three different interactions between the chains (Fig. 19c). Firstly, weak π-stacking can be observed. Secondly, as in **38**, metal-metal interactions are present. Again, the Ag−Ag distance is the shortest contact between the two chains with 3.408(6) Å, which is however by 0.3 Å longer than in **38**. An inversion centre is found in the geometric middle of the metal-metal contact. Thirdly, as mentioned above, weak anion coordination is observed. In fact, the two silver cations are held together by two bridging NO₃⁻ anions, acting as bidentate ligands.

Between the pairs of chains in **39**, a new kind of interaction is observed, which is not present in **37** or **38**: Ag-π-interactions with distances of 3.477 Å between the metal ion of one pair and the centre of the pyridine ring of a next pair, leading to a layer structure of chains. The remaining

space between such layers is filled with four water molecules per double-chain unit. These water molecules are linked via the nitrate anions in order to build ribbons of H-bonds running parallel to the layers.

The three compounds **37**, **38** and **39** have in principal one general structural feature in common, that is the presence of one-dimensional coordination polymer chains made of Ag^+ and L. The presence and the different number of water molecules in **38** and **39** lead to severe changes in the arrangement of the chains with respect to each other compared to **37**, as well as in the ligand conformation as far as **38** is concerned. Thus, compounds **38** and **39** also feature metal-metal contacts, leading to pairs of chains. Weak interactions are, in their sum, responsible for their formation. Aromatic π-π-stacking is observed in all three compounds. However, two major facts can be found which are responsible for the formation of different solid state structures. One is evidenced in the ligand conformation. In **39**, it adopts anti conformation, whereas in **38**, gauche arrangement is observed. The second point is the presence of different amounts of water molecules per asymmetric unit. Thus, the factor influencing the overall arrangement of the double-chains to each other in the crystal seems to be the number of water molecules and the resulting number of possible hydrogen bonds. The H-bonds also influence the fact that the chains run parallel in **39**, or cross each other in **38**, and that the ligand adopts two different conformations in **38** and **39**. Very probably, the Ag-π contacts in **39** are also responsible for inducing the parallel packing of the chains in this structure. Energies of such stacking interactions may be similar to coordinate bond energies for some heavy metals such as Tl^+, Ag^+ and Pb^{2+} and have roughly been estimated to up to 40 kJ/mol [37−39]. From Cu^I coordination compounds **35** and **36** with the same ligand L, it can be concluded that the H-bonds toward solvent molecules such as THF of H_2O may induce deformation of the ligand L, whereas in absence of solvent molecules, the ligand has so far always adopted the anti conformation as in the free ligand. The here observed coordination polymers for Cu and Ag are schematically represented in Scheme 4.

Representative examples of other coordination networks in which weak interactions also play a role and a survey of π-π-interactions in crystal engineering can be found in the literature as well [40, 41].

Many other coordination polymers are possible with our ligand, varying the reaction conditions such as counter ions, solvents, concentrations and also the size of the ligand along the spacer and the position of the nitrogen atom in the aromatic ring. Currently under investigation, these results will give rise to more publications in the field of crystal engineering before continuing the initial idea of combining such polymers via a second metal ion coordinated to the oxygen donor part of the ligand.

5 Applications

Among the above results, some were found to exhibit interesting properties. Thus, the one-dimensional [Ca(diglyme)₂-
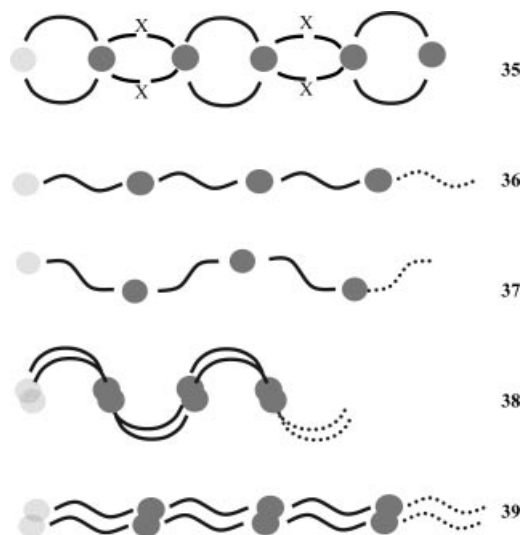
Scheme 4 Schematic representation of the here observed coordination polymers.
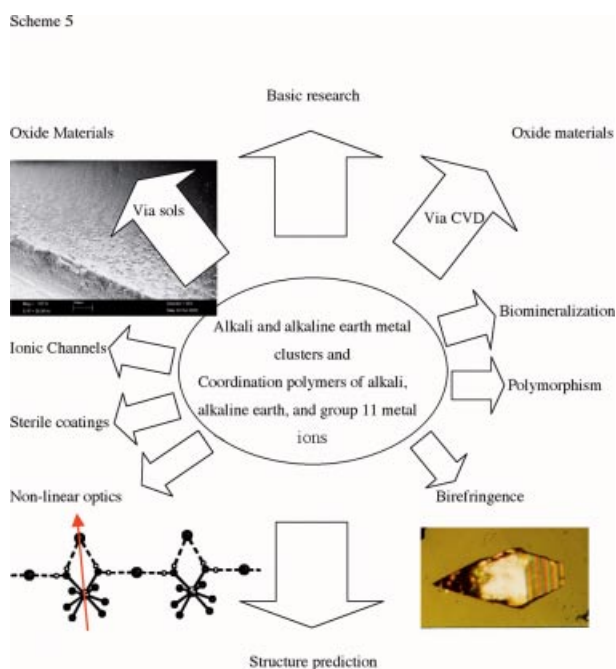
Scheme 5 Overview on possible application of our chemistry

$(H_2O)_2]I_2$ (**17**) crystallizes in the polar space group Cc, leading to the physical properties of i. e. non-linear optics (NLO) and piezoelectronics. For this compound, we were able to show that it is capable to produce second harmonics when irradiated with the fundamental wave length of a laser. The effect is weaker than in the classically used KH_2PO_4, however, good materials for NLO based on inorganic coordination compounds with a long-time resistance against heat and light are in the focus of actual research for certain applications. The compounds [Na⊂(DB18C6)I(L)], **6** and **7**, crystallize in acentric space groups as well, and the

crystals are observed to be birefringent under the polarizing microscope.

[IBa(O^{t}Bu)$_4${Li(thf)}$_4$(μ_4-OH)] (=„BaLi$_4$") (**33**), being volatile, it seemed to us a suitable precursor for barium oxide. Solution studies of the cluster, especially by NMR, revealed that the cluster retains its structure in solution, except for a fast exchange of THF ligands in d$_8$-THF. We then brought **33** onto a substrate of SrTiO$_3$ via a dip-coating method consisting of slowly withdrawing the substrate from the solution and let the solvent evaporate. At room temperature, the partially crystalline material was shown to be indeed the cluster of **33**. After thermal treatment as used in the synthesis of superconductors, only BaO was shown to be left on the surface, thus proving the possibility to use **33** as precursor for CVD of metal oxides. The two pure alkaline earth metal clusters, **27** and **28**, were not only shown to form sols on hydrolysis, but also the corresponding carbonates upon reaction with air. We now investigate the formation of CaCO$_3$ in the context of biomineralization.

Among the coordination polymers, we are interested in the disinfectant properties of silver compounds. As known from literature, they could be used as coating for catheters and other biocompatible materials in order to avoid bacteria to develop on such surfaces. Our compounds are currently being tested for such applications [37].

Conclusion

For alkali and alkaline earth metal compounds, we are able to present results in different contexts concerning low dimensional polymer, based on direct metal−halide contacts as well as on a supramolecular approach. For the latter, we continue our investigations with the goal of further contributions to crystal engineering and structure prediction. A new access to alkali and alkaline earth metal clusters is established and still leads to new results in this field. A recent review article deals with the importance of such oxygen donor based alkali and alkaline earth compounds [42]. Our results have shown that alkali and alkaline earth metal chemistry is not restrained to the ionic behaviour in water as solvent, but that substitution reactions and coordination chemistry similar to transition metals is possible.

Recently, we got involved in group 11 chemistry, and especially the coordination polymers of Cu$^{I/II}$ and Ag^I. This has led us into the field of polymorphism and gives also a contribution to crystal engineering and structure prediction. Some of our results present interesting physical properties, which we are investigating together with cooperation partners from physics, biology and medicine.

References

[1] K. M. Fromm, *Angew. Chem.* **1997**, *109*, 24, 2876−2878, *Angew. Chem. Int. Ed. Engl.* **1997**, *36*, 2799−2801.

[2] K. M. Fromm, *Cryst. Eng. Comm.* **2002**, *4(57)*, 318−322.

[3] K. M. Fromm, G. Bernardinelli, *Z. Anorg. Allg. Chem.* **2001**, *627*, 1626−1630.

[4] K. Boumizane, M. H. Herzog-Cance, D. J. Jones, J. L. Pascal, J. Potier, J. Roziere, *Polyhedron* **1991**, *10*, 2757−2769.

[5] A. D. Frankland, P. B. Hitchcock, M. F. Lappert, G. A. Lawless, *J. Chem. Soc., Chem. Commun.* **1994**, 2435−2436.

[6] K. M. Fromm, E. D. Gueneau, J.-P. Rivera, G. Bernardinelli, H. Goesmann, *Z. Anorg. Allg. Chem.* **2002**, *628*, 171−178.

[7] K. M. Fromm, E. D. Gueneau, H. Goesmann, C. Bochet, *Z. Anorg. Allg. Chem.* **2003**, *629*, 597−600.

[8] M. Dulak, R. Bergougnant, K. M. Fromm, H. R. Hagemann, A. Y. Robin, T. A. Wesolowski, submitted.

[9] S. Rashid, S. S. Turner, P. Day, M. E. Light, M. B. Hursthouse, S. Firth, R. J. H. Clark, *Chem. Commun.* **2001**, 1462−1463.

[10] U. Radius, *Z. Anorg. Allg. Chem.* **2004**, *630*, 848−857.

[11] E. D. Gueneau, K. M. Fromm, H. Goesmann, *Chem. Eur. J.* **2003**, *9*, 509−514.

[12] J. L. Atwood, P. C. Junk, S. M. Lawrence, C. L. Raston, *Supramol. Chem.* **1996**, *7*, 15−17.

[13] J. Amicangelo, P. B. Armentrout, *J. Phys. Chem. A* **2000**, *104*, 11420−11432.

[14] R. Bergougnant, A. Y. Robin, K. M. Fromm, submitted.

[15] K. M. Fromm, G. Bernardinelli, H. Goesmann, M.-J. Mayor-Lopez, J. Weber, *Z. Anorg. Allg. Chem.* **2000**, *626*, 1685−1691.

[16] K. M. Fromm, G. Bernardinelli, H. Goesmann, *Polyhedron* **2000**, *19*, 1783−1789.

[17] K. M. Fromm, *Chem. Eur. J.* **2001**, *7*, 2236−2244.

[18] K. M. Fromm, H. Goesmann, *Acta Crystallogr.* **2000**, *C56*, 1179−1180.

[19] D. G. Kurth, K. M. Fromm, J.-M. Lehn, *Eur. J. Inorg. Chem.* **2001**, 1523−1526.

[20] K. M. Fromm, W. Maudez, to be published.

[21] K. M. Fromm, E. D. Gueneau, G. Bernardinelli, H. Goesmann, J. Weber, M.-J. Mayor-López, P. Boulet, H. Chermette, *J. Am. Chem. Soc.* **2003**, *125*, 3593−3604 and therein.

[22] K. M. Fromm, *Chimia* **2002**, *56*, 676−680.

[23] Z. Xie, K. Chiu, B. Wu, T. C. W. Mak, *Inorg. Chem.* **1996**, *35*, 5957−5958; W. J. Evans, T. S. Gummersheimer, J. W. Ziller, *J. Am. Chem. Soc.* **1995**, *117*, 8999−9002; G. Heckmann, M. Niemeyer, *J. Am. Chem. Soc.* **2000**, *122*, 4227−4228; L. Huebner, A. Kornienko, T. J. Emge, J. G. Brennan, *Inorg. Chem.* **2004**, *43*, 5659−5664; M. Niemeyer, *Acta Crystallogr. Sect. E: Struct. Rep. Online* **2001**, *E57*, m363−m364.

[24] K. F. Tesh, D. J. Burkey, T. P. Hanusa, *J. Am. Chem. Soc.* **1994**, *116*, 2409−2417.

[25] K. M. Fromm, *Chimia* **2003**, *57*, 175−178.

[26] K. M. Fromm, *Cryst. Eng. Comm.* **2002**, *4*, 318−322.

[27] K. M. Fromm, W. Maudez, *Eur. J. Inorg. Chem.* **2003**, *18*, 3440−3444.

[28] R. J. Gillespie, E. A. Robinson, *Angew. Chem.* **1996**, *108*, 539−560; *Angew. Chem. Int. Ed. Engl.* **1996**, *35*, 495−514.

[29] E. D. Brady, T. P. Hanusa, M. Pink, V. G. Young, Jr., *Inorg. Chem.* **2000**, *39*, 6028−6037.

[30] K. M. Fromm, *Chem. Comm.* **1999**, *17*, 1659−1660.

[31] H. Nekola, F. Olbrich, U. Behrens, *Z. Anorg. Allg. Chem.* **2002**, *628*, 2067−2070.

[32] E. D. Gueneau, K. M. Fromm, unpublished results.

[33] R. D. Thomas, S. G. Bott, P. W. Gravelle, H. D. Nguyen, Book of Abstracts, 215th ACS National Meeting, Dallas, March 29th-April 2nd (1998).

[34] W. Maudez, K. M. Fromm, to be published.

[35] K. M. Fromm, E. D. Gueneau, H. Goesmann, *Chem. Comm.* **2000**, 2187−2188

[36] A. Y. Robin, K. M. Fromm, H. Goesmann, G. Bernardinelli, *Cryst. Eng. Comm.* **2003**, *5*, 405−410.

[37] A. Y. Robin, M. Meuwly, K. M. Fromm, H. Goesmann, G. Bernardinelli, *Cryst. Eng. Comm.* **2004**, *6*, 336−343.

[38] J. M. Harrowfield, B. J. Peachey, B. W. Skelton, A. H. White, *Aust. J. Chem.* **1995**, *48*, 1349−1356.

[39] L. Troxler, G. Wipff, J. M. Harrowfield, *J. Phys. Chem.* **1998**, *A102*, 6821−6830.

[40] Some examples: A. P. Cote, G. K. H. Shimizu, *Inorg. Chem.* **2004**, *43*, 6663−6673; Q. Chu, L. MacGillivray, Abstracts of Papers, 228th ACS National Meeting, Philadelphia, PA, United States, August 22−26, 2004 (2004), INOR-724; P. I. Richards, A. Steiner, *Inorg. Chem.* **2004**, *43*, 2810−2817; H. W. Roesky, M. Andruh, *Coord. Chem. Rev.* **2003**, *236*, 91−119; A. J. Blake, N. R. Champness, A. N. Khlobystov, D. A. Lemenovskii, W.-S. Li, M. Schroder, *Chem. Commun.* **1997**, *15*, 1339−1340.

[41] C. G. Claessens, J. F. Stoddart, *J. Phys. Org. Chem.* **1997**, *10*, 254−272.

[42] K. M. Fromm, E. D. Gueneau, *Polyhedron* **2004**, *23*, 1479−1504.

Jorge Luis Sague Doimeadios

Landoltstrasse 64
3007 Bern
Switzerland

Email: jorge.sague@unifr.ch
Home Phone: +41 (0) 31 371 34 82
Work Phone: +41 (0) 26 300 87 36

PERSONAL DETAILS

Marital status: Married.
Place of Birth: Holguín, Cuba.
Date of Birth: 11/10/1975.

Languages: English, French, German, Spanish (all fluent, spoken and written).

EDUCATION

1993-1998:
Studies of Chemistry, Faculty of Chemistry, University of Havana, La Havana, Cuba.

1998:
Thesis Degree on chemistry, "*Synthesis of new vegetal hormone based on human steroids precursor.*" Faculty of Chemistry, University of Havana, La Havana, Cuba.

2002-2006:
PhD.-studies: "*Silver Coordination Compounds with a Family of Ditopic Ligands of Varying Flexibility: about Chains, Rings, Helices and Polycatenanes*".
Supervisor Prof. K. M. Fromm. Department of Chemistry, University of Basel, Switzerland.
The thesis was awarded as *Magna Cum Laude*

EMPLOYMENT

6/1999-5/2001: **Development/Research**, *Spectroscopy and analytical Techniques*.
National Center for Scientific Research (NCSR), La Havana, Cuba.

10/1998-5/1999: **Research**, *Evaluation of the effects of synthetic hormones in plants*.
Center of Vegetal Biotechnology, Holguín, Cuba.

2006-present day: **Postdoctoral position**. *Synthesis and characterization of new materials for catalysis and NLO applications*.
University of Fribourg, Switzerland.
Supervisor Prof. K. M. Fromm., Department of Chemistry, University of Fribourg, Switzerland.

PUBLICATIONS

1) *Recent advances in the chemistry of "clusters" and coordination polymers of alkali, alkaline earth metal and group 11 compounds.* Fromm, Katharina M.; Gueneau, Estelle D.; Robin, Adeline Y.; Maudez, William; Sague, Jorge; Bergougnant, Remi., Zeitschrift fuer Anorganische und Allgemeine Chemie (2005), 631(10), 1725-1740.

2) *Concomitant crystallization of two polymorphs - a ring and a helix: concentration effect on supramolecular isomerism.* Fromm, Katharina M.; Doimeadios, Jorge L. Sague; Robin, Adeline Y., Chemical Communications (Cambridge, United Kingdom) (2005), (36), 4548-4550.

3) *On the coordination behaviour of NO₃⁻ in coordination compounds with Ag⁺ Part 1. Solubility effect on the formation of coordination polymer networks between AgNO₃ and L (L = ethanediyl bis(isonicotinate) as a function of solvent.* A. Y. Robin, J. L. Sague. D, K. M. Fromm, *Cryst.Eng.Comm.* 2006. 8(5): p. 403-416.

4) *The First Two-Dimensional Polycatenane: A New Type of Robust Network Obtained by Ag-Connected One-Dimensional Polycatenanes.* Sague, J.L. and Fromm, K.M., *Crystal Growth & Design.* 2006. 6(7): p. 1566-1568.

5) *Structure–property relationships: Polymorphism, solvates, and clay behavior in the one-dimensional coordination polymer chains [Ag(L)(NO3)](H2O)n, L = ethanediyl bis(isonicotinate), n = 0, and 2*. A. Y. Robin, J. L. Sague, A. Neels, T. Vig Slenters, K. M. Fromm. *Inorganica Chimica Acta* 360 (2007) 212–220.

ORAL PRESENTATIONS

03/2004	Third Swiss Snow Symposium 2005, Swiss young chemists' association. *Switzerland.*
2003-2006	Seminars in the Department of Inorganic Chemistry, *Uni Basel, Switzerland.*
07/2007	Workshop: "Simulation, design and crystal engineering of metal-organic frameworks". *University of Lyon, France*
09/2007	Conference in the Fall Meeting of the Swiss Chemical Society. *EPFL, Lausanne, Switzerland. (Accepted)*

LAB/ TECHNICAL SKILLS.

- Large experience in crystallization techniques, studies and characterization of polymorphs.
- Crystallography.
- Single mono-crystal and powder X-ray measures, singles X-ray structures resolution.
- Advanced Techniques in analytical, synthetic organic and inorganic chemistry.
- Organic, inorganic and analytical chemistry.
- Spectroscopy (Mass, UV, IR, NMR, X-ray diffraction) and Chromatography (TLC, GC, HPLC) techniques.
- Thermogravimetric techniques (SDTA, TG).
- Making reports.

ATTENDED CONFERENCES

XIII Scientific Seminar of the National Center for Scientific Research. *(June 2000. Cuba).*
V Caribbean and Centro American Environmental Analytical Chemistry Symposium. *(November 2000. Cuba).*
Seventh Latin American Conference on the Applications of the Mossbauer Effect. *(November 2000. Venezuela).*
Conferences from the Swiss Chemical Society (*from 2003 to 2006*)
GDCh- Jahrestagung Chemie 2003. *(October 2003. München, Germany).*
XXXVIth International Conference on Coordination Chemistry. *(July 2004. Mérida, Mexico).*
Summer school on advanced materials. *(September 2005. Villars-sur-Ollon, Switzerland)*
Dalton Discussion 9: Functional Molecular Assemblies. *(April 2006. University of Manchester, England)*
Summer school on Fundamental of Kinetics and Thermodynamics in (metallo)Supramolecular Assemblies. *(September 2006. Villars-sur-Ollon, Switzerland)*
CECAM workshop "Simulation, design and crystal engineering of metal-organic frameworks". *(July 2007, University of Lyon, France)*
Zürich Crystallography School 2007 (*August 2007, University of Zürich, Switzerland*)

POSTER PRESENTATIONS

1)*"Molecular Tectons as Building Blocks in Ag supramolecular Chemistry."* GDCh- Jahrestagung Chemie 2003. October 2003. München, Germany.

2)*"Coordination chemistry of polydentate ligands containing N and O donor functions."* XXXVIth International Conference on Coordination Chemistry. July 2004. Mérida, Mexico.

3)*"The amazing world of silver coordination polymers."* Herbstversammlung 2004. October 2004. Zürich. Switzerland.

4) *"Toward Complexity in Co-ordination Polymer Networks: Isomerism with Silver Salts."* Dalton Discussion 9. Manchester. England

TEACHING

06/2003-08/2004	**Demonstrator of Inorganic Chemistry for Chemistry Students**, University of Basel, Switzerland.
10/2004-02/2005	**General Chemistry Tutorial I for Biology Students**, University of Basel, Switzerland.
03/2005-07/2005	**Demonstrator of Inorganic Chemistry for Chemistry Students**, University of Basel, Switzerland.
10/2005-07/2006	**Analytical Chemistry Tutorial I for Pharmacy Students**, University of Basel, Switzerland.
10/2006-02/2007	**Organic Chemistry Tutorial I for Chemistry Students**, University of Fribourg, Switzerland.
03/2007-present	**Analytical Chemistry Tutorial II for Chemistry Students**, University of Fribourg, Switzerland.
06/2007-present	**Introduction to crystallography for Chemistry Students**, University of Fribourg, Switzerland.

Excellent inter-personal skills. Self-motivated, organized and independent in work habits.

References.

Prof. Edwin C. Constable

University of Basel
Department of Chemistry
Spitalstrasse 51.
CH-4056 Basel, Switzerland

Telf. +41 (0) 61 267 10 01

e-mail. Edwin.constable@unibas.ch

Prof. Katharina M. Fromm

University of Fribourg
Department of Chemistry
Rue du Musée 9.
CH-1700 Fribourg, Switzerland

Telf. +41 (0) 26 300 87 32

e-mail. Katharina.fromm@unifr.ch